THE PLANETARY BOUNDARY-LAYER OF THE ATMOSPHERE

F. Wippermann

Professor of Meteorology
Technical University Darmstadt, Germany

With Contributions by
D. ETLING, H. LEYKAUF and D. YORDANOV

DEUTSCHER WETTERDIENST
Offenbach a. M. 1973

Annalen der Meteorologie

(Neue Folge)
Nr. 7

Bisher erschienen:

		Erscheinungsjahr
Nr. 1	H. G. Cannegieter: The history of the International Meteorological Organization 1872–1951	1963
Nr. 2	A. Hofmann: Der internationale Stand des Problems der Langfrist-Vorhersage	1963
Nr. 3	Die Meteorologen-Tagung in München vom 27.–30. April 1966	1967
Nr. 4	Meteorologen-Geophysiker-Tagung in Hamburg vom 1.–6. April 1968, Meteorologische Vorträge	1969
Nr. 5	XI. Internationale Tagung für Alpine Meteorologie in Oberstdorf 22.–26. September 1970	1971
Nr. 6	Meteorologische Vorträge, gehalten auf der 36. Physikertagung 1971 in Essen	1973

Herausgeber und Verlag:
Deutscher Wetterdienst, Zentralamt, 6050 Offenbach a. M., Frankfurter Straße 135

Mit der Annahme des Manuskriptes und seiner Veröffentlichung durch den Deutschen Wetterdienst geht das Verlagsrecht für alle Sprachen und Länder einschließlich des Rechtes der photomechanischen Wiedergabe oder einer sonstigen Vervielfältigung an den Deutschen Wetterdienst über; für seinen Inhalt ist der Verfasser verantwortlich.

Zur Einführung

Der Deutsche Wetterdienst gibt seit 1963 die „Annalen der Meteorologie (Neue Folge)" heraus. In dieser Schriftenreihe werden Arbeiten über Teilgebiete der Meteorologie veröffentlicht, deren jeweiliger Stand in übersichtlicher und möglichst abgeschlossener Form dargestellt ist, sowie Vorträge von Meteorologentagungen.

In dem hier vorgelegten Band Nr. 7 gibt der Autor einen Überblick über den Stand der Forschung auf dem Gebiet der planetarischen Grenzschicht. Für den praktischen Wetterdienst sind diese Forschungen deshalb besonders aktuell, weil sie unter anderm auch Lösungen zum Problem der Parameterisierung von (kleinräumigen) Grenzschichteffekten in großräumigen numerischen Vorhersagemodellen beisteuern.

Die Art der in diesem Band gewählten Darstellung ist etwas ungewöhnlich. Aus verschiedenen Gründen, nicht zuletzt wegen der Kosteneinsparung, enthält sie eine Reihe Abdrucke von Publikationen des Autors in wissenschaftlichen Fachzeitschriften aus den letzten drei Jahren; diese sind zusammengestellt und mit einem verbindenden Text in Kapiteln angeordnet worden. Hierdurch mag zwar die Einheitlichkeit und Geschlossenheit bis zu einem gewissen Grade verlorengegangen sein, der Leser hat dafür andererseits die Gewähr, daß ihm nur neueste Ergebnisse dargeboten werden.

Dr. E. Süssenberger
Präsident des
Deutschen Wetterdienstes

Preface

Since 1963 the Deutscher Wetterdienst has been issuing the „Annalen der Meteorologie (New series)." In this series not only papers are published about different branches of meteorology, the actual status of which is represented clearly and in a possible completed form, but also proceedings of meteorological meetings.

In the present volume 7 the author gives a survey of the status of the research activities in the field of the planetary boundary layer. For the practical meteorological service these research activities are of particular interest as they contribute among others also solutions to the problem of the parameterization of (small-scale) boundary layer effects in large-scale numerical forecast models.

The representation used in this volume is somewhat unusual. For different reasons, last not least because of saving costs, it contains a number of reprints of publications of the author in scientific journals from the past 3 years; they are compiled and arranged in chapters with a connecting text. Thus the uniformity and completeness may be lost to a certain degree but on the other hand the reader may be sure that the latest results only are offered to him.

Dr. E. Süssenberger
President
Deutscher Wetterdienst

Contents

Preface v

Contents vii

Foreword 1

Chapter 1

The Planetary Boundary-Layer : Definitions and Equations 7

Chapter 2

Some Problems in Modelling the Planetary Boundary-Layer 25

The Problem of Closing the System of the PBL-Equations 26

Models Based on a Hypothesis for the Profile of the Eddy Viscosity 34

Models Based on a Hypothesis for the Mixing-Length 40

A Mixing-Length Hypothesis for the Planetary Boundary-Layer Flow in the Atmosphere
Beitr. Phys. Atm. 44, 215-226, 1971 46

Note on the Upper Boundary Conditions 58

A Note on a Method for Solving the Planetary Boundary-Layer Equations
Beitr. Phys. Atm. 44, 293-296, 1971 59

Chapter 3

The Structure of the Planetary Boundary-Layer 63

The Eddy Viscosity in a Barotropic Planetary Boundary-Layer as Related to the Turbulent Kinetic Energy
Beitr. Phys. Atm. 44, 127-136, 1971 66

Rossby-Number Similarity in the Planetary Boundary-Layer 76

A Note on the Rossby Similarity for Flows of Barotropic Planetary Boundary-Layers (with D.YORDANOV)
Beitr. Phys. Atm. 45, 66-71, 1972 89

Universal Profiles in the Barotropic Planetary Boundary-Layer
Beitr. Phys. Atm. 45, 148-163, 1972 95

Note on the Energy Budget in the PBL 111

Layers with a Reduced Eddy Viscosity Caused by the Baroclinicity (with D.YORDANOV)
Beitr. Phys. Atm. 45, 267-275, 1972 120

The Wind Profile Very Close to the Ground
Beitr. Phys. Atm. 46, 57-63, 1973 129

Numerical Study on the Effects Controlling the Low-Level Jet
Beitr. Phys. Atm. 46, 137-154, 1973 136

Chapter 4

The Parameterization of PBL-Effects with the Aid of the Resistance Law 154

The Resistance Law for the Planetary Boundary Layer 157

The Two Constants in the Resistance Law for a Neutral Barotropic Boundary Layer of the Atmosphere
Beitr. Phys. Atm. 43, 133-140, 1970 167

Note on a paper by F. Wippermann "The Two Constants in the Resistance Law for a Neutral Barotropic Boundary Layer of the Atmosphere"
by R.J. TAYLOR
Beitr. Phys. Atm. 44, 69, 1971 175
Reply by F. Wippermann 176

Empirical Formulae for the Universal Functions $M_m(\mu)$ and $N(\mu)$ in the Resistance Law for a Barotropic and Diabatic Planetary Boundary Layer
Beitr. Phys. Atm. 45, 305-311, 1972 177

The Parameterization of the Turbulent Fluxes of Momentum, Heat and Moisture at the Ground in a Baroclinic Planetary Boundary Layer (with D.YORDANOV)
Beitr. Phys. Atm. 45, 58-65, 1972 184

Baroclinic Effects on the Resistance Law for the Planetary Boundary Layer of the Atmosphere
Beitr. Phys. Atm. 45, 244-259, 1972 192

A Note on the Parameterization of the Large - Scale Wind Stress at the Sea Surface
Beitr. Phys. Atm. 45, 260-266, 1972 208

Problems which still have to be solved before the resistance laws can be applied 215

Chapter 5

Non-Stationary and/or Horizontally Non-Homogeneous Boundary-Layers 220

The Effects of Non-Stationarity on the Planetary Boundary-Layer (with D.ETLING and H. LEYKAUF)
Beitr. Phys. Atm. 46, 34-56, 1973 222

Boundary-Layers with a Change in the Roughness - Length and/or in the Temperature:
A Bibliographical Survey 245

Chapter 6

The Dynamic Instability of the Atmospheric Boundary Layer 255

The Orientation of Vortices Due to Instability of the Ekman Boundary-Layer
Beitr. Phys. Atm. 42, 225-244, 1969 260

The Stability of an Ekman Boundary-Layer Flow as Influenced by the Thermal Stratification (in Germ.)
by D. ETLING
Beitr. Phys. Atm. 44, 168-186, 1971 280

Chapter 7

The Dispersion of Windborne Material in the Planetary Boundary-Layer 299

A Perspective for a Routine Prediction of Concentration Patterns
(with D. YORDANOV)
Atm. Environm. 6, 877-888, 1972 301

Time-Dependent Concentrations of Dispersed Material Compared with those of the Corresponding Stationary Cases (in Germ.)
Meteor. Rdsch. 26, 11-18, 1973 314

Meteorological Parameters Relevant in a Statistical Analysis of Air Quality Data 322

List of Symbols 333

Author Index 343

Foreword

During the last ten years, approximately, the number of scientists interested in the boundary layer of the atmosphere has considerably increased; the number of papers in this field has increased likewise. There are several reasons for this development. One of these certainly is the need of a parameterization of the boundary layer effects in models for the numerical weather prediction or in models for the simulation of the general atmospheric circulation. Such models have been improved in recent years to a state, in which the incorporation of a more detailed description of the boundary layer is indispensable.

By this time there exist several monographs and review papers on the atmospheric boundary layer. The first book to be mentioned in this field was issued 1961 by LAIKHTMAN, a second revised and enlarged edition of it followed in 1970. ZILITINKEVICH, LAIKHTMAN and MONIN published a review paper in 1967 in the Proceedings (Izv.) of the Academy of Science USSR. In 1970 a monograph by ZILITINKEVICH appeared and in the same year a review paper by MONIN in the Annual Reviews of Fluid Mechanics, which is the first comprehensive

paper in English. One year later, in 1971, the U.S. Atomic Energy Commission edited the monograph by PLATE.

As far as the surface layer is concerned two earlier monographs should also be mentioned, that by PRIESTLEY 1959 and another one by LUMLEY and PANOFSKY 1964.

Very recently the American Meteorological Society published the lecture notes (ed. D.A.HAUGEN) of a workshop on micrometeorology, held at Boston, Mass., in August 1972.

All these books and papers have in common to treat the surface layer at full length but the whole planetary boundary layer to a much less extent. This is clear since the processes in the surface layer are much better understood than those in the planetary boundary layer; they can be measured by instruments mounted at masts or at towers and they may be predicted theoretically more easily on the basis of simplifying assumptions (e.g. constant fluxes) valid only in the surface layer.

In the present book the atmospheric boundary layer is treated as an entity and a subdivision of the planetary boundary layer into the surface layer and an outer layer is avoided deliberately.

The title of the present monograph "The Planetary Boundary Layer of the Atmosphere" possibly looks pretentious. However, in the first chapter, a definition of the planetary boundary layer (PBL) is given, showing it as an abstraction; it is based on several conditions, which will certainly not be satisfied in the real boundary layer of the atmosphere. Rather one has to assume that the real boundary layer differs only a little from a PBL and that the results obtained for the PBL can be applied to the real boundary layer.

For the purpose of a parameterization of boundary layer effects a restriction to the surface layer is pos-

sible only in such cases where the numerical prediction model, for the sake of which the parameterization is made, calculates the large-scale variables in a level located at the top of the surface layer (i.e. very roughly at 30 m). In most prediction models, however, the lowest layer, at which large-scale variables are computed, is located at a much higher level, often not below the top of the planetary boundary layer. For this reason, the processes in the whole boundary layer have to be understood, if a parameterization of boundary layer effects is attempted. Since in this book the main emphasis is laid upon the possibilities of a parameterization, the whole planetary boundary layer must be taken into consideration.

In this respect the fourth chapter is of principal importance, it is devoted to the parameterization of boundary layer effects by applying the so-called resistance laws. Obviously, this central part of the book has to be preceeded by some introductory chapters (one to three), in which the definition of a planetary boundary layer is given, the problems of modelling it are discussed, and the structure of the planetary boundary layer is studied. In chapter five the consequences of the assumptions of horizontal homogeneity and stationarity in the boundary layer are investigated, which were required for the purpose of the parameterization based on the resistance laws. Such a parameterization will probably also fail, when the boundary layer is dynamically unstable, i.e. when large longitudinal vortices are formed in the boundary layer. Vortices of this kind are investigated in chapter six.

Chapter seven, about the turbulent diffusion in the planetary boundary layer, is restricted to such problems of the turbulent diffusion, in which parameters of the planetary boundary layer are involved.

This book consists mainly of a collection of papers of the period 1970 - 1973. Some of these papers have been published jointly with Dr. D. YORDANOV of the Academy of Science of Bulgaria in Sofia. They date from the period (1970-1971), which I remember gratefully and with pleasure as two years of a fruitful cooperation with Dr. YORDANOV, when he stayed at Darmstadt as a research fellow of the A. v.Humboldt-Foundation. Another paper of this book has been published jointly with D. ETLING and H. LEYKAUF. The book also contains the diploma-thesis (in German) of D. ETLING, a paper for which he obtained the award for young scientists 1971 of the German Meteorological Society.

Since the book is mainly a collection of recently published papers, the symbols are not completely uniform. In the list of symbols at the end of the book all those symbols are entered, which have been mainly used; I tried to indicate different symbols for the same quantity.

The pages are numbered at the top throughout the book. The page numbers of the original papers have been retained (at the bottom of the pages). It was not possible to number the equations consecutively; they are numbered beginning with (1) in each of the reprinted papers.

With respect to the English: I did my very best. The reader is kindly requested to overlook mistakes and inaccuracies.

Nearly all of the published papers appeared in the "Beiträge zur Physik der Atmosphäre"; thanks are given to the VERLAG F. VIEWEG in Braunschweig, Germany, for the permission to reproduce these papers. Another paper appeared in the journal "Atmospheric Environment" and still another one in the "Meteorologische Rundschau". The permission for the reproduction of these papers has been granted by PERGAMON PRESS OXFORD and the SPRINGER VERLAG HEIDELBERG; this is

gratefully acknowledged.

I wish to express my gratitude particularly to Dr. E. SUESSENBERGER, the President of the Deutscher Wetterdienst; he gave his permission to publish this book by his organization. Dipl.-Met. M. SCHLEGEL, the Chief of the library und publishing section of the Deutscher Wetterdienst, provided me with his helpful assistance, which I acknowledge thankfully.

Darmstadt
July 1973

F. Wippermann

References:

AMERICAN METEOROLOGICAL SOCIETY 1973 Workshop on Micrometeorology (Ed. D.A.HAUGEN), Lecture Notes prepared for the workshop at Boston, Mass., August 1972, pp 392

LAIKHTMAN, D.L. 1961 Physics of the Atmospheric Boundary Layer (in Russ.) Hydrometeorological Press Leningrad
1970 Second edition (revised and enlarged), pp 341

LUMLEY, J.L. PANOFSKY, H.A. 1964 The Structure of the Atmospheric Turbulence Interscience Monographs and Texts Vol. XII, Interscience Publishers New York, pp 239 + XI

MONIN, A.S. 1970 The Atmospheric Boundary Layer Annual Reviews of Fluid Mechanics 2, 225 - 250

PLATE, E.J. 1971 Aerodynamic Characteristics of the Atmospheric Boundary Layer AEC Critical Review Series U.S. Atomic Energy Commission pp 190 + VIII

PRIESTLEY, C.H.B. 1959 Turbulent Transfer in the Lower Atmosphere The University of Chicago Press, Chicago, pp 130 + VII

ZILITINKEVICH, S.S. LAIKHTMAN, D.L. MONIN, A.S. 1967 Dynamics of the Atmospheric Boundary Layer, Review (in Russ.) Proc.(Izv.) Acad. Sci. USSR., Atm. Ocean. Phys. 3(3), 297-333 (Engl. transl. 170-191)

ZILITINKEVICH, S.S. 1970 Dynamics of the Atmospheric Boundary Layer (in Russ.) Hydrometeorological Press Leningrad, pp 291

CHAPTER 1

The Planetary Boundary-Layer: Definitions and Equations

As pointed out already in the foreword the planetary boundary layer (PBL) is an abstraction; it is a special (theoretical) case of the atmospheric boundary layer with conditions, which in reality are never satisfied simultaneously.

The purpose of this first chapter is to give the definition of the PBL; this is done by the following equations (8), (9) and the inequalities (10a') - (10c') and (20).

In this chapter the equations governing the PBL should also be given; they are derived by starting with the basic equations and applying the conditions of the PBL. This is done not only for the mean quantities $\hat{u}$, $\hat{v}$, $\hat{\vartheta}$ and $\hat{s}$ but also for the different kinds of energy as the kinetic energy $\bar{\varrho}\,\hat{\mathbb{v}}^2/2$ of the mean motion, the turbulent kinetic energy $\overline{\varrho(\mathbb{v}'')^2}/2$, the internal and potential energy $\bar{\varrho}(c_v\hat{T}+\phi)$ and the latent heat $\bar{\varrho}L^*\hat{s}$. A set of energy equations is derived showing the transformations between different kinds of energy. The energy budget of the PBL, however, based on this set of energy equations, is considered in chapter 3.

1. The Basic Equations

The starting point for the formulation of the boundary layer equations is the set of the basic equations, namely the equation of motion

$$\frac{\partial \mathbf{v}}{\partial t} + (\mathbf{v}\cdot\nabla)\mathbf{v} + 2\boldsymbol{\Omega}\times\mathbf{v} = -\nabla\Phi - \frac{1}{\varrho}\nabla p + \frac{1}{\varrho}(\nabla\cdot\mathbf{F}) \tag{1}$$

$$\mathbb{F} = \varrho\nu\left\{\nabla\mathbf{v} + \mathbf{v}\nabla - \frac{2}{3}(\nabla\cdot\mathbf{v})\,\mathbb{E}\right\}$$

$$\mathbb{E} = \mathbb{i}\mathbb{i} + \mathbb{j}\mathbb{j} + \mathbb{k}\mathbb{k}$$

the continuity equation

$$\frac{\partial\varrho}{\partial t} + \nabla\cdot\{\varrho\,\mathbf{v}\} = 0 \tag{2}$$

the thermodynamic energy equation

$$\frac{\partial T}{\partial t} + (\mathbf{v}\cdot\nabla)T + \left\{\frac{c_p}{c_v} - 1\right\}T(\nabla\cdot\mathbf{v}) = \frac{\delta Q^*}{c_v} \tag{3}$$

and the equation of state

$$p = R\,\varrho\,T \tag{4}$$

where $\mathbf{v}$ with the components u, v, w is the instantaneous velocity, p is the pressure, ϱ the density and T the temperature; δQ^* is the diabatic heating per unit mass per unit time, R is the gas constant for air, c_p is the specific heat at constant pressure, c_v is the specific heat at constant volume, Φ is the geopotential ($\nabla\Phi = \mathbb{k}\,g$ with g the gravitational acceleration), ν is the kinematic viscosity and $\boldsymbol{\Omega}$ is the vector of the earth's rotation.

The set of eqs. (1)-(4) contains six equations for the six variables u, v, w, p, ϱ, T; the system is closed, if δQ^* is given.

2. The Definition of the Planetary Boundary Layer (PBL)

The boundary-layer of the atmosphere is called a Planetary Boundary Layer (PBL), if

(a) the boundary-layer flow is turbulent

(b) the mean flow and the turbulence properties are stationary

(c) the mean flow and the turbulence properties are horizontally homogeneous

(d) the molecular transport of momentum, heat or moisture can be neglected, as being small compared with the corresponding turbulent transport.

Condition (a) requires to consider an averaged motion; an average with time will be applied, either the arithmetical mean or the barycentric one (i.e. weighted by the density)

$$\overline{\psi}(t) = \frac{1}{2\Delta t}\int_{-\Delta t}^{+\Delta t} \psi(t+\tau)\, d\tau \tag{5a}$$

with

$$\psi = \overline{\psi} + \psi' , \qquad \overline{\psi'} = 0 \tag{5b}$$

or

$$\widehat{\psi}(t) = \frac{1}{\overline{\varrho}\, 2\Delta t}\int_{-\Delta t}^{+\Delta t} \varrho\, \psi(t+\tau)\, d\tau \tag{6a}$$

with

$$\psi = \hat{\psi} + \psi'' , \qquad \widehat{\psi''} = 0 \tag{6b}$$

These two averages and their deviations are interrelated by

$$\overline{\varrho\psi} = \overline{\varrho}\hat{\psi} , \qquad \widehat{\overline{\psi}} = \overline{\psi} , \qquad \overline{\hat{\psi}} = \hat{\psi} \tag{7a}$$

$$\hat{\psi} - \overline{\psi} = \widehat{\psi'} = -\overline{\psi''} \tag{7b}$$

The conditions (b), (c) and (d) mentioned before may be

written as follows:
The condition of stationarity

$$\frac{\partial}{\partial t}\,\overline{\{\cdots\cdots\}} = \frac{\partial}{\partial t}\,\widehat{\{\cdots\cdots\}} = 0 \tag{8}$$

The condition of horizontal homogeneity

$$\nabla_h\,\overline{\{\cdots\cdots\}} = \nabla_h\,\widehat{\{\cdots\cdots\}} = 0 \tag{9}$$

$$\text{except} \quad \nabla_h \bar{p} = -f\,\bar{\varrho}\,\mathbb{k} \times \hat{\mathbb{v}}_g$$

$$\text{and} \quad \nabla_h \hat{T} \approx -\frac{f}{g}\,\hat{T}\,\mathbb{k} \times d\,\hat{\mathbb{v}}_g/dz$$

The neglect of the molecular transports in comparison with the turbulent transports of momentum

$$\left|\nabla\cdot\overline{\mathbb{F}}\right| << \left|\left(\nabla\cdot\{\overline{\varrho\,\mathbb{v}''\mathbb{v}''}\}\right)\right| \tag{10a}$$

of heat

$$\nu_h\left|\nabla^2\{c_v\,\bar{\varrho}\,\hat{T}\}\right| << c_p\left|\nabla\cdot\{\overline{\varrho\,\mathbb{v}''\vartheta''}\}\right| \tag{10b}$$

and of moisture

$$\nu_s\left|\nabla^2\{\bar{\varrho}\,\hat{s}\}\right| << \left|\nabla\cdot\{\overline{\varrho\,\mathbb{v}''s''}\}\right| \tag{10c}$$

or in the PBL respectively

$$\left|\frac{d\,\mathbb{F}_z}{dz}\right| << \left|\frac{d}{dz}\{\overline{\varrho\,w''\mathbb{v}''}\}\right| \tag{10a'}$$

$$\nu_h\left|\frac{d^2}{dz^2}\{c_v\,\bar{\varrho}\,\hat{T}\}\right| << c_p\left|\frac{d}{dz}\{\overline{\varrho\,\mathbb{v}''\vartheta''}\}\right| \tag{10b'}$$

$$\nu_s\left|\frac{d^2}{dz^2}\{\bar{\varrho}\,\hat{s}\}\right. << \left|\frac{d}{dz}\{\overline{\varrho\,\mathbb{v}''s''}\}\right| \tag{10c'}$$

The index h means either "heat" or "horizontal", the in-

dex s means moisture and the index g geostrophic; $f = 2\Omega \sin(\varphi)$ is the Coriolisparameter and $\mathbb{k}$ the unit vector in the vertical. The two inequalities (10b') and (10c') will be explained later.

A consequence of the conditions (8) and (9) is

$$\hat{w} = 0 \tag{11}$$

which can be seen by applying the averaging procedure (5a) to the continuity equation (2); one gets

$$\frac{\partial \bar{\varrho}}{\partial t} + \nabla \cdot \left\{ \bar{\varrho}\, \hat{\mathbb{v}} \right\} = 0 \tag{12}$$

Considering the conditions (8) and (9) it remains

$$\frac{d}{dz} \left\{ \bar{\varrho}\, \hat{w} \right\} = 0 \tag{13}$$

or $\bar{\varrho}\hat{w}$ = const.. This constant must be zero since the earth surface can act neither as a source of mass nor as a sink; it follows eq. (11).

3. The PBL-Equations

From eq.(1) together with eq.(2) an equation for the momentum can be obtained, which reads after an averaging according to (5a) as

$$\begin{aligned} \frac{\partial}{\partial t} \left\{ \bar{\varrho}\, \hat{\mathbb{v}} \right\} + \nabla \cdot \left\{ \bar{\varrho}\, \hat{\mathbb{v}}\, \hat{\mathbb{v}} \right\} + 2\Omega \times \hat{\mathbb{v}}\, \bar{\varrho} &= \\ = - \bar{\varrho} \nabla \Phi - \nabla \bar{p} + (\nabla \cdot \overline{\mathbb{F}}) - (\nabla \cdot \overline{\varrho\, \mathbb{v}''\mathbb{v}''}) \end{aligned} \tag{14}$$

One gets from that by using eq.(12) the averaged equation of motion in the form

$$\frac{\partial}{\partial t} \hat{\mathbb{v}} + (\hat{\mathbb{v}} \cdot \nabla) \hat{\mathbb{v}} + 2\Omega \times \hat{\mathbb{v}} = -\nabla \Phi - \frac{1}{\bar{\varrho}} \nabla \bar{p} + \frac{1}{\bar{\varrho}} \nabla \cdot \left\{ \overline{\mathbb{F}} - \overline{\varrho\, \mathbb{v}''\mathbb{v}''} \right\} \tag{15}$$

This equation is reduced in the PBL by the conditions (8), (9),(10a') and (11) to

$$f\,\mathbb{k} \times \left\{\hat{\mathbb{v}}_h - \hat{\mathbb{v}}_g\right\} = -\frac{1}{\bar{\varrho}}\frac{d}{dz}\left\{\overline{\varrho\, w''\mathbb{v}''}\right\} \tag{16}$$

$$\frac{\partial \bar{p}}{\partial z} + g\,\bar{\varrho} = f^*\,\hat{\mathbb{v}}_{h,WE} - \frac{1}{\bar{\varrho}}\frac{d}{dz}\left\{\overline{\varrho (w'')^2}\right\} \tag{17}$$

$f^* = 2\Omega\cos(\varphi)$, w is the vertical velocity and $\mathbb{v}_h$ is the horizontal velocity; the index WE means the west-east component.

In eq.(17) the two terms on the left-hand side are of the order of $1\ g\ cm^{-2}\ sec^{-2}$, the terms on the right-hand side are of the order of $10^{-1} - 10^{-2}\ g\ cm^{-2}\ sec^{-2}$ and may therefore be neglected; the remaining left-hand side is the hydrostatic equation.

Eq.(16) is written in components as

$$f\left\{\hat{u} - \hat{u}_g\right\} = \frac{d}{dz}\left\{\frac{\tau_y}{\bar{\varrho}}\right\} + \frac{\tau_y}{\bar{\varrho}^2}\frac{d}{dz}\bar{\varrho} \tag{18a}$$

$$-f\left\{\hat{v} - \hat{v}_g\right\} = \frac{d}{dz}\left\{\frac{\tau_x}{\bar{\varrho}}\right\} + \frac{\tau_x}{\bar{\varrho}^2}\frac{d}{dz}\bar{\varrho} \tag{18b}$$

where

$$\tau_x = -\overline{\varrho\, u''w''} \quad , \quad \tau_y = -\overline{\varrho\, v''w''} \tag{19}$$

The orientation of the horizontal coordinates is not yet fixed.

The terms appearing in (18a) and (18b) are the largest at the lower boundary; there the first term on the right - hand side is $5\cdot 10^{-2} - 1\cdot 10^{-1}$ cm sec^{-2}, but the second term on the right-hand side is $1\cdot 10^{-3} - 5\cdot 10^{-3}$ cm sec^{-2} only, i.e.

$$\left|\frac{1}{\bar{\varrho}}\frac{d\bar{\varrho}}{dz}\right| << \left|\frac{1}{\tau}\frac{d\tau}{dz}\right| \tag{20}$$

The neglected vertical gradient of density can be written

also

$$\frac{1}{\bar{\varrho}}\frac{d\bar{\varrho}}{dz} = -\frac{c_v}{c_p}\frac{g}{R\,\hat{T}} - \frac{1}{\hat{\vartheta}}\frac{d\hat{\vartheta}}{dz} \tag{21}$$

where

$$\vartheta = T\left(\frac{p_o}{p}\right)^k , \quad k = (c_p - c_v)/c_p$$

is the potential temperature.

With the neglect mentioned before the PBL-equations are

$$f\left\{\hat{u} - \hat{u}_g\right\} = \frac{d}{dz}\left\{\frac{\tau_y}{\bar{\varrho}}\right\} \tag{22a}$$

$$-f\left\{\hat{v} - \hat{v}_g\right\} = \frac{d}{dz}\left\{\frac{\tau_x}{\bar{\varrho}}\right\} \tag{22b}$$

The boundary conditions are at the lower boundary

$$z = z_o : \qquad \hat{u} = \hat{v} = 0 \tag{23a}$$

$$\tau_x = \tau_{xo} , \quad \tau_y = \tau_{yo} \tag{23b}$$

and at the upper boundary

$$z = z_T : \qquad \hat{u} = (\hat{u}_g)_T , \quad \hat{v} = (\hat{v}_g)_T \tag{23c}$$

$$\tau_x = \tau_y = 0 \tag{23d}$$

where z_o is the roughness-length; it is that fictive height above the ground (z = 0) to which the lower boundary must be elevated because of the existence of roughness elements. z_T means the height of the upper border of the boundary-layer, at which the velocity defect ($\hat{v} - \hat{v}_g$) as well as the Reynolds stress vanishes*). In most cases this height is not known; therefore in PBL-models this height is often shifted to infinity.

A third PBL-equation can be derived from the thermodyna-

*) in a barotropic PBL

mic energy equation. However, instead of eq. (3) the form

$$\frac{\partial}{\partial t}\vartheta + (\mathbf{v}\cdot\nabla)\vartheta = \frac{1}{c_p}\frac{\vartheta}{T}\delta Q^* \tag{24}$$

will be used with the potential temperature ϑ as defined in eq.(21). An averaging of that eq. (24) yields

$$\frac{\partial}{\partial t}\hat{\vartheta} + (\hat{\mathbf{v}}\cdot\nabla)\hat{\vartheta} = \frac{1}{c_p}\overline{\left\{\frac{\vartheta}{T}\delta Q^*\right\}} - \frac{1}{\bar{\varrho}}\nabla\cdot\{\overline{\varrho\,\mathbf{v}''\vartheta''}\} \tag{25}$$

The diabatic heating δQ^* consists of several parts

$$\overline{(\varrho\,\delta Q^*)}_{I} = \nu_h\nabla^2\{c_v\,\bar{\varrho}\,\hat{T}\} \tag{26a}$$

$$\overline{(\varrho\,\delta Q^*)}_{II} = \overline{\mathbb{F}}\cdot\cdot\nabla\hat{\mathbf{v}} = \bar{\varrho}\,\varepsilon_m\,, \qquad \varepsilon_m > 0 \tag{26b}$$

$$\overline{(\varrho\,\delta Q^*)}_{III} = \overline{\mathbb{F}\cdot\cdot\nabla\mathbf{v}''} = \bar{\varrho}\,\varepsilon_t\,, \qquad \varepsilon_t > 0 \tag{26c}$$

$$\overline{(\varrho\,\delta Q^*)}_{IV} = -(\nabla\cdot\overline{\mathbb{R}}) \tag{26d}$$

$$\overline{(\varrho\,\delta Q^*)}_{V} = -\bar{\varrho}\,L^*\,\delta\hat{s} \tag{26e}$$

ν_h $[\mathrm{cm}^2\ \mathrm{sec}^{-1}]$ is the coefficient of molecular heat transfer (the thermal conductivity), ε $[\mathrm{cm}^2\ \mathrm{sec}^{-3}]$ is the rate of kinetic energy, which is dissipated per unit volume and per unit time and converted into heat (the index m indicates the mean flow, the index t the turbulence); $\mathbb{R}$ $[\mathrm{cal}\ \mathrm{cm}^{-2}\ \mathrm{sec}^{-1}]$ is the radiative flux and L^* $[\mathrm{cal}\ \mathrm{g}^{-1}]$ is the condensation heat per unit mass. δs is the amount of water vapor condensated ($\delta s < 0$) or evaporated ($\delta s > 0$) per unit time.(The mechanical equivalent of heat is needed for a comparison of these five parts, it is $A^* = 2.389\ 10^{-8}$ cal $\mathrm{g}^{-1}\ \mathrm{cm}^{-2}\ \mathrm{sec}^2$).

Part I represents the divergence of the molecular heat flux; in a PBL the horizontal divergence of this flux vani-

shes according to condition (9), the remaining vertical divergence can be neglected in comparison with the vertical divergence of the turbulent heat flux, see condition (10b'). The exception in eq. (9), the horizontal temperature gradient being different from zero in baroclinic cases, does not mean that a divergence of the horizontal molecular heat flux can exist in such cases: the horizontal homogeneity of the baroclinicity requires that the second derivatives of $\hat{T}$ vanish with respect to the horizontal coordinates.

Part II and III represent the conversion of kinetic energy into heat; since the shear of the flow is involved, see eq.(1), the dissipation of kinetic energy of the mean flow is much smaller than the dissipation of the turbulent kinetic energy

$$\varepsilon_m \ll \varepsilon_t \tag{27}$$

but even the turbulent kinetic energy contributes a very small amount to the internal energy (compared with the other heating terms) and therefore may be neglected too (in the equation (25), of course not in the equation for the turbulent kinetic energy).

Part IV reduces in a PBL to the vertical divergence only

$$\overline{(\varrho\, \delta Q^*)}_{IV,PBL} = -\frac{d\bar{R}_z}{dz} \tag{28}$$

The radiative flux R_z consists of the short wave part and the long wave part, where the latter is the more important one.

By writing

$$\overline{\left(\frac{\vartheta}{T}\, \delta Q^*\right)} = R\, \overline{\left(\frac{\vartheta}{p}\, \varrho\, \delta Q^*\right)} \approx R\, \overline{\left(\frac{\vartheta}{p}\right)}\, \overline{(\varrho\, \delta Q^*)} \tag{29}$$

$$\approx R\, \left(\frac{\hat{\vartheta}}{\bar{p}}\right)\, \overline{(\varrho\, \delta Q^*)}$$

the five expressions of (26) can be used in the eq. (25). One gets for this equation with the PBL-conditions (8),(9), (10b') and (11)

$$c_p \frac{d}{dz} \{\overline{\varrho\, w''\vartheta''}\} + \frac{\hat{\vartheta}}{\hat{T}} \frac{d\bar{R}_z}{dz} + \frac{\hat{\vartheta}}{\hat{T}} \bar{\varrho}\, L^* \delta\hat{s} = 0 \qquad (30)$$

A divergence of the turbulent flux of sensible heat can be compensated either by a convergence of the radiative flux or by a heat release of condensating water vapor.
For the turbulent flux of sensible heat the abbreviation

$$q = c_p\, \overline{\varrho\, w''\vartheta''} \qquad (31)$$

will be used. In a non-radiative ($\bar{R}_z$=0) and dry ($\hat{s}$=0) PBL the turbulent flux q of sensible heat must be constant with height as follows from eqs. (30) and (31)

$$q = q_o = \text{const} \qquad (32)$$

According to condition (9) the horizontal gradient of the averaged temperature can be different from zero (baroclinic PBL). Setting $\nabla_h \hat{T} \approx \nabla_h \hat{\vartheta}$ one gets an additional term in eq. (30) for baroclinic cases

$$\frac{dq}{dz} = - c_p\, \bar{\varrho}\, \hat{T}\, \frac{f}{q}\, \mathbb{k} \cdot \left[\hat{\mathbb{v}}_h \times d\, \hat{\mathbb{v}}_g/dz\right] \qquad (33)$$

This convergence or divergence of the turbulent heat flux in the baroclinic case compensates the temperature advection due to the cross-isobaric flow, which takes place mainly in the lower part of the PBL.
Evaluating the turbulent heat flux q by integrating the eq. (33) numerically with a $\hat{\mathbb{v}}_h$-profile obtained from a PBL model and with a given baroclinicity ($d\,\hat{\mathbb{v}}_g/dz$ = const) one finds a variation of q through the whole boundary-layer which amounts to very few percent of q_o only (if usual values of the baroclinicity are chosen). Therefore this ef-

fect can be neglected too.

Finally a fourth equation can be derived for the turbulent transport of moisture; we start with an equation for the conservation of moisture

$$\frac{ds}{dt} = \frac{\nu_s}{\varrho} \nabla^2 \{\varrho\, s\} + \delta s \tag{34}$$

where s is the water vapor (the specific humidity or the mixing-ratio) and ν_s is the molecular transport coefficient for water vapor. The first term on the right-hand side represents the divergence of the molecular transport of water vapor; the second term represents the source or sink of water vapor by a change of phase, where δs is the amount of water vapor, which is lost per unit time by condensation or sublimation ($\delta s < 0$) or gained per unit time by evaporation ($\delta s > 0$).

Combining eq. (34) with the continuity eq. (2) and averaging one gets

$$\frac{\partial \hat{s}}{\partial t} + (\hat{\mathbf{v}} \cdot \nabla)\hat{s} = \frac{\nu_s}{\bar{\varrho}} \nabla^2 \{\bar{\varrho}\, \hat{s}\} + \delta\hat{s} - \frac{1}{\bar{\varrho}} \nabla \cdot \{\overline{\varrho\, \mathbf{w}'' s''}\} \tag{35}$$

With the PBL-conditions (8),(9),(10c') and (11) this equation reduces to

$$\frac{d}{dz}\{\overline{\varrho\, w'' s''}\} = \bar{\varrho}\, \delta\hat{s} \tag{36}$$

The turbulent moisture flux should be abbreviated by

$$j = \overline{\varrho\, w'' s''} \tag{37}$$

Now one has the following set of PBL-equations for the turbulent fluxes of momentum, sensible heat and moisture

$$\frac{d}{dz}\left(\frac{\tau_x}{\bar{\varrho}}\right) = - f\{\hat{v} - \hat{v}_g\} \tag{38a}$$

$$\frac{d}{dz}\left(\frac{\tau_y}{\bar{\varrho}}\right) = f\left\{\hat{u} - \hat{u}_g\right\} \tag{38b}$$

$$\frac{d}{dz}(q) = -\frac{\hat{\vartheta}}{\hat{T}}\frac{d}{dz}(\bar{R}_z) - \frac{\hat{\vartheta}}{\hat{T}}\bar{\varrho}\, L^* \delta\hat{s} \tag{38c}$$

$$\frac{d}{dz}(j) = \bar{\varrho}\, \delta\hat{s} \tag{38d}$$

with the boundary conditions

$$\left.\begin{array}{lll} z = z_o : & \tau_x = (\tau_x)_o \;, & \tau_y = (\tau_y)_o \\ & q = q_o \;, & j = j_o \\ & \hat{u} = \hat{v} = 0 & \end{array}\right\} \tag{39a}$$

$$\left.\begin{array}{lll} z = z_T : & \tau_x = (\tau_x)_T \;, & \tau_y = (\tau_y)_T \\ & q = q_T \;, & j = j_T \\ & \hat{u} = (\hat{u}_g)_T \;, & \hat{v} = (\hat{v}_g)_T \end{array}\right\} \tag{39b}$$

In the barotropic case is

$$(\tau_x)_T = (\tau_y)_T = 0$$

$$(\hat{u}_g)_T = (\hat{u}_g)_o \;, \quad (\hat{v}_g)_T = (\hat{v}_g)_o$$

Almost all efforts to solve the boundary layer problem are concentrated up to now still on that part, eqs. (38a) and (38b), which is concerned with the momentum. Of course the stress profiles $\tau_x(z)$ and $\tau_y(z)$ one wishes to obtain depend certainly on the thermal stratification and by that they are related also to the eqs. (38c) and (38d). However, up to now only such cases are solved for which q is constant with height, i.e. cases of a non-radiative and dry planetary boundary layer.

4. The Energy Equations for a PBL

A set of four equations can be derived for the kinetic energy of the mean motion, for the turbulent kinetic energy, for the sum of the internal and the potential energy and finally for the latent heat. It should be studied how these equations are reduced in a PBL, what the gains and losses of a kind of energy are in a PBL and which energy transformations occur in a PBL.

We start with the averaged equation of motion in the form of eq. (15), we multiply that by $\bar{\varrho}\,\hat{\mathbf{v}}$ and add to it the averaged continuity equation (12), which itself is multiplied by $\hat{\mathbf{v}}^2/2$; one obtains an equation for the total kinetic energy (per unit volume) of the mean motion:

$$\frac{\partial}{\partial t}\left\{\bar{\varrho}\,\frac{\hat{\mathbf{v}}^2}{2}\right\} + \nabla\cdot\left\{\bar{\varrho}\,\hat{\mathbf{v}}\,\frac{\hat{\mathbf{v}}^2}{2}\right\} = \tag{40}$$

$$= -\bar{\varrho}\,\hat{\mathbf{v}}\cdot\nabla\Phi - \hat{\mathbf{v}}\cdot\nabla\bar{p} + \hat{\mathbf{v}}\,\nabla\cdot\cdot\left\{\overline{\mathbb{F}} - \overline{\varrho\,\mathbf{v}''\mathbf{v}''}\right\}$$

where the last term may be written as

$$\hat{\mathbf{v}}\nabla\cdot\cdot\left\{\overline{\mathbb{F}} - \overline{\varrho\,\mathbf{v}''\mathbf{v}''}\right\} = \nabla\left\{\hat{\mathbf{v}}\cdot\cdot\,\overline{\mathbb{F}}\right\} - \nabla\left\{\hat{\mathbf{v}}\cdot\cdot\,\overline{\varrho\,\mathbf{v}''\mathbf{v}''}\right\} -$$

$$- \bar{\varrho}\,\varepsilon_m + \overline{\varrho\,\mathbf{v}''\mathbf{v}''}\cdot\cdot\,\nabla\hat{\mathbf{v}} \tag{41}$$

In the third term on the right-hand side the abbreviation (26b) has been used.

In order to get an equation for the turbulent kinetic energy the equation for the total kinetic energy will be derived and from this the eq. (40) will be subtracted. Starting with eq.(1), which has been multiplied by $\varrho\,\mathbf{v}$ and to which the continuity equation (2) multiplied by $\mathbf{v}^2/2$ has been added, one gets

$$\frac{\partial}{\partial t}\left\{\overline{\varrho\,\frac{\mathbf{v}^2}{2}}\right\} + \nabla\cdot\left\{\overline{\varrho\,\mathbf{v}\,\frac{\mathbf{v}^2}{2}}\right\} = -\bar{\varrho}\,\hat{\mathbf{v}}\cdot\nabla\Phi - \overline{\mathbf{v}\cdot\nabla p} + \overline{\mathbf{v}\,\nabla\cdot\cdot\,\mathbb{F}} \tag{42}$$

or partitioned into the two kinds of kinetic energy

$$\frac{\partial}{\partial t}\left\{\bar{\varrho}\,\frac{\hat{\mathbf{v}}^2}{2}\right\} + \frac{\partial}{\partial t}\left\{\overline{\varrho\,\frac{(\mathbf{v}'')^2}{2}}\right\} + \nabla\cdot\left\{\bar{\varrho}\,\hat{\mathbf{v}}\,\frac{\hat{\mathbf{v}}^2}{2}\right\} + \nabla\cdot\left\{\hat{\mathbf{v}}\,\overline{\varrho\,\frac{(\mathbf{v}'')^2}{2}}\right\}$$

$$+ \nabla\cdot\left\{\overline{\varrho\,\mathbf{v}''\frac{(\mathbf{v}'')^2}{2}}\right\} + \nabla\left\{\hat{\mathbf{v}}\cdot\cdot\left(-\bar{\mathbb{F}} + \overline{\varrho\,\mathbf{v}''\mathbf{v}''}\right)\right\} -$$

$$- \nabla\left\{\overline{\mathbf{v}''\cdot\cdot\,\mathbb{F}}\right\} = \tag{43}$$

$$= -\bar{\varrho}\,\hat{\mathbf{v}}\cdot\nabla\Phi - \hat{\mathbf{v}}\cdot\nabla\bar{p} - \overline{\mathbf{v}''\cdot\nabla p} - \bar{\varrho}\,\varepsilon_m - \bar{\varrho}\,\varepsilon_t$$

Subtracting eq. (40) with (41) from eq. (43) one obtains an equation for the turbulent kinetic energy

$$\frac{\partial}{\partial t}\left\{\overline{\varrho\,\frac{(\mathbf{v}'')^2}{2}}\right\} + \nabla\cdot\left\{\hat{\mathbf{v}}\,\overline{\varrho\,\frac{(\mathbf{v}'')^2}{2}}\right\} + \nabla\cdot\left\{\overline{\varrho\,\mathbf{v}''\frac{(\mathbf{v}'')^2}{2}}\right\} -$$

$$- \nabla\left\{\overline{\mathbf{v}''\cdot\cdot\,\mathbb{F}}\right\} = \tag{44}$$

$$= -\overline{\mathbf{v}''\cdot\nabla p} - \bar{\varrho}\,\varepsilon_t - \overline{\varrho\,\mathbf{v}''\mathbf{v}''}\cdot\cdot\nabla\hat{\mathbf{v}}$$

An equation for the internal energy is given by (3); of course, it has to be averaged after being multiplied by ϱ and combined with the continuity equation (2), which itself is multiplied by T. It results

$$\frac{\partial}{\partial t}\left\{c_v\,\bar{\varrho}\,\hat{T}\right\} + \nabla\cdot\left\{c_p\,\bar{\varrho}\,\hat{\mathbf{v}}\,\hat{T}\right\} + \nabla\cdot\left\{c_p\,\overline{\varrho\,\mathbf{v}''T''}\right\} =$$

$$= \bar{\varrho}\,\hat{\mathbf{v}}\cdot\nabla\Phi + \hat{\mathbf{v}}\cdot\nabla\bar{p} + \overline{\mathbf{v}''\cdot\nabla p} + \overline{\varrho\,\delta Q^*} \tag{45}$$

where

$$\overline{\varrho\,\delta Q^*} = \nu_h\nabla^2\left\{c_v\,\bar{\varrho}\,\hat{T}\right\} + \bar{\varrho}\,\varepsilon_m + \bar{\varrho}\,\varepsilon_t -$$

$$- \nabla\cdot\bar{\mathbb{R}} - \bar{\varrho}\,L^*\delta\hat{s}$$

as explained in the notes following eq. (26).

An equation for the latent heat is already given by eq. (35); it contains the moisture per unit mass. In order to have an equation for the moisture per unit volume eq. (35) must be multiplied by $\bar{\varrho}$ and combined with the averaged continuity equation (12), which itself is multiplied by $\hat{s}$. One gets

$$\frac{\partial}{\partial t}\{\bar{\varrho}\,\hat{s}\} + \nabla\cdot\{\bar{\varrho}\,\hat{\mathbb{v}}\,\hat{s}\} + \nabla\cdot\{\overline{\varrho\,\mathbb{v}''s''}\} - \nu_s\,\nabla^2\{\bar{\varrho}\,\hat{s}\} = \bar{\varrho}\,\delta\hat{s} \tag{46}$$

The resulting set of equations (40),(44),(45) and (46) is given on top of page 22 in a somewhat rearranged form. The four equations contain as first term the variation with time of the considered kind of energy; the next three terms in each equation are the divergences of the energy transports by the averaged motion, by the turbulent motion and by the molecular motion. The terms on the right-hand side of the four equations appear twice (except $\nabla\cdot\bar{\mathbb{R}}$) with an opposite sign. These are the rates of conversion of energy from one kind into another.

In the lower part of page 22, eqs. (47) - (50), the same set of energy equations is given, but reduced by applying the PBL-conditions (8) - (11). On the left-hand side are the divergences of the turbulent vertical fluxes of the four energies; the quantity $\overline{\varrho\,w''\mathbb{v}_h''}\cdot\hat{\mathbb{v}}_h = -(\tau\cdot\hat{\mathbb{v}}_h)$ in eq. (47) can be interpreted indeed as the turbulent vertical flux of the kinetic energy of the mean motion. In the conversion term (a) on the right-hand side the geostrophic wind equation has been used, see in condition (9). The conversion terms (b) and (c) originate from the term $\overline{(\mathbb{v}''\cdot\nabla)p}$, which can be transformed in the following way

$$\overline{(\mathbb{v}''\cdot\nabla)p} = \overline{(\mathbb{v}\cdot\nabla)p} - (\hat{\mathbb{v}}\cdot\nabla)\bar{p}$$

Divergence of the transport by the

	averaged motion	turbulent motion	molecular motion	Energy conversions			
$\frac{\partial}{\partial t}\left\{\bar{\varrho}\frac{\hat{\mathbf{v}}^2}{2}\right\}$	$+\ \nabla\cdot\left\{\hat{\mathbf{v}}\bar{\varrho}\frac{\hat{\mathbf{v}}^2}{2}\right\}$	$+\ \nabla\left\{\hat{\mathbf{v}}\cdot\cdot\,\overline{\varrho\mathbf{v}''\mathbf{v}''}\right\}$	$-\ \nabla\left\{\hat{\mathbf{v}}\cdot\cdot\,\overline{\mathbb{F}}\right\}$	$=\ -\bar{\varrho}\hat{\mathbf{v}}\cdot\nabla\Phi$	$-\ \hat{\mathbf{v}}\cdot\nabla\bar{p}$	$-\ \bar{\varrho}\varepsilon_m$	$+\ \overline{\varrho\mathbf{v}''\mathbf{v}''}\cdot\cdot\,\nabla\hat{\mathbf{v}}$
$\frac{\partial}{\partial t}\left\{\overline{\varrho\frac{(\mathbf{v}'')^2}{2}}\right\}$	$+\ \nabla\cdot\left\{\hat{\mathbf{v}}\,\overline{\varrho\frac{(\mathbf{v}'')^2}{2}}\right\}$	$+\ \nabla\cdot\left\{\overline{\varrho\mathbf{v}''\frac{(\mathbf{v}'')^2}{2}}\right\}$	$-\ \nabla\left\{\overline{\mathbf{v}''\cdot\cdot\,\mathbb{F}}\right\}$	$=$	$-\ \overline{\mathbf{v}''\cdot\nabla p}$	$-\ \bar{\varrho}\varepsilon_t$	$-\ \overline{\varrho\mathbf{v}''\mathbf{v}''}\cdot\cdot\,\nabla\hat{\mathbf{v}}$
$\frac{\partial}{\partial t}\left\{\bar{\varrho}(c_v\hat{T}+\Phi)\right\}$	$+\ \nabla\cdot\left\{\hat{\mathbf{v}}\bar{\varrho}(c_p\hat{T}+\Phi)\right\}$	$+\ \nabla\cdot\left\{c_p\overline{\varrho\mathbf{v}''T''}\right\}$	$-\ \nu_h c_v\nabla^2\left\{\bar{\varrho}\hat{T}\right\}$	$=\ +\bar{\varrho}\hat{\mathbf{v}}\cdot\nabla\Phi$	$+\ \hat{\mathbf{v}}\cdot\nabla\bar{p}$	$+\ \overline{\mathbf{v}''\cdot\nabla p}\ +\ \bar{\varrho}\varepsilon_m$	$+\ \bar{\varrho}\varepsilon_t\ \ -L^*\bar{\varrho}\,\delta\hat{s}\ -\nabla\cdot\overline{\mathbb{R}}$
$\frac{\partial}{\partial t}\left\{\bar{\varrho}L^*\hat{s}\right\}$	$+\ \nabla\cdot\left\{\hat{\mathbf{v}}\bar{\varrho}L^*\hat{s}\right\}$	$+\ \nabla\cdot\left\{L^*\overline{\varrho\mathbf{v}''s''}\right\}$	$-\ \nu_s L^*\nabla^2\left\{\bar{\varrho}\hat{s}\right\}$	$=$			$+\ L^*\bar{\varrho}\,\delta\hat{s}$

PBL:

$$-\frac{d}{dz}(\boldsymbol{\tau}\cdot\hat{\mathbf{v}}_h) = -f\,\bar{\varrho}\,\mathbb{k}\cdot[\hat{\mathbf{v}}_h\times\hat{\mathbf{v}}_g] - \bar{\varrho}\varepsilon_m - \left(\boldsymbol{\tau}\cdot\frac{d\hat{\mathbf{v}}_h}{dz}\right) \tag{47}$$

$$\frac{d}{dz}\left\{\overline{\varrho w''\frac{(\mathbf{v}'')^2}{2}}\right\} = -g\,\overline{\varrho' w'} - \frac{d}{dz}\{\overline{w'p'}\} - \bar{\varrho}\varepsilon_t + \left(\boldsymbol{\tau}\cdot\frac{d\hat{\mathbf{v}}_h}{dz}\right) \tag{48}$$

$$\frac{d}{dz}\left\{c_p\overline{\varrho w''T''}\right\} = +f\,\bar{\varrho}\,\mathbb{k}\cdot[\hat{\mathbf{v}}_h\times\hat{\mathbf{v}}_g] + \overline{g\varrho' w'} + \frac{d}{dz}\{\overline{w'p'}\} + \bar{\varrho}\varepsilon_m - \bar{\varrho}\varepsilon_t - L^*\bar{\varrho}\,\delta\hat{s} - \frac{d\overline{R}_z}{dz} \tag{49}$$

$$\frac{d}{dz}\left\{L^*\overline{\varrho w''s''}\right\} = +L^*\bar{\varrho}\,\delta\hat{s} \tag{50}$$

a b c d e f g h

$$= (\bar{\mathbf{v}}\cdot\nabla)\bar{p} + \overline{(\mathbf{v}'\cdot\nabla)p'} - \frac{1}{\bar{\varrho}}\overline{\varrho(\mathbf{v}\cdot\nabla)p}$$

$$= \nabla\cdot\{\overline{\mathbf{v}'p'}\} - \overline{p'(\nabla\cdot\mathbf{v}')} - \frac{1}{\bar{\varrho}}\overline{\varrho'(\mathbf{v}'\cdot\nabla)\bar{p}} \qquad (51)$$

the term $\overline{p'(\nabla\cdot v')}$ is assumed to be zero; however this can not be proved. In the atmospheric macro-turbulence this correlation certainly is different from zero but in the micro - turbulence it possibly vanishes.

With the PBL-conditions and the before-mentioned assumptions the eq. (51) reads

$$\overline{(\mathbf{v}''\cdot\nabla)p} = -\frac{1}{\bar{\varrho}}\overline{\varrho' w'}\frac{\partial\bar{p}}{\partial z} + \frac{d}{dz}\{\overline{w'p'}\}$$

and by applying the hydrostatic equation

$$\overline{(\mathbf{v}''\cdot\nabla)p} = g\,\overline{\varrho' w'} + \frac{d}{dz}\{\overline{w'p'}\} \qquad (52)$$

This equation has been used in order to obtain the conversion terms (b) and (c) in the eqs. (48) and (49). The terms (d), (e), (g) and (h) remain unchanged when the PBL-conditiones are imposed. The conversion term (f) reduces to the scalar product $(\tau\cdot d\hat{\mathbf{v}}_h/dz)$, where the abbreviation (19) has been used.

In order to get eq. (48) in the usual form of the budget of turbulent kinetic energy in the equlibrium

$$\left(\tau\cdot\frac{d\hat{\mathbf{v}}_h}{dz}\right) + \frac{g}{\bar{T}}\overline{\varrho w' T'} - \frac{d}{dz}\left\{\overline{\varrho w''\frac{(\mathbf{v}'')^2}{2}}\right\} - \frac{d}{dz}\{\overline{w'p'}\} - \bar{\varrho}\,\varepsilon_t = 0 \qquad (53)$$

some more assumptions have to be made beside that one already made

$$\overline{p'(\nabla\cdot\mathbf{v}')} = 0 \qquad (54a)$$

namely

$$\frac{p'}{p} << \frac{T'}{T}, \text{ i.e. } \frac{\varrho'}{\bar{\varrho}} \approx -\frac{T'}{\bar{T}} \qquad (54b)$$

by which

$$g\,\overline{\varrho' w'} \approx -g\frac{\bar{\varrho}}{\bar{T}}\overline{w'T'}$$

Furthermore must be assumed

$$\bar{\varrho}\,\overline{w'T'} \approx \overline{\varrho\, w'T'} \qquad (54c)$$

The result eq. (53) can be reached also when one starts with the Boussinesq approximation in the beginning, i.e. the assumptions (54a), (54b) and (54c) are the main constituents of the Boussinesq approximation. In order to be able to apply the flux-gradient relation the turbulent heat flux should be expressed by fluctuations of the p o t e n t i a l temperature. This requires two assumptions more

$$\overline{\varrho\, w'T'} \approx \overline{\varrho\, w'\vartheta'} \qquad (54d)$$

$$\approx \overline{\varrho\, w''\vartheta''} = q/c_p \qquad (54e)$$

The term (b) in eqs. (48) and (49) or the second term in eq. (53) represents the rate of energy converted from internal energy into turbulent kinetic energy and vice versa, it is one of the two most important terms in the budget of turbulent kinetic energy. One notices some contradiction with the condition (13) valid in a PBL when this term is used in eq. (53).

It is worth noting that a "balanced" form of a set of energy equations (such as the four equations on top of page 22) requires a representation of the turbulent flux of sensible heat by $\overline{\varrho w''T''}$ and not by $\overline{\varrho w''\vartheta''}$; however, the dilemma is that the relation between flux and gradient can be applied only when the heat flux is represented by the fluctuations of the potential temperature.

In order to be more correct, the eq. (45) should be called the equation for the sensible heat (instead of the internal energy) as long as the latent heat, eq. (46), is considered separately; the latter is a constituent of the internal energy too.

Chapter 2

Some Problems in Modelling the Planetary Boundary Layer

The PBL can be studied either by evaluating measurements made in the atmospheric boundary layer (eliminating in some way the effects being not consistent with the PBL conditions of stationarity and horizontal homogeneity) and in laboratory experiments or by carrying out numerical experiments with theoretical PBL-models. For the last possibility one needs a theoretical model, which should resemble to the true PBL as much as possible, i.e. as few assumptions as possible should be made for the purpose of simplification.

This chapter deals with some problems occuring in the development of a theoretical PBL-model.
The first part is concerned with the problem of closing the PBL-equations in general. Two sections follow with reviews of two types of models, namely those based on a hypothesis for the eddy viscosity and others based on a hypothesis for the mixing-length. The last two parts of this chapter deal with a special model developed by the author himself: another mixing-length hypothesis is presented as well as a method for solving the PBL-equations.

The Problem of Closing the System of the PBL-Equations

A PBL without radiative effects and without phase changes of the water vapor is governed by the set of eqs. (38a) - (38d) on the pages 17 and 18

$$\frac{d}{dz}\left\{\frac{\tau_x}{\bar{\varrho}}\right\} = -f\{\hat{v} - \hat{v}_g\} \tag{1a}$$

$$\frac{d}{dz}\left\{\frac{\tau_y}{\bar{\varrho}}\right\} = f\{\hat{u} - \hat{u}_g\} \tag{1b}$$

$$\frac{dq}{dz} = 0 \tag{1c}$$

$$\frac{dj}{dz} = 0 \tag{1d}$$

The eqs. (1a) and (1b) represent the dynamic part, they contain the four variables $\tau_x/\bar{\varrho}$, $\tau_y/\bar{\varrho}$, $\hat{u}$, $\hat{v}$. Therefore two equations more are needed for a closure of this partial system; since such two equations are not available the completion has to be made by two hypotheses.
The second part, eqs. (1c) and (1d), does not state anything about the vertical profiles of the potential temperature $\hat{\vartheta}(z)$ and of the moisture $\hat{s}(z)$ in which one is interested. Therefore one has to combine by two hypotheses the turbulent heat flux $q(z)$ with the temperature profile $\hat{\vartheta}(z)$ and the turbulent moisture flux $j(z)$ with the moisture profile $\hat{s}(z)$. Such hypotheses would be the flux - gradient relations, wich are applicable also to the eqs. (1a) and (1b); they are

$$\tau_x = \bar{\varrho}\, k_m\, d\hat{u}/dz \tag{2a}$$

$$\tau_y = \bar{\varrho}\, k_m\, d\hat{v}/dz \tag{2b}$$

$$-q = c_p\, \bar{\varrho}\, k_h\, d\hat{\vartheta}/dz \tag{2c}$$

$$-j = \bar{\varrho}\, k_s\, d\hat{s}/dz \tag{2d}$$

k_m , k_h , k_s are the turbulent diffusion coefficients for momentum, heat and moisture.

With these flux - gradient relations one gets for the eqs. (1a) - (1d)

$$\frac{d}{dz}\left\{ k_m \frac{d\hat{u}}{dz} \right\} = - f \{ \hat{v} - \hat{v}_g \} \tag{3a}$$

$$\frac{d}{dz}\left\{ k_m \frac{d\hat{v}}{dz} \right\} = f \{ \hat{u} - \hat{u}_g \} \tag{3b}$$

$$\frac{d}{dz}\left\{ k_h \frac{d\hat{\vartheta}}{dz} \right\} = 0 \tag{3c}$$

$$\frac{d}{dz}\left\{ k_s \frac{d\hat{s}}{dz} \right\} = 0 \tag{3d}$$

In the eqs. (3c) and (3d) the vertical variation of the density has been neglected as being small compared with the vertical temperature variation; compare with the inequality (20) on page 12 (of course, the difference can not be as large as in the case of the Reynolds stress).

In the four equations (3a) - (3d) now appear $\hat{\vartheta}$ and $\hat{s}$; but the four equations contain seven variables $\hat{u}$, $\hat{v}$, $\hat{\vartheta}$, $\hat{s}$, k_m , k_h , k_s , i.e. three additional equations are needed; with regard to the closing problem the situation is even worse than before.

Fortunately this is not true for the pure dynamical part of the problem, i.e. for the first two equations, (3a) and (3b); they contain the three variables $\hat{u}$, $\hat{v}$, k_m only. For the dynamics the set of equations can be closed by one hypothesis only, for instance by prescribing the vertical profile of the eddy viscosity

$$\boxed{\begin{aligned} \frac{d}{dz}\left\{ k_m \frac{d\hat{u}}{dz} \right\} &= - f \{ \hat{v} - \hat{v}_g \} && (4a) \\ \frac{d}{dz}\left\{ k_m \frac{d\hat{v}}{dz} \right\} &= f \{ \hat{u} - \hat{u}_g \} && (4b) \\ k_m &= \text{prescribed as } k_m(z) && (4c) \end{aligned}}$$

In the second part of this chapter a list is given of 23 models based on a hypothesis for $k_m(z)$.
Of course a closing in that manner is possible only by the additional hypothesis, that the eddy diffusion coefficients for τ_x and τ_y are the same; this is implied in eqs. (2a) and (2b). Actually one has the flux - gradient relations

$$\tau_x = \bar{\varrho}\, k_{m,x}\, d\hat{u}/dz \quad , \quad \tau_y = \bar{\varrho}\, k_{m,y}\, d\hat{v}/dz$$

and one has to assume

$$k_{m,x} = k_{m,y} = k_m \; .$$

An assumption for $k_m(z)$ is not the only possibility to close the system. k_m can be related to another variable and then a hypothesis has to be made for this variable; it can be the mixing-length for instance. In this case the necessary relation would be Prandtl's mixing-length relation

$$k_m = l^2 \left| \frac{d\hat{v}}{dz} \right| \tag{5}$$

If this eq. (5) is used, either the vertical profile $l(z)$ of the mixing-length has to be prescribed or an equation containing the mixing-length has to be hypothesized.
Then the set of equations is

$$\frac{d}{dz}\left\{ l^2 \frac{d\hat{u}}{dz} \left| \frac{d\hat{v}}{dz} \right| \right\} = - f \{ \hat{v} - \hat{v}_g \} \tag{6a}$$

$$\frac{d}{dz}\left\{ l^2 \frac{d\hat{v}}{dz} \left| \frac{d\hat{v}}{dz} \right| \right\} = f \{ \hat{u} - \hat{u}_g \} \tag{6b}$$

$$\left| \frac{d\hat{v}}{dz} \right| = \sqrt{\left(\frac{d\hat{u}}{dz}\right)^2 + \left(\frac{d\hat{v}}{dz}\right)^2} \tag{6c}$$

l = prescribed as $l(z)$ or (6d)
any hypothesis combining l with other variables which already
appear in the equations (6d')

These four equations (containing the four variables $\hat{u}$, $\hat{v}$ $|d\hat{v}/dz|$, l) are non-linear; models based on the eqs. (6a) - (6d) are more intricate.
In the third part of this chapter a list of models is given which are based on a hypothesis for the mixing-length; the advantages and disadvantages of such models are noted in this part too.

Sometimes k_m is related to the mixing-length l and to b , the turbulent kinetic energy per mass unit $[\, b = \overline{\rho (v'')^2}/(2\bar{\rho})\,]$ { instead of relating to l and to $|d\hat{v}/dz|$ as in eq. (5) }

$$k_m = l\, b^{1/2} \tag{7}$$

This means that beside l another new variable appears and that for the closure two hypotheses have to be made, one for l and another one for b. In such cases mostly the equation of turbulent kinetic energy is used

$$k_m \left[\frac{d\hat{v}}{dz}\right]^2 - k_h \frac{g}{\hat{\vartheta}} \frac{d\hat{\vartheta}}{dz} - \frac{d}{dz}\left\{k_b \frac{db}{dz}\right\} - \varepsilon_t = 0 \tag{8a}$$

(see eq. 53 on page 23), in which k_b is the turbulent diffusion coefficient for the turbulent kinetic energy and ε_t is the dissipation rate of this energy. Eq. (8a) involves two new variables, k_b and ε_t , for which one assumes

$$k_b = k_h \tag{8b}$$

$$\varepsilon_t = c\, l^{-1}\, b^{3/2} \tag{8c}$$

Such models are also listed in the third part; they are not necessarily restricted to the dynamics, they include the eq. (3c) and a further hypothesis for k_h .

If the dynamics of the PBL, the eqs. (3a) and (3b), are uncoupled from the system, the two eqs. (3c) and (3d) remain; they contain the four variables $\hat{\vartheta}$, $\hat{s}$, k_h and k_s . In order to close also this part of the system first one

puts

$$k_s = k_h \tag{9}$$

The turbulent diffusion coefficient for matter is certainly more similar to the turbulent diffusion coefficient for heat than that for momentum. Not at least this can be concluded from the same structure of the eqs. (3c) and (3d) which are different from the eqs. (3a) and (3b) containing k_m. The main reason, however, is that the heat and the moisture (matter) are transported quantities whereas the momentum is as well a transported as a transporting quantity.

In place of the second missing equation the vertical profile of k_h/k_m may be used such as it is observed in the boundary layer. Quite good profiles of k_h/k_m have been obtained for the surface layer by BUSINGER et al.(1971) evaluating the Kansas data of 1968

$$a_h = k_h/k_m \tag{10}$$

$$a_h(z) = \frac{1.0 + 4.7\ z/L_*}{0.74 + 4.7\ z/L_*} \quad , \quad L_* > 0 \tag{11a}$$

$$a_h(z) = \frac{(1 - 9\ z/L_*)^{1/2}}{(1 - 15\ z/L_*)^{1/4}} \quad , \quad L_* < 0 \tag{11b}$$

L_* is the Monin-Obukhov stability-length ($L_* > 0$ stable conditions, $L_* < 0$ unstable ones). If the relations (10), (11a) and (11b) are used one must assume that the profiles should be valid in the whole PBL, not in the surface layer only, where they have been obtained by measurements. This does not mean that the profiles $k_h(z)$ and $k_m(z)$ are extrapolated from the surface layer to the whole PBL; only the ratio of both is extrapolated.

Eq.(3c) requires that $k_h\ d\hat{\vartheta}/dz = \text{const}$. Since $d\hat{\vartheta}/dz \longrightarrow 0$ at the top (z_T) of the boundary layer it follows that $k_h \longrightarrow \infty$ for $z \longrightarrow z_T$. On the other side $k_m \longrightarrow 0$ for

$z \longrightarrow z_T$ *). (Of course, the dynamic height of the PBL, where $\hat{v} \longrightarrow (\hat{v}_g)_T$, must not be necessarily the same as the thermal height of the PBL, where $\hat{\vartheta} \longrightarrow \hat{\vartheta}_T$). One can conclude

$$z \longrightarrow z_T \quad (\text{resp. } z \longrightarrow \infty) : \quad a_h \longrightarrow \infty \;^{*)} \tag{12}$$

The empirical formula (11b), for the unstable case, satisfies this requirement (12), but the formula (11a) for stable conditions does not satisfy it. Therefore difficulties have to be expected in solving the equations when eq. (11a) is used to close the system; at least the results will be partly wrong.
The often used assumption

$$k_h = k_m \tag{13}$$

implies the same error.

The second part, eqs. (3c) and (3d), of the set of eqs. (3a) - (3d) cannot be closed separately but only when used together with the first part, the dynamic one; both parts are coupled by the variable k_m. The first part however can be closed separately as shown by the set (4a) - (4c) or (6a) - (6d).

On the whole the system of the PBL equations can not be closed without any hypothesis. Different hypotheses are possible; those given above are the most often used ones.

Another method of closing should still be mentioned, it has recently been attempted by several authors. The two stress components $\tau_x = -\varrho\overline{u''w''}$ and $\tau_y = -\varrho\overline{v''w''}$ appearing in the eqs. (1a) and (1b) are not parameterized, but an additional equation for each of these two stress components is derived. These equations are under the conditions of a PBL (steady state, horizontally homogeneous) the eqs. (14a) and (14b) on the next page.

*) in the barotropic case

$$\frac{d}{dz}\left\{\hat{u}\overline{\varrho(w'')^2} + \overline{\varrho u''(w'')^2}\right\} - f\overline{\varrho v''w''} - f^*\left\{\bar{\varrho}\hat{u}^2 + \overline{\varrho(u'')^2}\right\} + \tag{14a}$$
$$+ g\overline{\varrho' u'} + \overline{u'\frac{\partial p'}{\partial z}} + \overline{w''\frac{\partial p}{\partial x}} - D_{xz} = 0$$

$$\frac{d}{dz}\left\{\hat{v}\overline{\varrho(w'')^2} + \overline{\varrho v''(w'')^2}\right\} + f\overline{\varrho u''w''} - f^*\left\{\bar{\varrho}\hat{u}\hat{v} + \overline{\varrho u''v''}\right\} + \tag{14b}$$
$$+ g\overline{\varrho' v'} + \overline{v'\frac{\partial p'}{\partial z}} + \overline{w''\frac{\partial p}{\partial y}} - D_{yz} = 0$$

Herein D_{xz} and D_{yz} are abbreviations for the terms containing the molecular friction; these terms probably can be neglected in comparison with the corresponding turbulent terms. $f^* = 2\Omega\cos(\varphi)$ is the other Coriolis parameter. The second term in both equations is $f\tau_y$ and $f'\tau_x$, respectively. If all the other terms in the equations are known, τ_x and τ_y can be computed. However, now the parameterization problem arises for these other terms in which only $\hat{u}$ and $\hat{v}$ are variables of the other equations.
The paper by WYNGAARD, COTÉ and RAO (1973) should be cited as an example for making such a parameterization. These authors use a procedure presented by LUMLEY and KHAJEH-NOURI (1973), by which the terms to be parameterized are replaced by their values in an isotropic turbulence field and in addition by a series of terms representing corrections for anisotropy.

In such a procedure hypotheses have to be made for

$$\overline{\varrho\,(u'')^2} \quad , \quad \overline{\varrho u''v''}$$
$$\overline{\varrho \mathbf{v}_h''(w'')^2}$$
$$\overline{\varrho' \mathbf{v}_h'}$$
$$\overline{\mathbf{v}_h'\frac{\partial p'}{\partial z}} \quad , \quad \overline{w''\nabla_h p}$$

where $\overline{\varrho u''v''}$ probably vanishes in a PBL. Making so many hy-

potheses it is doubtful if such a closing procedure is an improved one indeed. The results obtained by models using such a closure are at least not better (at the present time) than those obtained by models using other, more conventional, closing hypotheses.

References:

BUSINGER, J.A. WYNGAARD, J.C. IZUMI, Y. BRADLEY, E.F.	1971	Flux - Profile Relationships in the Atmospheric Surface Layer J. Atm. Sci. 28 (2), 181-189
LUMLEY, J.L. KHAJEH-NOURI, B.	1973	Computational Modeling of Turbulent Transport Proc. 2nd IUTAM-IUGG Symposium on Turbulent Diffusion, Charlottesville Virg., USA April 8-14, 1973 To appear in "Advances in Geophysics"
WYNGAARD, J.C. COTÉ, O.R. RAO, K.S.	1973	Modeling the Atmospheric Boundary Layer Proc. 2nd IUTAM-IUGG Symposium on Turbulent Diffusion, Charlottesville Virg., USA April 8-14, 1973 To appear in "Advances in Geophysics"

Models Based on a Hypothesis for the Profile of the Eddy Viscosity

For more than sixty years (1905-1967) attempts have been made to model the PBL by prescribing the vertical profile of the eddy viscosity in the PBL-equations. In the fifteen last years only electronic computers have been available to carry out numerical integrations of the PBL-equations; one was forced in the time before to get a closed solution. The assumed profiles $k_m(z)$ are therefore as simple as possible and sometimes in a poor agreement with reality; nevertheless the wind spirals and the stress spirals obtained as solution describe the main structure of the PBL correctly. Even the simplest model, that by EKMAN (1905), gives fairly good results and is still often used to get some estimates. A brief survey of these models should be given:

01	k_m = const	1905 EKMAN, V.W. On the Influence of the Earth's Rotation on Ocean Currents Arkiv Math. Astr. och Fysik 2, Nr. 11, Uppsala, Sweden
02	k_m = const	1908 AKERBLOM, F.A. Recherches sur les courantes les plus bas de l'atmosphere au-dessus de Paris Nova Acta Reg. Soc. Sci. Uppsalensias 4, Nr.2
03	k_m = const	1915 TAYLOR, G.I. Eddy Motion in the Atmosphere Phil. Trans. Roy. Soc. London A 215, 1-26 (Slip condition at the lower boundary; herewith a precondition for the construction of a two-layer model is given)

04 $k_m \propto z^p$

1924 PRANDTL, L.
1924 TOLLMIEN, W
Die Windverteilung über dem Erdboden, errechnet aus den Gesetzen der Rohrströmung
Z. f. Geophys. 1, 47-55

(p = 0.843 is used according to results of pipe flows; in this paper, for the first time, the external parameters are combined to the surface Rossby number - not with that name of course. For the first time the geostrophic drag coefficient is computed and a "resistance law" being

$$C_g = 0.148\ (RO_o)^{-0.119}$$

is obtained)

05 $k_m = \text{const}$

1928 SAKAKIBARA, S.
On the Transverse Eddy Resistance in Moving Air in the Lower Atmosphere
Geophys. Mag. Tokyo 1, 130 - 149

06 $k_m \propto z^2$

07 $k_m \propto \exp(a\ z)$

1930 TAKAYA, S.
On the Coefficient of Eddy Viscosity in the Lower Atmosphere
Mem. Imp. Marine Obs. Kobe Japan, 4 (1)

08 $k_m \propto z$

1931 MÖLLER, F.
Austausch und Wind
Meteor. Z. 48 (2), 69 - 80

09 $k_m \propto (1 - \frac{z}{z_*})^2$
$z \leqq z_*$

1932 ROSSBY, C.G.
A Generalisation of the Theory of the Mixing-Length with Applications to Atmospheric and Oceanic Turbulence
MIT, Meteor. Pap. I (4), pp 36

(A hypothesis for the mixing-length is made with the consequence that $|d\hat{v}/dz|$ = const, i.e. the model remains linear. The mixing-length

hypothesis implies the hypothesis 09 for the eddy viscosity. The model is suitable as the upper part of a two-layer model, see model 11)

10 $k_m \propto z^p$

1933 KÖHLER, H.

Meteorologische Turbulenzuntersuchungen
Kungl. Svenska Wetenkapsakad. Handl. Tredje Ser. 13, 1-54
(The effect of a different thermal stratification is investigated with a variation of the power p . For the cross-isobar angle is obtained $\alpha_o = \pi/2\ (1-p)/(2-p)$)

11 $k_m \propto (1-\frac{z}{z_*})^2$
$z_1 \leqq z \leqq z_*$
$k_m \propto z$
$z_o \leqq z \leqq z_1$

1935 ROSSBY, C.G.
MONTGOMERY, R.B.

The Layers of Frictional Influence in Wind and Ocean Currents
Pap. Phys. Oceanogr. Meteor. MIT & WHOI 3 (3), pp 1o1
(First two-layer model of the PBL as a combination of the models 08 and 09; also first model which considers a maximum of k_m)

12 $k_m \propto z$

1937 BLINOVA, E.N.
KIBEL, I.A.

Application of the Theory of Turbulence to the Question of Distribution of Wind with Altitude (in Russ.)
in: Dynamic Meteorology (Ed. by B.I. Izvezkov and N.E. Kochin), Gidrometeoizdat

13 $k_m = \text{const}$
$z_1 \leqq z$
$k_m \propto z$
$z_o \leqq z \leqq z_1$

1940 YUDIN, M.I.
SVETZ, M.E.

A Stationary Model of Wind Distribution with Altitude in a Turbulent Atmosphere (in Russ.)
Trudy GGO Nr. 31 (8), 42-52
(The simplest kind of a two-layer

model, even today still used for getting estimates of wind profiles and stress profiles)

14 $k_m \propto 1 - \exp(-az)$

1944 SVETZ, M.E.

Determination of the Coefficient of Turbulent Viscosity for Atmospheric Motions (In Russ.) Dokl.Acad.Sci.USSR, 30 (8) and

The Turbulent Boundary Layer in the Atmosphere (in Russ.) Bull.(Izv.) Acad.Sci.USSR, Geogr. Geophys. Ser. 5, Nr.3

15 $k_m = \text{const}$ $z \geqq z_1$

$k_m \propto z^p$ $z \leqq z_1$

1947 BERLIAND, M.E.

The Boundary Layer of the Atmosphere (in Russ.) Trudy NIU GUGMS I, Nr.25, 14-67

16 $k_m \propto z^p$

1948 FROST, R.

Atmospheric Turbulence Q.J.Roy.Met.Soc. 74, 316-338

(Model 10 is extended by regarding the roughness-length z_o; a resistance law results

$$C_g = 0.206\ (RO_o)^{-0.111}\ .$$

In the neutral case p = 0.857, to be compared with p = 0.843 in model 04. As in model 10 the variation of α_o with the thermal stratification is studied)

17 $k_m \propto z$

1956 ELLISON, T.H.

Atmospheric Turbulence in: Surveys in Mechanics, ed. by G.K.Batchelor and R.M. Davies. Cambridge University Press, 400-430

(The same model almost as 08. For the determination of a constant the log-profile is used at the lower boundary; this enables to

derive the resistance law by this model. The main difference to model 08 is the extension for baroclinic PBLs; it is the first model which considers the baroclinicity of the PBL)

18 $k_m = \text{const}$ $z \geqq z_1$

$k_m \propto z^p$ $z \leqq z_1$

1960 TSEITIN, G.Kh.
ORLENKO, L.R.

The Stationary Distribution of Wind, Temperature and Turbulent Exchange in the Boundary Layer of the Atmosphere under Various Stability Conditions (in Russ.)
Trudy GGO 94, 8 – 28
AFCRL-Translation T-R-387

(Extension of model 15: in order to get a relationship between p and $d\hat{\vartheta}/dz$ the equation for the budget of turbulent kinetic energy - without the divergence term - has been used. C_3 and α_0 are obtained depending on the thermal stratification)

19 $k_m = \dfrac{\varkappa u_* z}{1+Sz+aS^2z^2}$

1963 KOVETZ, A.
NEUMANN, J.
SUZI, R.

Extension of Ekmans Spiral to Conditions of Near-Neutral Static Stability and a Constant Horizontal Temperature Gradient
Beitr.Phys.Atm. 36, 201-212

(Similar to model 17; however the thermal stratification is considered by the factor S, which is inversely proportional to the Monin-Obukhov stability length. Baroclinicity is also taken into consideration. Approximative solutions for small z only)

20 $k_m = \text{const}$ $z \geqq z_1$

$k_m \propto z$ $z \leqq z_1$

1965 BLACKADAR, A.K.

A Simplified Two-Layer-Model of the Baroclinic Neutral Atmospheric Boundary Layer

Final Rep. AFCRL-65-531 Part III, 49-65, ed. by A.K.Blackadar e.a.Pennsylv. State Univ. Dept. of Meteorol.
(Extension of model 13 to consider the baroclinicity also; the thermal wind is assumed to be constant with height)

21 $k_m \propto \exp(-az)$ $z \geqq z_1$
$k_m \propto z^p$ $z \leqq z_1$

1965 KLYUCHNIKOVA, L.A.
LAIKHTMAN, D.L.
TSEITIN, G.Kh.
Calculations of the Vertical Wind Profile in the Atmospheric Boundary Layer (in Russ.)
Trudy GGO 167, 3-28

22 $k_m \propto z^q$ $z \geqq z_1$
$k_m \propto z^p$ $z \leqq z_1$

23 $k_m \propto \exp(az)$ $z \geqq z_1$
$k_m \propto z^p$ $z \leqq z_1$

1967 GODEV, H.
YORDANOV, D.
On Models for the Study of the Variation of the Wind Velocity with Height in the Planetary Boundary Layer (in Bulgar.)
Comt. Rend. Acad. Bulgar. Sci. 20 (9), 911-913

Models Based on a Hypothesis for the Mixing-Length

As shown in the first part of this chapter ("The Problem of Closing the System of the PBL-Equations") there are two ways by which the mixing-length l can be introduced into the PBL-equations, namely either using Prandtl's mixing-length relation

A) $$k_m = l^2 \left| d\hat{w}/dz \right| \tag{1}$$

or using the relation between k_m, l and b (the turbulent kinetic energy $b = \overline{\varrho(w'')^2}/(2\bar{\varrho})$) together with three additional equations for b , ε_t and $\hat{\vartheta}$

B)
$$k_m = l\, b^{1/2} \tag{2}$$

$$k_m\left(\frac{d\hat{w}}{dz}\right)^2 - k_h \frac{g}{\bar{\vartheta}} \frac{d\hat{\vartheta}}{dz} - \frac{d}{dz}\left\{k_b \frac{db}{dz}\right\} - \varepsilon_t = 0 \tag{3}$$

$$\frac{d}{dz}\left\{k_h \frac{d\hat{\vartheta}}{dz}\right\} = 0 \tag{4}$$

$$\varepsilon_t = c\, b^{3/2}\, l^{-1} \tag{5}$$

In addition to that two hypotheses more have to be made in this way, namely for $k_h(z)$ and $k_b(z)$,and another assumption for the factor c in the eq.(5).

In both ways, (A) and (B) , the set of the PBL-equations can be closed by a hypothesis for the mixing-length l(z). Presumably such a procedure of closure is more advanced than a closure by a hypothesis of $k_m(z)$; the mixing - length l(z) increases monotonically with height starting with a very small value l_o at $z = z_o$ up to l_∞ at the top of the PBL; therefore it can be prescribed in a relative good agreement with reality. On the contrary, the profile $k_m(z)$ has a maximum at a certain height, it is therefore much more difficult to specify that than the profile

$l(z)$. This is the reason for believing that models with a $l(z)$-hypothesis are more realistic than models based on a hypothesis for $k_m(z)$. On the other hand the equations become non-linear when a mixing-length hypothesis is used, solutions can be obtained by numerical integrations only. This implies the use of electronic computers and it is the reason why such models have not been developed before the early sixties.

In most of the hypotheses the mixing-length profile $l(z)$ is prescribed, i.e. the mixing-length is related to the independent variable z. In other hypotheses the mixing-length is related to dependent variables as those appearing in the turbulent kinetic energy equation (3), see models 08, 10 or 11, or to the Reynolds stress, see model 12.

As it will be pointed out in the section about Rossby number similarity, Chapter 3, a mixing-length hypothesis has to be made in such a way that the mixing-length itself (non-dimensionalized by the internal scale height of the PBL $H = \kappa u_*/f$) remains independent of any external parameter. This requirement of Rossby-number similarity has not been observed in all hypotheses.

A brief survey of models based on a hypothesis of the mixing-length is following (The category A or B is indicated in each case).

01	$l = \kappa z$ (B)	1950 MONIN, A.S. Dynamic Turbulence in the Atmosphere (in Russ.) Bull.(Izv.) Acad.Sci.USSR Geogr. Geophys. Ser. 14 (3) 232-254 (Models restricted to the neutral case; the second term in eq.(3) vanishes just as eq.(4) remains unconsidered. $k_h/k_m = a_h$ as well as $k_b/k_m = a_b$ are assumed to be

constant. No numerical integration; solutions are obtained by expansion in series for small z only.

o2 $l = \kappa z/(1+\kappa z/l_\infty)$

$l_\infty = 2.7\ 10^{-4}|\hat{v}_{g0}|/f$

(A)

1962 BLACKADAR, A.K.

The Vertical Distribution of Wind and Turbulent Exchange in a Neutral Atmosphere
J.Geophys.Res. 67, 3095-3102

(The mixing-length nondimensionalized for Rossby-number similarity $L = \kappa Z/(1 + \kappa Z/L_\infty)$ has an asymptotic value

$$L_\infty = 6.75\ 10^{-4}\ C_g^{-1}$$

which is not independent of external parameters; the requirements of Rossby-number similarity are not satisfied)

03 $l = \kappa z/(1+a_1 z^{5/4})$

(A)

1962 LETTAU, H.H.

Theoretical Wind Spirals in the Boundary Layer of a Barotropic Atmosphere
Beitr.Phys.Atm. 35, 195-212

(This hypothesis is made in analogy to results obtained for duct flows. The mixing-length nondimensionalized by the internal scale height

$$L = \kappa Z/(1 + 33.62\ Z^{5/4})$$

is independent of external parameters. Unlike other hypotheses this one specifies a profile l(z) with a maximum; above the maximum l decreases to zero with increasing height)

04 $l = l_\infty\{1-\exp(\kappa z/l_\infty)\}$

(A)

1963 RUSZIN, M.I.

The Vertical Profile of the Exchange Coefficient in the Planetary Boundary Layer (in Russ.)
Trudy W.N.M.S. 7, 63-72
Gidrometeoroizdat
and

1963 RUSZIN, M.I.
BOLDIZEVA, N.A.
SABELEVA, T.A.

Some Results of Computations of the Exchange Coefficient in the Planetary Boundary Layer (in Russ.)
Trudy L.G.M.I. B 15, 66-68

05 $l = l_\infty \{1-\exp(\kappa z/l_\infty)\}$
(A)

1964 APPLEBY, J.F.
OHMSTEDE, W.D.

Numerical Solutions of the Distributions of Wind and Turbulence in the Planetary Boundary Layer
Meteor. Res. Note Nr.8, Meteor. Dept. USAERDA, Fort Huachuca, Ariz., Sept. 1964

06 $l = \kappa z/(1+\kappa z/l_\infty)$
$l_\infty = 2.7\ 10^{-4}|\hat{v}_{g0}|/f$
(A)

1965 BLACKADAR, A.K.

A Single Layer Theory of the Vertical Distribution of the Wind in a Baroclinic Neutral Atmospheric Boundary Layer
Final Rep. AFCRL-65-531,1-22 ed. by A.K.Blackadar et al., Pennsylv.State Univ.,Dept. of Meteor., 31 July 1965
(The same hypothesis as 02; it is applied here to baroclinic PBLs too)

07 $l = \kappa z/(1+\kappa z/l_\infty)F(L_*)$
$l_\infty = 2.7\ 10^{-4}|\hat{v}_{g0}|/f$
(A)

1965 BLACKADAR, A.K.
CHING, J.K.

Wind Distribution in a Steady-State Planetary Boundary Layer of the Atmosphere with Upward Turbulent Heat Flux
Final Rep. AFCRL-65-531,23-48 ed. by A.K.Blackadar et al., Pennsylv. State Univ., Dept. of Meteor., 31 July 1965
(The same hypothesis as 02 but extended to diabatic cases. The dependence on the stratification is obtained by using the KEYPS-equ., i.e. really valid only in the surface layer)

08 $l = c_1 \psi / (d\psi/dz)$
$\psi = \varepsilon_t / k_m$
(B)

1965 BOBILEVA, I.M.
ZILITINKEVICH, S.S.
LAIKHTMAN, D.L.

Turbulent Exchange in the Thermally Stratified Planetary Boundary Layer of the Atmosphere (Russ./Engl.) Intern. Colloqu. on Fine - Scale Structure of the Atmosphere, Moscow 1965

(This is the only type B model, which makes use of the complete equations (2)-(5) as given above)

09 $l = \varkappa z / \Phi_m$
(A)

1968 YAMAMOTO, G.
YASUDA, N.
SHIMANUKI, A.

The Effect of Thermal Stratification on the Ekman Boundary Layer
J.Meteor.Soc.Japan 46,442-455

(The non-dimensional profile function Φ_m is obtained from a modified KEYPS-equation, which has been improved for stable stratification; really valid only in the surface layer. The linear increase of l is damped for large z by the profile function Φ_m)

10 $l = \varkappa \, |d\hat{w}/dz| / |d^2\hat{w}/dz^2|$
(B)

1969 SMITH, F.B.

The Vertical Transfer of Momentum through the Boundary Layer
AGARD Conf.Proc. Nr. 48,Pap. Nr. 19, pp 8

(The mixing-length hypothesis is an extension of v.Karman's, which is applicable to the surface layer only)

11 $l = c_1 \psi / (d\psi/dz)$
$\psi = \varepsilon_t / k_m$
(B)

1970 KUROSAKI, A.

A Theoretical Study of the Structure of the Ekman Boundary Layer,(I) Mixing-Length Theory
Pap. in Meteor. & Geophys. 21 (2), 89-112

(Essentially the same model as 08; for the surface layer an adaption is made to satisfy the KEYPS-equation. Results for stable cases are not obtained)

12 $l = l_\infty - (l_\infty - l_o)\left(\frac{\tau}{\tau_o}\right)^p$

$$p = -\frac{\kappa \tau_o}{\{d\tau/dz\}_o (l_\infty - l_o)}$$

(A)

1971 WIPPERMANN, F.

A Mixing-Length Hypothesis for the Planetary Boundary Layer Flow in the Atmosphere
Beitr. Phys. Atm. 44, 215-226
and

1972 WIPPERMANN, F.

Universal Profiles in the Barotropic Planetary Boundary Layer
Beitr. Phys. Atm. 45, 148-163

(The power p contains $\{d\tau/dz\}_o$, which has to be determined in the model iteratively. Numerical results are presented in the second paper)

13 $l = \frac{\kappa z}{\Phi_m (1 + \kappa z / l_*)}$

$$l_* = c \frac{u_*}{f} \exp(-a\mu)$$

(A)

1972 FIEDLER, F.

The Effect of Baroclinicity on the Resistance Law in a Diabatic Ekman Layer
Beitr. Phys. Atm. 45, 164-173

(For the profile function Φ_m empirical formulae are used having been obtained from observations. In these formulae z/L_* is replaced by $1/(\kappa L_*)$, so that l appears once more in the denominator of (13))

Beiträge zur Physik der Atmosphäre, 44. Band, 1971, S. 215–226

A Mixing-Length Hypothesis for the Planetary Boundary Layer Flow in the Atmosphere *)

Eine Mischungsweg-Hypothese für die Strömung in der planetarischen Grenzschicht der Atmosphäre

F. Wippermann

Technical University, Darmstadt, Germany, Department of Meteorology

Received August 2, 1971

Summary: First of all a short review of several mixing-length hypotheses is given. Then a new hypothesis is presented which relates the increase of the mixing-length with height to the decrease of the Reynolds stress, i.e. the variation of l depends on an internal fluid parameter and not on the independent variable z (coordinate for the height above the ground). The hypothesis allows to compute the maximum value of the eddy viscosity K_m; values for that are given in table 2. The expression for the mixing-length contains only two parameters, namely K_{m0} and L_∞. The first one reflects the influence of the surface Rossby number, the later one the influence of the thermal stratification. An empirical relation is given between the parameter L_∞ (the asymptotic value of the nondimensional mixing-length) and the internal parameter μ for the stratification of the planetary boundary layer.

Zusammenfassung: Zunächst erfolgt ein kurzer Überblick über die bislang vorhandenen Mischungsweg-Hypothesen. Sodann wird eine neue Hypothese gegeben, derzufolge das Anwachsen des Mischungsweges mit der Höhe abhängt vom Abfall der Reynolds'schen Schubspannung mit der Höhe; d.h. die Veränderlichkeit des Mischungsweges hängt von einem internen Strömungsparameter ab und nicht direkt von der Vertikalkoordinate. Die Hypothese gestattet es, den Maximalwert des turbulenten Diffusionskoeffizienten K_m zu berechnen, in Tabelle 2 sind einige Werte hierfür angegeben.
Der Ausdruck für den Mischungsweg enthält nur zwei Parameter, nämlich K_{m0} und L_∞; der erste gibt den Einfluß der Oberflächen – Rossby-Zahl wieder, der zweite denjenigen der thermischen Schichtung. Es wird eine empirische Beziehung gewonnen zwischen dem Parameter L_∞ (dem asymptotischen Wert des dimensionslosen Mischungsweges) und dem internen Parameter μ für die hydrostatische Stabilität der Grenzschicht.

Résumé: On passe d'abord en revue diverses hypothèses en longueur de mélange. Ensuite, une nouvelle hypothèse est présentée, qui lie l'accroissement de la longueur de mélange avec la hauteur à la décroissance de la tension de Reynolds: la variation de l dépend d'un paramètre interne du fluide et non de la variable indépendante z (coordonnée pour la hauteur au-dessus de la surface). Cette hypothèse permet de calculer la valeur maximum de la viscosité turbulente K_m (valeurs au tableau 2).

L'expression de la longueur de mélange contient seulement deux paramètres, K_{m0} et L_∞. Le premier reflète l'influence du nombre de Rossby en surface, le second l'influence de la stratification thermique. On donne une relation empirique entre le paramètre L_∞ (valeur asymptotique de la longueur de mélange non-dimensionnelle) et le paramètre interne μ relatif à la stratification de la couche limite planétaire.

*) Paper presented at the Xth Symposium on Advenced Methods and Problems in Fluid Dynamics, Rynia, Poland, 05-11 September 1971.

1. Introduction

In the planetary boundary layer (PBL), i.e. an atmospheric boundary layer with the assumption of steadiness and horizontal homogeneity, the proportionality between the Reynolds-stress τ and the vertical wind shear $d\hat{v}/dz$ is almost ever used

$$\tau = \bar{\rho}\, k_m\, |d\hat{v}/dz| \tag{1}$$

where k_m is the eddy diffusion coefficient for momentum. According to PRANDTL the mixing-length l may be introduced into k_m

$$k_m = l^2 |d\hat{v}/dz| . \tag{2}$$

Very close to the ground l increases linearly with height z

$$l = \kappa z \tag{3}$$

(κ = von Karmán's constant); as far as observations can be evaluated l seems to approach a constant value l_∞. Figure 1 gives an evaluation of the Leipzig wind profile after APPLEBY and OHMSTEDE (1964) in which the two highest points are uncertain.

By using the friction velocity $u_* \doteq (|\tau_0|/\bar{\rho})^{1/2}$ and the scale height of the PBL $H = \kappa u_*/f$, where f is the Coriolis parameter, all quantities can be made dimensionless

$$Z \equiv z/H, \qquad Z_0 \equiv z_0/H = 1/(\kappa\, C_d\, Ro_0), \qquad L \equiv l/H \tag{4a}$$

$$U \equiv \kappa\, \hat{u}/u_*, \qquad V \equiv \kappa\, \hat{v}/u_*, \qquad 1/C_d \equiv |\hat{v}_g|/u_* \tag{4b}$$

$$T = \tau/\tau_0 = \tau/\bar{\rho} u_*^2, \quad K_m = k_m/(H^2 \cdot f), \qquad B^2 = b^2/u_*^2 \tag{4c}$$

$$Ro_0 = |\hat{v}_g|(f \cdot z_0) \tag{4d}$$

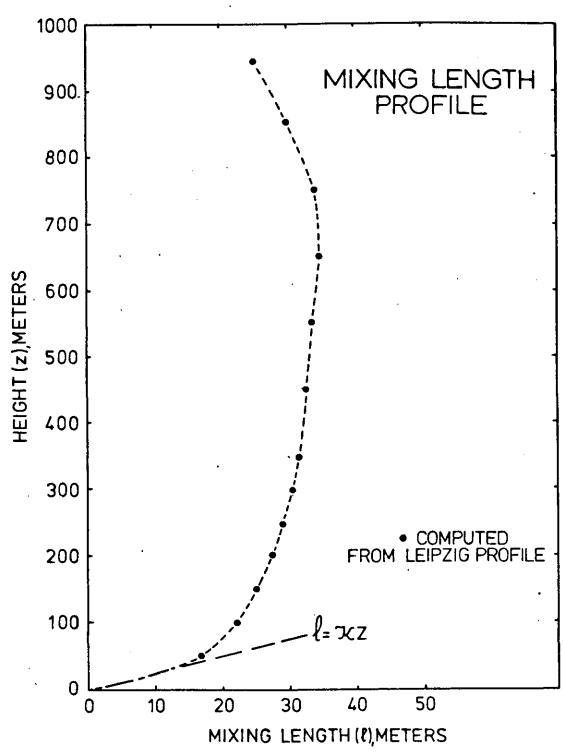

Fig. 1
The profile of the mixing-length computed from the Leipzig wind profile (after APPLEBY and OHMSTEDE 1964)

Bild 1
Das Mischungswegprofil berechnet aus dem Leipziger Windprofil (nach APPLEBY und OHMSTEDE 1964)

where C_d is called the geostrophic drag coefficient, Ro_0 the surface Rossby number and $b^2 = \overline{(u_i'')^2}/2$ the turbulent kinetic energy per mass unit. The relations (1) and (2) are in the nondimensional notation

$$T = K_m \, |d\mathbb{V}/dZ| \tag{5}$$

$$K_m = (L^2/\kappa^2)\,|d\mathbb{V}/dZ| \,. \tag{6}$$

Eliminating of the wind shear yields

$$K_m = (L/\kappa)\,T^{1/2} \,. \tag{7}$$

At the ground $(Z = Z_0)$ is $T = 1$; it follows from eq. (7)

$$K_{m0} = L_0/\kappa \,. \tag{8}$$

Several hypotheses have been made for the mixing-length L during the last decade. The hypothesis by BLACKADAR (1962) is

$$l = \kappa \cdot z/[1 + (\kappa z/l_\infty)] \qquad l_\infty = 2.7 \cdot 10^{-4}\,|\hat{v}_g|/f \tag{9a}$$

or in dimensionless notation

$$L = \kappa Z/[1 + (\kappa Z/L_\infty)] \qquad L_\infty = 6.75 \cdot 10^{-4}/C_d \tag{9b}$$

which shows, that L_∞ depends on the geostrophic drag coefficient C_d and therefore on the surface Rossby number Ro_0. This variation of L_∞ with Ro_0 can be shown by using the empirical relationship between C_d and Ro_0 given by KUNG (1966), see table 1.

Table 1 / Tabelle 1

$\log_{10}(Ro_0)$	4	5	6	7	8	9	10
C_d	0.060	0.046	0.038	0.032	0.028	0.024	0.022
L_∞ (BLKDR)	0.011	0.015	0.018	0.021	0.024	0.028	0.031

For $Z \gg Z_0$ the Rossby similarity requires, that dU/dZ and dV/dZ is independent of Z_0 and therefore (see eq. (4a)) independent of Ro_0. Then the equations for the PBL tell us that also d^2X/dZ^2 and d^2Y/dZ^2 $(X \equiv \tau_x/\tau_0, Y \equiv \tau_y/\tau_0)$ must be independent of Ro_0 or because of the fixed boundary values of X and Y these itself must be independent of Ro_0, i.e. T is independent of Ro_0. From eq. (5) follows then that for $Z \gg Z_0$ also $K_m(Z)$ must be independent of Ro_0 and according to eq. (6) finally $L(Z)$ must be independent of Ro_0. That means, that BLACKADARs hypothesis with $L_\infty = f_1(C_d)$ or $L_\infty = f_2(Ro_0)$ does not meet the widely accepted requirements of Rossby similarity.

Also in 1962 LETTAU made a hypothesis for the mixing-lingth in the PBL by extending a relationship for duct flows

$$l = \kappa z/[1 + 4(z/H')^{5/4}] \tag{10a}$$

where H' is LETTAUs scale height, which equals 0.182 H the scale height introduced above. In nondimensional notation eq. (10a) is

$$L = \kappa Z/[1 + 33.62\, Z^{5/4}] \,. \tag{10b}$$

This mixing-length is independent of Ro_0 as required by Rossby similarity for $Z \gg Z_0$, but it does not approach a constant value L_∞; for $Z \to \infty$ one has $L \to 0$. The maximum of L will be found at $Z = 0.18$ with the value $L_{max} = 0.014$. With the observational data available at the present time one is unable to decide wether $L \to 0$ or $L \to L_\infty$ for $Z \to \infty$.

Another hypothesis is proposed by RUSIN, BOLDIZEVA and SABELEVA (1963) and used by APPLEBY and OHMSTEDE (1964) in computations. It is

$$l = l_\infty [1 - \exp(-\kappa z/l_\infty)] \tag{11a}$$

which is in the nondimensional form

$$L = L_\infty [1 - \exp(-\kappa Z/L_\infty)] . \tag{11b}$$

In a further paper (1966) OHMSTEDE gives in his figure 3 the variation of l_∞/D with varying Ro_0, where $D = |\hat{v}_g|/f$ is the external scale height of the PBL; $l_\infty/D = L_\infty \kappa C_d$. Since the curve does not reflect the variation of C_d with Ro_0 only, also L_∞ must depend on Ro_0. However this should not be so. Another defect of this hypothesis seems to be, that the values for L at the ground $(Z = Z_0)$ are unrealistic and also dependent on L_∞.

BOBILEVA, ZILITINKEVICH and LAIKHTMAN (1965) in their boundary layer model are using four hypotheses, in which the first one is an extension of v. Karmán's mixing-length hypothesis

$$l = -\kappa \psi/(d\psi/dz) \tag{12a}$$

$$\psi = \epsilon/k_m \tag{12b}$$

$$\epsilon = c_1 b^3/l \tag{12c}$$

$$k_m = bl \tag{12d}$$

where ϵ [$cm^2 sec^{-3}$] is the rate of energy dissipation per unit mass. For the mixing-length it results

$$l = -\frac{\kappa}{\left(\frac{1}{b^2}\frac{db^2}{dz} - \frac{2}{l}\frac{dl}{dz}\right)}$$

which can be written as a first order ordinary differential equation for L (in nondimensional notation)

$$dL/dZ - L\,d(\ln B)/dZ = \kappa/2 \tag{13}$$

with the solution

$$L = \frac{B}{B_0}\left\{L_0 + \frac{\kappa}{2}\int_{Z_0}^{Z} \frac{dZ}{B/B_0}\right\} \tag{14}$$

The hypothesis (12d) is in nondimensional notation

$$K_m = (L/\kappa)B \tag{15}$$

and a comparison with eq. (7) yields

$$B^2 = T . \tag{16}$$

(The authors, of course, have not made use of Prandtl's mixing-length hypothesis eq. (6); nevertheless its validity is widely accepted and therefore as a consequence also eq. (16) has to be accepted.) If eq. (16) is inserted in eq. (14) one notices the variation of L with the stress T as well. Eq. (14) may be better understood if an example is chosen for T (or for B^2), for instance

$$T(Z) = \exp\{-m(Z - Z_0)\}$$

which is the stress profile belonging to an Ekman spiral; one obtaines

$$L = L_0 \exp[-\kappa(Z - Z_0)/2L_\infty] + L_\infty\{1 - \exp[-\kappa(Z - Z_0)/2L_\infty]\} . \tag{17}$$

In this case is $L_\infty = \kappa/m$. This example shows that the mixing-length hypothesis (12a) is very similar to that one by APPLEBY and OHMSTEDE, see eq. (11b). Since T(Z) has allways to be a monotonically decreasing function of height Z, see WIPPERMANN (1971), on can conclude, that also in the non-Ekman cases L(Z) will not differ very much from the profile given in eq. (17).

Another approach has been made by SMITH (1969). He uses the geostrophic wind speed and the scale height $D = |\hat{w}_g|/f$ as external parameters to nondimensionalize the velocities and the height z. If the quantities are made dimensionless as in the other examples, namely by (4a) and (4b), the hypothesis by SMITH is

$$L = \kappa\left[\left(\frac{dU}{dZ}\right)^2 + \left(\frac{dV}{dZ}\right)^2\right]^{1/2} \Big/ \left[\left(\frac{d^2U}{dZ^2}\right)^2 + \left(\frac{d^2V}{dZ^2}\right)^2\right]^{1/2} \tag{18}$$

which is chosen as an extension of v. Karmán's mixing-length hypothesis applicable in the constant stress layer; hereby in the denominator $|d^2\mathbb{V}/dZ^2|$ has been placed instead $d(|d\mathbb{V}/dZ|)/dZ$. The results of the model which uses this mixing-length hypothesis are not very encouraging.

Recently KUROSAKI (1970) made a hypothesis for the mixing-length which is almost the same as that one by BOBILEVA et al. (1965) but near the ground it is adapted to the KEYPS-law. Computations with this mixing-length hypothesis do not show an improvement of the results by BOBILEVA et al., even in cases of stable stratification the computational method did not converge and results have been obtained not at all for stable stratification.

The hypothesis by BLACKADAR (1962) as well that one by LETTAU (1962) or by APPLEBY and OHMSTEDE (1964) prescribes the mixing-length l as a function of z. Models of the PBL using these hypotheses are considered to be "a priori-models", since to some extent the vertical variation of the mixing-length can be hypothesized in such a way that the expected boundary layer characteristics will be obtained. This is not true for the mixing-length hypothesis by BOBILEVA et al. (1965), by SMITH (1969) and by KUROSAKI (1970) because by these hypotheses the mixing-length is given as depending on an internal fluid parameter, i.e. the vertical wind shear or the turbulent kinetic energy. The disadvantage of these last mentioned hypotheses is the need for additional hypotheses, for instance (12c) and (12d) and others for k_h/k_m and k_b/k_m. In the following section a mixing-length hypothesis shall be presented according to which the mixing-length depends on an internal fluid parameter only, namely on the Reynolds-stress.

2. The hypothesis; the maximum of eddy viscosity

As to be seen in fig. 1 the mixing-length increases with height and possibly approaches a constant value l_∞ asymptotically. The only one assumption which should be made is, that that increase can be described by the decrease of the Reynolds-stress with height. The hypothesis is:

$$\boxed{\begin{aligned} L &= L_\infty - (L_\infty - \kappa K_{m0})\,T^p \\ p &= -\kappa\,\frac{1 - K_{m0}\{2(dT/dZ)_0^2 + (dT/dZ)_0/2\}}{(dT/dZ)_0\{L_\infty - \kappa K_{m0}\}} \end{aligned}} \tag{19}$$

With respect to the lower boundary condition ($Z = Z_0$: $T = T_0 = 1$) eq. (8) tells that $\kappa K_{m0} = L_0$, so that

$$Z = Z_0: \quad (T = 1) \quad L = L_0 \tag{20a}$$

$$Z \to \infty: \quad (T \to 0) \quad L \to L_\infty. \tag{20b}$$

We know, YORDANOV and WIPPERMANN (1972), that $(dT/dZ)_0$ depends only on an internal parameter of the static stability and on two internal parameters for the baroclinicity, but $(dT/dZ)_0$ is independent of any external parameters as for instance Ro_0. In a neutral and barotropic PBL it is a universal constant

$$-(dT/dZ)_0 = N \tag{21}$$

the value of which is about 4.5, see WIPPERMANN (1970). For an application of the hypothesis (19) in a PBL-model $(dT/dZ)_0$ is not yet known but has to be determined iteratively.

By differentiating eq. (19) with respect to Z one obtaines

$$(dL/dZ)_0 = \kappa\,[1 - K_{m0}\{2(dT/dZ)_0^2 + (dT/dZ)_0/2\}]\,. \tag{22}$$

In the observed range of surface Rossby numbers, from $1 \cdot 10^5$ to $1 \cdot 10^9$, the values of K_{m0} vary between $5 \cdot 10^{-4}$ and $1 \cdot 10^{-7}$ approximately; therefore in this range

$$K_{m0}\{2(dT/dZ)_0^2 + (dT/dZ)_0/2\} \ll 1$$

which means that very close to the ground the mixing-length (19) behaves in the same way as in PRANDTLs hypothesis ($k_m = \kappa z$).

Let's consider the resulting eddy viscosity K_m. If one inserts the mixing-length (19) into eq. (7) and differentiates that with respect to Z it results

$$\frac{dK_m}{dZ} = T^{-1/2}\,\frac{dT/dZ}{(dT/dZ)_0}\,[T^p\{1 - K_{m0}A_1\} + A_2] \tag{23}$$

with

$$A_1 = 2(dT/dZ)_0^2 + (dT/dZ)_0\,L_\infty/(2\kappa\,K_{m0})$$

$$A_2 = (dT/dZ)_0\,L_\infty/(2\kappa)\,.$$

At the lower boundary ($Z = Z_0$: $T = 1$) one gets

$$(dK_m/dZ)_0 = 1 - K_{m0}\,2(dT/dZ)_0^2\,. \tag{24}$$

As argued before K_{m0} is very small in the observed range of external parameters, therefore the vertical variation of K_m very close to the ground is the same as in a Prandtl layer:

$$K_m = Z\,. \tag{25}$$

In the case of an Ekman spiral, i.e. $T_E(Z) = \exp\{(dT/dZ)_0\,Z\}$, $K_{mE}(Z) = 1/\{2(dT/dZ)_0^2\} = \text{const}$, one notices from eq. (24) that the mixing-length hypothesis (19) satisfies the condition of constant eddy viscosity at least very close to the ground. In the case of an Ekman spiral K_{m0} is not longer as small as mentioned before ($5 \cdot 10^{-4}$ to $1 \cdot 10^{-7}$) but about $2.35 \cdot 10^{-2}$; this is the order of magnitude of the maximum of K_m. Probably in the case $K_{m0} = K_{mE} = 2.35 \cdot 10^{-2}$ the maximum of K_m is at the ground and therefore $(dK_m/dZ)_0 = 0$.

The conditions for a PBL (i.e.: the steady state and horizontal homogeneity) require that T decreases monotonically from $T = 1$ at $Z = Z_0$ to $T \to 0$ for $Z \to \infty$; that means that for finite Z $dT/dZ \neq 0$. Herwith and using the condition $dK_m/dZ = 0$ the stress $T_{K\text{-max}}$ at the level where K_m has its maximum can be computed, one obtains:

$$T_{K\text{-max}} = \left[\frac{-(dT/dZ)_0\,L_\infty}{2\kappa\{1 - K_{m0}A_1\}}\right]^q \tag{26}$$

$$q = -\frac{(dT/dZ)_0}{\kappa}\,\frac{L_\infty - \kappa\,K_{m0}}{1 - K_{m0}A_3}$$

$$A_3 = 2(dT/dZ)_0^2 + (dT/dZ)_0/2\,.$$

If one replaces T in eq. (19) by T_{K-max} as obtained by eq. (26) one gets the mixing-length L_{K-max} in the level where K_m has its maximum:

$$L_{K-max} = L_\infty r, \quad r = \frac{1 - K_{m0} A_3}{1 - K_{m0} A_1} \tag{27}$$

Finally $K_{m,max}$ the maximum value of K_m is obtained by making use of eq. (26) and eq. (27) in eq. (7); one obtains

$$K_{m,max} = - \frac{2\,[1 - K_{m0} A_3]}{(dT/dZ)_0\,[1 - \{1 - 2(dT/dZ)_0^2\, K_{m0}\}\, A_4]^{1/r}} \tag{28}$$

$$A_4 = 2\kappa/\{(dT/dZ)_0\, L_\infty\}$$

As to be seen $K_{m,max}$ depends only on K_{m0} and on L_∞. In the case of Rossby similarity, i.e. for $K_{m0} < 1 \cdot 10^{-3}$, the profiles $K_m(Z)$ and therefore also $K_{m,max}$ should be independent of Z_0 (or K_{m0}) (as long as $Z \gg Z_0$). In these cases $K_{m,max}$ in eq. (28) reduces to

$$K_{m,max} = - \frac{2}{(dT/dZ)_0\,[1 - 2\kappa/(dT/dZ)_0\, L_\infty]^{1-s}} \tag{29}$$

with

$$s = (dT/dZ)_0\, L_\infty/(2\kappa)\,.$$

In table 2 the values of L_{K-max} according to eq. (27) are listed, also the values of T_{K-max} according to eq. (26) and the values of $K_{m,max}$ according to eq. (28). All these quantities are computed for eight different values of K_{m0} and for each of these again for four values of L_∞, namely 0.0100, 0.0125, 0.0150, 0.0175. These values are chosen because it is expected that L_∞ for the case of neutral stratification is somewhere in this range; observations show: $L_\infty = 0.0135$ (Leipzig), $L_\infty = 0.0126$ (Scilly), see lower part of table 2. The values of K_{m0} vary from $2.50 \cdot 10^{-7}$ up to $2.35 \cdot 10^{-2}$; the upper border corresponds to K_{m0} for the case of a pure Ekman spiral. In this case is

$$K_{m0} = K_{mE} = 1/\{2(dT/dZ)_0^2\}$$

for which the value mentioned above results with -4.5 for $(dT/dZ)_0$ in neutral stratification. However the mixing-length (19) inserted in eq. (7) with this special value $K_{m0} = 2.35 \cdot 10^{-2}$ does not allow for K_m being constant with height as necessary in the case of an Ekman spiral, rather K_m will decrease with height and only K_{m0} (which is at the same time the maximum value $K_{m,max}$) has the correct value $1/\{2(dT/dZ)_0^2\}$.

From table 2 it can be noticed, that $K_{m,max}$ is independent of K_{m0}, if $K_{m0} < 1 \cdot 10^{-3}$. As concluded already before this is the range of K_{m0} for which Rossby similarity for the $K_m(Z)$-profiles ($Z \gg Z_0$) is given or for which the so-called auto-model hypothesis is valid. In this range of K_{m0} also a Prandtl layer relation $k_m = \kappa\, u_* z$, or in nondimensional notation $K_m = Z$ is valid very close to the ground. That means with regard to eq. (4a)

$$K_{m0} = Z_0 = 1/(\kappa\, C_d\, Ro_0) \tag{30}$$

which is a direct relationship between K_{m0} and the external parameters combined in Ro_0. A short table with approximated values of Ro_0 corresponding to Z_0 can be given if one uses once more the empirical relationship by KUNG (1966)

$$C_d(Ro_0) = 0.205/\{\log_{10}(Ro_0) - 0.556\} \qquad \text{(neutral case)}$$

used already following to eq. (9b). It is obtained:

Table 2 / Tabelle 2

$K_{m,0}$	L_∞	$\frac{L_{K\text{-max}}}{L_\infty}$	$T_{K\text{-max}}$	$K_{m,max}$	$Z_{K\text{-max}}$	Ro_0 (approx.)
$2.35 \cdot 10^{-2}$	0.0100	0.945	0.989	0.0235		
	0.0125	0.768	0.957	0.0235		
	0.0150	0.648	0.936	0.0235		
	0.0175	0.561	0.920	0.0235		
$2.00 \cdot 10^{-2}$	0.0100	0.946	0.861	0.0219		
	0.0125	0.882	0.743	0.0239		
	0.0150	0.832	0.662	0.0254		
	0.0175	0.786	0.602	0.0267		
$1.25 \cdot 10^{-2}$	0.0100	0.946	0.775	0.0208		
	0.0125	0.920	0.705	0.0242		
	0.0150	0.896	0.651	0.0271		
	0.0175	0.874	0.607	0.0280		
$2.50 \cdot 10^{-3}$	0.0100	0.946	0.724	0.0201		$1.6 \cdot 10^4$
	0.0125	0.931	0.683	0.0241		
	0.0150	0.917	0.647	0.0277		
	0.0175	0.904	0.617	0.0311		
$2.50 \cdot 10^{-4}$	0.0100	0.946	0.716	0.0200		$2.3 \cdot 10^5$
	0.0125	0.932	0.679	0.0240		
	0.0.150	0.918	0.646	0.0277		
	0.0175	0.905	0.618	0.0312		
$2.50 \cdot 10^{-5}$	0.0100	0.946	0.716	0.0200		$2.9 \cdot 10^6$
	0.0125	0.932	0.678	0.0240		
	0.0150	0.919	0.646	0.0277		
	0.0175	0.906	0.618	0.0312		
$2.50 \cdot 10^{-6}$	0.0100	0.946	0.715	0.0200		$3.5 \cdot 10^7$
	0.0125	0.933	0.678	0.0240		
	0.0150	0.920	0.646	0.0277		
	0.0175	0.907	0.618	0.0312		
$2.50 \cdot 10^{-7}$	0.0100	0.946	0.715	0.0200		$4.0 \cdot 10^8$
	0.0125	0.933	0.678	0.0240		
	0.0150	0.921	0.646	0.0277		
	0.0175	0.908	0.618	0.0312		
observed Leipzig	0.0134		0.51	0.0223	0.0986	
observed Scilly	0.0126			0.0242	0.0974	
Theor. Model LETTAU 1962	0.0146	0.932	0.660	0.0277 *)	0.0915 *)	

*) for $Ro_0 = 1 \cdot 10^7$

Table 3 / Tabelle 3

$\log_{10}(Ro_0)$	4	5	6	7	8	9
Z_0 or K_{m0}	$4.2 \cdot 10^{-3}$	$5.4 \cdot 10^{-4}$	$6.6 \cdot 10^{-5}$	$7.9 \cdot 10^{-6}$	$9.1 \cdot 10^{-7}$	$1.0 \cdot 10^{-7}$

The last column of table 2 contains such approximated surface Rossby numbers which correspond to the chosen values of K_{m0}.

3. The effect of the thermal stratification on the mixing-length

As mentioned already in section 2 the Rossby similarity is given when $K_{m0} < 1 \cdot 10^{-3}$; then the profile of the nondimensional eddy viscosity (as long as $Z \gg Z_0$) depends only on the thermal stratification expressed by the nondimensional internal stability parameter

$$\mu = H/L_* \tag{31}$$

where L_* is the MONIN-OBUKHOV stability length

$$L_* = -c_p \bar{\rho} u_*^3 / \{\kappa \beta q_0\}$$

and on two nondimensional parameters for the baroclinicity; however this is not relevant here since a barotropic PBL should be considered only.

It can be seen that the same must be true for the profile of the mixing-length when nondimensionalized by the internal scale height H. Since Rossby similarity means that the profile is independent of Ro_0 (and therefore independent of K_{m0} or of L_0) the only way to consider a variation of L with the stability parameter μ is by relating the parameter L_∞ to the parameter μ. That means a relationship has to be established between L_∞ and μ; this can be done only empirically. In order to obtain such a relationship a set of integrations of the PBL-equations has been carried out for $Z_0 = K_{m0} = 1 \cdot 10^{-5}$ but for different values of L_∞ varying in the range from $1 \cdot 10^{-4}$ to 1.0. For each case the values of the universal functions $M(\mu)$ and $N(\mu)$ have been computed, which appear in the well-known resistance law of a barotropic PBL

$$\frac{\kappa}{C_d} \cos(\alpha_0) = -M(\mu) + \ln(Ro_0 \cdot C_d) \tag{32a}$$

$$\frac{\kappa}{C_d} \sin(|\alpha_0|) = N(\mu) . \tag{32b}$$

Actually the universal functions $M(\mu)$ and $N(\mu)$ can be obtained by measurements only. Unfortunately the available data are very poor; up to now evaluations have been made only by MONIN and ZILITINKEVICH (1967) and by CLARKE (1970). Since the evaluated measurements give data for M and N which scatter broadly, it is difficult to determine these functions; therefore such evaluations have to be considered as very preliminary. This is true also for a relationship between L_∞ and μ, which is derived from such evaluations.

For the purpose to establish a relationship between L_∞ and μ the later one has been adapted to L_∞ in such a manner that the experimental data of $M(\mu)$ and $N(\mu)$ are fitted in the best way by the values of M and N computed for different L_∞ as mentioned before. The relationship obtained hereby is:

$$\mu = -44.2 - 24.4 \log_{10}(L_\infty) . \tag{33}$$

The following table 4 gives some of the corresponding values of L_∞ and μ:

Table 4 / Tabelle 4

L_∞	$1 \cdot 10^{-5}$	$5 \cdot 10^{-5}$	$1 \cdot 10^{-4}$	$5 \cdot 10^{-4}$	$1 \cdot 10^{-3}$	$5 \cdot 10^{-3}$
μ	+ 77.8	+ 60.8	+ 53.4	+ 36.0	+ 29.0	+ 12.1
L_∞	$1 \cdot 10^{-2}$	$1.5 \cdot 10^{-2}$	$5 \cdot 10^{-2}$	$1 \cdot 10^{-1}$	$5 \cdot 10^{-1}$	1.0
μ	+ 4.6	0	- 12.2	- 19.8	- 36.6	- 44.2

The value for extremly stable stratification ($\mu = +77.8$) is $L_\infty = 1 \cdot 10^{-5}$, it is only 2.5 times the value of L_0 (see eq. (8)) chosen for the computations in this case. That means that the mixing-length grows from 4 mm at $Z = Z_0$ up to only 1 cm (as the asymptotic value) when the scale height H is about 1 km. The maximum of K_m will be found very close to Z_0 in this case. For neutral stratification L_∞ is about 15 m (for H = 1 km) and for extremly unstable stratification the mixing-length may grow up to the height of the PBL itself.

In figure 2 and 3 is shown how the functions $M(L_\infty)$ and $N(L_\infty)$ obtained by the numerical integrations of the PBL-equations (solid line) fit the observational results when the relationship (33) is applied; the broken curve is the best fit given by MONIN and ZILITINKEVICH (1967).

As mentioned before the established relationship (33) and the table 4 should be considered as very preliminary; it should be improved as soon as new and better measurements are available, which allow evaluations of the universal functions $M(\mu)$ and $N(\mu)$.

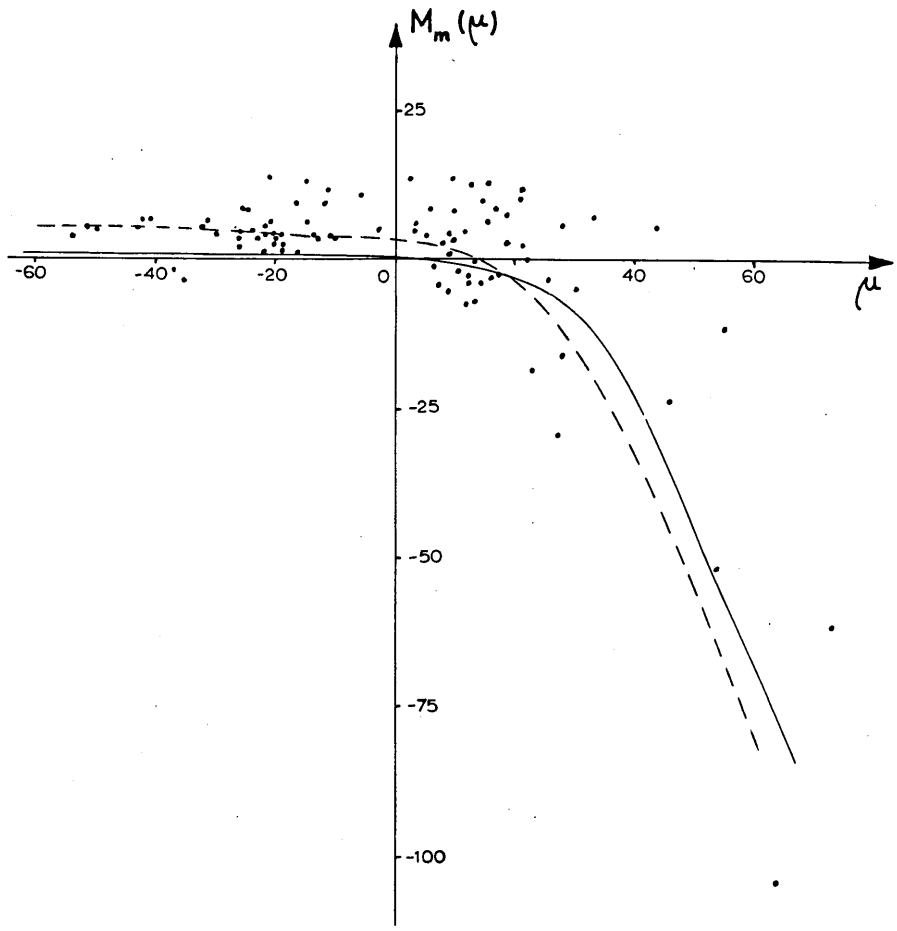

Fig. 2. The universal function $M_m(\mu)$ as evaluated by MONIN and ZILITINKEVICH (1967) (broken line) and the result of integrations of the PBL-equations (solid line) by using the empirical relationship (33)

Bild 2. Die universelle Funktion $M_m(\mu)$ nach Auswertungen von MONIN und ZILITINKEVICH (1967) (gestrichelte Kurve) sowie das Ergebnis von Integrationen der Grenzschichtgleichungen (ausgezogene Kurve) nach Anwendung der empirischen Beziehung (33)

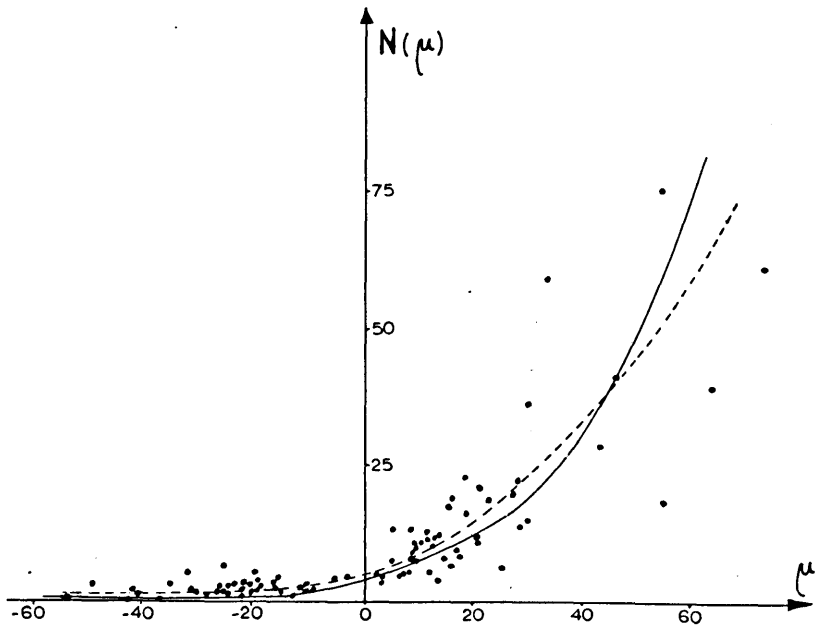

Fig. 3. See legend to fig. 2 but applied to $N(\mu)$

Bild 3. Siehe Erläuterung zu Bild 2, jetzt jedoch gültig für $N(\mu)$

The stability parameter μ is an internal one, it contains the turbulent heat flux. Mostly this parameter will not be available and has to be replaced therefore by an external stability parameter σ (also often called S) which contains the temperature difference from the top to the bottom of the PBL. A relation between the two stability parameters can be found in the paper by YORDANOV and WIPPERMANN (1972).

4. The closing of the system of equations for the barotropic PBL

The equations for the PBL are

$$f(\hat{u} - \hat{u}_g) = d(\tau_y/\bar{\rho})/dz \tag{34a}$$

$$f(\hat{v} - \hat{v}_g) = -d(\tau_x/\bar{\rho})/dz\,. \tag{34b}$$

By differentiating these equations with respect to z, by applying eq. (1) for each component and using the nondimensional notation (4a)–(4d) one gets the two equations

$$d^2Y/dZ^2 = X/K_m \tag{35}$$

$$d^2X/dZ^2 = -Y/K_m \tag{36}$$

where

$$X \equiv \tau_x/\tau_0,\quad Y \equiv \tau_y/\tau_0\,,\quad T = (X^2 + Y^2)^{1/2}\,. \tag{37}$$

Together with eq. (7) and the mixing-length hypothesis (19) one has a system of four eq. (35, (36), (7), (19) for the four dependent variables X, Y, K_m, L. Only two parameters occur in this set of equations, namely K_{m0} (= Z_0) and L_∞. According to eq. (30) the first one reflects the influence of the surface Rossby number, the second one according to eq. (33) may be replaced by the internal stability parameter μ.

The boundary conditions are

$$Z = Z_0: \quad X = 1, \quad Y = 0, \quad K_m = K_{m0} \tag{38a}$$

$$Z \to \infty: \quad X \to 0, \quad Y \to 0, \quad K_m \to 0. \tag{38b}$$

The system (35), (36), (7), (19) with the boundary conditions (38a), (38b) is closed, integrations can be carried out. A method to solve this system has been given by WIPPERMANN (1971).

References

APPLEBY, J. F., W. D. OHMSTEDE, 1964: Numerical solution of the distribution of wind and turbulence in the planetary boundary layer. Meteor. Res. Note Nr. 8, Meteorolog. Dept. USAERDA, Fort Huachuca, Ariz.

BLACKADAR, A. K., 1962: The vertical distribution of wind and turbulent exchange in a neutral atmosphere. J. Geophys. Res. 67, 3095–3102.

BOBILEVA, I. M., S. S. ZILITINKEVICH, D. L. LAIKHTMAN, 1965: Turbulent exchange in the thermally stratified planetary boundary layer of the atmosphere. Preprint Inter. Colloqu. on Fine-Scale Structure of the Atmosphere. Acad. Sci. USSR Moscow 1965, pp 21.

CLARKE, R. M., 1970: Observational studies in the atmospheric boundary layer. Q.J.R.M.S. 96, 91–114.

KUNG, E. C., 1966: On the momentum exchange between the atmosphere and earth over the northern hemisphere. Month. Wea. Rev. 96 (6), 337–341.

KUROSAKI, A., 1970: A theoretical study of the structure of the Ekman boundary layer (I), Mixing length theory. Pap. in Meteor. and Geophys. 21 (2), 89–112.

LETTAU, H. H., 1962: Theoretical wind spirals in the boundary layer of a barotropic atmosphere. Beitr. Phys. Atm. 35, 195–212.

MONIN, A. S., S. S. ZILITINKEVICH, 1967: Planetary boundary layer and large scale atmospheric dynamics. GARP Study Conf., Stockholm 28.6.–11.7.1967, Append. V, 37 pp.

OHMSTEDE, W. D., 1966: Numerical solution of the transport and energy equations in the planetary boundary layer. Techn. Rep. ECOM-6020, AD 633694, Atm. Sci. Lab., Fort Huachuca, Ariz., pp 152, April 1966.

RUSIN, M. I., N. A. BOLDIZEVA, T. A. SABELEVA, 1963: Some results of the computations of the exchange coefficient in the planetary boundary layer. Trudy L.G.M.I., B 15, 66–68 (in russian).

SMITH, F. B., 1969: The vertical transfer of momentum through the boundary layer. AGARD Conf. "Aerodynamics of Atmospheric Shear Flows" Munich 15–17 Sept. 1969. AGARD Conf. Proc. No. 48, Pap. 19, pp 8.

WIPPERMANN, F., 1970: The two constants in the resistance law for a neutral barotropic boundary layer of the atmosphere. Beitr. Phys. Atm. 43, 133–140.

WIPPERMANN, F., 1971: The eddy viscosity in a barotropic planetary boundary layer as related to the turbulent kinetic energy. Beitr. Phys. Atm. 44, 127–136.

WIPPERMANN, F., 1971: A note on a method for solving the planetary boundary layer equations. Submitt. for publ.: Beitr. Phys. Atm. 44.

YORDANOV, D., F. WIPPERMANN, 1972: The parametrization of the turbulent fluxes of momentum, heat and moisture at the ground in a baroclinic planetary boundary layer. Submitted for publ.: Beitr. Phys. Atm. 45.

Note added in proof: The eqs. (13) and (14) are identical with the eqs. (8) and (9) in the paper by LYKOSOV and GUTMAN, Izv. Acad. Sci. USSR, Atm. Ocean. Phys. 6 (12), 1238–1254, 1970; engl. transl. 738–746.

Note on the Upper Boundary Conditions

The upper boundary conditions at $Z \longrightarrow Z_T$ depend on the hypothesis made for the mixing-length. For the different mixing-length hypotheses discussed on the pages 48 - 50 different sets of upper boundary conditions can be distinguished

$Z \longrightarrow Z_T$ (or $Z \longrightarrow \infty$) :

$X \longrightarrow 0$	$X \longrightarrow \frac{L_\infty^2}{\kappa^2} \lambda_x (\lambda_x^2 + \lambda_y^2)^{1/2}$	$X \longrightarrow X_T(L_\infty, \lambda_x, \lambda_y)$
$Y \longrightarrow 0$	$Y \longrightarrow \frac{L_\infty^2}{\kappa^2} \lambda_y (\lambda_x^2 + \lambda_y^2)^{1/2}$	$Y \longrightarrow Y_T(L_\infty, \lambda_x, \lambda_y)$
$K_m \longrightarrow 0$	$K_m \longrightarrow \frac{L_\infty^2}{\kappa^2} (\lambda_x^2 + \lambda_y^2)^{1/2}$	$K_m \longrightarrow K_{mT}(L_\infty, \lambda_x, \lambda_y)$
$L \longrightarrow 0$	$L \longrightarrow L_\infty$	$L \longrightarrow L_T(L_\infty, \lambda_x, \lambda_y)$
(1)	(2)	(3)

If $L \longrightarrow 0$ for $Z \longrightarrow Z_T$ as for instance in LETTAU's hypothesis, eq. (10b) on page 48, also $X \longrightarrow 0$, $Y \longrightarrow 0$ and $K_m \longrightarrow 0$, see the set (1); This happens even for baroclinic cases, where $X_T \neq 0$ or $Y_T \neq 0$ or both.

If the hypothesis requires $L \longrightarrow L_\infty$ for $Z \longrightarrow Z_T$ the X , Y and K_m approach values given in the set (2). Examples for such hypotheses are those by BLACKADAR, eq. (9b) on page 48, by APPLEBY and OHMSTEDE, eq. (11b) on page 49, and others. L_∞ is the asymptotic mixing-length and simultaneously the parameter governing the thermal stratification.

In the mixing-length hypothesis by WIPPERMANN, eq. (19) on page 50, L_∞ is indeed the parameter for the thermal stratification, but it is not the mixing-length L_T at the top of the PBL; in the barotropic case only they are the same. So far the validity of the boundary condition (20b) on page 50 is restricted to barotropic cases. In a baroclinic case the value L_T has to be found iteratively; this of course reduces the usefulness of the mixing-length hypotheses of the kind $l = l(\tau)$.
In this sense the table on page 83 has to be corrected: the upper boundary conditions (30a) - (30d) are only valid for $L = L(Z)$ in (29) but not for $L = L(X,Y)$.

Beiträge zur Physik der Atmosphäre, 44. Band, 1971, S. 293–296

A Note on a Method for Solving the Planetary Boundary-Layer Equations

Kurze Mitteilung über ein Lösungsverfahren für die Gleichungen der planetarischen Grenzschicht

F. Wippermann

Technical University, Darmstadt, Germany, Department of Meteorology

Eingegangen am 22. Juli 1971

The following dimensionless notation may be used

$$H \equiv \kappa\, u_*/f \qquad Z \equiv z/H \qquad L \equiv l/H \tag{1a}$$

$$X \equiv \tau_x/\tau_0 \qquad Y \equiv \tau_y/\tau_0 \qquad K \equiv k_m/(H^2 f) \tag{1b}$$

$$P \equiv \kappa\,(\hat{u}-\hat{u}_g)/u_* \qquad Q \equiv \kappa\,(\hat{v}-\hat{v}_g)/u_* \tag{1c}$$

where H is the internal scale height of the planetary boundary layer (PBL), u_* is the friction velocity at the grond ($z = z_0$), f is the Coriolis parameter, l the mixing-length, τ the Reynolds stress, k_m the eddy viscosity and κ the Karman constant. The index $_0$ indicates values at the ground and the index $_g$ geostrophic winds.

From the PBL-equations (steady state and horizontal homogeneous) for a barotropic PBL and from the flux-gradient relations the components of the wind defect can be eliminated, one gets two ordinary second order differential equations

$$d^2Y/dZ^2 = X/K \tag{2a}$$

$$d^2X/dZ^2 = -Y/K \tag{2b}$$

with the boundary conditions

$$Z = Z_0: \qquad X = 1 \qquad Y = 0 \tag{3a}$$

$$Z \to \infty: \qquad X \to 0 \qquad Y \to 0\,. \tag{3b}$$

One recognizes from condition (3a) that the coordinate system is orientated with the x-axis into the direction of the Reynolds stress at the ground. In order to close the system of equations a hypothesis has to be made for K, possibly by a hypothesis for the mixing-length. With the flux-gradient relation

$$\tau/\bar{\rho} = k_m\, |d\hat{w}/dz|$$

and with PRANDTLs equation

$$k_m = l^2\, |d\hat{w}/dz|$$

one obtains in dimensionless notation

$$K = (X^2 + Y^2)^{1/4}\, L/\kappa\,. \tag{4}$$

If herein L is given by a mixing-length hypothesis either as $L(Z)$ or as $L(X, Y)$ the system (2a), (2b) can be closed and a numerical integration is possible.

Considerable difficulties encounter in solving the system (2a), (2b), (4) and the additional hypothesis for L, although it looks rather simple. LETTAU (1962) is forced to postulate the solution at a fixed height in order to integrate from there upwards and downwards; APPLEBY and OHMSTEDE (1964) achieved a solution "more by utilizing physical intuition than mathematical prowess". BLACKADAR (1962) selects trial values for $(dX/dZ)_0$ and $(dY/dZ)_0$ and carries out an integration with these using a finite difference scheme; a solution is obtained by refining the trial values and repeating the calculation until the upper boundary condition is considered to be sufficiently well satisfied. This method yields useful results as long as the integrations are carried out for the rather insensitive quantities P and Q (as done by BLACKADAR), for which the differential equations are of the same type; but this method would fail for the equations above containing the very sensitive quantities X and Y. Recently ESTOQUE and BHUMRALKAR (1970) gave an iterative method by applying a matrix inversion for each iterative step; this method has the disadvantage to be usuable only for a very restricted number of points along the Z-coordinate.

Therefore it seems to be worthwile to report a recently developed method which allows to obtain iteratively solutions of the system of equations mentioned above with the desired degree of accuracy.

First it is necessary to assume that X and Y became negligible at a finite but large height Z^* rather than at infinity. That means the boundary condition (3b) has to be changed into

$$Z \to Z^*: \qquad X \to 0 \qquad Y \to 0 . \tag{5}$$

Certainly it is high enough when Z^* is chosen to be 10, which roughly corresponds to a height of $z = 10$ km. Since for the highest possible surface Rossby number the value of Z_0 is about $1 \cdot 10^{-8}$ the possible range of the vertical coordinate may cover nine orders of magnitude; therefore it seems to be useful to transform the equation (2a) and (2b) for a logarithmic vertical coordinate

$$\xi = \log_{10} Z, \qquad d\xi/dZ = a/Z \qquad a = 0.4343 \tag{6}$$

$$d^2Y/d\xi^2 - 1/a\, dY/d\xi = 10^{2\xi}\, X/(a^2 K) \tag{7a}$$

$$d^2X/d\xi^2 - 1/a\, dX/d\xi = -10^{2\xi}\, Y/(a^2 K) . \tag{7b}$$

After the discretisation the integer of the points along the coordinate ξ may be called n

$$\xi_n = \xi_0 + n\,\Delta\xi .$$

By using centered differences in the eqs. (7a) and (7b) one gets for X_n and Y_n

$$X_n = 1/2\,\{[1 - \Delta\xi/(2\,a)]\,X_{n+1} + [1 + \Delta\xi/(2\,a)]\,X_{n-1} + (\Delta\xi)^2\, 10^{2\xi}\, Y_n/(a^2 K_n)\} \tag{8a}$$

$$Y_n = 1/2\,\{[1 - \Delta\xi/(2\,a)]\,Y_{n+1} + [1 + \Delta\xi/(2\,a)]\,Y_{n-1} - (\Delta\xi)^2\, 10^{2\xi}\, X_n/(a^2 K_n)\} . \tag{8b}$$

The two equations (7a), (7b) or (8a), (8b) have to be solved simultaneously. For the purpose of applying a relaxation procedure Y_n in eq. (8a) and X_n in eq. (8b) have to be expressed by the values of the neighbouring points; this can be done by using eq. (8b) for Y_n in eq. (8a) and vice versa.

$$X_n = 1/(2 + \Gamma_n^2)\,\{c_1\, X_{n+1} + c_2\, X_{n-1} + c_1\, \Gamma_n\, Y_{n+1} + c_2\, \Gamma_n\, Y_{n-1}\} \tag{9a}$$

$$Y_n = 1/(2 + \Gamma_n^2)\,\{c_1\, Y_{n+1} + c_2\, Y_{n-1} - c_1\, \Gamma_n\, X_{n+1} - c_2\, \Gamma_n\, X_{n-1}\} \tag{9b}$$

$$\left.\begin{aligned} \Gamma_n &\equiv (\Delta\xi)^2\, 10^{2\xi}/(a^2\, K_n) \\ c_1 &\equiv 1 - \Delta\xi/(2\,a) \\ c_2 &\equiv 1 + \Delta\xi/(2\,a) \end{aligned}\right\} \tag{9c}$$

If a first approximation $(q = 1)$ is given for $X(\xi)$ and $Y(\xi)$, for instance the profiles in the case of an Ekman spiral

$$\overset{(1)}{X}(\xi) = \exp\{-N(10^{\xi} - 10^{\xi_0})\}\cos\{N(10^{\xi} - 10^{\xi_0})\} \tag{10a}$$

$$\overset{(1)}{Y}(\xi) = -\exp\{-N(10^{\xi} - 10^{\xi_0})\}\sin\{N(10^{\xi} - 10^{\xi_0})\} \tag{10b}$$

$$\overset{(0)}{K}(\xi) = \text{const} = 1/(2N^2), \quad N = 4.6 \tag{10c}$$

the profile $\overset{(1)}{K}(\xi)$ can be computed from eq. (4) by using an additional mixing-length hypothesis. With $\overset{(1)}{K}(\xi)$ also $\overset{(1)}{\Gamma}(\xi)$ can be computed; therefore for each point the values $\overset{(1)}{X}_n$, $\overset{(1)}{Y}_n$ and $\overset{(1)}{\Gamma}_n$ can be defined. Now a onedimensional relaxation method can be applied in a single step procedure, i.e. in a modified LIEBMANN procedure (without over-relaxation). Here it is important that the iterations r for the relaxation process are made allways for X_n and Y_n at the same level n and that one proceedes to the next level $(n + 1)$ only when X_n as well as Y_n has been improved at the level n. If one goes upwards from $n = 1$ (one point above ξ_0) to $n = n^* - 1$ (one point below ξ^*) an improved $(r \to r + 1)$ value of X_n and Y_n is computed according to eqs. (9a) and (9b) as follows

$$\overset{(q+1)}{X}{}^{(r+1)}_n = 1/(2 + \overset{(q)}{\Gamma}_n)\left\{ c_1 \overset{(q+1)}{X}{}^{(r)}_{n+1} + c_2 \overset{(q+1)}{X}{}^{(r+1)}_{n-1} + c_1 \overset{(q)}{\Gamma}_n \overset{(q+1)}{Y}{}^{(r)}_{n+1} + c_2 \overset{(q)}{\Gamma}_n \overset{(q+1)}{Y}{}^{(r+1)}_{n-1} \right\} \tag{11a}$$

$$\overset{(q+1)}{Y}{}^{(r+1)}_n = 1/(2 + \overset{(q)}{\Gamma}_n)\left\{ c_1 \overset{(q+1)}{Y}{}^{(r)}_{n+1} + c_2 \overset{(q+1)}{Y}{}^{(r+1)}_{n-1} - c_1 \overset{(q)}{\Gamma}_n \overset{(q+1)}{X}{}^{(r)}_{n+1} - c_2 \overset{(q)}{\Gamma}_n \overset{(q+1)}{X}{}^{(r+1)}_{n-1} \right\} \tag{11b}$$

If one proceedes downwards instead upwards one would compute new values at the point n by using already improved values at the neighbouring points above but values of the last iteration at the neighbouring points below.

By going r^* times through the $n^* - 1$ interior points one is close enough to the solution of the equations with the qth approximation of K (or Γ). With that the $(q + 1)^{th}$ approximation of X and Y is obtained, now the $(q + 1)^{th}$ approximation of K (or by eq. (9c) of Γ) can be computed by making use of eq. (4). Then the relaxation procedure with the r-iterations starts again and will be carried out until one obtains after r^* passages the next approximation of X and Y. This process should be repeated until the $(q^*)^{th}$ approximation is reached, i.e. until the maximum of the difference $\overset{(q)}{K}_n - \overset{(q-1)}{K}_n$ is smaller than a given value. It is recommended to carry out the r^* passages for the relaxation process alternating upwards and downwards.

For integrations which have been carried out betwenn $\xi_0 = -8$ and $\xi^* = 1$ (roughly between 1/100 mm and 10 km) $\Delta\xi = 5 \cdot 10^{-2}$ has been chosen, i.e. 179 interior points have been used. With $q^* = 10$ iterations and during each iteration $r^* = 1000$ relaxation steps (passages) profiles of X and Y could be obtained which differ from the correct solution for less than one thousandth.

After having obtained the profiles $X(\xi)$ and $Y(\xi)$ any other profile in the PBL, for instance $P(\xi)$ and $Q(\xi)$ can easily be obtained, see WIPPERMANN (1971).

References

APPLEBY, J. F., W. D. OHMSTEDE, 1964: Numerical solution of the distribution of wind and turbulence in the planetary boundary layer. Meteor. Res. Note No. 8 Meteor. Departm. USAERDA Fort Huachuca, Ariz., Sept. 1964.

BLACKADAR, A. K., 1962: The vertical distribution of wind and turbulent exchange in a neutral atmosphere. J. Geophys. Res. 67 (8), 3095–3102.

ESTOQUE, M. A., CH. M. BHUMRALKAR, 1970: A method for solving the planetary boundary-layer equations. Boundary Layer Meteorology 1, 169–194.

LETTAU, H. H., 1962: Theoretical wind spirals in the boundary layer of a barotropic atmosphere. Beitr. Phys. Atm. 35, 195–212.

WIPPERMANN, F., 1971: The eddy viscosity in a barotropic planetary boundary layer as related to the turbulent kinetic energy. Beitr. Phys. Atm. 44, 127–136.

Correction

The following errors were noted in the article "A Note on a Method for Solving the Planetary Boundary-Layer Equations" by F. WIPPERMANN (Beiträge zur Physik der Atmosphäre 44, 293–296):

Page 294: Equations (9a) and (9b) should read:

$$X_n = 1/(2 + \Gamma_n^2/2)\,\{c_1 X_{n+1} + c_2 X_{n-1} + c_1 \Gamma_n Y_{n+1}/2 + c_2 \Gamma_n Y_{n-1}/2\}$$

$$Y_n = 1/(2 + \Gamma_n^2/2)\,\{c_1 Y_{n+1} + c_2 Y_{n-1} - c_1 \Gamma_n X_{n+1}/2 - c_2 \Gamma_n X_{n-1}/2\}$$

Page 295: Equations (11a) and (11b) should read:

$$\overset{(q+1)}{\underset{(r+1)}{X_n}} = 1/(2 + \Gamma_n^2/2)\left\{c_1 \overset{(q+1)}{\underset{(r)}{X_{n+1}}} + c_2 \overset{(q+1)}{\underset{(r+1)}{X_{n-1}}} + c_1 \overset{(q)}{\Gamma_n} \overset{(q+1)}{\underset{(r)}{Y_{n+1}}}/2 + c_2 \overset{(q)}{\Gamma_n} \overset{(q+1)}{\underset{(r+1)}{Y_{n-1}}}/2\right\}$$

$$\overset{(q+1)}{\underset{(r+1)}{Y_n}} = 1/(2 + \Gamma_n^2/2)\left\{c_1 \overset{(q+1)}{\underset{(r)}{Y_{n+1}}} + c_2 \overset{(q+1)}{\underset{(r+1)}{Y_{n-1}}} - c_1 \overset{(q)}{\Gamma_n} \overset{(q+1)}{\underset{(r)}{X_{n+1}}}/2 - c_2 \overset{(q)}{\Gamma_n} \overset{(q+1)}{\underset{(r+1)}{X_{n-1}}}/2\right\}$$

Chapter 3

The Structur of the Planetary Boundary-Layer

This chapter deals with several aspects of the structure of a PBL.

The first part is concerned with a relation between the eddy viscosity and the turbulent kinetic energy; it can be used as another additional relation needed for closing the sytem of the PBL-equations. Therefore this paper would likewise correctly be placed in the first section of chapter 2 . However it contains also some examples of vertical stress-profiles together with the corresponding profiles of the eddy viscosity and some considerations of the angular characteristics of several wind spirals distinguishing between equiangular and variangular spirals. For this reason this paper is placed in chapter 3 .

Two contributions follow, which are concerned with the Rossby-number similarity. Whereas the first contribution

proves the existence of the Rossby-number similarity by considering the PBL-equations and the boundary conditions, the second note investigates the height z_R above which Rossby number similarity is valid.

The fourth part of this chapter is concerned with universal profiles in a barotropic PBL; profiles obtained by a PBL-model are presented for the velocity-defect, the stress, the eddy viscosity and for the rate of energy dissipation. These profiles vary with the thermal stratification only.As a by-product an empirical formula has been developed for the vertical profile of the (non-dimensional) eddy viscosity; it possibly is useful for parameterization purposes.

In the next part the energy budget of a PBL is studied; here the vertical energy transports and their divergences as well as the energy transformations are considered varying with height. In addition to the previous part it is shown which profiles of energy-transports and energy-transformations are universal (in the sense of Rossby-number similarity) and which are not.

The sixth contribution in this chapter extends the results of the fourth to baroclinic cases. Again universal profiles of the stress, of the potential temperature and mainly of the eddy viscosity are presented for selected baroclinic cases. For special baroclinicities the eddy viscosity has a minimum in a rather thin layer, which acts like a barrier for turbulent diffusion in the vertical direction. This may be important for pollution problems (assuming $k_s = k_m$), when this layer is located at a rather low altitude.

In part seven the wind profile very close to the ground is considered; it is shown without any additional assumption or hypothesis that the profile very close to the ground is a logarithmic one. This result is important for the deri-

vation of the so-called resistance law dealt in chapter 4 This derivation namely requires that the wind profile has to be logarithmic in that lowest layer $z_o \leqq z \leqq z_R$, in which Rossby-number similarity does not exist.

In the final contribution the low-level jet is studied with the aid of a numerical boundary-layer model. Since the LLJ is a phenomenon of the atmospheric boundary layer, it cannot be disregarded, when the structure of the PBL is considered. This paper contains also a short review of the present knowledge of the LLJ and a bibliography on this subject.

Beiträge zur Physik der Atmosphäre, 44. Band, 1971 S. 127–136

The Eddy Viscosity in a Barotropic Planetary Boundary Layer as related to the Turbulent Kinetic Energy*)

F. Wippermann

Technical University Darmstadt, Germany, Department of Meteorology

Eingegangen am 12. Dezember 1970

Zusammenfassung: Für eine planetarische Grenzschicht mit den üblichen Voraussetzung (a) der Stationarität, (b) der horizontalen Homogenität und (c) vernachlässigbar kleiner vertikaler Dichteänderungen und mit der zusätzlichen Voraussetzung der Barotropie wird eine Beziehung abgeleitet, welche den turbulenten Diffusionskoeffizienten $k_m(z)$ als nur von der Schubspannung τ und deren vertikalen Ableitungen abhängend gibt. Wenn man die beiden Hypothesen für den turbulenten Diffusionskoeffizienten von PRANDTL und von MONIN gleichzeitig gelten läßt, kann eine Formel erhalten werden, nach welcher der turbulente Diffusionskoeffizient nur von der Turbulenzenergie und deren vertikalen Ableitungen abhängt.

Es werden außerdem die Winkelverhältnisse der Windspiralen und ihr Zusammenhang mit dem Vertikalprofil des turbulenten Diffusionskoeffizienten betrachtet.

Summary: For a planetary boundary layer with the usual assumptions of (a) stationarity, (b) horizontal homogeneity, and (c) neglected vertical variation of density and with the additional assumption of barotropy a relation is derived giving the eddy viscosity $k_m(z)$ as depending on the stress τ and its vertical derivatives only. With the hypotheses of PRANDTL and of MONIN for the eddy viscosity a formula can be obtained relating the eddy viscosity to the turbulent kinetic energy and its vertical derivates only.

Also some angular characteristics of wind spirals and their relations to the profile of the eddy viscosity are considered.

Résumé: Pour une couche limite planétaire, grâce aux hypothèses habituelles: a) d'état stationnaire b) d'homogénéité horizontale et c) de variations verticales négligeables de la masse volumique, ainsi qu'à l'hypothèse de la barotropie, on déduit une relation dans laquelle le coefficient de diffusion turbulente $\kappa_m(z)$ de la quantité de mouvement ne dépend que de la tension tangentielle horizontale et de sa dérivée suivant la verticale.

Quand on utilise simultanément les hypothèses de PRANDTL et de MONIN relatives au coefficient de diffusion turbulente, on arrive à une formule suivant laquelle ce coefficient de diffusion turbulente ne dépend que de l'énergie cinétique de la turbulence et de sa dérivée suivant la verticale.

L'auteur examine, en outre, les caractéristiques angulaires des spirales de vent et leur relation avec le profil vertical du coefficient de diffusion turbulente.

I. Introduction

The planetary boundary layer (PBL) is usually defined by the following assumptions: (a) stationarity, (b) horizontal homogeneity and (c) the vertical variation of the horizontally averaged density can be neglected.

The additional assumption of barotropy involves a geostrophic wind constant with height.

*) Paper presented at the International Conference on Meteorology (A.M.S. – I. M. S.) 30. Nov. – 4. Dec. 1970 Tel Aviv / Jerusalem

The PBL-equations are:

$$f\,[\bar{u} - u_g] = \left(\frac{\tau_y}{\bar{\rho}}\right)' \tag{1a}$$

$$f\,[\bar{v} - v_g] = -\left(\frac{\tau_x}{\bar{\rho}}\right)' \tag{1b}$$

where the usual notations are used and the prime symbolizes a derivative with respect to z. The coordinate system should be orientated with the x-axis in the direction of the surface stress, see fig. 1, i.e. $(\tau_x)_0 = \rho\, u_*^2$, $(\tau_y)_0 = 0$ and the components of the geostrophic wind are $u_g = |v_g| \cos(\alpha_0)$, $v_g = -|v_g| \sin(|\alpha_0|)$.

The four unknowns in eqs. (1a, 1b) may be reduced to three by assuming a gradient flux

$$\tau_x = \bar{\rho}\, k_m\, \bar{u}', \quad \tau_y = \bar{\rho}\, k_m\, \bar{v}'$$

but in order to close the system a fourth relation still has to be assumed.

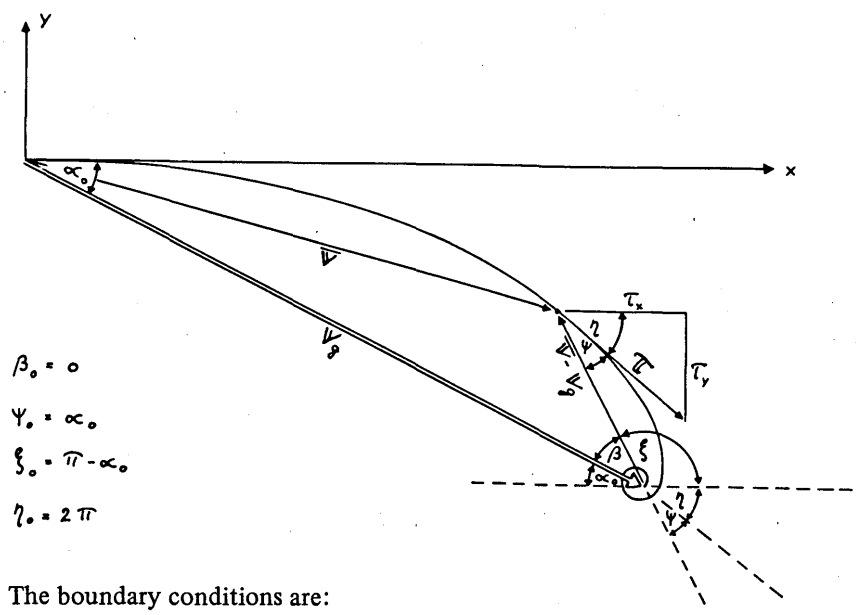

The boundary conditions are:

$$z = z_0: \quad \bar{u} = \bar{v} = 0 \tag{3a}$$

$$\tau_x = \bar{\rho}\, u_*^2, \quad \tau_y = 0 \tag{3b}$$

$$z \to \infty: \quad \bar{u} \to o, \quad \bar{v} \to 0 \tag{3c}$$

$$\tau_x \to 0, \quad \tau_y \to 0 \tag{3d}$$

Without a closure of the system and without solving it an information about the stress vector at the level z_0 can be obtained by the resistance law for a barotropic and neutral PBL, which was first derived by KAZANSKII and MONIN (1961):

$$\ln(Ro_0) = M - \ln(C_d) + \sqrt{\frac{\kappa^2}{C_d^2} - N^2} \tag{4a}$$

$$\kappa \sin(|\alpha_0|) = N\, C_d \tag{4b}$$

wherein $Ro_0 = |\mathbf{v}_g| / (f\, z_0)$ is the surface Rossby-Number, $C_d = u_* / |\mathbf{v}_g|$ is the geostrophic drag coefficient, α_0 is the cross-isobar angle and κ the Karman-constant; M and N are universal constants, the values of which are not yet exactly known but may be given, see WIPPERMANN (1970), by:

$$M = 0.90, \quad N = 4.50 \tag{5}$$

The constant N will be used in the following derivations.

II. A relationship between eddy viscosity and stress

Using the angle $\eta(z)$ between the x-axis and the stress vector $\tau(z)$, see fig. 1, one has

$$\tau_x = \tau \cos(\eta), \qquad \tau_y = \tau \sin(\eta)$$

by which the right-hand sides of eqs. (1a, 1b) should be replaced. By differentiation of these two equations with respect to z the two left-hand sides give

$$f u' = f\, |\bar{\mathbf{v}}'| \cos(\eta), \qquad f v' = f\, |\bar{\mathbf{v}}'| \sin(\eta)$$

and contain therefore also the angle η. By division of the equations and after some rearrangements the following two equations will result

$$\frac{1}{\tau}\, \tau'' = (\eta')^2 \tag{6}$$

$$\rho\, f\, |\bar{\mathbf{v}}'| = |2\, \eta' \tau' + \eta'' \tau| \tag{7}$$

From eq. (6) follows, that for any height z

$$\tau''(z) \geqq 0 \tag{8}$$

and from this with respect to the boundary conditions (3b, 3d)

$$\tau'(z) \leqq 0 \tag{9}$$

According to eq. (2) is the eddy viscosity

$$k_m = \frac{\tau}{\bar{\rho}\, |\bar{\mathbf{v}}'|} \tag{10}$$

It can be obtained therefore by dividing the expression $f\,\tau$ by the right-hand side of eq. (7), in which before η' and η'' have been replaced; this can be done with the aid of eq. (6) in the undifferentiated form as well as in differentiated form. One gets

$$\boxed{\frac{k_m}{2f} = \frac{\tau \sqrt{\tau\, \tau''}}{|3\, \tau' \tau'' + \tau\, \tau'''|}} \tag{11}$$

Very close to the ground ($z = z_0$) it is possible to obtain the approximated stress profile, since the first, the second and the third derivative of τ is known:

The eqs. (1a, 1b) can be written with the aid of the angle η

$$\bar{\rho}\, f\, [\bar{u} - u_g] = \tau' \sin(\eta) + \tau\, \eta' \cos(\eta) \tag{12a}$$

$$-\bar{\rho}\, f\, [\bar{v} - v_g] = \tau' \cos(\eta) - \tau\, \eta' \sin(\eta) \tag{12b}$$

According to the boundary condition (3a) the velocity components $\bar{u}$ and $\bar{v}$ vanish at the ground ($z = z_0$); furthermore $\eta_0 = 0$. This means

$$(\eta')_0 = -\frac{1}{\tau_0}\,\bar{\rho}\,f\,u_g \tag{13a}$$

$$(\tau')_0 = \bar{\rho}\,f\,v_g \tag{13b}$$

The later relation can be transformed with the aid of $v_g = -|\mathbb{v}_g|\sin(|\alpha_0|)$ and with the aid of eq. (4b) into

$$(\tau')_0 = -\frac{\bar{\rho}\,f\,u_*}{\kappa}\,N$$

or with the usual scaling height H

$$H \equiv \frac{\kappa\,u_*}{f} \tag{14}$$

into

$$(\tau')_0 = -\frac{\tau_0}{H}\,N \tag{15}$$

From the eqs. (12a, 12b) one gets

$$\bar{\rho}^2 f^2\,|\bar{\mathbb{v}} - \mathbb{v}_g|^2 = (\tau')^2 + \tau^2\,(\eta')^2$$

in which $(\eta')^2$ is replaced by eq. (6); a relation for τ'' is obtained

$$\tau'' = \frac{\bar{\rho}^2 f^2}{\tau}\,|\bar{\mathbb{v}} - \mathbb{v}_g|^2 - \frac{(\tau')^2}{\tau}$$

or with eqs. (3a), (14) and (15) at $z = z_0$

$$(\tau'')_0 = \frac{\tau_0}{H^2}\left\{\frac{\kappa^2}{C_d^2} - N^2\right\} = \frac{\tau_0}{H^2}\,N^2\,\mathrm{cotg}^2(|\alpha_0|) \tag{16}$$

In order to get $(\tau''')_0$ the eq. (11) will be used, in which $(k_m)_0 = \kappa\,u_*\,z$ is set according to results for the Prandtl-layer. Since according to the eqs. (15) and (16) the $(\tau')_0$ and $(\tau'')_0$ are finite, $(k_m)_0$ can only be zero when $(\tau''')_0 \to \infty$; therefore it is reasonable to assume the very small value given by the Prandtl-layer theory. From eq. (11) one gets

$$\tau''' = -\frac{2f}{k_m}\,\sqrt{\tau\tau''} - 3\,\frac{\tau'\tau''}{\tau}$$

At the ground ($z = z_0$) we replace $(\tau')_0$ and $(\tau'')_0$ by the eqs. (15) and (16) and we obtain:

$$(\tau''')_0 = -2\,\frac{\tau_0}{H^3}\sqrt{\frac{\kappa^2}{C_d^2} - N^2}\left\{\frac{H}{z_0} - \frac{3}{2}\,N\sqrt{\frac{\kappa^2}{C_d^2} - N^2}\right\} \tag{17}$$

Since

$$\frac{H}{z_0} \gg \frac{3}{2}\,N\sqrt{\frac{\kappa^2}{C_d^2} - N^2} = \frac{3}{2}\,N^2\,\mathrm{cotg}(|\alpha_0|)$$

the second term in the brackets may be neglected. It remains therefore

$$(\tau''')_0 = -\frac{\tau_0}{H^2\,z_0}\,2\,N\,\mathrm{cotg}(|\alpha_0|) \tag{18}$$

In summary it has been found:

$$\tau_0 = \bar{\rho}\, u_*^2 \tag{19a}$$

$$(\tau')_0 = -\frac{\tau_0}{H} N \tag{19b}$$

$$(\tau'')_0 = \frac{\tau_0}{H^2} N^2 \operatorname{cotg}^2 (\,|\alpha_0|\,) \tag{19c}$$

$$(\tau''')_0 = -\frac{\tau_0}{H^2 z_0} 2 N \operatorname{cotg} (\,|\alpha_0|\,) \tag{19d}$$

III. The height of the Prandtl-layer

In the lowest decameters of the PBL very often a Prandtl-layer is postulated, that means the stress τ is assumed to be constant with height. But according to condition (9) the stress can not be constant and actually it varies most rapidly just within the layer which is assumed to be a Prandtl-layer. In order to define a Prandtl-layer in spite of that one considers as Prandtl-layer the lowest layer up to a depth h at which the surface stress τ_0 is decreased for 10 %:

$$\tau(h) = 0.9\, \tau_0 \tag{20}$$

The stress τ (h) can be represented by

$$\tau\left(\frac{h}{H}\right) = \tau_0 + (\tau^*)_0 \frac{h}{H} + \frac{1}{2} (\tau^{**})_0 \frac{h^2}{H^2} + \ldots \tag{21}$$

in which h/H is the dimensionless height of the Prandtl-layer and (. . .)* symbolizes the derivation with respect to the dimensionless vertical coordinate $Z \equiv z/H$; for instance $(\tau^*)_0 = -\tau_0 N$. The height h/H is very small, it ranges probably between 0.02 and 0.05; therefore terms of second and higher order may be neglected in eq. (21). By combining the eqs. (21) and (20) one obtaines

$$\frac{h}{H} = -\frac{0.1\, \tau_0}{(\tau^*)_0} = \frac{0.1}{N}$$

or

$$h = 0.022\, H \tag{22}$$

If the scale height H is about 1000 m, which can be considered as a rough mean value, the height of the Prandtl-layer would be about 20 m.

IV. Some examples for the stress profile

It seems to be usefull to look at some analytical profiles τ (z) which satisfy the conditions (8) and (9) and the boundary condition (3d). By using eq. (11) the corresponding profile of the eddy viscosity may be considered. This has been done for the following four cases

A. $$\tau(z) = \tau_0 \exp\{-m(z - z_0)\}, \quad m > 0 \tag{23a}$$

$$k_m(z) = \text{const.} = \frac{f}{2\, m^2} \tag{23b}$$

B. $$\tau(z) = \tau_0 \left(\frac{z}{z_0}\right)^{-n}, \qquad n > 0 \tag{24a}$$

$$k_m(z) = \frac{f\sqrt{n(1+n)}\, z^2}{2n^3 + 3n^2 + n} \tag{24b}$$

C. $$\tau(z) = \tau_0 \exp\{-\mu(z - z_0)\} \left(\frac{z}{z_0}\right)^{-\nu} \qquad \mu > 0, \quad \nu > 0 \tag{25a}$$

$$k_m(z) = \frac{f\sqrt{(\mu z + \nu)^2 + \nu}\; z^2}{2(\mu z + \nu)^3 + 3\nu(\mu z + \nu) + \nu} \tag{25b}$$

D. $$\tau(z) = \tau_0 \frac{2}{\pi} \operatorname{arccotg}\{\lambda(z - z_0)\} \tag{26a}$$

$$k_m(z) = \frac{f\sqrt{2\lambda(z - z_0)}\,[1 + \lambda^2 (z - z_0)^2]^2 \{\operatorname{arccotg}[\lambda(z - z_0)]\}^{3/2}}{\lambda^2 \{ |[1 - 3\lambda^2 (z - z_0)^2] \operatorname{arccotg}[\lambda(z - z_0)] - 3\lambda(z - z_0)| \}} \tag{26b}$$

The stress profile in the case A corresponds to the original model by Ekman having an eddy viscosity constant with height. In the case B the profile of the eddy viscosity [$k_m(z) \propto z^2$] is also very unrealistic; lateron it will be shown, that a stress profile of typ B belongs to the equiangular wind spirals. To the stress profile D a profile of the eddy viscosity belongs, which shows a maximum in the lower part with a minimum above it; but above that k_m tends to infinity as $z \to \infty$. Only the lower part can be regarded as similar to observed profiles. The profile of the eddy viscosity belonging to the stress profile C shows at least a reasonable behaviour for very large z; in the lower part k_m increases with height and tends then to a constant value asymptotically.

V. Eddy viscosity and turbulent kinetic energy

At least two hypotheses are known for the eddy viscosity, namely one by PRANDTL (1932)

$$k_m = l^2 \left| \frac{d\bar{v}}{dz} \right| \tag{27}$$

where l is the mixing length, and the other by MONIN (1950) based on two papers by KOLMOGOROV and by OBUCHOV in the early forties

$$k_m = c_1\, l\, b^{1/2} \tag{28}$$

with $b = (\sigma_u^2 + \sigma_v^2 + \sigma_w^2)$, i.e. twice the value of the turbulent kinetic energy per mass unit; c_1 is a constant. By eliminating l from the eqs. (27) and (28) and making use of eq. (2) one gets

$$\frac{\tau}{\bar{\rho}} = c_1^2\, b \tag{29}$$

If in eq. (11) the stress τ is replaced by eq. (29) the relation between the eddy viscosity and the turbulent kinetic energy is obtained:

$$\boxed{k_m = 2f \frac{b\sqrt{bb''}}{|3b'b'' + bb'''|}} \tag{30}$$

In contrast to eq. (11), which is valid in a barotropic PBL without any additional assumption, the eq. (30) is only valid, when both hypotheses (27) and (28) are accepted. This of course, is done mostly.

VI. On the angular characteristics of several wind spirals in the PBL

A characteristic angle of the wind spiral is the angle ψ, see fig. 1, which is formed by the geostrophic departure $\bar{w} - w_g$ and the stress vector π. One notices from the figure 1 that

$$\psi_0 = \alpha_0 \tag{31}$$

and also that

$$\pi - \alpha_0 - \beta = \eta - \psi - \pi$$

or

$$\alpha_0 + \beta + \eta = 2\pi + \psi \tag{32}$$

For the decomposition of the vector $\bar{w} - w_g$ in its components the angle ξ, see fig. 1, will be used, where

$$\xi = \pi - \alpha_0 - \beta \tag{33}$$

with $\beta_0 = 0$.
Replacing in the eqs (1a) and (1b) the geostrophic departure in the form

$$\bar{u} - u_g = -|\bar{w} - w_g| \cos(\alpha_0 + \beta)$$

$$\bar{v} - v_g = |\bar{w} - w_g| \sin(\alpha_0 + \beta)$$

one obtains by making use of eq. (32)

$$\frac{1}{\tau}\tau' = \mathrm{r}\,\eta' \tag{34}$$

where r is the abbreviation for

$$\mathrm{r} \equiv \mathrm{tang}(\psi) \tag{35}$$

By eliminating η' between the eqs. (34) and (6) it follows

$$\left(\frac{\tau'}{\tau}\right)^2 = \mathrm{r}^2 \frac{\tau''}{\tau} \tag{36a}$$

or

$$\left(\frac{\tau'}{\tau}\right)' = \frac{1 - \mathrm{r}^2}{\mathrm{r}^2}\left(\frac{\tau'}{\tau}\right)^2 \tag{36b}$$

which can be integrated between z_0 and z; one gets

$$\frac{\tau'}{\tau} = \frac{1}{\left(\frac{\tau}{\tau'}\right)_0 - \int_{z_0}^{z} \frac{dz}{r^2} + (z - z_0)} \tag{37}$$

Considering eq. (15) and integrating once more between z_0 and z the following formula will result:

$$\boxed{\tau(z) = \tau_0 \exp \int_{z_0}^{z} \frac{dz}{z - z_0 - \frac{H}{N} - \int_{z_0}^{z} \frac{dz}{r^2}}} \tag{38}$$

or the same equation for b(z) when eq. (29) is considered. With the use of the stress τ as given by eq. (38) in the eq. (11) a relation can be obtained giving the eddy viscosity as depending on the angle ψ

$$\boxed{k_m = f \frac{r^3 \left\{ z - z_0 - \frac{H}{N} - \int_{z_0}^{z} \frac{dz}{r^2} \right\}^2}{\left| 1 + r^2 - \frac{1}{2} (r')^2 \left\{ z - z_0 - \frac{H}{N} - \int_{z_0}^{z} \frac{dz}{r^2} \right\} \right|}} \tag{39}$$

The two formulae may be applied to the equiangular wind spirals ($r = r_0 = \text{const.}$, $r' = 0$) as well as to the variangular spirals ($r' \neq 0$).

For the equiangular spiral is

$$z - z_0 - \frac{H}{N} - \int_{z_0}^{z} \frac{dz}{r^2} = \left[1 - \frac{1}{r_0^2}\right](z - z_0) - \frac{H}{N} \tag{40}$$

One has to destinguish two cases of equiangular spirals, namely

(a) $r_0 = 1$ (i.e.: $\psi_0 = \alpha_0 = \pi/4$)

(b) $r_0 \neq 1$

First the case (a) will be considered:

From eq. (38) with the aid of eq. (40) one gets

$$\tau(z) = \tau_0 \exp \left\{ - \frac{N}{H} (z - z_0) \right\} \tag{41a}$$

$$k_m = \frac{f}{2} \left(\frac{H}{N}\right)^2 = 3.95 \cdot 10^{-3} \frac{u_*^2}{f} \tag{41b}$$

If one compares this result with that of case A in section IV, see eqs. (23a), (23b), one notices that $r_0 = 1$ means the Ekmanmodel with $m = N/H$. The factor $3.95\ 10^{-3}$ obtained in eq. (41b) is only half the value estimated by HANNA (1969).

Also the geostrophic wind level, z_G, where the actual wind reaches for the first time the direction of the geostrophic wind, can be easily obtained:
The condition $\beta_G = \pi$ means $\eta_G = \pi + \psi_G - \alpha_0$ (because of eq. 32) or in this special case with regard of $\psi_G = \psi_0 = \alpha_0$

$$\eta_G = \pi \qquad (\text{for } r_0 = 1) \tag{42}$$

On the other hand η is obtained by integration of eq. (34)

$$\eta_G - \eta_0 = -\frac{N}{H}(z_G - z_0) \tag{43}$$

Elimination of η_G between the eqs. (42) and (43) gives with respect to $\eta_0 = 2\pi$

$$z_G = \frac{\pi}{N} H = 0.7\,H \tag{44}$$

In the case (b) with $r_0 \neq 1$ it is

$$\int_{z_0}^{z} \frac{dz}{1 - \frac{1}{\tau_0^2}(z - z_0) - \frac{H}{N}} = ln \left\{ 1 - \frac{r_0^2 - 1}{r_0^2} \frac{N}{H}(z - z_0) \right\}^{\frac{r_0^2}{r_0^2 - 1}}$$

With that one gets from eq. (38)

$$\tau(z) = \tau_0 \left\{ 1 - \frac{r_0^2 - 1}{r_0^2} \frac{N}{H}(z - z_0) \right\}^{\frac{r_0^2}{r_0^2 - 1}} \tag{45}$$

The condition (9) is only satisfied for

$$r_0^2 < 1 \qquad (\text{i.e.: } 0 < \alpha_0 < \frac{\pi}{4}$$

or for

$$r_0^2 > 1 \qquad (\text{i.e.: } \alpha_0 > \frac{\pi}{4}), \text{ but with the additional}$$

condition

$$z - z_0 \leqslant \frac{r_0^2}{r_0^2 - 1} \frac{H}{N}$$

From (39) it is obtained for the eddy viscosity

$$k_m = f \frac{r_0 \left\{ (r_0^2 - 1)(z - z_0) - \frac{r_0^2 H}{N} \right\}^2}{1 + r_0^2} \tag{46}$$

This eq. (46) shows that for equiangular spirals with $r_0 \neq 1$ the profile of the eddy viscosity is given by a second order curve as this has been shown already by LETTAU and DABERDT (1970). An eddy viscosity coefficient decreasing with height is only obtained in the case $r_0 > 1$, i.e. $\alpha_0 > \frac{\pi}{4}$, but only up to a height $z - z_0 = H/N\, r_0^2 / (r_0^2 - 1)$; above this height the eddy viscosity increases again, which can not be seen from the figures of LETTAU and DABBERDT.

In the variangular case an arbitrary behaviour of $r(z)$ can be assumed and used in the formulae (38) and (39), but very soon difficulties will arise in carrying out the integrations.
As an example it may be given

$$r^2(z) = \frac{1}{1 + \{a_1 + a_2(z - z_0)\} \exp\{a_3(z - z_0)\}} \tag{47}$$

for which at $z = z_0$ $r_0^2 = 1/(1 + a_1)$; r increases with height up to a maximum at $z = z_M$, which is

$$z_M = -\frac{1}{a_3} - \frac{a_1}{a_2}$$

The value at the maximum is

$$r^2(z_M) = \frac{1}{1 - \frac{a_2}{a_3} \exp\left\{-(1 + \frac{a_1 a_3}{a_2})\right\}}$$

The three constants a_1, a_2 and a_3 in eq. (47) are determined by r_0, z_M and $r(z_M)$. Above the maximum $r(z)$ decreases asymptotically to $r(\infty) = 1$, the same value as in the Ekman case.
The corresponding k_m-profile is obtained by eq. (39)

$$k_m = f \frac{\Phi^{3/2}\left[\frac{H}{N} + \frac{a_3}{a_2}(z - z_0)\right]^2}{\left|(1+\Phi)\exp\left\{-2a_3(z-z_0)\right\} - \frac{1}{2}\Phi^2\left[a_1 a_3 + a_2 a_3(z - z_0) + a_2\right]\left[\frac{H}{N} + \frac{a_2}{a_3}(z - z_0)\right]\right|} \tag{48}$$

where Φ is an abbreviation for

$$\Phi = \frac{1}{1 + [a_1 + a_2(z - z_0)] \exp\{a_3(z - z_0)\}}$$

For other $r(z)$ one runs soon into difficulties of carrying out the integrations in eq. (39).

References

HANNA, S. R. (1969): Characteristics of winds and turbulence in the planetary boundary layer
Tech. Mem. ERLTM–ARL 8, 61 pp, January 1969 Oak Ridge, Ten. USA

KAZANSKII, A. B., MONIN, A. S. (1961): On the dynamic interaction between the atmosphere and the earth surface
Bull. (Izv.) Acad. Sci. USSR, Geophys. Ser. (5) 786–788, engl. transl. 514–515

LETTAU, H. H., DABBERDT, W. F. (1970): Variangular wind spirals. Boundary Layer Meteorology 1 (1), 64–79

MONIN, A. S. (1950): Dynamic turbulence in the atmosphere. Bull. (Izv.) Acad. Sci. USSR, 14 (3), 232–254 Geograph. a. Geophysic. Ser.. (russ.)

PRANDTL, L. (1932): Zur turbulenten Strömung in Rohren und längs Platten.
Ergebn. Aerodyn. Versuchsanst. Göttingen 4, 18–29

WIPPERMANN, F. (1970): The two constants in the resistance law for a neutral barotropic boundary layer of the atmosphere
Beitr. Phys. Atm. 43, 133–140

Rossby - Number Similarity

in the Planetary Boundary - Layer

A possibility to realize the existence of Rossby-number similarity in the PBL is given by considering the PBL-equations non-dimensionalized in different ways. For only one set of the equations, namely that one with the correct non - dimensionalization, every thing becomes independent of the external parameters; in this case Rossby-number similarity exists.

Let us start with the PBL-equations given as eqs. (22a) and (22b) on page 13

$$f\{\hat{u} - \hat{u}_g\} = d(\tau_y/\bar{\varrho})/dz \tag{1a}$$

$$-f\{\hat{v} - \hat{v}_g\} = d(\tau_x/\bar{\varrho})/dz \tag{1b}$$

With the flux - gradient relations

$$\tau_x = \bar{\varrho}\, k_m\, d\hat{u}/dz \tag{2a}$$

$$\tau_y = \bar{\varrho}\, k_m\, d\hat{v}/dz \tag{2b}$$

and with the assumption of a thermal wind constant with height

$$\hat{u}_g(z) = \hat{u}_{go} + (d\hat{u}_g/dz)_c\{z - z_o\} \tag{3a}$$

$$\hat{v}_g(z) = \hat{v}_{go} + (d\hat{v}_g/dz)_c\{z - z_o\} \tag{3b}$$

one gets from eqs. (1a) and (1b) by differentiation

$$d^2(\tau_x/\bar{\varrho})/dz^2 + f\,\tau_y/(\bar{\varrho}\, k_m) - f\,(d\hat{v}_g/dz)_c = 0 \tag{4a}$$

$$d^2(\tau_y/\bar{\varrho})/dz^2 - f\,\tau_x/(\bar{\varrho}\, k_m) + f\,(d\hat{u}_g/dz)_c = 0 \tag{4b}$$

It is not yet decided how the coordinate system should be orientated; this will be done together with the nondimensionalization.

Let us consider the following two ways to non-dimensionalize the eqs. (4a) and (4b): the first way (I) by using i n - t e r n a l parameters, the second way (II) by e x t e r - n a l ones:

I	II
The velocity for the non-dimensionalization is	
u_*	$\lvert\hat{\mathbb{v}}_{go}\rvert$
the friction velocity	the geostrophic wind speed at the ground

The ratio of these two velocities $C_g = u_*/\lvert\hat{\mathbb{v}}_{go}\rvert$ is called the geostrophic drag coefficient.

The length for non-dimensionalization is formed with these velocities

$H = \kappa u_*/f$	$D = \kappa^5\lvert\hat{\mathbb{v}}_{go}\rvert/f$	(5)
the internal scale height of the PBL	the external scale height of the PBL	

The variables are non-dimensionalized in the following manner (the index n indicated the way II):

$Z = z/H$	$Z_n = z/D$	(6)
$K_m = k_m/(H^2 f)$	$K_{mn} = k_m/(D^2 f)$	(7)
$U = \kappa\hat{u}/u_*$	$U_n = \hat{u}/\lvert\hat{\mathbb{v}}_{go}\rvert$	(8a)
$V = \kappa\hat{v}/u_*$	$V_n = \hat{v}/\lvert\hat{\mathbb{v}}_{go}\rvert$	(8b)
$X = \tau_x/(\bar{\varrho}\, u_*^2)$	$X_n = \tau_x/(\bar{\varrho}\kappa^8\lvert\hat{\mathbb{v}}_{go}\rvert^2)$	(9a)
$Y = \tau_y/(\bar{\varrho}\, u_*^2)$	$Y_n = \tau_y/(\bar{\varrho}\kappa^8\lvert\hat{\mathbb{v}}_{go}\rvert^2)$	(9b)

Multiplying the equations (4a) and (4b) by the factor $(\kappa/f)^2$ one obtains

either	or
$\frac{d^2X}{dZ^2} + \frac{Y}{K_m} - \left\{\frac{dV_g}{dZ}\right\}_c = 0$	$\frac{d^2X_n}{dZ_n^2} + \frac{Y_n}{K_{mn}} - \left\{\frac{dV_{gn}}{dZ_n}\right\}_c = 0$ (10a)
$\frac{d^2Y}{dZ^2} - \frac{X}{K_m} + \left\{\frac{dU_g}{dZ}\right\}_c = 0$	$\frac{d^2Y_n}{dZ_n^2} - \frac{X_n}{K_{mn}} + \left\{\frac{dU_{gn}}{dZ_n}\right\}_c = 0$ (10b)

Now the orientation of the coordinate system should be fixed. In the case I the x-axis should have the direction of the surface stress τ_o , in the case II this axis should be directed along the surface geostrophic wind $\hat{\mathbb{v}}_{go}$.

$X_o = 1$	$X_{no} = \frac{u_*^2}{\kappa^8 \lvert\hat{\mathbb{v}}_{go}\rvert} \cos(\alpha_o) = \frac{C_g^2}{\kappa^8} \cos(\alpha_o)$ (11a)
$Y_o = 0$	$Y_{no} = \frac{u_*^2}{\kappa^8 \lvert\hat{\mathbb{v}}_{go}\rvert} \sin(\lvert\alpha_o\rvert) = \frac{C_g^2}{\kappa^8} \sin(\lvert\alpha_o\rvert)$ (11b)
$U_{go} = \kappa \frac{\lvert\hat{\mathbb{v}}_{go}\rvert}{u_*} \cos(\alpha_o) = \frac{\kappa}{C_g} \cos(\alpha_o)$	$U_{gno} = 1$ (11c)
$V_{go} = \kappa \frac{\lvert\hat{\mathbb{v}}_{go}\rvert}{u_*} \sin(\alpha_o) = -\frac{\kappa}{C_g} \sin(\lvert\alpha_o\rvert)$	$V_{gno} = 0$ (11d)

Also the components of the vector of baroclinicity are formed in both cases (I and II):

$$\frac{dU_g}{dZ} = \frac{\kappa^2}{f}\,\tau_o^\circ \cdot \left\{\frac{d\hat{v}_g}{dz}\right\}_c = \lambda_x \qquad \left\{\frac{dU_g}{dZ}\right\}_n = \frac{\kappa^2}{f}\,\hat{v}_{g\circ}^\circ \cdot \left\{\frac{d\hat{v}_g}{dz}\right\}_c = \eta_x \tag{11e}$$

$$\frac{dV_g}{dZ} = \frac{\kappa^2}{f}\,\mathbb{k}\cdot\left[\tau_o^\circ \times \left\{\frac{d\hat{v}_g}{dz}\right\}_c\right] = \lambda_y \qquad \left\{\frac{dV_g}{dZ}\right\}_n = \frac{\kappa^2}{f}\,\mathbb{k}\cdot\left[\hat{v}_{g\circ}^\circ \times \left\{\frac{d\hat{v}_g}{dz}\right\}_c\right] = \eta_y \tag{11f}$$

Whereas the equations (10a) and (10b) do not differ with regard to the orientation of the coordinate system the lower boundary conditions in both cases will be completely different. The boundary conditions are

$$\left.\begin{array}{l} z \longrightarrow z_T \\ (\text{or } z \longrightarrow \infty) \end{array}\right\} : \quad \hat{u} \longrightarrow (\hat{u}_g)_T\,, \quad \hat{v} \longrightarrow (\hat{v}_g)_T \tag{12a}$$

$$\tau_x \longrightarrow \bar{\varrho}\, k_{m\infty}\, (d\hat{u}_g/dz)_c$$

$$\tau_y \longrightarrow \bar{\varrho}\, k_{m\infty}\, (d\hat{v}_g/dz)_c \tag{12b}$$

$$k_m \longrightarrow k_{m\infty} = l_\infty^2\, |d\,\hat{v}_g/dz| \tag{12c}$$

$$z = z_o : \quad \hat{u} = \hat{v} = 0 \tag{13a}$$

$$\tau_x = \tau_{xo}\,, \quad \tau_y = \tau_{yo} \tag{13b}$$

$$\sqrt{(\tau_{xo})^2 + (\tau_{yo})^2} = \bar{\varrho}\, u_*^2$$

$$k_m = k_{mo} = \kappa\, u_* z_o \tag{13c}$$

In the condition (12c) l_∞ is the asymptotic mixing-length; in the barotropic case conditions (12b) and (12c) become

$$\tau_x \longrightarrow 0\,, \quad \tau_y \longrightarrow 0\,, \quad k_m \longrightarrow 0\,, \quad l \longrightarrow l_\infty$$

In non-dimensional form the boundary conditions are

$Z \longrightarrow Z_T$:
$\longrightarrow \infty$

$$U \longrightarrow (U_g)_T$$

$$V \longrightarrow (V_g)_T$$

$$X \longrightarrow K_{m\infty}\,\lambda_x$$

$$Y \longrightarrow K_{m\infty}\,\lambda_y$$

$$K_m \longrightarrow K_{m\infty} = \frac{L_\infty^2}{\kappa^2}\sqrt{\lambda_x^2+\lambda_y^2}$$

$Z = Z_o$:

$$U = U_o = 0$$

$$V = V_o = 0$$

$$X = X_o = 1$$

$$Y = Y_o = 0$$

$$K_m = K_{mo} = Z_o$$

$Z_n \longrightarrow Z_{nT}$:
$\longrightarrow \infty$

$$\left.\begin{aligned} U_n &\longrightarrow (U_{gn})_T \\ V_n &\longrightarrow (V_{gn})_T \end{aligned}\right\} \quad (14a)$$

$$\left.\begin{aligned} X_n &\longrightarrow K_{mn\infty}\,\eta_{x^*} \\ Y_n &\longrightarrow K_{mn\infty}\,\eta_{y^*} \end{aligned}\right\} \quad (14b)$$

$$\left.\begin{aligned} K_{mn} &\longrightarrow K_{mn\infty} = \\ &= \frac{L_{n\infty}^2}{\kappa^2}\sqrt{\eta_{x^*}^2+\eta_{y^*}^2} \end{aligned}\right\} \quad (14c)$$

$Z_n = Z_{no}$:

$$\left.\begin{aligned} U_n &= U_{no} = 0 \\ V_n &= V_{no} = 0 \end{aligned}\right\} \quad (15a)$$

$$\left.\begin{aligned} X_n &= X_{no} = \\ &= \frac{C_g^2}{\kappa^6}\cos(\alpha_o) \\ Y_n &= Y_{no} = \\ &= \frac{C_g^2}{\kappa^6}\sin(|\alpha_o|) \end{aligned}\right\} \quad (15b)$$

$$K_{mn} = K_{mno} = Z_{no}\frac{C_g}{\kappa^4} \quad (15c)$$

The boundary conditions (15b) and (15c) for II contain the geostrophic drag coefficient $C_g = u_*/|\hat{v}_{go}|$, which is not yet known but should be obtained by solving the set of the eqs. (10a) and (10b), after a closure. In order to avoid the appearance of C_g in the boundary conditions the first derivatives $(dX_n/dZ_n)_o$ and $(dY_n/dZ_n)_o$ can be used instead of

the values X_{no} and Y_{no} itself. The eqs. (1a) and (1b) together with the condition (13a) give

$$\{d(\tau_y/\bar{\varrho})/dz\}_o = - f\,\hat{u}_{go} \tag{16a}$$

$$\{d(\tau_x/\bar{\varrho})/dz\}_o = f\,\hat{v}_{go} \tag{16b}$$

This is in non-dimensional form (type II) :

$$(dY_n/dZ_n)_o = - U_{go}/\kappa^3 = -\kappa^{-3} \tag{17a}$$

$$(dX_n/dZ_n)_o = V_{go}/\kappa^3 = 0 \tag{17b}$$

In a similar way the condition (15c) for I and II can be changed into

$$(dK_m/dZ)_o = 1 \qquad \Big| \qquad (dK_{mn}/dZ_n)_o = C_g/\kappa^4 \quad \begin{matrix}(18a)\\(18b)\end{matrix}$$

In order to close the system of equations first one can use the flux - gradient relations (2a),(2b)

$$X = K_m\, dU/dZ \qquad \Big| \qquad X_n = \frac{1}{\kappa^3} K_{mn}\, dU_n/dZ_n \tag{19a}$$

$$Y = K_m\, dV/dZ \qquad \Big| \qquad Y_n = \frac{1}{\kappa^3} K_{mn}\, dV_n/dZ_n \tag{19b}$$

If one combines these (i.e. 2a, 2b or 19a, 19b) with Prandtl's mixing-length relation (l = mixing-length)

$$k_m = l^2\, |d\,\hat{\mathbb{V}}/dz| \tag{20}$$

or in non-dimensional notation

$$K_m = \frac{L^2}{\kappa^2}\, |d\,\mathbb{V}/dZ| \qquad \Big| \qquad K_{mn} = \frac{L_n^{\,2}}{\kappa^5}\, |d\,\mathbb{V}_n/dZ_n| \tag{21}$$

one obtains

$$k_m = l\,(\tau/\bar{\varrho})^{1/2} \tag{22}$$

or in the non-dimensional notation

$$K_m = \frac{L}{\varkappa}\{X^2 + Y^2\}^{1/4} \quad \Big| \quad K_{mn} = \frac{L_n}{\varkappa}\{X_n^{\ 2} + Y_n^{\ 2}\}^{1/4} \qquad (23)$$

For the four variables $\tau_x(z)$, $\tau_y(z)$, $k_m(z)$ and $l(z)$ one has only three equations, namely (4a) , (4b) and (22). For the missing fourth equation a hypothesis has to be made, which must contain the mixing-length

$$l = l(z, l_\infty) \quad \text{or} \quad l = l(\tau, l_\infty) \qquad (24)$$

or in non-dimensional form

$$\begin{array}{lll|lll} L = L(Z, L_\infty) & \text{or} & & L_n = L_n(Z_n, L_{n\infty}) & \text{or} & \\ L = L(X, Y, L_\infty) & & & L_n = L_n(X_n, Y_n, L_{n\infty}) & & \end{array} \qquad (25)$$

Finally one has a set of equations and boundary conditions, which are non-dimensionalized in two different ways. These are presented in the two tables on the following page.

The set of eqs. (26)-(29) depends on three parameters only, namely the internal parameters L_∞ , λ_x , λ_y in the system I or the external parameters $L_{n\infty}$, η_{x*} , η_{y*} in the system II (where $L_{n\infty}$, of course, is not a pure external parameter since it implies the regard of internal parameters, such as u_* and ϑ_* , too).
L_∞ (in the system I) is the asymptotic mixing-length and at the same time the parameter governing the thermal stratification, which otherwise is described by the parameter $\mu = H/L_*$ the ratio of the internal scale height H of the PBL to the Monin-Obukhov stability length. For a relationship between L_∞ and μ see page 183. In the system II the stratification parameter is $L_{n\infty}$.
λ_x and λ_y in the system I are the internal parameters for the baroclinicity, η_{x*} and η_{y*} in system II are the external parameters for the baroclinicity.

The same as for the eqs. (26)-(29) is true for the upper boundary conditions (30a)-(30d).

$\frac{d^2X}{dZ^2} + \frac{Y}{K_m} - \lambda_x = 0$	$\frac{d^2X_n}{dZ_n^2} + \frac{Y_n}{K_{mn}} - \eta_{x*} = 0$	(26)
$\frac{d^2Y}{dZ^2} - \frac{X}{K_m} + \lambda_y = 0$	$\frac{d^2Y_n}{dZ_n^2} - \frac{X_n}{K_{mn}} + \eta_{y*} = 0$	(27)
$K_m = \frac{L}{\varkappa}\{X^2 + Y^2\}^{1/4}$	$K_{mn} = \frac{L_n}{\varkappa}\{X_n^2 + Y_n^2\}^{1/4}$	(28)
$L = L(Z, L_\infty)$ or $L = L(X, Y, L_\infty)$	$L_n = L_n(Z_n, L_{n\infty})$ or $L_n = L_n(X_n, Y_n, L_{n\infty})$	(29)
$Z \longrightarrow \infty$:	$Z_n \longrightarrow \infty$:	
$X \longrightarrow K_{m\infty}\,\lambda_x$	$X_n \longrightarrow K_{mn\infty}\,\eta_{x*}$	(30a)
$Y \longrightarrow K_{m\infty}\,\lambda_y$	$Y_n \longrightarrow K_{mn\infty}\,\eta_{y*}$	(30b)
$K_m \longrightarrow K_{m\infty} = \frac{L_\infty^2}{\varkappa^2}\{\lambda_x^2 + \lambda_y^2\}^{1/2}$	$K_{mn} \longrightarrow K_{mn\infty} = \frac{L_{n\infty}^2}{\varkappa^2}\{\eta_{x*}^2 + \eta_{y*}^2\}^{1/2}$	(30c)
$L \longrightarrow L_\infty$	$L_n \longrightarrow L_{n\infty}$	(30d)
$Z = Z_o$:	$Z_n = Z_{no}$:	
$X = X_o = 1$	$X_n = X_{no} = \frac{C_q^2}{\varkappa^8}\cos(\alpha_o)$	(31a)
$Y = Y_o = 0$	$Y_n = Y_{no} = \frac{C_q^2}{\varkappa^8}\sin(\lvert\alpha_o\rvert)$	(31b)
$K_m = K_{mo} = Z_o$	$K_{mn} = K_{mno} = Z_{no}\frac{C_q}{\varkappa^4}$	(31c)
$L = L_o = \varkappa Z_o$	$L_n = L_{no} = \varkappa Z_{no}$	(31d)

For the upper boundary conditions (30a)-(30d) see the last phrase on page 58 .

Considering the lower boundary one notices that in the system I only two conditions, (31c) and (31d), depend on a parameter. This is the parameter Z_o, the non-dimensional roughness-length, which contains internal as well as external parameters; by the several definitions made in the beginning

$$Z_o = (\varkappa C_g RO_o)^{-1} \tag{32}$$

(whereas $Z_{no} = \varkappa^{-5} RO_o^{-1}$) with

$$RO_o = |\hat{v}_{go}|/(f z_o) \tag{33}$$

the surface Rossby-number, a non-dimensional combination of the external parameters $|\hat{v}_{go}|$, f and z_o. However the dependence of K_m and L on Z_o (i.e. on the external parameters) exists only at the lower boundary and in its neighbourhood, it is not relevant at larger heights $Z >> Z_o$. This can be seen for instance by comparing the maximal values of K_m and L with those at $Z = Z_o$; $K_{m'max}$ ranges from about $5 \cdot 10^{-3}$ for a very stable stratification to $2 \cdot 10^{-1}$ in a very unstable one. The roughness-length z_o varies between $1 \cdot 10^{-2}$ cm and $1 \cdot 10^{1}$ cm, which means roughly, that

$$1 \cdot 10^{-7} < Z_o = K_{mo} < 1 \cdot 10^{-4}$$

Therefore

$$2 \cdot 10^{-2} > K_{mo}/K_{m'max} > 5 \cdot 10^{-7}$$

and a similar range for L_o/L_{max} (but the values multiplied by the factor 0.4) . From this it can be concluded, that in the system I the boundary conditions (31c) and (31d) do not affect the profiles $K_m(Z)$ and $L(Z)$ for $Z >> Z_o$ and therefore neither the profiles $X(Z)$ and $Y(Z)$. The profiles would be completely unaffected by the boundary conditions, if

$$Z_o \longrightarrow 0 \text{ , i.e. if } \qquad RO_o \longrightarrow \infty \tag{34}$$

In this case in the system I the equations as well as the boundary conditions would be completely independent of any external parameter; this is called (Surface-) Rossby Number Similarity. It means that the profiles $X(Z)$, $Y(Z)$, $K_m(Z)$ and $L(Z)$ are u n i v e r s a l , they are valid (if non-dimensionalized correctly, i.e. like the system I) for arbitrary external parameters and depend only on three internal parameters, namely L_∞ (or μ) for the thermal stratification, λ_x and λ_y for the baroclinicity.

As mentioned before such a Rossby-number similarity exists in a PBL only for $Z \gg Z_o$, the neighbourhood of Z_o must be excluded. This happens not only with respect to the lower boundary conditions (31c) and (31d) but also with respect to the fact, that the position itself of the lower boundary depends on the external parameters. (In this sense the boundary conditions 31a and 31b are also dependent on external parameters).

WIPPERMANN and YORDANOV (1972) have investigated the height Z_R above which Rossby-number similarity is given; their result was

$$Z_R \approx 10 \cdot Z_o \tag{35}$$

One notices that the range to be excluded is very small.

All these considerations imply that the mixing-length hypothesis (29), which has to be made in order to close the set of equations, is independent of the external parameters.

The situation for the system II is completely different. Here the equations (26) - (29) depend on two external parameters (η_{x*}, η_{y*}) for the baroclinicity and on the stratification parameter $L_{n\infty}$, which contains internal as well as external parameters. The same is true for the upper boundary. Also the lower boundary conditions (31a) - (31c) con-

tain external parameters as well as internal ones; the appearing geostrophic drag coefficient is the ratio of the internal velocity u_* to the external velocity $|\hat{v}_{go}|$. This dependence is less important in the condition (31c), because the same argument as in the system I (conditions 31c and 31d) is valid for Z_{no}. In the conditions (31a) and (31b) C_g does not longer appear when the form (17a),(17b) is used. This, however, does not remove the difficulties: instead of the values X_{no} and Y_{no} the derivatives $(dX_n/dZ_n)_o$ and $(dY_n/dZ_n)_o$ are now prescribed; nevertheless the values X_{no} and Y_{no}, which will adjust in a solution, clearly continue to depend on C_g.

Apparently the system II is unable to give universal profiles, these can be obtained only in the system I, i.e. if all variables are non-dimensionalized by internal parameters. Any other kind of non-dimensionalization would have the same defect as the system II.

As shown Rossby-number similarity exists for the profiles

$$X(Z) \quad , \quad Y(Z) \quad , \quad K_m(Z) \quad , \quad L(Z) \quad .$$

There are, of course, more variables having universal profiles; they can be obtained by the four profiles mentioned before. For instance the eqs. (19a) and (19b) of the system I tell, that also the profiles

$$\frac{dU}{dZ}(Z) \quad \text{and} \quad \frac{dV}{dZ}(Z)$$

must be universal; one should notice that this is valid for the wind shear only and not for the velocities itself. (An integration of the universal shear profile in order to get a velocity profile has to be carried out starting at the lower boundary which depends on external parameters; by this the universality will be lost).
However the velocity-defect has a universal profile. Eqs.

(1a) and (1b) are in the non-dimensional form of the system I :

$$P = dY/dZ \tag{36a}$$

$$Q = - dX/dZ \tag{36b}$$

where $P = \kappa(\hat{u}-\hat{u}_g)/u_*$ and $Q = \kappa(\hat{v}-\hat{v}_g)/u_*$ are the components of the velocity defect. According to the eqs. (36a), (36b) $P(Z)$ and $Q(Z)$ must be universal profiles, since the right-hand sides of these two equations are also universal.

Rossby-number similarity exists for more variables, for instance also for the non-dimensional dissipation rate of the turbulent kinetic energy, for the non-dimensional vertical temperature gradient, for the non-dimensional vertical moisture gradient and for others. Probably the Rossby-number similarity exists also for the spectral density functions of several turbulence characteristics in the boundary layer. Of course, in each case the non-dimensionalization has to be done by correctly chosen internal parameters.

A similarity hypothesis of this kind has been applied for the first time by MONIN and OBUKHOV (1954) in order to obtain the profiles in the surface layer. Since then this similarity principle has often been used in the surface layer, sometimes it is named the "auto-model hypothesis". LETTAU (1962) was the first to show the existence of such a similarity in the whole boundary layer, he computed universal profiles. (He also named in 1959 the non-dimensional combination of the external parameters the Surface Rossby-Number). Since then numerous authors have been concerned with the Rossby-number similarity in the planetary boundary layer.

The eqs. (26) - (29) together with the boundary conditions (30a) - (30d), (31a) - (31d) show clearly that such a similarity must exist for $Z >> Z_o$ and that it would be complete, if the surface Rossby-number tends to infinity.

References

LETTAU, H.H. 1959 Wind Profile, Surface Stress and Geostrophic Drag Coefficient in the Atmospheric Surface Layer
Adv. in Geophys. 6, 241-257

LETTAU, H.H. 1962 Theoretical Wind Spirals in the Boundary Layer of a Barotropic Atmosphere
Beitr. Phys. Atm. 35, 195-212

MONIN, A.S.
OBUKHOV, A.M. 1954 Fundamental Laws of the Turbulent Exchange in the Surface Layer of the Atmosphere (in Russ.)
Rep. (Trudy) Geophys. Inst. Acad. Sci. USSR, Nr. 24 (151), 163-187
Germ. Transl. in "Sammelband zur Statistischen Theorie der Turbulenz", Akademie-Verlag Berlin 1958 199-224

WIPPERMANN, F.
YORDANOV, D. 1972 A Note on the Rossby Similarity for Flows of Barotropic Planetary Boundary Layers
Beitr. Phys. Atm. 45, 66-71

A Note on the Rossby Similarity for Flows of Barotropic Planetary Boundary Layers

Kurze Mitteilung zur Frage der Rossby-Ähnlichkeit von Strömungen barotroper planetarischer Grenzschichten

F. Wippermann and D. Yordanov*)

Technical University, Darmstadt, Germany, Department of Meteorology

With 1 figure
Received September 2, 1971

Summary: It is investigated for which nondimensional quantities Rossby similarity can be obtained and in which range of the height it does exist.

Zusammenfassung: Es wird untersucht, für welche dimensionslosen Größen und in welchem Höhenbereich Rossby-Ähnlichkeit auftreten kann.

Résumé: On recherche pour quelles grandeurs non-dimensionnelles et dans quelle gamme de hauteur la similitude de Rossby peut se présenter.

In recent years several authors (KAZANSKII and MONIN 1961, GILL 1967, MONIN and ZILITINKEVICH 1967, BLACKADAR and TENNEKES 1968) derived the resistance law for a barotropic planetary boundary layer (PBL) by making use of the so-called Rossby similarity (or Rossby-number similarity), sometimes called the auto-model hypothesis. In this note an investigation shall be reported on the limitations of this Rossby similarity.

The equations for the barotropic PBL may be written in a nondimensional notation

$$X = K_m d^2Y/dZ^2 \tag{1a}$$

$$Y = -K_m d^2X/dZ^2 \tag{1b}$$

$$K_m = (X^2+Y^2)^{1/4}L/\kappa \tag{1c}$$

$$L = f(X,Y,L_0,L_\infty); \quad L_0 = \kappa Z_0; \quad \partial L_\infty/\partial(Ro_0) = 0 \tag{1d}$$

with the boundary conditions

$$Z = Z_0: \; X = 1, \quad Y = 0, \quad L = L_0 \tag{2a}$$

$$Z \to \infty: \; X \to 0, \quad Y \to 0, \quad L \to L_\infty \tag{2b}$$

Herein are $X \equiv \tau_x/\tau_0$ and $Y \equiv \tau_y/\tau_0$ the components of the Reynolds stress made dimensionless by the value of the stress $\tau_0 = \bar{\rho} u_*^2$ at the ground, with u_* the friction velocity. The boundary condition (2a) shows that the coordinate system is orientated with the x-axis in the direction of the stress at the ground.

*) On leave from the Bulgarean Academy of Science, Department of Geophysics, Sofia, on a fellowship by the A. v. Humboldt-Foundation

$K_m \equiv k_m/(H^2 f)$ is the nondimensional eddy viscosity, $H = \kappa u_*/f$ is the scale height of the PBL with κ the Karman constant and f the Coriolis parameter. $Z = z/H$ is the nondimensional height coordinate and $Z_0 = z_0/H$ the nondimensional roughness length; with the aid of the definitions above one has

$$Z_0 = (\kappa C_d Ro_0)^{-1} \tag{3}$$

where $C_d = u_*/|\hat{v}_g|$ is the geostrophic drag coefficient with $|\hat{v}_g|$ the geostrophic wind speed and $Ro_0 = |\hat{v}_g|/(z_0 f)$ is the surface Rossby number. $L = l/H$ is the nondimensional mixing-length.

It is important to state, that all quantities are made dimensionless by internal parameters; the classification of internal and external parameters will be discussed later.

The eqs. (1a) and (1b) are the PBL equations combined with the flux-gradient relations, eq. (1c) is Prandtl's mixing-length equation $k_m = l^2 |d\hat{v}/dz|$ also combined with the flux-gradient relation and finally eq. (1d) stands for any mixing-length hypothesis which has to be made in order to close the system of the equations. Such a mixing-length hypothesis may be made by giving the direct dependency of L on Z (as for instance done by LETTAU 1962, BLACKADAR 1962 or APPLEBY and OHMSTEDE 1964) or by giving a relationship between L and certain flow parameters, for instance X and Y (WIPPERMANN 1972a). The mixing-length hypothesis should satisfy the condition $\partial L_\infty/\partial(Ro_0) = 0$, which is a physically reasonable condition.

One notices from eq. (3) that Z_0 depends on Ro_0. If Z_0 would be zero the eqs. (1a) - (1d) and the boundary conditions (2a), (2b) would be independent of Ro_0, i. e. in this case the profiles X(Z), Y(Z), K_m (Z) and L(Z) must be independent of Ro_0; this is called Rossby similarity. However in a PBL the Rossby number remains finite since the roughness length z_0 is different from zero although it is very small compared with the scale height of the PBL

$$Z_0 \ll 1 \tag{4}$$

That means that for different values of Z_0 the boundary condition (2a) has to be satisfied at different heights which of course are very close together compared with the scale height H of the PBL. From that it can be concluded, that Rossby similarity is not existent in the very lowest layer, the depth of which is in the order of the possible roughness length z_0.

In order to demonstrate this the eqs. (1a) - (1d) have been integrated with the boundary conditions (2a), (2b) for varying surface Rossby numbers, i. e. for varying Z_0. As the mixing-length hypothesis (1d) that one by WIPPERMANN (1972a)

$$L = L_\infty - (L_\infty - L_0)\ (X^2 + Y^2)^{q/2} \tag{5}$$

$$q = -\frac{\kappa - L_0\ \{(dX/dZ)_0^2 + (dX/dZ)_0/2\}}{(dX/dZ)_0\ \{L_\infty - L_0\}}$$

(with L = 0.015 for neutral stratification) has been used; the integration method is described in an other paper, WIPPERMANN (1972b). Figure 1 shows the results: the solid curves give the vertical profiles of the nondimensional Reynolds stress, in the figure shown as the deviation from the value at Z_0, i. e. as $1 - (X^2 + Y^2)^{1/2}$. These profiles have been computed for different values of Z_0 namely for $1 \cdot 10^{-2}$, $1 \cdot 10^{-3}$, $1 \cdot 10^{-4}$, $1 \cdot 10^{-5}$, $1 \cdot 10^{-6}$ and $1 \cdot 10^{-7}$. All profiles coincide in the upper part (which means that Rossby similarity exists here), they are splitted in the lower part where Rossby similarity is not existent. The figure 1 shows that the height Z_R above which the Rossby similarity exists is roughly

$$Z_R \approx 10 \cdot Z_{0,\,max} \tag{6}$$

where $Z_{0,\,max}$ is the largest possible value of the nondimensional roughness length. The largest value used in the computations, $Z_0 = 1 \cdot 10^{-2}$, is a very large roughness length corresponding roughly to $z_0 \approx 10$ m,

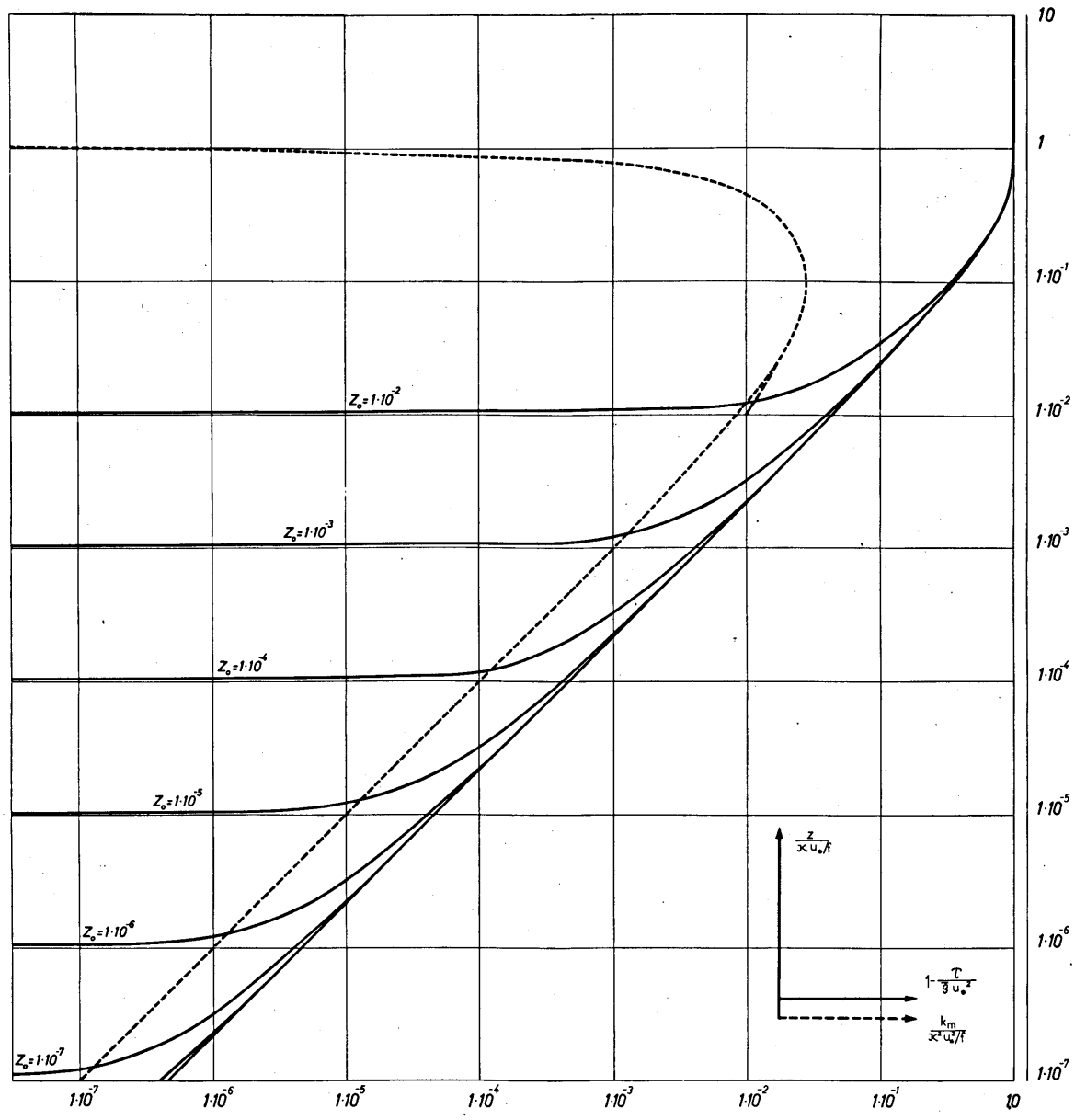

Fig. 1. Vertical profiles of the nondimensional Reynolds' stress (solid) and the nondimensional eddy viscosity (broken) for various values of the nondimensional roughness length Z_0 in the case of neutral stratification

Bild 1. Vertikalprofile der dimensionslosen Reynolds'schen Schubspannung (ausgezogen) und des turbulenten Diffusionskoeffizienten (gestrichelt) bei unterschiedlichen Werten der dimensionslosen Rauhigkeitslänge Z_0 im Falle neutraler Schichtung

it will not be found in usual cases. For $Z_0 = 1 \cdot 10^{-3}$, still a large roughness length ($z_0 \approx 1$ m for H = 1 km), Rossby similarity would exist above $Z_R \approx 1 \cdot 10^{-2}$ (roughly above 10 m). In this sense the condition (6) gives the advise that data measured in the Prandtl-layer are useful for similarity considerations only when

measured at a height larger than 10 times z_0. (Of course, a correct Prandtl-layer with $dX/dZ = 0$, $Y = 0$ does not exist; if one calls as "Prandtl-layer" the lowest layer, in which the stress $(X^2 + Y^2)^{1/2}$ decreases for only 10 %, 15 % or 20 %, the height Z_p of such a "Prandtl-layer" can be read from the figure 1 being $Z_p = 0.024$, 0.037 or 0.050.)

The broken curves represent the vertical profiles of the nondimensional eddy viscosity K_m for the six different values of Z_0 mentioned before. One notices that all profiles coincide completely except that one for $Z_0 = 1 \cdot 10^{-2}$. That is different from the profiles X(Z) and Y(Z) which are splitted in the lowest layer, it can be explained by the mixing-length hypothesis (1d) in which $L_0 = \kappa Z_0$ together with eq. (1c) requires that

$$K_{m0} = Z_0 \tag{7}$$

which is Prandtl's hypothesis $k_m = \kappa u_* z$ for $z = z_0$. This hypothesized relation (7) causes the complete coincidation of the various K_m-profiles in the lowest part.

The maximum value of K_m is $2.77\ 10^{-2}$, it will be found at $Z = 0.10$.

According to eq. (6) the height range, in which Rossby similarity exists, reaches as farer down as smaller Z_0 is, or – with respect to eq. (3) – as larger the surface Rossby number is. Complete Rossby similarity would to be expected for $Ro_0 \to \infty$; however there is a lower limit for Z_0 (or an upper limit for Ro_0) too. Since $K_m = k_m f/(\kappa^2 u_*^2)$ cannot be smaller than $\nu f/(\kappa^2 u_*^2)$ where $\nu \approx 0.13$ cm^2 sec^{-1} is the kinematic viscosity of the air, it follows from eq. (7)

$$Z_{0,\,min} = \nu f/(\kappa^2 u_*^2) \quad \text{or} \quad z_{0,\,min} = \nu/(\kappa u_*) \tag{8}$$

One sees that $z_{0,\,min}$ is also a measure for the depth of the viscous sublayer. For assumed smallest and largest values of u_* being 10 cm sec^{-1} and 50 cm sec^{-1} one gets for $z_{0,\,min} = 3.2\ 10^{-2}$ cm or $6.4\ 10^{-3}$ cm respectively. A reasonable mean value would be $z_{0,\,min} \approx 1 \cdot 10^{-2}$ cm which corresponds to $Z_{0,\,min} = 1 \cdot 10^{-7}$ (for H = 1 km). That corresponds (for neutral and barotropic conditions) to $(Ro_0)_{max} = 1 \cdot 10^{-9}$, see WIPPERMANN (1972a) table 3.

For the time being it has been shown that Rossby similarity exists for the profiles X(Z) and Y(Z) as long as $Z \geqslant Z_R$ and for the profiles $K_m(Z)$ and L(Z) for any height Z, when the condition $\partial L_\infty/\partial(Ro_0) = 0$ is satisfied. Rossby similarity cannot be used for the nondimensional components of the velocity but it exists for the nondimensional components of the wind shear. That can be understood from the flux – gradient relations in nondimensional notation

$$X = K_m dU/dZ \tag{9a}$$

$$Y = K_m dV/dZ \tag{9b}$$

where $U = \kappa \hat{u}/u_*$ and $V = \kappa \hat{v}/u_*$. Rossby similarity for X and Y as well as for K_m requires that for dU/dZ and dV/dZ too. The so-called auto-model hypothesis states that the dimensionless vertical differences of the velocity components

$$\kappa(\hat{u}_2 - \hat{u}_1)/u_*, \quad \kappa(\hat{v}_2 - \hat{v}_1)/u_* \tag{10}$$

are independent of the surface Rossby number, i. e. for this velocity differences exists Rossby similarity. (The heights z_2 and z_1 have to be made dimensionless by the scale height H.)

This auto-model hypothesis means nothing else than that Rossby similarity exists for the nondimensional shear components dU/dZ and dV/dZ. It has been applied for the first time by MONIN and OBUKHOV (1954) in order to compute the profiles in the surface layer; lateron the application has been extended to a barotropic PBL by KAZANSKII and MONIN (1960).

If the height Z_1 is chosen at the upper border of the PBL the velocity components there become the geostrophic ones, $\hat{u}_1 \to \hat{u}_g$, $\hat{v}_1 \to \hat{v}_g$. That means according to the expressions (10), that the nondimensional velocity defects

$$P = \kappa(\hat{u} - \hat{u}_g)/u_*, \quad Q = \kappa(\hat{v} - \hat{v}_g)/u_* \tag{11}$$

are subjected to Rossby similarity too.

Likewise Rossby similarity exists for the nondimensional vertical gradient of the potential temperature $d\Theta/dZ = d(\hat{\vartheta}/\vartheta_*)/d(z/H)$ with $\vartheta_* = -q_0/(\kappa c_p \bar{\rho} u_*)$; q_0 is the turbulent vertical heat flux being constant with height in a PBL. The existence of Rossby similarity for $d\Theta/dZ$ can be shown in a quite analogous way as for the velocity gradients. Because of $dq_0/dz = 0$ the thermal equation corresponding to the eqs. (9a), (9b) is

$$a_h K_m \, d\Theta/dZ = 1 \tag{12}$$

where $a_h = K_h/K_m$. It can be assumed that $a_h(Z)$ is independent of Z_0 and therefore independent of Ro_0; it can be concluded from eq. (12) that Rossby similarity must exist for $d\Theta/dZ$ as long as $Z \geqslant Z_R$. Completely the same conclusion can be drawn for the Rossby similarity of the nondimensional vertical gradient dS/dZ of the moisture $\hat{s}$; it is $S \equiv \hat{s}/s_*$ with $s_* = -j_0/(\kappa \bar{\rho} u_*)$ where j_0 is the turbulent vertical flow of moisture being constant with height in a PBL.

The nondimensional dissipation rate of kinetic energy $\mathcal{E} \equiv \epsilon\kappa^2/(u_*^2 f)$ is

$$\mathcal{E} = c K_m^3 L^{-4} \tag{13}$$

and must therefore also be subjected to Rossby similarity.

In the following table all quantities are listed for which Rossby similarity exists in a PBL:

$X = \tau_x/\bar{\rho} u_*^2$	$Y = \tau_y/\bar{\rho} u_*^2$
$L = l/(\kappa u_*/f)$	$K_m = k_m/(\kappa^2 u_*^2/f)$
$K_h = k_h/(\kappa^2 u_*^2/f)$	$K_s = k_s/(\kappa^2 u_*^2/f)$
$dU/dZ = \kappa^2/f \, d\hat{u}/dz$	$\kappa(\hat{u}_2 - \hat{u}_1)/u_*$
$dV/dZ = \kappa^2/f \, d\hat{v}/dz$	$\kappa(\hat{v}_2 - \hat{v}_1)/u_*$
$P \equiv \kappa(\hat{u} - \hat{u}_g)/u_*$	$Q \equiv \kappa(\hat{v} - \hat{v}_g)/u_*$
$d\Theta/dZ = \kappa u_*/(f\vartheta_*) \, d\hat{\vartheta}/dz$	$(\hat{\vartheta}_2 - \hat{\vartheta}_1)/\vartheta_*$
$dS/dZ = \kappa u_*/(f s_*) \, d\hat{s}/dz$	$(\hat{s}_2 - \hat{s}_1)/s_*$
$\mathcal{E} = \epsilon\kappa^2/(u_*^2 f)$	

It should be stated once more, that the eqs. (1a) - (1d) and the boundary conditions (2a), (2b) are independent of Ro_0 only if all quantities are made dimensionless by so-called internal parameters, i. e. only in that case Rossby similarity can be obtained for X(Z) and Y(Z) and the other quantities listed above. For instance if the quantities are made dimensionless by the velocity $|\hat{v}_g|$ and/or by the length $|\hat{v}_g|/f$ Rossby similarity cannot be obtained; that is easy to see since the boundary condition (2a) would be in that case: $X_0 = C_d^2$, $Y_0 = 0$ and therefore depend on Ro_0. $|\hat{v}_g|$ and $|\hat{v}_g|/f$ are so-called external parameters which are useless for such considerations. External and internal parameters have been discussed and listed in a table presented in a paper by YORDANOV and WIPPERMANN (1972).

In order to support all the foregoing conclusions the integrations mentioned before have been carried out, the results of which are displayed in figure 1. These integrations have been done for $L_\infty = 0.015$ which correspond to the neutral case, but there is not a general restriction to that case. They can be carried out

for any stratification when L_∞ is chosen appropriately to that stratification. Although the integrations have been made for a barotropic PBL only there is no general restriction to barotropic PBLs; Rossby similarity or the auto-model hypothesis may be extended to baroclinic PBLs as well, see YORDANOV and WIPPERMANN (1972). In this case the surface Rossby number must be formed as a combination of z_0, f and $|\hat{v}_{g0}|$ where the index o indicates the value at the ground.

It can be considered as one of the main advantages of Rossby similarity that it enables to derive the resistance law for a PBL giving C_d and α_0 as depending on Ro_0 (α_0 is the cross-isobar angle):

$$ln(Ro_0) = M - ln(C_d) + (\kappa^2/C_d^2 - N^2)^{1/2} \tag{14a}$$

$$\kappa \sin(|\alpha_0|)/C_d = N$$

where M and N are universal functions of internal parameters for the static stability and for the baroclinicity. Derivations have been given by the authors cited at the beginning of this note. For the first time the resistance law has been derived by ROSSBY and MONTGOMERY (1935) for the barotropic and neutral case; they obtained M = 0.92, N = 4.42 and also they had a factor 0.882 before the root in eq. (14a). That may be the reason that the dimensionless combination of the external parameters (z_0, f, $|\hat{v}_g|$) has been named after Rossby; this combination has been introduced and used for the first time already by PRANDTL and TOLLMIEN in 1924.

A thermal "resistance law" and one for the moisture can be derived just so by applying Rossby similarity.

References

APPLEBY, J. F. and W. D. OHMSTEDE, 1964: Numerical solution of the distribution of wind and turbulence in the planetary boundary layer; Meteor. Res. Note No. 8, Meteor. Dept. USAERDA Fort Huachuca, Ariz., Sept. 1964

BLACKADAR, A. K., 1962: The vertical distribution of wind and turbulent exchange in a neutral atmosphere; J. Geophys. Res. 67, 3095–3102

BLACKADAR, A. K. and H. TENNEKES, 1968: Asymptotic similarity in neutral barotropic planetary boundary layers J. Atm. Sci. 25, 1015–1020

CSANADY, G. T., 1967: On the "resistance law" of a turbulent Ekman layer; J. Atm. Sci. 24, 467–471

GILL, A. E., 1967: The turbulent Ekman layer; Unpubl. Manuscr., Dept. Appl. Math. Theor. Phys. University of Cambridge

KAZANSKII, A. B. and A. S. MONIN, 1960: The turbulent regime above the ground layer of the atmosphere, Izv. Acad. Sci. USSR, Ser. Geophys. No. 1, 165–168

KAZANSKII, A. B. and A. S. MONIN, 1961: On the dynamical interaction between the atmosphere and the earth surface, Izv. Acad. Sci. USSR, Ser. Geophys. No. 5, 786–788, engl. transl. 514–515

LETTAU, H. H., 1962: Theoretical wind spirals in the boundary layer of a barotropic atmosphere, Beitr. Phys. Atm. 35, 195–212

MONIN, A. S. and S. S. ZILITINKEVICH, 1967: Planetary boundary layer and large scale atmospheric dynamics, Rep. Study Conf. on GARP, Stockholm Append. V, pp 37

PRANDTL, L. and W. TOLLMIEN, 1924: Die Windverteilung über dem Erdboden, errechnet aus den Gesetzen der Rohrströmung, Z. f. Geophys. 1, 47–55

ROSSBY, C. G. and R. B. MONTGOMERY, 1935: The layers of frictional influence in wind and ocean currents, Pap. in Physic. Oceanogr. Meteor. MIT and WHOI 3(3), pp. 101

WIPPERMANN, F., 1972a: A mixing-length hypothesis for the planetary boundary layer flow in the atmosphere, Beitr. Phys. Atm. 45, to be published

WIPPERMANN, F., 1972b: A note on a method for solving the planetary boundary layer equations, Beitr. Phys. Atm. 45, 83–86

YORDANOV, D. and F. WIPPERMANN, 1972: The parametrization of the turbulent fluxes of momentum, heat and moisture at the ground in a baroclinic planetary boundary layer, Beitr. Phys. Atm., 45, 58–65

Universal Profiles in the Barotropic Planetary Boundary Layer*)

Universelle Profile in der barotropen planetarischen Grenzschicht

F. Wippermann

Technical University Darmstadt, Germany, Department of Meteorology

Received November 19, 1971

Summary: The system of the equations for the planetary boundary layer has been closed by a mixing-length hypothesis. Then integrations have been carried out for different thermal stratifications giving universal profiles of the variables, which have been made dimensionless by the appropriate internal parameter. Such profiles have been obtained for the deviation from the geostrophic wind, for the Reynolds stress, for the eddy viscosity and for the dissipation rate of turbulent kinetic energy.

Beside some other results of the integrations it will be reported also on evaluations of the universal functions $M_m(\mu)$ and $N(\mu)$ which appear in the resistance law for a barotropic planetary boundary layer.

Zusammenfassung: Das Gleichungssystem für die planetarische Grenzschicht wird durch eine Mischungsweghypothese geschlossen. Integrationen des Systems für unterschiedliche thermische Schichtungen liefern dann universelle Profile, wenn die betrachteten Variablen mit den zugehörigen inneren Parametern dimensionslos gemacht worden sind. Solche Vertikalprofile werden berechnet und dargestellt für die Abweichung vom geostrophischen Wind, für die Reynolds'sche Schubspannung, für den turbulenten Diffusionskoeffizienten und für die Dissipationsrate turbulenter kinetischer Energie.

Neben andern Ergebnissen der Integrationen werden auch noch Auswertungen der im Widerstandsgesetz auftretenden universellen Funktionen $M_m(\mu)$ und $N(\mu)$ mitgeteilt.

Résumé: On réalise un système fermé d'équations pour la couchelimite planétaire à l'aide d'une hypothèse en longueur de mélange. L'intégration du système pour différentes stratifications thermiques fournit alors les profils universels, où les variables ont été rendues non dimensionnelles à l'aide des paramètres internes appropriés. De tels profils verticaux sont obtenus pour l'écart par rapport au vent géostrophique, pour la tension de Reynolds, pour les coefficients de diffusion turbulente et pour le taux de dissipation de l'énergie cinétique de turbulence.

Outre d'autres résultats des intégrations, on donne des évaluations des fonctions universelles $M_m(\mu)$ et $N(\mu)$, qui apparaissent dans la loi de résistance pour une couche-limite planétaire barotrope.

I. Introduction

A boundary layer is called a planetary boundary layer (PBL), if the conditions of stationarity and horizontal homogeneity are satisfied and if the variation of the density with height can be considered to be very small. It can be shown by arguments of Rossby similarity that in such a PBL the vertical profiles of the Reynolds stress, of the velocity defect, of the eddy viscosity or of other variables are universal ($Z \gg Z_0$), if these variables are nondimensionalized by internal flow parameters; such variables are listed in a paper by WIPPERMANN and YORDANOV (1972). Universal profile means that such a vertical profile is valid for any combination of the external parameters, it varies only with the thermal stratification and, of course, in the baroclinic case it depends on two internal parameters of the baroclinicity, see YORDANOV and WIPPERMANN (1972).

*) Paper presented at the meeting of the German Meteorological Society in Essen 27 Sept. – 2 Oct. 1971

The universal profiles can be obtained either by the evaluation of measurements in the atmospheric boundary layer (assuming that the conditions for a PBL are satisfied) or by integrating the boundary layer equations using a model for the PBL. The measurements are still very few and rather imperfect, in almost all cases the thermal stratification and the baroclinicity have not been determined. Computations with a two-layer model of the PBL have been made first by ROSSBY and MONTGOMERY (1935), then by YUDIN and SHVETZ in 1940, with a single-layer model by BLACKADAR (1962) and LETTAU (1962) and later on by a few others. The profiles obtained by these computations can be made dimensionless by the correct internal parameters, then they will be the universal profiles. The disadvantage of such results is the use of so-called "a priori-models", i.e. models for which the system of equations has been closed by a mixing-length hypothesis pre-assigning the vertical mixing-length profile. The single-layer model by BOBILEVA, ZILITINKEVICH and LAIKHTMAN (1965) avoids this disadvantage, but it seems to have some others; the universal profile obtained by this model differ considerably from observations (for instance: the maximum of eddy viscosity appears at $Z > 1$ in the neutral case but it is observed at $Z \approx 0.1$).

In the present paper the universal profiles will be computed by a single-layer model which avoids the aforementioned disadvantages. For this model the system of equations is closed by a mixing-length hypothesis, which relates the mixing-length to an internal variable, namely the Reynolds' stress.

The set of the equations is:

$$d^2Y/dZ^2 = X/K_m \tag{1a}$$

$$d^2X/dZ^2 = -Y/K_m \tag{1b}$$

$$K_m = T^{1/2}L/\kappa\,, \qquad T = (X^2 + Y^2)^{1/2} \tag{2}$$

$$L = L_\infty - (L_\infty - \kappa K_{mo})\,T^p \tag{3}$$

$$p = -\kappa\,\frac{1 - K_{mo}\{2(dT/dZ)_0^2 + (dT/dZ)_0/2\}}{(dT/dZ)_0 \quad L_\infty - \kappa K_{mo}}$$

The boundary conditions are:

$$Z = Z_0:\ \ X_0 = 1,\ \ Y_0 = 0,\ \ K_{mo} = Z_0,\ \ L_0 = \kappa K_{mo} \tag{4a}$$

$$Z \to \infty:\ \ X \to 0,\ \ \ Y \to 0,\ \ K_m \to 0,\ \ \ L \to L_\infty \tag{4b}$$

The following notation is used:

$$H = \kappa u_*/f,\quad L = l/H \tag{5a}$$

$$Z = z/H,\quad Z_0 = z_0/H = 1/(\kappa C_g Ro_0) \tag{5b}$$

$$X = \tau_x/(\bar{\rho} u_*^2),\quad Y = \tau_y/(\bar{\rho} u_*^2),\quad K_m = k_m/(H^2 f) \tag{5c}$$

H is the internal scale height of the PBL, l the mixing-length, z the vertical coordinate and z_0 the roughness-length, τ_x and τ_y are the components of the Reynolds' stress, k_m is the eddy viscosity, u_* the friction velocity, ρ the density, f the Coriolis parameter and κ is the Karman constant. $|\hat{w}_g|$ is the geostrophic wind speed, $C_g = u_*/|\hat{w}_g|$ is the geostrophic drag coefficient and $Ro_0 = |\hat{w}_g|/(z_0 f)$ is the surface Rossby number.

The two second order ordinary differential equations (1a) and (1b) are the PBL-equations after elimination of the velocity components; eq. (2) is a combination of the flux-gradient relation and Prandtl's mixing-length equation and eq. (3) is the aforementioned mixing-length hypothesis by WIPPERMANN (1971a). From the boundary condition (4a) one notices that the x-axis has the direction of the surface stress. For an integration of the eqs. (1a)–(3) between Z_0 and infinity there is only one free parameter, namely L_∞ being the asymptotic mixing-length. With respect to Rossby similarity this parameter L_∞ must be determined by the thermal stratification only (and in the baroclinic case by the baroclinicity probably), i.e. L_∞ has to satisfy the following reasonable condition

$$\partial L_\infty / \partial (Ro_0) = 0$$

An empirical formula relating L_∞ to the internal parameter μ of the thermal stratification has been given by WIPPERMANN (1971a):

$$\mu = -44.2 - 24.4 \log_{10}(L_\infty) \tag{6}$$

where μ is defined as

$$\mu = H/L_* \tag{7}$$

with L_* being the Monin-Obukhov stability-length. The relationship (6) allows to apply the system of the eqs. (1a)–(3) for different thermal stratifications μ; however the relationship (6) should be considered as a very preliminary one.

For the integrations of the system of the eqs. (1a)–(3) the lower boundary has been chosen at $Z_0 = 1 \cdot 10^{-5}$ which corresponds very roughly to $z_0 = 1$ cm or to a surface Rossby number between $1 \cdot 10^6$ and $1 \cdot 10^7$ according to eq. (5b). It has been assumed that X and Y become negligible at a finite but large height Z^* rather than at infinity; that means the boundary condition (4b) has to be changed into

$$Z \to Z^*, \quad X \to 0, \quad Y \to 0, \quad K_m \to 0, \quad L \to L_\infty \tag{8}$$

Z^* has been chosen to be 10 which roughly corresponds to a height of z = 10 km and which is certainly high enough. The eqs. (1a)–(3) and the boundary conditions (4a) and (8) have been transformed using the logarithmic vertical coordinate $\xi = \log_{10}(Z)$, discretization has been done by chosing $\Delta\xi = 0.05$, i.e. 179 interior points. The solution is obtained by an iterative method described by WIPPERMANN (1971b).

Integrations have been carried out for the following values of L_∞: $1 \cdot 10^{-4}$, $5 \cdot 10^{-4}$, $1 \cdot 10^{-3}$, $1 \cdot 10^{-2}$, $1.5 \cdot 10^{-2}$, $2 \cdot 10^{-2}$, $5 \cdot 10^{-2}$, $1 \cdot 10^{-1}$ and 1.0. The first two cases give an unrealistic stable stratification, the asymptotic mixing-length L_∞ is only 10 times (resp. 50 times) the roughness-length, i.e. very roughly 10 cm, resp. 50 cm (for H = 1 km). In the most unstable case the mixing-length increases with height to a length L_∞ which equals the scale height of the PBL.

The solution of the eqs. (1a)–(3) consists of the four profiles X(Z), Y(Z), $K_m(Z)$ and L(Z); from these other profiles can be derived. For instance the profiles of the two components of the nondimensional departures from the geostrophic wind

$$P = \kappa\,(\hat{u} - \hat{u}_g)/u_*, \quad Q = \kappa\,(\hat{v} - \hat{v}_g)/u_* \tag{9}$$

can be obtained by using the stress profiles X(Z) and Y(Z) in the two basic equations of the PBL

$$P = dY/dZ, \quad Q = -dX/dZ \tag{10a,b}$$

It should be mentioned, that with respect to the lower boundary condition for the velocities

$$z = z_0: \quad \hat{u} = \hat{v} = 0 \tag{11}$$

one has at $Z = Z_0$

$$P_0 = -\kappa\,|\hat{w}_g|\,\cos(\alpha_0)/u_* = -\kappa\cos(\alpha_0)/C_g \tag{12a}$$

$$Q_0 = -\kappa\,|\hat{w}_g|\,\sin(\alpha_0)/u_* = \kappa\sin(|\alpha_0|)/C_g \tag{12b}$$

where α_0 is the cross-isobar angle. The resistance law for a barotropic PBL is

$$\ln(Ro_0) = M_m(\mu) - \ln(C_g) + \kappa\cos(\alpha_0)/C_g \tag{13a}$$

$$N(\mu) = \kappa\sin(|\alpha_0|)/C_g \tag{13b}$$

Herein $M_m(\mu)$ and $N(\mu)$ are universal functions of the thermal stratification μ (and in the baroclinic case also of two internal parameters for the baroclinicity); they can be determined by measurements only or for a given boundary layer model by an integration of the boundary layer equations. In addition to the universal profiles the integrations described above gave also the universal functions $M_m(\mu)$ and $N(\mu)$ for the PBL-model used in this paper.

One notices from eqs. (10b) and (13b) that

$$Q_0 = -(dX/dZ)_0 = N \tag{14}$$

depends only on the thermal stratification but is independent of the surface Rossby number, i.e. it is independent of the external parameters. But on the other hand P_0 depends on the surface Rossby number, this can be seen by regarding eqs. (10a) and (13a); one gets

$$P_0 = (dY/dZ)_0 = M_m - \ln(C_g\,Ro_0) \tag{15a}$$

or with respect to the definitions (5a) and (5b)

$$P_0 = (dY/dZ)_0 = M_m + \ln(\kappa) + \ln(Z_0) \tag{15b}$$

It will be referred to this eq. (15b) in the next section.

II. The profiles of the velocity components

First the results are presented as hodographs in figure 1 for four different thermal stratifications ($L_\infty = 0.001, 0.01, 0.1$ and 1.0). The numbers at the four spirals give the height Z. Close to the ground ($Z_0 = 1 \cdot 10^{-5}$) the hodographs are almost parallel to the P-axis, i.e. $Q = \text{const} = Q_0$. This is the range, in which the wind does not turn with height (surface layer), it has always the direction of the surface stress π_0. The windvector $\kappa\,\hat{w}/u_*$ at any height Z is given as the straight line connecting the end-point of the hodograph ($Z_0 = 1 \cdot 10^{-5}$) with the height Z in question. If any other roughness-length Z_0 would be chosen as the lower boundary of the integration range one would find this other end-point on that part of the hodograph for which $Q = Q_0$; the spiral itself remains unchanged. This expresses the existence of

Rossby similarity, see WIPPERMANN and YORDANOV (1972). The vector of the geostrophic wind $\kappa\,\hat{w}_g/u_*$ is obtained by the straight line which connects the end-point of the hodograph with the point (P = 0, Q = 0), the angle between this straight line and the hodograph is the cross-isobar anlge α_0.

Such a universal spiral has been derived first by LETTAU (1962) for the neutral case. LETTAU uses another mixing-length hypothesis, but his results differ only very little from the results obtained here. This shows, that in the neutral and barotropic case the velocity profiles are not very sensitive to different mixing-length hypotheses.

One notices from the hodograph curves, that the height Z_g varies with the thermal stratification; Z_g is the (nondimensional) height, at which the wind $\hat{w}$ reaches the direction of the geostrophic wind for the first time. The values of Z_g obtained by the integrations are listed in table 1.

Table 1/Tabelle 1

Stratification	L_∞	N	Z_g	Z_{gE}	c
extremely stable	$1 \cdot 10^{-3}$	16.1	0.17	0.19	45.5
stable	$1 \cdot 10^{-2}$	5.39	0.52	0.58	9.9
neutral	$1.5 \cdot 10^{-2}$	4.53	0.66	0.69	7.6
unstable	$1 \cdot 10^{-1}$	2.58	1.42	1.22	2.4
extremely unstable	1.0	2.22	1.59	1.41	1.3

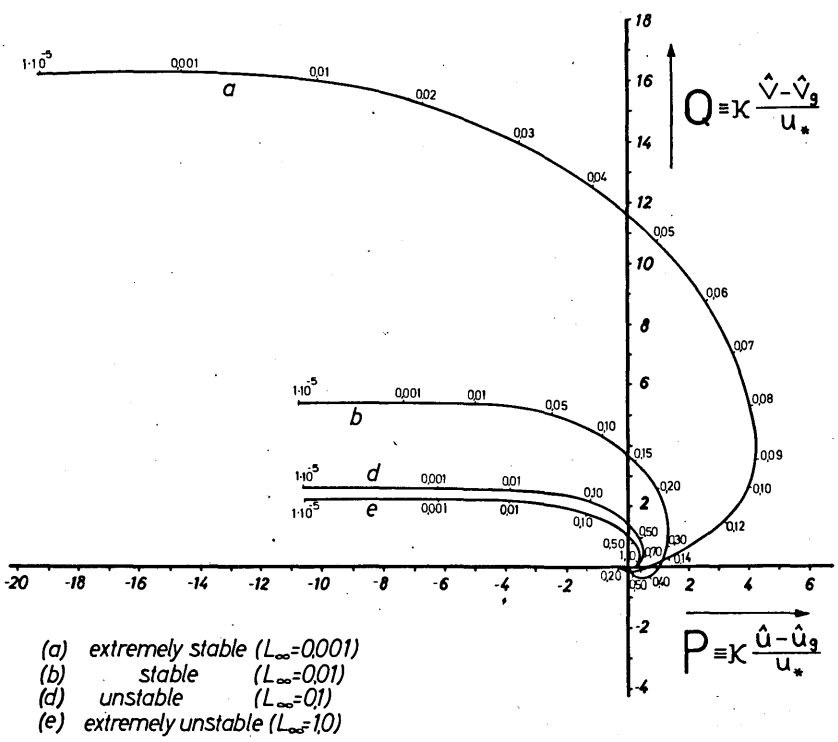

Figure 1. Universal wind spirals for four different thermal stratifications. The numbers give the non-dimensional height Z.

Bild 1. Universelle Windspiralen für vier verschiedene Schichtungen. Die Zahlen geben die jeweilige dimensionslose Höhe Z an.

It is interesting to compare these heights Z_g with those heights Z_{gE} obtained from the simple Ekman solution; it is

$$Z_{gE} = \pi/N \tag{16}$$

where N is the universal function appearing in the resistance law (13b). The values of N and Z_{gE} are included likewise in the table 1.

For the neutral case ($L_\infty = 0.015$) the two universal profiles P(Z) and Q(Z) are shown in figure 2. The dots are the values from the Leipzig wind profile as given by GILL (1967). This figure shows a very good agreement between the observations and the theory; it shows also that the choice of $L_\infty = 0.015$ is correct for the neutral stratification ($\mu = 0$) or for a stratification very close to the neutral one. The Leipzig wind profile is supposed to be neutral or almost neutral.

The lower part of the curve P(Z) in figure 2 reaches asymptotically the logarithmic wind profile, which is shown as a broken line in figure 3 for three different stratifications.

The logarithmic wind profile

$$\kappa \hat{u}/u_* = \ln(z/z_0)$$

is in the nondimensional notation (considering the definition 5b for Z_0)

$$U_L = \ln(Z) + \ln(\kappa C_g Ro_0) \tag{17}$$

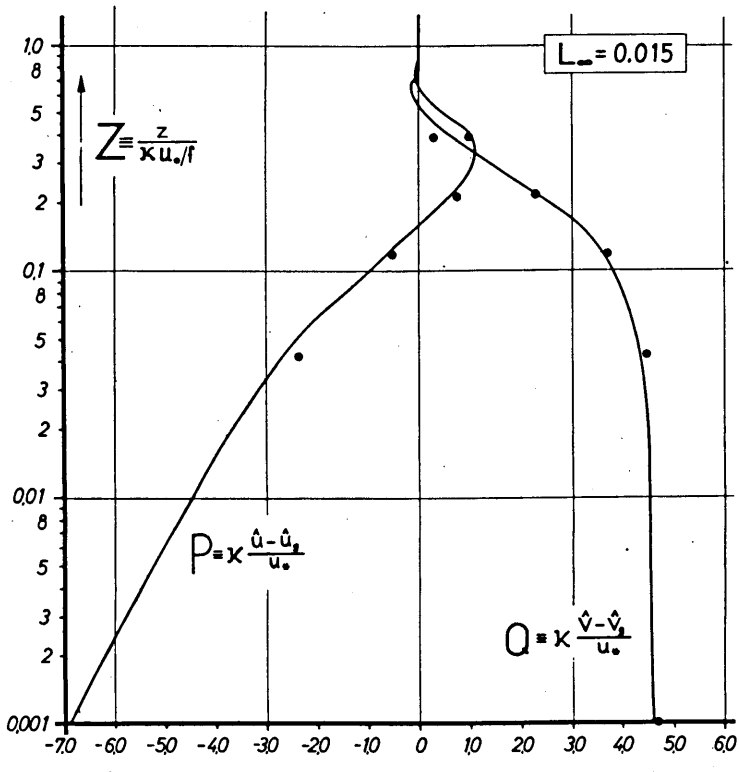

Figure 2. The two components P(Z) and Q(Z) of the universal wind profile in the neutral case. The dots are values of the Leipzig wind profile as given by GILL (1967)

Bild 2. Die beiden Komponenten P(Z) und Q(Z) des universellen Windprofiles im Falle adiabatischer Schichtung. Die Punkte sind Werte, welche GILL (1967) dem Leipziger Windprofil entnommen hat

or written as the departure from the geostrophic wind

$$P_L = \ln(Z) + \ln(\kappa C_g Ro_0) - U_g$$

Because of $U_g = \kappa \cos(\alpha_0)/C_g$ the last two terms may be written as $\ln(\kappa) + M_m(\mu)$, which results from the resistance law (13a). It is obtained

$$P_L = \ln(Z) + M_m(\mu) + \ln(\kappa) \tag{18}$$

A comparison of (15b), which results from the resistance law, and (18) shows, that the resistance law assumes a logarithmic profile at $Z = Z_0$.

At $Z = 1.0$ one gets

$$M_m(\mu) = -\ln(\kappa) + P_L(1.0) \tag{19}$$

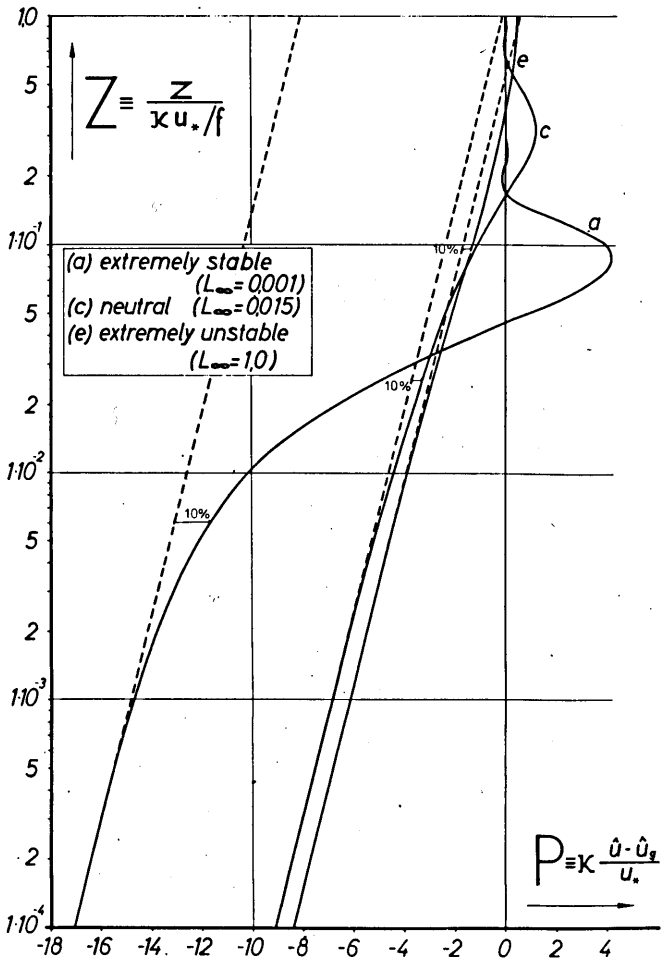

Figure 3. The component P(Z) of the universal wind profile (solid line) compared with the logarithmic wind profile (broken line) for three different thermal stratifications

Bild 3. Die Komponente P(Z) des universellen Windprofiles (ausgezogene Linie) im Vergleich mit dem logarithmischen Windprofil (gestrichelte Linie) für drei verschiedene thermische Schichtungen

In another paper WIPPERMANN (1970) has supposed (and incorrectly derived, see TAYLOR 1971), that in the neutral case $M_m(0) = -\ln(\kappa)$, which requires with respect to eq. (19) $P_L(Z = 1.0; \mu = 0) = 0$. Figure 3 shows, that $P_L(1.0; 0)$ is almost zero indeed for the PBL-model used in these integrations. The value obtained for $M_m(L_\infty = 0.015)$ equals 1.06 which differs only a little from $-\ln(\kappa) = 0.92$. Perhaps the value of L_∞ for $\mu = 0$ can be determined by the condition $P_L(1.0; 0) = 0$.

Figure 3 shows also the difference between $P(Z)$ and $P_L(Z)$, i.e. the difference between the corresponding solid and broken lines. For the three stratifications (a) extremely stable ($L_\infty = 0.001$), (c) neutral ($L_\infty = 0.015$) and (e) extremely unstable ($L_\infty = 1.0$) the heights are indicated, for which this difference $P(Z) - P_L(Z)$ equals 10 % of $P(Z)$. These heights are $Z = 5.8\ 10^{-3}$ in case (a), $Z = 2.3\ 10^{-2}$ in case (c) and $Z = 6.0\ 10^{-2}$ in the extremely unstable case (e), respectively. In the neutral case this height is very close to the height Z_P of the Prandtl-layer defined as the height in which the stress is reduced to 0.9 of the stress at the ground; see WIPPERMANN (1971c). One would expect, that the difference $P(Z) - P_L(Z)$ is smallest in the neutral case and larger in the stable as well as in the unstable case; but this expectation is not met by the results of the model.

Here a real defect of the mixing-length hypothesis (3) appears, a defect which also other mixing-length hypotheses possess as for instance that one by BLACKADAR (1962), LETTAU (1962) or APPLEBY and OHMSTEDE (1964). The defect can be shown most easily with the aid of the mixing-length hypothesis by BLACKADAR (1962).

$$L_{BL}(Z) = \kappa Z/(1 + \kappa Z/L_\infty) \tag{20}$$

(here it is unimportant that BLACKADAR's L_∞ depends also on Ro_0, what it shouldn't do.) We know from observations, that very close to the ground ($Z \ll 1$) the mixing-length is

$$l = \kappa z/\Phi_m \quad \text{or} \quad L = \kappa Z/\Phi_m \tag{21}$$

where Φ_m is the nondimensional shear function

$$\Phi_m = 1 + \gamma z/L_* = 1 + \gamma \mu Z \tag{22}$$

γ is a constant, which has different values in stable ($L_* > 0$) and in unstable ($L_* < 0$) stratification. If one replaces Φ_m in eq. (21) by eq. (22) and compares the two mixing-length one gets

$$L_\infty = \kappa/(\gamma \mu) \tag{23}$$

Eq. (23) shows clearly, that because of $L_\infty > 0$ only a stable stratification is possible. For the neutral case an appropriate value of the asymptotic mixing length is $L_\infty = 0.015$; that means, that all mixing-length hypotheses mentioned before (including the hypothesis (3) used in this paper) in the unstable case have an asymptotic value L_∞ between 0.015 and L_0. Because of this defect it is impossible to determine the parameter μ of the thermal stratification by the wind profile in the surface layer.

In figure 4 the vertical profiles of the horizontal wind speed are drawn for an extremely stable stratification (a), for a neutral one (c) and for an extremely unstable stratification (e). As in the other figures also in this figure the height z is made dimensionless by the internal height scale H; but here the horizontal wind speed is made dimensionless by the geostrophic wind, which is an external parameter:

$$|\hat{w}|/|\hat{w}_g| = C_g/\kappa \sqrt{(P - P_0)^2 + (Q - Q_0)^2} \tag{24}$$

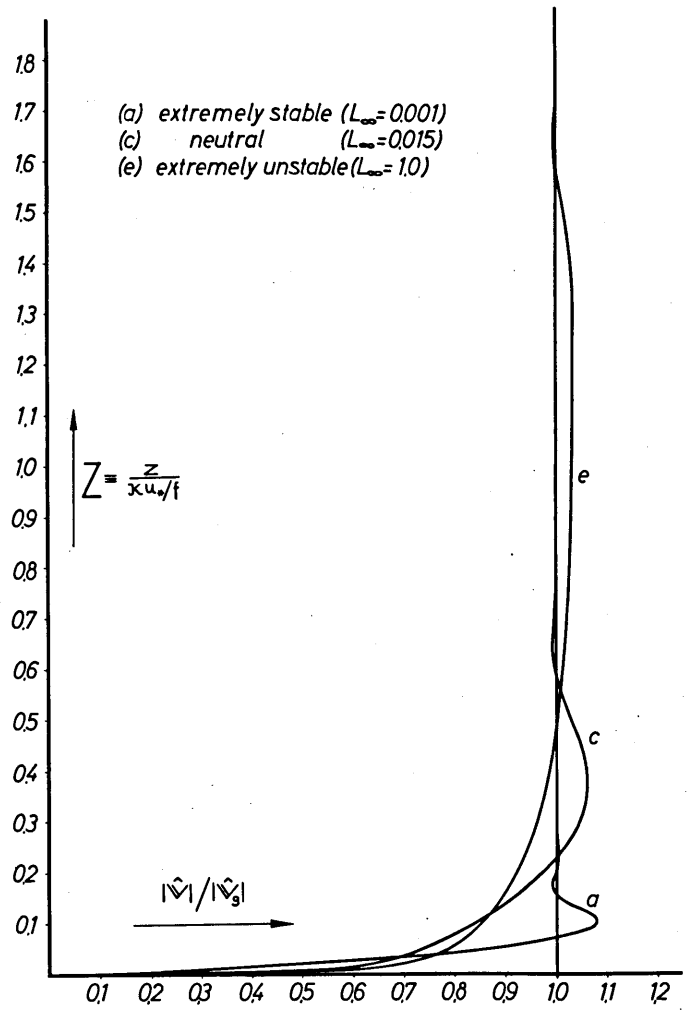

Figure 4. The influence of the thermal stratification on the overshooting of the geostrophic wind

Bild 4. Der Einfluß unterschiedlicher thermischer Schichtung auf das Überschreiten des geostrophischen Windes durch den Horizontalwind

It is true that Q_0 is independent of the surface Rossby number, i.e. independent of the external parameters (except the thermal stratification); this can be seen from eqs. (13b) and (14). But P_0 as well as C_g are dependent on Ro_0 as eq. (15) tells us. Therefore $|\hat{w}|/|\hat{w}_g|$ varies with Ro_0, in the figure 4 it is given for a surface Rossby number between $1 \cdot 10^6$ and $1 \cdot 10^7$ (namely for $Z_0 = 1 \cdot 10^{-5}$). One notices, that in the case of stable stratification the overshooting over the geostrophic wind is strongest (~ 8 %), it is very weak (~ 3 %) in the case of an extremely unstable stratification. In the stable case this overshooting is concentrated in a rather thin layer (roughly 50–100 m), for unstable stratification it exists in a layer of several hundred meters.

III. The profiles of stress, eddy viscosity and the rate of energy dissipation

Figure 5 shows the stress spirals for the same thermal stratifications as used for the velocity spirals in figure 1. For an extremely stable stratification (a) the stress becomes zero already at a height $Z \approx 0.2$, but in an extremely unstable stratification the stress spiral is bulged out more and the stress vanishes at a height $Z \approx 2$; in this case the stress profile reaches a height about ten times larger than in the extremely stable case.

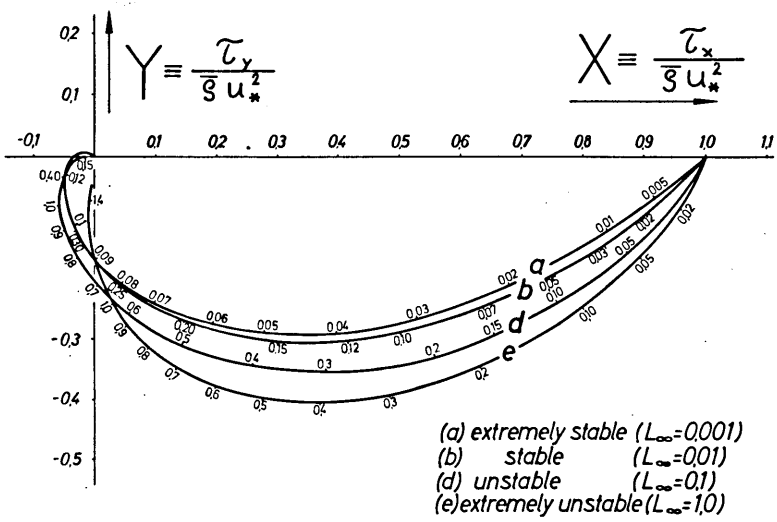

Figure 5. Universal stress spirals for four different thermal stratifications. The numbers give the non-dimensional height Z.

Bild 5. Universelle Spiralen der Schubspannung für vier unterschiedliche thermische Schichtungen. Die Zahlen geben die jeweilige dimensionslose Höhe Z an

From the PBL-equation applied to the height $z = z_0$, ($\hat{w} = 0$),

$$(d\,\tau/dz)_0 = f[\hat{w}_g \times \mathbb{k}] \tag{24a}$$

or in the non-dimensional notation

$$(d\,\tau/dZ)_0 = [\hat{w}_g^0 \times \mathbb{k}]\kappa/C_g \tag{24b}$$

one notices that at the ground ($X = 1$, $Y = 0$) the spiral is perpendicular to the geostrophic wind.

The more unstable the stratification the larger is the angle between the stress spiral and the x-axis, i.e. as smaller is the cross-isobar angle α_0.

Dimensionless stress spirals showing this variation with the thermal stratification have already been shown also by YAMAMOTO, YASUDA and SHIMANUKI (1968). However these spirals are made dimensionless by the external parameter $|\hat{w}_g|$ and are therefore not universal in this case.

The integration of the system of the equation (1a)–(3) gives also the non-dimensional eddy viscosity K_m. In figure 6 the profiles $K_m(Z)$ are presented for five different thermal stratifications. In the extremely stable case the maximum of K_m is weak and appears very low ($Z \approx 0.01$), in the neutral case it has the value $K_{m,max} = 0.027$ and will be found near $Z = 0.1$ (very roughly near 100 m) and in the extremely unstable case the maximum of K_m is very large and displaced upwards to the upper border of the PBL. The broken line in figure 6 gives the vertical profile of K_m as evaluated from the Leipzig wind profile, see LETTAU (1950). The very good agreement between the K_m-profile Leipzig and the K_m-profile obtained for $L_\infty = 0.015$ shows, that this value has been chosen well for the stratification belonging to the Leipzig wind profile; this stratification has not been measured but it is assumed to be neutral. Probalbly the value $L_\infty = 0.014$ or $L_\infty = 0.0135$ would give a still better agreement with the Leipzig wind profile.

In the diagram (figure 6) the maxima of K_m for different thermal stratifications seem to be almost on a straight line; that means the amount of the maximum of K_m is proportional to the height $Z_{(K,max)}$, at which it appears. The relation is

$$K_{m,max} = 0.27\, Z_{(K,max)} \tag{25}$$

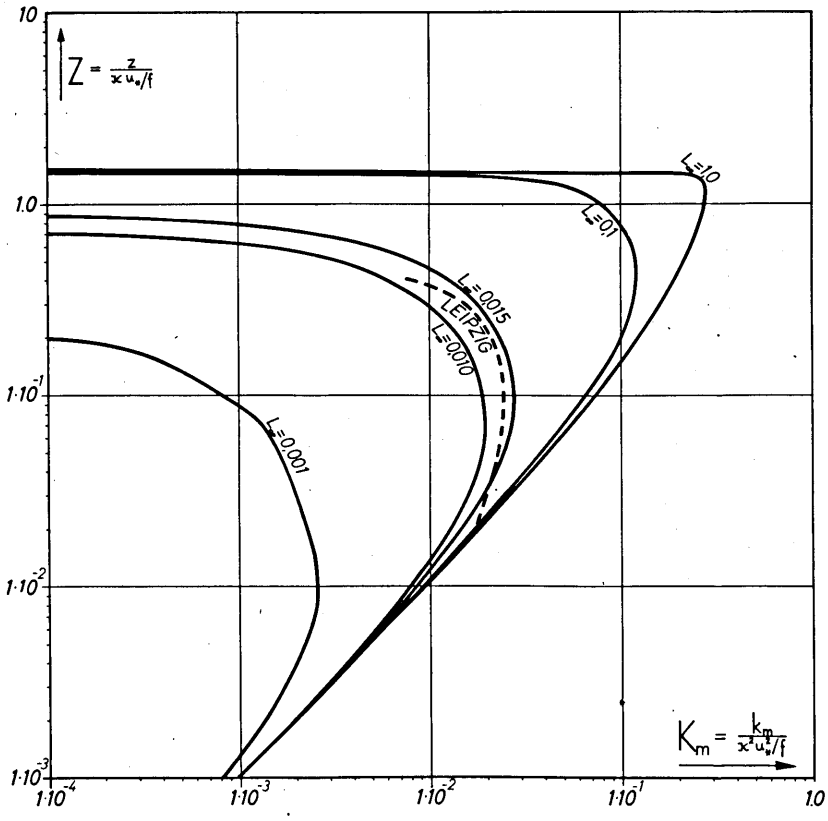

Figure 6. Universal profiles of the non-dimensional eddy viscosity K_m for five different thermal stratifications. The broken line is the K_m-profile obtained from the Leipzig wind profile by LETTAU (1950)

Bild 6. Universelle Profile des dimensionslosen turbulenten Diffusionskoeffizienten K_m für fünf verschiedene thermische Schichtungen. Die gestrichtelte Kurve gibt das Profil $K_m(Z)$, welches LETTAU (1950) aus dem Leipziger Windprofil erhalten hat

The differences between the $K_{m,max}$ obtained by the integrations and the $K_{m,max}$ computed by the relationship (25) are very small, even in the case of an extremely stable stratification where this difference is largest it is 6 % only. Of course the relationship (25) is valid only in the barotropic case; if a relationship of this kind would also exist in baroclinic cases, the factor certainly would depend on the two parameters for the baroclinicity $d\hat{u}_g/dz$ and $d\hat{v}_g/dz$.

For some purposes it may be useful to have the profile of the eddy viscosity in an functional form; such one has been determined as

$$K_{mF}(Z) = Z\exp\{-c\,Z^{0.764}\} \tag{26}$$

where c is a factor depending on the thermal stratification, i.e. on L_∞. Some values of c are given in the last column of table 1. The function (26) satisfies the empirical relation (25). The difference between K_{mF} (according to eq. 26) and K_m obtained by the integration of the PBL-equations is displayed in figure 7, this difference is given in portions of $K_{m,max}$. One notices that for $Z < 1.0$ the largest deviation is about 15 %, except for the extremely stable case, in which the difference reaches 50 % of $K_{m,max}$ in the height range between $Z = 0.05$ and $Z = 0.07$.

Universal profiles of the dissipation rate of the kinetic energy can be obtained also, if the dissipation rate is made dimensionless correctly, namely by internal parameters

$$\mathcal{E} = \epsilon/\epsilon_N, \qquad \epsilon_N = u_*^2 f/\kappa^2$$

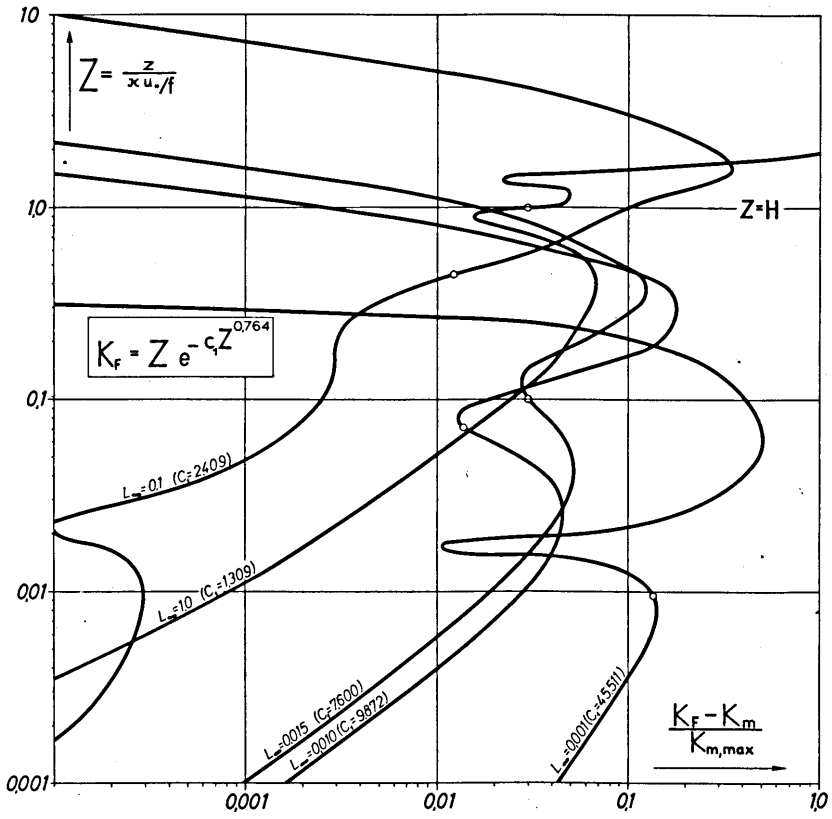

Figure 7. The deviations of the eddy viscosity K_{mF} according to eq. (26) from K_m as obtained by the integrations of the PBL-equations. These deviations are given in portions of $K_{m,\,max}$
The small circles indicate the height at which K_m has its maximum

Bild 7. Die Abweichungen des turbulenten Diffusionskoeffizienten K_{mF} berechnet nach Gl. (26) von den K_m-Werten, wie sie durch die Integration der Grenzschichtgleichungen erhalten wurden. Die Abweichungen sind in Teilen von $K_{m,\,max}$ angegeben. Die kleinen Kreise zeigen diejenigen Höhen an, in denen das Maximum des K_m-Profiles auftritt

The equation for the turbulent kinetic energy is in non-dimensional notation

$$\mathcal{E} = T^2/K_m - \mu + d/dZ\,\{K_b\, dB^2/dZ\} - d/dZ\,\{\overline{W p_N}\} \tag{28}$$

where $B^2 = b^2/u_*^2$ with $b^2 = \overline{(u_i')^2}$; K_b is the eddy diffusion coefficient for the turbulent kinetic energy b^2. In the last term of eq. (28) there appears the correlation product of the nondimensional vertical velocity $W = \kappa w/u_*$ and the non-dimensional pressure $p_N = p/\tau_0$. It is usual to neglect this last term by the following two reasons: firstly one is unable to handle this term and secondly this term is believed to be much smaller than the others. The third term on the right-hand side is the divergence of the vertical turbulent flux of the turbulent kinetic energy; also this term is very often neglected as small compared with three remaining terms. With these neglections eq. (28) is reduced to

$$\mathcal{E} = T^2/K_m - \mu$$

According to this equation the profiles $\mathcal{E}(Z)$ have been computed for different stratifications, they are presented in figure 8. An evaluation of $\mathcal{E}(Z)$ from the described integrations requires an identification of the used value of L_∞ with a certain thermal stratification given by the internal parameter μ; for this the empirical relation (6) has been applied.
Since with increasing height T^2 goes faster to zero than K_m

$$\lim_{Z \to \infty} \mathcal{E} = -\mu \tag{30}$$

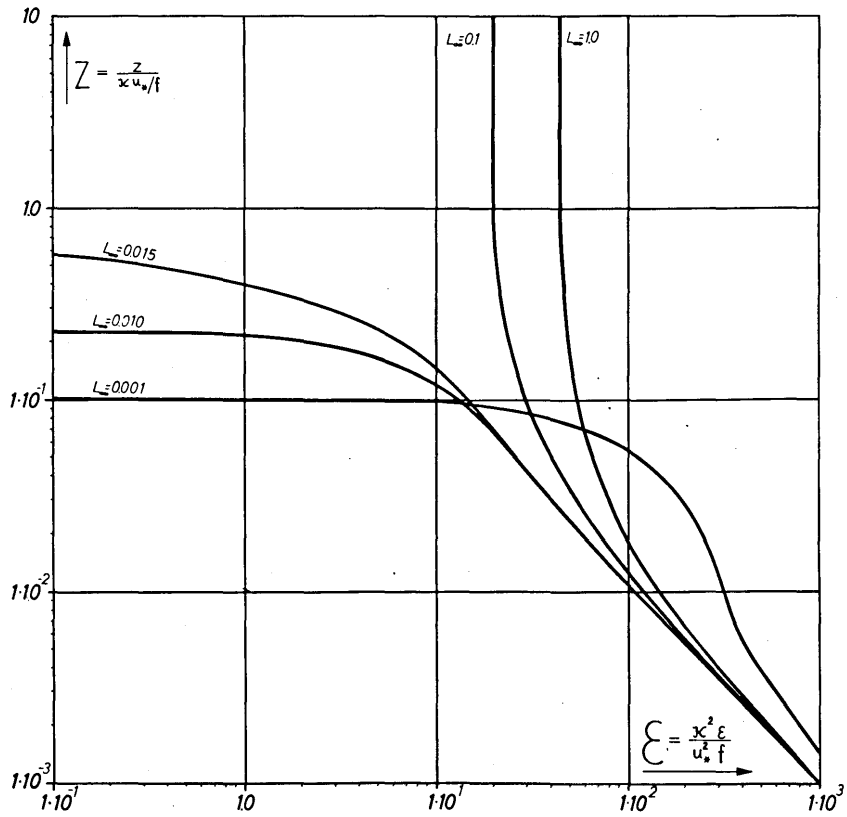

Figure 8. Universal profiles of the non-dimensional dissipation rate $\mathcal{E}$ of the turbulent kinetic energy for five different thermal stratifications

Bild 8. Universelle Vertikalprofile für den (dimensionslosen) Betrag der Vernichtung $\mathcal{E}$ turbulenter kinetischer Energie pro Zeiteinheit für fünf unterschiedliche thermische Schichtungen.

That means, that for a stable stratification ($\mu > 0$) and for large heights Z the non-dimensional dissipation rate of turbulent kinetic energy will become negative, i.e. a generation of turbulent kinetic energy would occur. This of course is not possible and the profile $\mathcal{E}(Z)$ can be considered as valid only in a range of heights in which $\mathcal{E} > 0$. An explanation is given by ZILITINKEVICH in his book (1970). One notices in figure 8 that the profile ($L_\infty = 0.1$) for the unstable case and the profile ($L_\infty = 1.0$) for the extremely unstable case almost reach the asymptotic value $-\mu$; for the stable case ($L_\infty = 0.01$) and for the extremely stable case ($L_\infty = 0.001$) the profiles show a very rapid decrease of $\mathcal{E}$ with height, these curves tend to go to negative values of $\mathcal{E}$. Qualitatively the diagram obtained by BOBILEVA et al. (1965) is completly the same as that one in figure 8.

IV. The universal functions $M_m(\mu)$ and $N(\mu)$ in the resistance law for a barotropic PBL

In the resistance law (13a), (13b) the two universal functions $M_m(\mu)$ and $N(\mu)$ appear, from which some values have been evaluated by the integrations of the model equations. According to the eqs. (14) and (15a) they are obtained as the derivatives of the stress components at the ground:

$$N = -(dX/dZ)_0 \tag{31a}$$

$$M = (dY/dZ)_0 + \ln(C_g Ro_0) \tag{31b}$$

Values of M_m and N are given in table 2; this table contains also the corresponding values of C_g and α_0. With L_∞ the corresponding values of μ are listed according to the empirical formula (6). All integrations have been carried out with a lower boundary at $Z_0 = 1 \cdot 10^{-5}$ corresponding to a surface Rossby number between $1 \cdot 10^6$ and $1 \cdot 10^7$

Table 2/Tabelle 2

L	μ	M_m	N	C_g	α_0
$5 \cdot 10^{-4}$	+ 36	- 12.0	22.8	0.012	43.0°
$1 \cdot 10^{-3}$	+ 29	- 6.8	16.1	0.016	40.0°
$1 \cdot 10^{-2}$	+ 5	- 0.6	5.4	0.031	24.5°
$1.5 \cdot 10^{-1}$	0	1.1	4.5	0.033	21.7°
$2 \cdot 10^{-1}$	- 3	1.3	4.0	0.034	19.9°
$5 \cdot 10^{-2}$	- 12	1.7	3.0	0.036	15.5°
$1 \cdot 10^{-1}$	- 20	1.8	2.6	0.036	13.6°
1.0	- 44	1.8	2.2	0.037	11.7°

M_m and N are independent of Ro_0 and therefore independent of Z_0 (according to 5b). A series of integrations with different Z_0 has been carried out in order to test the independency of M_m and N on Ro_0 for the model used in this paper. These integrations have been made for the neutral case ($L_\infty = 0.015$), some of the results are summarized in table 3

Table 3/Tabelle 3

Z_0	M_m	N	C_g	α_0
$1\ 10^{-3}$	0.91	4.5	0.049	33.2°
$1\ 10^{-4}$	1.0	4.5	0.039	26.4°
$1\ 10^{-5}$	1.1	4.5	0.033	21.7°
$1\ 10^{-6}$	1.1	4.5	0.028	18.4°
$1\ 10^{-7}$	1.2	4.5	0.024	15.9°

N is completely independent of Ro_0, M_m varies only a little. C_g and α_0 of course depend on Ro_0 (and therefore also on Z_0), they must show a variation with varying Z_0.

The largest Z_0 of table 3, namely $Z_0 = 1 \cdot 10^{-3}$ (roughly corresponding to $z_0 = 1$ m), is probably unrealistic large and may better be dropped. In this case also the variation of the remaining M_m is very small so that the independency of M_m and N on Ro_0 is verified for the model in the neutral case.

It is interesting to compare the values of $M_m(\mu)$ and $N(\mu)$ obtained by the model as $M_m(L_\infty)$ and $N(L_\infty)$ with those values evaluated from observations. Unfortunately there are only two sets of observations which are sufficient for an evaluation of $M_m(\mu)$ and $N(\mu)$. These are the O'Neil data evaluated by MONIN and ZILITINKEVICH (1967) and re-evaluated by ZILITINKEVICH (1970) and secondly the Kerang and Hay data evaluated by CLARKE (1970). These evaluations are presented in figure 9, the values from table 3 (indicated by WI'71) also are shown. For a comparison figure 9 also contains the results of a single-layer model by FIEDLER (1971) and those of a two-layer model by ZILITINKEVICH (1970).

The crossed circles marke the point for the neutral case. For the model WI'71 one has $M_m(0) = 1.1$, $N(0) = 4.5$ which is very close to the values $\{M_m(0) = 0.90, N(0) = 4.50\}$ evaluated by WIPPERMANN (1970) from the available observations as well as from different adiabatic models.

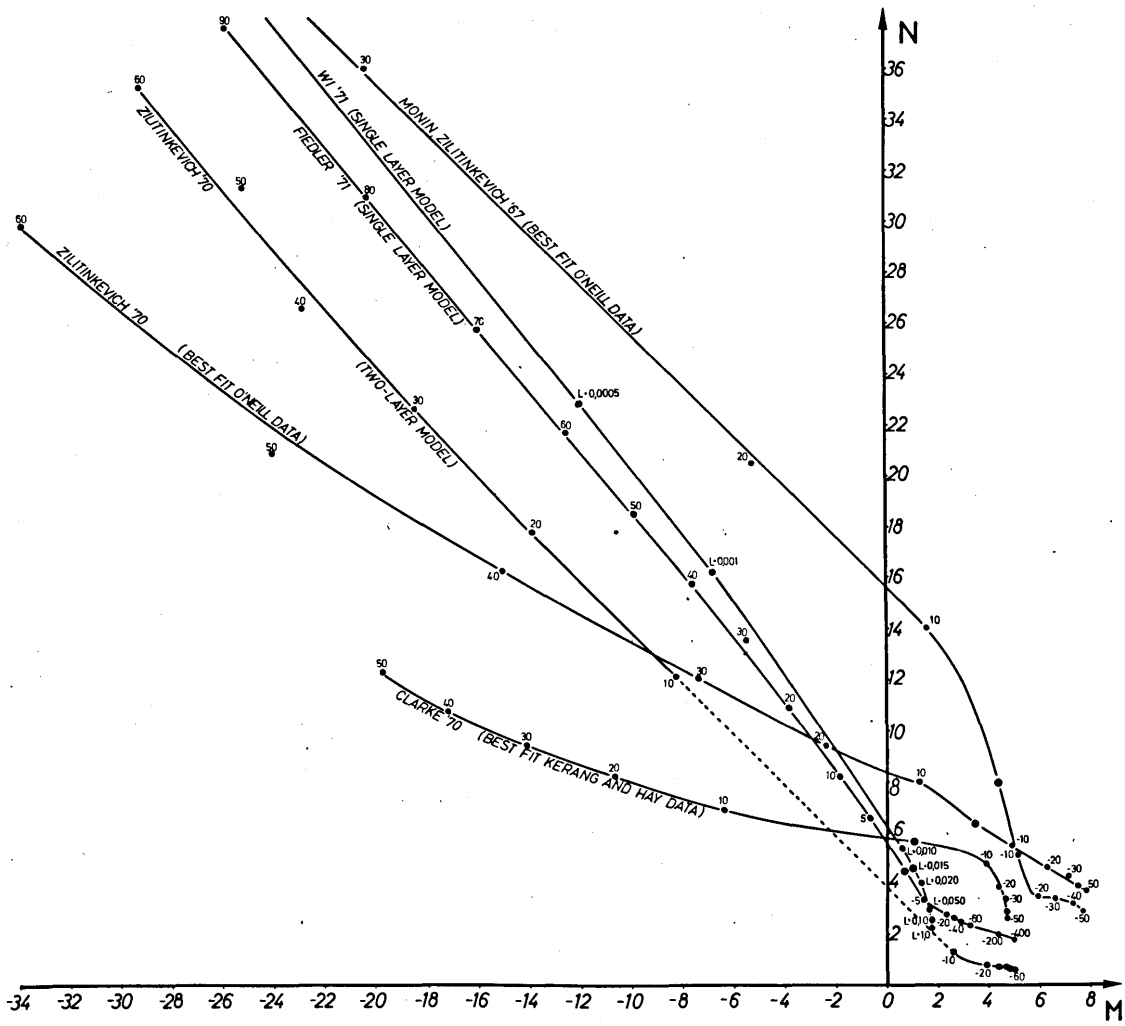

Figure 9. M_m and N varying with the stratification parameter μ according to the evaluations of observational data and to the integrations for several PBL-models

Bild 9. M_m und N für sich ändernden Parameter μ der thermischen Schichtung nach den Auswertungen von Beobachtungen und nach den Integrationsergebnissen verschiedener PBL-Modelle

The values of M_m and N for an unstable stratification ($\mu < 0$, $L_\infty > 0.015$) are found in the lower right corner of the diagram. Here the values obtained by various models as well as the values obtained by measurements don't differ very much.

The curvature in the lower part of the line representing the model WI'71 is to the left. This is similar to the curve representing CLARKE's evaluation of data. The other curves are in the lower part either straight or they have a curvature to the right. It is supposed that the opposite curvature of the result WI'71 is caused by the defect of the mixing-length hypothesis described in section II, eq. (23). But the mentioned influence of this defect seems to be not severe with respect to the large scatter of the observations and of the results of different models.

V. Acknowledgements

The author wishes to thank Dr. YORDANOV for many stimulating and helpful discussions and Mr. ETLING for doing the work of programming.

VI. References

BACKADAR, A. K. 1962, The vertical distribution of wind and turbulent exchange in a neutral atmosphere, J. Geophys. Res. **67**, 3095–3102.

BOBILEVA, I. M., ZILITINKEVICH, S. S., LAIKHTMAN, D. L. 1965, Turbulent exchange in the thermally stratified planetary boundary layer of the atmosphere. Int. Colloqu. on Fine-Scale Structure of the Atmosphere. Moscow 1965, pp. 21.

CLARKE, R. H. 1970, Observational studies in the atmospheric boundary layer, Quart. J. Roy. Meteor. Soc. **96**, pp. 91–114.

FIEDLER, H. 1971, Modelluntersuchungen zur Ekmanschicht, Pap. pres. at the meeting of the German Meteor. Soc. Essen, 27 Sept.–2. Oct. 1971.

GILL, A. E. 1967, The turbulent Ekman layer, Unpubl. Manuscr. Dept. Appl. Math. & Theor. Phys., Univers. of Cambridge.

LETTAU, H. H. 1950, A re-examination of the "Leipzig wind profile" considering some relations between wind and turbulence in the friction layer. Tellus **2** (2), pp. 125–129.

LETTAU, H. H. 1962, Theoretical wind spirals in the boundary layer of a barotropic atmosphere. Beitr. Phys. Atm. **35**, pp. 195–212.

MONIN, A. S., ZILITINKEVICH, S. S. 1967, Planetary boundary layer and large scale atmospheric dynamics. IUGG/WMO Rep. Study Conf. GARP Stockholm Append. V, pp. 37.

ROSSBY, C. G., MONTGOMERY, R. B. 1935, The layers of frictional influence in wind and ocean currents. Papers in Phys. Oceanogr. M. I. T. and W. H. O. I. **3** (3), pp. 101.

TAYLOR, R. J. 1971, A note on a paper by F. Wippermann: "The two constants in the resistance law for a neutral barotropic boundary layer of the atmosphere", Beitr. Phys. Atm. **44**, pp. 69–70.

WIPPERMANN, F. 1970, The two constants in the resistance law for a neutral barotropic boundary layer of the atmosphere. Beitr. Phys. Atm. **43**, pp. 133–140.

WIPPERMANN, F. 1971a, A mixing-length hypothesis for the planetary boundary layer flow in the atmosphere, Beitr. Phys. Atm. **44**, 215–226.

WIPPERMANN, F. 1971b, A note on a method for solving the planetary boundary layer equations. Beitr. Phys. Atm., **44**, 293–296.

WIPPERMANN, F. 1971c, Eddy viscosity in a barotropic planetary boundary layer as related to the turbulent kinetic energy. Beitr. Phys. Atm. **44**, pp. 127–136.

WIPPERMANN, F., YORDANOV, D. 1972, A note on the Rossby similarity for flows of barotropic planetary boundary layers. Beitr. Phys. Atm. **45**, 66–71

YAMAMOTO, G., YASUDA, N., SHIMANUKI, A. 1968, Effect of thermal stratification on the Ekman layer. J. Meteor. Soc. Japan **XXXXIV** (6), pp. 442–455.

YORDANOV, D., WIPPERMANN, F. , The parametrization of the turbulent fluxes of momentum, heat and moisture at the ground in a baroclinic planetary boundary layer. Beitr. Phys. Atm. **45**, 58–65

YUDIN, M. I., SHVETZ, M. E., 1940, A stationary model of wind distribution with altitude in a turbulent atmosphere. Trudy Glav. Geofiz. Obs. (GGO), No. **31** (8), pp. 42–52 (in russian)

ZILITINKEVICH, S. S. 1970, The dynamics of the boundary layer of the atmosphere. pp. 291, Leningrad, Gidrometeor. Isd. (in russian).

Note on the Energy Budget in the PBL

A set of energy equations, (47) - (50), for the PBL is derived in the first chapter (see page 22); it shows the energy conversions, which are possible among the four different kinds of energy. These equations are repeated here; in the eqs. (48) and (49) the term $-g\overline{\varrho' w'}$ has been transformed to $g/\bar{T}\ \overline{\varrho w' T'}$ according to eqs. (54a) - (54c), page 23,

$I = \bar{\varrho}\{c_v\hat{T}+\Phi\}$	$b_m = \bar{\varrho}\,\frac{\hat{\mathbb{v}}^2}{2}$	$b_t = \overline{\varrho\,\frac{(\mathbb{v}'')^2}{2}}$	$\bar{\varrho}\,L^*\hat{s}$
$-\frac{d}{dz}\{c_p\overline{\varrho w'' T''} - \overline{w'p'}\}$	$+\frac{d}{dz}(\tau\cdot\hat{\mathbb{v}}_h)$	$-\frac{d}{dz}\{\overline{\varrho w''\frac{(\mathbb{v}'')^2}{2}} + \overline{w'p'}\}$	$-\frac{d}{dz}\{L^*\overline{\varrho w'' s''}\}$
$+f\bar{\varrho}\,\mathbb{k}\cdot[\hat{\mathbb{v}}_h\times\hat{\mathbb{v}}_g]$	$-f\bar{\varrho}\,\mathbb{k}\cdot[\hat{\mathbb{v}}_h\times\hat{\mathbb{v}}_g]$		
$-\frac{g}{\bar{T}}\overline{\varrho w' T'}$		$+\frac{g}{\bar{T}}\overline{\varrho w' T'}$	
$+\bar{\varrho}\,\varepsilon_m$	$-\bar{\varrho}\,\varepsilon_m$		
$+\bar{\varrho}\,\varepsilon_t$		$-\bar{\varrho}\,\varepsilon_t$	
	$-(\tau\cdot\frac{d\hat{\mathbb{v}}_h}{dz})$	$+(\tau\cdot\frac{d\hat{\mathbb{v}}_h}{dz})$	
$-L^*\bar{\varrho}\,\delta\hat{s}$			$+L^*\bar{\varrho}\,\delta\hat{s}$
$-\frac{d}{dz}\bar{R}_z$			
$= 0$	$= 0$	$= 0$	$= 0$
(1)	(2)	(3)	(4)

In the book by LUMLEY and PANOFSKY (1964) the discussions about the terms are summarized, which appear in the bud-

get of turbulent kinetic energy, eq. (3); estimates of these terms are also given in this book. However they are almost all restricted to the surface layer. Since that time some more investigations have been published discussing measurements of these terms, but they are also restricted to the surface layer. The most detailed discussion is given by WYNGAARD and COTÉ (1971) using the set of the Kansas 1968 Field Program Data, see IZUMI (1971).

Some of the terms in the budget of the kinetic energy of the mean motion, eq. (2), have been evaluated as profiles for the whole boundary layer by LETTAU and HOEBER (1964) from pilot balloon ascents on the island Helgoland. KRAUS (1972) has plotted the profiles of these terms (except the dissipation rate $\bar{\varrho}\,\varepsilon_m$) after two of these Helgoland wind profiles; he discusses also the effect of the thermal stratification on these terms.

In this note some general considerations should be made on the conversions among the four different kinds of energy.

The schematic figure on page 113 shows the variation of the energy conversions for a dry PBL in the neutral case. Let us denote the internal and potential energy $\bar{\varrho}\,\{c_v\hat{T} + \Phi\}$ with an I, the kinetic energy of the mean motion $\bar{\varrho}\,\hat{\mathbb{v}}^2/2$ with a b_m and the turbulent kinetic energy $\overline{\varrho(\mathbb{v}'')^2}/2$ with b_t. The conversion per unit time from energy E_1 into energy E_2 should be denoted with $C\langle E_1,E_2\rangle$.
The following energy conversions have to be taken into consideration:

$$C\langle I,b_m\rangle = -(\hat{\mathbb{v}}\cdot\nabla)\bar{p} = -f\,\bar{\varrho}\,\mathbb{k}\cdot\left[\hat{\mathbb{v}}_h\times\hat{\mathbb{v}}_g\right] \tag{5}$$

$$C\langle I,b_m\rangle = -\bar{\varrho}\,\varepsilon_m \tag{6}$$

$$C\langle I,b_t\rangle = g/\bar{T}\,\overline{\varrho w'T'} \tag{7}$$

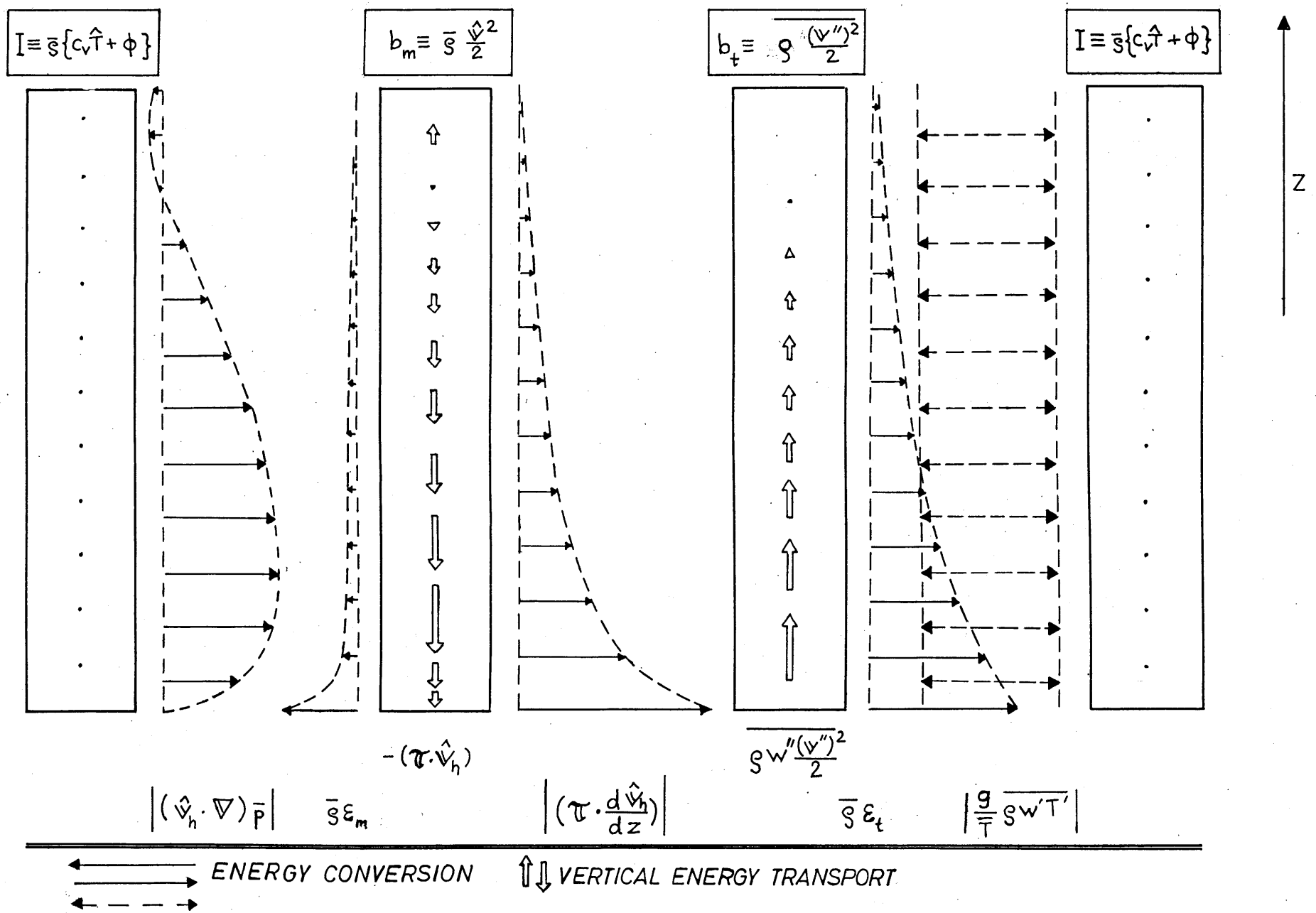
$I \equiv \bar{\varrho}\{c_v\hat{T} + \phi\}$
$b_m \equiv \bar{\varrho}\,\frac{\hat{v}^2}{2}$
$b_t \equiv \overline{\varrho\,\frac{(v'')^2}{2}}$
$I \equiv \bar{\varrho}\{c_v\hat{T} + \phi\}$
Z
$-(\tau\cdot\hat{v}_h)$
$\overline{\varrho w''\frac{(v'')^2}{2}}$
$|(\hat{v}_h\cdot\nabla)\bar{p}|$
$\bar{\varrho}\varepsilon_m$
$|(\tau\cdot\frac{d\hat{v}_h}{dz})|$
$\bar{\varrho}\varepsilon_t$
$|\frac{g}{\bar{T}}\overline{\varrho w'T'}|$
ENERGY CONVERSION
VERTICAL ENERGY TRANSPORT

$$C\left\langle I,b_t\right\rangle = -\bar{\varrho}\,\varepsilon_t \tag{8}$$

$$C\left\langle b_m,b_t\right\rangle = \left(\tau\cdot\frac{d\,\hat{v}_h}{dz}\right) \tag{9}$$

The conversion rate $C_{(5)}\left\langle I,b_m\right\rangle$ is positive in the largest part of the PBL, since the horizontal wind deviates to the left of the geostrophic wind in the largest part of the PBL; only in the upper part, where the wind has veered into a direction to the right of the geostrophic wind, the $C_{(5)}\left\langle I,b_m\right\rangle < 0$. The maximum of $C_{(5)}\left\langle I,b_m\right\rangle$ occurs very roughly in about 100 m; there the velocity $\hat{v}_h$ has almost reached the value of $\left|\hat{v}_g\right|$ and the cross-isobar angle α is still large.

The energy conversion rate $C_{(6)}\left\langle I,b_m\right\rangle$ has its maximum at the ground, it decreases very rapidly with height and has a very small amount only. Since $\varepsilon_m > 0$ the conversion rate $C_{(6)}\left\langle I,b_m\right\rangle < 0$: the dissipated kinetic energy of the mean motion is always transformed into heat.

The kinetic energy of the mean motion is lost by the conversion $C_{(9)}\left\langle b_m,b_t\right\rangle$ in lower layers than it is gained by $C_{(5)}\left\langle I,b_m\right\rangle + C_{(6)}\left\langle I,b_m\right\rangle$. Therefore a turbulent vertical energy flux must exist in order to transport the energy b_m into those layers where it is needed for the conversion $C_{(9)}\left\langle b_m,b_t\right\rangle$. This turbulent energy flux is directed downward, it is indicated in the figure (page 113) by the double arrows; this flux reaches its maximum in an altitude of very roughly 30 m. KRAUS (1972) proposes to define this level (at which the maximum of the downward flux $\tau\cdot\hat{v}_h$ occurs) as the top of the surface layer. The quantity $\tau\cdot\hat{v}_h$ can be interpreted indeed as the turbulent flux of the kinetic energy b_m .

The conversion $C_{(9)}\left\langle b_m,b_t\right\rangle$ is always positive, its maximum is at the ground. This conversion rate decreases

very rapidly with height.

The dissipation of the kinetic energy b_t of the turbulence is very similar to the gain of this kind of energy by the conversion $C_{(9)}\langle b_m, b_t\rangle$. For the neutral case they are very often put equal

$$(\tau \cdot \frac{d\,\hat{v}_h}{dz}) = \bar{\varrho}\,\varepsilon_t \tag{10}$$

which means that

$$\frac{d}{dz}\left\{\overline{\varrho w'' \frac{(v'')^2}{2}} + \overline{w'p'}\right\} = 0 \tag{11}$$

Indeed the few existing estimates for this divergence indicate, that it is very small. In the figure this turbulent flux of turbulent kinetic energy (double arrows) is sketched as directed upward while $\overline{w'p'}$ is neglected. There is no doubt, that such a turbulent flux of b_t exists and that it is directed upward; there is the question if this flux is convergent or divergent. In the figure a convergence is indicated; that means that the decrease of ε_t with height is less than the decrease of $(\tau \cdot \frac{d\,\hat{v}_h}{dz})$.

In the diabatic case exists an additional energy conversion, the rate of which is $C_{(7)}\langle I, b_t\rangle$; it is indicated in the figure by broken arrows and it is directed from I to b_t in the case of an unstable stratification ($\overline{\varrho w'T'} > 0$) and from b_t to I in stable conditions ($\overline{\varrho w'T'} < 0$). As shown in chapter 1 (eq. 32 on page 16) a PBL without radiative effects and without phase changes of the water vapor requires that the turbulent vertical flux of sensible heat is constant with height. That means that in unstable conditions the gain of energy b_t by the conversion $C_{(7)}\langle I, b_t\rangle > 0$ must be compensated by a loss at the top of the PBL. Such a loss is given by the turbulent vertical flux of b_t going through the upper border of the PBL; this flux must

therefore increase with height (it has a divergence). The opposite occurs in the stable case: almost all of the amount of energy, which is converted from b_t into I by the conversion term $-\overline{\varrho w'T'}\, g/\bar{T}$ must be put into the PBL through its upper border by $\overline{\varrho w''(v'')^2}/2$. That means that the turbulent vertical flux of b_t must be directed downward and has a convergence. The height, at which this flux changes its direction is possibly very low (for large $\overline{\varrho w'T'}$), but in the lowest part the flux is always directed upward.

It is quite interesting to look at the energy conversion rates as being "universal" (in the sense of universal profiles for Rossby-number similarity). If one non-dimensionalizes the eqs. (1) - (4) by multiplying these with the factor $\varkappa^2/(\bar{\varrho}\, f\, u_*^2)$ one obtains the eqs. (12) - (15) given on page 117.
Herein is $\mu = H/L_*$ the internal stability parameter (with $H = \varkappa u_*/f$ the internal scale height of the PBL and L_* the Monin-Obukhov stability-length), $\mathcal{E} = \varepsilon\varkappa^2/(f u_*^2)$, $\mathbb{V}_h = \varkappa \hat{v}/u_*$ $Z = z/H$, $\mathbb{T} = \tau/(\bar{\varrho} u_*^2)$, $B_t = b_t/(\bar{\varrho} u_*^2)$, $W = \varkappa w/u_*$ and $p_N = p/(\bar{\varrho} u_*^2)$. The budget for the turbulent kinetic energy, eq. (14), is in non-dimensional form

$$\frac{d}{dZ}\left\{\overline{W'B_t} + \overline{W'p_N'}\right\} + \mu + \mathcal{E}_t - \left(\mathbb{T}\cdot\frac{d\,\mathbb{V}_h}{dZ}\right) = 0 \qquad (16)$$

$|\mathbb{T}|$ as well as $|d\,\mathbb{V}_h/dZ|$ are universal profiles, i.e. profiles for which Rossby-number similarity exists. In the case of a vanishing divergence (first term in eq. 16) $\mathcal{E}_t(Z)$ must also be a universal profile since μ is constant with height in the PBL. $\mathcal{E}_t(Z)$ is generally considered to be a quantity the profile of which is universal even in the case that the divergence does not vanish. Presumably the first term in eq. (16) is also such a quantity for which Rossby - number similarity exists, since it consists of a vertical derivative. This would mean that all terms in eq. (16) are

$I = \bar{\varrho}\{c_v\hat{T}+\hat{\Phi}\}$	$b_m = \bar{\varrho}\,\frac{\hat{\mathbb{V}}^2}{2}$	$b_t = \varrho\,\overline{\frac{(v'')^2}{2}}$	$\bar{\varrho}\,L^*\,\hat{s}$
$-\frac{\varkappa}{u_*^3}\frac{d}{dZ}\{c_p\widehat{w''T''}\}$	$\frac{d}{dZ}(\mathbb{T}\cdot\mathbb{V}_h)$	$-\frac{d}{dZ}\{\overline{W''B_t}$	$-\frac{\varkappa}{u_*}\frac{d}{dZ}\{L^*\widehat{w''s''}\}$
$+\ d/dZ\{\overline{W'p_N'}\}$		$+\ \overline{W'p_N'}\}$	
$\mathbb{k}\cdot[\mathbb{V}_h\times\mathbb{V}_g]$	$-\ \mathbb{k}\cdot[\mathbb{V}_h\times\mathbb{V}_g]$		
μ		$-\ \mu$	
$\mathcal{E}_m$	$-\ \mathcal{E}_m$		
$\mathcal{E}_t$		$-\ \mathcal{E}_t$	
	$-\ (\mathbb{T}\cdot\frac{d\,\mathbb{V}_h}{dZ})$	$+\ (\mathbb{T}\cdot\frac{d\,\mathbb{V}_h}{dZ})$	
$-\frac{\varkappa^2 L^*}{f\,u_*^2}\,\delta\hat{s}$			$\frac{\varkappa^2 L^*}{f\,u_*^2}\,\delta\hat{s}$
$-\ \frac{\varkappa}{u_*^3}\frac{d}{dZ}\{\bar{R}_z/\bar{\varrho}\}$			
$= 0$	$= 0$	$= 0$	$= 0$
(12)	(13)	(14)	(15)

universal profiles. This is different for the budget, eq. (13), of the kinetic energy of the mean motion:

$$\left(\mathbb{V}_h\cdot\frac{d\,\mathbb{T}}{dZ}\right) - \mathbb{k}\cdot[\mathbb{V}_h\times\mathbb{V}_g] - \mathcal{E}_m = 0 \qquad (17)$$

The third term in this equation is very small compared with the two other terms, it can be neglected. The two first terms both contain $\mathbb{V}_h(Z)$ which of course is not a universal pro-

file but depends still on the external parameters.(The vertical derivative of the non-dimensional velocity only is a quantity for which Rossby-number similarity exists). The two non-dimensional velocity components are

$$U = P - M_m(\mu, \lambda_x, \lambda_y) + \lambda_x Z + \ln(C_g\ RO_o) \tag{18a}$$

$$V = Q - N(\mu, \lambda_x, \lambda_y) + \lambda_y Z \tag{18b}$$

where $U = \varkappa \hat{u}/u_*$, $V = \varkappa \hat{v}/u_*$, $P = \varkappa(\hat{u}-\hat{u}_g)/u_*$ and $Q = \varkappa(\hat{v}-\hat{v}_g)/u_*$; $\lambda_x = \varkappa^2/f\ d\hat{u}_g/dz$ and $\lambda_y = \varkappa^2/f\ d\hat{v}_g/dz$ are the internal parameters for the baroclinicity. M_m and N are universal functions which appear in the resistance law of a PBL. $C_g = u_*/|\hat{v}_{go}|$ is the geostrophic drag coefficient and $RO_o = |\hat{v}_{go}|/(f\ z_o)$ is the surface Rossby-number. The coordinate system is orientated with the x-axis in the direction of the surface stress τ_o .
The influence of the external parameters appears in the last term of eq. (18a).
Although the budget of the turbulent kinetic energy (nondimensionalized by internal parameters) is "universal", i.e. is independent of external parameters, the budget of the kinetic energy of the mean motion depends on external parameters.

A final remark should be made referring to the Richardson-number. The Richardson-flux-number is obtained by dividing the second term in eq. (16) by the fourth term of this equation

$$Ri_f = \frac{\mu}{\left(\mathbb{T} \cdot \frac{d\mathbb{V}_h}{dZ}\right)} \tag{19}$$

Since in a barotropic PBL the two quantities $\mathbb{T}(Z)$ as well as $d\mathbb{V}_h/dZ\ (Z)$ decrease with height, the Richardson-flux-number must increase monotonically with height and become infinite at the top of the PBL.

To each stratification parameter μ belongs a "universal" profile $Ri_f(Z)$, i.e. a profile, which is independent of the external parameters.

References:

BERNHARDT, K. 1972 Zum Energieumsatz in der atmosphärischen Grenzschicht
Gerl. Beitr. Geophys.,Leipzig (GDR) 81, 341-354

IZUMI, Y. 1971 Kansas 1968 Field Program Data Report
AFCRL Meteor.Lab., Bedford Mass., Proj. 7655, Envir.Res.Pap. Nr. 379 pp 79+VIII

KRAUS, H. 1972 A Note on the Definition of the Surface Boundary Layer
Beitr.Phys.Atm. 45, 185-195

LETTAU, H.H.
HOEBER, H. 1964 Über die Bestimmung der Höhenverteilung von Schubspannung und Austauschkoeffizient in der atmosphärischen Reibungsschicht
Beitr.Phys.Atm. 37, 105-118

LUMLEY, J.L.
PANOFSKY, H.A. 1964 The Structure of Atmospheric Turbulence
Interscience Publishers, New York pp 239 + XI; p 120-126

WYNGAARD, J.C.
COTÉ, O.R. 1971 The Budget of Turbulent Kinetic Energy and Temperature Variance in the Atmospheric Surface Layer
J.Atm.Sci. 28, 190-201

Layers with a Reduced Eddy Viscosity Caused by the Baroclinicity

Schichten mit vermindertem Austausch verursacht durch Baroklinität

F. Wippermann and D. Yordanov*)

Technical University Darmstadt, Germany, Department of Meteorology

Received December 21, 1971

Summary: Investigations with a model of the planetary boundary layer have shown that certain baroclinicities cause a minimum in the vertical profile of the Reynolds' stress. Such a minimum occurs together with one in the vertical profile of the eddy viscosity. The height, at which it occurs, and the rate, by which K_m is reduced, depend on the direction and on the value of the thermal wind as well as on the thermal stratification.

The results have been verified by observations.

Zusammenfassung: Durch Untersuchungen mit einem Modell für die planetarische Grenzschicht ließ sich zeigen, daß für bestimmte Baroklinitäten ein Minimum im Vertikalprofil der Reynolds'schen Schubspannung auftritt. Dieses Minimum ist gekoppelt mit einem solchen im Vertikalprofil des Austausches K_m. Die Höhe, in welcher es auftritt, und sein Betrag hängen ab von Richtung und Betrag des thermischen Windes und von der thermischen Schichtung.

Die Ergebnisse wurden mit Beobachtungen belegt.

Résumé: Des recherches avec un modèle de couche-limite planétaire ont montré que, pour certaines baroclinies, un minimum apparaît dans le profil vertical de la tension de Reynolds. Ce minimum est associé à un minimum dans le profil vertical de la viscosité turbulente K_m. La hauteur où cela se produit et le taux de réduction de K_m dépendent de la direction et de l'intensité du vent thermique, ainsi que de la stratification thermique. Les résultats ont été confirmés par les observations.

Computations with a numerical model for a diabatic and baroclinic planetary boundary layer (PBL) have shown, that for special baroclinic structures a pronounced minimum appears in the vertical profile of the eddy viscosity. Such a minimum occurs mostly in a relatively thin layer, the layers are observed in the upper part of the PBL above a height of 200–300 m. Since they can act as a barriere for a process of turbulent diffusion in the vertical direction, this may be important mainly for diffusion processes from tall stacks. Besides others this is one reason why it seems to be useful to present some considerations about such minima in the eddy viscosity.

---

*) On leave from the Bulgarean Academy of Science, Department of Geophysics, Sofia, on a fellowship by the A. v. Humboldt-Foundation.

The PBL-model consists of the following equations:

$$d^2Y/dZ^2 = X/K_m - \lambda_x \tag{1}$$

$$d^2X/dZ^2 = -Y/K_m + \lambda_y \tag{2}$$

$$K_m = T^{1/2}\, L/\kappa, \quad T = (X^2 + Y^2)^{1/2} \tag{3}$$

$$L = L_\infty - (L_\infty - L_0)\, T^p \tag{4}$$

$$p = -\frac{\kappa - L_0\,[2\,(dT/dZ)_0^2 + (dT/dZ)_0/2]}{(dT/dZ)_0\,[L_\infty - L_0]}$$

Eq. (1) and eq. (2) are the equations for a baroclinic PBL (steady state, horizontally homogeneous) after elimination of the velocity components. Eq. (3) is a combination of the flux-gradient relation

$$T = K_m\, |dV/dZ| \tag{5}$$

and of Prandtl's mixing-length equation

$$K_m = L^2/\kappa^2\, |dV/dZ| \tag{6}$$

Finally eq. (4) is a mixing-length hypothesis, WIPPERMANN (1971), it is made in order to close the system of the equations.

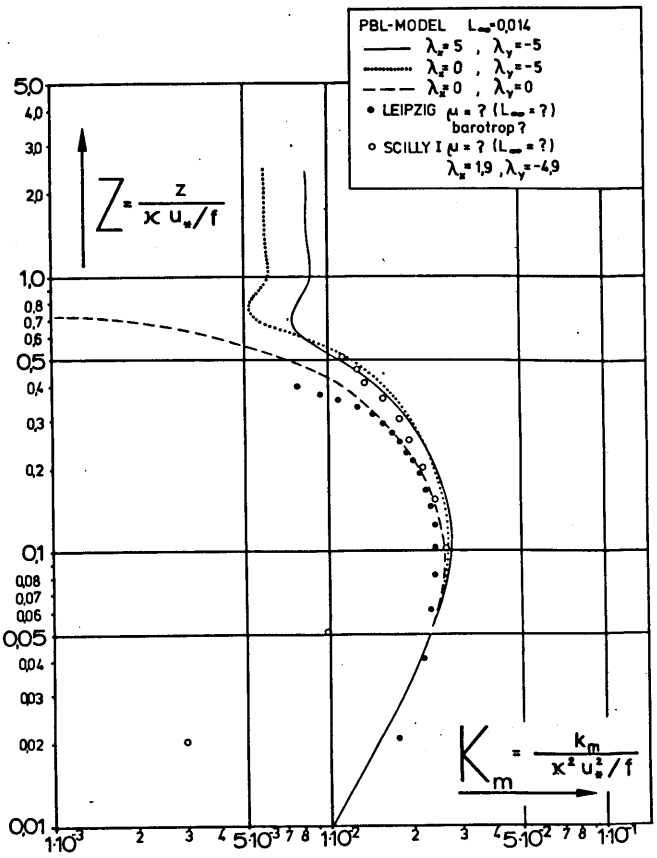

Fig. 1/Bild 1

The symbols have the following meaning: $X=\tau_x/\bar{\rho}u_*^2$ and $Y=\tau_y/\bar{\rho}u_*^2$ are the two non-dimensional components of the Reynolds' stress with u_* the friction velocity, $K_m=k_m/(\kappa^2 u_*^2/f)$ is the non-dimensional eddy viscosity and $Z=z/H$ is the non-dimensional height coordinate with $H=\kappa u_*/f$ the internal scale height of the PBL. $\lambda_x=dU_g/dZ$ and $\lambda_y=dV_g/dZ$ are the internal parameters for the baroclinicity assumed (in the model) to be constant with height. $U_g=\kappa u_g/u_*$ and $V_g=\kappa v_g/u_*$ are the non-dimensional components of the geostrophic wind. The coordinate system is orientated with the x-axis in the direction of the surface stress vector τ_0. It is $L=l/H$ the non-dimensional mixing-length, which has the value L_0 at the lower boundary ($Z=Z_0$) and approaches the asymptotic value L_∞ for $Z\to\infty$. It is the value of L_∞ which governs the influence of the thermal stratification on $K_m(Z)$, $T(Z)$ and the other vertical profiles. κ denotes the Karman constant.

At the upper boundary ($Z\to\infty$) is in the baroclinic case

$$|dV/dZ| = |dV_g/dZ| = (\lambda_x^2+\lambda_y^2)^{1/2}$$

and therefore according to eq. (6)

$$K_{m,\infty} = L_\infty^2/\kappa^2(\lambda_x^2+\lambda_y^2)^{1/2} \tag{7}$$

This asymptotic value of K_m has been given by BLACKADAR (1965) already. Using this value in eq. (5) one obtains

$$T_\infty = L_\infty^2/\kappa^2(\lambda_x^2+\lambda_y^2) \tag{8}$$

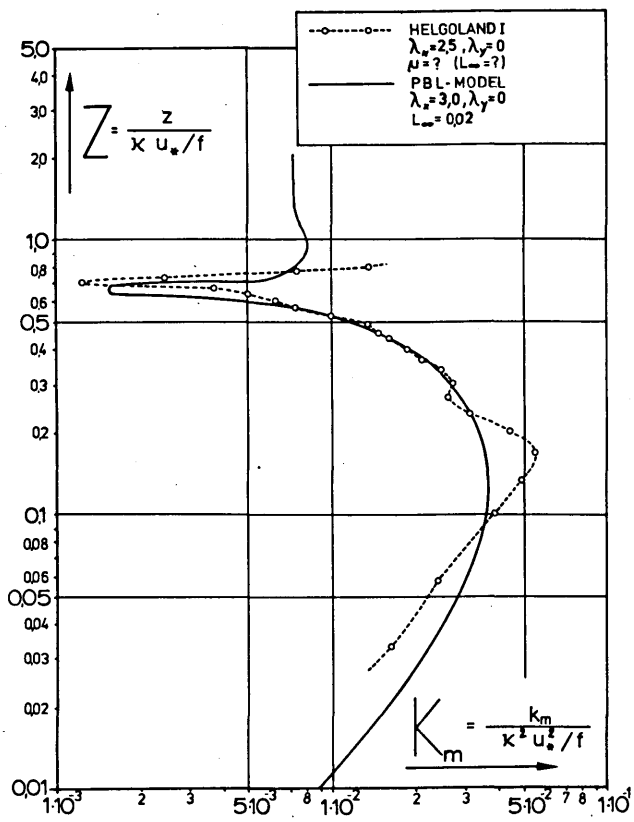

Fig. 2/Bild 2

which is a asymptotic value of the Reynolds' stress for $Z \to \infty$. The lower boundary condition for the stress T is

$$Z = Z_0: \; T_0 = 1, \quad (dT/dZ)_0 = -N \tag{9}$$

where N is a universal function (of the thermal stratification and of the baroclinicity) almost every time positive appearing in the resistance law for a PBL, see YORDANOV and WIPPERMANN (1972).

In a barotropic ($\lambda_x = \lambda_y = 0$) PBL it can be shown (WIPPERMANN 1971), that T decreases monotonically with height and approaches the asymptotic value $T_\infty = 0$, see eq. (8). In the baroclinic case, however, it is possible, that $T_\infty \geqslant T_0$; this means with respect to the condition (9) that at least one minimum of T must occur.

Regarding eq. (3) one can expect, that a minimum of T implies also a minimum of K_m, since the mixing-length L has almost reached its asymptotic value L_∞ in the height of the minimum. Because of the mixing-length hypothesis (4), which contains the stress T itself, the minimum in K_m will be less pronounced than the minimum obtained with a mixing-length hypothesis $L = L(Z)$, for instance BLACKADAR (1962). This is one of the advantages the authors see for the mixing-length hypothesis eq. (4).

The figures 1–7 show some results obtained by numerical integrations with the PBL-model mentioned before.

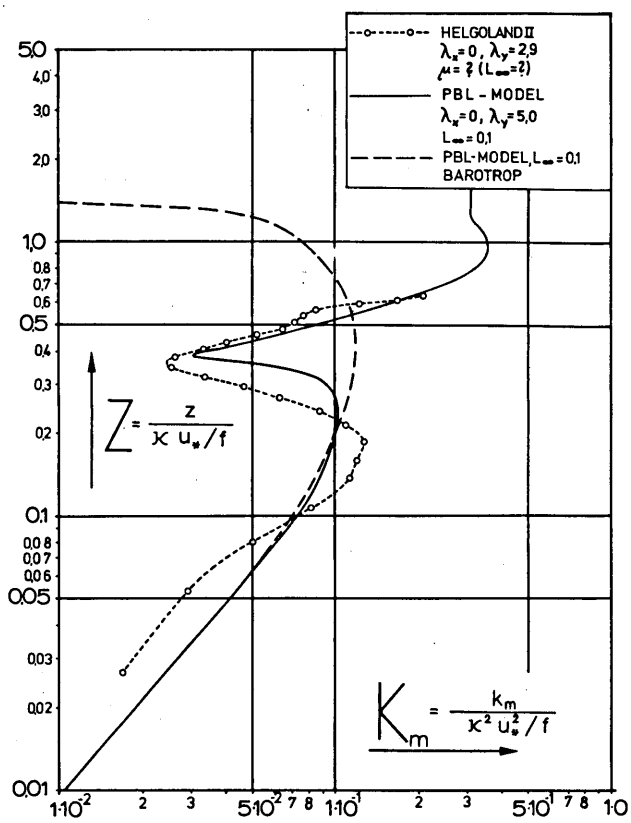

Fig. 3/Bild 3

Figure 1 shows for a neutral PBL the differences in the K_m-profiles for the barotropic case (broken line) and two baroclinic cases (solid line and dotted line). The eddy viscosity as well as the height Z are non-dimensionalized by internal parameters, which means that the K_m-profiles can be considered as universal, see YORDANOV and WIPPERMANN (1972). This enables to compare such profiles with any set of observational data, if these data are made dimensionless in the same way. In the figure 1 the full circles are observations, the Leipzig wind profile (MILDNER 1932), evaluated by LETTAU (1950), the open circles are observations from the Scilly Island (SHEPPARD, CHARNOCK, FRANCIS 1952) also evaluated by LETTAU (1957).

In figure 2 and figure 3 the circles represent (nondimensional) observational data obtained from the wind profiles Helgoland I and Helgoland II by LETTAU and HOEBER (1964). They are compared with the universal profiles $K_m(Z)$ obtained by the PBL-model for an appropriate thermal stratification. The thermal stratification has not been measured or determined for the two wind profiles, but the comparison with the model shows, that for Helgoland I a slightly unstable stratification ($L_\infty = 0.02$) and for Helgoland II an unstable stratification ($L_\infty = 0.1$) must be assumed.

One notices from figure 3 that the eddy viscosity in the minimum is redúced to a value of about 1/3 of the value in the barotropic case. The minimum of the K_m-profile Helgoland II is located at $Z = 0.35$, i. e. in this case 320–330 m.

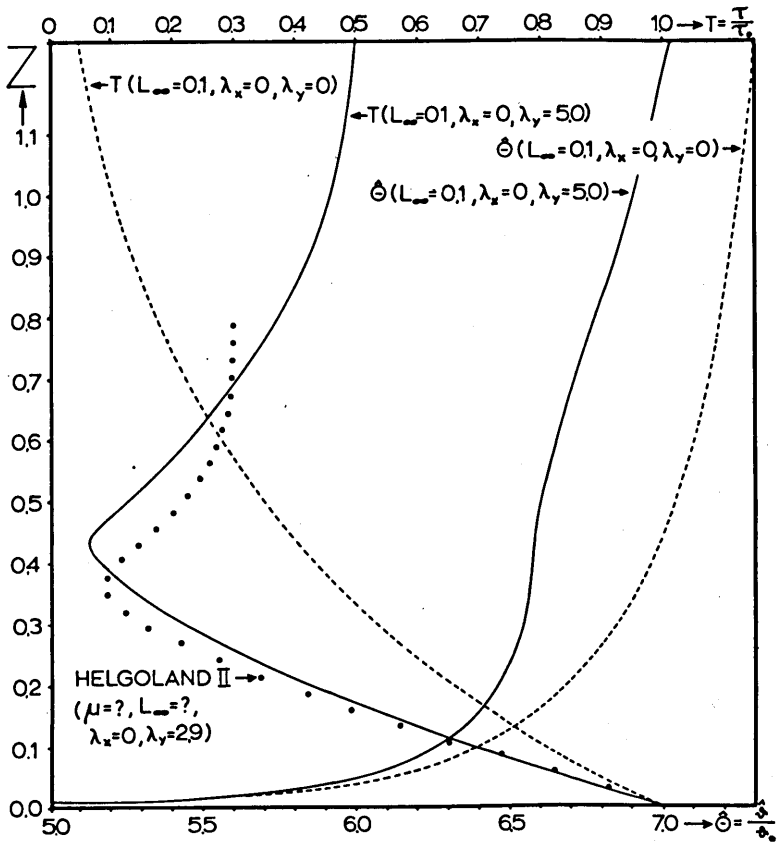

Fig. 4/Bild 4

In figure 4 the stress profile Helgoland II is shown by the dots; it is compared with the universal stress profile for a baroclinic ($\lambda_x = 0$, $\lambda_y = 5.0$) PBL and for a barotropic ($\lambda_x = \lambda_y = 0$) one, both obtained by the PBL-model. One notices that the baroclinic stress profile, observed as well as computed, has also a minimum at the height, where K_m is a minimum. Figure 4 contains also two universal profiles $\hat{\Theta} = \hat{\vartheta}/\vartheta_*$ representing the non-dimensional deviation of the potential temperature from the temperature at the ground ($Z = Z_0$). The broken line is the profile for the barotropic case, the solid line that one for the baroclinic ($\lambda_x = 0$, $\lambda_y = 5.0$) case. Since the temperature for the non-dimensionalization $\vartheta_* = -q_0/(\kappa c_p \bar{\rho} u_*)$ is negative in the unstable case ($L_\infty = 0.1$, $q_0 > 0$), the two profiles mean, that the potential temperature decreases monotonically with height. This decreasing is fastest in the surface layer, at the top of the PBL the profile (in the barotropic case) tends to a neutral one, i. e. $\hat{\Theta}$ approaches a constant value. In the baroclinic case the thermal stratification is less unstable and almost neutral in that layer in which K_m and T have their minimum. However, it is impossible to get a temperature inversion in this layer; this means, that a reduced eddy viscosity of this kind and therefore also a reduced turbulent diffusion is caused by the baroclinicity only and not by the thermal stratification.

The universal profiles of the potential temperature have been computed by the formula

$$\hat{\Theta}(Z) - \hat{\Theta}(Z_0) = \int_{Z_0}^{Z} \frac{\Phi_h}{\Phi_m} \frac{T}{K_m} \, dZ \tag{10}$$

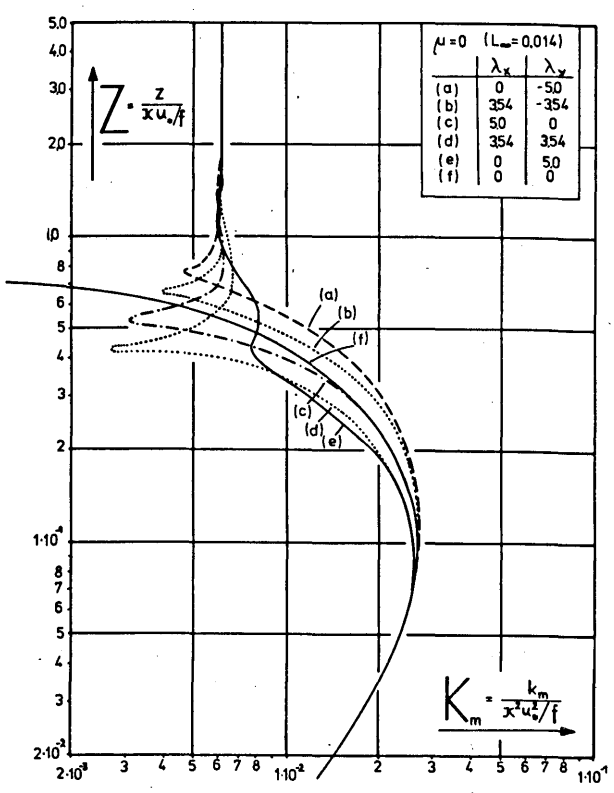

Fig. 5/Bild 5

with

$$\frac{\Phi_h}{\Phi_m} = 0.74\,\frac{1+6.35\,\mu Z}{1+4.7\,\mu Z} \quad \text{stable } (\mu>0)$$

$$\frac{\Phi_h}{\Phi_m} = 0.74\,\frac{[1-15\,\mu Z]^{1/4}}{[1-9\,\mu Z]^{1/2}} \quad \text{unstable } (\mu<0)$$

where μ is the internal parameter for the thermal stratification

$$\mu = H/L_* \tag{11}$$

L_* is the Monin-Obukhov stability-length. The derivation and a discussion of formula (10) will be given in another paper.

The minimum in the K_m-profile is caused by the baroclinicity, since a certain baroclinicity dV_g/dZ diminishes the vertical wind shear dV/dZ of the PBL. This effect is modified by the thermal stratification. In the figures 5, 6 and 7 the influence of the baroclinicity as well as of the thermal stratification is considered.

In figure 5 the K_m-profiles are displayed for the neutral case ($\mu=0$) but for different baroclinicities. One notices that the influence of the baroclinicity disappears below $Z \sim 0.07$ whereas the influence of the thermal stratification reaches farer down, see figure 6 and 7. In the neutral case (fig. 5) the minimum

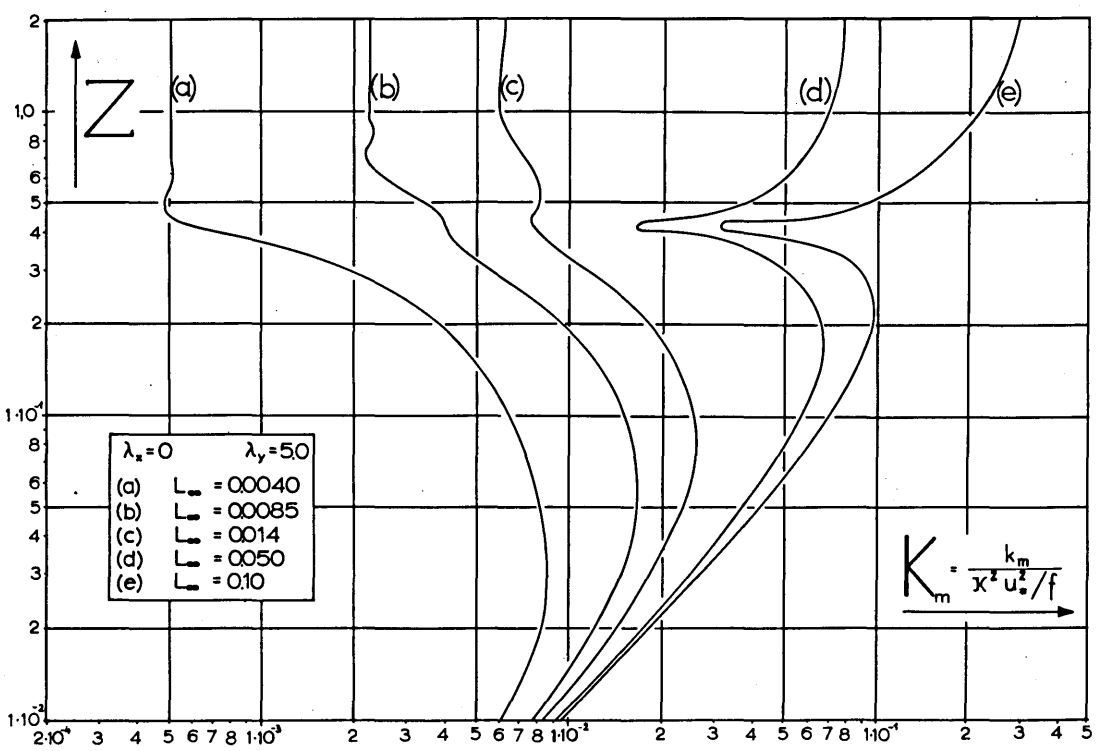

Fig. 6/Bild 6

is most pronounced for the baroclinic condition (d) where the thermal wind is directed to the left of the geostrophic wind $\hat{\mathbb{V}}_{g0}$ (cold air advection). As more as the thermal wind turns to the right (passing through the direction of the geostrophic wind $\hat{\mathbb{V}}_{g0}$), the minimum becomes weaker and it is located at a higher level. It should be mentioned, that the direction of the x-axis does not coincide with the direction of the geostrophic wind $\hat{v}_{g0}$ but differs from it by the cross-isobar angle α_0. For the purpose of a comparison also the K_m-profile in the barotropic case (f) is given.

In figure 6 ($\lambda_x = 0$, $\lambda_y = 5.0$; cold air advection) and in figure 7 ($\lambda_x = 5.0$, $\lambda_y = 0$; thermal wind parallel to the surface wind) the influence of the thermal stratification is investigated. The case (a), $L_\infty = 0.0040$, means an extremely stable stratification, (b) with $L_\infty = 0.0085$ a stable one and (c), $L_\infty = 0.014$, the neutral case. $L_\infty = 0.050$ denotes an unstable case (d) and finally $L_\infty = 0.10$ (e) a rather strong unstable stratification. For the considered cold air advection (fig. 6) the minimum in the K_m-profile occurs only for an unstable stratification, in the neutral case it is not strongly marked and it disappears for the stable stratifications. However in the case of a thermal wind parallel to the surface wind (fig. 7) the minimum occurs only for a neutral (c) and for a slightly stable (b) stratification.

Acknowledgments

The authors wish to thank Dipl. Met. ETLING and Dipl. Met. LEYKAUF for doing the computational work.

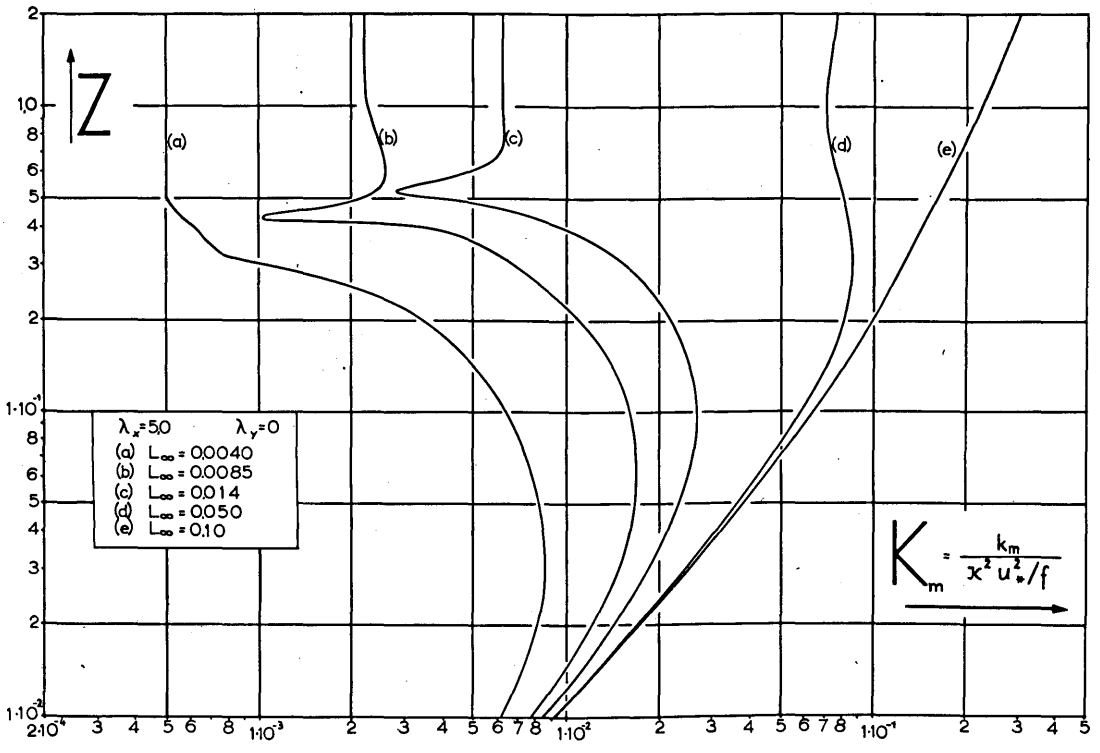

Fig. 7/Bild 7

References

BLACKADAR, A. K. (1962): The vertical distribution of wind and turbulent exchange in a neutral atmosphere. J. Geophys. Res. **67**, 3095–3102

BLACKADAR, A. K. (1965): A single layer theory of the vertical distribution of wind in a baroclinic neutral atmospheric boundary layer. Final Rep. AFCRL–65–531 Part I, 1–22, Pensyl. State Univ., Dept. of Meteor.

LETTAU, H. H. (1950): A re-examination of the "Leipzig wind profile" considering some relations between wind and turbulence in the frictional layer. Tellus **2**, 125–129

LETTAU, H. H. (1957): Windprofil, Innere Reibung und Energieumsatz in den unteren 500 m über dem Meer. Beitr. Phys. Atm. **30**, 78–96

LETTAU, H.H. and HOEBER, H. (1964): Über die Bestimmung der Höhenverteilung von Schubspannung und Austauschkoeffizient in der atmosphärischen Reibungsschicht. Beitr. Phys. Atm. **37**(2), 105–118

WIPPERMANN, F. (1971): The eddy viscosity in a barotropic planetary boundary layer as related to the turbulent kinetic energy. Beitr. Phys. Atm. **44**, 127–136

WIPPERMANN, F. (1971): A mixing-length hypothesis for the planetary boundary layer flow in the atmosphere. Beitr. Phys. Atm. **44(4)**, 215–226

YORDANOV, D. and WIPPERMANN, F. (1972): The parameterization of the turbulent fluxes of momentum, heat and moisture at the ground in a baroclinic planetary boundary layer. Beitr. Phys. Atm. **45(1)**, 58–65.

The Wind Profile Very Close to the Ground

Das Windprofil in unmittelbarer Nähe des Erdbodens

F. Wippermann

Technical University Darmstadt, Germany

Received 4 January 1973

Summary: The wind profile in a planetary boundary layer (steady state, horizontally homogenenous) is logarithmic (or log + linear for the diabatic case) in the nearest neighbourhood of the ground. This result is derived without any additional hypothesis but only using the boundary layer equations. Since the stress is not constant with height in the planetary boundary layer, the eddy viscosity k_m cannot increase linearly with height as required for a constant stress layer; this will be discussed.

Zusammenfassung: In einer planetarischen Grenzschicht (stationär, horizontal homogen) hat das Windprofil in unmittelbarer Nähe des Erdbodens eine logarithmische Form bzw. bei nicht-neutraler Schichtung diejenige eines log + linear Profiles. Dieses Ergebnis wird ohne eine weitere Hypothese abgeleitet, es werden nur die Grenzschichtgleichungen benutzt. Da in der planetarischen Grenzschicht die Schubspannung nicht konstant mit der Höhe ist, kann sich auch der turbulente Diffusionskoeffizient k_m nicht linear mit der Höhe ändern, wie das bei Vorgabe einer höhenkonstanten Schubspannung erforderlich wäre; diese Verhältnisse werden erörtert.

Résumé: Dans une couche limite planétaire (stationnaire, horizontalement homogène) le profil du vent à proximité immédiate du sol a une forme logarithmique, resp., dans le cas d'une disposition par couches non-adiabatiques, celle d'un profil log + linéaire. Ce résultat est déduit sans autre hypothèse; seules des equations de couches linéaires ont été employées. Comme dans une couche limite planétaire l'effort de cisaillement n'est pas constant dans la verticale, le coefficient de diffusion turbulente k_m ne peut se modifier de facon linéaire dans la verticale, comme exigé par un effort de cisaillement constant. Ces rapports sont discutes.

1. List of symbols

$C_g =$ $u_*/|\hat{v}_{go}|$ Geostrophic drag coefficient

$d =$ Zero-plane displacement

$f =$ Coriolis parameter

$H =$ $\kappa\, u_*/f$ Internal scale height of the planetary boundary layer

$k_m =$ Eddy viscosity

$K_m =$ $k_m/(H^2 f)$ Non-dimensional eddy viscosity

$L_* =$ Monin-Obukhov stability length

$\left.\begin{matrix} M_m \\ N \end{matrix}\right\} = \left\{\begin{matrix} \text{Universal functions in the resistance law of the planetary} \\ \text{boundary layer} \end{matrix}\right.$

$P =$ $\kappa\,(\hat{u} - \hat{u}_g)/u_*$ Non-dimensional velocity defect, x-component

$Q =$ $\kappa\,(\hat{v} - \hat{v}_g)/u_*$ Non-dimensional velocity defect, y-component

$Ro_0 =$ $|\hat{v}_{go}|/(f\, z_0)$ Surface Rossby number

Beiträge zur Physik der Atmosphäre, 46. Band, 1973, S. 57–63

$U =$ $\kappa\, \hat{u}/u_*$ Non-dimensional velocity, x-component
$u_* =$ friction velocity
$V =$ $\kappa\, \hat{v}/u_*$ Non-dimensional velocity, y-component
$\hat{u}, \hat{v} =$ Velocity components
$X =$ $\tau_x/(\bar{\rho}\, u_*^2)$ Non-dimensional stress, x-component
$Y =$ $\tau_y/(\bar{\rho}\, u_*^2)$ Non-dimensional stress, y-component
$x, y =$ Horizontal coordinates, x has the direction of the surface stress
$z =$ Vertical coordinate
$Z =$ z/H Non-dimensional vertical coordinate
$\alpha_0 =$ Cross-isobar angle
$\eta =$ $(Z - Z_0)/K_{mo}$
$\kappa =$ Von Karman's constant
$\lambda_x =$ dU_g/dZ } Internal parameter for the baroclinicity
$\lambda_y =$ dV_g/dZ }
$\rho =$ Density
$\mu =$ H/L_* Internal parameter for the thermal stratification
$\phi_m =$ $Z\, dU/dZ$ Non-dimensional profile function
$\tau_x, \tau_y =$ Components of the Reynolds stress

Indices:

ad = adiabatic g = geostrophic
o = at the ground m = for momentum

Differentiation:

$(\,)' = d(\,)/dZ$, $(\,)^{(n)} = d^n(\,)/dZ^n$

2. Introduction

Almost all authors in the field of the atmospheric boundary layer claim that the wind profile is logarithmic in the layer close to the ground if this layer has a neutral stratification and is barotropic. In order to derive the logarithmic profile they use assumptions beside the usual ones (stationarity, horizontal homogeneity); by such assumptions or hypotheses the logarithmic form of the profile is already implied. Examples of such assumptions are: no variation of wind direction with height, constant stress and/or linear variation of the mixing-length with height, the auto-model hypothesis or other similarity arguments. One does not find any derivation which makes use of the boundary layer equations

$$f\,\bar{\rho}(\hat{u} - \hat{u}_g) = d\,\tau_y/dz \tag{1a}$$

$$-f\,\bar{\rho}(\hat{v} - \hat{v}_g) = d\,\tau_x/dz \tag{1b}$$

or in the non-dimensional notation

$$P = Y' \tag{2a}$$

$$Q = -X' \tag{2b}$$

Of course the system (2a), (2b) is not closed, even not when in addition the two equations of the flux-gradient relation

$$\tau_x = \bar{\rho}\, k_m\, d\hat{u}/dz \tag{3a}$$

$$\tau_y = \bar{\rho}\, k_m\, d\hat{v}/dz \tag{3b}$$

or in non-dimensional notation

$$X = K_m (P' + \lambda_x) \tag{4a}$$

$$Y = K_m (Q' + \lambda_y) \tag{4b}$$

are used; a hypothesis is still necessary to close the system. However if one restricts the consideration to the profile very close to the ground this profile can be derived without a further hypothesis. It is the purpose of this paper to show that.

3. The derivatives of the stress components at $z = z_0$

The lower boundary conditions belonging to the eqs. (1a), (1b) are:

$$z = z_0: \quad \hat{u} = \hat{v} = 0 \tag{5a}$$

$$\tau_x = \bar{\rho}\, u_*^2,\ \tau_y = 0 \tag{5b}$$

or in the non-dimensional notation

$$Z = Z_0: \quad U = V = 0 \tag{6a}$$

$$X_0 = 1 \tag{6b}$$

$$Y_0 = 0 \tag{6c}$$

The condition (6a) implies

$$P_0 = -U_{go} = -\kappa/u_* \,|\hat{w}_{go}|\cos(\alpha_0) = -\kappa/C_g \cos(\alpha_0) = \\ = M_m(\mu, \lambda_x, \lambda_y) - \ln(Ro_0\, C_g) \tag{7a}$$

$$Q_0 = -V_{go} = -\kappa/u_* \,|\hat{w}_{go}|\sin(\alpha_0) = \kappa/C_g \sin(|\alpha_0|) = N(\mu, \lambda_x, \lambda_y) \tag{7b}$$

In the eqs. (7a), (7b) the "resistance law" of a diabatic baroclinic planetary boundary layer has been used, see YORDANOV and WIPPERMANN (1972). It states that M_m and N are universal functions, i.e. they do not depend on any external parameter but depend only on the internal parameter μ for the thermal stratification and on two internal parameters λ_x and λ_y for the baroclinicity. – One should remember that the derivation of the resistance law itself makes use of a logarithmic wind profile at least at $z = z_0$. However this is insignificant for the further derivation here.

The first derivatives of the stress components are given by (2a) and (2b), namely $X'_0 = -Q_0$ and $Y'_0 = P_0$. In order to obtain the higher derivatives the velocity defect P should be eliminated in the eqs. (2a) and (4a) and the defect Q in the eqs. (2b) and (4b); one gets

$$X'' = -Y/K_m + \lambda_y \tag{8a}$$

$$Y'' = X/K_m - \lambda_x \tag{8b}$$

The second derivatives are therefore: $X''_0 = \lambda_y$ and $Y''_0 = 1/K_{mo} - \lambda_x$. Higher derivatives are obtained by differentiationg the eqs. (8a) and (8b); of course in the obtained expressions appear K_{mo} and derivatives of it, which one does not know. One obtains:

$$\left.\begin{array}{ll}
X_0 = 1 & Y_0 = 0 \\
X'_0 = -Q_0 & Y'_0 = P_0 \\
X''_0 = \lambda_y & Y''_0 = 1/K_{mo} - \lambda_x \\
X'''_0 = -P_0/K_{mo} & Y'''_0 = -Q_0/K_{mo} - K'_{mo}/K^2_{mo} \\
X^{IV}_0 = 2P_0K'_{mo}/K^2_{mo} - & Y^{IV}_0 = 2Q_0K'_{mo}/K^2_{mo} + 2(K'_{mo})^2/K^3_{mo} - \\
\quad - 1/K^2_{mo} + \lambda_x/K_{mo} & \quad - K''_{mo}/K^2_{mo} + \lambda_y/K_{mo}
\end{array}\right\} \quad (9)\,(10)$$

4. The wind profile close to the ground

Let's consider first the wind component in the direction of the surface stress. U(Z) can be expanded in a Taylor serie at the point $Z = Z_0$:

$$U(Z) = \sum_n U_0^{(n)} (Z - Z_0)^n/n! \qquad n = 1, 2, 3, \ldots \tag{11a}$$

The undifferentiated velocity vanishes because of eq. (6a). In the barotropic case ($\lambda_x = \lambda_y = 0$), which now will be assumed, $U^{(n)} = P^{(n)}$ and with eq. (2a) one has $U^{(n)} = Y^{(n+1)}$; it follows

$$U(Z) = \sum_n Y_0^{(n+1)} (Z - Z_0)^n/n! \qquad n = 1, 2, 3, \ldots \tag{11b}$$

Using the expressions (10) in eq. (11b) one obtains with the abbreviation $\eta \equiv (Z - Z_0)/K_{mo}$

$$\begin{aligned} U(Z) = {} & \eta - [Q_0K_{mo} + K'_{mo}]\,\eta^2/2 + \\ & + K'_{mo}\,[Q_0K_{mo} + K'_{mo}]\,\eta^3/3 - K''_{mo}K_{mo}\,\eta^3/6 \pm \ldots \end{aligned} \tag{11c}$$

Adding and subtracting the term $[Q_0K_{mo} + K'_{mo}]\,\eta$ one finds the expansion of the $\ln(1 + \eta)$; it results

$$\begin{aligned} U(Z) = {} & [Q_0K_{mo} + K'_{mo}]\ln(1 + \eta) + [1 - Q_0K_{mo} - K'_{mo}]\,\eta - \\ & - [K''_{mo}K_{mo}/2 + (1 - K_{mo})[Q_0K_{mo} + K'_{mo}]]\,\eta^3/3 + 0(\eta^4) \end{aligned} \tag{12}$$

Actually this profile (12) is valid only in the nearest neighbourhood of Z_0 since the expansion for the $\ln(1 + \eta)$ converges only if $\eta \leqslant 1$, this means because of $K_{mo} \approx Z_0$ for the range $Z_0 \leqslant Z < 2Z_0$. Unfortunately one does know neither the value of K_{mo}, which probably varies

with the thermal stratification, nor the values of the derivatives K'_{mo} and K''_{mo}. Therefore it is reasonable to use the profile function ϕ_m instead K_m since one has some observational evidence for the former. ϕ_m is defined as

$$\phi_m = \kappa z/u_* \, d\hat{u}/dz \tag{13a}$$

or in the non-dimensional notation

$$\phi_m = Z\,U' \tag{13b}$$

Eq. (4a) is in the barotropic case reduced to

$$X = K_m\,P' = K_m\,U' \tag{14}$$

Eliminating U' from the eqs. (13b) and (14) one gets

$$K_m = Z\,X/\phi_m \tag{15}$$

which is with respect to eq. (6b) at $Z = Z_o$

$$K_{mo} = Z_o/\phi_{mo} \tag{16}$$

Differentiating eq. (15) and making use of the eqs. (6b), (9) together with (7b), (16) one obtains

$$K'_{mo} = \{1 - [N(\mu) + \phi'_{mo}/\phi_{mo}]\,Z_0\}/\phi_{mo} \tag{17}$$

The expressions (16) and (17) are used to replace K_{mo} and K'_{mo} in eq. (12); the argument of the logarithme has to be transformed also:

$$1 + \eta = 1 + (Z - Z_o)/K_{mo} = \phi_{mo}\,[Z - Z_o\,(1 - 1/\phi_{mo})]/Z_o \tag{18}$$

If the second term in the interior brackets is considered as a zero-plane displacement d

$$d = Z_o - Z_{oo} = Z_o\,[1 - 1/\phi_{mo}] \tag{19a}$$

it follows

$$Z_o = \phi_{mo}\,Z_{oo} \tag{19b}$$

Using the eqs. (16), (17), (19a) and (19b) in eq. (12) this equation reads then:

$$\begin{aligned} U(Z) = {} & 1/\phi_{mo}\,\{1 - Z_o\,\phi'_{mo}/\phi_{mo}\}\,\ln[(Z - d)/Z_{oo}] + \\ & + [(\phi_{mo} - 1)/Z_o + \phi'_{mo}/\phi_{mo}]\,(Z - Z_o) + 0(\eta^3) \end{aligned} \tag{20}$$

The term containing the second derivative of K_{mo} has been not considered any more, since nothing is known about this second derivative. Its value is probably very small, in a constant stress layer it would be exactly zero. Also the other term associated with η^3 remains disregarded, since $1 - K'_{mo}$ is very small; it vanishes in a constant stress layer. The power of the disregarded terms is lowered therefore by one.

In a procedure analog to (11a)–(11c) the following profile of the V-component is obtained

$$\begin{aligned} V(Z) = {} & -P_oZ_o/\phi_{mo}\,\{1/2\,[\phi_{mo}\,(Z - Z_o)/Z_o]^2 + 1/3\,[\phi_{mo}\,(Z - Z_o)/Z_o]^3\,[1 - \\ & - N(\mu)\,Z_o + \phi'_{mo}/\phi_{mo}\,Z_o - \phi'_{mo}/2P_o]/\phi_{mo}\} + 0(\eta^4) \end{aligned} \tag{21}$$

It is worth noting, that there is a remarkable difference between the U(Z) and the V(Z), the latter profile does not contain a linear term; its lowest order of $(Z - Z_o)$ is quadratic. The V-component is much smaller than the U-component.

5. The profile function ϕ_m and its first derivative at $z = z_o$

An extensive study of the profile function ϕ_m has been made recently by BUSINGER, WYNGAARD, IZUMI and BRADLEY (1971) using the data obtained in Kansas in summer 1968. The authors obtained for a neutral stratification $\phi_{mo,ad} = 1.15$ and they concluded that the von Karman constant must be 0.35 instead 0.40 which value is commonly used. This conclusion is made since $\phi_{mo,ad} = 1.0$ is required; of course this requirement is based on the assumption of a constant stress layer with a logarithmic wind profile. Such a requirement cannot be maintained in the planetary boundary layer, where the stress has its largest decrease with height at the ground. However also eq. (20), valid in a planetary boundary layer with decreasing stress, requires $\phi_{mo,ad} = 1.0$; differentiating eq. (20) once and inserting U′ in eq. (13b) applied at $Z = Z_o$ gives

$$\phi_{mo,ad} = Z_o \{\phi_{mo,ad} [Z_o - d]\}^{-1} = 1.0 \tag{22}$$

Eq. (22) has the consequence that the zero-plane displacement d vanishes and $Z_o = Z_{oo}$.

In order to get the first derivative of ϕ_m at $Z = Z_o$ the empirical formula obtained by BUSINGER et al. (1971) for the range $-0.08 < z/L_* = \mu Z < +0.08$, namely

$$\phi_m = 1 + 3.0\,\mu Z + 10.2\,\mu^2 Z^2 \tag{23}$$

may be used. One gets

$$\phi'_{mo} = 3.0\,\mu + 20.4\,\mu^2 Z_o \tag{24}$$

Since Z_o is very small, 10^{-6} to 10^{-4}, the second term on the right hand side in eq. (24) may be neglected even for very large values of the stratification parameter μ, as is for instance $|\mu| = 100$. Eq. (23) shows that at $Z = Z_o$ the term reflecting the influence of the thermal stratification are very small compared with 1.0 and therefore they may be neglected. This means

$$\phi_{mo} \approx \phi_{mo,ad} = 1.0 \tag{25}$$

6. Discussion of the results

Replacing in eqs. (20) and (21) the ϕ_{mo} by eq. (25) and ϕ'_{mo} by eq. (24) one gets for the velocity components the following profiles in the neighbourhood of Z_o

$$U(Z) = \ln(Z/Z_o) + 3.0\,\mu(Z - Z_o) + 0\,\{(Z - Z_o)^3/Z_o^3\} \qquad Z_o \leqslant Z < 2Z_o \tag{26}$$

$$V(Z) = -P_o Z_o \{(Z - Z_o)^2/(2Z_o^2) + (Z - Z_o)^3/(3Z_o^3)\,[1 - 1/2P_o]\} + \\ + 0\,\{(Z - Z_o)^4/Z_o^4\} \tag{27}$$

In eq. (27) $Z_o\,[N(\mu) + 3.0\,\mu]$ is neglected as very small compared with 1.0; P_o in this equation has to be replaced by the expression given in eq. (7a).

One notices from eq. (26) that the wind profile has the form of a log + linear profile at the lower boundary of the planetary boundary layer. This has been shown here by using the equations of the planetary boundary layer only without any additional hypothesis. Admittedly this result is almost irrelevant to any practical application of wind profiles. Nevertheless it is an interesting result from the theoretical point of view. For instance the derivation of the "resistance law" of the planetary boundary layer requires the existence of the log-profile at $Z = Z_o$ at least. Up to now such a profile has been assumed or was derived with the aid of some additional hypotheses, which are now not longer necessary.

If the stress is assumed to be constant with height, one can conclude from eq. (4a) that $K_m = Z$ and therefore $K'_m = 1$. Since in the planetary boundary layer the stress varies with height (even at $Z = Z_o$ this variation is largest), K_m cannot vary linearly with height and it must be $K'_m \neq 1$. According to eq. (17) and with regard to eqs. (24) and (25) one gets for K'_{mo}

$$K'_{mo} = 1 - [N(\mu) + 3.0\,\mu]\,Z_o \tag{28}$$

The difference to 1.0 exists indeed but it is very small at $Z = Z_o$; it may reach 0.01 for a very large roughness-length and a very large parameter μ of the thermal stratification. However this difference increases with increasing height Z under the consideration and may grow (outside the range bounded by $2Z_o$) to an amount which cannot longer be neglected.

One notices also that the increase of K_m with height is smaller in stable conditions ($\mu > 0$) than in unstable conditions ($\mu < 0$). In the latter the factor of proportionality between K_m and Z even may be larger than 1.0.

For the universal function $N(\mu)$ in eq. (28) WIPPERMANN (1972) has proposed an empirical formula.

The derivation of the log + linear profile presented in section 4 does not tell up to which height Z and with which error the log + linear profile can be applied; the derivation is valid only for the range $Z_o \leqslant Z < 2Z_o$. However many investigations about the log + linear profile show that it is applicable with a reasonable error within the total surface layer, let's say up to $Z \sim 0.02$ if the thermal stratification does not deviate to much from the neutral one.

References

BUSINGER, J.A., WYNGAARD, J. C., IZUMI, Y., BRADLEY, E. F., 1971: Flux – profile relationships in the atmospheric surface layer. J. Atm. Sci. **28** (2), 181–189.

WIPPERMANN, F., 1972: Empirical formulae for the universal functions $M_m(\mu)$ and $N(\mu)$ in the resistance law for a barotropic and diabatic planetary boundary layer. Beitr. Phys. Atm. **45** (4), 305–311.

YORDANOV, D., WIPPERMANN, F., 1972: The parameterization of the turbulent fluxes of momentum, heat and moisture at the ground in a baroclinic planetary boundary layer. Beitr. Phys. Atm. **45** (1), 58–65.

Numerical Study on the Effects Controlling the Low-Level Jet

Numerische Untersuchung der für den bodennahen Strahlstrom verantwortlichen Effekte

F. Wippermann

Technical University Darmstadt, Germany

Manuscript received 16 March 1973

Summary: At first the phenomenology of the low-level jet (LLJ) is reviewed briefly. Then results are reported which have been obtained by numerical models of the planetary boundary layer, they allow to study the effect of the thermal stratification, of the baroclinicity and of the non-stationarity on the development of a LLJ. It will be shown, that the development of a LLJ is favoured in a very stable boundary layer; the same is true for a baroclinicity, for which the thermal wind is opposite to the geostrophic wind at the ground. Finally it can be shown that the non-stationarity at night has the effect to intensify the supergeostrophic flow in the LLJ-level whereas the wind maximum is weakened in the day time. The correspondence of these effects with the observations is discussed. The paper is followed by a bibliography on the LLJ.

Zusammenfassung: Nach einem kurzen Überblick über die Phaenomenologie des bodennahen Strahlstromes wird über Ergebnisse berichtet, die mit numerischen Modellen der planetarischen Grenzschicht erhalten wurden. Sie erlauben es, den Einfluß der thermischen Schichtung, der Baroklinität der Grenzschicht und der Instationarität auf die Ausbildung eines LLJ zu untersuchen. Es zeigt sich, daß eine möglichst stabile Schichtung die Ausbildung eines LLJ begünstigt, ebenso eine Baroklinität, bei welcher der thermische Wind entgegengesetzt dem geostrophischen Wind am Boden ist. Schließlich zeigt sich, daß die Instationarität gerade in der Nacht die Wirkung hat, die Geschwindigkeit im LLJ-Niveau zu verstärken, während sie diese tagsüber abschwächt. Die Übereinstimmung dieser Effekte mit den Beobachtungen wird erörtert. Der Arbeit ist eine Bibliographie zum LLJ angehängt.

Résumé: Après un aperçu sur la phénoménologie du courant-jet de la couche limite (low-level jet, LLJ), on donne des résultats qui ont été obtenus à l'aide de modèles numériques de la couche limite planétaire et qui permettent d'étudier l'effet de la stratification thermique, de la baroclinie et du caractère non stationnaire sur la formation du LLJ.

On constate qu'une stratification très stable de la couche limite favorise le développement d'un LLJ; il en est de même d'une baroclinie où le vent thermique est opposé au vent géostrophique en surface. Enfin, on montre que le caractère non stationnaire a comme effet d'intensifier le courant au niveau du LLJ pendant la nuit et au contraire de l'affaiblir pendant le jour.

On analyse la concordance de ces effets avec les observations et on termine par une bibliographie sur le LLJ.

I. Introduction

The low-level jet (LLJ) is different from the jet-stream which generally occurs in the upper part of the troposphere. The difference is given not only by the height, at which it occurs, but also by the effects causing these phenomena. The jet-stream of the upper troposphere is due to the tropospheric baroclinicity mostly concentrated in rather narrow bands; the jet-stream is a phenomenon of the synoptic scale.

The LLJ however is a boundary layer phenomenon, it is primarily caused by the overshooting of the horizontal wind over the geostrophic wind in the upper part of the boundary layer. This overshooting occurs only in fluids in rotating systems, where one has a three-dimensional boundary layer and where the "external" velocity (the geostrophic one) is perpendicular to the acting horizontal pressure gradient.

Beiträge zur Physik der Atmosphäre, 46. Band, 1973, S. 137–154

The overshooting can be intensified or weakened by the thermal stratification of the boundary layer, by the baroclinicity of the boundary layer and/or by the non-stationarity. If this overshooting is strong and occurs in a rather thin layer, it appears as a LLJ; mostly the overshooting is very weak and distributed over a larger height interval.

It belongs to a planetary boundary layer and occurs permanently. This can be seen immediately from the equations for the planetary boundary layer (PBL), i. e. for a stationary and horizontally homogeneous boundary layer

$$f\bar{\rho}\{\hat{u}-\hat{u}_g\} = d\tau_y/dz \tag{1}$$

$$-f\bar{\rho}\{\hat{v}-\hat{v}_g\} = d\tau_x/dz \tag{2}$$

The notation is the usual one: f is the Coriolis parameter, ρ the density, $\hat{u}$ and $\hat{v}$ the velocity components, $\hat{u}_g$ and $\hat{v}_g$ the components of the geostrophic wind, τ_x and τ_y the components of the Reynolds' stress and z is the vertical coordinate. The boundary conditions are in the barotropic case

$$z = z_0: \quad \hat{u} = \hat{v} = 0 \tag{3a}$$

$$\tau_x = \bar{\rho}\, u_*^2, \quad \tau_y = 0 \tag{3b}$$

$$z = z_T: \quad \hat{u} = \hat{u}_g, \quad \hat{v} = \hat{v}_g \tag{4a}$$

$$\tau_x = \tau_y = 0 \tag{4b}$$

Here z_0 is the roughness-length, z_T is the height of the top of the PBL, u_* is the friction velocity. The condition (3b) shows that the coordinate system is orientated with the x-axis parallel to the vector $\boldsymbol{\tau}_0$, the Reynolds' stress at the ground. Integrating the eqs. (1) and (2) from z_0 to z_T one obtains

$$\int_{z_0}^{z_T} \{\hat{u}-\hat{u}_g\}\, dz = 0 \tag{5}$$

$$\int_{z_0}^{z_T} \{\hat{v}-\hat{v}_g\}\, dz = u_*^2/f \tag{6}$$

Because of the condition (3a) the integral in eq. (5) can vanish only if $\hat{u} > \hat{u}_g$ in some hight interval; this is the overshooting at least for the u-component which itself amounts to more than $0.95\,|\hat{v}_g|$ already. In a neutral and barotropic boundary layer the wind speed exceeds the geostrophic one in the maximum by about 6 % and the supergeostrophic flow is not concentrated within a rather thin layer; one would call this not yet a LLJ, it requires a much more pronounced velocity maximum. Therefore a definition of the LLJ is needed and a criterion when a wind maximum is considered to be a low-level jet observation. Such a criterion does not yet exist which is generally accepted; different authors gave different criteria, for instance BLACKADAR (1957), BONNER (1968), RIDER and ARMENDARIZ (1971). As an example the second criterion by BONNER (1968) may be mentioned here: The wind maximum must be located within the lowest 1500 m. The wind at the level of the maximum must equal or exceed 16 m/s and must decrease by at least 8 m/s to the next higher minimum or to the 3 km-level, whichever is lower.

Before the effects will be discussed, which modify the overshooting, some of the observational facts of the LLJ should be reviewed.

II. Phenomenology of the LLJ, a brief review

a) Examples for LLJ-observations

The LLJ is known now for about twenty years. In this time many observations of it have been made, many examples could be given. Only four examples should be presented here, three of which have been recently published by RIDER and ARMENDARIZ (1971). The vertical profiles shown in the figures 1–3 have been measured at the White Sands Missile Range, New Mexico; they are grouped by the authors according to the wind direction, northerly winds in fig. 1, westerly in fig. 2 and southerly winds in fig. 3; according to that RIDER and ARMENDARIZ distinguish three types of LLJs (I, II and III). Of course, this classification is for the present valid only at the site where the measurements have been made. These examples are chosen since they show also the simultaneous vertical profiles of the temperature. Another example may be given in figure 4, it shows the vertical profiles of the wind speed (average of 16 cases) at 0300 and 1500 CT in January 1953 in San Antonio, Tex. as presented by BLACKADAR (1957). This figure also contains the vertical profile of the geostrophic wind; one notices the considerable overshooting.

b) Geographical distribution of the LLJ-occurence

The LLJ has been observed in many parts of the world, for instance in the USA, by many authors (see references), Canada by ROCKE (1965), West-Peru by LETTAU (1967), Sahara (Tchad) by GOUALT (1938), Kenya by FINDLATER (1967), Tropical Africa by FARQUHARSON (1939), Soviet Union by TSVERAVA (1967), Indian Ocean by FINDLATER (1969) and the Antarctic Plateau by SCHWERDTFEGER and MAHRT (1968).

The greater part of the LLJ-observations have been made in the USA. BONNER (1968) examined two years of LLJ-data from 47 stations in the USA and presented a climatology of the LLJ; he obtained interesting and very informative results. Only two of his numerous figures can be reproduced here. Figure 5 shows the isolines of the frequency of LLJs in the two years period Jan. 59 through Dec. 60. The hatched area at the left has an elevation of more than 1000 m above sea level, it can be considered very roughly as the mountain area. The zone of maximum frequency of LLJ-observations is roughly parallel to the Rocky Mountains, it occurs over the Great Plains; east of the Mississippi River the frequency drops off sharply.

Figure 6 shows the isotach pattern for an averaged LLJ (from 28 jet cases which have been centered) east of the Rocky Mountains. One notices from this figure that the LLJ has a similar configuration as the jet-stream in the upper troposphere but on a smaller scale; the ratio of the transverse dimensions is 1/2 according to BONNER (1968).

c) The height of the LLJ

RIDER and ARMENDARIZ (1971) gave for the three types of LLJs over White Sands Missile Range the following heights of the wind maxima

Type I (northerly winds) 100–400 m
Type II (westerly winds) 600–1000 m
Type III (southerly winds) 400–600 m

In his climatology of the LLJ BONNER (1968) devided the boundary layer in three layers (0–500 m, 500–1000 m, 1000–1500 m); he found that the maximum of wind occurs more often in the layer 0–500 m than in the two other layers together.

In general the LLJ-observations are still to sparse and not enough systematic to make a sound statement about the height of the wind maximum.

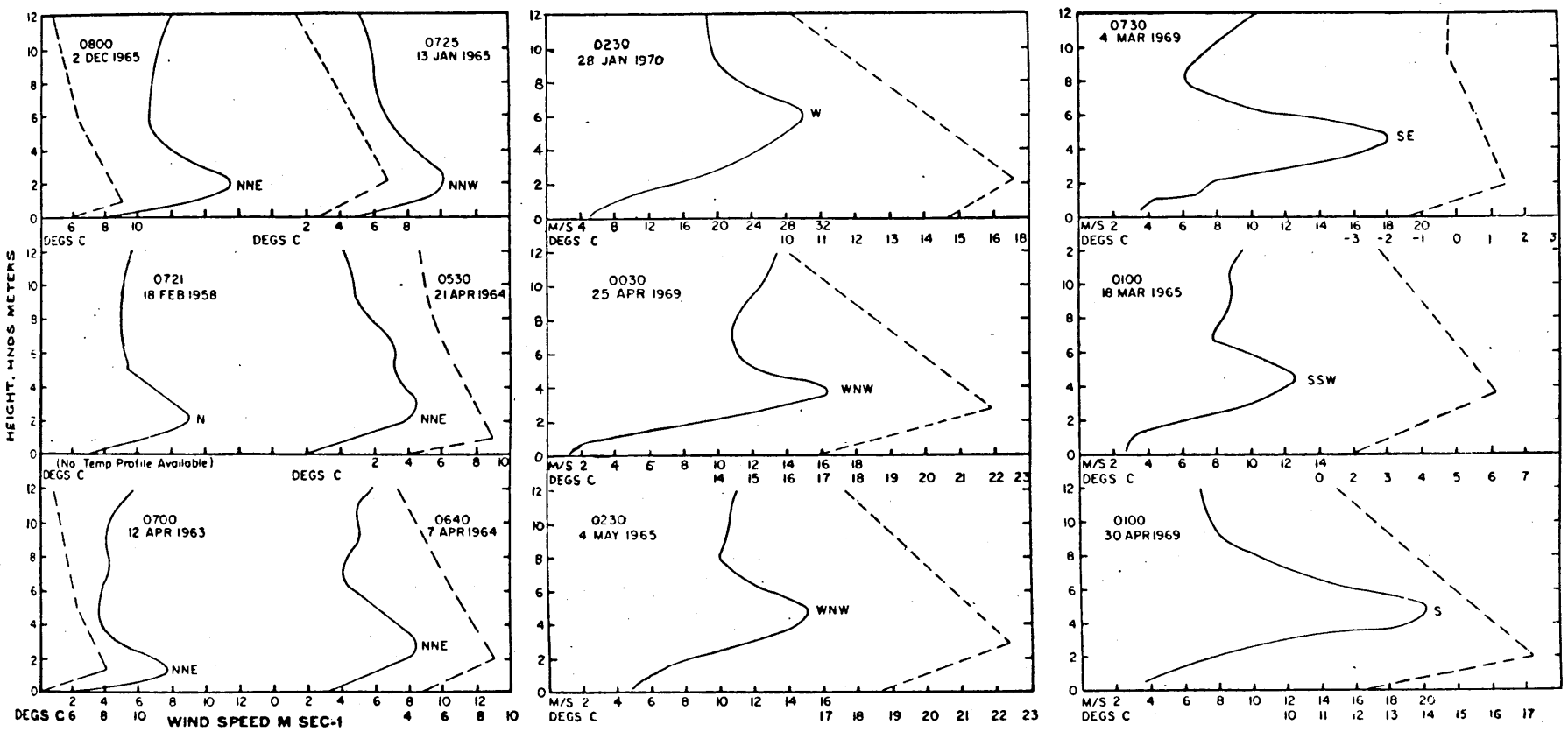

- **Figure 1–3** Examples for vertical profiles of the wind speed and of the temperature measured at White Sands Missile Range (After RIDER and ARMENDARIZ, 1971). The examples are grouped for three types according to the wind direction.

- **Bild 1–3** Beispiele für die Vertikalprofile der Windgeschwindigkeit und der Temperatur gemessen in der White Sands Missile Range (nach RIDER und ARMENDARIZ, 1971). Die Beispiele sind entsprechend der Windrichtung in drei Typen aufgeteilt.

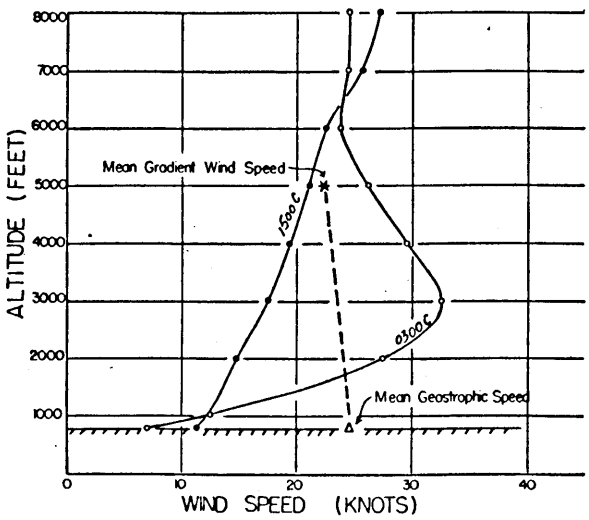

- **Figure 4** Two averaged vertical profiles of the wind speed (16 cases in January 1953) in San Antonio, Tex. (After BLACKADAR, 1957).

- **Bild 4** Zwei gemittelte Vertikalprofile der Windgeschwindigkeit (16 Fälle im Januar 1953) in San Antonio, Tex. (nach BLACKADAR, 1957).

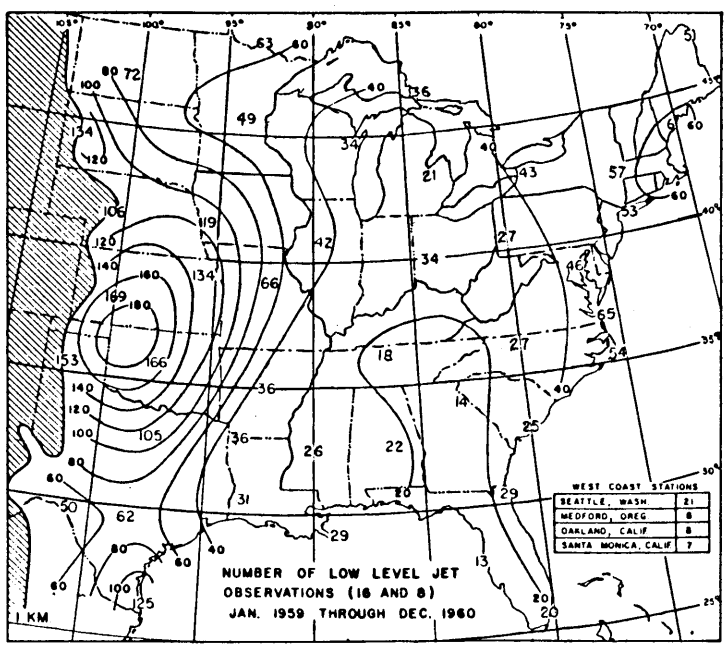

- **Figure 5** Isolines of the frequency of LLJ in the two years period Jan. 59. – Dec. 60. (After BONNER, 1968).

- **Bild 5** Isolinien der Häufigkeit des Auftretens eines LLJ in der Zweijahresperiode Jan. 1959 – Dez. 1960 (nach BONNER, 1968).

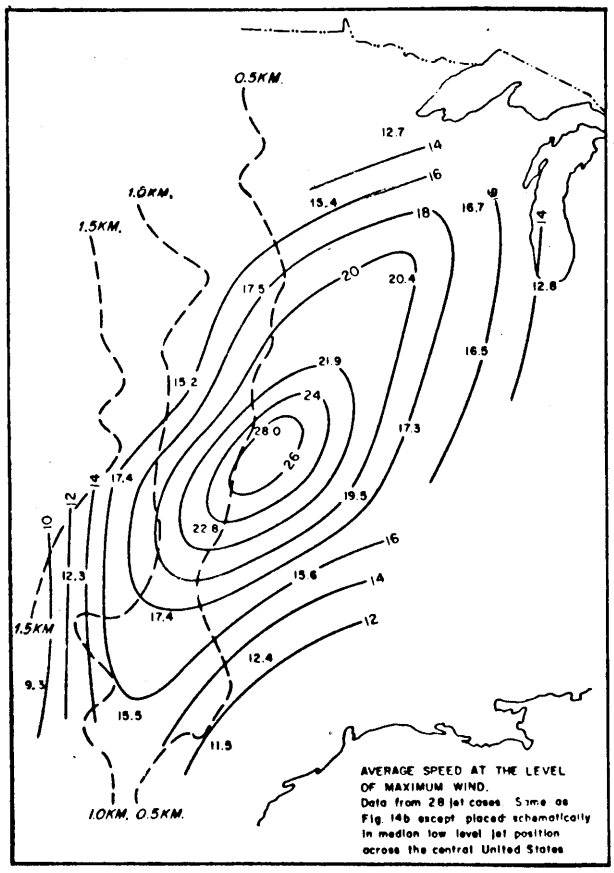

● **Figure 6** Mean isotach pattern (m sec^{-1}) at the level of maximum wind (28 cases, centered at its median position and orientated along the median jet axis). Left of the line 1.0 km is the hatched area of figure 5. (After BONNER, 1968).

● **Bild 6** Mittleres Isotachenfeld (m sec^{-1}) im Niveau des Geschwindigkeitsmaximums (28 Fälle, zentriert nach der mittleren Position und ausgerichtet entlang der Achse des mittleren Jets). Das gestrichelte Gebiet des Bildes 5 befindet sich links der Linie 1.0 km (nach BONNER, 1968).

d) Time of occurence of the wind maximum

In a theoretical study KRISHNA (1968) found that the wind maximum should occur as later as farer south the wind profile is measured; he gives the following local times.

■ **Table 1/Tabelle 1**

φ	50°	40°	30°	20°	10°
local time	22	23	01	05	09

This agrees qualitatively with an earlier result by LETTAU (1967). According to table 1 the wind maximum at the White Sands Missile Range (φ = 32° N) must be expected at midnight. However RIDER

and ARMENDARIZ (1971) give the following frequencies for the time intervals of the occurence of the wind maximum:

20.00–24.00 MST 10 %
24.00–04.00 MST 56 %
04.00–08.00 MST 34 %

The theoretical result mentioned before can not be verified by the observational data available at the present time.

e) The simultaneous temperature profile

Only few LLJ-observations exist for which the simultaneous temperature profile has been measured. Almost all of the temperature profiles show a significant inversion. The top of this inversion, of course, does not coincide with the wind maximum; it is located in most cases somewhere below the level of the wind maximum. The figures 1–3 give some examples for the temperature profile.

The measurements of the simultaneous temperature profiles also are to sparse and to sporadic yet for any sound conclusion.

One should have in mind the observed existence of a strong temperature inversion in the LLJ-cases, when lateron the effect of the thermal stratification is investigated using a PBL-model. Because of the two assumptions for the PBL (stationarity, horizontal homogeneity) each PBL-model must consider the turbulent heat flux as being constant with height. That involves vertical temperature profiles, for which the temperature increases or decreases monotonically with height; a PBL-model (as long as radiative effects are excluded) does not know temperature inversions.

III. The PBL-model

The model for a non-stationary, barotropic and diabatic PBL is described by WIPPERMANN, ETLING and LEYKAUF (1973), that one for a stationary, baroclinic and diabatic PBL by WIPPERMANN (1972). Both models use essentially the same equations, namely

$$\partial^2 Y/\partial Z^2 = X/K_m - \lambda_x + \partial/\partial F\,(Y/K_m) \tag{7}$$

$$\partial^2 X/\partial Z^2 = -\,Y/K_m + \lambda_y + \partial/\partial F\,(X/K_m) \tag{8}$$

$$K_m = L\,\{X^2 + Y^2\}^{1/4}/\kappa \tag{9}$$

$$L = L_\infty - (L_\infty - \kappa\,K_{mo})\,\{X^2 + Y^2\}^{p/2},\quad p = -\frac{\kappa}{(\partial X/\partial Z)_0\,\{L_\infty - \kappa\,K_{mo}\}} \tag{10}$$

The two independent variables are $F = ft$ the non-dimensional time and $Z = z/H$ the non-dimensional vertical coordinate, where $H = \kappa\,u_*/f$ is the internal scale height of the PBL. The four dependent variables are $X = \tau_x/(\bar{\rho}\,u_*^2)$, $Y = \tau_y/(\bar{\rho}\,u_*^2)$, $L = l/H$ and $K_m = k_m/(H^2 f)$, i. e. the non-dimensional components of the Reynolds' stress, the non-dimensional mixing-length and the nondimensional eddy viscosity. κ is the Karman constant. Four free parameters appear in these equations: K_{mo}, L_∞, λ_x and λ_y. The first describes the influence of the external parameters via the surface Rossby number; it is

$$K_{mo} = Z_0 = (\kappa\,C_g\,Ro_0)^{-1} \tag{11}$$

Herein $Z_0 = z_0/H$ is the nondimensional roughness-length, $Ro_0 = |\hat{v}_{go}|/(f z_0)$ the surface Rossby number with $|\hat{v}_{go}|$ the geostrophic wind speed at the ground and $C_g = u_*/|\hat{v}_{go}|$ the geostrophic drag coefficient. The second of the free parameters, L_∞, governs the thermal stratification; it is related to the internal parameter μ for the thermal stratification ($\mu = H/L_*$, L_* = Monin-Obukhov stability length) by the empirical formula

$$\mu = -53.4 - 28.8 \log_{10}(L_\infty) \tag{12}$$

The third and the fourth parameter, λ_x and λ_y, describe the baroclinicity, which is assumed to be constant with height; $\lambda_x = \kappa^2/f\, d\hat{u}_g/dz$, $\lambda_y = \kappa^2/f\, d\hat{v}_g/dz$ are internal parameters for the baroclinicity because of the orientation of the co-ordinate system, the x-axis has the direction of the (internal) vector τ_0.

The eqs. (7) and (8) are the same as eqs. (1) and (2) for the non-stationary case, but the flux-gradient relation has been used and the velocity components are eliminated. Eq. (9) is a combination of the flux-gradient relation with Prandtl's mixing-length relation. Eq. (10) is a mixing-length hypothesis by WIPPERMANN (1971); in the stationary case instead of eq. (10) a modified mixing-length hypothesis by APPLEBY and OHMSTEDE has been used

$$L(Z) = L_\infty \{1 - \exp[-\kappa (Z - Z_0)/L_\infty]\} \tag{13}$$

The boundary conditions are

$$Z = Z_0: \quad X_0 = 1, \; Y_0 = 0 \tag{14a}$$

$$L_0 = \kappa Z_0, K_{m0} = Z_0 \tag{14b}$$

$$Z \to \infty \quad X \to X_\infty = \frac{L_\infty^2}{\kappa^2} \lambda_x \{\lambda_x^2 + \lambda_y^2\}^{1/2} \tag{15a}$$

$$Y \to Y_\infty = \frac{L_\infty^2}{\kappa^2} \lambda_y \{\lambda_x^2 + \lambda_y^2\}^{1/2} \tag{15b}$$

$$L \to L_\infty \tag{15c}$$

$$K_m \to K_{m\infty} = \frac{L_\infty^2}{\kappa^2} \{\lambda_x^2 + \lambda_y^2\}^{1/2} \tag{15d}$$

The solution of the system (7)–(10) for the stationary case gives the four universal profiles

$$\left.\begin{array}{r} X(Z, \mu, \lambda_x, \lambda_y) \\ Y(Z, \mu, \lambda_x, \lambda_y) \\ L(Z, \mu, \lambda_x, \lambda_y) \\ K_m(Z, \mu, \lambda_x, \lambda_y) \end{array}\right\} Z \gg Z_0 \qquad \begin{array}{r} (16a) \\ (16b) \\ (16c) \\ (16d) \end{array}$$

they are called universal since they are completely independent of the external parameters $|\hat{v}_{go}|$, f and z_0; only in the neighbourhood of z_0 they depend on Ro_0, in which the external parameters are combined.

For a consideration of the LLJ the velocities are needed; the velocity defects can be obtained by differentiating the stress profiles, see eq. (1) and (2):

$$P = dY/dZ, \qquad Q = -dX/dZ \tag{17a), (17b}$$

where $P = \kappa \dfrac{\hat{u} - u_g}{u_*}$, $Q = \kappa \dfrac{\hat{v} - v_g}{u_*}$. The profiles P (Z) and Q (Z) are also universal for $Z \gg Z_0$. However this

is valid only for the velocity defect, not for the velocity itself. In order to obtain the velocities the defects have to be multiplied by C_g/κ

$$\hat{u}/|\hat{v}_{go}| = (P - P_0)\, C_g/\kappa \tag{18a}$$

$$\hat{v}/|\hat{v}_{go}| = (Q - Q_0)\, C_g/\kappa \tag{18b}$$

$$|\hat{v}|/|\hat{v}_{go}| = \{(P - P_0)^2 + (Q - Q_0)^2\}^{1/2}\, C_g/\kappa \tag{19}$$

P_0 and Q_0 can be obtained with regard to the boundary condition (3a) from the definition of the defects; it is

$$P_0 = -\kappa \cos(\alpha_0)/C_g = M_m(\mu, \lambda_x, \lambda_y) - \ln(C_g\, Ro_0) \tag{20}$$

$$Q_0 = \kappa \sin(|\alpha_0|)/C_g = N(\mu, \lambda_x, \lambda_y) \tag{21}$$

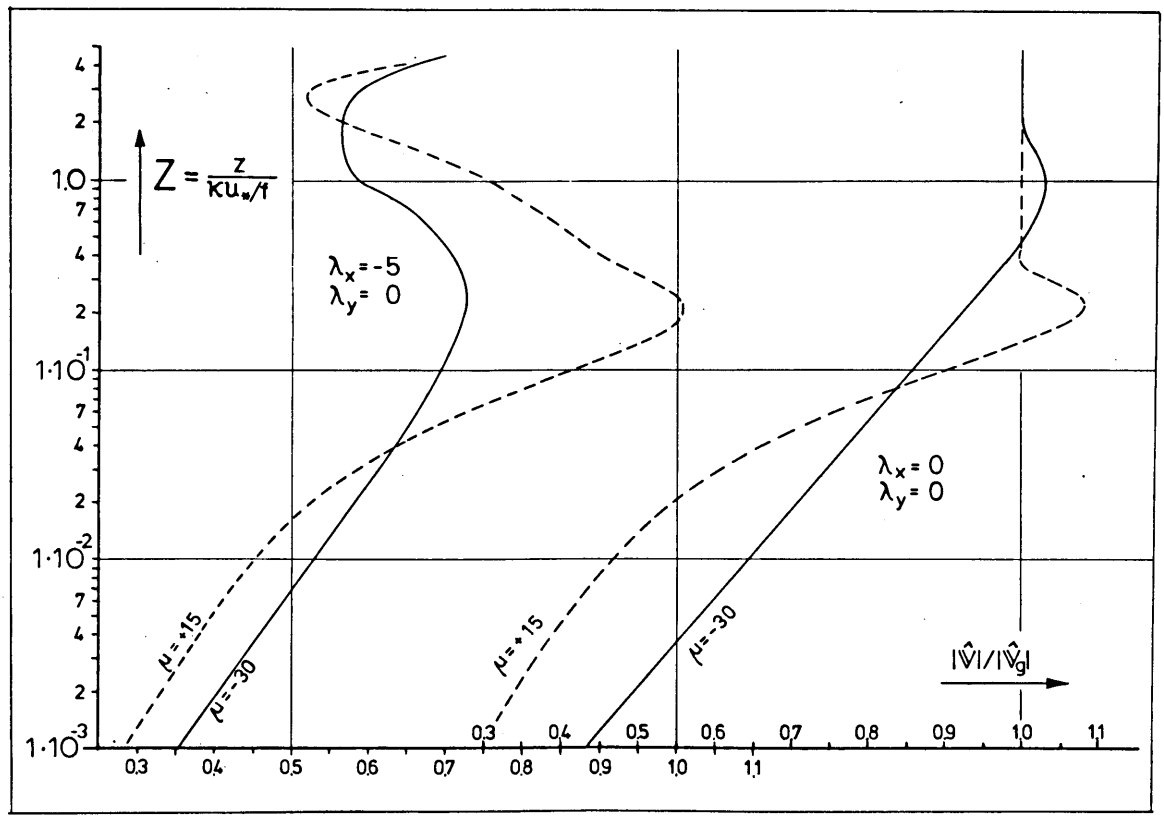

- **Figure 7** Comparison of vertical wind profiles for a stable ($\mu = +15$) and an unstable ($\mu = -30$) stratification in the barotropic case ($\lambda_x = \lambda_y = 0$) right and a baroclinic case ($\lambda_x = -5$, $\lambda_y = 0$) left.

- **Bild 7** Vergleich von vertikalen Windprofilen für eine stabile ($\mu = +15$) und eine instabile ($\mu = -30$) Schichtung im barotropen Fall ($\lambda_x = \lambda_y = 0$) rechte Hälfte und in einem baroklinen Fall ($\lambda_x = -5$, $\lambda_y = 0$) linke Hälfte.

where on the right-hand side the so-called resistance law of the PBL is applied; $M_m(\mu, \lambda_x, \lambda_y)$ and $N(\mu, \lambda_x, \lambda_y)$ are universal functions. Since P_0 depends also on C_g and Ro_0 the wind speed $|\hat{v}|/|\hat{v}_{go}|$ in eq. (19) must depend on these external parameters too.

In the non-stationary case the profiles $|\hat{v}|(Z)/|\hat{v}_{go}|$ at different times must be comparable. This is not so as long as the heigh z and the velocities are non-dimensionalized by u_*, which varies with time. Therefore $C_{g*} = u_{**}/|\hat{v}_{go}|$, which is C_g for $\mu = 0$, $\lambda_x = 0$, $\lambda_y = 0$ and for stationarity, has been used for the non-dimensionalization. Other details should be seen in the two papers mentioned above.

IV. The effect of the thermal stratification

Figure 7 shows some of the obtained vertical wind profiles for different thermal stratifications (very stable $\mu = +15$, moderately unstable $\mu = -30$). The profiles on the right are valid for the barotropic case ($\lambda_x = \lambda_y = 0$), those on the left for a baroclinic case ($\lambda_x = -5$, $\lambda_y = 0$, i. e. the thermal wind is directed opposite to the surface stress). One notices very well the overshooting in the barotropic case, which is more pronounced (about 8 %) in stable stratification than in the unstable one, where it is only about 3 %. The position of the wind maximum is about Z = 0.25 (very roughly 250 m) in the stable case but about Z = 0.9 in the unstable case. Both maxima in the barotropic case can not be considered as LLJs. However in the baroclinic case a sharp wind maximum appears at about Z = 0.25 in the case of stable stratification; this profile would satisfy a LLJ-criterion. In the level of the maximum the wind speed exceeds a little the speed of the geostrophic wind at the ground, above the level the speed decreases to about half the maximum value at $Z \approx 3$ (very roughly 3 km). In the unstable case one has also a maximum of the wind, but the decrease of wind speed above the level of the maximum is too small for satisfying a LLJ-criterion.

The comparison shows how important a stable stratification is for the development of a LLJ; in unstable conditions the vertical mixing tends to equalize the momentum and to remove a maximum.

For the same baroclinicity ($\lambda_x = -5$, $\lambda_y = 0$) as in the left-hand side of figure 5 vertical wind profiles have been computed for five different stratifications; they are presented in figure 8. The heavy line is the profile of the (nondimensional) geostrophic wind, it is approached by all other profiles at different heights. This figure shows very clearly that the wind maximum is as more pronounced as the stratification is more stable. One notices also that the position of the wind maximum is as lower as the stratification is more stable. Some values of the height of the maximum are given in table 2.

■ **Table 2** Heights of the wind maxima for different thermal stratifications μ (baroclinicity $\lambda_x = -5$, $\lambda_y = 0$)

■ **Tabelle 2** Höhe der Windmaxima für verschiedene thermische Schichtung μ (bei der Baroklinität $\lambda_x = -5$, $\lambda_y = 0$).

μ	-30	-25	-20	-15	-10	-5	0	+5	+10	+15
Z_{max}	1.00	0.88	0.76	0.65	0.56	0.47	0.40	0.33	0.28	0.22

For the purpose of orientation: the non-dimensional height Z is very roughly equivalent to the given number in kilometer (for the neutral case, a little more in stable and a little less in unstable conditions).

The effect of the stable stratification is certainly one of the reasons why the LLJ occurs mainly at night.

V. The effect of the baroclinicity

In the barotropic case the hodograph has the well-known form of a spiral, however in the baroclinic case the hodograph approaches that one of the geostrophic wind, which is a straight line according to the assumption of a thermal wind constant with height. Figure 9 gives four examples.

In this diagram the x-axis has the direction of the surface stress τ_0. The vector $\hat{v}_{go}$ of the geostrophic wind has the length 1.0, it starts at the point (0.0) and is turned to the right of the x-axis by the angle α_0 (cross-isobar angle). Since α_0 itself depends on the baroclinicity the orientation of the vector $\hat{v}_{go}$ is slightly different in the four cases chosen as examples. At low heights ($Z < 0.5$, very roughly $z < 500$ m) the hodographs tend to have a spiralic form as in the barotropic case, at larger heights ($Z > 1.0$) the four curves are rectilinear, their directions give the direction of the thermal wind in the respective example.

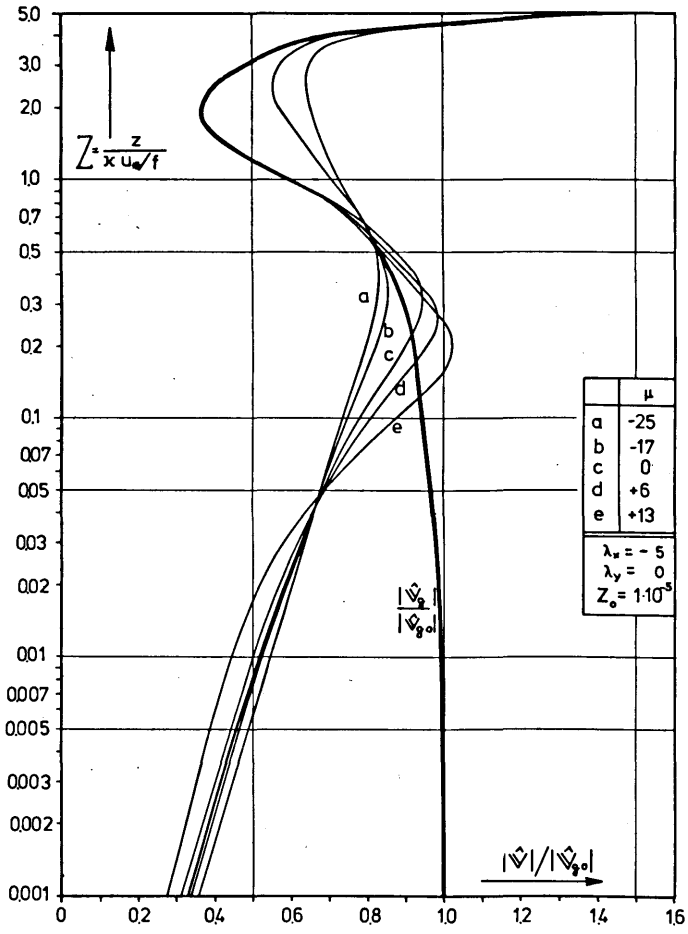

- **Figure 8** Comparison of vertical wind profiles for different thermal stratifications μ in a baroclinic case ($\lambda_x = -5$, $\lambda_y = 0$). The heavy curve gives the profile of the geostrophic wind speed.

- **Bild 8** Vergleich vertikaler Windprofile für verschiedene thermische Schichtung μ in einem baroklinen Fall ($\lambda_x = -5$, $\lambda_y = 0$). Die kräftige Kurve stellt das Vertikalprofil der geostrophischen Windgeschwindigkeit dar.

One notices from the figure 9 that the wind maximum is best developed, when the thermal wind is directed into the quadrat II, i. e. if the baroclinicity is $\lambda_x < 0, \lambda_y > 0$. The wind maximum is most pronounced, when the decrease of wind speed above the maximum is very strong; this happens, when the thermal wind is very strong and is directed opposite to the vector $\hat{v}_{go}$. The height of the wind maximum (in stable conditions as chosen here) is then between Z = 0.2 and Z = 0.3.

In figure 10 vertical wind profiles are presented for four baroclinic cases, in which the thermal wind has the same direction (along the x-axis, $\lambda_y = 0$) but varies in magnitude ($\lambda_x = +5, 0, -5$ and -10); the stratification again is stable ($\mu = +15$). One notices that the wind maximum is as more developed as larger the decrease is of the geostrophic wind with height. In the cases (a) and (b), where the thermal wind is opposite to the vector $\hat{v}_{go}$, a remarkable LLJ is formed, whereas in the barotropic case (c) only the original overshooting can be seen; in the case (d) (the thermal wind has the same direction as $\hat{v}_{go}$) a very weak secondary maximum occurs.

One reason for the high frequency of LLJ over the Great Plains (BONNER, 1968) can be an indirect effect of the slope of the terrain. The diurnal temperature variation has a larger amplitude in the layer close to the ground of the elevated western part of the plains than in the free atmosphere over the eastern part. This causes a horizontal temperature gradient directed to the west in the daytime and directed to the east at night. This means that a thermal wind should be observed, which is directed to the north at night. Such a baroclinicity would be an effect of the horizontally inhomogeneous heating and cooling over the sloped terrain; it would cause a LLJ preferably when the geostrophic wind is opposite to the thermal wind, i. e. when it is northerly at night.

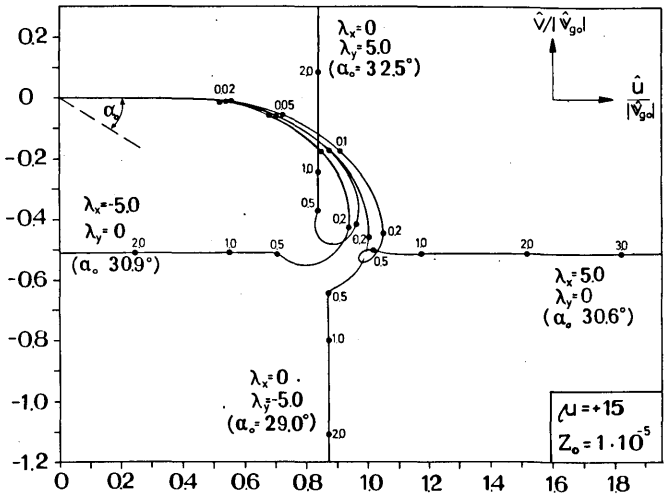

- **Figure 9** Hodographs for four baroclinic cases, stable conditions ($\mu = +15$). The numbers give the non-dimensional height Z. The orientation of the vector of the geostrophic wind $\hat{v}_{go}$ at the ground is given by the cross-isobar angle α_0 which varies slightly with the baroclinicity. The length of this vector is 1.0.

- **Bild 9** Hodographenkurven für vier barokline Fälle bei stabiler Schichtung ($\mu = +16$). Die Zahlen bedeuten die dimensionslose Höhe Z. Die Orientierung des geostrophischen Windvektors $\hat{v}_{go}$ am Boden wird durch den Ablenkungswinkel α_0 gegeben; dieser ändert sich leicht mit sich ändernder Baroklinität. Die Länge dieses Vektors ist 1.0.

However it is a definite observational result, that most of the LLJs (about 2/3) over the Great Plains occur with southerly winds and that the wind maximum is best developed for southerly LLJs, see fig. 1–3. Nevertheless this is not necessarily a contradiction to the explanation given above. It is possible, that the thermal wind caused by the sloped terrain is directed to the north in the layer from bottom up to the level of maximum wind and directed to the south in the layer above the wind maximum (A thermal wind directed to the south has been found by BONNER (1968) in the layer above the wind maximum). Such a baroclinicity would cause some jet-like profile for a southerly geostrophic wind already; certainly it would intensify the maximum of the LLJ.

VI. The effect of the non-stationarity

In the paper by WIPPERMANN, ETLING and LEYKAUF (1973) the input for the time-dependent model has been shown, it can not be given here. The input is the diurnal variation of the internal stratification parameter μ. From the picture given in the cited paper one can realize that the assumed diurnal variation of μ is in good agreement with measurements on a normal clear day.

Here only two results of the integration with the barotropic time-dependent model will be reproduced: Figure 11 gives the isopleths for the non-dimensional wind speed in a height – time – diagram. Inspite of the input of μ, which is completely symmetric to 12 local time, the pattern of the resulting $|\hat{v}|/|\hat{v}_{go}|$ are quite unsymmetric. It can be seen that the wind speed is largest at night in the height of about Z = 0.2 (very roughly 200 m). Between 23 and 02 local time the wind speed exceeds the geostrophic one by more than 20 %; this is an effect of the non-stationarity.

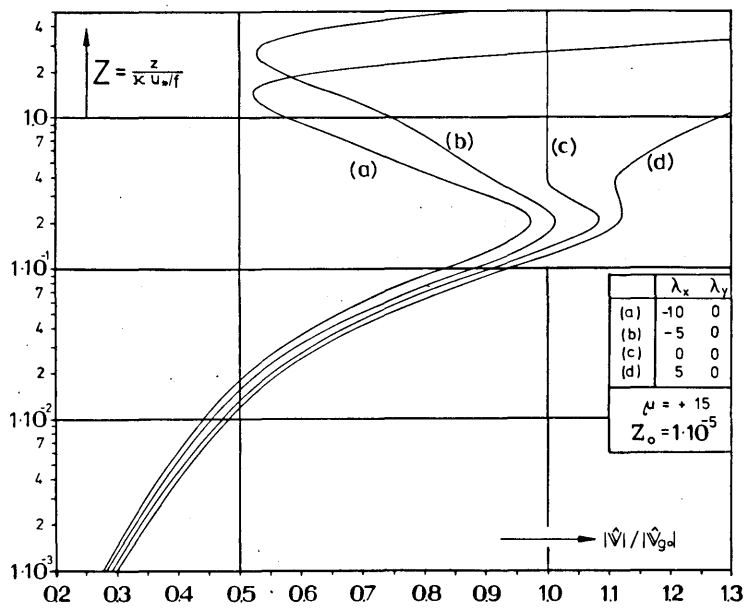

- **Figure 10** Vertical wind profiles for baroclinic cases, in which the thermal wind has the same direction but a different magnitude.
- **Bild 10** Vertikale Windprofile für barokline Fälle, in denen der thermische Wind zwar die gleiche Richtung hat aber seine Stärke ändert.

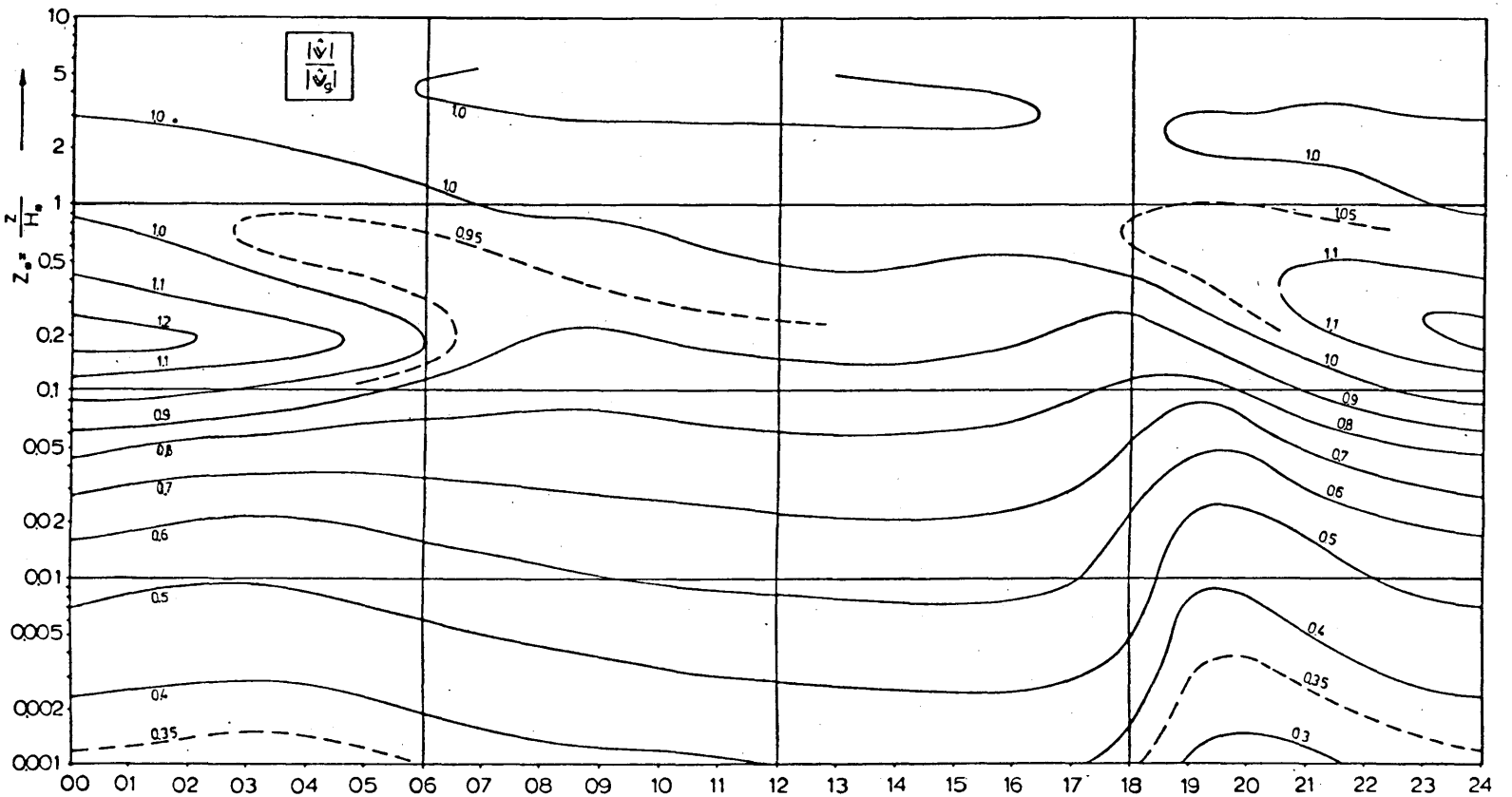

- **Figure 11** Isopleths of $|\hat{v}|/|\hat{v}_{go}|$ obtained with a time-dependent boundary-layer model using as input the diurnal variation of the internal stratification parameter μ for a clear day.

- **Bild 11** Isoplethen des Verhältnisses $|\hat{v}|/|\hat{v}_{go}|$ erhalten mit einem zeitabhängigen Grenzschichtmodell, welches als Vorgabe den Tagesgang des internen Schichtungsparameters μ für einen Strahlungstrag enthält.

In figure 12 a comparison is made between the vertical wind profile in the non-stationary case and that one in the corresponding stationary case. The "corresponding" stationary case means that one, which has the same thermal stratification as the considered non-stationary case. At night the wind speed exceeds the geostrophic one by more than 20 % in the non-stationary case but by 8 % only in the stationary case. This shows very clearly how the non-stationarity supports the development of a LLJ at night. At noon the non-stationary wind speed is less than the geostrophic speed but the difference is very small. Probably it is again the stable stratification at night which makes possible the large difference whereas at noon the strong vertical mixing smoothes the changes with time in different layers and produces almost the profile of the stationary case.

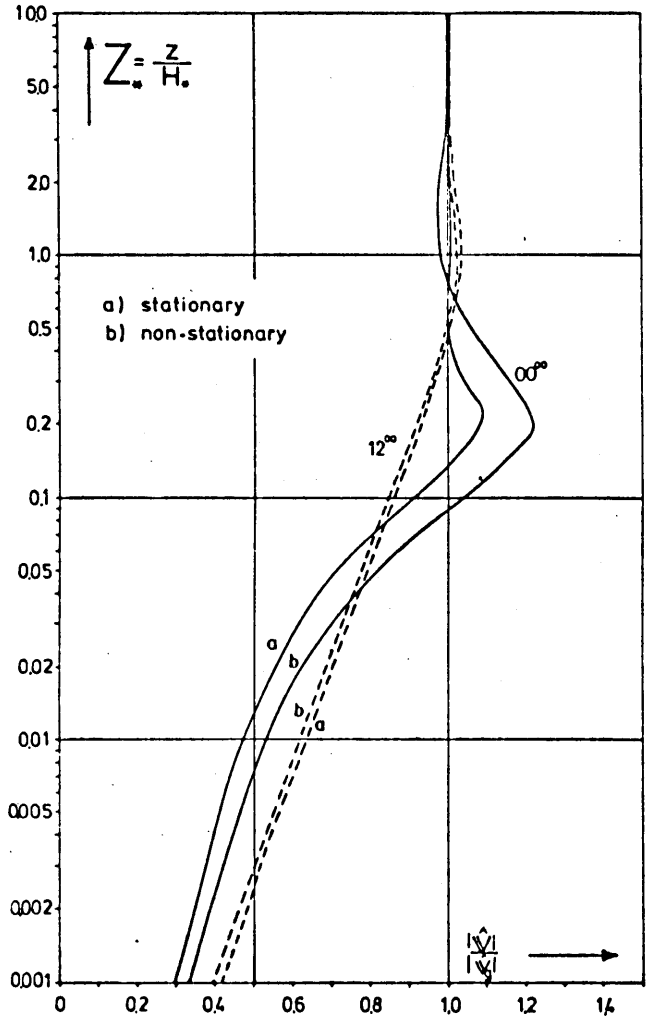

- **Figure 12** Comparison of vertical wind profiles in the non-stationary case with those of the stationary case having the same thermal stratification.

- **Bild 12** Vergleich der vertikalen Windprofile im nicht-stationären Fall mit denjenigen im stationären Fall, die die gleiche thermische Schichtung haben.

VII. LLJ Bibliography

a) Phenomenology: observations, statistics

BLACKADAR, A. K., 1955: The low-level jet phenomenon. Inst. of Aeronaut. Sci., Reprint No. 519.

BLACKADAR, A. K., 1957: Boundary layer wind maxima and their significance for the growth of nocturnal inversions. Bull. Amer. Meteor. Soc. 83, 283–290.

BONNER, W. D., 1965: Statistical and kinematical properties of the low-level jet stream. Mesometerology Research Papers 38, 54 pp. Univers. of Chicago.

BONNER, W. D., 1968: Climatology of the low-level jet. Month. Weather Rev. 96, 833–850.

BONNER, W. D., ESBENSEN, S., GREENBERG, R., 1968: Kinematics of the low-level jet J. Appl. Meteor. 7 (3), 339–347.

BUNKER, A. F., 1965: The low-level jet produced by air, sea- and land interactions. Techn. Note ESSA Weath. Bur. 9-SAIL-1.

FARQUHARSON, S. J., 1939: The diurnal variations of wind over Tropical Africa. Quart. J. Roy. Meteor. Soc. 65, 165–183.

FINDLATER, J., 1969: A major low-level air current near the Indian Ocean during the northern summer. Quart. J. Roy. Meteor. Soc. 95 (404), 362–380; 1970: Discussion. Quart. J. Roy. Meteor. Soc. 96 (409), 551–554.

FINDLATER, J., 1966: Cross-equatorial jet streams at low level over Kenya. Meteor. Mag. 95 (1133), 353–364.

FINDLATER, J., 1967: Some further evidence of cross-equatorial jet streams at low level over Kenya. Meteor. Mag. 96 (1140), 216–219.

FRENZEL, C. W., 1962: Diurnal wind variations in Central California. J. Appl. Meteor. 1, 405–412.

GERHARDT, J. R., 1962: An example of a nocturnal low-level jet stream. J. Atm. Sci. 19, 116–118.

GERHARDT, J. R., 1963: Mesoscale association of a low-level jet stream with a squall-line cold-front situation. J. Appl. Meteor. 2 (1), 49–55.

GIFFORD, F. A., 1952: The breakdown of a low-level inversion studied by means of detailed soundings with a modified radiosonde. Bull. Amer. Meteor. Soc. 33, 373–379.

GOUALT, J., 1938: Vents en altitude a Fort Lamy (Tchad). Ann. de Phys. du Globe de la France d'Outre-Mer, 5, 70–91.

HERING, W. S., BORDEN, Jr., T. R., 1962: Diurnal variations in the summer wind field over the Central United States. J. Atm. Sci. 19 (1), 81–86.

HOECKER, W. H., 1963: Three southerly low-level jet systems delineated by the weather bureau special pibal network of 1961. Month. Weath. Rev. 91, 573–582.

HOECKER, W. H., 1965: Comparative physical behaviour of southerly boundary layer wind jets. Month. Weath. Rev. 93, 133–144.

IZUMI, Y., 1964: The evolution of temperature and velocity profiles during breakdown of a nocturnal inversion and a low-level jet. J. Appl. Meteor. 3, 70–82.

IZUMI, Y., BROWN, H. A., 1966: Temperature, humidity and wind variations during dissipation of a low-level jet. J. Appl. Meteor. 5, 36–42.

JEHN, K. H., DURIE, S. J., 1963: Boundary layer wind maxima and associated temperature distributions as observed on the 1400-foot television tower near Dallas, Texas 1961–1962. Rept. No. 4-09 AF 19 (604)-2459, 1 Oct. 1963, pp. 14, The Univ. of Texas, Electr. Eng. Res. Lab., Austin Tex.

KAIMAL, J. C., IZUMI, Y., 1965: Vertical velocity fluctuations in a nocturnal low-level jet. J. Appl. Meteor. 4 (5), 576–584.

LETTAU, H. H., 1954: Graphs and illustrations of diverse atmospheric states and processes observed during the seventh test period of the great plains turbulence field program. Occas. Rept. No. 1, Atm. Analys. Lab., A. F. Cambridge Res. Center.

LETTAU, H. H., DAVIDSON, B., 1957: Exploring the atmosphere's first mile. Two Vol., Pergamon Press, New York and London.

LHERMITTE, R. M., 1966: Probing air motion by Doppler analysis of radar clear air return. J. Atm. Sci. 23, 575–591.

LINDEMANN, C., 1968: Äquatoriale Strahlströme in niedrigen Höhen über Kenia. Berliner Wettterkarte, Beil. 81, So. 18, pp. 4.

MENDENHALL, B. R., 1967: A statistical study of frictional veering in the planetary boundary layer. Colorado State Univ., Atm. Sci. Pap. No. 116, pp. 57.

NOVOZHILOV, N. I., 1961: Troposphärische Mesoströmungen (in russ.). Ser. Geofiz., Izv. Acad. Sci. UdSSR, No. 2, 334–336.

NOVOZHILOV, N. I., 1963: Eddy inversion as a consequence of the mesojet. (in russ.) Meteor. i Gidrol. No. 10, 33–36, Moscow; 1968: engl. transl.: Dept. of Transport, Toronto (Ont.), Meteorol. Branch. Meteor. Transl. Nr. 13, pp. 7.

RIDER, L. J., 1966: Low-level jet at White Sand Missile Range. J. Appl. Meteor. 5, 283–287.

RIDER, L. J., ARMENDARIZ, M., 1966: Low-level jet winds at Green River, Utah. J. Appl. Meteor. 5, 733–736.

RIDER, L. J., ARMENDARIZ, M., 1971: Nocturnal maximum winds in the planetary boundary layer at White Sands Missile Range, New Mexico. J. Appl. Meteor. 10, 1154–1161.

ROOKE, F. H., 1965: Low-level jets over Montreal. Unpubl. Rept., Dept. of Transport, Meteor. Branch, Toronto (Ont.), Canada, pp. 11.

SANGSTER, W. E., 1967: Diurnal surface geostrophic wind variations over the Great Plains. Proc. Fifth Conf. "Severe Local Storms". St. Louis, Mo. Oct. 19–20, 1967, pp. 8.

SCHWERDTFEGER, W., MAHRT, L. J., 1968: The relation between terrain features, thermal wind and surface wind over Antarctica. Antarctic Journ. of the U. S. 3, 190–191.

SCHWERDTFEGER, W., 1972: The vertical variation of the wind through the friction layer over the Greenland ice cap. Tellus XXIV (1), 14–16.

De SOUZA, R. L., ASPLIDEN, C. I., GARSTANG, M., LASEUR, N. E., 1971: A low-level jet in the tropics. Month. Weath. Rev. 99 (7), 559–563.

TSVERAVA, V. G., 1967: Jet-streams in the boundary layer of the atmosphere (in russ.). Meteor. i Gidrol. No. 10, 71–75.

b) Interpretations and theoretical explanations, models

BUAJITTI, K., BLACKADAR, A. K., 1957: Theoretical studies of diurnal wind variations in the planetary boundary layer. Quart. J. Roy. Meteor. Soc. 83, 486–500.

CHARNEY, J. G., 1955: The Gulf stream as an inertial boundary layer. Proc. Nat. Acad. Sci. 41, No. 10, 731–740. Univ. of Chicago Press.

CHING, J. K. S., BUSINGER, J. A., 1968: The response of the planetary boundary layer to time varying pressure gradient force. J. Atm. Sci. 25, 1021–1025.

DARKOW, G. L., THOMPSON, O. E., 1968: Diurnal oscillations of the tropospheric wind field above a low-level jet. J. Atm. Sci. 25 (1), 39–46.

ESTOQUE, M. A., 1963: A numerical model of the atmospheric boundary layer. J. Geophys. Res. 68, 1103–1113.

HOLTON, J. R., 1967: The diurnal boundary layer wind oscillation above sloping terrain. Tellus XIX, 199–205.

McKAY, Jr., K. P., 1970: Thermo-tidal winds over sloping terrain. Ph. D.-Thesis Univ. of Wisconsin, Dept. of Meteor., Madison, pp. 92.

KRISHNA, K., 1968: A numerical study of the diurnal variation of meteorological parameters in the planetary boundary layer. I. Diurnal variation of winds. Month. Weath. Rev. 96, 269–276.

KUROSAKI, A., 1970: A theoretical study on the structure of the Ekman boundary layer. I. Mixing length theory. Pap. Meteor. Geophys. 21 (2), 89–112.

LAIKHTMAN, D. L., BYUTNEV, E. K., 1964: Turbulence in jet streams with turning geostrophic winds (in russ.). Trudy Glavn. Geofiz. Obs. Voeikova 150, 63–68.

LETTAU, H. H., 1964: Preliminary note on the effects of terrain slope on low level jets and thermal winds in the planetary boundary layer. Sect. 4 of "Studies of the effects of variations in boundary conditions on the atmospheric boundary layer" Ann. Rept. DA-36-039-AMC-00878 Univ. of Wisc., Dept. of Meteor., Madison, Wisc.

LETTAU, H. H., 1967: Small to large scale features of boundary layer structures over mountain slopes. Proc. Symp. on Mountain Meteorology, Colorado State University, pp. 1–74.

LYKOSOV, V. N., 1972: Unsteady state in the planetary boundary layer of the atmosphere. Izv. Atm. Ocean. Phys. 8 (2), 142–155. engl. transl.: 85–91.

NEUMANN, J., MAHRER, Y., 1971: A theoretical study of the land and sea breeze circulation. J. Atm. Sci. 28, 532–542.

OKADA, T., YAMADA, T., 1926–1928: On the effect of topography on the diurnal variation of wind direction. The Geophys. Magaz. I, 105–129, Tokyo 1926-28.

ORLANSKI, I., 1969: The influence of bottom topography on the stability of jets in a baroclinic fluid. J. Atm. Sci. **26** (6), 1216–1232.

PAEGLE, J., 1970: Studies of diurnally periodic boundary layer winds. U.C.L.A., Dept. of Meteor., Techn. Rept. NSF-Grant 698.

PANDOLFO, J. P., BROWN, P. S., 1967: Inertial oscillations in an Ekman layer containing a horizontal discontinuity surface. J. Marine Res. **25**, 10–28.

PETERSON, E. W., 1971: Comment on "A numerical study of the effect of coastal irregularity on the sea breeze" by McPherson. J. Appl. Meteor. **10**, 559–560. Reply by McPherson: J. Appl. Meteor. **10**, 560–561.

McPHERSON, R. D., 1970: A numerical study of the effect of a coastal irregularity on the sea breeze. J. Appl. Meteor. **9**, 767–777.

SASAMORI, T., 1970: A numerical study of atmospheric and soil boundary layers. J. Atm. Sci. **27** (8), 1122–1137.

SHEIH, C. M., 1972: A theoretical study of the diurnal wind variations in the planetary boundary layer. J. Atm. Sci. **29**, 995–998.

USHIJIMA, T., 1969: Analytical study of the low-level jet stream. J. Meteor. Soc. Japan **47** (1), 13–22.

VORONTSOV, P. A., 1967: Jet streams in the atmospheric boundary layer (in russ.). Trudy Glavn. Geofiz. Obs. Voeikova **205**, 77–92; engl. transl.: AF-Systems Command, Wright-Patterson AF Base Ohio, AD 681619 13 Aug. 1968.

WAGNER, A., 1936: Zur Theorie des täglichen Ganges der Windverhältnisse. Gerlands Beitr. Geophys. **47**, 172–202.

WAGNER, A., 1939: Über die Tageswinde in der freien Atmosphäre. Beitr. Phys. d. freien Atm. **25**, 145–170.

WIPPERMANN, F., 1972: Universal profiles in the barotropic planetary boundary layer. Beitr. Phys. Atm. **45**, 148–163.

WIPPERMANN, F., ETLING, D., LEYKAUF, H., 1973: The effects of non-stationarity on the planetary boundary layer. Beitr. Phys. Atm. **46** (1), in press.

WEXLER, H., 1961: A boundary layer interpretation of the low-level jet. Tellus XIII (3), 368–378.

CHAPTER 4

The Parameterization of PBL-Effects with the Aid of the Resistance Law

The so-called resistance law of the PBL combines small-scale PBL-effects (the turbulent vertical fluxes of momentum, heat and moisture at the ground) with the large - scale parameters of the boundary layer, i.e. $\hat{v}_{go}$, $d\hat{v}_g/dz$ (assumed to be constant with height) , $\delta\hat{\vartheta}$ and $\delta\hat{s}$. The last two parameters are the differences of the potential temperature $\hat{\vartheta}$ and the moisture $\hat{s}$ at the top and the bottom of the PBL. Of course, some local parameters as f (Coriolis parameter) , z_o (roughness-length) and $\beta = g/\tilde{\vartheta}$ have to be given; at sea z_o is not a fixed local parameter but depends on the surface stress itself making an application more difficult.

The resistance law offers a possibility to parameterize the three turbulent fluxes τ_o , q_o and j_o mentioned before to be used in numerical models of large-scale atmospheric motions such as models for the numerical weather prediction or models for a simulation of the general circulation of the atmosphere. However, one should keep in mind

that the resistance law is valid in a PBL only, i.e. in an atmospheric boundary-layer, which is steady state and horizontally homogeneous. That means that by making a parameterization with the aid of the resistance law one has to assume horizontal homogeneity and stationarity. The first assumption will be violated all the less the larger the horizontal grid spacing of the numerical model is chosen. The second assumption requires that the variation with time has to be considered as a sequence of stationary states. A more detailed consideration of these problems will be given in chapter 5.

In the first section of this chapter two different derivations of the resistance law are presented, also an additional note on the modification of the resistance law due to a moving lower surface as one has at sea.

The second section is concerned with the two universal constants appearing in the resistance law for a barotropic and neutral PBL. I tried to determine these constants from observations. However all observations available at that time have been used without discriminating with respect to the thermal stratification and to the baroclinicity (because these two additional informations are not available for most of the data); therefore the obtained values scatter very much. In the same paper an attempt has been made to give a physical interpretation of the two constants. One (N) has been identified as the non-dimensional reciprocal displacement thickness of the boundary-layer; the derivation of the result $\{M \approx -\ln(\kappa)\}$ for the other constant contains a mistake as R.J.TAYLOR pointed out in a note, which follows this paper. In the reply to this note an additional condition is formulated which must be satisfied in order to support this result. On page 101 some results of computations with a PBL-model are presented; they show that this additional conditi-

on is almost satisfied in a PBL.

At the time when this paper ("The two constants...") was published the author had not yet an acces to the report of the GARP Study Conference in Stockholm (1967) which among others contains also a contribution by MONIN and ZILITINKEVICH. These authors have evaluated the O'Neill data and obtained not only the values $M_m(0)$, $M_h(0)$, $M_s(0)$ and $N(0)$ for the neutral case, but also their variation with the parameter μ for the thermal stratification. (M_h and M_s are universal constants or universal functions, respectively, appearing in the relationships for the heat- and the moisture - transfer). A similar evaluation by CLARKE using the Kerang and the Hay data was also published in 1970. These evaluations together with the results of several boundary layer models have been used to construct empirical formulae at least for $M_m(\mu)$ and $N(\mu)$; they can be found in the third section of this chapter.

In the next section ("The Parameterization of the Turbulent Fluxes ...") the resistance law is extended to baroclinic cases; an empirical formula for the deviation of the two universal functions $M_m(\mu)$ and $N(\mu)$ in the baroclinic case from the barotropic one are given.

The final section of this chapter is concerned with the parameterization of the large-scale wind-stress at the sea surface. It is an application of the resistance law but in addition CHARNOCK's (1955) relation between z_o and u_* is used in order to eliminate the parameter z_o .

The Resistance Law for the Planetary Boundary Layer

The resistance law was first derived by KAZANSKII and MONIN (1961) for the barotropic and neutral case and for the determination of the momentum flux only. It has been extended to diabatic cases by BLACKADAR (1967) and simultaneously by MONIN and ZILITINKEVICH (1967), who also made possible the determination of the turbulent heat flux and the turbulent moisture flux. Other derivations are given by CSANADY (1967) and GILL (1967,1968) as well as by BLACKADAR and TENNEKES (1968). YORDANOV and WIPPERMANN (1972) extended the resistance law to baroclinic PBLs.

The "classical" derivation by KAZANSKII and MONIN shows best the assumptions which have to be made and for which the resistance law is valid. This derivation may be repeated here with the notation used in the other chapters of this book.

The two quantities in which one is interested are the geostrophic drag coefficient $C_g = u_*/|\hat{v}_{go}|$ and the cross - isobar angle α_o . Both are related to the non-dimensional velocity defect at the ground by the lower boundary condition, see eqs. (12a),(12b) on page 98,

$$P_o = - \varkappa \cos(\alpha_o)/ C_g \tag{1a}$$

$$Q_o = \varkappa \sin(|\alpha_o|)/ C_g \tag{1b}$$

On the other side the velocity defects are given by the non-dimensional PBL-equations

$$P(Z) = dY/dZ \tag{2a}$$

$$Q(Z) = - dX/dZ \tag{2b}$$

see eqs. (10a),(10b) on page 97; therefore one has

$$\varkappa \cos(\alpha_o)/ C_g = - (dY/dZ)_o \tag{3a}$$

$$\varkappa \sin(|\alpha_o|)/ C_g = - (dX/dZ)_o \tag{3b}$$

$Z = z/H$ is the non-dimensional vertical coordinate with the internal scale height of the PBL $H = \varkappa u_*/f$ and with u_* the friction velocity; $X = \tau_x/(\bar{\varrho} u_*^2)$ and $Y = \tau_y/(\bar{\varrho} u_*^2)$ are the components of the non-dimensional Reynolds stress, $\varkappa$ is von Karman's constant.

In order to get C_g and α_o from the eqs. (3a),(3b) one has to know $(dY/dZ)_o$ and $(dX/dZ)_o$; these can be obtained in the following way:
Using the flux - gradient relation and eliminating the velocity defect components, the PBL-equations can be written as

$$d^2Y/dZ^2 = X/ K_m \tag{4a}$$

$$d^2X/dZ^2 = - Y/ K_m \tag{4b}$$

where $K_m = k_m/(H^2 f)$ is the non-dimensional eddy diffusion coefficient. From the eqs. (4a),(4b) one gets by integration

$$- (dY/dZ)_o = \int_{Z_o}^{Z_T}(X/ K_m)\, dZ = \int_{Z_o}^{Z_R}(X/ K_m)\, dZ + \int_{Z_R}^{Z_T}(X/ K_m)\, dZ \tag{5a}$$

$$(dX/dZ)_o = \int_{Z_o}^{Z_T}(Y/ K_m)\, dZ = \int_{Z_o}^{Z_R}(Y/ K_m)\, dZ + \int_{Z_R}^{Z_T}(Y/ K_m)\, dZ \tag{5b}$$

In the eqs. (5a),(5b) use is made of the upper boundary condition at $Z = Z_T$ (for the barotropic case) in the form

$$Z \longrightarrow Z_T : \quad dY/dZ \longrightarrow 0 \quad , \quad dX/dZ \longrightarrow 0 \tag{6}$$

Z_R is the height above which Rossby-number similarity is valid, which means very roughly ten times the roughness - length Z_o (according to the results on page 90). In the

layer below Z_R a Prandtl-layer must be assumed to be valid, i.e. the wind profile must be assumed to be logarithmic in the layer $Z_o \leqq Z \leqq Z_R$. It can be shown, WIPPERMANN (1973), that in the PBL very close to the ground such a Prandtl-layer exists. Therefore no additional assumption is necessary, except that the layer in which this is proved ($Z_o \leqq Z \leqq 2\ Z_o$) must be extended upward to Z_R.
It follows

$$Z_o \leqq Z \leqq Z_R : \qquad X(Z) = 1 \tag{7a}$$

$$Y(Z) = 0 \tag{7b}$$

(i.e.: the coordinate system is orientated with the x-axis in the direction of the surface stress)

$$K_m(Z) = Z \tag{7c}$$

$$Z \geqq Z_R : \qquad \left.\begin{array}{l} X(Z) \\ Y(Z) \\ K_m(Z) \end{array}\right\} \text{Universal profiles} \qquad \begin{array}{l} (8a) \\ (8b) \\ (8c) \end{array}$$

Therefore each of the last integrals in eqs. (5a) and (5b) must be an universal constant

$$\int_{Z_R}^{Z_T} (X/\ K_m)\ dZ = c_1 \quad , \qquad \int_{Z_R}^{Z_T} (Y/\ K_m)\ dZ = c_2 \qquad \begin{array}{l} (9a) \\ (9b) \end{array}$$

i.e.: c_1 and c_2 are constants which are independent of any external parameter.
Furthermore one has with (7a) - (7c)

$$\int_{Z_o}^{Z_R} (X/\ K_m)\ dZ = \ln(Z_R) - \ln(Z_o) \tag{10a}$$

$$\int_{Z_o}^{Z_R} (Y/\ K_m)\ dZ = 0 \tag{10b}$$

or by inserting the eqs. (3a),(3b) into the eqs. (5a),(5b)

$$\varkappa \cos(\alpha_o)/ C_g = \ln(Z_R) - \ln(Z_o) + c_1 \tag{11a}$$

$$\varkappa \sin(|\alpha_o|)/ C_g = - c_2 \tag{11b}$$

In the largest part of the PBl the component Y is negative, therefore $c_2 < 0$; the constant c_2 should be called $- N$. The non-dimensional height Z_R can be chosen as a fixed value; by this reason $\ln(Z_R)$ is a constant. According to the definitions made for the nondimensionalization the non-dimensional roughness-length Z_o is related to the geostrophic drag coefficient and to the surface Rossby-number RO_o by

$$Z_o = (\varkappa C_g RO_o)^{-1} \tag{13}$$

where the surface Rossby-number is defined as

$$RO_o = |\hat{w}_g|/(f z_o) \tag{14}$$

$\ln(\varkappa)$ can be split from $\ln(Z_o)$ in eq. (11a) and combined with $\ln(Z_R)$ and with c_1 to a new constant $- M_m$

$$\ln(Z_R) + \ln(\varkappa) + c_1 = - M_m \tag{15}$$

Now the resistance law results in the following form

$$\frac{\varkappa}{C_g} \cos(\alpha_o) = \ln(C_g RO_o) - M_m \tag{16a}$$

$$\frac{\varkappa}{C_g} \sin(|\alpha_o|) = N \tag{16b}$$

The derivation of the resistance law by BLACKADAR in 1967 uses the method of matching the velocity profiles of the surface layer with those of the outer boundary layer. In the surface layer one has

$$\varkappa\, \hat{u}/u_* = U(\zeta) \tag{17a}$$

$$\varkappa\, \hat{v}/u_* = 0 \tag{17b}$$

with $\zeta = z/z_o$, ($Z = \zeta\, Z_o$)
but in the outer boundary layer

$$\varkappa\, (\hat{u} - \hat{u}_g)/u_* = P(Z) \tag{18a}$$

$$\varkappa\, (\hat{v} - \hat{v}_g)/u_* = Q(Z) \tag{18b}$$

By matching the $\hat{u}$-component in (17a) and (18a) one obtains

$$P(Z) = P(\zeta\, Z_o) = U(\zeta) - \varkappa\, \hat{u}_g/u_* \tag{19}$$

Differentiating eq. (19) with respect to ζ keeping RO_o constant and differentiating it with respect to RO_o at constant ζ one gets

$$Z_o\, \partial P/\partial(\zeta\, Z_o) = \partial U/\partial\zeta \tag{20a}$$

$$\zeta\, \partial P/\partial(\zeta\, Z_o)\ \partial Z_o/\partial(RO_o) = \\ = -\varkappa\, \partial(\hat{u}_g/u_*)/\partial(RO_o) \tag{20b}$$

Eliminating $\partial P/\partial(\zeta\, Z_o)$ from the eqs. (20a) and (20b) gives

$$\zeta\, \partial U/\partial\zeta = -\frac{Z_o}{\partial Z_o/\partial(RO_o)}\, \varkappa\, \frac{\partial}{\partial(RO_o)}\left\{\frac{\hat{u}_g}{u_*}\right\} \tag{21}$$

Each side of this equation must be a constant, since the left-hand side depends only on ζ and the right-hand side only on RO_o . This constant is chosen to be 1 . Integration of these two equations originated from (21) gives

$$U = \ln(\zeta) \tag{22}$$

$$\varkappa\, \hat{u}_g/u_* = \ln(C_g\, RO_o) - M_m \tag{23}$$

where $M_m = c_2 - \ln(\varkappa)$.
In the same way one obtains from (17b) and (18b)

$$\varkappa\, \hat{v}_g/u_* = -N \tag{24}$$

Considering $\hat{u}_g = |\hat{\mathbf{v}}_g|\cos(\alpha_o)$ and $\hat{v}_g = -|\hat{\mathbf{v}}_g|\sin(|\alpha_o|)$ one has with the eqs. (23) and (24) the result (16a) and (16b); the eq. (22) gives the well-known logarithmic wind profile in the surface layer.

These results can be obtained more directly if the existence of the logarithmic wind profile in the surface layer is assumed in the beginning. This is the way of derivation used by MONIN and ZILITINKEVICH (1967). They assume Rossby-number similarity in the outer boundary layer not only for the components of the velocity defect $P(Z)$ and $Q(Z)$ but also for $1/\vartheta_*\, d\hat{\vartheta}/dZ$ and for $1/s_*\, d\hat{s}/dZ$. Here $\hat{\vartheta}$ is the potential temperature and $\hat{s}$ the specific humidity or the mixing-ratio. $\vartheta_* = -q_o/(c_p\, \bar{\varrho}\, \varkappa\, u_*)$ with $q_o = c_p(\varrho\overline{w''\vartheta''})_o$ and $s_* = -j_o/(\bar{\varrho}\, \varkappa\, u_*)$ with $j_o = (\varrho\overline{w''s''})_o$. In order to be able to make the matching one has to assume that the potential temperature as well as the moisture have a logarithmic profile below the height of matching

$$a_{ho}\{\hat{\vartheta}(Z) - \hat{\vartheta}_o\}/\vartheta_* = \ln(Z/Z_o) \tag{25a}$$

$$a_{so}\{\hat{s}(Z) - \hat{s}_o\}/s_* = \ln(Z/Z_o) \tag{25b}$$

where $a_{ho} = (k_h/k_m)_o$ and $a_{so} = (k_s/k_m)_o$.

This kind of derivation by applying similarity arguments has been used also by YORDANOV and WIPPERMANN (1972); they allow the PBL to be baroclinic (of course a baroclinicity only, which corresponds to a thermal wind constant with height). The resulting relations are:

$$\sin(|\alpha_o|)\,\kappa/C_g = N(\mu, \lambda_x, \lambda_y) \tag{26a}$$

$$\cos(\alpha_o)\,\kappa/C_g = \ln(C_g\, RO_o) - M_m(\mu, \lambda_x, \lambda_y) \tag{26b}$$

$$a_{ho}/C_{th} = \ln(C_g\, RO_o) - M_h(\mu, \lambda_x, \lambda_y) \tag{26c}$$

$$a_{so}/C_s = \ln(C_g\, RO_o) - M_s(\mu, \lambda_x, \lambda_y) \tag{26d}$$

Herein $C_{th} = \vartheta_*/(\hat{\vartheta}_T - \hat{\vartheta}_o)$ is a Stanton-number; in this case it expresses the ratio of the characteristic temperature fluctuation ϑ_* (an internal parameter) to the temperature difference between top and bottom of the PBL; this difference is an external parameter. In the analogous manner C_s is defined as $C_s = s_*/(\hat{s}_T - \hat{s}_o)$.

On the right-hand side appear four universal functions M_m, M_h, M_s and N; these are functions which are completely independent of any external parameter, they depend only on the three internal parameters μ, λ_x, λ_y. The first one is the internal parameter for the thermal stratification; it is defined as $\mu = H/L_*$, where H is the internal scale height of the PBL and L_* is the Monin - Obukhov stability length ($L_* = - c_p\, \bar{\varrho}\, u_*^3/\{\beta\, \kappa\, q_o\}$). The two parameters $\lambda_x = d\hat{u}_g/dz\ \kappa^2/f$ and $\lambda_y = d\hat{v}_g/dz\ \kappa^2/f$ govern the baroclinicity; they are internal parameters, since the two components of the baroclinicity are those in the direction of the surface stress (internal parameter) and perpendicular to it.

The resistance law (26a) - (26d) with $C_g = u_*/|\hat{\mathbb{v}}_{go}|$ is valid only for a fixed surface at the lower boundary as on land. If this surface is moving as at sea (with the velocity $\hat{\mathbb{v}}_s$), the drag-coefficient should be defined as

$$C_g = u_*/(|\hat{v}_{go} - \hat{v}_s|) \tag{27}$$

and α_o must be the angle between the vectors $\hat{v}_{go} - \hat{v}_s$ and τ_o. Of course, the definition of the surface Rossby-number has also to be changed slightly; instead of eq.(14) one has

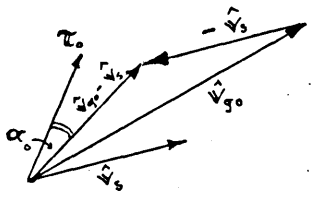

$$RO_o = (|\hat{v}_{go} - \hat{v}_s|)/(f\, z_o) \tag{28}$$

In order to show that we follow CSANADY's (1967) derivation (in vector notation). In the surface layer one has

$$\kappa\,(\hat{v} - \hat{v}_s)/u_* = \mathbf{i}\, \ln(z/z_o) \tag{29a}$$

and in the outer boundary layer

$$\kappa\,(\hat{v} - \hat{v}_g)/u_* = \mathbf{i}\, P(z/H) + \mathbf{j}\, Q(z/H) \tag{29b}$$

Herein $\mathbf{i}$ is the unit vector in the direction of the surface stress and $\mathbf{j}$ the unit vector perpendicular to it. A matching requires for the matching height z_M

$$P(z_M/H) = \ln(z_M/H) + c_2$$

$$Q(z_M/H) = c_3$$

$$\mathbf{c} = \mathbf{i}\, c_2 + \mathbf{j}\, c_3$$

One obtains the vector equation

$$\mathbf{i}\, \ln(z_o/H) + \mathbf{c} + \kappa\,(\hat{v}_{go} - \hat{v}_s)/u_* = 0 \tag{30}$$

With eq. (13) and the above definition for α_o one gets for the two components the resistance law (16a),(16b); it is

$$c_2 - \ln(\kappa) = M_m$$

$$c_3 = N$$

An application of the relations (26a) - (26d) in order to determine α_o, C_g, C_{th} and C_s for a given RO_o is possible only if the four universal functions M_m, M_h, M_s and N are known. The only way to obtain these functions is the evaluation of measurements, but unfortunately suitable data are very sparse. Some of the following sections are concerned with the determination of these functions.

References

BLACKADAR, A.K. 1967 External Parameters of the Wind Flow in the Barotropic Boundary Layer of the Atmosphere
Proc. GARP Study Conf. Stockholm
Append. IV, pp 11

BLACKADAR, A.K.
TENNEKES, H. 1968 Asymptotic Similarity in Neutral Barotropic Boundary Layers
J. Atm. Sci. 25, 1015-1020

CSANADY, C.T. 1967 On the "Resistance Law" of a Turbulent Ekman Layer
J. Atm. Sci. 24, 467-471

GILL, A.E. 1967 The Turbulent Ekman Layer
Unpubl. Manuscr., Univ. Cambridge
Dept. Math. & Theor. Phys.

GILL, A.E. 1968 Similarity Theory and Geostrophic Adjustment
Quart. J. Roy. Met. Soc. 94, 586-588

KAZANSKII, A.B.
MONIN, A.S. 1961 On the Dynamic Interaction between the Atmosphere and the Earth Surface (in Russ.)
Bull. (Izv.) Acad. Sci. USSR, Geophys. Ser. Nr. 5, 786-788
(engl. transl. 514-515)

MONIN, A.S.
ZILITINKEVICH, S.S. 1967 Planetary Boundary Layer and Large Scale Atmospheric Dynamics
Proc. GARP Study Conf. Stockholm
Append. V, pp 37

YORDANOV, D.
WIPPERMANN, F.
1972 The Parameterization of Turbulent Fluxes of Momentum, Heat and Moisture at the Ground in a Baroclinic Planetary Boundary Layer
Beitr. Phys. Atm. 45, 58-65

Beiträge zur Physik der Atmosphäre, 43. Band, 1970, S. 133–140

The Two Constants in the Resistance Law for a Neutral Barotropic Boundary Layer of the Atmosphere *)

Die beiden Konstanten im Widerstandsgesetz für eine neutrale und barotrope Grenzschicht der Atmosphäre

Friedrich Wippermann

Institut für Meteorologie der Technischen Hochschule Darmstadt

With 1 Figure

Received February 20. 1970

Summary: Two constants M and N appear in the resistance law for a neutral barotropic boundary layer

$$\ln(Ro_0) = M - \ln(C_d) + [\kappa^2/C_d^2 - N^2]^{1/2}$$

and

$$\kappa \sin(|\alpha_0|) = N\, C_d \ ,$$

where Ro_0 = surface Rossby number, $C_d = u_*/|\mathbf{v}_g|$ the geostrophic drag coefficient, κ = Karman constant, α_0 = cross-isobar angle. The numerical values of M and N are investigated with the aid of several boundary layer models and checked by observations. A theoretical value $M \approx -\ln(\kappa) = 0.90$ is derived and an interpretation of N in terms of flow parameters is given.

Zusammenfassung: In dem Widerstandsgesetz für eine neutrale barotrope Grenzschicht

$$\ln(Ro_0) = M - \ln(C_d) + [\kappa^2/C_d^2 - N^2]^{1/2}$$

and

$$\kappa \sin(|\alpha_0|) = N\, C_d \ ,$$

worin Ro_0 die Oberflächen-Rossby-Zahl, $C_d = u_*/|\mathbf{v}_g|$ den geostrophischen 'drag'-Koeffizienten, κ die Karmansche Konstante und α_0 den Ablenkungswinkel gegenüber den Isobaren bedeuten, treten die beiden Konstanten M und N auf. Deren numerischer Wert wird mit Hilfe verschiedener Grenzschicht-Modelle untersucht, außerdem mit denjenigen verglichen, die durch die Auswertung von Beobachtungen erhalten werden. Für M kann ein theoretischer Wert abgeleitet werden, nämlich $M \approx -\ln(\kappa) = 0{,}90$, während N sich als Reziprokwert der (dimensionslosen) Verdrängungsdicke der Grenzschicht erweist.

Résumé: La loi de résistance dans le cas d'une couche limite barotrope neutre, s'exprime à l'aide des formules

$$\ln(Ro_0) = M - \ln(C_d) + [\kappa^2/C_d^2 - N^2]^{1/2} \text{ et}$$

$\kappa \sin(|\alpha_0|) = N\, C_d$ où Ro_0 représente le nombre de Rossby à la surface, $C_d = u_*/|V_g|$ le coefficient de frottement géostrophique. κ la constante de Karman et α_0 l'angle de déviation par rapport aux isobares. Deux constantes M et N interviennent dans cette loi de résistance. Leur valeur numérique est examinée à l'aide de différents modèles de couche limite. En outre, ces valeurs sont comparées avec celles résultant du traitement d'observations. Il en découle pour M, une valeur théorique, $M = \approx -\ln(\kappa) = 0.90$ alors que N apparait comme étant l'invers d'un paramètre sans dimension représentant une épaisseur caractéristique de la couche limite.

*) SPAAZ – Contribution Nr. 5
Paper presented at the IUGG-IAMAP Symposium on Planetary Boundary Layers, Boulder, Col. March 18–21, 1970.

1. Introduction

KAZANSKII and MONIN (1962) have been the first who derived the resistance law for a neutral barotropic boundary layer of the atmosphere

$$\ln(Ro_0) = M - \ln(C_d) + [\kappa^2/C_d^2 - N^2]^{1/2} \tag{1a}$$

$$\kappa \sin(|\alpha_0|)/C_d = N \tag{1b}$$

where $Ro_0 = |\bar{v}_g|/(f z_0)$ is the surface Rossby number, $|\bar{v}_g|$ the geostrophic wind speed, f the Coriolis parameter and z_0 the roughness length; $C_d = u_*/|\bar{v}_g|$ is the geostrophic drag coefficient, u_* the friction velocity, α_0 the cross-isobar angle and κ the Karman constant. The same formulae have been derived in applying principles of asymptotic similarity by CSANADY (1967), GILL (1967, 1968) and by BLACKADAR and TENNEKES (1968). A review of the different methods of deriving these formulae is given by HANNA (1969).

M and N (in the western world mostly called A and B, in the russian literature B and A) are constants in a neutral boundary layer; M and N will of course depend on the thermal stratification in a diabatic boundary layer. The numerical values of these two constants are not yet determined exactly, their values obtained by evaluating observations scatter rather widely; their numerical values resulting from different boundary layer models vary also with the model assumptions.
It is the purpose of this paper to investigate the available observations and also the boundary layer models in order to find the most probable values of M and N.

2. The physical interpretation of the constants

In order to give an interpretation of the constant N in terms of flow parameters we start with the equations for a stationary and horizontally homogeneous flow for which the vertical variation of density can be neglected

$$\bar{u} - \bar{u}_g = 1/f\, d/dz(\tau_y/\bar{\rho}) \qquad \bar{v} - \bar{v}_g = -1/f\, d/dz(\tau_x/\bar{\rho}) \ . \tag{2}$$

In a coordinate system whose x-axis has the direction of the surface stress τ_x forming the cross-isobar angle α_0 with the geostrophic wind, i.e. when

$$\tau_x(z_0) = \bar{\rho}\, u_*^2 \qquad \tau_y(z_0) = 0 \tag{3}$$

$$\bar{u}_g = |\bar{v}_g| \cos(\alpha_0) \qquad \bar{v}_g = -|\bar{v}_g| \sin(|\alpha_0|) \tag{4}$$

the integrated equations (2) read

$$\int_{z_0}^{\infty} (\bar{u} - \bar{u}_g)\, dz = 0 \qquad \int_{z_0}^{\infty} (\bar{v} - \bar{v}_g)\, dz = u_*^2/f \ . \tag{5}$$

If we define a scale height H for the boundary layer

$$H = \kappa\, u_*/f \tag{6}$$

which is in normal conditions in the order of 1000 m, the displacement thickness δ^* defined as

$$\delta^* = \int_{z_0}^{\infty} (1 - \bar{v}/\bar{v}_g)\, dz \tag{7}$$

results to be

$$\delta^* = C_d H[\kappa \sin(|\alpha_0|)]^{-1} \tag{8}$$

or with regard to eq. (1b)

$$\boxed{N = \frac{1}{\delta^*/H}} \tag{9}$$

One notices that the constant N is the reciprocal of the dimensionless displacement thickness.

In order to give an explanation of the constant M we start from eqs. (2) in vector notation

$$d/dz\,(\pi/\bar{\rho}) = f\,|k \times (\bar{v} - \bar{v}_g) \quad . \tag{10}$$

By differentiating eq. (10) with respect to z and inserting the stress

$$\pi/\bar{\rho} = k_m\, d/dz(\bar{v}) \tag{11}$$

where k_m is the eddy viscosity, one obtains

$$d^2/dz^2(\pi/\bar{\rho}) = f/k_m\, |k \times \pi/\bar{\rho} \quad .$$

This reads in a dimensionless notation

$$d^2/dz^2(\mathbb{T}) = 1/K_m\, |k \times \mathbb{T} \tag{12}$$

where

$$Z \equiv z/H, \quad K_m \equiv k_m/(H^2 f), \quad \mathbb{T} \equiv \pi/(\bar{\rho}\, u_*^2) \tag{13}$$

with H as the scale height according to (6).

As long as a height z is considered within the surface layer ($z_0 < z < z_p$, z_p = height of the surface layer), the eddy viscosity is $k_m \approx \kappa\, u_* z$
or in dimensionless notation

$$K_m \approx Z \qquad (Z < Z_p) \quad . \tag{14}$$

After having inserted (14) into eq. (12) one gets by an integration

$$d/dZ\,(\mathbb{T})\Big|_Z - d/dZ(\mathbb{T})\Big|_{Z_0} \approx |k \times \tilde{\mathbb{T}} \ln(Z/Z_0) \tag{15}$$

where

$$\tilde{\mathbb{T}} = 1/(Z - Z_0) \int_{Z_0}^{Z} \mathbb{T}\, dZ \quad . \tag{16}$$

Since eq. (15) is valid at any height $Z < Z_p$ it can be concluded that

$$d/dZ\,(\mathbb{T})\Big|_{Z_0} \approx |k \times \tilde{\mathbb{T}} \ln(Z_0) \quad . \tag{17}$$

The conditions within the surface layer should be very close to a constant stress condition, therefore and because of eq. (3)

$$\tilde{\mathbb{T}} \approx i \cdot 1 \tag{18}$$

(if the coordinate system is orientated with the x-axis in the direction of the surface stress). With (18) in eq. (17) it follows

$$\left|d/dZ(\mathbb{T})\right|_y \approx \ln(Z_0) \quad . \tag{19}$$

If, on the other hand, the lower boundary condition

$$z \to z_0: \qquad \bar{V} \to 0 \tag{20}$$

is applied to eq. (10) this equation is in dimensionless notation

$$d/dZ\,(\mathbb{T}) = -\,\kappa/C_d\ |k \times (\bar{v}_g)^0 \qquad (Z = Z_0) \tag{21}$$

or

$$|d/dZ\,(\mathbb{T})|_y = -\,\kappa/C_d \cos(\alpha_0) \tag{22}$$

using eq. (4). Equating (19) and (22) one gets

$$\ln(Z_0) \approx -\,\kappa/C_d \cos(\alpha_0) \tag{23}$$

or after replacing the right hand side by eq. (1a)

$$\ln(Z_0) \approx M - \ln(C_d\, Ro_0)\ . \tag{24}$$

The dimensionsless roughness length Z_0 is by definition

$$Z_0 = 1/(\kappa\, C_d\, Ro_0)\ . \tag{25}$$

Inserting this into eq. (24) it follows

$$\boxed{M \approx -\ln(\kappa)} \tag{26}$$

Depending on the value of the Karman constant κ one obtains for $\kappa = 0.40$ $M \approx 0.92$ and for $\kappa = 0.41$ $M \approx 0.88$. The value $M = 0.90$ may be considered to be appropriate.

3. The numerical values of M and N as obtained by observations

In order to get the numerical values of the constants M and N from observations simultaneous measurements of Ro_0, C_d and α_0 are necessary, that means one has to know v_g, π_0, z_0 and f. Only few of such observations are available, they are collected and listed in extenso in a paper by APPLEBY and OHMSTEDE (1964). The resulting values of M and N are listed in table 1 containing also the observations made at Helgoland (key nr. 4 and 5), which are not contained in the aforementioned paper; they are published by LETTAU and HOEBER (1964) and reported in the paper by CSANADY (1967).

Table 1 / Tabelle 1

Key	Site	M	N
1	LEIPZIG	−0.21	4.91
2	SCILLY I	−1.45	4.30
3	SCILLY II	−1.53	2.82
4	HELGOLAND I	3.17	3.26
5	HELGOLAND II	2.39	3.58
6	ELLENDALE	0.81	3.75
7	DREXEL	−1.31	4.02
8	BROKEN ARROW	−1.84	4.62
9	GROESBECK	−2.14	4.20
10	Average	−0.32 ± 1.35	4.12 ± 0.58

The values for the various locations are indicated in figure 1 by the key number; one notices a very large scatter. As shown by the standard deviations the scatter of M is much larger than that one of N. This has been found also by CLARKE, reported by SHEPPARD (1969), evaluating the data from Kerang and Hay

field. Since the observations are only very few and these observations may also still reflect effects of baroclinicity as well as of a non-neutral straticifation one should not consider the averaged values of M and N as very significant. Instead of averaging the constants M and N it would be also possible to average the observations of C_d and α_0 for classes of Ro_0 and then to determine M and N from the averaged observations. In a similar way GILL (1967) obtained values of M and N located in the hatched quadrilateral in figure 1. It is centered at M = 1.70, N = 4.68.

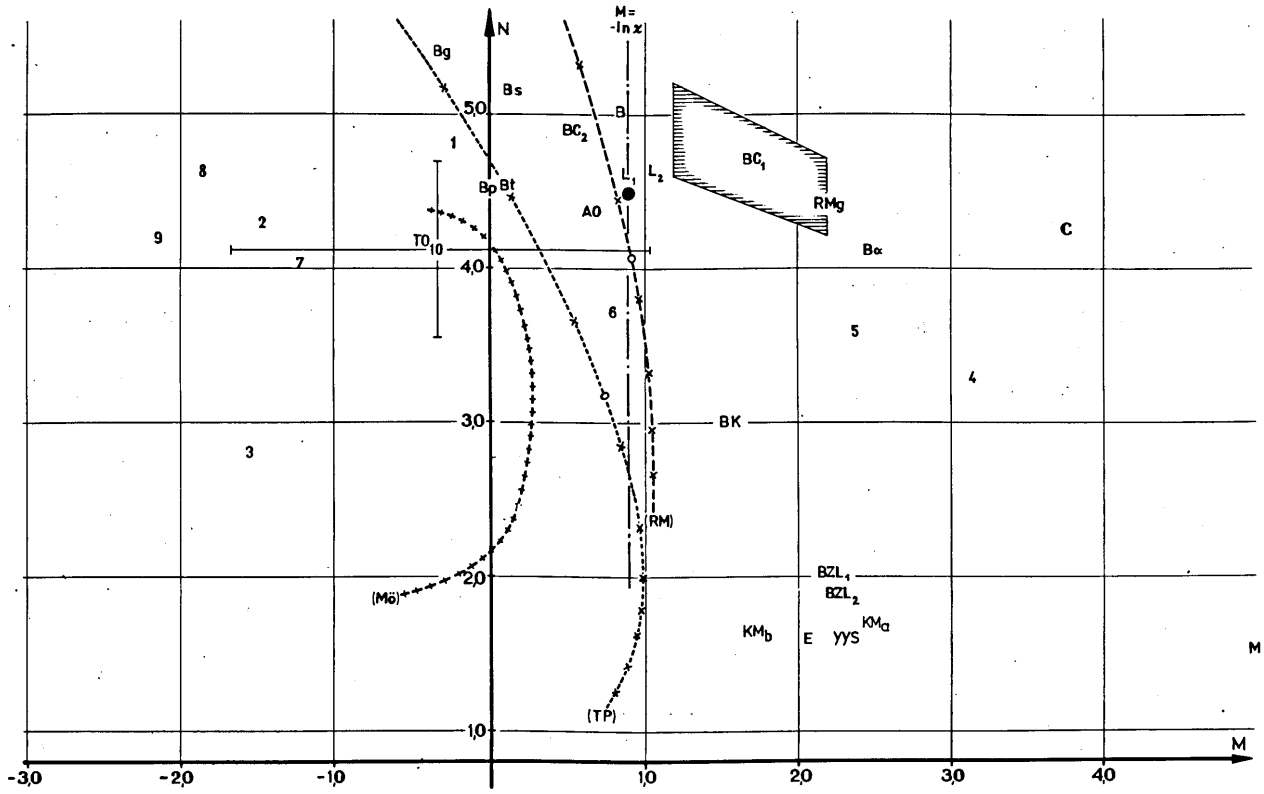

Fig. 1. The constants M and N as obtained by various boundary layer models [characters, see Table 2] and evaluated from observations [numbers, see Table 1]

Bild 1. Die Konstanten M und N wie sie aus verschiedenen Grenzschichtmodellen [Buchstaben, zur Erläuterung siehe Tabelle 2] und aus Beobachtungen [Zahlen, siehe Tabelle 1] erhalten werden

4. The numerical values of M and N as determined by boundary layer models

It is also very interesting to see which numerical values of M and N can be obtained by the various models of the planetary boundary layer. For five of such models the resulting values of M and N are already given in the review paper by ZILITINKEVICH, LAIKHTMAN and MONIN (1967). Several other models have been investigated, the obtained constants M and N are listed in table 2.

Table 2 / Tabelle 2

Key	Model	Source	M	N	Eva-luat.	Remarks
AO	APPLEBY and OHMSTEDE (1964)	R	0.66	4.37	W	
B	BLACKADAR (1962)	37	0.84	5.01	W	
Bα	BLACKADAR (1962)	37	2.5	4.1	ZLM	Using the dependence α_0 (Ro_0)
Bd	BLACKADAR (1962)	37	1.8	6.7	ZLM	Using the dependence C_d (Ro_0)
Bg	BLACKADAR (1962)	37	−0.3	5.4	→	evaluated by GILL (1967)
BC_1	BLACKADAR and CHING (1965)	R	1.7	4.7	A	reported by HANNA (1969)
BC_2	BLACKADAR and CHING (1965)	R	0.53	4.90	W	neutral case
Bs	BLACKADAR (1965) single layer baroclinic	R	0.11	5.15	W	barotropic case
Bt	BLACKADAR (1965) two layer baroclinic	R	0.25	4.51	W	barotropic case
Bp	BLACKADAR (1968)	R	0	4.5	A	by similarity considerations and "patching"
BK	BLINOVA and KIBEL (1937)	10	2.99	1.57	ZLM	$M = 2\ln(\gamma/\kappa)$, $N = \pi/2$ $\gamma = 1{\cdot}7811...$ Euler's const.
BZL_1	BOBYLEVA, ZILITINKEVICH and LAIKHTMAN (1965)	39	2.2	2.0	ZLM	
BZL_2	BOBYLEVA, ZILITINKEVICH and LAIKHTMAN (1965)	39	2.26	1.88	W	
C	CSANADY (1967)	R	3.8	4.28	A	Estimates by using obervational data
E	ELLISON (1956)	20	2.07	1.57	W	barotropic case
KMa	KAZANSKII and MONIN (1961)	60	2.49	1.69	A	k_m has a max., $k_m \to 0$ as $z \to \infty$
KMb	KAZANSKII and MONIN (1961)	60	1.7	1.81	A	$k_m \to$ const. as $z \to \infty$
L_1	LETTAU (1962)	44	0.9	4.6	ZLM	
L_2	LETTAU (1962)	44	1.07	4.62	W	
M	MONIN (1950)	30	5.0	1.5	ZLM	for $\beta = 0.1885$
RMg	ROSSBY and MONTGOMERY (1935)	15	2.2	4.4	→	evaluated by GILL (1967) using $z_p = 0.044\, u_*/f$
TO	TSEITIN and ORLENKO (1960)	26	−0.42	4.17	W	Average of 6 values of the near-neutral stability classes $m = -0.05$ and $m = 0.05$
YYS	YAMAMOTO, YASUDA and SHIMANUKI (1968)	R	2.3	1.6	W	neutral case, average for the range of Rossby numbers $1 \cdot 10^5 \leqslant Ro \leqslant 1 \cdot 10^9$
(TP)	TAYLOR (1915) "patched" with a Prandtl layer (Bt is a special case of this model, corresponding to $\lambda \approx 0.004$)	4	--------		W	$N = \kappa/\sqrt{2\lambda}$ $M = \ln(\kappa/\lambda) - N$ The crosses (upwards) give the values for $\lambda = 0.050$, 0.040, 0.030, 0.025, 0.020, 0.015, 0.010, 0.006, 0.004 the circle is valid for HANNA's (1968) value $\lambda = 0.008$
RM	ROSSBY (1932) ROSSBY and MONTGOMERY (1935)	19 15	– – – –		W	$N = 2\kappa/(3r)$, $M = \sqrt{2}\kappa/3r^2 - N/\sqrt{2}$ The crosses (upwards) give the values for $r = 0.10$, 0.09, 0.08, 0.07, 0.06, 0.05, 0.04, the circle is valid for Rossby's value $r = 0.065$
(Mö)	MOELLER (1931) (with modified lower boundary condition)	R	+ + + + +		W	for $z_p = 0.02$ and values of b ranging from 0.6 (lower end) to 0.06 (upper end)

In order to avoid a presentation of the references of all the investigated models the corresponding reference number in the aforementioned review article by ZILITINKEVICH et al. (1967), where a complete citation is made, has been indicated in the third column of table 2. Only for the models (indicated by R), which are not cited in the aforementioned review article, references are given at the end of this paper.
In the sixth column of table 2 is indicated who evaluated the constants M and N; A means the author of the model, ZLM means ZILITINKEVICH, LAIKHTMAN and MONIN (1967) and W stands for the author of this paper.

For many of the models M and N as given in table 2 are averages of the values obtained for the five surface Rossby numbers $1 \cdot 10^n$, n = 5, 6, 7, 8 and 9, for which the constants scatter slightly. Only for few models the two constants M and N show a distinct dependence on the surface Rossby number what they should not do; these are probably the models (for example: B, BC, Bs) for which the variation of the mixing length with height is assumed to depend also on the surface Rossby number itself.

Figure 1 shows, that the numerical constants obtained by some of the models (BZL_1, BZL_2, E, KM_a, KM_b, YYS) are grouped rather close together in an area $1.7 < M < 2.5$, $1.5 < N < 2.0$. It is believed, that these values are not very realistic. This may depend on the assumed linear increase of the eddy viscosity with height in some of these models.

Because of these and other reasons it cannot be believed that averages of the various values of M as well as of N do give a significant information. (The averages are M = 1.61, N = 3.73 .)

5. Conclusions

The observations available up to now are much too spare to allow an accurate evaluation of the numerical values of M and N; nevertheless it seems to be possible to fix the range in which thes values should be expected.

The various models of the planetary boundary layer are based on different assumptions of the vertical variation of the eddy viscosity; therefore different values of M and N result. Also for these values the scatter is rather large.

After a critical survey of all the data listed in the two tables and with regard to the theoretical result eq. (26) it is proposed to consider

$$M = 0.90 \qquad N = 4.50$$

as the most appropriate values at the present time.

References

APPLEBY, J. F., OHMSTEDE, W. D., 1964: Numerical solution of the distribution of wind and turbulence in the planetary boundary layer. Meteor. Res. Note No. 8 Meteor. Dept. USAERDA, Fort Huachuca, Ariz.

BLACKADAR, A. K., 1965: A single layer theory of the vertical distribution of wind in a baroclinic neutral atmospheric boundary layer Final. Rep. AFCRL-65-531, pp. 1–22. Pennsylvania State Univ., Dept. of Meteor.

BLACKADAR, A. K., CHING, J. K., 1965: Wind distribution in a steady state planetary boundary layer of the atmosphere with upward turbulent heat flux. Final. Rep. AFCRL-65-531, pp. 23–48, Pennsylvania State Univ., Dept. of Meteor.

BLACKADAR, A. K. 1965: A simplified two layer model of the baroclinic neutral atmospheric boundary layer. Final. Rep. AFCRL-65-531, pp. 49–65, Pennsylvania State Univ., Dept. of Meteor.

BLACKADAR, A. K., TENNEKES, H. 1968: Asymptotic similarity in neutral barotropic boundary layers. J. Atm. Sci. **25**, 1015–1020.

CSANADY, G. T. 1967: On the 'resistance law' of a turbulent Ekman layer. J. Atm. Sci. **24**, 467–471.

GILL, A. E. 1967: The turbulent Ekman layer Unpubl. Manuscr., Univ. of Cambridge, Dept. Appl. Math. a. Theor. Phys.

GILL, A. E. 1968: Similarity theory and geostrophic adjustment. Quart. J. Roy. Met. Soc. **94**, 586–588.

HANNA, S. R., 1969: Characteristics of winds and turbulence in the planetary boundary layer. ESSA Techn. Mem. ERLTM-ARL 8, Oak Ridge Tenn., pp. 61.

KAZANSKII, A. B., MONIN, A. S., 1961: On the dynamic interaction between the atmosphere and earth surface. Bull. (Izv.) Acad. Sci. USSR, Geophys. Ser. Nr. 5 pp. 786–788, engl. transl. pp. 514–515.

LETTAU, H. H., HOEBER, H., 1964: Über die Bestimmung der Höhenverteilung von Schubspannung und Austauschkoeffizient in der atmosphärischen Reibungsschicht. Beitr. Phys. Atm. **37**, 105–118.

MOELLER, F., 1931: Austausch und Wind. Met. Z. **48** (2), 69–80.

SHEPPARD, P. A., 1969: The atmospheric boundary layer in relation to large scale dynamics. Pap. present. at the meeting on the General Circulation of the Atmosphere, London, August 1969. (To be publ. in the Proceed.)

YAMAMOTO, G., YASUDA, N., SHIMANUKI, A., 1969: Effect of thermal stratification of the Ekman layer. J. Met. Soc. Japan **46**, 442–455.

ZILITINKEVICH, G., LAIKHTMAN, D. L., MONIN, A. S., 1967: Dynamics of the atmospheric boundary layer. Izv. Acad. Sci. USSR **3** (3), 297–333, Atmosph. and Oceanic Physics. (Engl. transl. pp. 170–191.)

Note added in proof:

Recently (J. Atm. Sci., **26**, 763–767, 1969) DEARDORFF found the values M = 1.3, N = 3.0 by simulating boundary layer turbulence with a numerical model.

Beiträge zur Physik der Atmosphäre, 44. Band, 1971, S. 69–70

A note on a paper by F. Wippermann, „The two constants in the resistance law for a neutral barotropic boundary layer of the atmosphere"

R. J. Taylor

C. S. I. R. O., Division of Meteorological Physics, Station Street, Aspendale, Vic. 3195, Australia

WIPPERMANN (1970) discusses the values of M and N, two constants occurring in the resistance law for a neutral barotropic boundary layer, and gives a completely theoretical derivation of the value of the former, equating it to $-\ln \kappa$, where κ is von Karman's constant.

Unfortunately it is necessary to point out that the derivation is invalid and the step from WIPPERMANN's equation (15) to his equation (17) cannot be justified. Equation (15)

$$\left.\frac{d\mathbb{T}}{dZ}\right|_Z - \left.\frac{d\mathbb{T}}{dZ}\right|_{Z_0} \approx \mathbb{k} \times \tilde{\mathbb{T}} \ln \frac{Z}{Z_0}, \tag{15}$$

together with the fact that it is valid for all Z within a certain range, is said to imply that

$$\left.\frac{d\mathbb{T}}{dZ}\right|_{Z_0} \approx \mathbb{k} \times \tilde{\mathbb{T}} \ln Z_0 \tag{17}$$

and it would follow that

$$\left.\frac{d\mathbb{T}}{dZ}\right|_Z \approx \mathbb{k} \times \tilde{\mathbb{T}} \ln Z .$$

However eq. (15) is equally well satisfied by

$$\left.\frac{d\mathbb{T}}{dZ}\right|_{Z_0} \approx \mathbb{k} \times \tilde{\mathbb{T}} (\ln Z_0 + C)$$

$$\left.\frac{d\mathbb{T}}{dZ}\right|_Z \approx \mathbb{k} \times \tilde{\mathbb{T}} (\ln Z + C)$$

where C is any arbitrary constant whatever.

Instead of quation (17) we would then have

$$\left.\frac{d\mathbb{T}}{dZ}\right|_{Z_0} = \mathbb{k} \times \tilde{\mathbb{T}} \ln \beta Z_0$$

leading to

$$M = \ln \frac{\beta}{\kappa} .$$

The only restrictions on β are that it be independent of height so as to satisfy equation (15) and that it be independent of wind speed so as not to violate the principles of similarity from which the resistance law is derived.

WIPPERMANN, F. (1970), Beiträge zur Physik der Atmosphäre, 43 Band, S. 133–140.

Reply

As R. J. Taylor pointed out the derivation is incorrect between eq. (15) and eq. (17) because the constant c (or $\ln \beta$) is missing in eq. (17).

However, the result eq. (26) would be still valid if one could prove that this constant is zero or at least is small enough to be neglected comparing it with $\ln (1/\kappa)$. A more detailed analysis recently done in order to give this proof has shown that an additional condition is needed, which must concern a height $z > z_p$. Such a condition can not be formulated unless one makes use of the (hypothesized) properties of a boundary layer model. One of such hypotheses could be the following:

Be definition it should be

$$\bar{u}_p(z) = \frac{u}{\kappa} \ln \frac{z}{z_0} \tag{27}$$

where $\bar{u}_p = \bar{u}$ in the surface layer $z_0 \leqslant z \leqslant z_p$; also z_g is defined as the height ($> z_p$), where $\bar{u}_p$ equals the x-component of the geostrophic wind

$$\bar{u}_p(z_g) = \bar{u}_g \tag{28}$$

z_g should not be mixed up with the geostrophic wind level z_G, where for the first time the actual wind reaches the direction of the geostrophic wind. The hypothesis

$$z_g = H \tag{29}$$

is an other expression for the resistance law and at the same time implies $C = 0$ or $\beta = 1.0$. This, of course, does not prove $C = 0$ but may be able to show to some extent what $C = 0$ means physically.

On this occasion it may be usefull to give an other evaluation of experimental data. KUNG (1966) has given empirical formulae for C_d and α_0

$$C_d = \frac{0.205}{\log_{10}(Ro_0) - 0.556} \tag{30a}$$

$$\alpha_0 = \frac{173.58}{\log_{10}(Ro_0)} - 3.03 \tag{30b}$$

which allow to evaluate the constants M and N. This has been done for the range $1 \cdot 10^5 \leqslant Ro_0 \leqslant 1 \cdot 10^9$, one gets

$$\begin{aligned} M &= 1.038 \pm 0.061 \\ N &= 4.636 \pm 0.027 \end{aligned} \tag{31}$$

The rather small standard deviation for both constants shows that the C_d and α_0 obtained by (30a) and (30b) meet very well the resistance law. I think one can have some confidence in these values (31).
$M = 1.038$ means $\beta = 1.13$ or with the negative standard deviation $M = 0.977$ one has $\beta = 1.06$.

I thank Dr. Taylor for his comment.

KUNG, E. C., 1966, Month. Weath. Rev. **96**, 327–341.

F. Wippermann

Empirical Formulae for the Universal Functions $M_m(\mu)$ and $N(\mu)$ in the Resistance Law for a Barotropic and Diabatic Planetary Boundary Layer

Empirische Formeln für die universellen Funktionen $M_m(\mu)$ und $N(\mu)$ im Widerstandsgesetz einer barotropen und diabatischen planetarischen Grenzschicht

F. Wippermann

Technical University Darmstadt, Germany, Department of Meteorology

Received 29 August, 1972

Abstract: The resistance law of the planetary boundary layer can be used only, if the two universal functions $M_m(\mu)$ and $N(\mu)$ are known, which appear in this law. The author proposes two empirical formulae, eqs. (4a) and (4b), for these functions; the formulae are more or less an average over the relationships given up to now Using these formulae the geostrophic drag coefficient C_g and the cross-isobar angle α_0 depending on the stability parameter μ and on the surface Rossby number Ro_0 can be computed. They are displayed in a diagram. The empirical formulae allow also a computation of the limit of the downward turbulent heat flux.

Zusammenfassung: Eine Anwendung des Widerstandsgesetzes für die planetarische Grenzschicht ist nur möglich, wenn die beiden darin auftretenden universellen Funktionen $M_m(\mu)$ und $N(\mu)$ bekannt sind. Für diese werden zwei empirische Formeln, Gln. (4a) und (4b), vorgeschlagen, welche mehr oder weniger ein Mittel der bisher vorliegenden Ergebnisse repräsentieren. Mit den Formeln läßt sich der geostrophische Widerstandskoeffizient C_g und der Ablenkungswinkel α_0 in Abhängigkeit vom Parameter μ für die thermische Schichtung und von der Surface-Rossby-Zahl Ro_0 berechnen; die Ergebnisse sind in einem Diagramm dargestellt. Die Verwendung der empirischen Formeln erlaubt außerdem eine Aussage über den Grenzwert des abwärts gerichteten turbulenten Wärmestromes.

Résumé: La loi de résistance pour la couche limite planétaire ne peut être utilisée que si les deux fonctions universelles $M_m(\mu)$ et $N(\mu)$, qui y figurent, sont connues. Pour celles-ci, l'auteur propose deux formules empiriques (équations 4a et 4b), qui représentent plus ou moins une moyenne des résultats existants. A l'aide de ces formules, on peut calculer le coefficient de frottement géostrophique C_g et l'angle de déviation par rapport aux isobares α_0, en fonction du paramètre de stabilité μ et du nombre de Rossby en surface R_0; les résultats sont représentés par un diagramme. Les formules empiriques permettent aussi d'estimer la valeur limite du flux turbulent de chaleur vers le bas.

I. The empirical formulae

In recent years the resistance law for a barotropic planetary boundary layer (PBL) has been derived in different ways. A first formulation for the neutral case was given by KAZANSKII and MONIN (1961), other derivations by GILL (1967) and CSANADY (1967). An extension to diabatic PBLs was given by MONIN and ZILITINKEVICH (1967), BLACKADAR (1967) as well as BLACKADAR and TENNEKES (1968); an extension to baroclinic cases was published by YORDANOV and WIPPERMANN (1972). In the resistance law

$$\kappa \sin(|\alpha_0|)/C_g = N(\mu, \lambda_x, \lambda_y) \tag{1a}$$

$$\kappa \cos(\alpha_0)/C_g = -M_m(\mu, \lambda_x, \lambda_y) + \ln(C_g Ro_0) \tag{1b}$$

means $Ro_0 = |\hat{v}_g|/(fz_0)$ the surface Rossby number, which is a non-dimensional combination of the given external parameters, namely the geostrophic wind speed $|\hat{v}_g|$, the Coriolis parameter f and the roughness-length z_0. In the usual notation is $C_g = u_*/|\hat{v}_g|$ the gestrophic drag coefficient with u_* the friction velocity, α_0 is the cross-isobar angle and κ is the von Karman constant. $M_m(\mu, \lambda_x, \lambda_y)$ and $N(\mu, \lambda_x, \lambda_y)$ are

the two universal functions of the internal stability parameter μ and of the two internal parameters λ_x and λ_y for the baroclinicity.

$$\mu = H/L_* \tag{2}$$

is the ratio of the scale height H of the PBL to the Monin-Obukhov stability length, where $H = \kappa\, u_*/f$. Since only barotropic PBLs should be considered the parameters λ_x and λ_y are not relevant in this context.

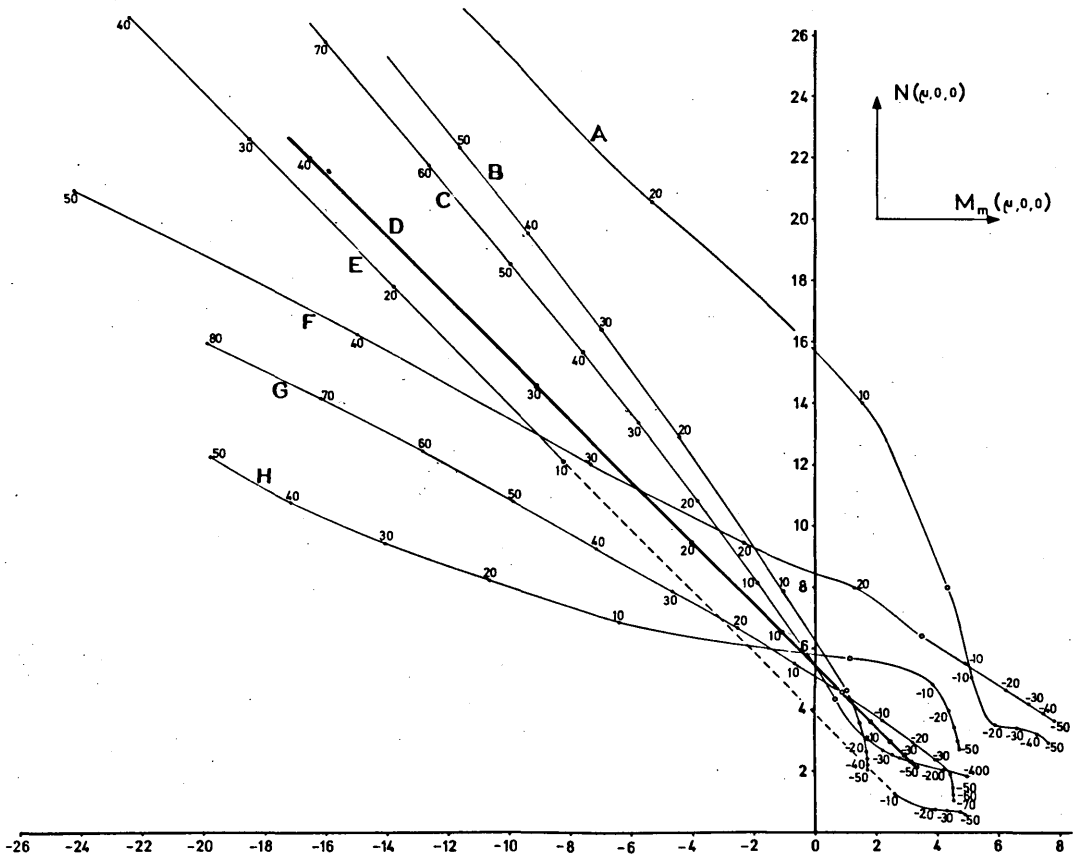

- **Fig. 1.** $M_m(\mu, 0, 0)$ and $N(\mu, 0, 0)$ in a (M_m, N)-plane according to observations and PBL-models. The numbers give the values of the stability parameter μ, the circles denote the neutral case.
  - A Best fit of the O'Neill data according to MONIN and ZILITINKEVICH 1967
  - B Single layer model WIPPERMANN 1972
  - C Single layer model FIEDLER 1972
  - D Empirical formulae (4a), (4b)
  - E Two layer model ZILITINKEVICH 1970
  - F Best fit of the O'Neill data according to ZILITINKEVICH 1970
  - G Empirical formulae PANOFSKY and FIEDLER 1972
  - H Best fit Kerang and Hay data CLARKE 1970

- **Bild 1.** $M_m(\mu, 0, 0)$ und $N(\mu, 0, 0)$ dargestellt in einer (M_m, N)-Ebene nach Beobachtungsauswertungen und nach PBL-Modellen. Die Zahlen an den Kurven geben den Wert des Stabilitätsparameters μ an, die kleinen Kreise bedeuten den neutralen Fall. Die Kurven A–H sind vorstehend erläutert.

For a practical use of the resistance law (1a), (1b) the two functions $M_m(\mu)$ and $N(\mu)$ both functions monotonous in μ have to be known. They can be determined only by an evaluation of observations or as an approximation by a model of the PBL. A collection of such evaluations of observations and of theoretical results was given by the author in a previous paper (WIPPERMANN 1972); This collection is represented by the curves A, B, C, E, F and H of the figure 1. In addition two recent empirical formulae (curve G) by PANOFSKY and FIEDLER (1972) are shown in this figure.

The curves in the (M_m, N)-plane scatter widely and it is not yet possible to get a correct formulation for the two functions. Therefore the author proposes the curve D in figure 1 showing N as function of M_m with parameter μ.

$$M_m(\mu, 0, 0) + N(\mu, 0, 0) = 5.5 \tag{3}$$

as a preliminary relation between $M_m(\mu)$ and $N(\mu)$; the curve represents more or less an average of the scattering results displayed in figure 1. Also the dependence on the stability parameter μ is chosen in accordance with the other results, the two empirical formulae are proposed:

$$N(\mu, 0, 0) = 1.83 + 2.77 \exp(\mu/20) \tag{4a}$$
$$M_m(\mu, 0, 0) = 3.67 - 2.77 \exp(\mu/20) \tag{4b}$$

Of course, these formulae have to be improved when more informations will be available by more suitable observations. But for the time being the formulae (4a), (4b) seem acceptable as preliminary results. The two curves (4a) and (4b) are shown in figure 2, some values are given in table 1

■ **Table 1/Tabelle 1.** (Because of the definition of L_∞ see section IV)

μ	+30	+20	+10	+5	0	−5	−10	−20	−30	−40	−50
M_m	−8.9	−3.9	−1.0	0	0.9	1.5	1.9	2.6	3.0	3.2.	3.4
N	14.4	9.4	6.5	5.5	4.6	4.0	3.6	2.9	2.5	2.3	2.1
L_∞	1.26 10^{-3}	2.28 10^{-3}	6.32 10^{-3}	9.94 10^{-3}	1.40 10^{-2}	2.09 10^{-2}	3.13 10^{-2}	6.40 10^{-2}	1.54 10^{-1}	3.43 10^{-1}	7.63 10^{-1}

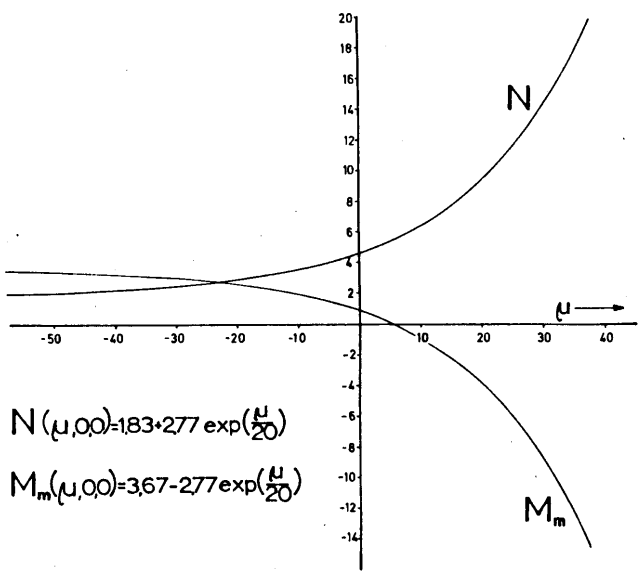

● **Fig. 2**
The two empirical formulae for $M_m(\mu, 0, 0)$ and $N(\mu. 0, 0)$ as given in eqs. (4a), (4b).

● **Bild 2**
Die beiden empirischen Formeln für $M_m(\mu, 0, 0)$ und $N(\mu, 0, 0)$ entsprechend den Gln. (4a), (4b).

With increasing instability the functions $M_m(\mu)$ and $N(\mu)$ approach very rapidly the limiting values for $\mu \to -\infty$

$$\lim_{\mu \to -\infty} M(\mu, 0, 0) = 1.83 \qquad \lim_{\mu \to -\infty} N(\mu, 0, 0) = 3.67 \tag{5}$$

for instance $M_m(-70) = 1.91$ and $N(-70) = 3.59$ already.

II. The drag coefficient and the cross-isobar angle

Two diagrams have been computed for $C_g(Ro_0, \mu)$ and $\alpha_0(Ro_0, \mu)$ by using the resistance law (1a), (1b) and the empirical formulae (4a), (4b) for the universal functions; these diagrams are shown in figure 3. It exist a set of observations for $C_g(Ro_0)$ and $\alpha_0(Ro_0)$, i. e. a collection of data by LETTAU (1959),

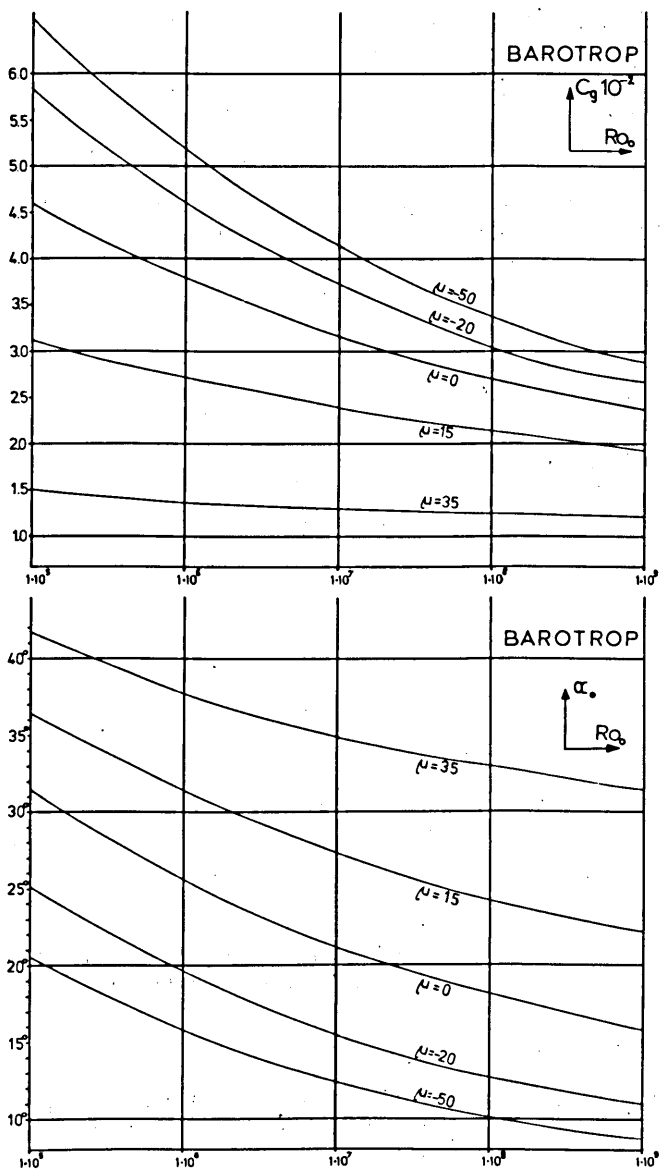

- **Fig. 3**
  $C_g(Ro_0, \mu)$ upper part and $\alpha_0(Ro_0, \mu)$ lower part as obtained by the resistance law eqs. (1a), (1b) using the empirical formulae (4a), (4b).

- **Bild 3**
  $C_g(Ro_0, \mu)$ im oberen Teil und $\alpha_0(Ro_0, \mu)$ im unteren Teil wie es sich nach dem Widerstandgesetz (1a), (1b) ergibt, wenn in diesem die empirischen Formenl (4a), (4b) verwendet werden.

an additional collection by BLACKADAR (1967) and other additions by ZILITINKEVICH (1970). Unfortunately the thermal stratification as well as the baroclinicity have not been determined accurately for any of these data. Therefore they are unsuitable for a proof of the results obtained by the resistance law and the empirical formulae.

III. The limit for the turbulent downward heat flux

The definition (2) of the internal stability parameter μ can be written also

$$\mu = -\frac{\kappa^2 \beta q_0}{f c_p \bar{\rho} u_*^2} \tag{6a}$$

or

$$\mu = -\frac{1}{a}\frac{q_0}{C_g^2} \quad \text{with } a = \frac{f c_p \bar{\rho} |\hat{v}_g|^2}{\kappa^2 \beta} \tag{6b}$$

where q_0 is the turbulent heat flux at the ground, ρ is the density and c_p the specific heat. $\beta = g/\tilde{\vartheta}$ contains the acceleration of gravity and a reference temperature. The abbreviation a in eq. (6b) consists of external parameters only, it has the dimension of a heat flux (cal cm^{-2} sec^{-1}) and is used to non-dimensionalize the turbulent heat flux q_0. This heat flux

$$q_0 = -a C_g^2 \mu \quad (\text{with } q_0 > 0 \text{ upward directed}) \tag{7}$$

increases for increasing instability (i. e. for increasing $|\mu|$; $\mu < 0$), since C_g increases with increasing instability. However for a stable stratification ($\mu > 0$) C_g decreases with increasing stability (i. e. with increasing μ); the increasing μ and the decreasing C_g in the stable range causes a maximum of q_0, which occurs at the stability μ_*. This stability depends on the surface Rossby number Ro_0. Figure 4 shows how the

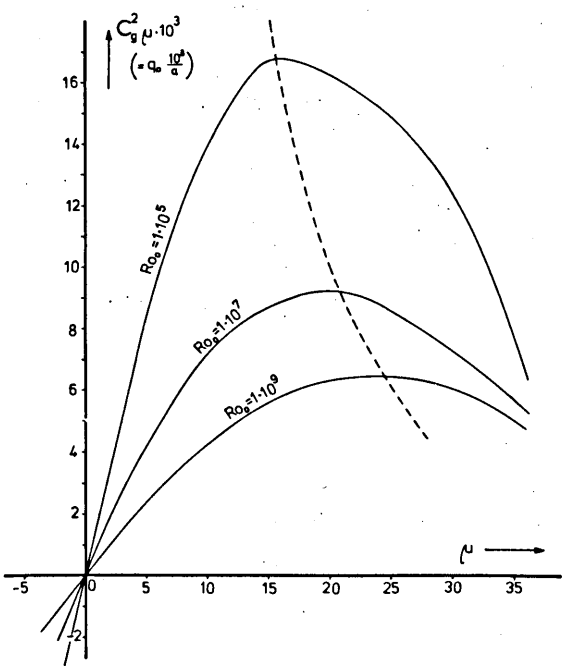

- **Fig. 4**
  The (nondimensional) turbulent downward heat flux depending on the stability parameter μ and on the surface Rossby number Ro_0.

- **Bild 4**
  Der (dimensionslose) abwärts gerichtete turbulente Wärmestrom in Abhängigkeit vom Stabilitätsparameter μ und der Surface Rossby-Zahl Ro_0.

(nondimensional) turbulent heat flux depends on the internal stability parameter μ and on the surface Rossby number Ro_0. Some values of μ_* and the corresponding values of $q_{0,max}$ are given in table 2 for two geostrophic wind velocities. (These wind velocities imply a roughness-length $z_0 = 89$ cm, resp. $z_0 = 44.5$ cm for $Ro_0 = 1 \cdot 10^5$ and a $z_0 = 0.089$ mm, resp. $z_0 = 0.0445$ mm for $Ro_0 = 1 \cdot 10^9$).

■ Table 2/Tabelle 2

Ro_0	μ_*	$\mu_* C_g^2(\mu_*)$	$q_{0,max}$ I [mcal cm^{-2} sec^{-1}]	$q_{0,max}$ II [mcal cm^{-2} sec^{-1}]
$1\ 10^5$	+ 16	$1.68\ 10^{-2}$	1.02	0.26
$1\ 10^6$	+ 18	$1.25\ 10^{-2}$	0.76	0.19
$1\ 10^7$	+ 21	$9.2\ 10^{-3}$	0.56	0.14
$1\ 10^8$	+ 23	$7.5\ 10^{-3}$	0.45	0.11
$1\ 10^9$	+ 24	$6.4\ 10^{-3}$	0.39	0.10
			I: $\lvert\hat{v}_g\rvert = 10$ m/s II: $\lvert\hat{v}_g\rvert = 5$ m/s $f = 1.13\ 10^{-4}$ sec^{-1} ($\varphi = 50°$) $\rho = 1.25\ 10^{-3}$ g cm^{-3}, $\tilde{\vartheta} = 280°$K	

The heat flux a used for nondimensionalization is a = 60.7 mcal cm^{-2} sec^{-1}, respectively a = 15.2 mcal cm^{-2} sec^{-1}.

For a physical interpretation of these results one may think, that a stable thermal stratification stronger than a critical one ($\mu > \mu_*$) dampens the turbulence and makes it more and more ineffective for transporting heat downward.

An application of the resistance law (1a), (1b) requires the use of horizontally (over a large area) averaged values in order to satisfy the conditions of horizontal homogeneity of the PBL. Such an averaged value of μ will exceed μ_* probably very seldom, so that in general increasing μ means increasing downward heat flux.

BERZ (1969) has published a one year-set of heat flux measurements (each averaged over 60 minutes) carried out near Munich, Germany, in the period 1 June 1964 – 31 May 1965. The largest downward heat flux measured during this period occured on 17 January 1965, 1530–1630 local time with 2.55 mcal cm^{-2} sec^{-1}. Of course, this value is larger as the values given in table 2; but one should have in mind, that this is a value obtained at a single point and averaged only over 60 minutes. It does not represent a horizontally averaged value as it should for the considerations here. It should be mentioned also, that the experimental station near Munich has an extrem large roughness-length; Ro_0 is therefore small and $q_{0,max}$ large.

The measured maximal downward heat flux aggrees quite well at least in the order of magnitude with the limit obtained by the resistance law.

IV. The asymptotic mixing-length depending on μ

In several mixing-length hypotheses appears a parameter L_∞ which represents the asymptotic mixing-length (to be approached at the top of the PBL) and reflects the influence of the thermal stratification on the eddy viscosity, see for example WIPPERMANN (1971). In this paper a preliminary empirical relationship has been given between the asymptotic mixing-length L_∞ and the parameter μ for the thermal stratification, namely

$$L_\infty = 10^{-\delta_1} H \quad \text{with} \quad \delta_1 = (\mu + 44.2)/24.4$$

The formulae (4a), (4b) enable us to improve this relationship. The author proposes now the formula

$$l_\infty = 10^{-\delta_2} H \quad \text{with} \quad \delta_2 = (\mu + 53.4)/28.8 \tag{8}$$

for which few values are listed in the last row of table 1, where $L_\infty = l_\infty / H$. One notices, that in the neutral case l_∞ amounts to 1.4 % of the scale height H of the PBL, i. e. $l_\infty(\mu = 0) = 14$ m if H = 1 km. In the extrem unstable case ($\mu = -50$) the asymptotic mixing-length $l_\infty = 0.76$ H, but in the very stable case ($\mu = +30$) l_∞ reaches only a little bit more than 1 $^0/_{00}$ of H.

References

BERZ, G. (1969): Untersuchungen zum Wärmehaushalt der Erdoberfläche und zum bodennahen atmosphärischen Transport. Wiss. Mittl. 16 Meteor. Inst. Univ. München, pp. 94.

BLACKADAR, A. K. (1965): A single layer theory of the vertical distribution of wind in a baroclinic neutral atmospheric boundary layer. Part I, pp 1–22, Final Report AFCRL-65-531, 31 July 1965, Pennsylvania State Univ., Dept. Meteorol., University Park.

BLACKADAR, A. K. (1967): External parameters of the wind flow in the barotropic boundary layer of the atmosphere, GARP Study Conference, Stockholm, Append. IV, pp. 11.

BLACKADAR, A. K. and TENNEKES, H. (1968): Asymptotic similarity in neutral barotropic boundary layers. J. Atm. Sci. 25, 1015–1020.

CLARKE, R. H. (1970): Observational studies in the atmospheric boundary layer. Quart. J. Roy. Meteor. Soc. 96, 91–114.

CSANADY, C. T. (1967): On the "resistance law" of a turbulent Ekman layer. J. Atm. Sci. 24, 467–471.

FIEDLER, F. (1972): The effect of baroclinicity on the resistance law in a diabatic Ekman layer. Beitr. Phys. Atm. 45, 164–173.

GILL, A. E. (1967): The turbulent Ekman layer. Unpubl. Manuscr., Univ. Cambridge, Dept. Appl. Math. & Theor. Phys.

KAZANSKII, A. B. and MONIN, A. S. (1961): On the dynamic interaction between the atmosphere and the earth surface. Bull. (Izv.) Acad. Sci. USSR, Geophys. Ser. Nr. 5, pp 786–788, engl. transl. pp 514–515.

LETTAU, H. H. (1959): Wind profile, surface stress and geostrophic drag coefficient in the atmospheric surface layer. Pp 241–257 Advances in Geophysics, Vol. 6, Academic Press, 471 pp.

MONIN, A. S. and ZILITINKEVICH, S. S. (1967): Planetary boundary layer and large scale atmospheric dynamics. GARP Study Conference Stockholm, Append. V, pp 37.

PANOFSKY, H. A. and FIEDLER, F. (1972): The geostrophic drag coefficient and the "effective" roughness-length. Quart. J. Roy. Meteor. Soc. 98, 213–220.

WIPPERMANN, F. (1971): A mixing-length hypothesis for the planetary boundary layer flow in the atmosphere. Beitr. Phys. Atm. 44, 215–226.

WIPPERMANN, F. (1972): Universal profiles in the barotropic planetary boundary layer. Beitr. Phys. Atm. 45, 148–163.

YORDANOV, D. and WIPPERMANN, F. (1972): The parameterization of turbulent fluxes of momentum, heat and moisture at the ground in a baroclinic planetary boundary layer. Beitr. Phys. Atm. 45, 58–65.

ZILITINKEVICH, S. S. (1970): The dynamics of the atmospheric boundary layer. Gidrometeor. Leningrad, pp 291 (in russ.).

The Parametrization of the Turbulent Fluxes of Momentum, Heat and Moisture at the Ground in a Baroclinic Planetary Boundary Layer

Die Parametrisierung der turbulenten Impuls-, Wärme- und Feuchteflüsse am Boden in einer baroklinen planetarischen Grenzschicht

D. Yordanov*) and F. Wippermann

Technische Hochschule Darmstadt, Germany, Department of Meteorology

Received July 14, 1971

Summary: In the same way as for a barotropic planetary boundary layer so-called resistance laws (a mechanical one, a thermal one and one for the moisture) can be derived for a baroclinic boundary layer. The form of these laws is completely the same as in the barotropic case, but in the baroclinic case the universal functions of the internal stability parameter μ are also universal functions of two internal parameters for the baroclinicity.

For a parametrization the available external parameters for the stability and for the baroclinicity have to be converted into the corresponding internal parameters which are needed.

Zusammenfassung: In der gleichen Weise wie für eine barotrope planetarische Grenzschicht können auch für eine barokline Grenzschicht sogenannte Widerstandsgesetze (ein mechanisches, ein thermisches und eines für die Feuchtigkeit) hergeleitet werden. Die Form dieser Gesetze ist völlig gleich derjenigen für den barotropen Fall, lediglich die auftretenden universellen Funktionen des internen Stabilitätsparameters sind im baroklinen Fall auch noch Funktionen von zwei internen Parametern für die Baroklinität.

Für eine Parametrisierung müssen die verfügbaren externen Parameter für die Stabilität und für die Baroklinität in die entsprechenden internen Parameter umgewandelt werden, welche man braucht.

Résumé: De la même façon que pour une couche limite planétaire barotrope, on peut établir pour une couche limite barocline des «lois de résistance»: une loi mécanique, une loi thermique et une autre pour l'humidité. La forme de ces lois est tout à fait la même que dans le cas barotrope mais, dans le cas barocline, les fonctions universelles du paramètre stabilité interne sont aussi fonctions de deux paramètres internes de baroclinie.

La paramétrisation exige que les paramètres externes de stabilité et de baroclinie dont on dispose soient convertis en paramètres internes correspondants.

1. Introduction

For the parametrization of the turbulent fluxes in a baroclinic planetary boundary layer (PBL) it seems to be sufficient to consider only a linear variation of the geostrophic wind with height

$$\hat{u}_g = \hat{u}_{go} + (d\,\hat{u}_g/dz)\,(z - z_o) \quad \text{with} \tag{1a}$$

$$d\,\hat{u}_g/dz = -\,g/(f\,\tilde{\vartheta})\,\partial\,\hat{\vartheta}/\partial y = \text{const} = -\,f\,B_y$$

$$\hat{v}_g = \hat{v}_{go} + (d\,\hat{v}_g/dz)\,(z - z_o) \quad \text{with} \tag{1b}$$

$$d\,\hat{v}_g/dz = g/(f\,\tilde{\vartheta})\,\partial\,\hat{\vartheta}/\partial x = \text{const} = f\,B_x$$

*) On leave from the Bulgarean Academy of Science, Department of Geophysics, Sofia, on a fellowship by the A.v. Humboldt-Foundation

where the index g indicates the geostrophic wind and the index o values at the ground ($z = z_o$); f is the Coriolis parameter, g the acceleration due to gravity and ϑ the virtual potential temperature ($\tilde{\vartheta}$ is a mean or reference value for the total PBL). The x-axis is orientated in the direction of τ_0, the Reynolds stress at the ground. With the assumption (1a, 1b) the equations for a baroclinic PBL, i.e. a baroclinic boundary layer with steadyness and horizontal homogeneity can be written:

$$f(\hat{v} - \hat{v}_g) + \frac{d}{dz}\{k_m\, d(\hat{u} - \hat{u}_g)/dz\} - g/(f\,\tilde{\vartheta})\,\partial\,\hat{\vartheta}/\partial x\, dk_m/dz = 0 \qquad (2)$$

$$-f(\hat{u} - \hat{u}_g) + \frac{d}{dz}\{k_m\, d(\hat{v} - \hat{v}_g)/dz\} + g/(f\,\tilde{\vartheta})\,\partial\,\hat{\vartheta}/\partial y\, dk_m/dz = 0 \qquad (3)$$

k_m is the coefficient of eddy viscosity. The assumption of a steady state requires that any turbulent transport q of sensible heat

$$q = -c_p\,\bar{\rho}\,k_H\,\partial\,\hat{\vartheta}/\partial z \qquad (4)$$

and/or any turbulent transport of moisture

$$j = -\bar{\rho}\,k_s\,\partial\hat{s}/\partial z \qquad (5)$$

has to be constant with height as long as a divergence of radiative fluxes is not effective and as long as condensation as well as evaporation is absent. k_H is the coefficient for the turbulent exchange of sensible heat and k_s that one for moisture, c_p is the specific heat and ρ the density.

In order to parameterize the PBL only the turbulent fluxes of momentum, sensible heat and moisture at the ground ($z = z_o$) are needed, i.e.

$$u_* = (\tau_0/\bar{\rho})^{1/2} \quad \text{and } \alpha_0 \qquad (6a) \qquad u_*$$

$$\vartheta_* = -\frac{q_o + q_{so}}{c_p\,\bar{\rho}\,\kappa\,u_*} \qquad (6b)$$

$$s_* = -\frac{j_o}{\bar{\rho}\,\kappa\,u_*} \qquad (6c)$$

u_* is the friction velocity, α_0 the cross-isobar angle, κ the von Karman constant and q_{so} the turbulent transport of latent heat at the ground. These four quantities (u_*, α_0, ϑ_*, s_*) can be obtained either by an integration of the four equations (2)–(5) with three additional equations gained by hypotheses for k_m, k_H and k_s or by application of the similarity theory. In the later case there remain four unknown universal functions of the static stability and of the baroclinicity which have to be determined by observations. In the following sections shall be shown how the four quantities u_*, α_0, ϑ_* and s_* can be determined by the application of the similarity theory in a baroclinic PBL.

2. Internal and external parameters

For an application of the similarity theory first all relevant parameters should be listed in the following table.

Explanation of the parameters: z_o is the roughness length, $\beta = g/\tilde{\vartheta}$, $|\hat{\mathbb{V}}_{go}|$ is the geostrophic wind speed at the ground, the components are $\hat{u}_{go} = |\hat{\mathbb{V}}_{go}|\cos(\alpha_0)$ and $\hat{v}_{go} = |\hat{\mathbb{V}}_{go}|\sin(|\alpha_0|)$. It is $\delta\,\hat{\vartheta} = \hat{\vartheta}(z = h) - \hat{\vartheta}(z = z_o)$ and $\delta\hat{s} = \hat{s}(z = h) - \hat{s}(z = z_o)$, here h is the height of the upper border of the PBL, a definition will be given later. $\nabla_2\,\hat{\vartheta}$ means the (twodimensional) horizontal gradient of $\hat{\vartheta}$ and γ is the angle between $\hat{\mathbb{V}}_{go}$ and $\nabla_2\,\hat{\vartheta}$.

$\hat{u}, \hat{v}, \hat{\vartheta}, \hat{s}, k_m, k_H, k_s, \tau, \ldots$		dependent variable
z		independent variable
z_o		local parameters
f		
β		
u_*	$\lvert\hat{V}_{go}\rvert$	internal (left) or external (right) fluid parameters for a barotropic PBL
ϑ_*	$\delta\hat{\vartheta}$	
s_*	$\delta\hat{s}$	
$\partial\hat{\vartheta}/\partial x$	$\lvert\nabla_2\hat{\vartheta}\rvert$	additional internal (left) or external (right) parameters for a baroclinic PBL
$\partial\hat{\vartheta}/\partial y$	γ	

The parameters listed in the table are considered to be relevant, i.e. the local parameters together with either the internal or with the external fluid parameters describe the turbulent state of the PBL as it is necessary for determining the vertical profiles of the dependent variables.

Since we have for each dependent variable one independent variable and 7 parameters the π-theorem requires for three basic dimensions (cm, sec, grad) that any dimensionless dependent variable should depend only on five dimensionless combinations of the parameters. Here it has been assumed that for any dependent variable, except for the moisture $\hat{s}$, the internal parameter s_* or the external parameter $\delta\hat{s}$ is not relevant; the dimensionless moisture depends on the same number (5) of dimensionless combinations of parameters because one more basic dimension (gramm) is involved.

Using the internal parameters these relations are:

$$\frac{\hat{u}}{u_*} = F_u\,(Z, Z_o, \mu, B_x, B_y) \tag{7a}$$

$$\frac{\hat{v}}{v_*} = F_v\,(Z, Z_o, \mu, B_x, B_y) \tag{7b}$$

$$\frac{\hat{\vartheta}}{\vartheta_*} = F_\vartheta\,(Z, Z_o, \mu, B_x, B_y) \tag{7c}$$

$$\frac{s}{s_*} = F_s\,(Z, Z_o, \mu, B_x, B_y) \tag{7d}$$

The meaning of the dimensionless combinations of parameters is:

$$Z \equiv z/H \qquad Z_o \equiv z_o/H \qquad H \equiv \kappa u_*/f \tag{8a}$$

where H is the internal scale height of the PBL. μ is called the internal stability parameter, it is defined as

$$\mu \equiv \kappa^3 \beta/f\, \vartheta_*/u_* = H/L_* \tag{8b}$$

with the Monin-Obukhov stability-length L_*

$$L_* \equiv -\frac{c_p\, \bar{\rho}\, u_*^3}{\kappa\, \beta\, (q_o + q_{so})} \tag{8c}$$

According to the definition in the equations (1a) and (1b)

$$B_x = \beta/f^2\ \partial\hat{\vartheta}/\partial x \qquad B_y = \beta/f^2 \partial\hat{\vartheta}/\partial y \tag{8d}$$

When instead the internal the external parameters are used one obtains for the relations:

$$\frac{\hat{u}}{|\hat{v}_{go}|} = G_u(z/\Lambda, Ro_0, S, B_n, \gamma) \tag{9a}$$

$$\frac{\hat{v}}{|\hat{v}_{go}|} = G_v(z/\Lambda, Ro_0, S, B_n, \gamma) \tag{9b}$$

$$\frac{\hat{\vartheta}}{\delta\hat{\vartheta}} = G_\vartheta(z/\Lambda, Ro_0, S, B_n, \gamma) \tag{9c}$$

$$\frac{\hat{s}}{\delta\hat{s}} = G_s(z/\Lambda, Ro_0, S, B_n, \gamma) \tag{9d}$$

In these equations the parameters and their dimensionless combinations are:

$$\Lambda = |\hat{v}_{go}|/f \tag{10a}$$

Λ is the external scale height of the PBL,

$$Ro_0 = |\hat{v}_{go}|/(fz_0) = (z_0/\Lambda)^{-1} \tag{10b}$$

is the surface Rossby number and S is the external stability parameter

$$S = \beta\delta\hat{\vartheta}/(f|\hat{v}_{go}|) \tag{10c}$$

The two external parameters for the baroclinicity are B_n and γ, the later is already explained in the table.

$$B_n = \beta|\nabla_2\hat{\vartheta}|/f^2 \tag{10d}$$

For the reason of application of certain similarity properties lateron only the eqs. (7a)–(7d) will be used, in which the internal fluid parameters are involved. This means for the practice of parametrization that relations have to be known between the internal and the external parameters; these relations are:

$$\frac{H}{\Lambda} = \kappa\frac{u_*}{|\hat{v}_{go}|} = \kappa.C_d \tag{11a}$$

where $C_d = u_*/|\hat{v}_{go}|$ is called the geostrophic drag coefficient,

$$\frac{\mu}{S} = \kappa^3\,\vartheta_*/\delta\hat{\vartheta}\,|\hat{v}_{go}|/u_* = \kappa^3\,C_{th}/C_d \tag{11b}$$

with $C_{th} = \vartheta_*/\delta\hat{\vartheta}$ the thermal drag coefficient and finally for the baroclinicity

$$\frac{B_y}{B_x} = \text{tang}\,(\alpha_0 + \gamma) \qquad \frac{B_x}{B_n} = \cos\,(\alpha_0 + \gamma) \tag{11c}$$

It should be noted, that the dimensionless roughness length Z_0 can be written

$$Z_0 = (\kappa\,C_d\,Ro_0)^{-1} \tag{12}$$

As mentioned before the turbulent state of the PBL is determined completely by either the internal or the external parameters listed in the table. That means that each internal parameter made dimensionless by the corresponding external parameter has to depend on all the dimensionless combinations of external parameters except on z/Λ:

$$\frac{u_*}{|\hat{\mathbb{V}}_{go}|} \equiv C_d = \psi_{C_d}(Ro_o, S, B_n, \gamma) \tag{13a}$$

$$\frac{\vartheta_*}{\delta\hat{\vartheta}} \equiv C_{th} = \psi_{C_{th}}(Ro_o, S, B_n, \gamma) \tag{13b}$$

$$\frac{s_*}{\delta\hat{s}} \equiv C_s = \psi_{C_s}(Ro_o, S, B_n, \gamma) \tag{13c}$$

$$\alpha_0 = \psi_\alpha(Ro_o, S, B_n, \gamma) \tag{13d}$$

The cross-isobar angle is itself dimensionless, for it can be drawn the same conclusion.

The eqs. (13a)–(13d) are the most important equations for the purpose of parametrization of the PBL. If one would know the functions ψ_{C_d}, $\psi_{C_{th}}$, ψ_{C_s} and ψ_α these equations would allow to compute the turbulent transports of momentum, heat and moisture at the ground when the four external parameters Ro_o, S, B_n and γ are given. The equations (13a)–(13d) are the resistance laws in a general form; in the next sections it shall be tried to get these four ψ-functions by applying the principle of Rossby-similarity and by using the logarithmic behaviour of the vertical profiles for $\hat{u}$, $\hat{\vartheta}$ and $\hat{s}$ in the immediate neighbourhood of z_o.

3. Rossby similarity

The main statement of the so-called auto-model hypothesis is, that the vertical variation of the velocity components, of the temperature of or the moisture, made dimensionless by the corresponding internal parameter, does not depend on the roughness length Z_o as long as the considered height Z is large compared with Z_o:

$$\kappa \frac{\hat{u}(Z_2) - \hat{u}(Z_1)}{u_*} = \psi_u(Z_2, \mu, B_x, B_y) - \psi_u(Z_1, \mu, B_x, B_y) \tag{14a}$$

$$\kappa \frac{\hat{v}(Z_2) - \hat{v}(Z_1)}{u_*} = \psi_v(Z_2, \mu, B_x, B_y) - \psi_v(Z_1, \mu, B_x, B_y) \tag{14b}$$

$$\frac{\hat{\vartheta}(Z_2) - \hat{\vartheta}(Z_1)}{\vartheta_*} = \psi_\vartheta(Z_2, \mu, B_x, B_y) - \psi_\vartheta(Z_1, \mu, B_x, B_y) \tag{14c}$$

$$\frac{\hat{s}(Z_2) - \hat{s}(Z_1)}{s_*} = \psi_s(Z_2, \mu, B_x, B_y) - \psi_s(Z_1, \mu, B_x, B_y) \tag{14d}$$

The range of height, in which the eqs. (14a)–(14d) are valid, is extended as farer down as smaller Z_0 is. According to eq. (12) $Z_0 \to 0$ means $Ro_0 \to \infty$, therefore the similarity of the profiles given in (14a)–(14d) is called Rossby similarity. It must be stated clearly that the profiles are independent of Z_0 only when internal parameters are used as done in (14a)–(14d). It can be concluded that also the profiles of k_m, k_H, k_s, τ and others as turbulent energy, dissipation rate, . . . (for the quantity itself, not for the vertical difference) with the same conditions are independent of Z_0 when the quantities are made dimensionless by internal parameters.

Now in the eqs. (14a)–(14d) Z_2 will be replaced by the variable Z and Z_1 by Z_h, where Z_h is the dimensionless height of the PBL, it is $Z_h = h/H$; if one assumes that the upper boundary condition (for $Z \to \infty$) is already satisfied to a certain degree at $Z = Z_h$ than with respect to the Rossby similarity it can be concluded, that Z_h is a universal function of the internal stability parameter μ and the two internal parameters B_x and B_y for the baroclinicity. Of course Z_h should be independent of Ro_0 and therefore it is not comparable with the quantities listed in eqs. (13a)–(13d).
With the forementioned specification for Z_2 and Z_1 the eqs. (14a)–(14d) will read:

$$\kappa \frac{\hat{u}(Z) - \hat{u}_{go}}{u_*} = \psi_u(Z, \mu, B_x, B_y) - \psi_u(Z_h, \mu, B_x, B_y) - \kappa^2 B_y Z_h = \varphi_u(Z, \mu, B_x, B_y) \tag{15a}$$

$$\kappa \frac{\hat{v}(Z) - \hat{v}_{go}}{u_*} = \psi_v(Z, \mu, B_x, B_y) - \psi_v(Z_h, \mu, B_x, B_y) + \kappa^2 B_x Z_h = \varphi_v(Z, \mu, B_x, B_y) \tag{15b}$$

$$\frac{\hat{\vartheta}(Z) - \hat{\vartheta}(Z_h)}{\vartheta_*} = \psi_\vartheta(Z, \mu, B_x, B_y) - \psi_\vartheta(Z_h, \mu, B_x, B_y) = \varphi_\vartheta(Z, \mu, B_x, B_y) \tag{15c}$$

$$\frac{\hat{s}(Z) - \hat{s}(Z_h)}{s_*} = \psi_s(Z, \mu, B_x, B_y) - \psi_s(Z_h, \mu, B_x, B_y) = \varphi_s(Z, \mu, B_x, B_y) \tag{15d}$$

4. The resistance laws in a baroclinic PBL

In the literature can be found different methods to derive the resistance laws, see KAZANSKII and MONIN (1961), CSANADY (1967), GILL (1967, 1968) as well as BLACKADAR and TENNEKES (1968); these all are based on the same idea to combine the profiles (15a)–(15d) obtained for Rossby similarity with some Prandtl layer properties at the ground. Here the simple method of matching the profiles (15a)–(15d) with the following logaithmic profiles should be applied.

$$\kappa \hat{u}(Z)/u_* = \ln(Z/Z_0) \tag{16a}$$

$$\kappa \hat{v}(Z)/u_* = 0 \tag{16b}$$

$$a_{Ho}(\hat{\vartheta}(Z) - \hat{\vartheta}_0)/\vartheta_* = \ln(Z/Z_0) \tag{16c}$$

$$a_{so}(\hat{s}(Z) - \hat{s}_0)/s_* = \ln(Z/Z_0) \tag{16d}$$

Herein is $a_{Ho} = k_H/k_m$ and $a_{so} = k_s/k_m$ at $Z = Z_0$. The matching gives:

$$\ln(Z_0) + \kappa\, \hat{u}_{go}/u_* = \ln(Z) - \varphi_u(Z, \mu, B_x, B_y) \tag{17a}$$

$$\kappa \hat{v}_{go}/u_* = -\varphi_v(Z, \mu, B_x, B_y) \tag{17b}$$

$$\ln(Z_0) + a_{Ho} \frac{\hat{\vartheta}_h - \hat{\vartheta}_0}{\vartheta_*} = \ln(Z) - \varphi_\vartheta(Z, \mu, B_x, B_y) \tag{17c}$$

$$\ln(Z_0) + a_{so} \frac{\hat{s}_h - \hat{s}_0}{s_*} = \ln(Z) - \varphi_s(Z, \mu, B_x, B_y) \tag{17d}$$

Since the left-hand side of the eqs. (17a)–(17d) is independent of Z, the right-hand side has to be also independent of Z; that means the left-hand side equals an universal function of the remaining dimensionless combinations of parameters:

$$\lim_{Z \to Z_0} \{ \varphi_u(Z, \mu, B_x, B_y) - \ln(Z) \} = M_m(\mu, B_x, B_y) + \ln(\kappa) \tag{18a}$$

$$\lim_{Z \to Z_0} \{ \varphi_v(Z, \mu, B_x, B_y) \} = N(\mu, B_x, B_y) \tag{18b}$$

$$\lim_{Z \to Z_0} \{ \varphi_\vartheta(Z, \mu, B_x, B_y) - \ln(Z) \} = M_H(\mu, B_x, B_y) + \ln(\kappa) \tag{18c}$$

$$\lim_{Z \to Z_0} \{ \varphi_s(Z, \mu, B_x, B_y) - \ln(Z) \} = M_s(\mu, B_x, B_y) + \ln(\kappa) \tag{18d}$$

If one replaces Z_0 in the eqs. (17a), (17c) and (17d) by eq. (12) and if one regards the eqs. (18a)–(18d) the resistance laws can be obtained in the following form:

$$\ln(Ro_0 \cdot C_d) - M_m(\mu, B_x, B_y) = [\kappa^2/(C_d)^2 - N^2(\mu, B_x, B_y)]^{1/2} \tag{19a}$$

$$N(\mu, B_x, B_y) = \kappa \sin(|\alpha_0|)/C_d \tag{19b}$$

$$\ln(Ro_0 \cdot C_d) - M_H(\mu, B_x, B_y) = a_{Ho} \frac{\hat{\vartheta}_h - \hat{\vartheta}_0}{\vartheta_*} = a_{Ho}/C_{th} \tag{19c}$$

$$\ln(Ro_0 \cdot C_d) - M_s(\mu, B_x, B_y) = a_{so} \frac{\hat{s}_h - \hat{s}_0}{s_*} = a_{so}/C_s \tag{19d}$$

The equations (19a) and (19b) give the mechanical resistance law, equation (19b) a thermal resistance law and (19d) such one for the moisture. These laws are the same as in the barotropic case but the universal functions M_m, M_H, M_s and N depend in the baroclinic case also on the (dimensionless) internal parameters for the baroclinicity.

5. Conclusions

It has been shown, that also for a baroclinic PBL the turbulent transports of momentum, heat and moisture at the ground, needed for the purpose of parametrization, can be obtained by three resistance laws, eqs. (19a)–(19d). These laws have the same form as in a barotropic PBL, but the universal function M_m, M_H, M_s and N depend not only on the (internal) stability parameter μ but also on the two (internal) parameters B_x and B_y for the baroclinicity. These universal functions can be determined only by measurements; the equations (19a)–(19d) show that evaluations of such measurements should be carried out for varying values of the internal parameters μ, B_x and B_y.

An application of the equations (19a)–(19d) for a parametrization of the turbulent transports in a baroclinic PBL (for instance in numerical models of the general circulation) requires that the internal parameters μ, B_x and B_y are available. However such a circulation model gives with its predicted large-scale fields only the corresponding external parameters S, B_n and γ. Therefore the available external parameters (S, B_n, γ) have to be converted into the corresponding internal parameters (μ, B_x, B_y), which are needed. For this conversion the equations (11a)–(11c) can be used when applied iteratively. Diagrams for this conversion of the available external parameters into the needed internal parameters are presented by CLARKE (1970) and ZILITINKEVICH (1970), but these diagrams are restricted to the barotropic case. For the baroclinic case it is not yet possible to construct such diagrams because of the lack of usefull measurements.

References

BLACKADAR, A. K., TENNEKES, H. (1968): Asymptotic similarity in neutral barotropic planetary boundary layers J. Atm. Sci. **25**, 1015–1020

CLARKE, R. H. (1970): Recommended methods for the treatment of the boundary layer in numerical models Austral. Meteor. Mag. **18** (2), 51–73

CSANADY, G. T. (1967): On the "resistance law" of a turbulent Ekman layer J. Atm. Sci. **24**, 467–471

GILL, A. E. (1967): The turbulent Ekman layer.Unpubl. Manuscr., Dept. Appl. Math. and Theor. Phys., University of Cambridge

GILL, A. E. (1968): Similarity theory and geostrophic adjustment Q. J. R. M. S. **94**, 586–588

KAZANSKII, A. B., MONIN, A. S. (1961): On the dynamical interaction between the atmosphere and earth's surface Izv. Akad. Nauk., Ser. Geofiz., 1961 (5), 786–788; engl. transl. 514–515

ZILITINKEVICH, S. S. (1970): The dynamics of the boundary layer of the atmosphere,Leningrad 1970, pp. 291, in russian

Correction

In the paper by D. YORDANOV and F. WIPPERMANN "The parameterization of the turbulent fluxes of momentum, heat and moisture at the ground in a baroclinic planetary boundary layer", Beitr. Phys. Atm. **45** (1), 58–65, 1972, the following corrections should be made: In the eqs. (17c) and (18c) $\varphi_\vartheta(\ldots)$ has to be replaced by $a_{Ho}\,\varphi_\vartheta(\ldots)$, in the eqs. (17d) and (18d) $\varphi_s(\ldots)$ has to be replaced by $a_{so}\,\varphi_s(\ldots)$. The final result eqs. (19a)–(19d) remains uneffected by these corrections.

Baroclinic Effects on the Resistance Law for the Planetary Boundary Layer of the Atmosphere

Die Berücksichtigung barokliner Effekte im Widerstandsgesetz für die planetarische Grenzschicht der Atmosphäre

F. Wippermann

Technical University Darmstadt, Germany, Department of Meteorology

Manuscript received 8 March 1972

Summary: If one wishes to apply the resistance law for the planetary boundary layer (PBL) the two functions $M_m(\mu, \lambda_x, \lambda_y)$ and $N(\mu, \lambda_x, \lambda_y)$ have to be known. (μ is the internal parameter of the thermal stratification, λ_x and λ_y are the internal parameters of the baroclinicity.) These functions have been determined by integrations with a baroclinic PBL-model, then a simple approximative formula is given for the effects of the baroclinicity on M_m and N, eq (29). This formula is independent of the surface Rossby number because of the use of the *internal* parameters λ_x and λ_y for the baroclinicity, but it would depend on Ro_0 if the *external* parameters η_{x*} and η_{y*} for the baroclinicity are used. These external parameters are those which are available for a practical application of the resistance law; therefore diagrams or tables are needed which contain $M_m(\eta_{x*}, \eta_{y*}, Ro_0)$ and $N(\eta_{x*}, \eta_{y*}, Ro_0)$ for each possible thermal stratification. An example of such a diagram is given for the neutral case and $Ro_0 = 7.7\ 10^6$; it is also based on the results of integrations with a baroclinic PBL-model.

Zusammenfassung: Eine Anwendung des Widerstandsgesetzes für eine planetarische Grenzschicht (PBL) ist nur möglich, wenn die beiden Funktionen $M_m(\mu, \lambda_x, \lambda_y)$ und $N(\mu, \lambda_x, \lambda_y)$ bekannt sind. (μ ist der interne Parameter für die thermische Schichtung, λ_x und λ_y sind die beiden internen Parameter für die Baroklinität.) Diese beiden Funktionen werden mit Hilfe der Ergebnisse von Integrationen eines PBL-Modelles ermittelt, sodann wird eine einfache Näherungsformel für die Effekte der Baroklinität auf M_m und N aufgestellt, Gl. (29). Solange die *internen* Parameter λ_x und λ_y für die Baroklinität verwendet werden, sind derartige Formeln unabhängig von der Boden-Rossby-Zahl, doch hängen sie von dieser ab, wenn die *externen* Parameter η_{x*} und η_{y*} für die Baroklinität Verwendung finden. Letztere sind aber gerade diejenigen, die für eine praktische Anwendung des Widerstandsgesetzes zur Verfügung stehen; es werden daher Diagramme oder Tabellen benötigt, welche für jede mögliche thermische Schichtung die Funktionen $M_m(\eta_{x*}, \eta_{y*}, Ro_0)$ und $N(\eta_{x*}, \eta_{y*}, Ro_0)$ enthalten. Als Beispiel für derartige Diagramme wird ein solches für den neutralen Fall und für $Ro_0 = 7.7\ 10^6$ gegeben; auch dieses wurde mittels der Ergebnisse von Integrationen des baroklinen PBL-Modelles erstellt.

Résumé: Si l'on désire appliquer la loi de résistance à la couche limite planétaire (PBL), il faut connaître les deux fonctions $M_m(\mu, \lambda_x, \lambda_y)$ et $N(\mu, \lambda_x, \lambda_y)$ – μ est le paramètre interne de la stratification thermique et λ_x, λ_y sont les paramètres internes de la baroclinie.

Ces fonctions ont été déterminées par intégrations à l'aide d'un modèle-PBL; une formule simple d'approximation donne les effets de la baroclinie sur M_m et N (éq. 29). Cette formule est indépendante du nombre de Rossby en surface si l'on utilise les paramètres internes λ_x et λ_y pour la baroclinie, mais elle en dépend si l'on emploie pour la baroclinie les paramètres externes η_{x*} et η_{y*}. Cependant, c'est de ceux-ci qu'on dispose pour une application pratique de la loi de résistance; par suite, il faut des diagrammes ou des tables qui fournissent, pour chaque stratification thermique possible, les fonctions $M_m(\eta_{x*}, \eta_{y*}, Ro_0)$ et $N(\eta_{x*}, \eta_{y*}, Ro_0)$. Comme exemple, un tel diagramme est donné dans le cas neutre et pour $Ro_0 = 7{,}7.\ 10^6$; il est basé sur les résultats d'intégration du modèle-PBL barocline.

Beiträge zur Physik der Atmosphäre, 45. Band, 1972, S. 244–259

I. Introduction

The resistance law for a barotropic planetray boundary layer (PBL) can be written

$$\kappa \cos(\alpha_o) / C_g = -M_m + \ln(C_g \, Ro_o) \tag{1a}$$

$$\kappa \sin(|\alpha_o|) / C_g = N \tag{1b}$$

It was first derived by KAZANSKII and MONIN (1961) and later on in different ways by GILL (1967), MONIN and ZILITINKEVICH (1967), CSANADY (1967) and by BLACKADAR and TENNEKES (1968). It allows to compute the geostrophic drag coefficient $C_g = u_*/|\hat{w}_{go}|$ (with u_* the friction velocity) and the cross-isobar angle α_0 for a given surface Rossby number Ro_0. This is a nondimensional combination of the external parameters z_0, the roughness-length, the Coriolisparameter f and $|\hat{w}_{go}|$, the geostrophic wind speed at the ground; $Ro_0 = |\hat{w}_{go}|/(f\, z_0)$. M_m and N have to be known; they are independent of the external parameters, but they are functions of a nondimensional internal parameter μ for the thermal stratification

$$\mu = H/L_* \tag{2}$$

where

$$H = \kappa\, u_*/f \tag{3}$$

is the internal scale-height of the PBL and

$$L_* = -c_p\, \bar{\rho}\, u_*^3 / (\kappa\, \beta\, q_0) \tag{4}$$

is the Monin-Obukhov stability-length. κ is the Karman constant, $\beta = g/\tilde{\vartheta}$ with g the acceleration of gravity and $\tilde{\vartheta}$ a reference temperature. $q_0 = c_p\, (\overline{\rho\, w''\, \vartheta''})_0$ is the turbulent heat flux at the ground, c_p is the specific heat and ρ is the density. The external parameter for the thermal stratification is

$$\sigma = \kappa^2\, \beta\, \delta\, \hat{\vartheta} / (f\, |\hat{w}_{go}|) \tag{5}$$

where $\delta\, \hat{\vartheta}$ is the difference of the potential temperature at the top of the PBL and at the ground.

In a recent paper by YORDANOV and WIPPERMANN (1972) it has been shown, that the resistance law (1a), (1b) remains unchanged in a baroclinic PBL, but the functions M_m and N should depend also on two nondimensional *internal* parameters for the baroclinicity

$$\lambda_x = \kappa^2/f\, d\hat{u}_g/dz \approx -\beta\, \kappa^2/f^2\, \partial\hat{\vartheta}/\partial y \tag{6a}$$

$$\lambda_y = \kappa^2/f\, d\hat{v}_g/dz \approx \beta\, \kappa^2/f^2\, \partial\hat{\vartheta}/\partial x \tag{6b}$$

as long as one assumes that $d^2\, \hat{w}_g/dz^2 = 0$. $\hat{\vartheta}$ is the potential temperature having a horizontal gradient in baroclinic cases. The x-axis has the direction of the surface stress $\tau_0 = -(\overline{\rho\, w''\, \hat{w}_h''})_0$, which is turned by the cross-isobar angle α_0 to the left (northern hemisphere, $f > 0$) of the direction of the geostrophic wind at the ground. Since the orientation of the coordinate system is fixed by the *internal* parameter τ_0, the parameters λ_x and λ_y for the baroclinicity must be also *internal* ones. They should not be mistaken with the *external* parameters for the baroclinicity

$$\eta_{x*} = \kappa^2/f\, (\hat{w}_{go}^0 \cdot d\, \hat{w}_g/dz) \tag{7a}$$

$$\eta_{y*} = \kappa^2/f\, [|k \times \hat{w}_{go}^0] \cdot d\, \hat{w}_g/dz \tag{7b}$$

These contain the components of the geostrophic wind shear in the direction of the geostrophic wind at the ground and perpendicular to it. $\hat{w}^0_{go}$ and $|\mathbf{k}$ are unit-vectors.

For a practical application of the resistance law (1a), (1b) only the external parameters σ, η_{x*}, η_{y*} are available but not the internal ones μ, λ_x, λ_y which are needed. This means that diagrams or tables have to be constructed which give M_m and N as depending on the external parameters, σ, η_{x*}, η_{y*}. Of course, the main disadvantage will be, that such diagrams or tables have to be constructed for each possible surface Rossby number. Only the use of the internal parameters μ, λ_x, λ_y has the advantage, that the functions $M_m(\mu, \lambda_x, \lambda_y)$ and $N(\mu, \lambda_y, \lambda_y)$ are universal ones, i.e. independent of the surface Rossby number. The aim of this paper is therefore to show how M_m and N depend on the internal parameters λ_x and λ_y for the baroclinicity. However in the final section also an example of a diagram will be given showing the dependence of M_m and N on the external parameters η_{x*} and η_{y*} for the baroclinicity; but this diagram is valid only for the neutral case and a surface Rossby number $Ro_0 = 7.7\ 10^6$.

II. How to obtain M_m and N from wind profiles or stress profiles

In the PBL the equations of motion are reduced to

$$f\bar{\rho}(\hat{u} - \hat{u}_g) = d\tau_y/dz \tag{8a}$$

$$f\bar{\rho}(\hat{v} - \hat{v}_g) = -d\tau_x/dz \tag{8b}$$

where τ_x and τ_y are the components of the Reynolds' stress. In a nondimensional notation eqs. (8a) and (8b) are

$$P = dY/dZ \qquad Q = -dX/dZ \tag{9a), (9b}$$

where P and Q are the components of the nondimensional velocity defect $P = \kappa\,(\hat{u} - \hat{u}_g)/u_*$ and $Q = \kappa\,(\hat{v} - \hat{v}_g)/u_*$, X and Y are the components of the nondimensional Reynolds' stress $X = \tau_x/(\bar{\rho} u_*^2)$ and $Y = \tau_y/(\bar{\rho}\, u_*^2)$. It is $Z = z/H$ the nondimensional height coordinate; a nondimensional roughness-length $Z_0 = z_0/H$ can be formed, which is by the definitions made before

$$Z_0 = (\kappa C_g\, Ro_0)^{-1} \tag{10}$$

With respect to the lower boundary condition

$$z = z_0: \qquad \hat{u} = \hat{v} = 0 \tag{11}$$

the eqs. (9a) and (9b) give at $z = z_0$

$$P_0 = -\kappa\,\hat{u}_{go}/u_* = -\kappa\,|\hat{w}_{go}|\cos(\alpha_0)/u_* = -\kappa\cos(\alpha_0)/C_g = (dY/dZ)_0 \tag{12a}$$

$$Q_0 = -\kappa\,\hat{v}_{go}/u_* = -\kappa\,|\hat{w}_{go}|\sin(\alpha_0)/u_* = \kappa\sin(|\alpha_0|)/C_g = -(dX/dZ)_0 \tag{12b}$$

If one replaces the third terms on the right-hand sides of the eqs. (12a) and (12b) by the eqs. (1a) and (1b), one obtains

$$M_m = P_0 - \ln(\kappa Z_0), \qquad N = Q_0 \qquad (13a), (13b)$$

$$M_m = (dY/dZ)_0 - \ln(\kappa Z_0), \qquad N = -(dX/dZ)_0 \qquad (14a), (14b)$$

For a given nondimensional roughness-length Z_0 the values of M_m and N may be obtained either from the nondimensional wind profile at the ground or from the nondimensional vertical gradient of the stress components at the ground. Since M_m and N are independent of Z_0 also Q_0 and $(dX/dZ)_0$ must be independent of Z_0, but P_0 and $(dY/dZ)_0$ depend on Z_0, they equalize $\ln(Z_0)$ apart from a constant.

As a kind of by-product N can be related to the eddy viscosity in the case of a pure Ekman spiral (k_{mE} = const.). In such a case the x-component of the Reynolds' stress is

$$\tau_{xE} = \tau_0 \exp\{-n(z - z_0)\} \cos\{n(z - z_0)\}$$

with

$$n = \sqrt{f/(2\, k_{mE})} \qquad (15)$$

where k_{mE} is the eddy viscosity in the case of an Ekman spiral, it is nondimensionalized in the form $K_{mE} = k_{mE}/(H^2 f)$. The first derivative of τ_x with respect ot z at $z = z_0$ is

$$(d\,\tau_{xE}/dz)_0 = -n\,\tau_0 \qquad \text{or} \qquad (dX_E/dZ)_0 = -nH \qquad (16)$$

Using eq. (14b) herein one obtains

$$N = (2\, K_{mE})^{-1/2} \qquad (17)$$

In eq. (17) N is related to the (nondimensional) constant eddy viscosity of an Ekman spiral which would correspond to the given case.

Instead of eq. (15) it can be written also

$$n = f/(\sqrt{2}\, u_*\, C_{gE}) \qquad (18)$$

This means with respect to eqs. (14b) and (16)

$$N = \kappa/(\sqrt{2}\, C_{gE}) \qquad (19)$$

Since N is independent of Ro_0, Z_0 or C_g, it can be concluded from eq. (19), that C_{gE} can not vary; it is a fixed value (varying only with N) as it is also the cross-isobar angle in the case of an Ekman spiral ($\alpha_{oE} = \pi/4$). Eq. (19) is nothing else than eq. (1b) for $\alpha_0 = \alpha_{oE}$. In the barotropic and neutral case (N = 4.6) the geostrophic drag coefficient in the case of an Ekman spiral is $C_{gE} = 0.062$; this is a rather large value.

III. $M_m(\mu, \lambda_x, \lambda_y)$ and $N(\mu, \lambda_x, \lambda_y)$ obtained from a PBL-model

A single-layer model of the PBL has been used in order to obtain $M_m(\mu, \lambda_x, \lambda_y)$ and $N(\mu, \lambda_x, \lambda_y)$. This model has been described for the barotropic case in a paper by WIPPERMANN (1972), now it is extended for baroclinic conditions. The model equations are obtained by differntiating the eqs. (9a), (9b) with respect to Z

$$dP/dZ = d^2Y/dZ^2 \qquad dQ/dZ = -d^2X/dZ^2 \qquad (20a), (20b)$$

and by replacing the left-hand sides in eqs. (20a), (20b) by the flux-gradient relations

$$X = K_m(dP/dZ + \lambda_x) \qquad Y = K_m(dQ/dZ + \lambda_y) \qquad (21a), (21b)$$

One gets

$$d^2Y/dZ^2 = X/K_m - \lambda_x \qquad (22a)$$

$$d^2X/dZ^2 = -Y/K_m + \lambda_y \qquad (22b)$$

Prandtl's relation for the eddy viscosity (in nondimensional notation)

$$K_m = L^2\{(dU/dZ)^2 + (dV/dZ)^2\}^{1/2}/\kappa^2 = L^2\{(dP/dZ + \lambda_x)^2 + (dQ/dZ + \lambda_y)^2\}^{1/2}/\kappa^2 \qquad (23)$$

together with the flux-gradient relations (21a), (21b) yields

$$K_m = L\{X^2 + Y^2\}^{1/4}/\kappa \qquad (24)$$

$L = l/H$ is the nondimensional mixing-length. In order to close the system of equations the following mixing-length hypothesis is made

$$L = L_\infty - (L_\infty - \kappa K_{mo})\{X^2 + Y^2\}^{p/2} \qquad (25)$$

$$p = -\kappa \frac{1 - K_{mo}\{2(dX/dZ)_0^2 + (dX/dZ)_0/2\}}{(dX/dZ)_0\{L_\infty - \kappa K_{mo}\}}$$

A detailed description of this mixing-length hypothesis is given by WIPPERMANN (1971a). The set of the four equations (22a), (22b), (24), (25) is a closed system for the four variables X, Y, L, K_m. The solutions of this system of equations are the vertical profiles of these four nondimensional variables X(Z), Y(Z), L(Z) and $K_m(Z)$. The boundary conditions are

$$Z = Z_0: \quad X = X_0 = 1 \qquad Y = Y_0 = 0 \qquad (26a), (26b)$$

$$L = L_0 = \kappa Z_0 \qquad K_m = K_{mo} = Z_0 \qquad (26c), (26d)$$

$$Z \to \infty: \quad X \to X_\infty = L_\infty^2/\kappa^2\, \lambda_x(\lambda_x^2 + \lambda_y^2)^{1/2} \qquad (27a)$$

$$Y \to Y_\infty = L_\infty^2/\kappa^2\, \lambda_y(\lambda_x^2 + \lambda_y^2)^{1/2} \qquad (27b)$$

$$L \to L_\infty \qquad (27c)$$

$$K_m \to K_{m\infty} = L_\infty^2/\kappa^2(\lambda_x^2 + \lambda_y^2)^{1/2} \qquad (27d)$$

The boundary condition (27d) is obtained by using eq. (27c) in eq. (24) together with the eqs. (21a), (21b) in which one puts $P_\infty = (dP/dZ)_\infty = Q_\infty = (dQ/dZ)_\infty = 0$. The conditions (27a), (27b) result from the eqs. (21a), (21b), in which $K_{m\infty}$ is replaced by eq. (27d).

Three free parameters appear in the system of eqs. (22a), (22b), (24), (25), namely λ_x and λ_y the internal parameters for the baroclinicity and L_∞ the asymptotic mixing-length, for which the mixing-length hypothesis asserts $\partial L_\infty/\partial(Ro_0) = 0$. This assymptotic ming-length L_∞ plays the role of the internal parameter μ for the thermal stratification; an empirical relationship between both is given by WIPPERMANN (1971a)

$$\mu = -44.2 - 24.4 \log_{10}(L_\infty) \tag{28}$$

An iterative method to solve the system of eqs. (22a), (22b), (24), (25) has been given by WIPPERMANN (1971b); it requires that the boundary conditions (27a)–(27d) are valid at a finite but large height Z^* rather than at infinity. Z^* has been chosen to equal 10.0, i.e. ten times the internal scale height of the PBL and very roughly corresponding to 10 km.

The solution gives the profiles X(Z) and Y(Z) in discreticized form, they allow to determine $(dX/dZ)_0$ and $(dY/dZ)_0$ and according to eqs. (14a), (14b) also M_m and N. Integrations have been carried out for the following six thermal stratifications

μ	−20	−12	0	7	15	30
L_∞	0.100	0.050	0.014	0.0085	0.0040	0.0010

For each of these thermal stratifications eight different baroclinicities have been considered, which are listed in the lower left-hand part of figure 1. All these baroclinicities correspond to the same amount of the thermal wind

$$|d\,\hat{v}_g/dz| = 5.0\, f/\kappa^2 = 3.5 \text{ m sec}^{-1}/1000 \text{ m} \qquad (\varphi = 50°)$$

or

$$|\nabla_h \vartheta| = 5.0\, f^2/(\kappa^2 \beta) = 1.2 \text{ grad}/100 \text{ km} \qquad (\tilde{\vartheta} = 290\ °K)$$

but the direction of the thermal wind varies. It should be mentioned, that this variation of the direction does not occur proceeding in equal steps of the azimut angle, since the (x, y)-coordinate system has a slightly different orientation for different baroclinicities. The internal parameters λ_x and λ_y for the baroclinicity are given in this coordinate system, the orientation of which depends on the baroclinicity itself.

Let us consider the influence of the baroclinicity on the functions M_m and N. For this purpose the differences $M_m(\mu, \lambda_x, \lambda_y) - M_m(\mu, 0, 0)$ and $N(\mu, \lambda_x, \lambda_y) - N(\mu, 0, 0)$ should be studied. Figure 1 shows the result of the integrations for three of the forementioned thermal stratifications in a plane of this two differences. The crosses connected by the broken lines represent the result for the eight different baroclinicities for each of the three thermal stratifications. As more stable the thermal stratification is as smaller are the two differences and as more symmetric to the origin are the differences in the plane given in figure 1. This symmetry suggests to evaluate the results of the integrations in order to determine the coefficients in a simple approximative formula

$$\boxed{\begin{aligned} M_m(\mu, \lambda_x, \lambda_y) - M_m(\mu, 0, 0) &= c_3(\mu)\,\lambda_x + c_2(\mu)\,\lambda_y \qquad (29a) \\ N(\mu, \lambda_x, \lambda_y) - N(\mu, 0, 0) &= -c_2(\mu)\,\lambda_x + c_3(\mu)\,\lambda_y \qquad (29b) \end{aligned}}$$

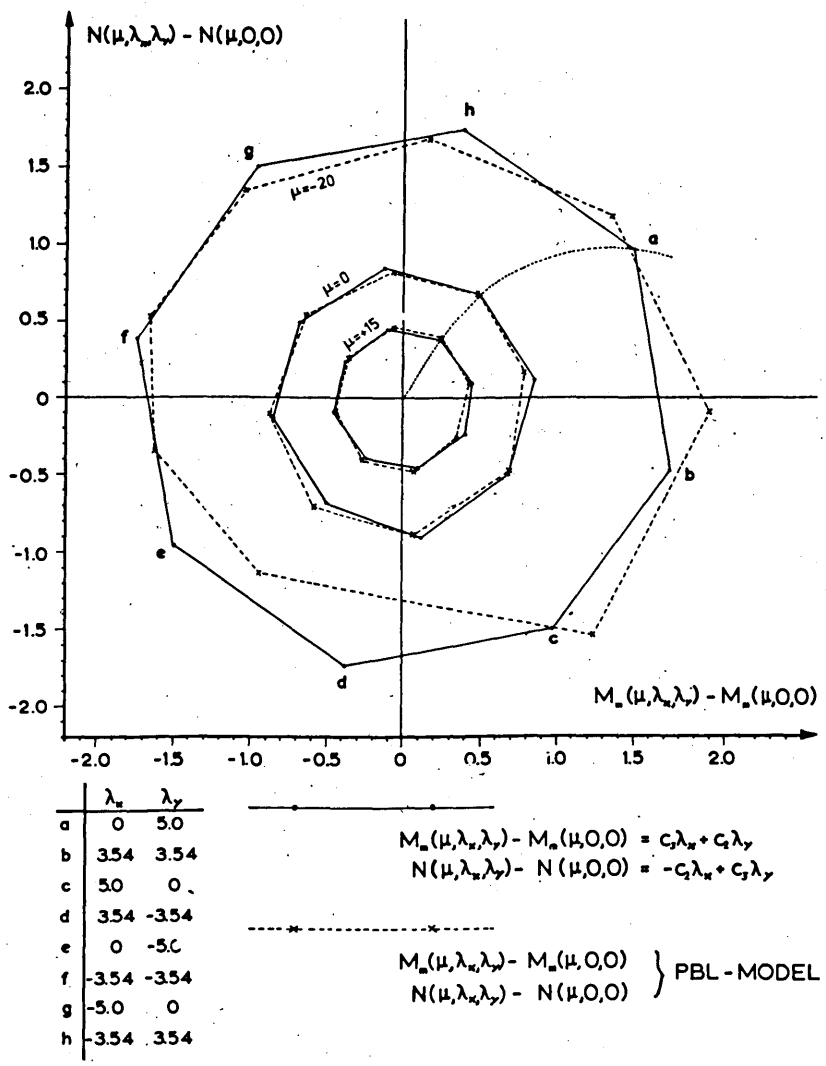

Figure 1. Values of the functions M_m and N, which appear in the resistance law for the PBL, for eight different baroclinicities (λ_x, λ_y) and three different thermal stratifications (μ). The values are obtained by a PBL-model (crosses) and by an approximative formula (dots).

Bild 1. Werte der beiden im Widerstandsgesetz für eine planetarische Grenzschicht auftretenden Funktionen M_m und N für acht verschiedene Baroklinitäten (λ_x, λ_y) und drei verschiedene thermische Schichtungen (μ). Die Werte wurden einerseits mit einem Grenzschichtmodell (Kreuze) erhalten, zum anderen mit einer approximativen Formel (Punkte).

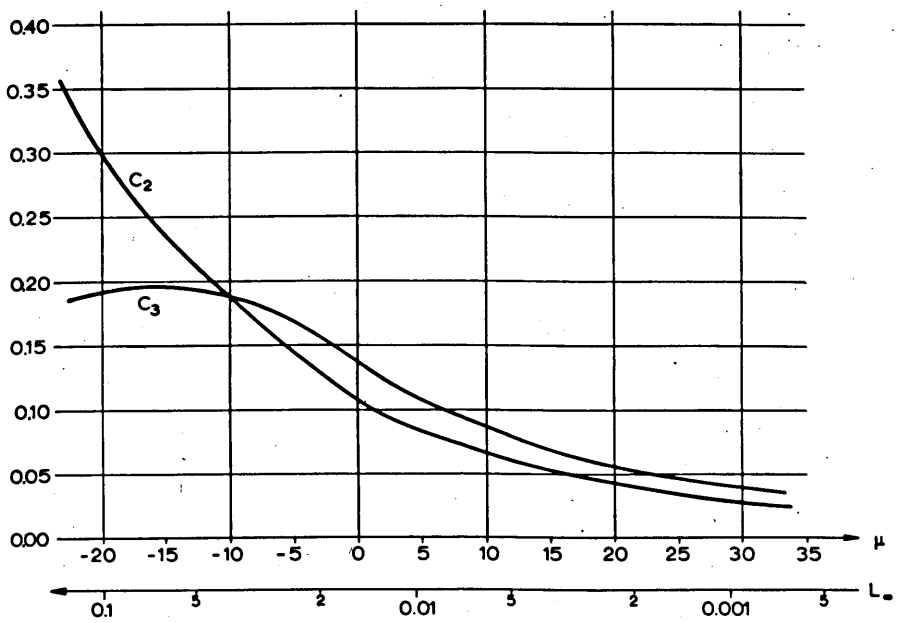

Figure 2. The coefficients c_2 and c_3, which appear in the approximative formula (29), as depending on the internal parameter μ for the thermal stratification.

Bild 2. Die beiden Koeffizienten c_2 und c_3, welche in der approximativen Formel (29) auftreten, in Abhängigkeit vom internen Schichtungsparameter μ.

Since the formulae (29a), (29b) have been established with the results for baroclinicities only of the amount $(\lambda_x^2 + \lambda_y^2)^{1/2} = 5.0$, the assumption is implied, that a linear proportionality exists between each of the two differences $M_m(\mu, \lambda_x, \lambda_y) - M_m(\mu, 0, 0)$, $N(\mu, \lambda_x, \lambda_y) - N(\mu, 0, 0)$ and the two internal parameters λ_x and λ_y for the baroclinicity. The coefficients c_2 and c_3 are evaluated for the six thermal stratifications mentioned before and interpolated in the whole range $-20 \leqslant \mu + 30$. The variation of c_2 and c_3 with μ is displayed in figure 2. The results obtained by the approximative formulae (29a), (29b) are shown in figure 1 by the dots connected by solid lines. It can be seen that the deviation of the result obtained by the approximative formulae (29a), (29b) from the result obtained by the PBL-model is very small in stable conditions, still small in the neutral case but growing with increasing instability of the thermal stratification. This can be demonstrated by some evaluations. For the sake of abbreviation the following notation may be used

$$\delta M_m = M_m(\mu, \lambda_x, \lambda_y) - M_m(\mu, 0, 0)$$

$$\delta N = N(\mu, \lambda_x, \lambda_y) - N(\mu, 0, 0)$$

and

$$\Delta|\delta M_m| = |\delta M_m|_{Model} - |\delta M_m|_{Eq.29}$$

$$\Delta|\delta N| = |\delta N|_{Model} - |\delta N|_{Eq.29}$$

$\overbrace{(\quad)}$ should denote an average over the eight different baroclinicities for a given μ. The obtained deviations have been listed in table 1:

Table 1 / Tabelle 1

μ	$\overbrace{\lvert\delta M_m\rvert}_{Mod}$	$\overbrace{\lvert\delta N\rvert}_{Mod}$	$\overbrace{\lvert(\Delta\lvert\delta M_m\rvert)\rvert}$	$\overbrace{\lvert(\Delta\lvert\delta N\rvert)\rvert}$
30	0.14	0.16	0.01	0.01
15	0.28	0.30	0.02	0.01
7	0.41	0.44	0.02	0.02
2	0.52	0.58	0.04	0.02
- 12	1,02	0.86	0.16	0.10
- 20	1.25	0.97	0.28	0.20

Table 1 demonstrates the usefulness of the formulae (29a), (29b) for a moderate baroclinicity. Few computations have been made to test the formulae also for an extremely large baroclinicity (in the neutral case); the results are listed in table 2.

Table 2 / Tabelle 2

		PBL-Model		Equ. (29)	
λ_x	λ_y	M_m	N	M_m	N
0	0	0.99	4.66		
0	15	2.26	6.62	3.03	6.26
0	- 15	- 1.24	2.78	- 1.05	3.06
- 15	0	- 0.83	6.39	- 0.61	6.70
15	0	2.76	2.93	2.59	2.62

Even for such unrealistic large baroclinicities as those in table 2 the formulae (29a), (29b) give satisfying results, except for $M_m(0;15)$ where the difference between the value of M_m obtained by the PBL-model and the value of M_m obtained by eq. (29) is about 1/3 M_m. However it should be mentioned that the value of $M_m(0;15)$ obtained by the PBL-model is possibly incorrect, since difficulties of convergence occured in the integration procedure for special cases of very large baroclinicity.

In a recent paper FIEDLER (1971) computed M_m and N as depending on the internal parameter μ of the thermal stratification for two special cases of baroclinicity; he found that in his case of cold-air advection only N is affected by the baroclinicity but M_m remains more or less unchanged and vice versa in the case of warm-air advection. These findings are valid only for the two very special cases of baroclinicity which have been chosen for the computations. This can be explained very easily with the aid of the eqs. (29a), (29b). The two cases treated by FIEDLER (9171) are

cold-air advection: $\lambda_x = -\sqrt{\lambda^2/2}$ $\quad \lambda_y = \sqrt{\lambda^2/2}$

warm-air advection: $\lambda_x = -\sqrt{\lambda^2/2}$ $\quad \lambda_y = -\sqrt{\lambda^2/2}$

By applying the formulae (29a), (29b) one gets

cold-air advection: $\delta M_m = (c_2 - c_3)\sqrt{\lambda^2/2}$

$\delta N = (c_2 + c_3)\sqrt{\lambda^2/2}$

warm-air advection: $\delta M_m = -(c_2 + c_3)\sqrt{\lambda^2/2}$

$\delta N = (c_2 - c_3)\sqrt{\lambda^2/2}$

In the neutral case for instance (as seen from figure 2) $c_2 + c_3 = 0.244$ and $|c_2 - c_3| = 0.028$, which means that $|\delta M_m|$ is about 10 % of $|\delta N|$ in the case of cold-air advection and vice versa in the case of warm-air advection. Since the difference $|c_2 - c_3|$ decreases with increasing stability $|\delta M_m|$ must decrease with increasing stability in the cold-air advection and $|\delta N|$ in the warm-air advection. But also $c_2 + c_3$ is very small in stable stratifications, for instance $c_2 + c_3 = 0.067$ for $\mu = 30$, therefore $|\delta N|$ in cold-air advection and $|\delta M_m|$ in warm-air advection are rather small for $\mu \gg 0$. For strong unstable stratifications $c_2 + c_3$ reaches large values causing a remarkable $|\delta N|$ in the case of cold-air advection and a remarkable $|\delta M_m|$ in the case of warm-air advection. This all is in complete agreement with FIEDLER's results. However it should be stated once more, that he considers only two very special cases of baroclinicity, the results of which can not be generalized.

Another aspect of the effects of baroclinicity is the possibility of the funktion $N(\mu, \lambda_x, \lambda_y)$ to be negative. It seems to be sure that $N(\mu, 0, 0) > 0$ even for largest instabilities of the stratification. (A collection of results, measurements as well as model computations, has been given in figure 9 of a paper by WIPPERMANN 1972). If it is accepted that $N(\mu, 0, 0) > 0$, a value $N < 0$ requires a large baroclinic effect; according to eq. (29b) $-c_2\lambda_x + c_3\lambda_y$ has to be very negative. For instance $N = -10$ at $\mu = 0$ requires $-c_2\lambda_x + c_3\lambda_y = -14.6$ considering that $N(0, 0, 0) = 4.6$. Assuming that $\lambda_x = \sqrt{\lambda^2/2}$, $\lambda_y = -\sqrt{\lambda^2/2}$ one finds $\lambda = 83.5$ corresponding to a shear of the geostrophic wind of 58.5 m sec^{-1}/1000 m. This is a unrealistic value which never will be observed.

By these reasons one should have some doubt on the evaluations of measurements reported by CLARKE (1970); 26 % of his N-values are negative, some even -18 or -19 in the near neutral case. Cases with $N < 0$ occur very seldom probably, they require a very strong warm-air advection and a strong unstable stratification.

With respect to eq. (14b) one can conclude that in cases with $N < 0$ the Reynolds' stress has to increase with height (at $z = z_0$). Eq. (13b) together with eq. (12b) tells, that for $N < 0$ the cross-isobar angle α_0 has to be positive, i.e. the direction of the surface stress is to the right of the direction of the geostrophic wind at the ground (northern hemisphere).

IV. The coefficients c_2 and c_3 in the equations (29a), (29b)

In this section some considerations will be given about the two coefficients appearing in the eqs. (29a), (29b).

By integrating the eqs. (22a), (22b) with respect to Z from Z_0 to infinity one obtains

$$(dY/dZ)_0 = -\int_{Z_0}^{\infty} (X/K_m - \lambda_x)\, dZ \tag{30a}$$

$$(dX/dZ)_0 = \int_{Z_0}^{\infty} (Y/K_m - \lambda_y)\, dZ \tag{30b}$$

where it has been considered that the stress components X and Y approach a constant value at infinity, see the boundary conditions (27a) and (27b). According to eqs. (14a), (14b) the left-hand sides in the eqs. (30a) and (30b) equal $M_m + \ln(\kappa Z_0)$ and $-N$ respectively. The integrals of the right-hand sides of the eqs. (30a), (30b) should be subdivided into three parts each, namely an integral from Z_0 to Z_R, one from Z_R to Z_T and a third one from Z_T to infinity. Z_R is a nondimensional height rather close to Z_0, above Z_R exists Rossby similarity. A determination of this height has been given in a study by WIPPERMANN and YORDANOV (1972). For the small range $Z_0 \leqslant Z \leqslant Z_R$ the following assumptions of a constant stress layer can be made

$$Z_0 \leqslant Z \leqslant Z_R: \qquad X \approx 1 \qquad Y \approx 0 \tag{31a), (31b}$$

$$K_m \approx Z \tag{31c}$$

With these assumptions and the relation (10) the lower part of the integrals in the eqs. (30a), (30b) is

$$\int_{Z_0}^{Z_R} (X/K_m - \lambda_x)dZ = \ln(Z_R/Z_0) - \lambda_x (Z_R - Z_0)$$
$$\approx \ln(\kappa Z_R) - \ln(C_g\, Ro_0) - \lambda_x Z_R \tag{32a}$$

$$\int_{Z_0}^{Z_R} (Y/K_m - \lambda_y)dZ = -\lambda_y (Z_R - Z_0) \approx -\lambda_y Z_R \tag{32b}$$

The nondimensional roughness-length Z_0 has been neglected compared with Z_R.

Z_T is the top of the PBL, i.e. the height at which the velocity defect is close enough to zero and the stress components have almost reached their constant value given by eq. (27a), (27b).

$$Z \geqslant Z_T: \quad P = dP/dZ = Q = dQ/dZ = 0 \tag{33}$$

Z_T certainly varies with μ the internal parameter for the thermal stratification. With the conditions (33) it follows from the eqs. (21a), (21b) that the upper part of each of the integrals vanishes.

The eqs. (30a), (30b) have now the form

$$M_m = -\ln(\kappa Z_R) - \int_{Z_R}^{Z_T} (X/K_m)dZ + \lambda_x Z_T \tag{34a}$$

$$N = -\int_{Z_R}^{Z_T} (Y/K_m)dZ + \lambda_y Z_T \tag{34b}$$

The integrals in eqs. (34a), (34b) vary with λ_x and λ_y, they do not retain the value of the barotropic case. In order to form the differences δM_m and δN as defined in section III the stress components in the barotropic case as well as the eddy viscosity should be indicated by a "b".

$$\delta M_m = -\int_{Z_R}^{Z_T} (X/K_m - X_b/K_{mb})dZ + \lambda_x Z_T = -I_x + \lambda_x Z_T \tag{35a}$$

$$\delta N = -\int_{Z_R}^{Z_T} (Y/K_m - Y_b/K_{mb})dZ + \lambda_y Z_T = -I_y + \lambda_y Z_T \tag{35b}$$

I_x and I_y are abbreviations for the integrals in the eqs. (35a), (35b). Assuming that the approximative formulae (29a), (29b) are correct, the eqs. (35a) and (35b) give a possibility to compute the coefficients c_2 and c_3 by evaluating the integrals I_x and I_y from given profiles $X(Z)$, $Y(Z)$, $K_m(Z)$ in the barotropic case and in any baroclinic case:

$$c_2 = (\lambda_x I_y - \lambda_y I_x) / (\lambda_x^2 + \lambda_y^2) \tag{36a}$$

$$c_3 = Z_T - (\lambda_x I_x + \lambda_y I_y) / (\lambda_x^2 + \lambda_y^2) \tag{36b}$$

As long as the approximative formulae (29a), (29b) give correct results, the constant c_2 or c_3, respectively, must be independent of the baroclinicity (λ_x, λ_y). Since eqs. (36a), (36b) must be valid for any baroclinicity, i.e. also for $\lambda_x = \lambda_y = 1$, these equations can be reduced to

$$c_2 = (I_y - I_x)/2 \tag{37a}$$

$$c_3 = Z_T - (I_x + I_y)/2 \tag{37b}$$

V. M_m and N as depending on the external parameters for the baroclinicity

For a practical application of the resistance law (1a), (1b) the internal parameters λ_x and λ_y, see (6a), (6b), are needed but not available. Instead of these the external parameters η_{x*} and η_{y*} are available, they are defined in eqs. (7a), (7b). Before an application of the resistance law these external parameters have to be converted into the internal ones, which can be done only iteratively.

Of course it can be done very easily if the cross-isobar angle α_0 is known

$$\lambda_x = \eta_{x*} \cos(\alpha_0) + \eta_{y*} \sin(|\alpha_0|) \tag{38a}$$

$$\lambda_y = -\eta_{x*} \sin(|\alpha_0|) + \eta_{y*} \cos(\alpha_0) \tag{38b}$$

For the cases of computations with the PBL-model, reported in section III, the cross-isobar angles have been obtained; for an example they are listed in table 3. Of course, for the purpose of converting the cross-isobar angles are needed for each possible stratification, for each possible baroclinicity and for each possible surface Rossby number.

One notices that the cross-isobar angle α_0 averaged over the eight baroclinic cases differs only very little from α_0 in the barotropic case, except for the most unstable case, where the difference is almost 2°. The averaged amount of the difference between α_0 in the baroclinic case and in the barotropic one

$$|\delta\alpha_0| = |\alpha_0(\mu, \lambda_x, \lambda_y) - \alpha_0(\mu, 0, 0)|$$

increases with decreasing stability of the thermal stratification.

Table 3: The cross-isobar angle α_0 obtained by a PBL-model for the barotropic and eight baroclinic cases in different thermal stratifications ($Ro_0 = 7.7\ 10^6$)

Tabelle 3: Der Ablenkungswinkel α_0, mit einem Grenzschichtmodell erhalten, im barotropen und in acht baroklinen Fällen für verschiedene thermische Schichtungen ($Ro_0 = 7.7\ 10^6$)

		μ					
λ_x	λ_y	30	15	7	0	-12	-20
0	0	40.0°	31.2°	25.7°	22.2°	15.5°	13.6°
0	5	40.5°	32.9°	28.5°	26.0°	22.2°	22.0°
3.54	3.54	40.4°	32.9°	27.4°	24.4°	18.0°	16.0°
5	0	40.0°	31.1°	25.1°	21.1°	10.6°	6.3°
3.54	-3.54	39.6°	29.9°	23.1°	18.4°	8.0°	7.1°
0	-5	39.4°	29.4°	22.7°	18.2°	11.0°	10.3°
-3.54	-3.54	39.6°	30.1°	24.1°	20.3°	15.0°	14.2°
-5	0	39.9°	31.4°	26.2°	23.3°	19.3°	18.6°
-3.54	3.54	40.3°	32.5°	28.0°	25.5°	22.5°	22.1°
$\overline{\alpha_0}$		39.96°	31.20°	25.64°	22.15°	15.92°	15.57°
$\overline{\lvert\delta\alpha_0\rvert}$		0.34°	1.08°	1.86°	2.64°	4.67°	5.25°

Cross-isobar angles as depending on the baroclinicity have been computed for the neutral case already 1965 by BLACKADAR with a two-layer model of the PBL.

For $Ro_0 = 7.7\ 10^6$ and for neutral stratification model integrations have been carried out for more baroclinicities, namely $\lambda = 3, 5, 7, 10$ and 15. The cross-isobar angles obtained by these integrations allow to construct a diagram giving M_m and N as depending on the external parameters η_{x*} and η_{y*}. This diagram is shown in figure 3. The isolines of M_m and N are almost straight and equidistant; the slight curvature is caused by the cross-isobar angle varying with the direction of the thermal wind.

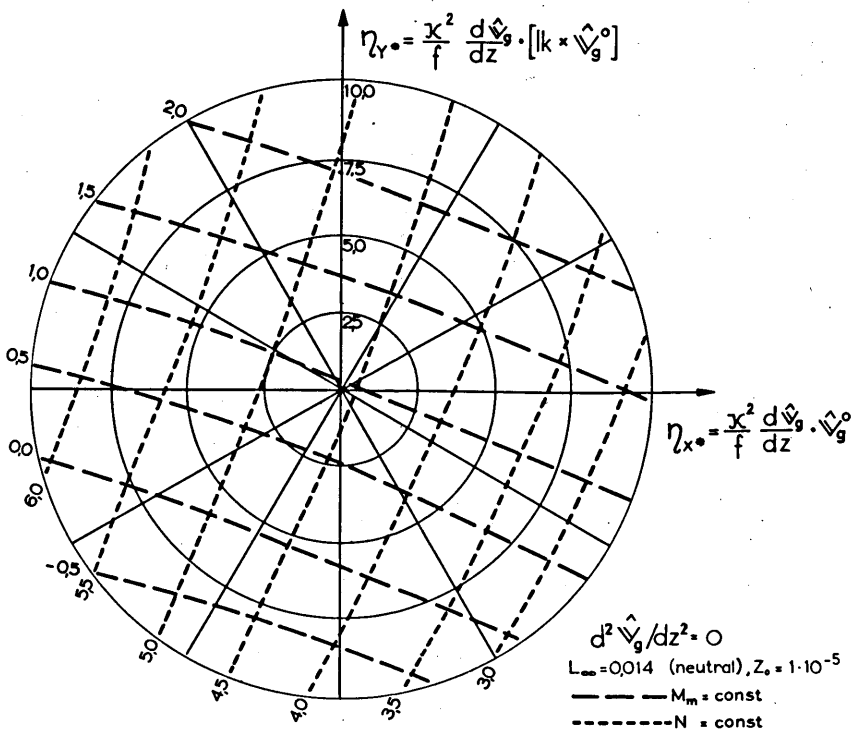

Figure 3. The functions M_m and N, which appear in the resistance law, as depending on the *external* parameters for the baroclinicity. The diagram is restricted to $\mu = 0$ and $Ro_0 = 7.7\ 10^6$.

Bild 3. Die beiden im Widerstandsgesetz auftretenden Funktionen M_m und N in ihrer Abhängigkeit von den *externen* Parametern für die Baroklinität. Das Diagramm gilt nur für $\mu = 0$ und $Ro_0 = 7.7\ 10^6$.

However it should be mentioned, that the table 3 as well as table 4 contain values which do not belong exactly to the surface Rossby number $7.7\ 10^6$ as said in the captions. The reason for that is the kind of the integrations, which have been carried out with a lower boundary chosen at $Z_0 = 1 \cdot 10^{-5}$. According to relation (10) is

$$Ro_0 = (\kappa Z_0 C_g)^{-1} \tag{39}$$

This shows that for a fixed nondimensional roughness-length the surface Rossby number varies with the geostrophic drag coefficient C_g; the later again varies with the baroclinicity. This will be demonstrated for eight different baroclinicities in table 4, section VI. Correctly spoken each point in the plane of figure 3 belongs to another surface Rossby number, the value of which in the barotropic case is $7.7\ 10^6$.

However the variation of Ro_0 with λ_x and λ_y or with η_{x*} and η_{y*} respectively are rather small. For a moderate baroclinicity ($\lambda = 5$), for instance, the largest deviations are $Ro_0 = 7.2\ 10^6$ ($\lambda_x = 0$; $C_g = 0.0346$) and $Ro_0 = 8.2\ 10^6$ ($\lambda_x = -3.54$, $\lambda_y = -3.54$; $C_g = 0.0305$). Therefore figure 3 as well as table 3 and table 4 are valid for approximately Ro_0 7.7 10^6; of course, the indication $Z_0 = 1 \cdot 10^{-5}$ in the diagram (figure 3) is exact.

A practical application of the resistance law (1a), (1b) is only possible, if for each μ and Ro_0 diagrams are available like that one which is shown in figure 3. However measurements in the atmospheric boundary layer are much to spare and to inaccurate to allow the construction of such diagrams, at best they are sufficient to prove in special cases the results obtained by a PBL-model. At the present time one is therefore able to construct such diagrams only with the aid of results obtained by integrations with a PBL-model.

In the two cases of the computations by FIEDLER (1971), mentioned with more details in section III, the thermal wind is chosen to have the direction either of the lines M_m = const or the lines N = const in the diagram figure 3. In this way he obtains the result, that in cold-air advection only N is affected by the baroclinicity and M_m remains unchanged and vice versa for warm air advection.

VI. The variation of the drag coefficient C_g with the baroclinicity

Eq. (39) shows, that it is necessary to know C_g in order to determine Ro_0 for a given Z_0.

In table 4 the values of the geostrophic drag coefficients C_g are listed for the same thermal stratifications and the same baroclinicities as it is done for the cross-isobar angle α_0 in table 3. These values of C_g are also obtained by the numerical integrations with the PBL-model described in section III.

Again the values in table 4 are given only as an example.

Table 4: The geostrophic drag coefficient $C_g\ 10^2$ obtained by the PBL-model for the barotropic and eight baroclinic cases in different thermal stratifications, ($Ro_0 = 7.7\ 10^6$).

Tabelle 4: Der geostrophische Widerstandskoeffizient $C_g\ 10^2$, mit einem Grenzschichtmodell erhalten, im barotropen und in acht baroklinen Fällen für verschiedene thermische Schichtungen, ($Ro_0 = 7.7\ 10^6$).

		μ					
λ_x	λ_y	30	15	7	0	-12	-20
0	0	1.59	2.52	2.99	3.24	3.59	3.64
0	5	1.59	2.52	3.01	3.28	3.80	3.99
3.54	3.54	1.60	2.57	3.10	3.42	4.08	4.43
5	0	1.61	2.59	3.14	3.46	4.04	4.21
3.54	-3.54	1.60	2.57	3.07	3.34	3.51	3.42
0	-5	1.59	2.52	2.96	3.16	3.21	3.20
-3.54	-3.54	1.58	2.47	2.87	3.05	3.13	3.15
-5	0	1.58	2.46	2.86	3.05	3.22	3.24
-3.54	3.54	1.58	2.48	2.91	3.14	3.47	3.53
$\widetilde{C_g} \cdot 10^2$		1.591	2.523	2.990	3.238	3.558	3.771
$\overline{\lvert\delta C_g\rvert} \cdot 10^2$		0.0090	0.040	0.090	0.138	0.320	0.419

Like the cross-isobar angle, see table 3, also the geostrophic drag coefficient $C_g\ 10^2$ averaged over the eight baroclinicities differs only slightly from $C_g\ 10^2$ in the barotropic case.

$$|\delta C_g| = |C_g(\mu, \lambda_x, \lambda_y) - C_g(\mu, 0, 0)|$$

averaged over the eight baroclinicities increases with decreasing stability of the thermal stratification.

VII. Acknowledgement

The author wishes to thank Dr. YORDANOV of the Bulgarean Academy of Science for many helpful and stimulating discussions and Mr. ETLING and Mr. LEYKAUF for doing the programming work in order to carry out the numerical integrations with the PBL-model.

VIII. References

BLACKADAR, A. K. 1965: A simplified two-layer model of the baroclinic neutral atmospheric boundary layer. Part III, p 49–65 of Final Report AFCRL-65-531, Contract AF (604)-6641 "Flux of heat and momentum in the planetary boundary layer of the atmosphere" Pennsylvania State University, Department of Meteorology.

BLACKADAR, A. K. and TENNEKES, H. 1968: Asymptotic similarity in neutral barotropic boundary layers. J. Atm. Sci. 25, 1015–1020.

CLARKE, R. M. 1970: Observational studies in the atmospheric boundary layer. Q.J.R.M.S. 96, 91–114.

CSANADY, G. T. 1967: On the "resistance law" of a turbulent Ekman layer. J. Atm. Sci., 24, 467–471.

FIEDLER, F. 1971: The effect of baroclinicity on the resistance law in a diabatic Ekman layer. Paper presented at the Meeting of the German Meteorological Society 26 Sept.–2 Oct., Essen.

GILL, A. E. 1967: The turbulent Ekman layer. Unpubl. Manuscr. Univ. of Cambridge, Departm. Appl. Mathem. and Theor. Physics.

KAZANSKII, A. B. and MONIN, A. S. 1961: On the dynamic interaction between the atmosphere and the earth surface. Bull. (Izv.) Acad. Sci. USSR, Geophys. Ser. Nr. 5 pp. 786–788, engl. transl. 514–515.

MONIN, A. S. and ZILITINKEVICH, S. S. 1967: Planetary boundary layer and large scale atmospheric dynamics. GARP Study Conf. Stockholm 28 June–11 July 1967, Appendix V, 37 pp.

WIPPERMANN, F. 1971a: A mixing-length hypothesis for the planetary boundary layer flow in the atmosphere. Beitr. Phys. Atm. 44, 215–226.

WIPPERMANN, F. 1971b: A note on a method for solving the planetary boundary layer equations. Beitr. Phys. Atm. 44, 293–296.

WIPPERMANN, F. 1972: Universal profiles in the barotropic planetary boundary layer. Beitr. Phys. Atm. 45(2), 148–163.

WIPPERMANN, F. and YORDANOV, D. 1972: A note on the Rossby similarity for flows of barotropic planetary boundary layers. Beitr. Phys. Atm. 45, 66–71.

YORDANOV, D. and WIPPERMANN, F. 1972: The parameterization of the turbulent fluxes of momentum, heat and moisture at the ground in a baroclinic planetary boundary layer. Beitr. Phys. Atm. 45, 58–65.

A Note on the Parameterization of the Large-Scale Wind Stress at the Sea-Surface

Kurze Mitteilung über die Parameterisierung der großräumigen windbedingten Schubspannung an der Meeresoberfläche

F. Wippermann

Technical University Darmstadt, Germany, Department of Meteorology

Received December 21, 1971

Summary: The variation of the geostrophic drag coefficient and of the cross-isobar angle with the geostrophic wind speed is derived by making use of the resistance law for the barotropic planetary boundary layer. The theoretical results have been compared with observations.

Zusammenfassung: Unter Verwendung des Widerstandsgesetzes für eine barotrope planetarische Grenzschicht wird die Abhängigkeit des geostrophischen Widerstandskoeffizienten und des Ablenkungswinkels von der geostrophischen Windgeschwindigkeit hergeleitet. Die theoretischen Ergebnisse werden mit Beobachtungen verglichen.

Résumé: En utilisant la loi de résistance pour une couche-limite planétaire barotrope, on établit la variation du coefficient de frottement géostrophique et de l'angle de déviation par rapport aux isobares, en fonction de la vitesse du vent géostrophique.
Les résultats théoriques ont été comparés aux observations.

The resistance law for a planetary boundary layer (PBL) enables us to compute the friction velocity u_* and the cross-isobar angle α_0 if the external parameters are given, namely the geostrophic wind speed $|\hat{V}_g|$, the Coriolis parameter f and the roughness length z_0. These external parameters can be combined to the nondimensional surface Rossby number $Ro_0 = |\hat{V}_g|/(f z_0)$. The resistance law was derived first by KAZANSKII und MONIN (1961) for a barotropic and neutral PBL, its general form is

$$\ln(Ro_0) = M_m(\mu, \lambda_x, \lambda_y) - \ln(C_g) + \kappa \cos(\alpha_0)/C_g \tag{1a}$$

$$N(\mu, \lambda_x, \lambda_y) = \kappa \sin(|\alpha_0|)/C_g \tag{1b}$$

$C_g = u_*/|\hat{V}_g|$ is the geostrophic drag coefficient, κ is the Karman constant and $M_m(\mu, \lambda_x, \lambda_y)$ as well as $N(\mu, \lambda_x, \lambda_y)$ are two universal functions of the internal stability parameter μ and of the two internal parameters λ_x, λ_y for the baroclinicity. These parameters are defined as

$$\mu = H/L_* \tag{2}$$

$$\lambda_x = dU_g/dZ, \quad \lambda_y = dV_g/dZ \tag{3a, 3b}$$

where $H = \kappa u_*/f$ is the internal scale-height of the PBL and L_* is the MONIN-OBUKHOV stability-length; $U_g = \kappa \hat{u}_g/u_*$, $V_g = \kappa \hat{v}_g/u_*$ and $Z = z/H$.

The functions $M_m(\mu, \lambda_x, \lambda_y)$ and $N(\mu, \lambda_x, \lambda_y)$ in the eqs. (1a), (1b) can be obtained by measurements only, approximated functions may be obtained for special models of the PBL by integrating the PBL-equations.

At sea the roughness-length z_0 depends on the friction velocity u_* itself. This means, that one external parameter, namely z_0, can be eliminated in the resistance law, if a relationship can be applied between z_0 and u_*. Such a relationship would be for instance a combination of CHARNOCK's (1955) formula

$$z_0 = u_*^2/(c_1 g) \tag{4}$$

and of the formula valid for very small velocities

$$z_0 = c_2 \nu / u_* \tag{5}$$

see ZILITINKEVICH (1970). g is the acceleration of gravity, the constant c_1 is 81 according to CHARNOCK (1955), BROCKS and KRUEGERMEYER (1970) obtained $c_1 = 28.5$ from the evaluations of observations and ZILITINKEVICH (1970) uses the value $c_1 = 20.8$ in the figure 1.6. of his book. $\nu = 0.13\ cm^2\ sec^{-1}$ is the kinematic viscosity and the constant c_2 should be 0.1 according to ZILITINKEVICH (1970). For very small values of u_* the roughness-length z_0 should be given by eq. (5) only, but for very large values of u_* by eq. (4) only. An additive combination of these two equations

$$z_0 = u_*^2/(c_1 g) + c_2 \nu / u_* \tag{6}$$

shows a minimum of z_0 at a friction velocity

$$u_*(z_0 = \min) = \left\{ \frac{c_1 c_2 \nu g}{2} \right\}^{1/3} \tag{7}$$

i. e. at $u_*(z_0 = \min) = 7.95\ cm\ sec^{-1}$ for the afore mentioned values of the constants.

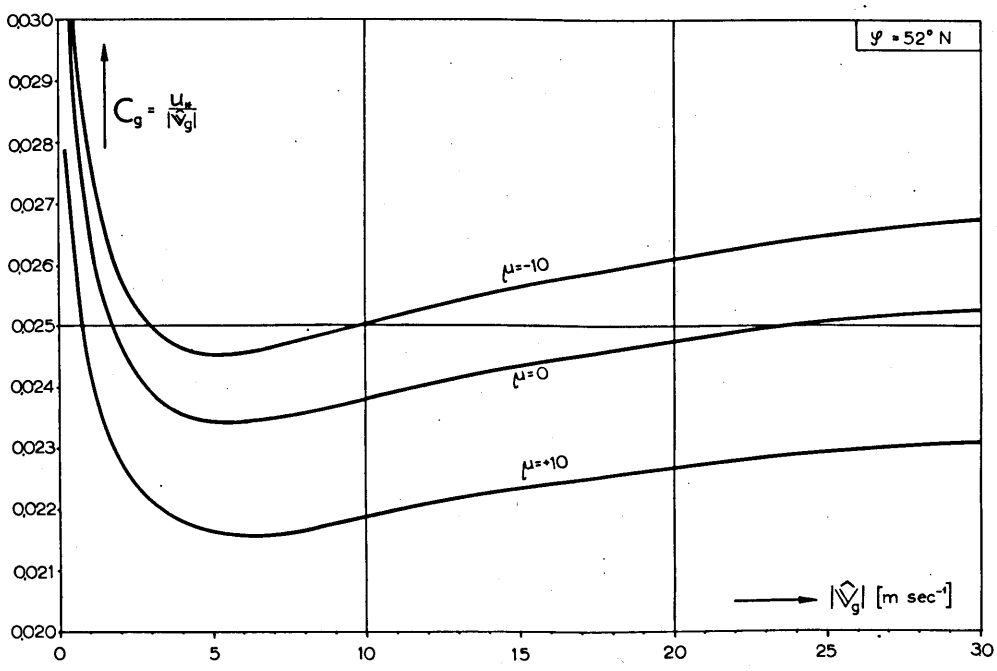

Fig. 1. The geostrophic drag coefficient at the sea surface as depending on the geostrophic wind speed for different thermal stratifications

Bild 1. Der geostrophische Widerstandskoeffizient auf dem Meere in Abhängigkeit von der geostrophischen Windgeschwindigkeit für verschiedene thermische Schichtungen

Eq. (1a) contains z_0 in the surface Rossby number on the left hand side; if one replaces this z_0 by eq. (6) the eq. (1a) can be re-written in the following form:

$$\widetilde{M}_m + (\kappa^2 |\hat{V}_g|^2 / u_*^2 - N^2)^{1/2} + \ln\{u_*/(c_1 g) + c_2 \nu / u_*^2\} = 0 \qquad (8)$$

where

$$\widetilde{M}_m = M_m + \ln(f)$$

For given $\widetilde{M}_m$ and N this equation together with eq. (1b) allows to compute the geostrophic drag coefficient C_g and the cross-isobar angle α_0 as depending on the geostrophic wind speed $|\hat{V}_g|$. For three different thermal stratifications the values of M_m and N have been obtained for a barotropic PBL-model (see WIPPERMANN 1972) and are listed in table I

Table I/Tabelle 1

μ	M_m	$\widetilde{M}_m$ ($\varphi = 52°$)	N	γ	$\gamma \mu c_3$
+10	0	9.1	6.2	4.7	13.5
0	1.0	8.1	4.6	0	0
−10	1.5	7.6	3.5	3.75	−10.8

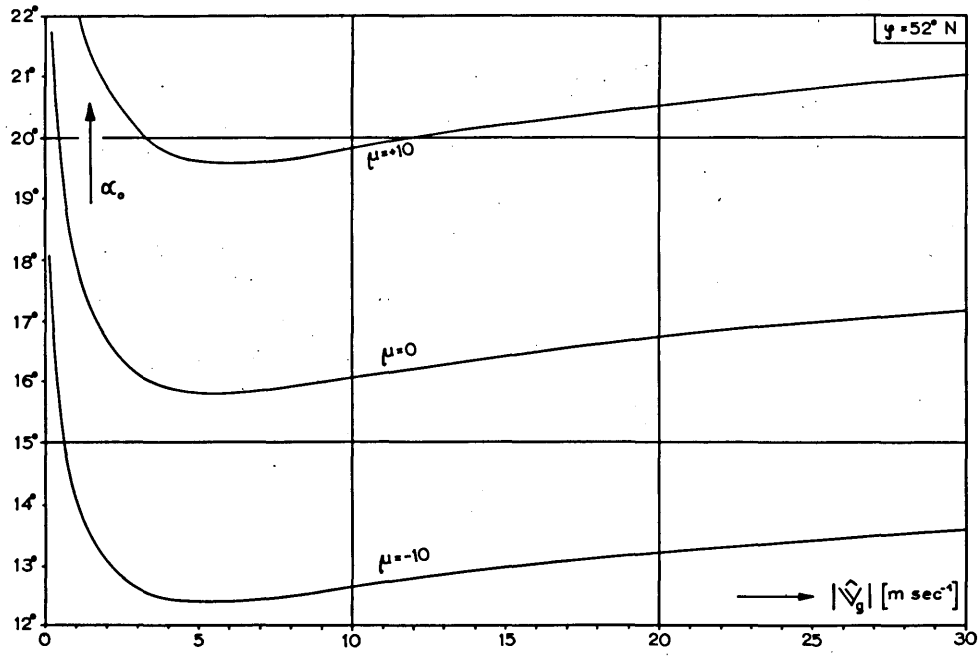

Fig. 2. The cross-isobar angle at the sea surface as depending on the geostrophic wind speed for different thermal stratifications

Bild 2. Der Ablenkungswinkel auf dem Meere in Abhängigkeit von der geostrophischen Windgeschwindigkeit für verschiedene thermische Schichtungen

As a result of such a computation figure 1 shows the variation of the geostrophic drag coefficient C_g with the geostrophic wind speed $|\hat{\mathbb{V}}_g|$. One notices a minimum of C_g at a geostrophic wind speed of about 6 m sec^{-1}. The variation of C_g with $|\hat{\mathbb{V}}_g|$ is rather small if one disregards geostrophic wind speeds $\leqslant 2$ m sec^{-1}. But there is a remarkable variation of C_g with the thermal stratification.

Almost the same patterns are obtained for the cross-isobar angle α_0, see Figure 2. As expected this angle is rather small at sea, for the considered stratifications it varies only between 12° and 22°. In stable conditions one has a large cross-isobar angle but a small geostrophic drag coefficient and vice versa in the unstable case.

When the geostrophic drag coefficient is obtained as depending on $|\hat{\mathbb{V}}_g|$ one is able to compute the roughness-length z_0 as depending on $|\hat{\mathbb{V}}_g|$ by applying eq. (6):

$$z_0 = C_g^2 \, |\hat{\mathbb{V}}_g|^2 / (c_1 g) + c_2 \, \nu / (C_g \, |\hat{\mathbb{V}}_g|) \tag{9}$$

The result is shown in figure 3. The roughness-length has a minimum of 2.4 10^{-2} mm, it appears with a geostrophic wind speed of about 4 m sec^{-1}. For smaller geostrophic wind speeds the roughness-length increases to more than 1/10 mm, it increases also for larger geostrophic wind speeds to almost 1 mm (for $|\hat{\mathbb{V}}_g| = 30$ m sec^{-1}). The variation with the thermal stratification is not very remarkable, but it should be mentioned, that cases with an extremely stratification, either unstable or stable, have not been considered.

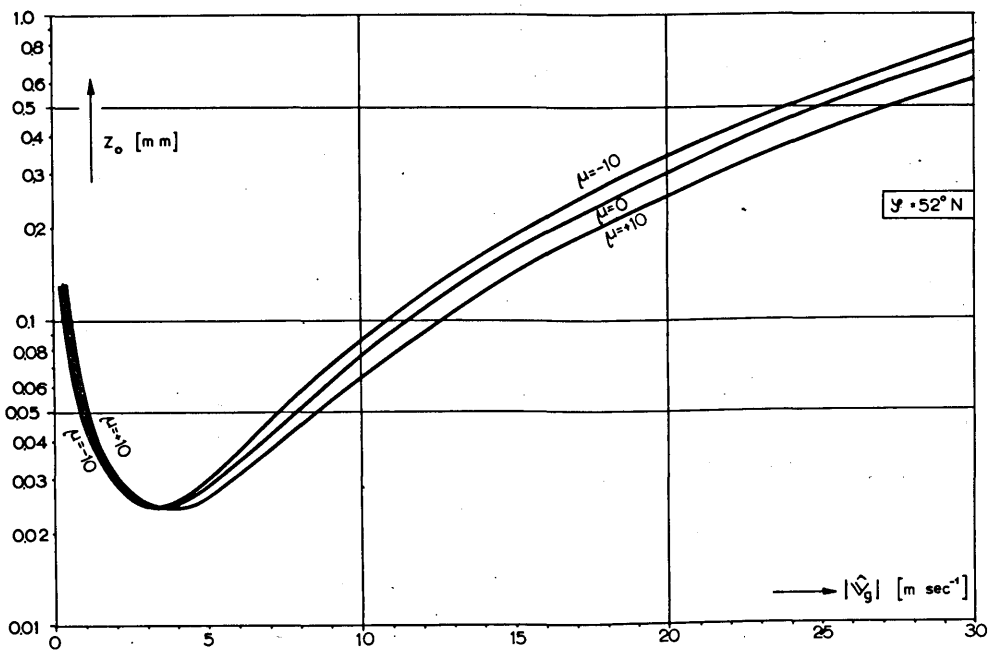

Fig. 3. The roughness-length of the sea surface as depending on the geostrophic wind speed for different thermal stratifications

Bild 3. Die Rauhigkeitslänge auf dem Meere in Abhängigkeit von der geostrophischen Windgeschwindigkeit bei verschiedenen thermischen Schichtungen

Unfortunately no observations are available suitable for proving such results. But there are some observations of the ratio $|\hat{\mathbb{V}}_{10}|/|\hat{\mathbb{V}}_g|$ i. e. the ratio of the "surface wind" (measured at 10 m) to the geostrophic wind. In order to make possible an application of such observations one has to compute $|\hat{\mathbb{V}}_{10}|$ from the friction velocity u_* obtained earlier. In doing that the so-called log-linear profile shoud be used to obtain the wind speed in 10 m

$$|\hat{\mathbb{V}}_{10}| = u_*/\kappa\,[\ln(z_{10}/z_0) + \gamma z_{10}/L_*] \tag{10}$$

Herein it may be written according to eq. (2)

$$\gamma z_{10}/L_* = \gamma \mu z_{10}/H = \gamma \mu z_{10} f/(\kappa u_*)$$

Replacing z_0 in eq. (10) by eq. (6) one gets

$$|\hat{\mathbb{V}}_{10}| = u_*/\kappa\,\{\ln(z_{10}/u_*) - \ln[u_*/(c_1 g) + c_2 \nu/u_*^2] + \gamma \mu c_3/u_*\} \tag{11}$$

where

$$c_3 = z_{10} f/\kappa = 0.288 \text{ cm sec}^{-1} \text{ (for } \varphi = 52°\text{N)}$$

Eq. (11) can be used to compute $|\hat{\mathbb{V}}_{10}|$ as depending on $|\hat{\mathbb{V}}_g|$, if u_* is replaced by $C_g\,|\hat{\mathbb{V}}_g|$ and the before computed geostrophic drag coefficients are used. In this way the solid lines in figure 4 have been obtained;

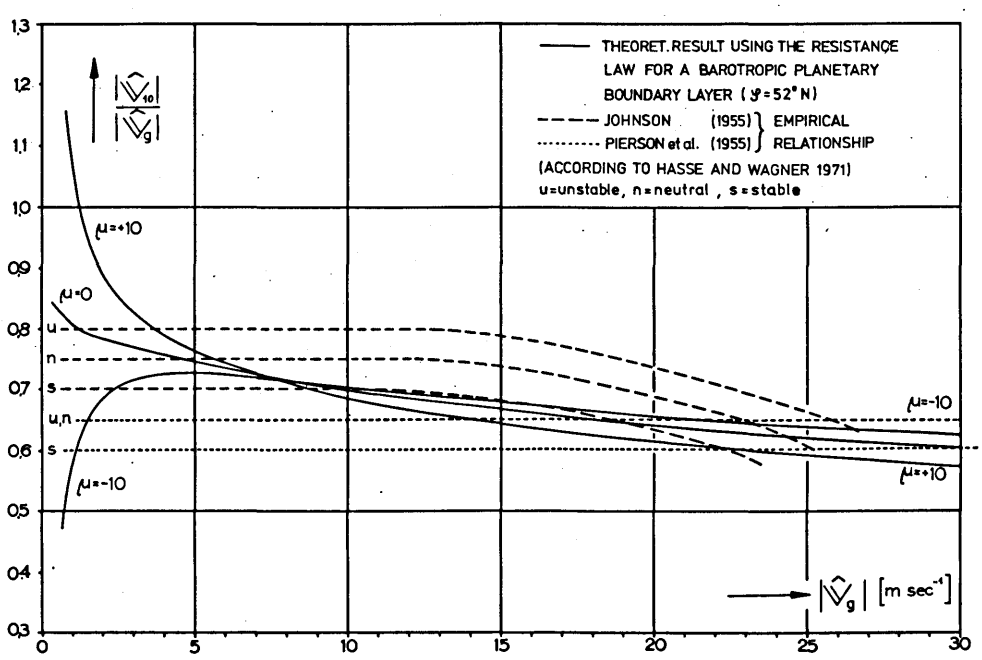

Fig. 4. The ratio of surface wind to geostrophic wind as depending on the geostrophic wind speed according to theoretical results (solid lines) and to empirical relationships (broken and dotted lines)

Bild 4. Das Verhältnis von Windgeschwindigkeit in 10 m Höhe zur geostrophischen Windgeschwindigkeit in Abhängigkeit von der letzteren als theoretisches Ergebnis (ausgezogene Linien) und als empirische Beziehungen (gestrichelte und gepunktete Linien)

they are drawn again for the three thermal stratifications $\mu = +10$, $\mu = 0$ and $\mu = -10$. These curves are compared with the empirical relationships by JOHNSON (1955), broken lines, and by PIERSON et al. (1955), dotted lines, as given by HASSE and WAGNER (1971). Disregarding the very small geostrophic wind speeds the theoretical curves are between the empirical ones by JOHNSON and by PIERSON et al. The agreement with the empirical relations can be considered as good.

HASSE and WAGNER (1971) used also wind observations from the light ship P8 in the German Bight together with the geostrophic wind obtained by the evaluation of measurements of the pressure. Their ratios $|\hat{\mathbb{V}}_{10}| / |\hat{\mathbb{V}}_g|$ are shown in figure 5 and compared with the theoretical results mentioned before. The agreement is good for geostrophic wind speeds > 15 m sec^{-1}, for lighter geostrophic winds the observations by HASSE and WAGNER show larger values than the theoretical ones. According to the observations evaluated by HASSE and WAGNER few of these ratios are almost 1.0 and some are even larger than 1.0 which is difficult to understand. A possible explanation (according to a private communication by one of the authors) is that for geostrophic winds < 15 m sec^{-1} the observations of the surface wind can contain pronounced micro- or meso-scale winds (of any direction), which cause the large ratio. The disagreement between the observations by HASSE und WAGNER and the theoretical results must not disprove necessarily the latter.

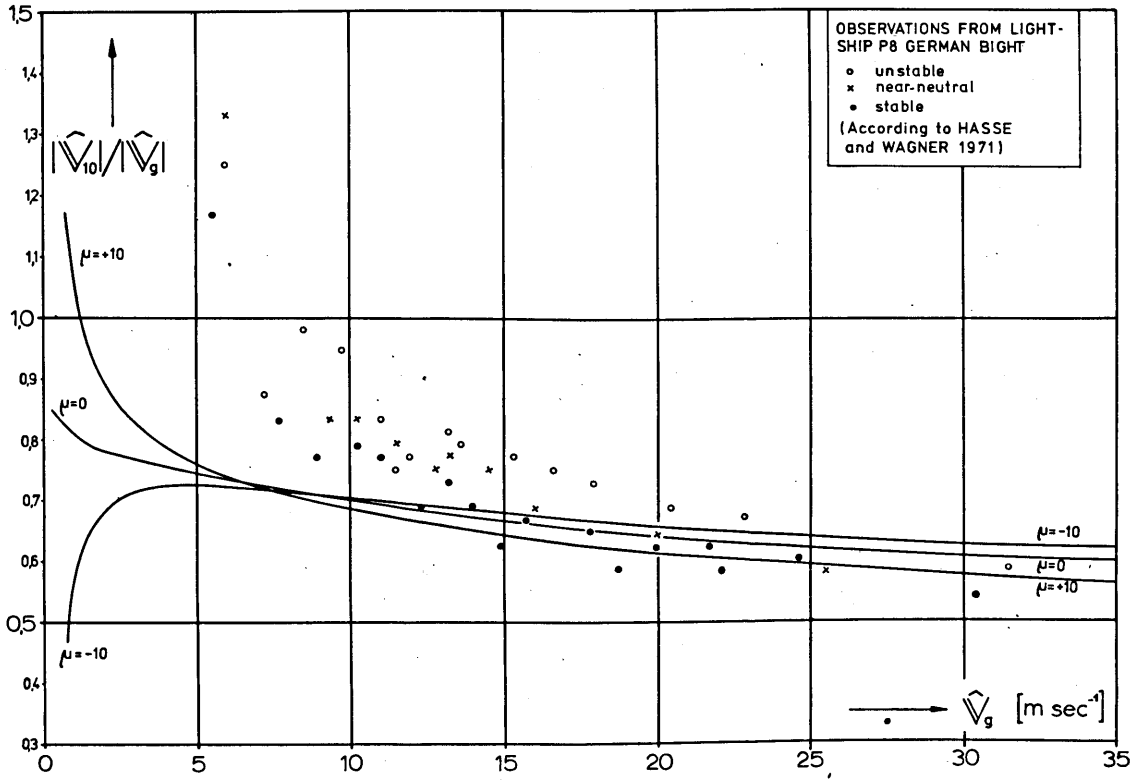

Fig. 5. The same as in figure 4, but the theoretical results are compared with observations (after HASSE and WAGNER)

Bild 5. Das gleiche wie in Bild 4, jedoch werden die theoretischen Ergebnisse jetzt mit Beobachtungen (nach HASSE und WAGNER) verglichen.

References

BROCKS, K. and KRUEGERMEYER, L. (1970): The hydrodynamic roughness of the sea surface. Ber. Inst. Radiometeor. Marit. Meteor. Nr. 14, Hamburg, pp 35

CHARNOCK, H. (1955): Wind stress on a water surface. Quart. J. Roy. Meteor. Soc. **81**, 639–642

HASSE, L. and WAGNER, V. (1971): On the relationship between the geostrophic and surface wind at sea. Monthly Wea. Rev. 99(4), 255–260

JOHNSON, P. W. (1955): The ratio of the sea surface wind to the gradient wind. Proc. 1st Conf. on Ships and Waves, Hoboken, N. J. Oct. 1954, Council on Wave Research, Berkeley, Calif., 104–110

KAZANSKII, A. B. and MONIN, A. S. (1961): On the dynamic interaction between the atmosphere and earth surface. Bull. (Izv.) Acad. Sci. USSR, Geophys. Ser., Nr. 5, 786–788, engl. transl. 514–515.

PIERSON, W. J., NEUMANN, G. and JAMES, R. J. (1955): Practical methods for observing and forecasting ocean waves by means of wave spectra and statistics. H. O. Publ. No. 603, pp 284, US Hydrographic Office Washington, D. C.

WIPPERMANN, F. (1972): Universal profiles in the barotropic planetary boundary layer. Beitr. Phys. Atm. **45**, 148–163

ZILITINKEVICH, S. S. (1970): The dynamics of the atmospheric boundary layer. Leningrad, pp 291 (in russ.)

Problems which still have to be solved before the resistance laws can be applied for the purpose of parameterization in numerical models for large-scale atmospheric motions:

(1) At sea the roughness-length z_o is not a given local parameter (constant with time) but it depends on the surface stress τ_o besides on some other variables and therefore it varies with time. How can z_o be determined at sea ?

(2) At the sea surface the temperature $\hat{\vartheta}_o$ and the moisture $\hat{s}_o$ are given; how should they be determined at land ?

(3) The values $\hat{\vartheta}_T$ and $\hat{s}_T$ at the top of the PBL have to be determined from the vertical $\hat{\vartheta}$-profile and the $\hat{s}$-profile, respectively, computed by the numerical model for the place under consideration. The question is: where is the level z_T at which these values $\hat{\vartheta}_T$ and $\hat{s}_T$ have to be read-off ?

(4) From the large-scale parameters computed by the numerical model one obtains the external stability parameter $\sigma = \beta\,\delta\hat{\vartheta}/(f\,|\hat{v}_{go}|)$. For an application of the resistance laws, however, one needs the internal stability parameter $\mu = H/L_*$. How can μ be obtained from σ ? (q_o and u_*, both contained in L_*, are not yet known; just these two should be determined with the aid of the resistance laws).

(5) From the large-scale parameters computed by the numerical model one obtains the two external parameters of the baroclinicity $\eta_{x*} = \kappa^2/f\; d\hat{v}_g/dz \cdot (\hat{v}_{go})^o$ and $\eta_{y*} = \kappa^2/f\; d\hat{v}_g/dz \cdot \mathbf{k} \times (\hat{v}_{go})^o$. For an application

of the resistance laws, however, one needs the two internal parameters for the baroclinicity, namely $\lambda_x = \kappa^2/f \; d\hat{v}_g/dz \cdot (\tau_o)^o$ and $\lambda_y = \kappa^2/f \; d\hat{v}_g/dz \cdot \cdot |k \times (\tau_o)^o$. How can λ_x and λ_y be obtained from η_{x*} and η_{y*} ? (τ_o is not yet known, just this should be determined with the aid of the resistance laws).

(6) The functions $M_m(\mu, \lambda_x, \lambda_y)$, $M_h(\mu, \lambda_x, \lambda_y)$, $M_s(\mu, \lambda_x, \lambda_y)$ and $N(\mu, \lambda_x, \lambda_y)$ have to be known. How do they look ?

(7) The resistance law is not applicable in the equatorial region where $f \longrightarrow 0$ and $RO_o \longrightarrow \infty$. What has to be done in order to parameterize the boundary layer effects with the aid of the resistance law in a global numerical model?

Comments on these problems:

ad (1) A relationship has to be established between the roughness of the sea (expressed by the roughness-length z_o) and the surface stress or the friction velocity, respectively. An example for such a relationship is the formula by CHARNOCK (1955)

$$z_o = u_*^2/(c_1 \; g)$$

applicable for rather large wind velocities or the well-known formula for very small velocities

$$z_o = c_2 \; \nu / u_*$$

Such relationships allow to eliminate z_o in the resistance law and to obtain the variations of C_g and

α_o with $|\hat{\mathbb{v}}_{go}|$ (of course for a given f). An example of such an application of the resistance law is given in the section on page 208 - 214 .

ad (2) For this purpose the heat budget at the earth surface has to be included in the numerical model. The water content of the soil must either be given depending on time or it must be computed by the model itself, which means that the model must also contain levels for computations at the earth surface and in the soil.

ad (3) Evaluations of observations show (as far as they can show it) that M_h is very similar to M_m , the same is true for M_s , see MONIN and ZILITINKEVICH (1967) and CLARKE (1970). If one puts

$$M_h = M_s = M_m$$

one gets the two equations

$$a_{ho} (\Theta_T - \Theta_o) = |\mathbb{V}_g| \cos(\alpha_o)$$

$$a_{so} (S_T - S_o) = |\mathbb{V}_g| \cos(\alpha_o)$$

where $\Theta = \hat{\vartheta}/\vartheta_*$ and $S = \hat{s}/s_*$. Using these two formulae it must be possible to compute the height Z_T for which $\Theta(Z_T) = \Theta_T$ and $S(Z_T) = S_T$ with the aid of a PBL-model. This height will depend on α_o and on the (non-dimensional) geostrophic wind speed at the ground.

ad (4) For a given σ the internal stratification parameter can be obtained iteratively only. In his monograph ZILITINKEVICH (1970) presents diagrams obtained by such an iterative procedure. These diagrams (after CHALIKOV 1968) allow to read-off the values of μ for given σ and RO_o.

ad (5) A similar procedure has to be applied for getting the λ_x and λ_y fom the η_{x*} and η_{y*} ; diagrams are not yet available. Since only α_o has to be known for the coordinate transformation, it is probably sufficient to use directly the known value of α_o which the numerical model has computed at the time one time step before.

ad (6) Some evaluations of observational data are available, see MONIN and ZILITINKEVICH (1967) and CLARKE (1970). These evaluations have been used, beside some results of PBL-models, to construct an empirical formula for $M_m(\mu,0,0)$ and $N(\mu,0,0)$ as presented in the section on page 177 - 183. The functions M_h and M_s possibly can be put equal to M_m , see ad (3). In the baroclinic case the differences $M_m(\mu, \lambda_x, \lambda_y)$ - $- M_m(\mu,0,0)$ and $N(\mu, \lambda_x, \lambda_y) - N(\mu,0,0)$ have been obtained by a PBL-model; empirical formulae for these differences are given in the section "Baroclinic Effects ..." on page 192 - 207.

ad (7) A procedure for extending the applicability of the resistance laws to the equatorial region is not yet presented; of course such an extension is not impossible.

References

CHARNOCK, H. 1955 Wind Stress on a Water Surface Quart. J. Roy. Meteor. Soc. 81, 639 - 642

CLARKE, R.H. 1970 Observational Studies in the Atmospheric Boundary Layer
Quart. J. Roy. Meteor. Soc.
96, 91 - 114

CHALIKOV, D.V. 1968 The Turbulent Fluxes at the Ground Derived from Synoptic Informations (in Russ.)
Meteorol. and Gidrol. Nr. 8, 10-19

MONIN, A.S.
ZILITINKEVICH, S.S. 1967 Planetary Boundary Layer and Large Scale Atmospheric Dynamics
Proc. GARP Study Conf. Stockholm
Append. V, pp 37

Chapter 5

Non-Stationary and/or Horizontally Non-Homogeneous Boundary Layers

The PBL is defined as a stationary and horizontally homogeneous boundary layer. The atmospheric boundary layer, however, is neither stationary nor horizontally homogeneous; it may therefore considerably deviate from a PBL.

If the resistance law for instance is applied to determine the turbulent fluxes τ_o , q_o and j_o in the real atmospheric boundary layer an error will be made since the assumptions of a PBL are not satisfied in reality. The first paper of this chapter ("The Effect of Non-Stationarity on the PBL") studies this error for the case the diurnal variation being that of a clear day in summer time. For this purpose a time-depending boundary-layer model has been integrated, the results are compared with those of the corresponding stationary cases, i.e. stationary cases having the same thermal stratification than the nonstationary ones.

Some other time-dependent models are cited at the end

of that paper, several more on the pages 152 and 153. In a part of these models are incorporated the divergences of the radiative fluxes, which are even more important for time - depending models than for stationary ones.

The second part of this chapter is concerned with the effects due to horizontal inhomogeneities of the surface roughness. Investigations of this topic are going on for almost forty years, but they all are still restricted to cases, in which the boundary flow passes a sudden change in the roughness (which is homogeneous in front of this change and behind it). An internal boundary layer develops, starting at the change of roughness, its height grows continuously in the downstream direction up to that distance, where the whole boundary layer is again in the equilibrium with respect to the changed roughness-length.
There are developed some models considering a sudden change in the temperature of the lower boundary; such a change causes a similar effect as a change in the roughness-length.

This second part of the chapter consists of a bibliographical survey only. It includes the Russian-language papers which have already been cited in the review paper on this topic by PANCHEV, DONEV and GODEV (1971), see page 252. More than half of this bibliography has already been given in the book by PLATE (1971), see page 6; it contains almost 50 references to internal boundary layers. This list has been completed and arranged chronologically.

The Effects of Non-Stationarity on the Planetary Boundary Layer

Der Einfluß der Instationarität auf eine planetarische Grenzschicht

F. Wippermann, D. Etling, H. Leykauf

Technical University Darmstadt, Germany, Department of Meteorology

Received November 7, 1972

Summary: The "resistance law" for a planetary boundary layer (a horizontally homogeneous and steady state boundary layer) can be applied only if the variation with time of the boundary layer is understood as a sequence of stationary cases. In this paper the difference is studied for boundary layer parameters in a non-stationary case on the one side and in the corresponding stationary case on the other side. For this purpose the equations of a non-stationary boundary layer model are integrated numerically for a given diurnal variation of the internal parameter μ of the thermal stratification. – The response of a planetary boundary layer to single point perturbations (variations with time) is investigated likewise.

Zusammenfassung: Das „Widerstandsgesetz" für eine planetarische Grenzschicht, d.h. eine horizontal homogene und stationäre Grenzschicht, kann nur angewandt werden, wenn die zeitliche Veränderung der Grenzschicht als eine Folge stationärer Zustände aufgefaßt wird. In dieser Arbeit werden die Unterschiede untersucht, die sich für Grenzschichtparameter ergeben einerseits im instationären Fall und zum andern im entsprechenden stationären. Zu diesem Zwecke werden die Gleichungen eines instationären Grenzschichtmodelles numerisch integriert, wobei die tägliche Änderung des internen Parameters μ für die thermische Schichtung vorgegeben wird. – Ebenfalls wird untersucht, in welcher Weise eine planetarische Grenzschicht auf punktförmige Störungen (Veränderungen mit der Zeit) anspricht.

Résumé: – La «loi de résistance» pour une couche limite planétaire (couche limite horizontalement homogène et stationnaire) ne peut être appliquée que si la variation avec le temps de la couche limite est conçue comme une suite d'états stationnaires. Dans cet article, on étudie les différences que manifestent les paramètres de la couche limite, d'une part, dans un cas non stationnaire et, d'autre part, dans le cas stationnaire correspondant. A cet effet, les équations d'un modèle de couche limite non stationnaire sont intégrées numériquement pour une variation diurne donnée du paramètre interne μ de la stratification thermique. On recherche également de quelle façon une couche limite planétaire répond à des perturbations ponctuelles (variations avec le temps).

I. Introduction

The planetary boundary layer (PBL) is defined as a steady state and horizontally homogeneous boundary layer of the atmosphere. By this definition the PBL is a rather crude model of the real boundary layer but it proves to be an excellent instrument for the parameterization of boundary layer effects, for instance for the incorporation of such effects into general circulation models. The parameterization can be done by applying the so-called resistance law. Since this law is valid in a PBL only, the variation with time of the boundary layer must be understood as a sequence of stationary states. Such a procedure is justified only if the effects of non-stationarity can be neglected. It is the object of the present paper to investigate these effects on a PBL by means of numerical integrations of a time dependent boundary layer model.

II. The time dependent model of the boundary layer

We shall start with the equations for a non-stationary horizontally homogeneous boundary layer

$$\partial\hat{u}/\partial t - f(\hat{v} - \hat{v}_g) = \partial(\tau_x/\bar{\rho})/\partial z \tag{1a}$$

$$\partial\hat{v}/\partial t + f(\hat{u} - \hat{u}_g) = \partial(\tau_y/\bar{\rho})/\partial z \tag{1b}$$

where u and v are the horizontal velocity components, τ_x and τ_y are the components of the Reynolds stress, f is the Coriolis parameter, ρ the density (the variation of $\bar{\rho}$ with z is neglected), t the time and z the vertical coordinate. The index g denotes the geostrophic wind, the bar means an average and the circumflex an average weighted by ρ. With the flux-gradient relation

$$\tau_x/\bar{\rho} = k_m\, \partial\hat{u}/\partial z \tag{2a}$$

$$\tau_y/\bar{\rho} = k_m\, \partial\hat{v}/\partial z \tag{2b}$$

where k_m is the eddy viscosity, the eqs. (1a), (1b) read in non-dimensional notation

$$\partial Q/\partial F + P = \partial/\partial Z\, [K_m\, \partial Q/\partial Z] + \lambda_y\, \partial K_m/\partial Z \tag{3a}$$

$$\partial P/\partial F - Q = \partial/\partial Z\, [K_m\, \partial P/\partial Z] + \lambda_x\, \partial K_m/\partial Z \tag{3b}$$

Herein is $Z = z/H$ the non-dimensional height with $H = \kappa u_*/f$ the scale height of the PBL; u_* is the friction velocity and κ von Karmans constant. $F = f \cdot t$ is the non-dimensional time, $P = \kappa(\hat{u} - \hat{u}_g)/u_*$ and $Q = \kappa(\hat{v} - \hat{v}_g)/u_*$ are the components of the non-dimensional velocity defect. $K_m = k_m/(H^2 f)$ is the non-dimensional eddy viscosity; $\lambda_x = \kappa^2/f\, \partial\hat{u}_g/\partial z$ and $\lambda_y = \kappa^2/f\, \partial\hat{v}_g/\partial z$ are two internal parameters for the baroclinicity.

Using the non-dimensionalized relations (2a), (2b)

$$X = K_m\, \partial U/\partial Z \tag{4a}$$

$$Y = K_m\, \partial V/\partial Z \tag{4b}$$

in the eqs. (3a), (3b) one obtains

$$\partial/\partial F\, [Y/K_m] + X/K_m - \lambda_x = \partial^2 Y/\partial Z^2 \tag{5a}$$

$$\partial/\partial F\, [X/K_m] - Y/K_m + \lambda_y = \partial^2 X/\partial Z^2 \tag{5b}$$

$U = \kappa\hat{u}/u_*$ and $V = \kappa\hat{v}/u_*$ denote the non-dimensional components of the velocity and $X = \tau_x/(\bar{\rho}\, u_*^2)$ as well as $Y = \tau_y/(\bar{\rho} u_*^2)$ the non-dimensional components of the Reynolds stress.

The two equations (5a), (5b) contain the three variables X, Y, K_m. In order to close this system of equations Prandtl's mixing-length relation

$$k_m = l^2\, |\partial\hat{v}/\partial z| \tag{6}$$

shall be used, which leads after elimination of the velocity gradients with the aid of (2a), (2b) to

$$K_m = T^{1/2}\, L/\kappa \tag{7}$$

Herein is $T = [X^2 + Y^2]^{1/2}$ and $L = l/H$ the non-dimensional mixing-length. For L a mixing-length hypothesis shall be used, which has been given by WIPPERMANN (1971a)

$$L = L_\infty - (L_\infty - L_0)\, T^p \tag{8}$$

$$p = -\kappa/[(\partial T/\partial Z)_0\, (L_\infty - L_0)]$$

The index 0 denotes values at the lower boundary. L_∞ is the asymptotic mixing-length for $z \to \infty$; this parameter governs the thermal stratification of the boundary layer. An empirical relationship between L_∞ and μ, the internal parameter for the thermal stratification, has been given in the paper mentioned before

$$\mu = -44.2 - 24.4 \log_{10}(L_\infty) \tag{9}$$

The definition of μ is $\mu = H/L_*$ with L_* the Monin-Obukhov stability length. The parameter L_0 in eq. (8) is the mixing-length at $Z = Z_0$, i.e. in the height of the non-dimensional roughness-length $Z_0 = z_0/H$. By applying the behaviour of $L(Z)$ as valid in the constant stress layer one gets at $Z = Z_0$

$$L_0 = \kappa Z_0 \tag{10}$$

With the mixing-length hypothesis (8) the system of the equations is now closed, for the four variables X, Y, K_m, L the four eqs. (5a), (5b), (7), (8) are available. The boundary conditions are

$$Z \to \infty: \quad X \to \lambda_x (\lambda_x^2 + \lambda_y^2)^{1/2} L_\infty^2/\kappa \tag{11a}$$

$$Y \to \lambda_y (\lambda_x^2 + \lambda_y^2)^{1/2} L_\infty^2/\kappa \tag{11b}$$

$$K_m \to (\lambda_x^2 + \lambda_y^2)^{1/2} L_\infty^2/\kappa \tag{11c}$$

$$L \to L_\infty \tag{11d}$$

$$Z = Z_0: \quad X = 1, \; Y = 0, \; K_m = Z_0, \; L = \kappa Z_0 \tag{12a–d}$$

Of course the conditions (12a), (12b) are correct only for an orientation of the coordinate system where the x-axis has the direction of the surface stress.

For any given variation with time of the thermal stratification represented by the parameter $L_\infty(F)$ one gets $X(Z, F)$, $Y(Z, F)$, $K_m(Z, F)$ and $L(Z, F)$ as the solution of the system of eqs. (5a), (5b), (7), (8) with the boundary conditions (11a)–(11d) and (12a)–(12d). With these four variables the velocity defects $P(Z, F)$ and $Q(Z, F)$ can be obtained by using the flux-gradient relations (4a), (4b) written for the defects

$$X = K_m \, [\partial P/\partial Z + \lambda_x] \tag{13a}$$

$$Y = K_m \, [\partial Q/\partial Z + \lambda_y] \tag{13b}$$

in integrated form

$$P(Z, F) = \int_{Z_0}^{Z} [X/K_m - \lambda_x] \, dZ' + P_0 \tag{14a}$$

$$Q(Z, F) = \int_{Z_0}^{Z} [Y/K_m - \lambda_y] \, dZ' + Q_0 \tag{14b}$$

Another interesting variable is $|\hat{\mathbf{v}}|/|\hat{\mathbf{v}}_g|$, which can be obtained from the velocity defects by

$$\frac{|\hat{\mathbf{v}}|}{|\hat{\mathbf{v}}_g|}(Z, F) = C_g/\kappa \, [(P - P_0 + \lambda_x Z)^2 + (Q - Q_0 + \lambda_y Z)^2]^{1/2} \tag{15}$$

Herein means $C_g = u_*/|\hat{\mathbf{v}}_{g0}|$ the geostrophic drag coefficient. P_0 and Q_0 are the velocity defects at $Z = Z_0$; because of the lower boundary conditions for the velocity components

$$z = z_0: \quad \hat{u} = \hat{v} = 0 \tag{16}$$

are

$$P_0 = -\kappa \hat{u}_{g0}/u_* = -\kappa\,|\hat{\mathbf{v}}_{g0}|\cos(\alpha_0)/u_* = -\kappa\,\cos(\alpha_0)/C_g \tag{17a}$$

$$Q_0 = -\kappa \hat{v}_{g0}/u_* = -\kappa\,|\hat{\mathbf{v}}_{g0}|\sin(\alpha_0)/u_* = \kappa\,\sin(|\alpha_0|)/C_g \tag{17b}$$

α_0 denotes the cross-isobar angle.

The time variation of the vertical profile of the potential temperature can be obtained from the X(Z, F), Y(Z, F) and K_m (Z, F). In order to get a formula for computation first the two profile functions ϕ_m and ϕ_h are defined

$$\phi_h = z/\vartheta_*\ \partial\hat{\vartheta}/\partial z = Z\partial\hat{\Theta}/\partial Z \tag{18a}$$

$$\phi_m = \kappa z/u_*\ |\partial\,\hat{\mathbf{v}}/\partial z| = Z|\partial\,\mathbf{V}/\partial Z| \tag{18b}$$

which are very often used in the constant stress layer. ϑ is the potential temperature and $\Theta = \vartheta/\vartheta_*$ the non-dimensional potential temperature, where $\vartheta_* = -q_0/(\kappa\, c_p\, \overline{\rho}\, u_*)$ is a characteristic fluctuation of the potential temperature, q_0 is the turbulent flux of sensible heat at the ground and c_p is the specific heat. The flux-gradient relationships for heat and momentum are

$$q = -c_p\, \overline{\rho}\, k_h\, \partial\hat{\vartheta}/\partial z \qquad q/q_0 = K_h\, \partial\hat{\Theta}/\partial Z \tag{19a,b}$$

$$\tau = \overline{\rho}\, k_m\, |\partial\,\hat{\mathbf{v}}/\partial z| \qquad T = K_m\, |\partial\,\mathbf{V}/\partial Z| \tag{20a,b}$$

k_h is the turbulent diffusion coefficient for sensible heat, $K_h = k_h/(H^2 f)$ is this coefficient in non-dimensional notation. For the ratio k_h/k_m can be written

$$a_h = k_h/k_m = K_h/K_m = q/q_0\ \phi_m/\phi_h\ 1/T \tag{21}$$

where the eqs. (18a), (18b), (19b) and (20b) have been used in order to eliminate the vertical gradients. Using eq. (21) in eq. (19b) one gets the vertical gradient of the potential temperature

$$\partial\hat{\Theta}/\partial Z = \phi_h/\phi_m\ T/K_m$$

or in integrated form

$$\hat{\Theta}(Z, F) = \hat{\Theta}(Z_T) - \int_Z^{Z_T} \phi_h/\phi_m\ T/K_m\, dZ' \tag{22}$$

The index $_T$ denotes the top of the PBL where the potential temperature should be kept constant with time.

In order to evaluate the profiles $\hat{\Theta}(Z)$ at various times F one has to know the ratio ϕ_h/ϕ_m. For this the hypothesis should be made that the ratio measured in the surface layer will be valid through the total PBL

$$\phi_h/\phi_m = (\phi_h/\phi_m)_{obs} \tag{23}$$

However, it may be accentuated that this assumption is made only for the ratio ϕ_h/ϕ_m not for the profile functions itself. It will be used

$$(\phi_h/\phi_m)_{obs} = \begin{cases} \dfrac{0.74 + 4.7\,\mu Z}{1 + 4.7\,\mu Z} & \mu > 0 \\[2ex] \dfrac{(1 - 15\,\mu Z)^{1/4}}{(1 - 9\,\mu Z)^{1/2}} & \mu < 0 \end{cases} \tag{24}$$

These are the relationships given by BUSINGER et al. (1971), they are obtained by evaluating the data measured at the Kansas site during summer 1968. According to eq. (21) the ratio of the diffusion coefficients at the ground is with the relationships (24)

$$a_{h0} = (K_h/K_m)_0 = (\phi_m/\phi_h)_0 = 1.35 \tag{25}$$

In order to get $K_h/K_m(Z, F)$ one has to know the ratio $q/q_0(Z, F)$ as to be seen from eq. (21). This can be obtained by using the equation for the internal energy in the form $d\vartheta/dt = -\nabla(\mathbb{R}/(\rho c_p))$ where $\mathbb{R}$ is the radiative flux. It reads in the PBL

$$c_p \bar{\rho}\, \partial\hat{\vartheta}/\partial t = -\partial(q + R_z)/\partial z \tag{26a}$$

or in non-dimensional notation

$$\partial\hat{\Theta}/\partial F = \partial(q/q_0 + R_z/q_0)/\partial Z \tag{26b}$$

In the integrated form (disregarding the divergence of the radiative flux) this equation

$$q/q_0(Z, F) = 1 + \int_{Z_0}^{Z} (\partial\hat{\Theta}/\partial F)\, dZ' \tag{27}$$

gives the ratio $q/q_0(Z, F)$ which is needed in eq. (21) to obtain $K_h/K_m(Z, F)$.

The model described here gives all the variables in the PBL one is interested in. A (numerical) solution of the system of the eqs. (5a), (5b), (7), (8) with the boundary conditions (11a)–(11d) and (12a)–(12d) lets obtain $X(Z, F)$, $Y(Z, F)$, $K_m(Z, F)$, $L(Z, F)$; with these $P(Z, F)$, $Q(Z, F)$ are obtained by using eqs. (14a), (14b) as well as $\hat{\Theta}(Z, F)$, $q/q_0(Z, F)$ and $K_h/K_m(Z, F)$ by using the eqs. (22), (27) and (21).

However the model has a severe disadvantage: all variables are non-dimensionalized by the *internal* parameters u_* and q_0 beside the local parameters f and $\bar{\rho}$. Both parameters u_* and q_0 vary with time, which means the non-dimensionalization varies with time including that of the independent variable Z; even the orientation of the coordinate system varies with time (for a geostrophic wind $\hat{v}_{g0}$ constant with time), since α_0 varies with time. This makes it almost impossible to discreticize the equations of the system (5a), (5b), (7), (8) in the usual way for a numerical solving procedure. This disadvantage could be avoided, if for the non-dimensionalization the *external* scale height $D = \kappa^5 |\hat{v}_{g0}|/f$ is used; then the height variable $Z_n = z/D$ will be constant with time and the direction of the coordinate system remains unchanged with time (the x-axis always has the direction of the geostrophic wind $\hat{v}_{g0}$). The variables would be $X_n = \tau_x/(\bar{\rho}\kappa^8 |\hat{v}_{g0}|^2)$, $Y_n = \tau_y/(\bar{\rho}\kappa^8 |\hat{v}_{g0}|^2)$, $K_{mn} = k_m/(D^2 f)$, $L_n = l/D$. The equations and boundary conditions corresponding to eqs. (5a), (5b), (7), (8), (11a)–(11d), (12a)–(12d) would be

$$\partial/\partial F\,[Y_n/K_{mn}] + X_n/K_{mn} - \eta_x = \partial^2 Y_n/\partial Z_n^2 \tag{28a}$$

$$\partial/\partial F\,[X_n/K_{mn}] - Y_n/K_{mn} + \eta_y = \partial^2 X_n/\partial Z_n^2 \tag{28b}$$

$$K_{mn} = T_n^{1/2} L_n/\kappa \tag{29}$$

$$L_n = L_{n\infty} - (L_{n0})\,(T_n/T_{n0})^{p_n} \tag{30}$$

$$p_n = \kappa^4 T_{n0}^2/[Y_{n0}(L_{n\infty} - L_{n0})]$$

$$Z_n \to \infty: X_n \to \eta_x(\eta_x^2 + \eta_y^2)^{1/2} L_{n\infty}^2/\kappa \tag{31a}$$

$$Y_n \to \eta_y(\eta_x^2 + \eta_y^2)^{1/2} L_{n\infty}^2/\kappa \tag{31b}$$

$$K_{mn} \rightarrow (\eta_x^2 + \eta_y^2)^{1/2} L_{n\infty}^2/\kappa \tag{31c}$$

$$L_n \rightarrow L_{n\infty} \tag{31d}$$

$$Z_n = Z_{n0}: \quad (\partial X_n/\partial Z_n)_0 = 0 \tag{32a}$$

$$(\partial Y_n/\partial Z_n)_0 = -1/\kappa^3 \tag{32b}$$

$$K_{mn} = Z_{n0}\, C_g/\kappa^4 \tag{32c}$$

$$L_{n0} = \kappa Z_{n0} \tag{32d}$$

$$\eta_x = \kappa^2/f\, d\, \hat{\mathbf{v}}_g/dz \cdot (\hat{\mathbf{v}}_{g0})^0 \text{ and } \eta_y = \kappa^2/f\, d\, \hat{\mathbf{v}}_g/dz \cdot [\mathbf{k} \times (\hat{\mathbf{v}}_{g0})^0]$$

are the external parameters for the baroclinicity.

The equations are the same in both systems but the boundary conditions at $Z = Z_0$ differ remarkably. In the condition (32c) appears the geostrophic drag coefficient C_g which is not yet known but to obtain from the solution at $Z = Z_0$ itself, namely $X_{n0} = C_g^2 \cdot \cos(\alpha_0)/\kappa^8$ and $Y_{n0} = C_g^2 \sin(|\alpha_0|)/\kappa^8$. This can be overcome by applying an iterative method starting with the known value of C_g in the stationary case. If one compares the boundary conditions (12a), (12b) for the system non-dimensionalized by internal parameters with those (32a), (32b) for the system non-dimensionalized by external parameters, one notices that in the former system the variables itself are given at the boundary but in the latter system the derivatives in the normal direction. An attempt of the numerical integration of this extended Neumann problem did fail, since the convergence was extremely slow. That was the reason to use the former system, in which the variation with time of the scaling parameters was taken into consideration iteratively.

III. Discretization and integration procedure

The vertical coordinate Z is transformed into ξ by $\xi = \log_{10}(Z)$. Using finite differences the increment be $\Delta\xi$ and the integer k running from $k = 0$ at $\xi = \xi_0$ up to k^* at an artificial upper boundary ξ^* which is high enough to have no influence on the PBL. The time increment be ΔF, the integer r. The method for solving the set of equations (5a), (5b), (7), (8) is the same as presented by WIPPERMANN (1971b) for the stationary case but now extended to non-stationarity by incorporating a backward directed finite difference with time. The equations for the iterative procedure are

$$\overset{(p+1)}{\overset{(s+1)}{Y_{k,r}}} = \frac{2 + \overset{(p)}{\Gamma_{k,r}}/\Delta F}{(2 + \overset{(p)}{\Gamma_{k,r}}/\Delta F)^2 + \overset{(p)}{\Gamma_{k,r}}} \left\{ c_1 \overset{(p+1)}{\overset{(s)}{Y_{k+1,r}}} + c_2 \overset{(p+1)}{\overset{(s)}{Y_{k-1,r}}} - \right. \tag{33a}$$

$$\left. - c_1 \overset{(p)}{G_{k,r}} \overset{(p+1)}{\overset{(s)}{X_{k+1,r}}} - c_2 \overset{(p)}{G_{k,r}} \overset{(p+1)}{\overset{(s)}{X_{k-1,r}}} + A_{k,r-1} - \overset{(p)}{G_{k,r}} B_{k,r-1} \right\}$$

$$\overset{(p+1)}{\overset{(s+1)}{X_{k,r}}} = \frac{2 + \overset{(p)}{\Gamma_{k,r}}/\Delta F}{(2 + \overset{(p)}{\Gamma_{k,r}}/\Delta F)^2 + \overset{(p)}{\Gamma_{k,r}}} \left\{ c_1 \overset{(p+1)}{\overset{(s)}{X_{k+1,r}}} + c_2 \overset{(p+1)}{\overset{(s)}{X_{k-1,r}}} + \right. \tag{33b}$$

$$\left. + c_1 \overset{(p)}{G_{k,r}} \overset{(p+1)}{\overset{(s)}{Y_{k+1,r}}} + c_2 \overset{(p)}{G_{k,r}} \overset{(p+1)}{\overset{(s)}{Y_{k-1,r}}} + B_{k,r-1} + \overset{(p)}{G_{k,r}} A_{k,r-1} \right\}$$

$$\overset{(p)}{\Gamma}_{k,r} = 10^{2\xi}(\Delta\xi)^2/a^2\ 1/(\overset{(p)}{K_m})_{k,r} \qquad a = 0.4343 \tag{33c}$$

$$A_{k,r-1} = \Gamma_{k,r-1}\,[Y_{k,r-1}/\Delta F + (K_m)_{k,r-1}\,\eta_x] \tag{33d}$$

$$B_{k,r-1} = \Gamma_{k,r-1}\,[X_{k,r-1}/\Delta F - (K_m)_{k,r-1}\,\eta_y] \tag{33e}$$

$$\overset{(p)}{G}_{k,r} = \overset{(p)}{\Gamma}_{k,r}/(2 + \overset{(p)}{\Gamma}_{k,r}/\Delta F) \tag{33f}$$

$$c_1 = 1 - \Delta\xi/(2a) \qquad c_2 = 1 + \Delta\xi/(2a) \tag{33g}$$

There are two iterations p and s running into one another. $(K_m)_{k,r}$ is formed by eq. (7) and (8) with the values $\overset{(p)}{X}_{k,r}$ and $\overset{(p)}{Y}_{k,r}$, it is kept constant during the s-iteration is carried out. (Using a single step relaxation procedure for the $X_{k+1,r}$ and $Y_{k+1,r}$ above the point k under consideration the (s + 1)th iteration may be used already by going downward or for the $X_{k-1,r}$ and $Y_{k-1,r}$ below the point under consideration by going upward respectively). After s* iterations a new $(K_m)_{k,r}$ should be formed with the values $\overset{(p+1)}{\underset{(s^*)}{X}}$ and $\overset{(p+1)}{\underset{(s^*)}{Y}}$ obtained then and the cycle of the s-iterations should be repeated.

The values $X_{k,r-1}$, $Y_{k,r-1}$ and $(K_m)_{k,r-1}$, the last one appearing in $\Gamma_{k,r-1}$, are the final values obtained at the time (r − 1), they remain constant during the whole iteration procedures. However they can be used in the eq. (33) only after having been corrected for the different scaling used at the time r. That means the vertical coordinate at the time (r − 1) has to be scaled by the same internal height H as at the time r

$$(Z_{k,r-1})_{corr} = Z_{k,r-1}\,(C_g)_{r-1}/(C_g)_r \tag{34}$$

where $(C_g)_{r-1}$ is known and $(C_g)_r$ can be determined allways after finishing the s-iteration cycle by

$$(\partial X/\partial Z)_{0,r} = -\kappa\,\sin(|\alpha_0|)/(C_g)_r \tag{35a}$$

$$(\partial Y/\partial Z)_{0,r} = -\kappa\,\cos(\alpha_0)/(C_g)_r \tag{35b}$$

It means also that the coordinate system at time (r − 1) has to be turned into the orientation of the coordinate system at the time r, which can be done with the known cross-isobar angle $(\alpha_0)_{r-1}$ and with the angle $(\alpha_0)_r$ obtained from the eqs. (35a), (35b). It means finally that the variables have to be scaled at the time (r − 1) by the scaling parameters used at the time r

$$(X_{k,r-1})_{corr} = X_{k,r-1}\,(C_g^2)_{r-1}/(C_g^2)_r \tag{36a}$$

$$(Y_{k,r-1})_{corr} = Y_{k,r-1}\,(C_g^2)_{r-1}/(C_g^2)_r \tag{36b}$$

$$(K_m)_{k,r-1;corr} = (K_m)_{k,r-1}\,(C_g^2)_{r-1}/(C_g^2)_r \tag{36c}$$

$$(P_{r-1})_{corr} = P_{r-1}\,(C_g)_{r-1}/(C_g)_r \tag{36d}$$

$$(Q_{r-1})_{corr} = Q_{r-1}\,(C_g)_{r-1}/(C_g)_r \tag{36e}$$

These three steps (stretching or shrinking of the vertical coordinate, turning the coordinate system, correcting the variables) have to be done each times when the s-iteration is finished with s* and before the new K_m-value is formed. After each s-iteration namely the value of C_g and α_0 has slightly changed and therefore a new scaling has to be done.

The same three steps have to be made when the computations are finished for all times. In order to make the results for different times comparable with each other they must be scaled by the same scaling parameter. For this purpose the scale height H_* and the crossisobar angle α_{0*} are chosen, which are obtained in the stationary, barotropic and neutral case (for the same surface Rossby number). The corrections are the same as in eqs. (34), (36a)–(36e) but instead $(C_g)_r$ now C_{g*} is to use. Also the coordinate system must be orientated with the angly α_{0*} at all times. The chosen values are

$$C_{g*} = 0.0324, \quad \alpha_{0*} = 22.2^0 \tag{37}$$

The final variables are $X_*(Z_*, F)$, $Y_*(Z_*, F)$, $K_{m*}(Z_*, F)$, $L_*(Z_*, F)$, $P_*(Z_*, F)$, $Q_*(Z_*, F)$, where the star denotes that for the non-dimensionalization the scale height H_* has been used. Since $Z_* = ZH/H_* = ZC_g/C_{g*}$ and $Z_n = ZH/D = ZC_g/\kappa^4$ one would have chosen best for C_{g*} the value $\kappa^4 = 0.0256$; in the way C_{g*} is chosen (eq. 37) one has $Z_* = 0.790\,Z_n$.

Since the integrations have been carried out with a constant (non-dimensional) roughness-length $Z_0 = 1 \cdot 10^{-5}$ the real roughness-length z_0 varies with time as the scaling parameter H varies with time; the error involved hereby is small, it should be considered later when the results of the integrations will be discussed.

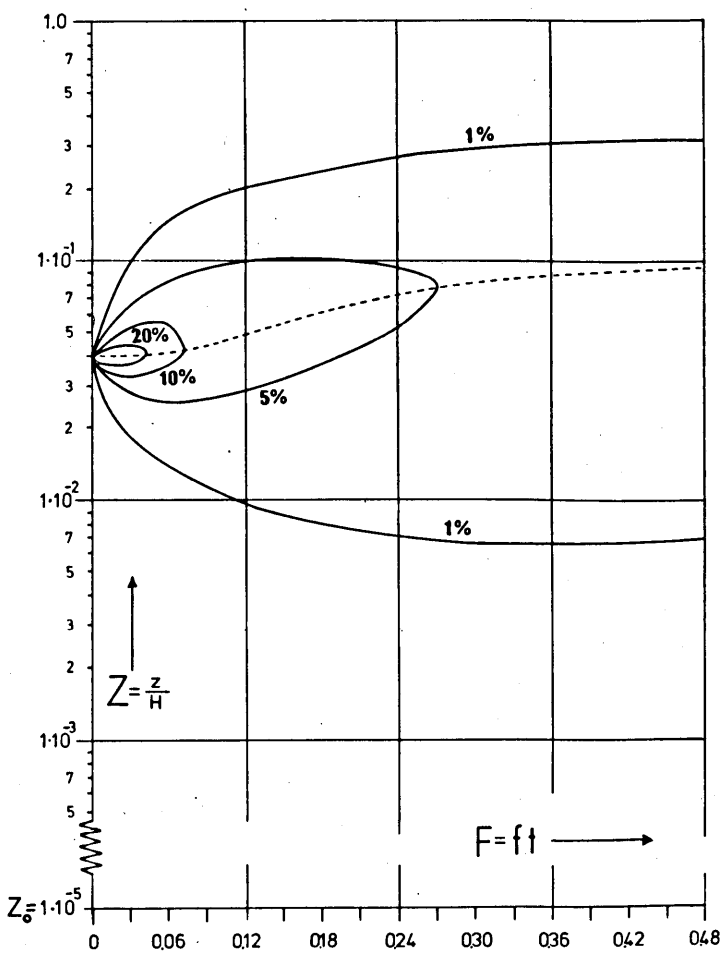

- **Figure 1**
  The decrease with time of the influence of a single point perturbation in the Reynolds stress T at Z = 0.04 in a barotropic and neutral PBL

- **Bild 1**
  Die Abnahme des Einflusses einer punktförmigen Störung der Reynolds'schen Schubspannung T bei Z = 0.04 in einer barotropen und neutralen PBL

Likewise the turbulent heat flux q_0 varies with time, it is used to non-dimensionalize the potential temperature. Therefore it is necessary to scale all potential temperatures with the same heat flux q_{0*} which is chosen to be

$$q_{0*} = +\ 1.0 \text{ mcal cm}^{-2} \text{ sec}^{-1} \tag{38}$$

The formula (22) reads then

$$\hat{\Theta}_*(Z_*, F) = \hat{\Theta}_*(Z_{*T}) + q_0/q_{0*} \int_{Z_*}^{Z_{*T}} \phi_h/\phi_m \, T_*/K_{m*} \, dZ'_* \tag{39}$$

IV. The response of the PBL to perturbations due to non-stationarity

In the first place the response of the PBL should be investigated to a single point perturbation in the Reynolds stress. For a barotropic and neutral PBL (i.e. steady state) the Reynolds' stress T has been increased at the height of the "point source" by 3 % of its original value. Then the model described

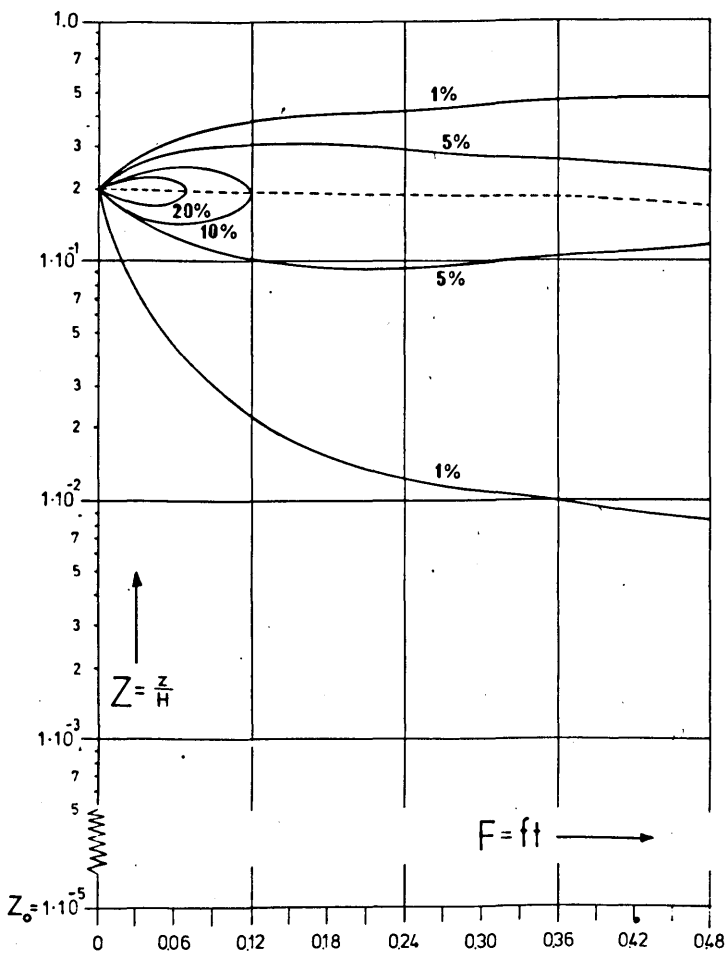

- **Figure 2**
  Same as in fig. 1, except Z = 0.20

- **Bild 2**
  Wie Bild 1, jedoch Z = 0.20

in section II and III was applied and the influence of the perturbation on the T-profiles at later times was studied. Two examples for the results are shown in figure 1 and 2. In the first case (Figure 1) the single point perturbation was located at Z = 0.04, in the second case (Figure 2) at Z = 0.2 which corresponds very roughly to 200 m. The K_m-profile is the same in both cases, the maximum of K_m appears at Z = 0.09. One notices that the dispersion of the perturbation is not symmetric in the vertical; the effect of the perturbation is more remarkable in the direction towards the maximum of K_m. It can also be seen, that the influence of the single point perturbation decreases very rapidly with time; it is less than 5 % after F = 0.26 (43 min for $f = 1 \cdot 10^{-4}\ sec^{-1}$) in case 1 and after F > 0.5 (corresponding to 83 min for $f = 1 \cdot 10^{-4}\ sec^{-1}$) in the case 2.

The results obtained for cases with stable stratification show that the influence of the single point perturbation remains more concentrated in the height of the source; in cases with unstable stratification the vertical dispersion of this influence is larger than in the neutral case.

The influence of an initially disturbed T-profile shows a much slower decrease with time as the influence of a single point perturbation. The result of such a computation is given in figure 3. As the initially perturbated T-profile it has been chosen that one which occurs during a diurnal variation

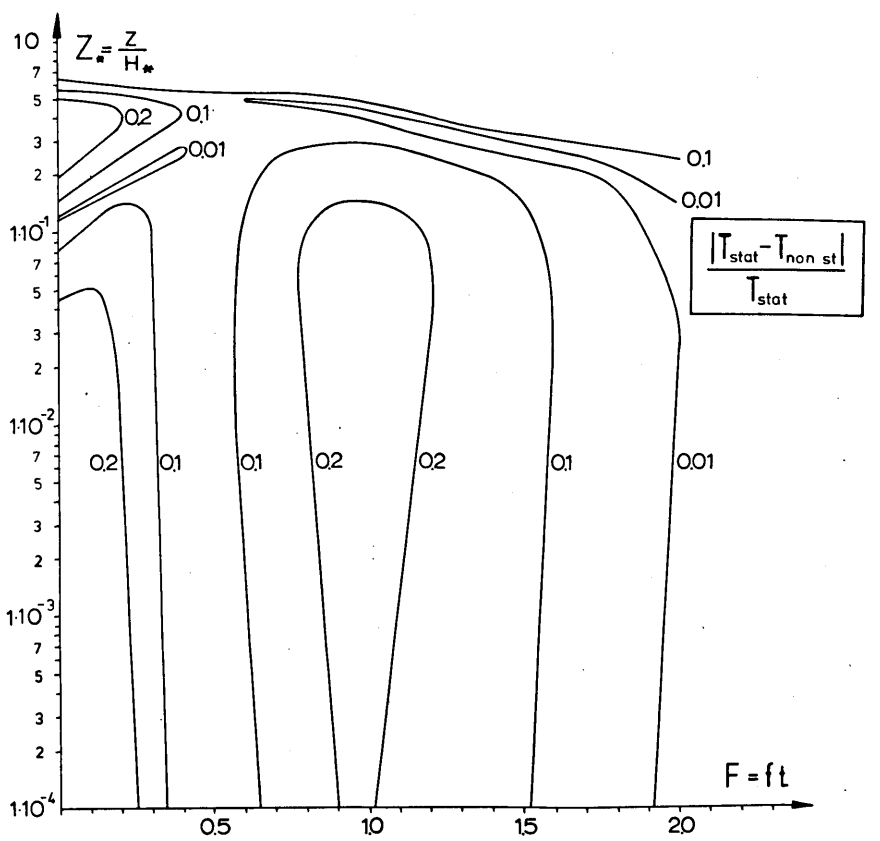

- **Figure 3.** The decrease with time of the influence of a initially disturbed T-profile in a barotropic and neutral PBL
- **Bild 3.** Das Abklingen des Einflusses eines anfänglich gestörten T-Profiles mit der Zeit in einer barotropen und neutralen PBL

(described in section V) at the time when the stratification is neutral. With that the profiles $T_{nonst}(Z)$ at later times have been computed under the condition, that the stratification remains neutral. It is studied how these profiles $T_{nonst}(Z)$ approach the profile $T_{st}(Z)$ which belongs to the corresponding barotropic and neutral PBL, see WIPPERMANN (1972). Fig. 3 shows the decrease with time of the influence of the initial perturbation; one notices that this influence is less than 5 % after F = 1.8 (corresponding to 5 hrs for $f = 1 \cdot 10^{-4}\ sec^{-1}$). This is considerably longer than in the case of a single point perturbation.

For the purpose of a parameterization of PBL-effects one is very interested to know how long it takes (for an initially disturbed T-profile) until the values of C_g and α_0 approach those of the stationary case. Computations as those described before (Fig. 3) have been carried out for different thermal stratifications: the T-profiles obtained during the diurnal variation at 06^{00}, 09^{00}, 18^{00} and 21^{00} are used as initially disturbed profiles, the integrations with time are carried out keeping the thermal stratification constant with time. Figure 4 shows these four cases. The dashed line gives the values of C_g and α_0 during the diurnal variation, the solid lines starting at 06^{00}, 09^{00}, 18^{00} and 21^{00} give the values during the approach to the corresponding stationary cases marked by double circles. It takes the longest time

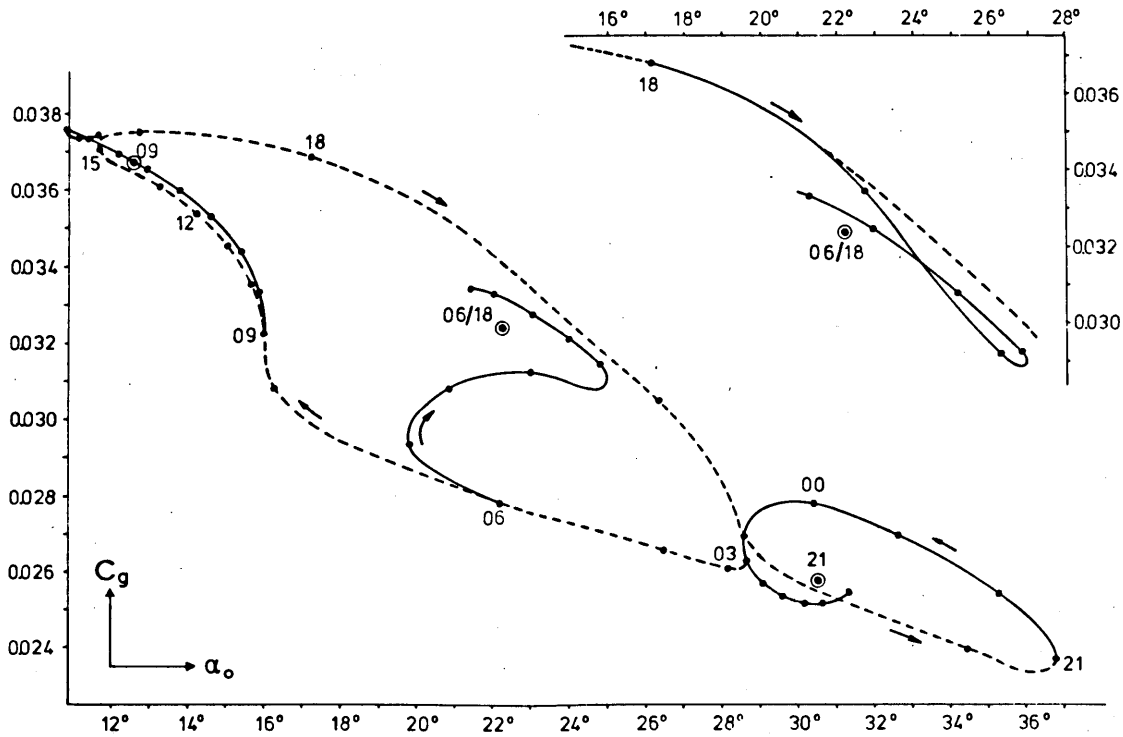

- **Figure 4.** Dashed line: Values of C_g and α_0 for a given diurnal variation of the thermal stratification. The numbers give the time of the day, the time between two dots is always 1 hr. Solid lines: values of C_g and α_0 for the thermal stratification kept constant; the values approach those in the stationary case marked by double circles.

- **Bild 4.** Punktierte Kurve: Werte von C_g und α_0 für einen vorgegebenen Tagesgang der thermischen Schichtung. Die Zahlen geben die Uhrzeit; zwischen zwei Punkten liegt eine Stunde. Ausgezogene Kurven: Werte von C_g und α_0 für den Fall, daß die thermische Schichtung konstant gehalten wird. Die Werte nähern sich denjenigen des stationären Falles, welche durch einen Doppelkreis gekennzeichnet sind.

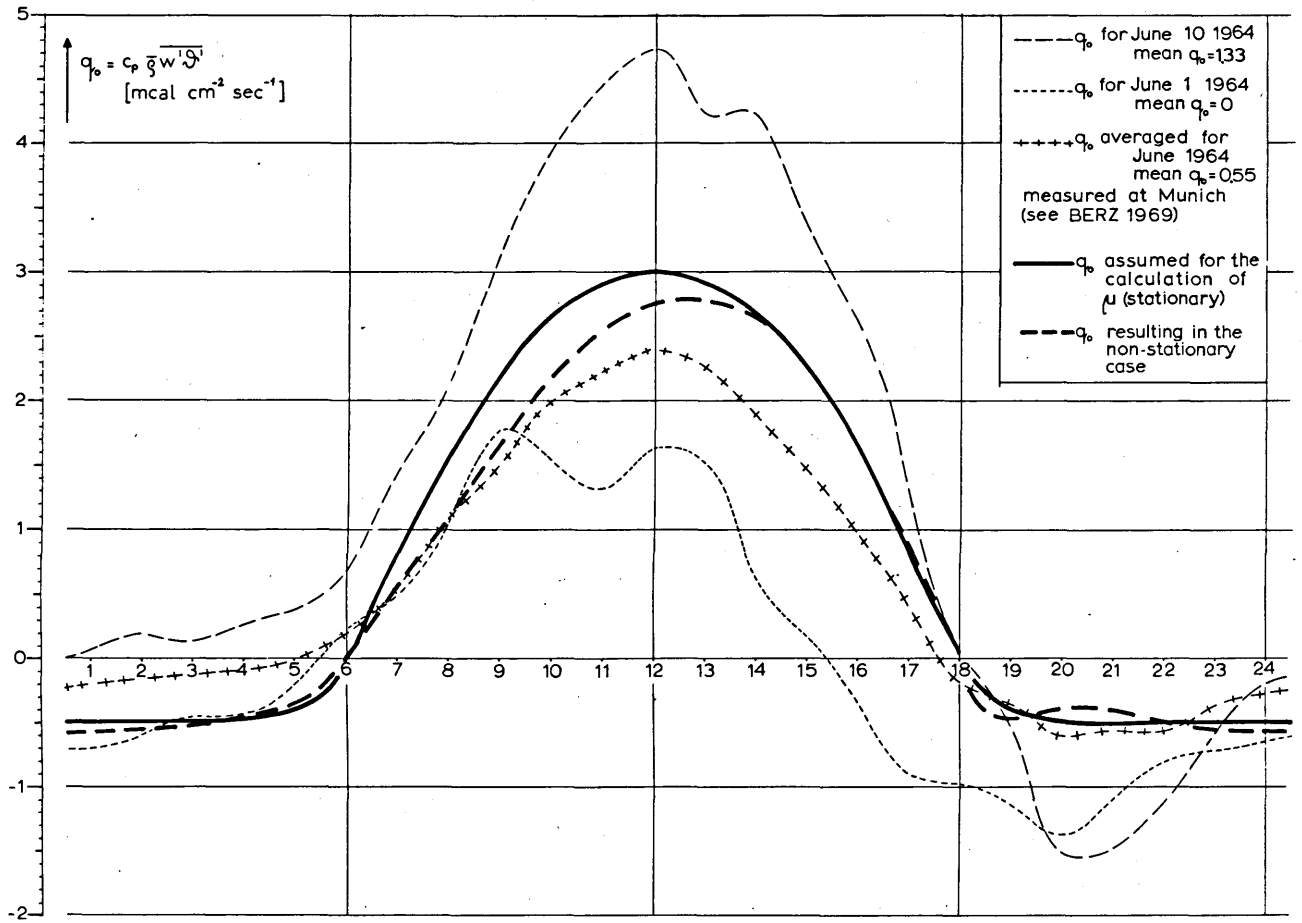

- **Figure 5.** The assumed diurnal variation of the turbulent heat flux q_0 compared with measurements.
- **Bild 5.** Der vorgegebene Tagesgang des turbulenten Wärmestromes am Boden verglichen mit Meßergebnissen.

to approach the value of the stationary case during the night (constant stable stratification also in the diurnal variation 21^{00}–03^{00}); even after 12 hrs the value of the stationary case is not yet reached. The shortest time for the approach is needed after 09^{00} when the stratification is unstable; already after 5 1/2 hrs the stationary value is reached, after that an overshooting occurs. The two cases 06^{00} and 18^{00} are those with the neutral stratification.

V. An example of the diurnal variation of the boundary layer

In order to simulate the diurnal variation of the PBL it is necessary to make assumptions for the diurnal variation of the thermal stratification represented by the internal parameter μ or the equivalent L_∞. However it is easier to make assumptions for the turbulent heat flux q_0 at the ground, because many measurements of that are available. The assumed diurnal variation of q_0 can be seen in figure 5 (solid line); it is symmetric to 12^{00} and it remains constant during the night for 6 hours. A comparison of the assumed diurnal variation with measurements by BERZ (1969) near Munich shows that the assumed variation is quite realistic.

The definition of μ following eq. (9) can be written also

$$\mu = -q_0/(b\,C_g^2) \tag{40}$$

where b is an abbreviation for

$$b = c_p\,\bar{\rho}\,f\,|\hat{v}_{g0}|^2/(\kappa^2\beta)$$

$\beta = g/\tilde{\vartheta}$ is a local parameter with g the acceleration of gravity and $\tilde{\vartheta}$ a reference temperature. With $f = 1.1 \cdot 10^{-4}\ \mathrm{sec}^{-1}$, $\bar{\rho} = 1.2\ 10^{-3}\ \mathrm{g\,cm}^{-3}$, $c_p = 0.24$ and $\beta = 3.5$ one gets $b = 0.566\ 10^{-7} \cdot |\hat{v}_{g0}|^2$ cal cm^{-4} sec, or assuming $|\hat{v}_{g0}| = 10$ m/s one gets $b = 56.6$ mcal $\mathrm{cm}^{-2}\ \mathrm{sec}^{-1}$. Using the assumed values of q_0, the forementioned value of b and the values of C_g as obtained in the stationary case the values of μ have been computed with the aid of eq. (40). They are listed in table 1

Table 1 / Tabelle 1

Time of the day	00 / 24	01 / 23	02 / 22	03 / 21	04 / 20	05 / 19	06 / 18	07 / 17	08 / 16	09 / 15	10 / 14	11 / 13	12
q_0 mcal $\mathrm{cm}^{-2}\,\mathrm{s}^{-1}$	-0.50	-0.50	-0.50	-0.50	-0.48	-0.40	0	+0.80	+1.56	+2.22	+2.66	+2.89	+3.00
μ	13.4	13.4	13.4	13.4	12.4	9.0	0	-11.0	-20.6	-29.1	-34.7	-37.7	-39.1
L_∞	0.0044	0.0044	0.0044	0.0044	0.0048	0.0062	0.014	0.043	0.106	0.237	0.405	0.535	0.605

The last row in table 1 gives the variation of L_∞, it is obtained from the values of μ using the relationship (9). L_∞ is the parameter which is actually needed in eq. (8).

Since the C_g-values obtained during the diurnal variation differ from those in the corresponding stationary case, a final q_0 results from eq. (40), which is no longer symmetric to 12^{00}. Also this q_0 is shown in figure 5.

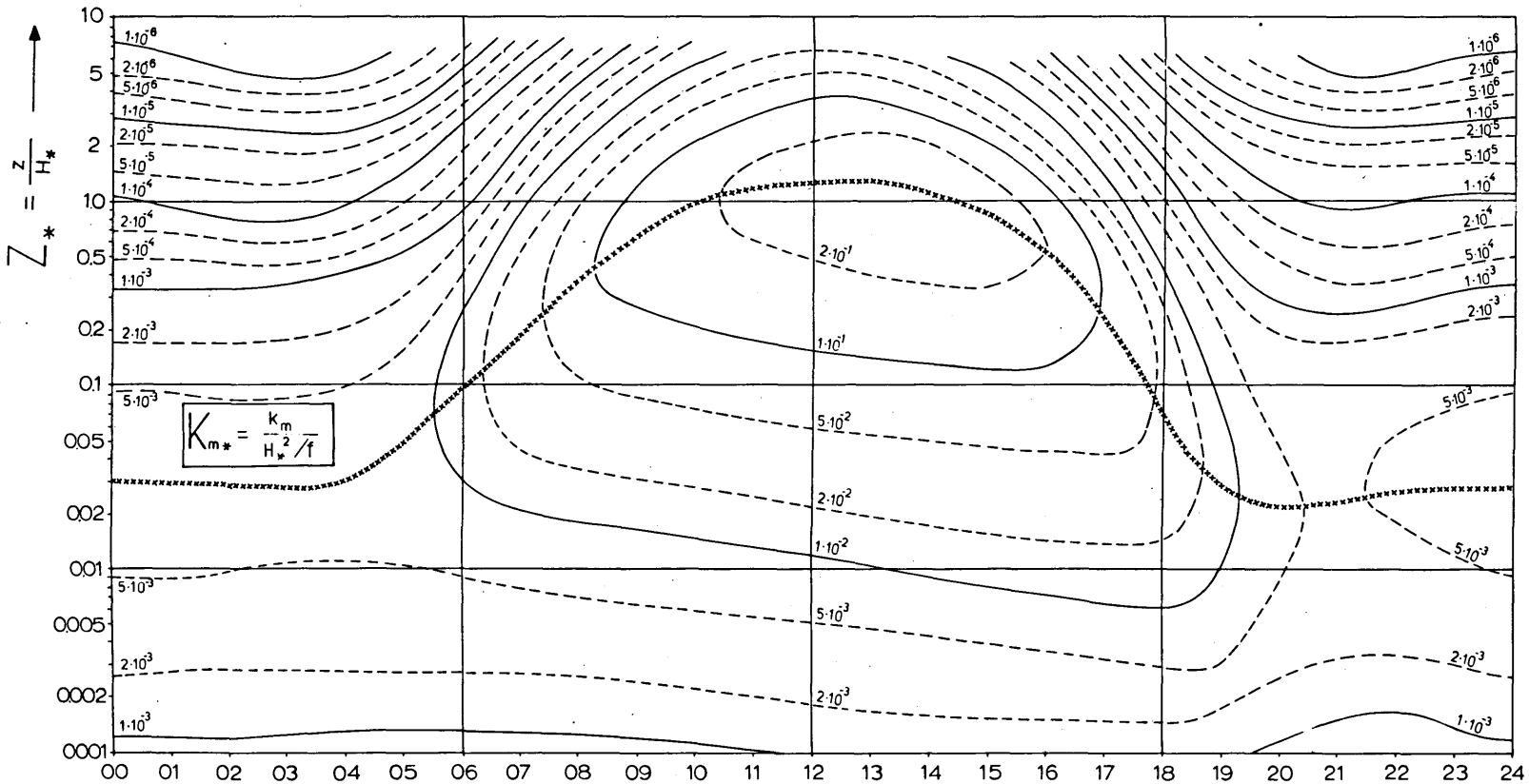

- **Figure 6.** Isopleths of the non-dimensional eddy viscosity K_{m*}. The heavy line indicates the position of the maximum

- **Bild 6.** Isoplethen des dimensionslosen turbulenten Diffusionskoeffizienten K_{m*}. Die hervorgehobene Linie gibt die jeweilige Lage des Maximums an.

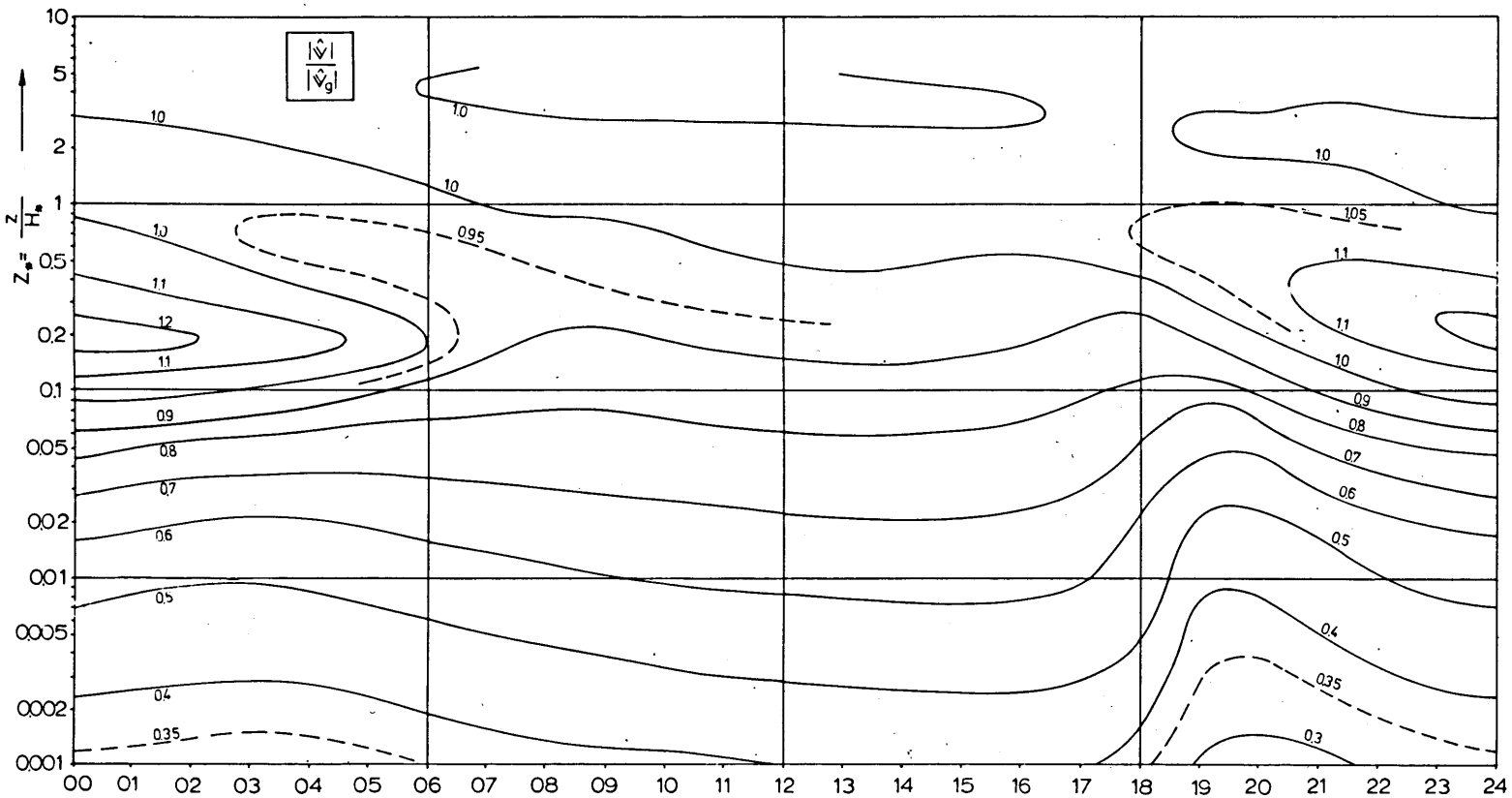

- **Figure 7.** Isopleths of the non-dimensional magnitude of the horizontal wind $|\hat{v}|/|\hat{v}_{g0}|$
- **Bild 7.** Isoplethen des dimensionslosen Betrages des Horizontalwindes $|\hat{v}|/|\hat{v}_{g0}|$

With the values of L_∞ listed in table 1 the system of eqs. (5a), (5b), (7), (8) has been solved 48 times during the day; the time interval of 30 min was chosen to $\Delta F = 0.2$, which is correct for $f = 1.11\ 10^{-4}\ sec^{-1}$. The 48 integrations during the day have been repeated three times (with the same assumption for the diurnal variation of the thermal stratification) in order to become uneffected by the arbitrary initial conditions at the time 00^{00} of the first day. It came out that the results of the second and of the third day had only very small and negligible differences. – All integrations have been carried out for the barotropic case ($\lambda_x = \lambda_y = 0$); the roughness-length was chosen $Z_0 = 1 \cdot 10^{-5}$. Some of the results are shown in the figures 6–10.

In figure 6 isopleths are plotted which show the variation of $K_{m*}(Z_*, t)$. The maximum in the vertical is located during the night at about $Z_* = 0.03$ and it is shifted at noontime to more than $Z_* = 1.0$ (which very roughly corresponds to 1 000 m). This does not agree with the result obtained by LYKOSOV (1972), who found the maximum at about 200 m also at noontime. – In spite of the symmetrical (to 12^{00}) input of the thermal stratification the distribution of $K_{m*}(Z_*)$ during the day is remarkably unsymmetric; this must be interpreted as an effect of the non-stationarity. For instance the maximum occurs about 1 1/2 hrs later than the most unstable stratification.

The magnitude of the horizontal wind $|\hat{v}|/|\hat{v}_{g0}|$ is displayed in figure 7. It shows the expected variation: the wind close to the ground increases during the day and has its maximum in the afternoon. In the evening hours a pronounced minimum occurs reaching upward to more than $Z_* = 0.1$; however at $Z_* = 0.2$ this minimum occurs 2–3 hours earlier. At 21^{00} starts the formation of a wind maximum at about $Z_* = 0.2$ (very roughly corresponding to 200 m) lasting until about 04^{00}. This maximum may be

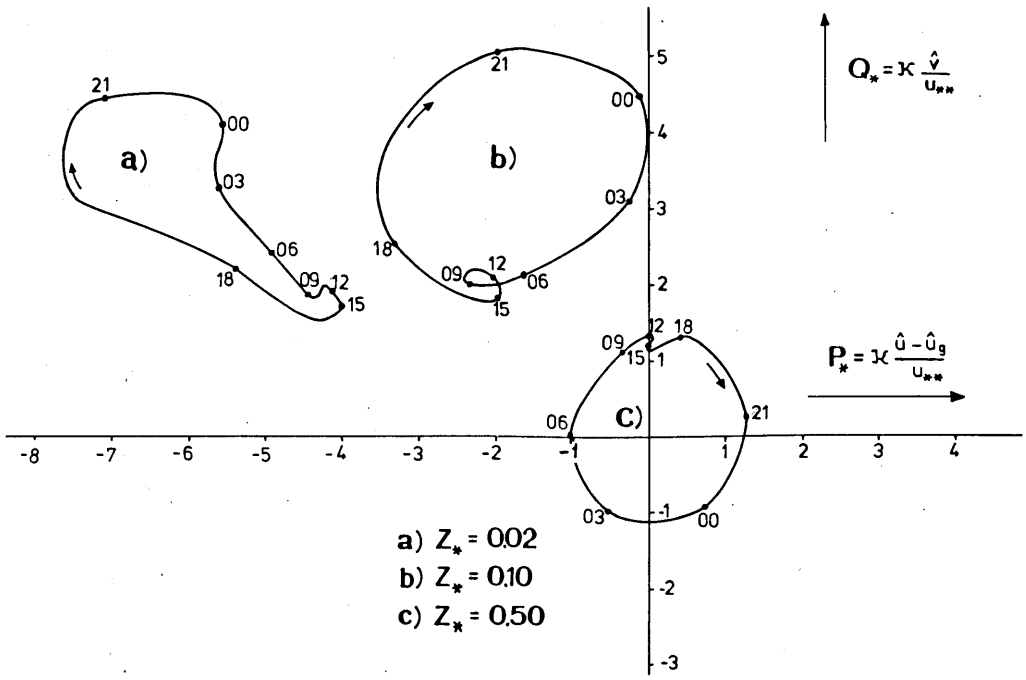

- **Figure 8.** Hodographs of the horizontal wind at three different heights. The numbers give the time of the day. (For the location of the geostrophic wind vector in this diagram see section V).

- **Bild 8.** Hodographenkurven für den Horizontalwind in drei verschiedenen Höhen; die Zahlen geben die Tageszeit an. (Zur Lage des Vektors des geostrophischen Windes in diesem Diagramm siehe Abschnitt V im Text).

explained as a low level jet. The field of isopleths is qualitatively the same as obtained by KUROSAKI (1970), who closed the system of equations with another mixing-length hypothesis; he also obtained a pronounced minimum of the wind close to the ground in the late afternoon. During the night the wind exceeds in the maximum the geostrophic wind by 16 % according to his results and by 22 % in our computations.

In figure 8 resulting hodograph curves are shown at three different heights. In this diagram the geostrophic wind vector $\hat{\mathbf{v}}_{g0}$ has the direction of the P_*-axis, it ends in the origin of the coordinate system and the point, where it begins on the negative P_*-axis, depends on C_g; the dimensionless geostrophic wind is namely $\kappa \mid \hat{\mathbf{v}}_{g0} \mid / u_* = \kappa / C_g$, for example with $C_g = C_{g*} = 0.0324$ according to (37) the vector of the non-dimensional geostrophic wind starts at $P_* = -12.3$, $Q_* = 0$. The results are in fairly good agreement with those by LYKOSOV (1972).

In figure 9 the vertical profiles of the potential temperature $\hat{\Theta}_*$ are shown as computed by eq. (22). Even in these non-stationary cases the potential temperature $\hat{\Theta}_*$ decreases (in unstable conditions) and increases (in stable conditions) monotonically with heigt to the temperature above the boundary layer; this is like the variation in a (stationary) PBL without radiative effects. It is one of the results of these computations, that the formation of temperature inversions is impossible in the used model even

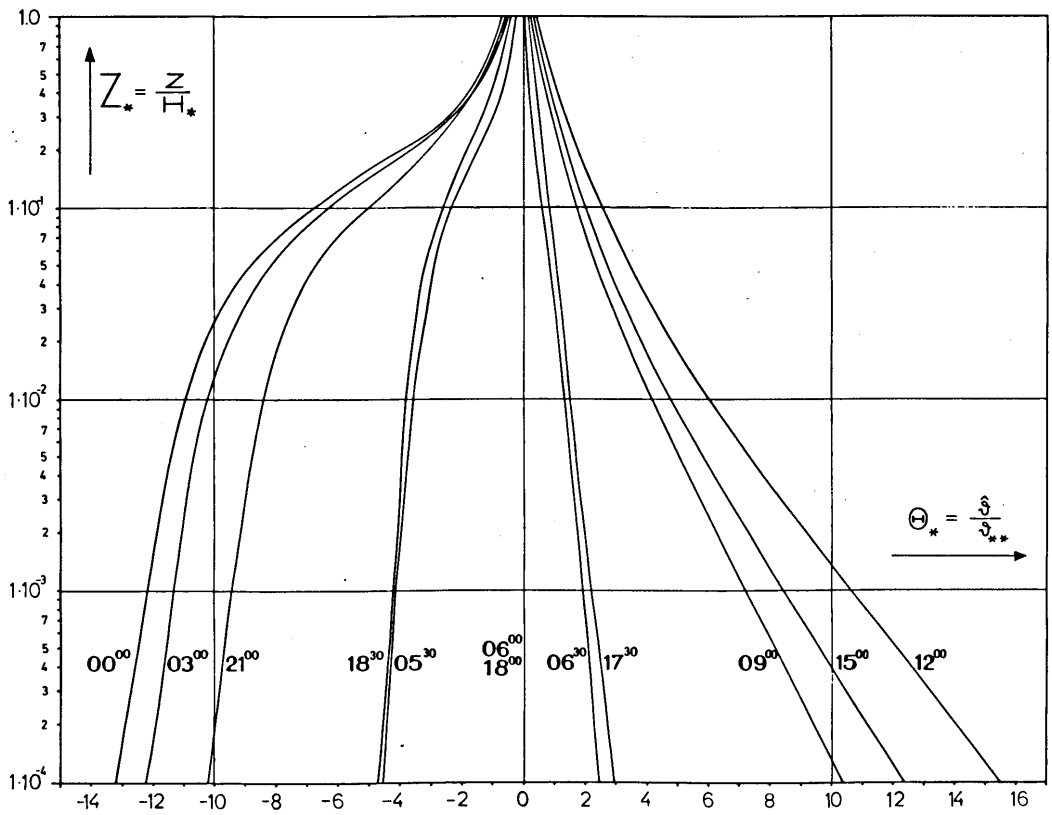

● **Figure 9.** Vertical profiles of the non-dimensional potential temperature $\hat{\Theta}_*$ at various times.

● **Bild 9.** Vertikalprofile der dimensionslosen potentiellen Temperatur $\hat{\Theta}_*$ zu verschiedenen Tageszeiten.

in the non-stationary case (without radiative effects). The profiles show an asymmetric behaviour in stable and unstable conditions, in the latter the deviation from the temperature above the boundary layer is concentrated more in the layers close to the ground. The effect of non-stationarity can be seen by comparing the profiles of 21^{00}, 00^{00} and 03^{00} which all have the same thermal stratification ($\mu = 13.4$); also the profiles at 09^{00} and 15^{00} can be compared which both belong to the unstable stratification $\mu = -29.1$.

In figure 10 the vertical profiles of the ratio k_h/k_m are shown for 00^{00}, 06^{00}, 12^{00}, 18^{00}. They have been computed by eq. (21) using for q/q_0 the eq. (27). An evaluation of the eq. (27) has shown, that the ratio q/q_0 remains almost constant with height similar to the case of the (stationary) PBL. The

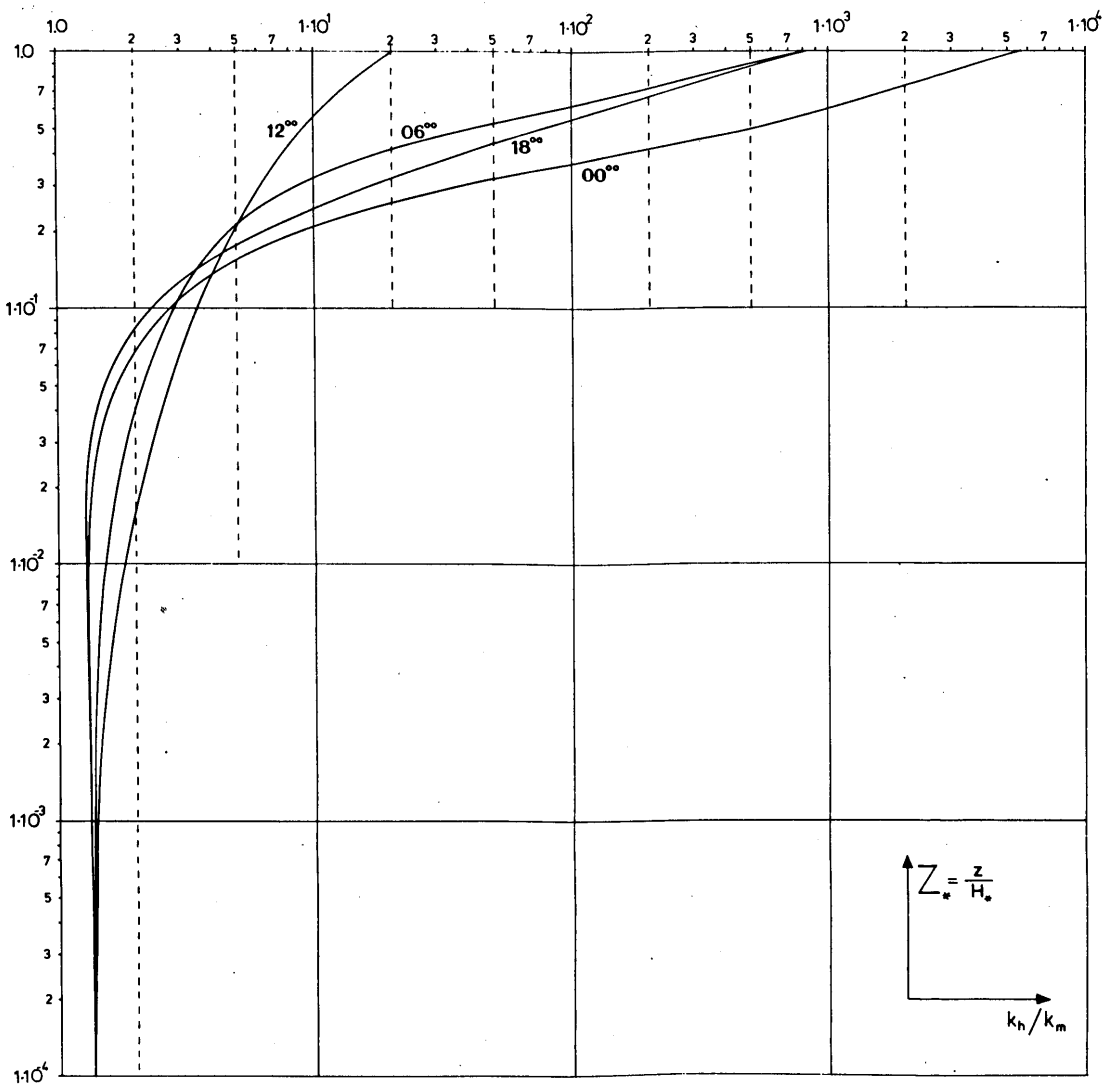

- **Figure 10.** Vertical profiles of k_h/k_m at various times.

- **Bild 10.** Vertikalprofile des Verhältnisses k_h/k_m zu verschiedenen Tageszeiten.

effect of non-stationarity changes this ratio for less than 2 %. This causes an increase of k_h/k_m with height as k_m decreases with height. – Close to the ground $k_h/k_m = 1.35$ according to eq. (25).

Few words should be said about z_0 in all these computations. As mentioned already earlier the lower boundary was fixed at $Z_0 = 1 \cdot 10^{-5}$ which means that z_0 varies during the day since the scaling height H varies with time. It is $Z_{*0} = Z_0 C_{g*}/C_g$ which varies between $0.87 \cdot 10^{-5}$ (at 17^{00}) and $1.38\ 10^{-5}$ (at 20^{30}). For $H_* = 1000$ m (which would occur for $|\hat{w}_{g0}| = 7.7$ m sec^{-7}, $f = 1 \cdot 10^{-4}$ sec^{-1}) one would have a variation of z_0 during the day between 0.9 cm and 1.4 cm. This is an error caused by the use of the equations non-dimensionalized by internal parameters.

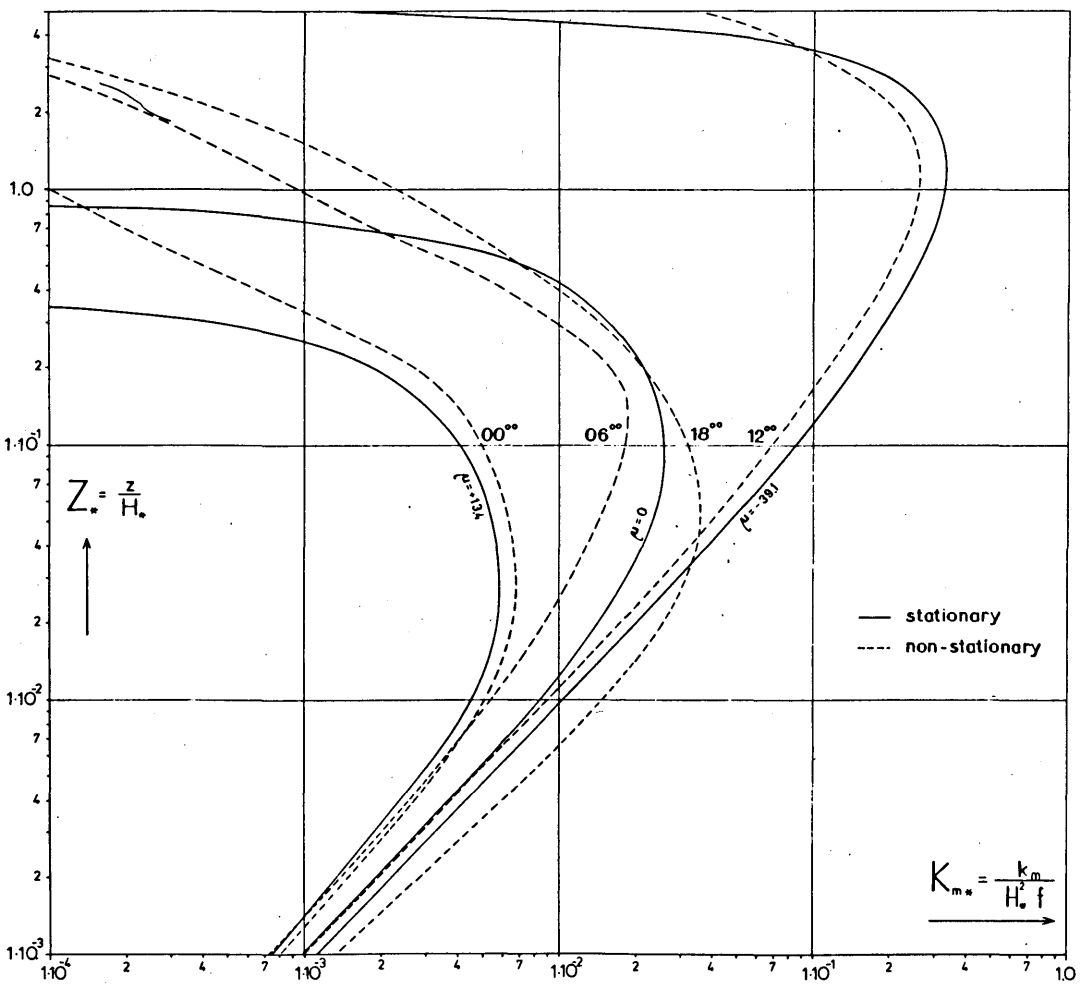

- **Figure 11.** Vertical profiles of K_{m*} at various times compared with the profiles of the corresponding stationary cases

- **Bild 11.** Vertikalprofile von K_{m*} zu verschiedenen Tageszeiten verglichen mit den Profilen für die entsprechenden stationären Fälle.

VI. A comparison between corresponding non-stationary and stationary cases

As mentioned in the introduction boundary layer effects can be parameterized by applying the so-called resistance law of a PBL. This means a variation with time of the boundary layer has to be understood as a sequence of stationary cases with different thermal stratification. For a justification of that one should know the differences of corresponding non-stationary and stationary cases. They can be studied by comparing the results for a diurnal variation described in section V with those obtained for the stationary cases.

Such a comparison for the K_{m*}-profiles is presented in figure 11. At 12^{00} K_{m*} is smaller (factor 0.8 in the maximum) as in the corresponding stationary case but at midnight it is larger (factor 1.17 in the maximum). At 06^{00} and 18^{00} one has neutral stratification ($\mu = 0$). Because of the retardation the non-stationary profile at 06^{00} are smaller than those of the corresponding stationary profile, at 18^{00} they are larger. Also the maximum for 06^{00} is located at $Z_* = 0.14$, for 18^{00} at $Z_* = 0.05$ but in the stationary case at $Z_* = 0.09$.

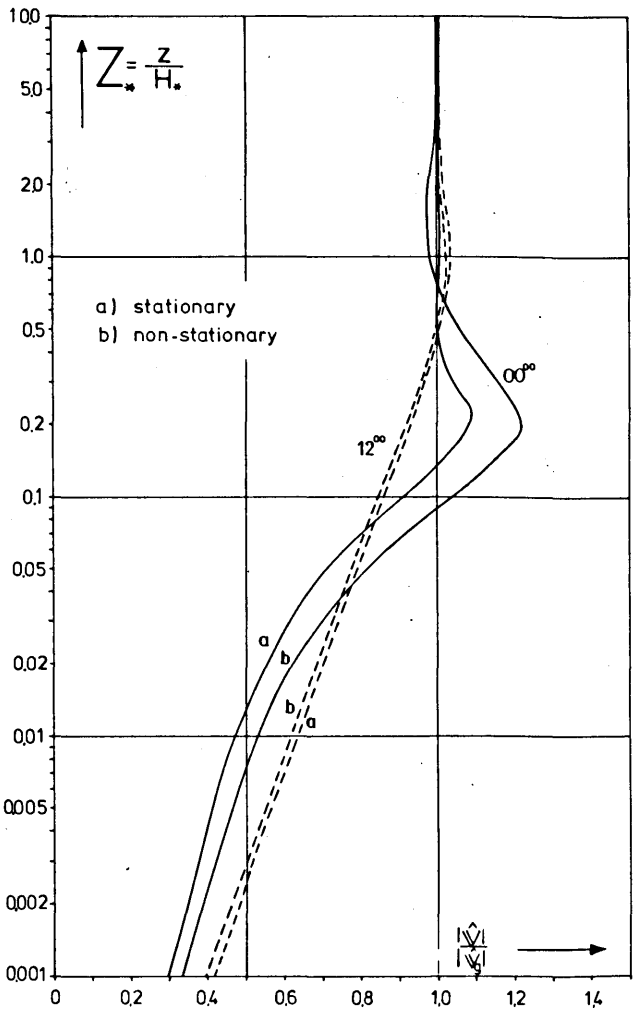

- **Figure 12**
  Vertical profiles of $|\hat{w}|/|\hat{w}_{g0}|$ at 00^{00} and 12^{00} compared with the profiles of the corresponding stationary cases.

- **Bild 12**
  Vertikalprofile von $|\hat{w}|/|\hat{w}_{g0}|$ für 00^{00} und 12^{00} verglichen mit den Profilen für die entsprechenden stationären Fälle.

Another comparison has been made for the non-dimensional horizontal wind $|\hat{v}|/|\hat{v}_{g0}|$. Figure 12 shows the profiles for 00^{00} and 12^{00} compared with the profiles in the corresponding stationary cases. During the night (stable stratification) a remarkable difference occurs: the maximum overshooting of the geostrophic wind is 9 % in the stationary case but 22 % in the non-stationary one. This may be an important result for the theory of the low level jet. At noontime the differences are very small probably due to the larger vertical mixing (unstable stratification).

The most important parameters in a parameterization procedure are C_g and α_0; these are plotted in the figures 13 and 14. In both figures a comparison is possible with the values of the corresponding stationary cases. The deviations are smaller for α_0 than for C_g. The maximum difference $|\alpha_{0,nonst} - \alpha_{0,st}|$ is about 15 % (daytime) and 23 % (night-time) of the total range in which α_0 varies; for C_g the maximum difference is 46 % during the day and 16 % in the night. Similar results can be found in the book by ZILITENKEVICH (1970), figure 2.35. The range in which α_0 varies is $11^0 - 37^0$ according to our results but $5^0 - 24^0$ in ZILITINKEVICH's figure. The range of variation of C_g is 0.025 – 0.037 and 0.024 – 0.038 respectively. The difference of the curves during the nighttime may be explained by the assumption that the thermal stratification remains constant from $21^{00} - 03^{00}$ whereas ZILITINKEVICH assumes a periodic variation of the temperature at the ground. In figure 14 C_g and α_0 are used as the coordinates. The rather curious shape of the curve can be understood by considering the developments with constant stratification as given in figure 4.

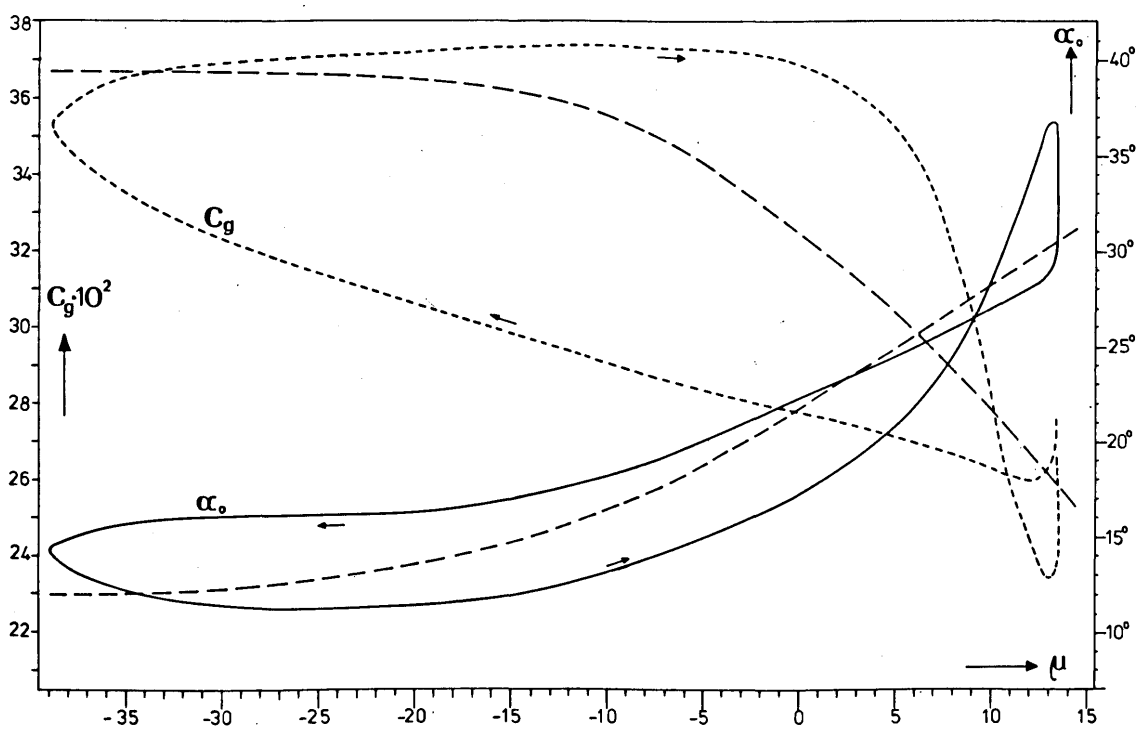

- **Figure 13.** $C_g(\mu)$, dotted line, and $\alpha_0(\mu)$, solid line, as obtained for the diurnal variation described in section V. The dashed lines give the curves for C_g and α_0 in the corresponding stationary cases.

- **Bild 13.** $C_g(\mu)$, punktierte Linie, und $\alpha_0(\mu)$, ausgezogene Linie, erhalten für den im Abschnitt V beschriebenen Tagesgang. Die gestrichelten Linien geben die Kurven für C_g und α_0 in den entsprechenden stationären Fällen.

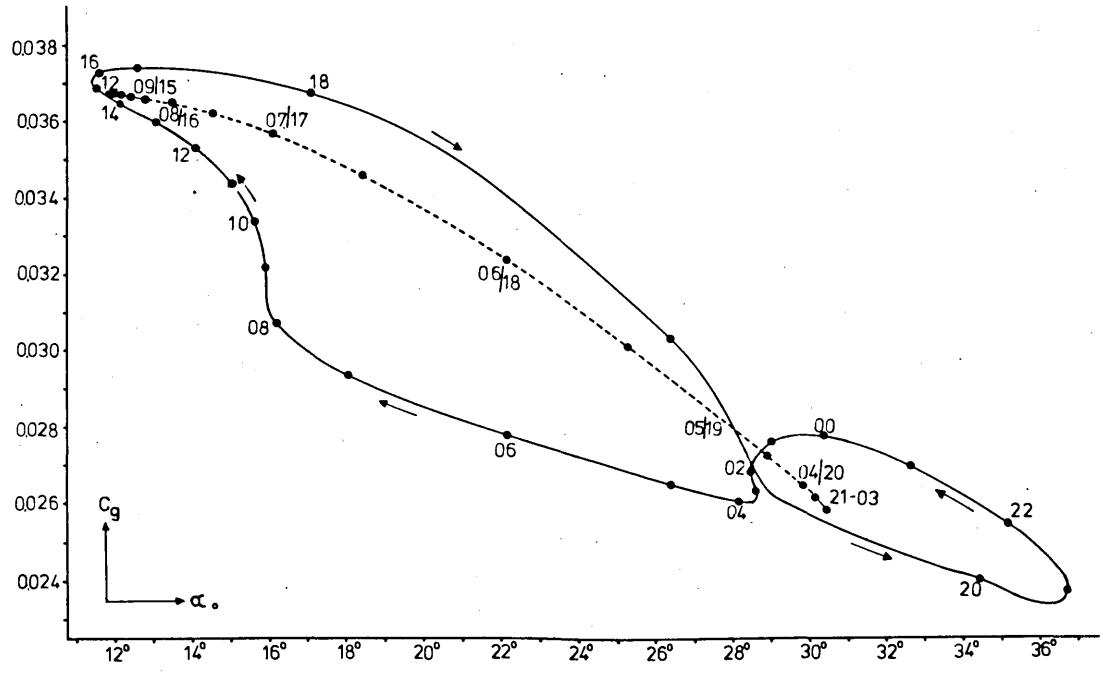

- **Figure 14.** The diurnal variation of C_g and α_0; the dashed line is valid for the corresponding stationary cases. The numbers are the times of the day.

- **Bild 14.** Der Tagesgang von C_g und α_0; die gestrichelte Kurve gilt für die entsprechenden stationären Fälle. Die Zahlen geben die Tageszeit an.

With the non-stationary values of C_g as given in figure 13 one is able to compute the turbulent heat flux q_0 at the ground by using eq. (40). Figure 15 shows the result of such a computation, it is very similar to the result obtained by ZILITINKEVICH (1970).

VII. Conclusions

It was the purpose of this investigation to get some knowledge about the differences of boundary layer parameters in corresponding non-stationary and stationary cases. It has been found that such differences cannot allways be neglected. For a parameterization of boundary layer effects by applying the resistance law of the PBL it will be necessary therefore to find (empirical) relationships which correct for the influence of non-stationarity.

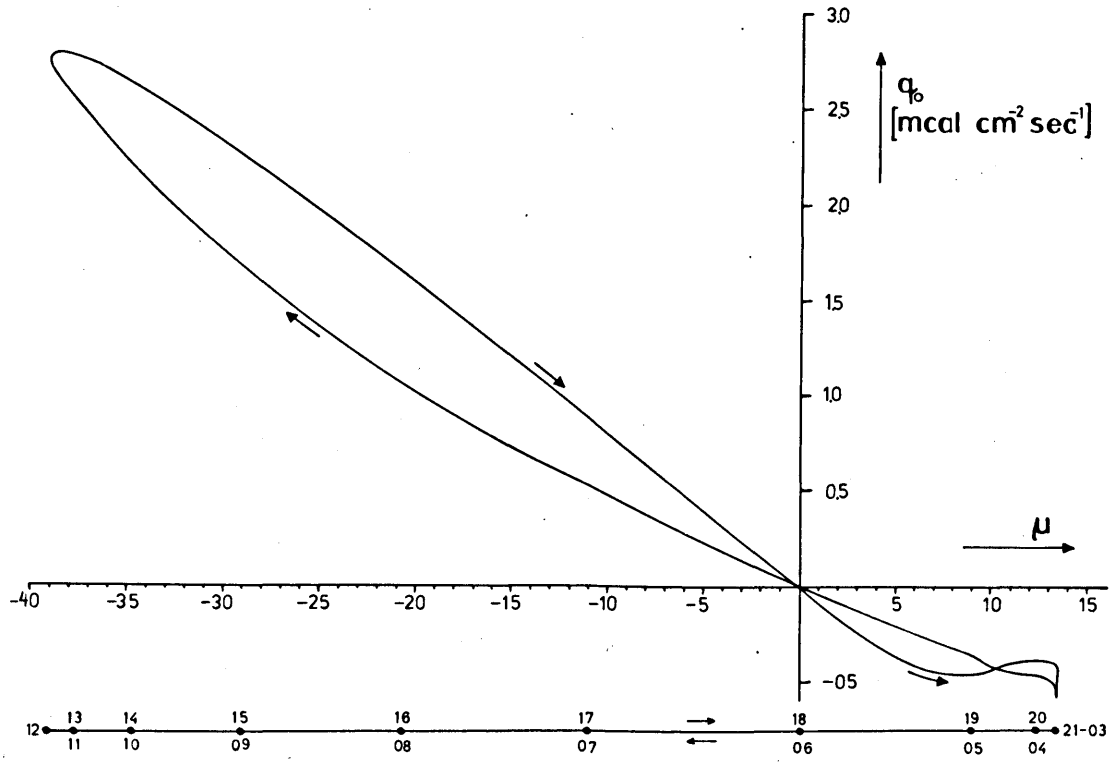

- **Figure 15.** The diurnal variation of the turbulent heat flux at the ground; the lower scale indicates the time of the day
- **Bild 15.** Der Tagesgang des turbulenten Wärmestromes am Boden; die untere Skala gibt die Tageszeiten an

References

BERZ, G. (1969): Untersuchungen zum Wärmehaushalt der Erdoberfläche und zum bodennahen atmosphärischen Transport. Wiss. Mitt. Nr. 16, Meteor. Inst. Univ. München, pp. 94.

BUSINGER, J. A., WYNGAARD, J. C., IZUMI, Y., BRADLEY, E. F. (1971): Flux-profile relationships in the atmospheric surface layer. J. Atm. Sci. 28 (2), 181–189.

LYKOSOV, V. N. (1972): Unsteady state of the planetary boundary layer of the atmosphere. Izv. Acad. Sci. USSR, Atmosph. Ocean. Phys. 8 (2), 142–155, engl. transl. 85–91.

KUROSAKI, A. (1970): A theoretical study of the structure of the Ekman boundary layer (I), Mixing-length theory. Pap. Meteor. Geophys. 21 (2), 89–112.

WIPPERMANN, F. (1971a): A mixing-length hypothesis for the planetary boundary layer flow in the atmosphere. Beitr. Phys. Atm. 44, 215–226.

WIPPERMANN, F. (1971b): A note on a method for solving the planetary boundary layer equations. Beitr. Phys. Atm. 44, 293–296 and 45, 275.

WIPPERMANN, F. (1972): Universal profiles in the barotropic planetary boundary layer. Beitr. Phys. Atm. 45, 148–163.

ZILITINKEVICH, S. S. (1970): Dynamics of the atmospheric boundary layer (in russ.) Leningrad, Gidrometeor. pp. 291.

Boundary-Layers with a Change in the Roughness-Length and/or in the Temperature: A Bibliographical Survey

1935

ROUX, L. Turbulente Windströmungen auf der rauhen Erdoberfläche
Z. Geophys. 11, 165-187

1939

JACOBS, W. Umformung eines trubulenten Geschwindig - profiles
Z. Angew. Math. Mech. 19, 87-100

1949

MERBT, H. Vereinfachte Theorie der örtlich und zeitlichveränderlichen atmosphärischen Reibungsschichten
Veröff. Geophys. Inst. Univ. Leipzig XV 138-146

1952

GANDIN, L.S. On the Transformation of the Wind Profile (in Russ.)
Trudy GGO 33, 71-84

1954

DMITRIEV, A.A.
SOKOLOVA, I.N. A Scheme for Evaluation of the Wind Velocity Changes in Airflow Passing over a Land-Sea Shore (in Russ.)
Trudy Hydrophys. Inst. IV, 87-93

1957

GLASER, A.H.
ELLIOTT, W.P.
DRUCE, A.J.
The Study of Small-Scale Modification of Air Passing over Inhomogeneous Surfaces
Texas A & M Res. Found., Contr. AF 19(604)-997 Final Rep., pp 36

1958

ELLIOTT, W.P.
The Growth of the Atmospheric Internal Boundary Layer
Trans. Amer. Geophys. Union 39, 1048-1054

1959

ARAGO, L.R.
On the Vertical Motions in the Atmosphere above a Thermally Inhomogeneous Surface (in Russ.)
Trudy GGO 99, 112-121

1961

BROOKS, F.A.
Need for Measuring Horizontal Gradients in Determining Vertical Eddy Transfers of Heat and Moisture
J. Meteor. 18, 589-596

KUTZBACH, J.
Investigations of the Modification of Wind Profiles by Artificially Controlled Surface Roughness
in Ann. Rep. "Studies of the Threedimensional Structure of the Planetary Boundary Layer", 71-113, Dept. of Meteor., Univ. of Wisconsin, Mdison, Wisc. USA

MIYAKE, M.
Transformation of the Atmospheric Boundary Layer Induced by Inhomogeneous Surfaces
M.Sc. Thesis, Univ. of Washington

1962

ESTOQUE, M.A.
A Sea Breeze as a Function of Prevailing Synoptic Situation
J. Atm. Sci. 19, 244-250

LETTAU, H.H. Studies of the Effects of Variations in Boundary Conditions on the Atmospheric Boundary Layer
Ann. Rep. Contr. DA-36-039-AMC-00878, pp 115
Dept. of Meteor., Univ. of Wisconsin, Madis.

TAYLOR, R.J. Small-Scale Advection and the Neutral Wind Profile
J. Fluid Mech. 13, 529-539

1963

DYER, A.J. Adjustment of Profiles and Eddy Fluxes
Quart. J. Roy. Met. Soc. 89, 276-280

LOGAN, E.
JONES, J.B. Flow in a Pipe Following an Abrupt Increase in Surface Roughness
Trans. Am. Soc. Mech. Eng., Ser. D,
J. Basi Eng. 85, 35-40

RIDER, N.E.
PHILIP, J.R.
BRADLEY, E.F. The horizontal Transport of Heat and Moisture - a Micrometeorological Study
Quart. J. Roy. Meteor. Soc. 89, 506-531
Discussion (1965) ibidem 91, 236-240

STEARNS, C.R.
LETTAU, H.H. Report on Two Windprofile Modification Experiments in Air Flow over the Ice of Lake Mendota
Ann. Rep. Contr. DA-36-039-AMC-00878
Dept. of Meteor., Univ of Wisconsin, Madison

ZAITSEV, A.S. Transformation of the Wind Profile with the Change of Turbulence Intensity (in Russ.)
Trudy GGO 95, 42-46

1964

NADEJDINA, E.D. On the Change of Meteorological Elements in Case of Air Flow Transformation (in Russ.)
Trudy GGO 150, 3-13

PANOFSKY, H.A.
TOWNSEND, A.A. Change of Terrain Roughness and Wind Profile
Quart. J. Roy. Meteor. Soc. 90, 147-155
Discussion (1965) ibidem 91, 241

STEARNS, C.R. Wind Profile Modification Experiments Using Fields of Christmas Trees on the Ice of Lake Mendota

Ann. Rep. Contr. DA-36-039-AMC-00878, pp 115 Dept. of Meteor., Univ. of Wisconsin, Madis.

1965

DYER, A.J.
CRAWFORD, T.V. Observations of the Modification of the Microclimate at a Leading Edge

Quart. J. Roy. Meteor. Soc. 91, 345-348

MIAYKE, M. Transformation of the Atmospheric Boundary Layer over Inhomogeneous Surfaces

Sci. Rep. Contr. 477(24)(Nr.307-252), pp 63 Dept. Atm. Sci., Univ. of Washington

MONIN, A.S. On the Atmospheric Boundary Layer with Inhomogeneous Temperature (in Russ.)

Bull. (Izv.) Acad. Sci. USSR, Atm. Ocean. Phys. 1, 490-500; engl. transl. 287-292

TOWNSEND, A.A. Self Preserving Flow inside a Turbulent Boundary Layer

J. Fluid Mech. 22, 773-797

TOWNSEND, A.A. The Response of a Turbulent Boundary Layer to Abrupt Change in Surface Conditions

J. Fluid Mech. 22, 799-822

TKACHENKO, A.V. Determination of the Eddy Coefficient in the Stationary Horizontally Inhomogeneous Atmospheric Surface Boundary Layer (in Russ.)

Kiev Ukrainskii N.-I. Gidrometeor. Inst. Trudy Nr. 48, 45-51

1966

NADEJDINA, E.D. The Use of the Energy Balance Equation in the Problem of Air Flow Transformation (in Russ.)

Trudy GGO 187, 69-76

TOWNSEND, A.A. The Flow in a Turbulent Boundary Layer after a Change in Surface Roughness

J. Fluid Mech. 26, 255

WAGNER, N.K. A Two-Dimensional Time-Dependent Numerical Model of Atmospheric Boundary Layer Flow over Inhomogeneous Terrain

in: "Theoretical Studies of the Atmospheric Boundary Layer" Final Rep. USAERDA, pp 1-80 Univ. of Hawaii, Institute of Geophysics

1967

BLACKADAR, A.K.
GLASS, P.E.
PANOFSKY, H.A.
A Theory of the Effects of Stability upon the Wind Profile under Conditions of Inhomogeneous Terrain Roughness

Proc. USAEC Meteor. Inform. Meeting, Chalk River Nucl. Lab Ontario
Canad. Rep. AECL - 2787, 453 - 461

BLACKADAR, A.K.
PANOFSKY, H.A.
GLASS, P.E.
BOOGARD, J.F.
Determination of the Effect of Roughness Change on the Wind Profile

Phys. Fluids 10 (9), pt 2, S 209 - S 211

BRADSHAW, P.
FERRIS, D.H.
ATWELL, N.P.
Calculation of Boundary Layer Development Using the Turbulent Energy Equation

J. Fluid Mech. 28, 593-616

MOROZ, W.J. Lake Breeze on the Eastern Shore of Lake Michigan: Observation and Model

J. Atm. Sci. 24, 337-355

PLATE, E.J.
HIDY, G.M.
Laboratory Study of Air Flow over a Smooth Surface onto Small Water Waves

J. Geophys. Res. 72 (18), 4627-4641

SMITH, F.B. Modification of the Wind Profile Due to Changes in Surface Roughness

Proc. USAEC Meteor. Inform. Meeting, Chalk River Nucl. Lab. Ontario
Canad. Rep. AECL - 2787, 463 - 475

TAYLOR, P.A. On Turbulent Wall Flows above a Change in Surface Roughness

Ph.D.Thesis, Univ. of Bristol

1968

BRADLEY, E.F. A Micrometeorological Study of Velocity Pro-

les and Surface Drag in the Region Modified by the Change in the Surface Roughness

Quart. J. Roy. Meteor. Soc. 94, 361-379

LETTAU, H.H.
ZABRANSKY, J.
Interrelated Changes of Wind Profile Structure and Richardson Number in Air Flow from Land to Inland Lakes

J. Atm. Sci. 25, 718-728

NICKERSON, E.C.
Boundary Layer Adjustment as an Initial Value Problem

J. Atm. Sci. 25, 207-213

ONISHI, G.
ESTOQUE, M.A.
Numerical Study on Atmospheric Boundary Layer Flow over Inhomogeneous Terrain

J. Meteor. Soc. Japan 46, 280-286

TANI, I.
Review of Some Experimental Results on the Response of a Turbulent Boundary to Sudden Perturbations

AFOSR-IFP-Stanford Conf. on Comput. of Turb. Bound. Layers 1, 483-494

1969

BLOM, J.
WARENTA, L.
The Influence of Changes in Roughness on the Development of the Turbulent Boundary Layer in the Lower Layers of the Atmosphere

J. Atm. Sci. 26, 255-265

BRADSHAW, P.
Comments on: On the Relation between the Shear Stress and the Velocity Profile after a Change in Surface Roughness (by E.W. Peterson)

J. Atm. Sci. 26, 1353-1354

ESTOQUE, M.A.
BHUMRALKAR, C.M.
Flow over a Localized Heat Source

Month. Weath. Rev. 97, 850-859

HANNA, S.R.
The Propagation of Internal Boundary Layers within the Planetary Boundary Layer

in: "Characteristics of Winds and Turbulence in the Planetary Boundary Layer" ESSA-Techn.-Mem. ERLTM-ARL 8, Oak Ridge, Tenn., 38-44

NADEJDINA, E.D. On the Change of the Characteristics of a Turbulent Flow Passing over a Land-Sea Shore (in Russ.)

Trudy GGO 241, 56-62

NOVIKOVA, S.P. On the Problem of Transformation of the Meteorological Elements (in Russ.)

Meteor. i Gidrol. 12, 89-93

PETERSON, E.W. A Numerical Model of the Mean Wind and Turbulent Energy Downstream of a Change in Surface Roughness

Rep. Nr. 102-69, Center for Air Environm. Stud., Penns. State Univ.

PETERSON, E.W. Modification of Mean Flow and Turbulent Energy by a Change in Surface Roughness under Conditions of Neutral Thermal Stability

Quart. J. Roy. Meteor. Soc. 95, 561-575

PETERSON, E.W. On the Relation between the Shear Stress and the Velocity Profile after a Change in Surface Roughness

J. Atm. Sci. 26, 773-774
Comment by P. BRADSHAW: J. Atm. Sci. 26, 1353-1354

RIGBY, D.C. The Reaction of a Fully Developed Turbulent Flow to a Sudden Change in Surface Roughness

M.A.Sc. Thesis, University of Toronto, Can.

TAYLOR, P.A. On Wind and Shear Stress Profiles above a Change in Surface Roughness

Quart. J. Roy. Meteor. Soc. 95, 77-91

TAYLOR, P.A. The Planetary Boundary Layer above a Change in Surface Roughness

J. Atm. Sci. 26, 432-440

1970

DONEV, E. Transformation of the Wind Profile in Neutrally Stratified Surface Layer (in Bulgar.)

Diploma-Thesis, Dept. of Meteor., Univ. of Sofia, Bulgaria

ECHOLS, W.T. Modification in Surface Boundary Layer Wind Structure with Onshore Flow

Rep. Nr. 23, Atm. Sci. Group, Univ. of Texas Austin, Tex., pp 59

ESTOQUE, M.A.
BHUMRALKAR, C.M. A Method for Solving the Planetary Boundary Layer Equations

Bound. Layer Meteor. 1, 169-194

KUNG, R. Boundary Layer Development over Equally Spaced Fences

Ph.D.Thesis, Dept. of Civil Eng.,Colorado Sate Univ., Ft. Collins, Col. USA

LAIKHTMAN, D.L. Change of Meteorological Fields Generated by the Uneveness of the Underlying Surface

Chapter 4 of the monograph:"Physics of the Boundary Layer of the Atmosphere" (in Russ.) Hydrometeorolog. Press Leningrad, pp 341

TAYLOR, P.A. A Numerical Model of Air Flow above Changes in Surface Heat Flux, Temperature and Roughness for Neutral and Unstable Conditions

Bound. Layer Meteor. 1, 18-39

1971

ANTONIA, R.A.
LUXTON, R.E. The Response of a Turbulent Boundary Layer to a Step Change in Surface Roughness, Part 1: Smooth to Rough

J. Fluid Mech. 48 (4), 721-761

COUNIHAN, J. Wind Tunnel Determination of the Roughness Length as a Function of the Fetch and the Roughness Density of Threedimensional Roughness Elements

Atmospheric Environm. 5, 637-642

PANCHEV, S.
DONEV, E.
GODEV, N. Wind Profile and Vertical Motions above an Abrupt Change in Surface Roughness and Temperature
(A review of Russian-language papers)

Bound. Layer Meteor. 2, 52-63

PETERSON, E.W. Predictions of the Momentum Exchange Coefficient for Flow over Heterogeneous Terrain
J. Appl. Meteor. 10, 958-961

RADIKEVICH, V.M. Modification of the Dynamic Characteristics of an Air Stream Due to Changes in Surface Roughness (in Russ.)
Bull. (Izv.) Acad. Sci. USSR, Atm. Ocean. Phys. 7, 1241-1250 (engl.transl. 813-818)

TAYLOR, P.A. Air Flow above Changes in Surface Heat Flux, Temperature and Roughness; an Extension to Include the Stable Case
Bound. Layer Meteor. 1, 474-497

1972

ANTONIA, R.A.
LUXTON, R.E. The Response of a Turbulent Boundary Layer to a Step Change in Surface Roughness Part 2: Rough to Smooth
J. Fluid Mech. 53, 737-757

ECHOLS, W.T.
WAGNER, E.K. Surface Roughness and Internal Boundary Layer near a Coastline
J. Appl. Meteor. 11, 658-662

SHIR, C.C. A Numerical Computation of Air Flow over a Sudden Change in Surface Roughness
J. Atm. Sci. 29, 304-310
Comment to that by E.W.PETERSON: ibidem 29, 1393-1394

TAYLOR, P.A. Some Comparisons between Mixing-Length and Turbulent Energy Equation Models for Flow above a Change in Surface Roughness
Pap. presented 3d Int. Conf. Numer. Meth. in Fluid Dynamics, Paris 1972

TAYLOR, P.A. Wind Profile Development above a Locally Adjusted Sea Surface
Bound. Layer Meteor. 2, 381-389

1973

ANTONIA, R.A.
LUXTON, R.E. Characteristics of Turbulence within an Internal Boundary Layer

Proc. 2nd IUTAM-IUGG Symposium on Turbulent Diffusion in Environmental Pollution, Charlottesville, Virg.,USA, April 8-14 1973
To appear in "Advances in Geophysics"

PETERSEN, E.L.
TAYLOR, P.A.
Some Comparisons between Observed Wind Profiles at Risö and Theoretical Predictions for Flow over Inhomogeneous Terrain
Quart. J. Roy. Meteor. Soc. 99, 329-336

CHAPTER 6

The Dynamic Instability of the Atmospheric Boundary Layer

In this chapter we can not retain the assumption of stationarity and horizontal homogeneity, therefore we treat now atmospheric boundary layers and no longer PBLs; in any case we consider boundary layers in rotating systems.

The atmospheric boundary layer is turbulent; a great many t h r e e - dimensional eddies of different sizes, of different locations and of different life-times transport the mean momentum downward. In order to do that the eddies have an asymmetric structure (possibly a horse - shoe form, or in unstable thermal stratification the form of an inclined rotating plume); nevertheless all these superimposed vortices give the well-known chaotic picture of the turbulence. The amount of mean momentum transported downward depends on the vertical shear of the mean wind; if this shear exceeds a critical value, the micro-scale turbulence is no longer capable to effect the necessary downward transport of mean momentum. Now this will be transported downward by a new system of meso-scale eddies which are formed; it consists of almost longitudinal vortex rolls, i.e. t w o-dimensional vortices, which appear "more organized" and less chaotic than the micro-scale eddies. They are superimposed

upon the basic boundary layer flow.

All theoretical investigations of the transition from the micro-turbulent state of the boundary layer to the meso-turbulent one (with vortex rolls) are made with the assumption of a mean boundary layer flow of the Ekman type and an eddy viscosity k_m being constant with height. This means that actually the transition is investigated from laminar to the (meso-) turbulent state.

FALLER and KAYLOR (1966), who have made experiments in rotating tanks as well as numerical studies, found two types of vortex rolls: the type I vortices have their axes orientated about 14° to the left of the direction of the basic flow, they are stationary or nearly so and have a relatively short wave length. For the type II vortex rolls the angle observed is more variable and lies between 20° to the right to 5° to the left of the basic flow; these vortices have a phase velocity which depends on their orientation and the wave length of these vortices is two to three times that of the type I rolls. In the case of a dynamically unstable boundary layer either the vortex rolls of type I (inflectional instability) exist or those of type II (parallel mode instability) or both.
There are observations made about such vortex rolls in the atmospheric boundary layer, they are visible by cloud streets, by strips of soaring sea-gulls or possibly by seif dunes too. A schematic picture of the generating process of these phenomena is on page 263; on the pages 261 and 262 there are also pictures of cloud streets and seif dunes, these pictures are taken from space vehicles. On page 264 a neph-analysis is given (after RONNE and MALKUS 1960) showing two systems of superimposed vortex rolls which have different wave lengths. In this special case, however, the axes of the two vortex systems are almost perpendicular to each other and

their orientation does not agree with the findings by FALLER and KAYLOR (1966).

In the following paper "The Orientation of Vortices Due to Instability of the Ekman Boundary Layer" the orientation is studied for the case that the two superimposed systems are orthogonal. In the same paper a physical interpretation of these vortices is attempted: it can be seen that the vertical component of the Coriolis acceleration acts in the same manner as the centrifugal acceleration in a flow along a concave wall producing Taylor-Görtler vortices or as the buoyancy acceleration in a flow along a heated wall also producing longitudinal vortex rolls. The latter effect certainly plays an important role in the atmospheric boundary layer too, possibly it is more often responsible for the development of cloud streets than the dynamic instability.

The transition to dynamic instability of the atmospheric boundary layer (idealized as an Ekman layer) has been investigated for different thermal stratifications by ETLING (1971); this paper is reproduced on the pages 280 - 298. According to his results the type I vortices appear preferably in the unstably stratified and in the neutral boundary layer, those of type II in a stably stratified boundary layer. The ratio of the wave length is $L_{II}/L_I \approx 2.6$, which is in very good agreement with the result by FALLER and KAYLOR. These authors found, that the type II vortices develop at a lower Reynolds number than the type I vortices. This result is in accordance with those by ETLING as long as a stably stratified or almost neutral boundary layer is considered. In the neutral case the critical Reynolds number is nearly the same for both types of vortices and in an unstably stratified boundary layer the critical Reynols number

for the type I vortices is lower. This is very clearly shown by the figure 9 on page 293.

In a later paper KAYLOR and FALLER (1972) have also investigated the dependence of the growth rate on the thermal stratification expressed by the Richardson-number (for stable stratification only). They obtained the expected variation except for large values of the Richardson-number, where a resonance is seen of the shear flow instability with internal gravity waves. The authors study also the energy transfer from the energy of the mean flow into that of the secondary flow. This has also been investigated by BROWN (1970) who shows the modification of the original Ekman spirals into hodographs exhibiting increased alignment with the geostrophic direction and supergeostrophic velocities. In both papers {KAYLOR and FALLER (1972) and BROWN (1970)} figures are presented showing numerically obtained cross-sections of the vortex rolls under different conditions; one recognizes in these figures the shape of the vortices which they must have in order to be able to transport the momentum downward.

The literature relevant to the dynamic instability of the boundary layer (till about 1970/71) is mainly cited in the references (pages 279, 296-297) of the two following reproduced papers. Some additional more recent papers are cited hereafter, they concern the theory as well as observational results:

ANGELL, J.K. 1971 Helical Circulations in the Planetary Boundary Layer
J. Atm. Sci. 28, 135-138

ANGELL, J.K. 1972 A Comparison of Circulations in Transverse and Longitudinal Planes in an Unstable Planetary Boundary Layer
J. Atm. Sci. 29, 1252-1261

BROWN, R.A. 1972 On the Inflection Point Instability of a Stratified Ekman Boundary Layer
J. Atm. Sci. 29, 850-859

HANNA, S.R.
HOECKER, W.H. 1971 The Response of Constant Density Balloons to Sinusoidal Variations of Vertical Wind Speeds
J. Appl. Meteor. 10, 601-604

HILL, G.E. 1968 One the Orientation of Cloud Bands
Tellus 20 (1), 132-137

GORDON, A.L. 1970 Vertical Momentum Flux Accomplished by Langmuir Circulation
J. Geophys. Res. 75 (21), 1477-1479

KAYLOR, R.
FALLER, A.J. 1972 Instability of the Stratified Ekman Boundary Layer and the Generation of Internal Waves
J. Atm. Sci. 29, 497-509

Beiträge zur Physik der Atmosphäre, 42. Band, 1969, S. 225–244

The Orientation of Vortices Due to Instability of the Ekman-Boundary Layer[1])

Die Lage der in einer instabilen Ekman-Grenzschicht entstandenen Wirbelrollen[1])

Friedrich Wippermann

Institut für Meteorologie der Technischen Hochschule Darmstadt

With 10 Figures

Received 14 June 1969

Summary: In an unstable EKMAN boundary layer vortex rolls are formed; their axes are orientated almost longitudinally, they include an angle ϵ of about 14° to the left with the direction of the geostrophic flow. The analogy of these vortices to the TAYLOR-GÖRTLER vortices on a concave wall and/or to the thermo-convective vortices due to a heated wall will be shown. Sometimes a superimposed second vortex system is observed whose axes are orientated in a more transversal direction. The spacing of these vortices is larger than that one of the more longitudinal vortices. The main part of this paper is concerned with deriving a formula relating the forementioned angle ϵ to the ratio of the wavenumbers of the two vortex systems. This formula has been verified by laboratory experiments.

An application of this formula to cloud streets and seif-dunes is given; the gross-features of the last ones can be explained by vortices due to EKMAN layer instability.

Zusammenfassung: Wenn eine EKMANsche Grenzschicht instabil wird, bilden sich horizontale Wirbelrollen; deren Achsen liegen nahezu in Strömungsrichtung, sie schließen mit der Richtung des geostrophischen Windes einen Winkel ϵ von etwa 14° (nach links) ein. Es wird gezeigt, daß diese Wirbelrollen den TAYLOR-GÖRTLER-Wirbeln an einer konkaven Wand oder auch den thermokonvektiven Wirbeln an einer geheizten Wand analog sind.

Manchmal beobachtet man ein überlagertes zweites Wirbelsystem, dessen Achsen mehr in transversaler Richtung liegen und dessen Abstand zwischen zwei Wirbelrollen größer ist als bei dem mehr longitudinal orientierten Wirbelsystem. Der Hauptteil dieser Arbeit beschäftigt sich mit der Ableitung einer Formel, durch welche der vorgenannte Winkel ϵ mit dem Verhältnis der Wirbeldurchmesser (Wellenzahlen) der beiden Wirbelsysteme verknüpft ist. Diese Formel wird anhand der Ergebnisse von Versuchen im Laboratorium geprüft.

Sie wird auf Wolkenstraßen und Seif-Dünen angewendet, wobei sich Schlüsse hinsichtlich der Orientierung derselben ziehen lassen; die wesentlichen Erscheinungsformen der Seif-Dünen lassen sich durch Wirbelrollen erklären, die sich aufgrund einer instabilen EKMAN-Schicht gebildet haben.

Résumé: Lorsque la couche limite d'EKMAN devient instable, il s'y forme des rouleaux (tourbillons à axes horizontaux) orientés presque dans le sens du courant. Les axes de ces rouleaux font avec le vent géostrophique un angle ϵ de l'ordre de 14°, à gauche de ce vent. L'auteur montre qu'il existe une analogie entre ces rouleaux et les tourbillons de TAYLOR-GÖRTLER en présence d'une paroi concave et les tourbillons thermoconvectifs au-dessus d'une surface réchauffée. Il apparait souvent au-dessus de ces rouleaux un second système de rouleaux dont les axes ont une orientation plus transversale. L'espacement entre ces derniers rouleaux est plus grand qu'entre les premiers dont les axes ont une orientation plus longitudinale. L'objet principal de cet article est d'établir une relation entre l'angle ϵ et le rapport des nombres d'onde des deux systèmes de rouleaux tourbillonnaires. La formule établie a été confirmée expérimentalement. Elle a été appliquée au cas des nuages en file et à celui de seif-dunes. On peut en déduire quelques conclusions quant à l'orientation de ces formations. Les grands traits de ces phénomènes trouvent leur explication dans la formation de rouleaux tourbillonnaires dans une couche limite d'EKMAN instable.

---

[1]) Paper presented at the AGARD Specialists Meeting on "The Aerodynamics of Atmospheric Shear Flows" sponsored by the Fluid Dynamics Panel at Munich, Germany during 15–17 Sept. 1969

I. Introduction

In recent years pictures from satellites, mainly those from Gemini and Apollo space vehicles flying in lower altitudes, have shown that clouds of the cumulus type are much more arranged in patterns of cloud rows (cloud streets) as one has thought before. Figure 1 gives such a picture of cloud streets over Georgia and South Carolina; the lateral distance of the cloud streets in this case averages to 3.2 km. They extend in the longitudinal direction for more than 150 km.

Fig. 1. Cloud streets over Georgia and South Carolina as seen from an Apollo space whicle.

Bild 1. Wolkenstraßen über Georgia und South Carolina von einem Apollo-Raumschiff aufgenommen

A very similar phenomenon seems to be given by the seif-dunes. These are straight and parallel chains of dunes extending often for more than 100 km in the longitudinal direction and having a lateral distance of a few kilometers too. Their height above the basis is mainly between 50 m and 100 m, they are called seif-dunes in Egypt, Yardangs in Persia, 'urgs in Arabia and alâb (sing.: elb) in Mauretania. Figure 2 shows a photograph of such dunes in the Arabian desert as seen from Gemini IV.

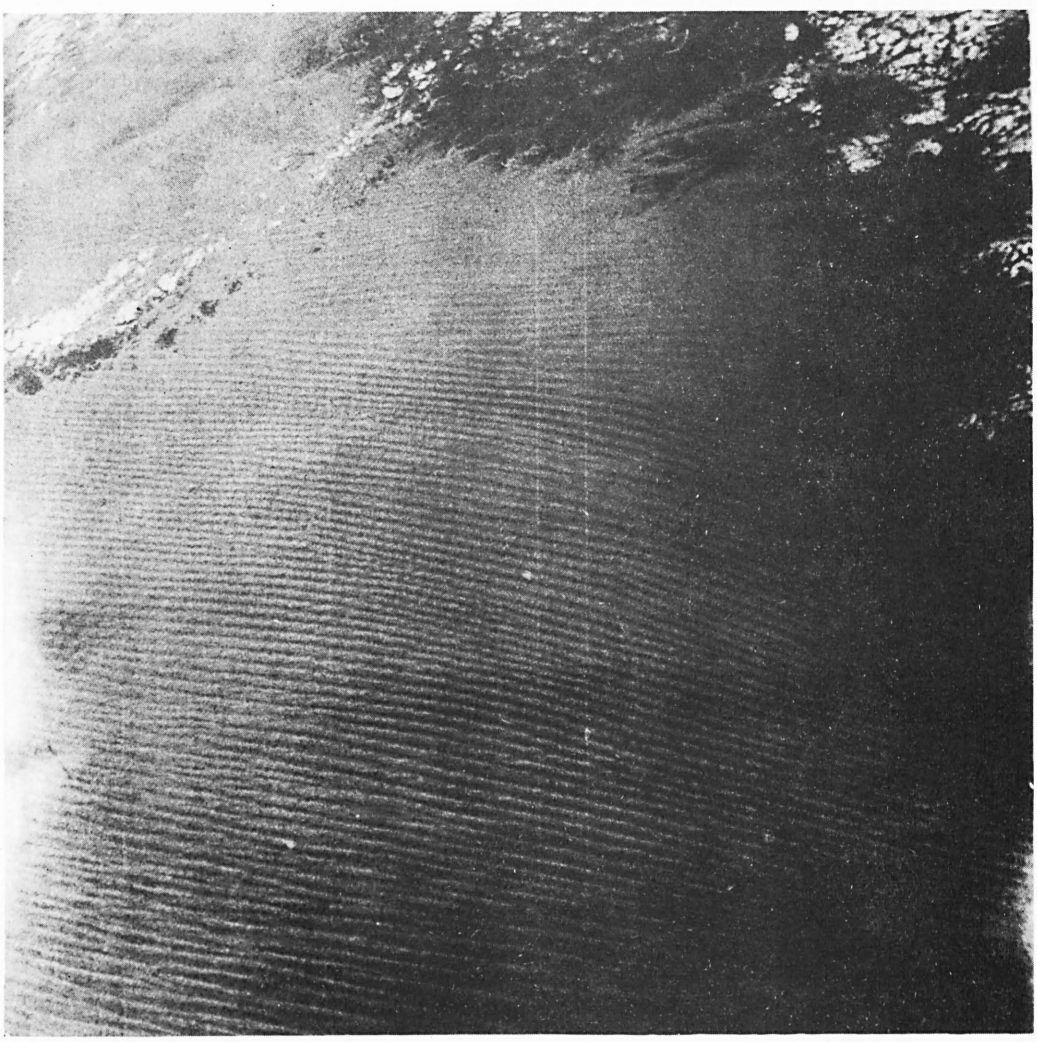

Fig. 2. Seif-dunes in the Arabian desert as seen from Gemini IV

Bild 2. Seif-Dünen in der Arabischen Wüste, aufgenommen von Gemini IV

For a possible explanation of the formation of cloud streets or seif-dunes the vortex rolls could be used, which are caused by an instability of the atmospheric boundary layer. As a rough approximation the flow in this boundary layer may be assumed to be of the EKMAN type. In the schematic figure 3 it is shown how the formation of cloud streets and/or seif-dunes by such vortex rolls could be understood. From the observations of sea gulls WOODCOCK (1940) has concluded, that parallel stripes of upward motion exist over the open ocean under certain atmospheric conditions. Such stripes of upwind may also be explained by the vortex rolls due to EKMAN layer instability.

For instance, for the formation of seif-dunes BAGNOLD (1945), p. 224, postulates a system of wind components perpendicular to the basic flow. The wind components given by the forementioned vortex rolls are exactly of that kind. The (doubled) diameter of such vortex rolls as obtained by theoretical investigations is in fair agreement with the observed lateral distance of cloud streets or seif-dunes.

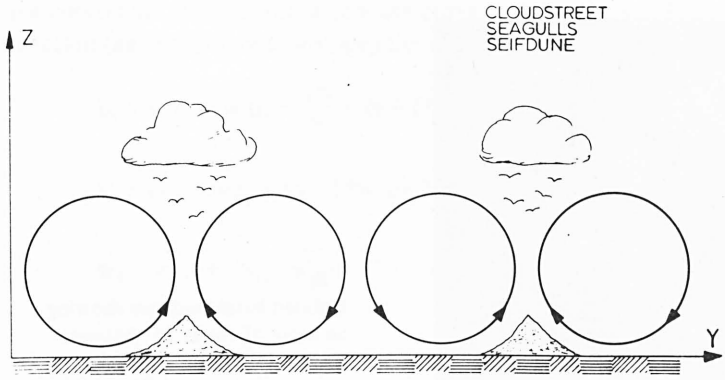

Fig. 3

The formation of cloud streets and seif-dunes by longitudinal vortex rolls (schematic).

Bild 3

Schematische Darstellung zur Bildung von Wolkenstraßen und Seifdünen durch longitudinale Wirbelrollen

The vortex rolls are more or less longitudinal vortices, their axis is orientated almost in the direction of the basic flow. The direction of the axis and the direction of the basic flow (geostrophic wind) form an angle to the left of the wind direction varying between 13° and 16°.

In an analysis of cloud patterns PLANCK (1966) found the angle ϵ between the direction of cloud rows and the wind in the cloud level to be 15°. ANGELL a.o. (1968) using tetroons studied the helical circulations due to such vortex rolls and found an angle ϵ between the axis of the helical motion and the geostrophic flow (in 500 mb) of 13°. In laboratory experiments the angle ϵ between the axis of the almost longitudinal vortex rolls and the basic flow has been found to be 14° by GREGORY a.o. (1955), to be 14.7° by FALLER (1963) and to be 13° 11′ by HORST (1969). As a theoretical result GREGORY a.o. (1955) gives ϵ = 13° 18′. FALLER and KAYLOR (1965) obtained ϵ theoretically depending on the Reynoldsnumber; the most frequently obtained value of ϵ is between 14° and 16°. Similar results show the numerical integrations by LILLY (1966).

Cloud streets will be reorientated immediately when the direction of the mean wind changes, in each case it should be possible to observe the angle ϵ. This angle cannot be observed for seif-dunes since these are fixed and cannot be reorientated for a changed direction of the prevailing winds. Figure 4 for instance shows a case of an alâb, where the prevailing wind coming from NE forms an angle of about 25° with the direction of the chain of dunes. The direction of the prevailing wind in this case may be seen from the direction of motion of the barchan dunes.

Sometimes a second vortex system is superimposed on the former system of "longitudinal" vortices. This is shown for example in figure 5 which gives a schematic representation of distribution of clouds in the neighbourhood of a troughline in the easterlies; the axes of vortices of the second system seem to be almost perpendicular to the axes of the more longitudinal vortices. One notices, that the wave-length in the wind direction is much larger than in the transversal direction as it should be according to one of the main results of a theoretical investigation by KUO (1963). FALLER and KAYLOR (1966) have obtained both these vortex systems in laboratory experiments; they found that the spacing of the transversal vortex rolls is two to three times that of the vortex rolls with axis in the more longitudinal direction. They also obtained cases with the two vortex systems existing simultaneously but these pictures are not very useful to measure the two spacings and the angle ϵ. Very recently the double system of vortices has been investigated in laboratory experiments by HORST (1969). He creates the instable boundary layer by decelerating a rotating cylindric tank. The experiments are similar to those described by STERN (1960). Figure 9 gives a photograph of one of his experiments; looking into the rotating cylinder filled with water, the two vortex systems in the boundary layer will be seen marked by sand on the ground.

The purpose of this paper is to show how the forementioned angle ϵ depends on the two wavelengths in the more longitudinal and the more transversal direction.

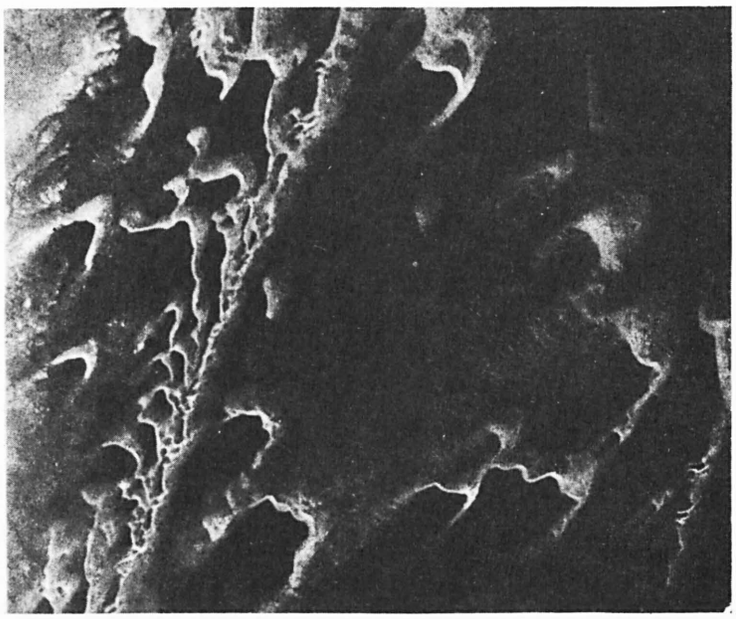

Fig. 4

Isolated barchan-dunes showing an angle of about 25° between the direction of the mean wind and an elb (after CLOS-ARCEDUC 1968).

Bild 4

Durch die Bewegungsrichtung einzelner Barchan-Dünen wird ein Winkel von etwa 25° zwischen der mittleren Windrichtung und einem Elb erkennbar (nach CLOS-ARCEDUC 1968)

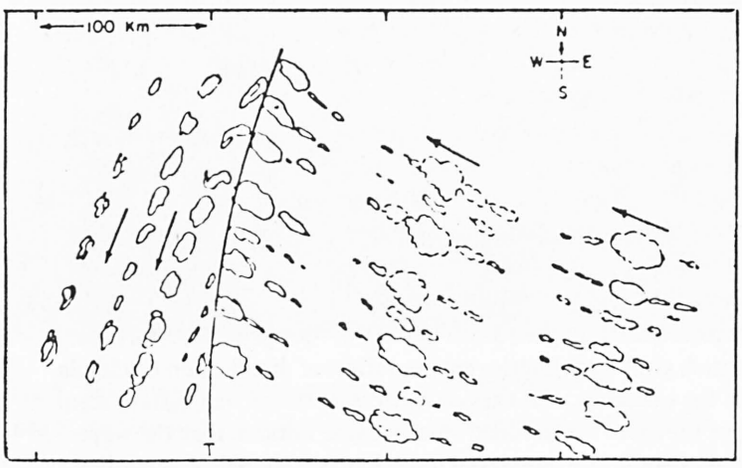

Fig. 5

Cloud distribution in the neighbourhood of a trough line in the easterlies (after MALKUS and RONNE 1960).

Bild 5

Wolkenverteilung im Bereich einer Troglinie in den Easterlies (nach MALKUS und RONNE 1960)

II. The analogy of the longitudinal vortex rolls to TAYLOR-GÖRTLER vortices and to thermo-convective vortex rolls

The longitudinal vortices caused by an instability of the EKMAN boundary layer are quite analogous to the TAYLOR-GÖRTLER vortices on a wall with concave curvature or to the vortex rolls on a plane but heated wall. The analogy between the latter two has been shown by GÖRTLER (1959). The (negative) centrifugal force in the case of a concave wall and/or the buoyancy force in the case of a heated wall have to be replaced by the Coriolis force in the atmosphere. This will be shown for an assumed parallel shear flow in the atmosphere (not for an EKMAN shear flow as it should be when Coriolis forces are acting).

In a coordinate system with a concave curved x-axis, the y-axis horizontal and the z-axis in the vertical direction (as usual in meteorology) the equations of motion and the continuity equation are:

$$u_t + v\,u_y + w\,u_z - \frac{uw}{R} - fv + f^*w\cos\lambda = +K\left(u_{yy} + u_{zz} - \frac{1}{R}u_z\right) \tag{1a}$$

$$v_t + vv_y + wv_z + fu - f^*w\sin\lambda = -\frac{1}{\rho}p_y + K\left(v_{yy} + v_{zz} - \frac{1}{R}v_z\right) \tag{1b}$$

$$w_t + vw_y + ww_z + \frac{u^2}{R} + f^*(v\sin\lambda - u\cos\lambda) = g\frac{T^*}{\bar{T}} - \frac{1}{\rho}p_z + K(w_{yy} + w_{zz}) \tag{1c}$$

$$v_y + w_z - \frac{w}{R} = 0 \tag{1d}$$

Herein all derivations with respect to x are put zero since the x-axis shall be the axis of symmetry for the longitudinal vortices; this means $\epsilon = 0$ for the purpose of showing the analogy. The symbols are chosen as usual, R is the radius of curvature of the x-axis, $f = 2\,\Omega\sin\varphi$ and $f^* = 2\,\Omega\cos\varphi$ the two Coriolisparameters with Ω the angular velocity of the earth and φ the geographical latitude, λ is the angle between the x-axis and the west-east direction and K is the coefficient of micro-turbulent diffusion assumed to be constant. Use has been made of the BOUSSINESQ-approximation, which enables to consider the buoyancy effect due to the heated wall; T^* is the temperature deviation from the mean value in the (x, y)-plane. To close the system for the five variables u, v, w, p, T^* one needs actually a fifth equation (the energy equation). This is avoided by assuming that T^* does not depend on z.

By restricting the considerations to a flow in the layer near the wall (i.e.: $z \ll R$) one has

$$\left|\frac{u}{R}\right| \ll |u_z|, \quad \left|\frac{v}{R}\right| \ll |v_z|, \quad \left|\frac{w}{R}\right| \ll |w_z|$$

by which all terms containing R may be neglected, except the term $\frac{u^2}{R}$ in the equation for w.

Using a basic current in the x-direction ($\bar{u} = \bar{u}(z)$, $\bar{v} = \bar{w} = 0$) one obtaines a set of four equations for the perturbations u', v', w', p'. These perturbations are assumed to be of the form

$$h'(y, z, t) = \hat{h}(z)\exp\{i\,k\,(y - ct)\}, \quad k = \frac{2\pi}{L} \quad \text{for } h' = u', v', w', p' \tag{2a}$$

$$T^*(y, t) = \hat{T}^*\exp\{i\,k\,(y - ct)\}\ ; \tag{2b}$$

one obtains the following wavenumber equations:

$$i\,k\,c\,\hat{u} + \bar{u}_z\,\hat{w} - f\,\hat{v} + f^*\hat{w}\cos\lambda = K(\hat{u}_{zz} - k^2\hat{u}) \tag{3a}$$

$$i\,k\,c\,\hat{v} + f\,\hat{u} - f^*\hat{w}\sin\lambda + i\,k\frac{\hat{p}}{\rho} = K(\hat{v}_{zz} - k^2\,\hat{v}) \tag{3b}$$

$$i\,k\,c\,\hat{w} + \frac{2}{R}\bar{u}\hat{u} + f^*(\hat{v}\sin\lambda - \hat{u}\cos\lambda) + \frac{1}{\rho}\hat{p}_z - g\frac{\hat{T}^*}{\bar{T}} = K(\hat{w}_{zz} - k^2\,\hat{w}) \tag{3c}$$

$$i\,k\,\hat{v} + \hat{w}_z = 0 \tag{3d}$$

After having eliminated $\hat{v}$ in (3a), (3b) und (3c) by making use of (3d) and having eliminated $\hat{p}$ by cross-derivation of (3b) and (3c) one obtains

$$\frac{K}{k^2}\hat{w}_{zzzz} - (i\frac{c}{k} + 2K)\hat{w}_{zz} + (Kk^2 + ikc)\hat{w} = -i\frac{f}{k}\hat{u}_z + f^*\hat{u}\cos\lambda - \frac{2}{R}\bar{u}\hat{u} + g\frac{\hat{T}^*}{\bar{T}} \tag{4a}$$

$$-K\hat{u}_{zz} + (Kk^2 + ikc)\hat{u} = i\frac{f}{k}\hat{w}_z - f^*\hat{w}\cos\lambda - \bar{u}_z\hat{w} \tag{4b}$$

The system (4a), (4b) for the two variables $\hat{w}$ and $\hat{u}$ shows the effects to be studied by the three last terms of the right hand side of equ. (4a):

$$f^*\hat{u}\cos\lambda - \frac{2}{R}\bar{u}\hat{u} + g\frac{\hat{T}^*}{\bar{T}} \tag{5}$$

This shows, that the *vertical* component of the Coriolis force acts in the same manner as the (negative) centrifugal force or the buoyancy force. This component of the Coriolis force is different from zero as long as the perturbated horizontal motion has a component parallel to the basic current and as long as the direction of the latter one is not exactly meridional.

The horizontal component of the Coriolis force appearing in (4a) belongs to the imaginary part of the equation, the term $\frac{if}{k}\hat{u}_z$ has the effect of coupling the two equations.

This conclusion is in contradiction to that one by BARCILON (1965) that the Coriolis-force does not effect the stability at least for large Reynoldsnumbers.

For the system (4a, 4b) three essential cases can be distinguished:

(a) $f = f^* = 0, \hat{T}^* = 0$ — flow along a concave wall; on the right-hand side of equ. (4a) only the third term is acting, representing the centrifugal forces. In this case (4a) and (4b) give exactly the equations (2.4.1) and (2.42) investigated by GÖRTLER (1940), if the real part c_r of the phase velocity vanishes and the imaginary part is put $c_i = -\frac{\beta}{k^2}$

(b) $f = f^* = 0, R \to \infty$ — flow along a plane wall which is heated ($\hat{T}^* > 0$). Only the last term on the right hand side of equ. (4a) is relevant

(c) $\hat{T}^* = 0, R \to \infty$ — flow along a plane and non-heated wall, Coriolis forces are acting; now the second term on the right-hand side of equ. (4a) plays an important role.

For the atmospheric boundary layer in general the conditions are those of case (c), but often (mainly over land) the buoyancy force due to the heated earth surface and the Coriolis force act together in producing longitudinal vortices in the unstable boundary layer flow. Photographs from satellites prove this in showing well developed cloud streets which are interrupted over large lakes, where thermal convection is prohibited.

For the conditions of case (b) longitudinal vortex rolls have been produced in laboratory experiments already by AVSEC (1939); it is worth while to mention that AVSEC has obtained also transversal vortex rolls, of course in separate experiments.

III. The longitudinal vortex rolls in the EKMAN boundary layer

In the EKMAN boundary layer ($|\bar{v}_g| = \bar{u}_g$, independent of height) the basic current is no longer parallel as assumed for the derivation of (4a) and (4b), but

$$\bar{u}(z) = |\bar{v}_g| \left\{ 1 - \exp\left(-\sqrt{\frac{f}{2K}}\, z\right) \cos\left(\sqrt{\frac{f}{2K}}\, z\right) \right\} \tag{6a}$$

$$\bar{v}(z) = |\bar{v}_g| \exp\left(-\sqrt{\frac{f}{2K}}\, z\right) \sin\left(\sqrt{\frac{f}{2K}}\, z\right) \tag{6b}$$

or in a coordinate system ($\overset{*}{x}, \overset{*}{y}, z$), which is rotated about an angle ϵ around the z-axis and whose $\overset{*}{x}$-axis forms therefore the angle ϵ with the direction of the geostrophic wind (x-axis)

$$\overset{*}{\bar{u}}(z) = |v_g| \left\{ \cos\epsilon - \exp\left(-\sqrt{\frac{f}{2K}}\, z\right) \cos\left(\sqrt{\frac{f}{2K}}\, z + \epsilon\right) \right\} \tag{7a}$$

$$\overset{*}{\bar{v}}(z) = |v_g| \left\{ \sin\epsilon - \exp\left(-\sqrt{\frac{f}{2K}}\, z\right) \sin\left(\sqrt{\frac{f}{2K}}\, z + \epsilon\right) \right\} \tag{7b}$$

In such a coordinate system, where the axis of the vortices has the direction of the $\overset{*}{x}$-axis (all the derivatives with respect to $\overset{*}{x}$ vanish) the set of wavenumber equations analogous to (4a, 4b) without regarding the effect of a curved wall and of thermo-convection is:

$$K\{\hat{\psi}_{zzzz} - 2k^2 \hat{\psi}_{zz} + k^4 \hat{\psi}\} - ik\{(\overset{*}{\bar{v}} - c)[\hat{\psi}_{zz} - k^2 \hat{\psi}] - \overset{*}{\bar{v}}_{zz} \hat{\psi}\} = -f \hat{\overset{*}{u}}_z - ikf^* \cos\lambda\, \hat{\overset{*}{u}} \tag{8a}$$

$$K\{\hat{\overset{*}{u}}_{zz} - k^2 \hat{\overset{*}{u}}\} - ik\{(\overset{*}{\bar{v}} - c)\hat{\overset{*}{u}} + \overset{*}{\bar{u}}_z \hat{\psi}\} = f \hat{\psi}_z + ikf^* \cos\lambda\, \hat{\psi} \tag{8b}$$

Herein ψ' is the perturbation of the streamfunction in the ($\overset{*}{y}$, z)-plane, $\overset{*}{u}'$ the deviation of the velocity component in the $\overset{*}{x}$-direction; for both these quantities the form of a moving harmonic wave is assumed

$$\psi'(y, z, t) = \hat{\psi}(z) \exp\{ik(y - ct)\} \tag{9a}$$

$$\overset{*}{u}'(y, z, t) = \hat{u}(z) \exp\{ik(y - ct)\} \tag{9b}$$

With respect to the small scale of the vortices the variation of f and f* with geographical latitude has been neglected ($f_y = f^*_y = 0$).

The lefthand side of (8a) is the ORR-SOMMERFELD equation for a motion in the ($\overset{*}{y}$, z)-plane; the two terms on the righthand side couple the two equations (8a, 8b).

For $\overset{*}{\bar{u}}$ and $\overset{*}{\bar{v}}$ and their derivatives with respect to z in (8a, 8b) the expressions (7a) and (7b) have to be used. This has been done by LILLY (1966), who solved the equations (8a, 8b) numerically in order to find critical values of the triple (Re, k, ϵ) for the transition ($c_i = 0$) from stable to unstable conditions of the EKMAN boundary layer. For the Reynoldsnumber

$$Re = \frac{|v_g|\, h_N}{K} \tag{10}$$

was used with $h_N = \sqrt{\frac{2K}{f}}$, see (6a, 6b).

LILLYs equations, of course, do not include the last term in (8a) and the last one in (8b); they are neglected as common in meteorology for large scale atmospheric motions. As shown in (4a) and (5) these terms may be important for the formation of the vortices; there is some doubt if neglection is justified in this case.

Apart from this the numerical results show an angle $\epsilon \neq 0$; since ϵ is also observed in the atmosphere and obtained in laboratory experiments, the question arises how this angle ϵ (between the axis of the vortex rolls and the geostrophic flow) can be understood.

IV. The angle between EKMAN-flow and the geostrophic flow

A simple explanation would be that this angle ϵ is determined by the direction of the actual flow averaged vertically over the total EKMAN layer. As height of the EKMAN layer one defines the height z_N, where $\bar{v}(z)$, see (6b), vanishes for the first time, i.e.:

$$z_N = \pi \sqrt{\frac{2K}{f}} = \pi h_N, \tag{11}$$

see (10). If the vertical mean value is symbolized by

$$\widehat{(\ldots)} = \frac{1}{\pi h_N} \int_0^{\pi h_N} (\ldots)\, dz$$

on gets for the averaged wind direction expressed by the angle δ

$$\widehat{\delta} = \text{arc tg} \widehat{\left(\frac{\bar{v}}{u}\right)} \simeq \text{arc tg} \frac{\widehat{\bar{v}}}{\widehat{\bar{u}}} \tag{12}$$

Using (6a) and 6b) in (12) one obtains

$$\widehat{\bar{u}} = |w_g| \{1 - \frac{1}{2\pi}(1 + e^{-\pi})\}$$

$$\widehat{\bar{v}} = |w_g| \frac{1}{2\pi}(1 + e^{-\pi})$$

and therefore

$$\widehat{\delta} = 11° \, 16' \tag{13a}$$

Another figure can be obtained for the angle between the geostrophic flow and the actual flow in the middle of the EKMAN layer, i.e. for $z = \pi \sqrt{\frac{K}{2f}}$. One gets

$$\delta_{\left(z=\pi\sqrt{\frac{K}{2f}}\right)} = 11° \, 42' \tag{13b}$$

These figures for ϵ are somewhat small compared with the angles obtained in laboratory experiments or observed in the atmosphere.

V. The angle between the axis of the more longitudinal vortices and the basic current

In this section it shall be shown how the angle ϵ is related to the wavelength of the more longitudinal vortices and also to the wavelength of a superimposed vortex system; it is assumed that the axes of the two vortex systems are orthogonal.

At least in this case of two existing (orthogonal) vortex systems it can be shown that also for a parallel shear flow ($\delta = 0$) the angle $\epsilon \neq 0$; this means ϵ cannot be explained by a $\widehat{\delta} \neq 0$ as tried in section IV.

In the laboratory the effect of Coriolis forces is most easily simulated by experiments with rotating disphans. This is also the reason for using a modified cylindrical coordinate system consisting of logarithmic spirals and spirals orthogonal to them as may be seen in figure 10; such spirals should be useful to handle the vortex axes deviating from the circular basic current. The NAVIER-STOKES equation and the continuity equation will be transformed into this coordinate system (σ, η, z) starting from a system of pure cylindrical coordinates (r, ϑ, z); the transformation relations are:

$$\sigma = (r\, e^{-\alpha\vartheta})^{\frac{1}{1+\alpha^2}} \tag{14a}$$

$$\eta = \frac{1}{1+\alpha^2}\,(\alpha \ln r + \vartheta) \tag{14b}$$

$$z = z \tag{14c}$$

The paramter α, more clear in the inverse relations

$$r = \sigma\, e^{\alpha\eta} \tag{15a}$$

$$\vartheta = \eta - \alpha \ln \sigma \tag{15b}$$

gives the angle γ between the logarithmic spiral and the circle by

$$\tau_1 = \text{arc tg}\,\frac{1}{\alpha} \tag{16a}$$

$$\tau_2 = \text{arc tg}\,\alpha \tag{16b}$$

$$\gamma = \text{arc cotg}\,\alpha \tag{16c}$$

see figure 6. In the following the abbreviation

$$\beta \equiv \frac{e^{-\alpha\eta}}{\sqrt{1+\alpha^2}} \tag{17}$$

will be used where

$$\frac{1}{\sqrt{1+\alpha^2}} = \cos(\tau_2), \qquad \frac{\alpha}{\sqrt{1+\alpha^2}} = \sin(\tau_2) \tag{18a, b}$$

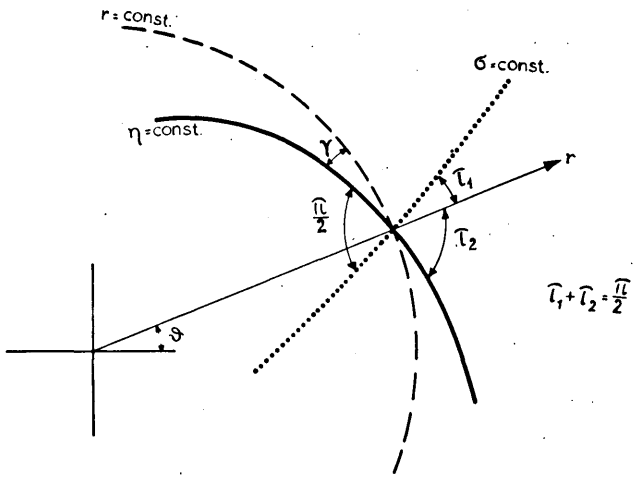

Fig. 6
Bild 6

From (15a), (17) and (18a) it is seen that

$$\frac{\beta}{\sigma} = \frac{\cos(\tau_2)}{r}$$

With the assumption K = const, necessary for an EKMAN layer, the equations of motion and the continuity equation in the (σ, η, z)-system are:

$$u_t + \beta\{u\,u_\sigma + \frac{v}{\sigma}u_\eta - \frac{v^2}{\sigma} + \alpha\frac{uv}{\sigma} + \frac{1}{\bar\rho}p_\sigma\} + w\,u_z - f_v + f^* w\cos(\eta - \alpha\ln\sigma - \tau_2) -$$

$$- K\beta^2\{u_{\sigma\sigma} + \frac{1}{\sigma^2}u_{\eta\eta} + \frac{1}{\sigma}u_\sigma - (1+\alpha^2)\frac{u}{\sigma^2} + \frac{2\alpha}{\sigma}v_\sigma - \frac{2}{\sigma^2}v_\eta\} - K\,u_{zz} = 0 \qquad (20a)$$

$$v_t + \beta\{u\,v_\sigma + \frac{v}{\sigma}v_\eta - \alpha\frac{u^2}{\sigma} + \frac{uv}{\sigma} + \frac{1}{\bar\rho\,\sigma}p_\eta\} + w\,v_z + f\,u - f^* w\sin(\eta - \alpha\ln\sigma - \tau_2) -$$

$$- K\beta^2\{v_{\sigma\sigma} + \frac{1}{\sigma^2}v_{\eta\eta} + \frac{1}{\sigma}v_\sigma - (1+\alpha^2)\frac{v}{\sigma^2} - \frac{2\alpha}{\sigma}u_\sigma + \frac{2}{\sigma^2}u_\eta\} - K\,v_{zz} = 0 \qquad (20b)$$

$$w_t + \beta\{u\,w_\sigma + \frac{v}{\sigma}w_\eta\} + w\,w_z + \frac{1}{\bar\rho}p_z + g - f^*\{v\sin(\eta - \alpha\ln\sigma - \tau_2) - u\cos(\eta - \alpha\ln\sigma - \tau_2)\} -$$

$$- K\beta^2\{w_{\sigma\sigma} + \frac{1}{\sigma^2}w_{\eta\eta} + \frac{1}{\sigma}w_\sigma\} - K\,w_{zz} = 0 \qquad (20c)$$

$$\beta\{u_\sigma + \frac{u}{\sigma} + \frac{1}{\sigma}v_\eta - \frac{\alpha}{\sigma}v\} + w_z = 0 \qquad (20d)$$

A homogeneous medium ($\rho = \bar\rho$) is considered. The three components of the vorticity are:

$$m = \frac{\beta}{\sigma}w_\eta - v_z \qquad (21a)$$

$$n = u_z - \beta\,w_\sigma \qquad (21b)$$

$$q = \frac{\beta}{\sigma}\{(\sigma v)_\sigma - u_\eta - \alpha u\} \qquad (21c)$$

where (21a) gives the component perpendicular to the (η, z)-plane and (21b) that one perpendicular to the (σ, z)-plane, see figure 10. By cross-derivation of (20c) and (20b) an equation for m is obtained, by cross derivation of (20c) and (20a) an equation for n; in both equations the pressure is eliminated. Considering averaged values and small perturbations (symbolized by bar and prime) one obtains the following linearized vorticity equations:

$$m'_t + \beta\{\bar u\,m'_\sigma + u'\bar m_\sigma + \frac{1}{\sigma}\bar v\,m'_\eta + \frac{1}{\sigma}v'\bar m_\eta + \frac{1}{\sigma}\bar m\,u' + \frac{1}{\sigma}m'\bar u + \frac{1}{\sigma}\bar m\,v'_\eta + \frac{1}{\sigma}m'\bar v_\eta +$$

$$+ \frac{\alpha}{\sigma}n'\bar u - \frac{1}{\sigma}n'\bar u_\eta + \frac{\alpha}{\sigma}\bar n\,u' - \frac{1}{\sigma}\bar n\,u'_\eta - \bar u_z\,q' - u'_z\,\bar q\} +$$

$$+ \bar w\,m'_z + w'\bar m_z + \bar m\,w'_z + m'\bar w_z - f\,u'_z + f^* w'_z\sin(\eta - \alpha\ln\sigma - \tau_2) +$$

$$+ \frac{\beta}{\sigma}[f^* v'\sin(\eta - \alpha\ln\sigma - \tau_2) - f^* u'\cos(\eta - \alpha\ln\sigma - \tau_2)]_\eta -$$

$$- K\beta^2\{m'_{\sigma\sigma} + \frac{1}{\sigma^2}m'_{\eta\eta} - \frac{1+\alpha^2}{\sigma^2}m' + \frac{1}{\sigma}m'_\sigma + \frac{2\alpha}{\sigma}n'_\sigma - \frac{2}{\sigma^2}n'_\eta\} - K\,m'_{zz} = 0 \qquad (22a)$$

$$n'_t + \beta \{\bar{u}\, n'_\sigma + u' \bar{n}_\sigma + \frac{1}{\sigma} \bar{v} n'_\eta + \frac{1}{\sigma} v' \bar{n}_\eta + \frac{\alpha}{\sigma} \bar{n} v' + \frac{\alpha}{\sigma} n' v + n \bar{u}'_\sigma + \bar{n} u'_\sigma + n' \bar{u}_\sigma +$$

$$+ \frac{1}{\sigma} m' \bar{v} - m' \bar{v}_\sigma + \frac{1}{\sigma} \bar{m} v' - \bar{m} v'_\sigma - \bar{v}_z\, q' - \bar{q} v'_z \} +$$

$$+ \bar{w}\, n'_z + w' \bar{n}_z + \bar{n} w'_z + n' \bar{w}_z - f v'_z + f^* w'_z \cos(\eta - \alpha \ln \sigma - \tau_2) -$$

$$- \beta\, [f^* v' \sin(\eta - \alpha \ln \sigma - \tau_2) - f^* u' \cos(\eta - \alpha \ln \sigma - \tau_2)]_\sigma -$$

$$- K \beta^2 \{ n'_{\sigma\sigma} + \frac{1}{\sigma^2} n'_{\eta\eta} - \frac{1 + \alpha^2}{\sigma^2} n' + \frac{1}{\sigma} n'_\sigma - \frac{2\alpha}{\sigma} m'_\sigma + \frac{2}{\sigma^2} m'_\eta \} - K\, n'_{zz} = 0 \tag{22b}$$

For the basic current the assumption of a circular flow constant in time is made

$$\bar{v}_{(\vartheta)} = \bar{v}_{(\vartheta)}\,(r, z) \tag{23a}$$

$$\bar{v}_{(r)} = \bar{v}_{(z)} = 0 \tag{23b}$$

which, of course, will not satisfy (20a) and (20b) for the mean values. One should be aware of that; the basic current (23) will be used for the sake of simplicity. Between the vector components in the two coordinate systems the following relationships are valid

$$A_{(\sigma)} = \frac{1}{\sqrt{1 + \alpha^2}} A_{(r)} - \frac{\alpha}{\sqrt{1 + \alpha^2}} A_{(\vartheta)} \tag{24a}$$

$$A_{(\eta)} = \frac{\alpha}{\sqrt{1 + \alpha^2}} A_{(r)} + \frac{1}{\sqrt{1 + \alpha^2}} A_{(\vartheta)} \tag{24b}$$

As a consequence hereof regarding (23b) one has

$$\bar{u} = -\alpha \bar{v} \tag{25}$$

(25) has been used to replace all the quantities $\bar{u}$, $\bar{m}$, $\bar{n}$, $\bar{q}$ and their derivatives by $\bar{v}$ or by the derivatives of $\bar{v}$. Because of (23b) $\bar{w} = 0$.

Considering the σ-spiral as the vortex axis and therefore as the axis of symmetry

$$(u'\sigma)_\sigma = 0 \tag{26a}$$

$$v'_\sigma = w'_\sigma = 0 \tag{26b}$$

the divergence in the (η, z)-plane will vanish

$$\frac{\beta}{\sigma} \{ v'_\eta - \alpha v' \} + w'_z = 0 \tag{27}$$

and a streamfunction $\psi'(\eta, z)$ can be used

$$w' = -\frac{\beta}{\sigma} \psi'_\eta - \alpha \frac{\beta}{\sigma} \psi' \tag{28a}$$

$$v' = \psi'_z \tag{28b}$$

by which (21a) becomes

$$m' = -\frac{\beta^2}{\sigma^2} \psi'_{\eta\eta} + \frac{\alpha^2 \beta^2}{\sigma^2} \psi' - \psi'_{zz} \tag{28c}$$

Quite analogous expressions are obtained when the η-spiral is considered as vortex axis. The derivations with respect to η have to vanish

$$(v' e^{-\alpha\eta})_\eta = 0 \tag{29a}$$

$$u'_\eta = w'_\eta = 0 \tag{29b}$$

The vanishing of the divergence in the (σ, z)-plane

$$\beta \{u'_\sigma + \frac{u'}{\sigma}\} + w'_\sigma = 0 \tag{30}$$

allows the use of a streamfunction $\varphi'(\sigma, z)$ by which

$$w' = -\beta \varphi'_\sigma + \frac{\beta}{\sigma} \varphi' \tag{31a}$$

$$u' = -\varphi'_z \tag{31b}$$

and according to (21b)

$$n' = -\beta^2 \varphi'_{\sigma\sigma} - \frac{\beta^2}{\sigma} \varphi'_\sigma + \frac{\beta^2}{\sigma^2} \varphi' - \varphi'_{zz} \tag{31c}$$

Making use of (28a), (28b) and (28c) in (22a) one obtains a differential equation for $\psi'(\eta, z, t)$ containing also $u'(\eta, z, t)$ as a further perturbation quantity.

In the same manner using (31a), (31b) and (31c) in (22b) a differential equation for $\varphi'(\sigma, z, t)$ is obtained which contains also $v'(\sigma, z, t)$. The two differential equations are:

$$\begin{aligned}
&\frac{\beta}{\sigma} \{-2\bar{v}[\psi'_{\eta zz} + (1+\alpha^2) u'_z] + \bar{v}_z [\alpha \psi'_z - 2(1+\alpha^2) u'] + \bar{v}_{zz} [\psi'_\eta + \alpha \psi']\} + \\
&+ \frac{\beta^2}{\sigma^2} \{-\psi'_{\eta\eta t} + \alpha^2 \psi'_t + K[2\psi'_{\eta\eta zz} - (1+2\alpha^2)\varphi'_{zz} + 2u'_{\eta z} + 2\alpha u'_z]\} + \\
&+ \frac{\beta^3}{\sigma^3} \{\bar{v}\alpha^2 \psi'_\eta - \bar{v}\psi'_{\eta\eta\eta}\} + \\
&+ \frac{\beta^4}{\sigma^4} K\{\psi'_{\eta\eta\eta\eta} - 4\alpha\psi'_{\eta\eta\eta} + (1+2\alpha^2)\psi'_{\eta\eta} - 2\alpha(1-2\alpha^2)\psi'_\eta - 3\alpha^2(1+\alpha^2)\psi'\} - \\
&- \psi'_{zzt} + K\psi'_{zzzz} = 0
\end{aligned} \tag{32a}$$

$$\begin{aligned}
&\frac{\beta}{\sigma} \{2\bar{v}[\alpha\sigma\varphi'_{\sigma zz} - (1+\alpha^2) v'_z] - \bar{v}_z [\alpha\varphi'_z + 2(1+\alpha^2) v'] - \bar{v}_{zz}\alpha[\sigma\varphi'_\sigma + \varphi']\} + \\
&+ \frac{\beta^2}{\sigma^2} \{-\sigma^2 \varphi'_{\sigma\sigma t} - \sigma\varphi'_{\sigma t} + \varphi'_t + K[2\sigma^2\varphi'_{\sigma\sigma zz} - (1+2\alpha^2)\varphi'_{zz} + 2\sigma\varphi'_{\sigma zz} - 2\alpha\sigma v'_{\sigma z} + 2\alpha v'_z]\} + \\
&+ \frac{\beta^3}{\sigma^3} \alpha\bar{v}\{\sigma^3\varphi'_{\sigma\sigma\sigma} + 3\sigma^2\varphi'_{\sigma\sigma}\} + \\
&+ \frac{\beta^4}{\sigma^4} K\{\sigma^4\varphi'_{\sigma\sigma\sigma\sigma} + 2\sigma^3\varphi'_{\sigma\sigma\sigma} - (3-\alpha^2)\sigma^2\varphi'_{\sigma\sigma} + (3-\alpha^2)\sigma\varphi'_\sigma - 3(1+\alpha^2)\varphi'\} - \\
&- \varphi'_{zzt} + K\varphi'_{zzzz} = 0
\end{aligned} \tag{32b}$$

According to (23a) the basic current has been specified as axi-symmetric; in addition stationarity is now postulated for the basic current and for its dependence on r it is assumed

$$\bar{v}_{(\vartheta)} = B(z)\, r \tag{33}$$

corresponding to the inner part of a RANKINE vortex. From (33) with (24b) and (15a) one gets

$$\bar{v}(\sigma, \eta, z) = \frac{\sigma}{\beta} \frac{B(z)}{1+\alpha^2} \tag{34}$$

Using the basic flow (34) in (32a) and (32b) in both these equations terms with β/σ as coefficient, terms with β^2/σ^2 and terms with β^4/σ^4 will appear but also terms which are free of β/σ. According to (19) β/σ is very small if r is very large. By the assumption of very large r (which may be in conflict with (33) valid only in the inner part of a RANKINE vortex) all the terms containing β^2/σ^2 and β^4/σ^4 may be neglected. Hereby the two equations are much simpler.

Equation (32a) contains ψ' and u', the second equation needed to close the system is equ. (20a) in linearized form for the perturbation u'; in this equation the conditions (26a) and (26b) have to be used and also $p_\sigma = 0$.

The form of a moving harmonic wave shall be assumed for the two perturbations

$$\psi'(\eta, z, t) = \Psi(z) \exp\{i\mu(\eta - c_1 t)\} \tag{35a}$$

$$u'(\eta, z, t) = U(z) \exp\{i\mu(\eta - c_1 t)\} \tag{35b}$$

Herewith one obtains for (32a) and the just described equation developed from (20a) the following set of two wave number equations:

$$K\Psi_{zzzz} + i\mu\left(c_1 - \frac{2}{1+\alpha^2} B\right)\Psi_{zz} + \frac{\alpha}{1+\alpha^2} B_z \Psi_z + \frac{i\mu+\alpha}{1+\alpha^2} B_{zz}\Psi - (2B+f)U_z - 2B_z U = 0 \tag{36}$$

$$-KU_{zz} + \left\{\frac{\alpha+i\mu}{1+\alpha^2} B - i\mu c_1\right\} U + \frac{i\mu+\alpha}{1+\alpha^2} \alpha B_z \Psi - (2B+f)\Psi_z = 0 \tag{37}$$

On the other hand equation (32b) contains φ' and v'; here (20b) in linearized form and with regard of (29a), (29b) and $p_\eta = 0$ gives the second equation needed to close the system. The form of a moving harmonic wave will also be assumed

$$\varphi'(\sigma, z, t) = -\Phi \exp\left\{i\nu\left(\frac{\ln\sigma}{\alpha} + c_2 t\right)\right\} \tag{38a}$$

$$v'(\sigma, z, t) = V \exp\left\{i\nu\left(\frac{\ln\sigma}{\alpha} + c_2 t\right)\right\} \tag{38b}$$

Herewith one obtains for (23b) and the forementioned equation originating from (20b) a set of the following two wavenumber equations:

$$-K\Phi_{zzzz} + i\nu\left(c_2 - \frac{2}{1+\alpha^2} B\right)\Phi_{zz} + \frac{\alpha}{1+\alpha^2} B_z \Phi_z + \frac{i\nu+\alpha}{1+\alpha^2} B_{zz}\Phi - (2B+f)V_z - 2B_z V = 0 \tag{39}$$

$$KV_{zz} + \left\{\frac{\alpha+i\nu}{1+\alpha^2} B - i\nu c_2\right\} V + \frac{i\nu+\alpha}{1+\alpha^2} \frac{1}{\alpha} B_z \Phi - (2B+f)\Phi_z = 0 \tag{40}$$

The two systems of wavenumber equations (36), (37) und (39), (40) are symmetric with the exception of the following deviations:

(a) The sign of the first term in (36) is opposite to the sign of the first term in (39)

(b) The sign of the first term in (37) is opposite to the sign of the first term in (40)

(c) In the third term of equation (37) appears the factor α but in the third term of (40) the factor $\frac{1}{\alpha}$

The first equations of each set namely (36) and (39) are completely symmetric in the inviscid case ($Re \to \infty$). Let us assume this for further comparison. This is justified by the argument that the terms containing Ψ_{zzzz} and/or Φ_{zzzz} are considered to be less important.

Then the amplitude functions $\Phi(z)$ and $V(z)$ obey the same differential equation as $\Psi(z)$ and $U(z)$; in both cases the transition to instability of the boundary layer depends on B, B_z, B_{zz} and f. If instability occurs vortex rolls of both systems should be formed where the wavenumber of the more longitudinal vortices is μ and of the more transversal vortex rolls is ν. For a comparison of these two wavenumbers one has to consider that ν should be counted along σ instead $\frac{\ln\sigma}{a}$

$$\nu_{\left(\frac{\ln\sigma}{a}\right)} = \alpha\, \nu_{(\sigma)} l \tag{41a}$$

where

$$l = \frac{\ln\sigma \Big|_{\vartheta=2\pi}^{\vartheta=0}}{\sigma \Big|_{\vartheta=2\pi}^{\vartheta=0}} = \frac{2\pi}{\alpha \exp\left(\frac{2\pi}{\alpha}\right)}$$

obtained with (15b) for η = const. Therefore (41a) is

$$\nu_{(\sigma)} = \frac{\exp\left\{\frac{2\pi}{\alpha}\right\}}{2\pi}\, \nu_{\left(\frac{\ln\sigma}{a}\right)} \tag{41b}$$

It has been concluded that the two wavenumbers $\mu_{(\sigma)}$ and $\nu_{\left(\frac{\ln\sigma}{a}\right)}$ become unstable at the same time and have to equal each other with respect to the symmetry of (36) and (39):

$$\mu_{(\sigma)} = \nu_{\left(\frac{\ln\sigma}{a}\right)} \tag{42}$$

(42) with (41b) gives the ratio of the two wave numbers (each on the same measure)

$$\frac{\nu}{\mu} = \frac{\exp\left\{\frac{2\pi}{\alpha}\right\}}{2\pi} \tag{43}$$

Since an axi-symmetric basic current has been chosen (23) one notices from figure 6, that $\gamma = \epsilon$ and $\epsilon = \frac{\pi}{2} - \tau_2$ or with use of (16b)

$$\epsilon = \operatorname{arc\,cotg} \alpha \tag{44}$$

Inserting (43) in (44) one gets the relationship between the angle ϵ and the wavenumber ratio

$$\boxed{\epsilon = \operatorname{arc\,tg}\left\{\frac{\ln\left(2\pi\frac{\nu}{\mu}\right)}{2\pi}\right\}} \tag{45}$$

The following table gives few values of the wavenumber ratio and the corresponding angle ϵ.

$\frac{\nu}{\mu}$	α	ϵ
0.5	5.51	11°10′
0.72	4.17	13°30′
1.00	3.41	16°20′
2.00	2.48	22°00′

It is seen that for an observed angle $\epsilon = 13°30'$ the wavelength in the longitudinal direction σ is larger than that one in the transversal direction η, it is $L_\sigma = 1.4\ L_\eta$. The experiments by FALLER and KAYLOR gave $2 \leqslant L_\sigma/L_\eta < 3$ which would imply $\epsilon \leqslant 11°$ according to formula (45).

VI. The verification of formula (45) by laboratory experiments

Recent experiments by HORST (1969), very briefly described in section I, see fig. 9, allow to measure the angle ϵ as well as the simultaneous wavenumbers μ and ν. This has been done for a total of 72 runs giving ϵ, μ, ν for varied experimental parameters (diameter of the cylinder, height of the fluid, initial circular velocity, viscosity). Using the measured values of the wavenumbers μ and ν in equation (45) a "theoretical" angle ϵ_{th} has been computed and has been compared with the measured angle ϵ. The result is shown in figure 7 where the rather large scattering of points is overcome by comprehending them for equally spaced stripes. Indead, one notices a systematic deviation, however the mean values agree very well

$$\tilde{\epsilon}_{EXP} = 13°11'; \quad \tilde{\epsilon}_{THEO} = 13°19'$$

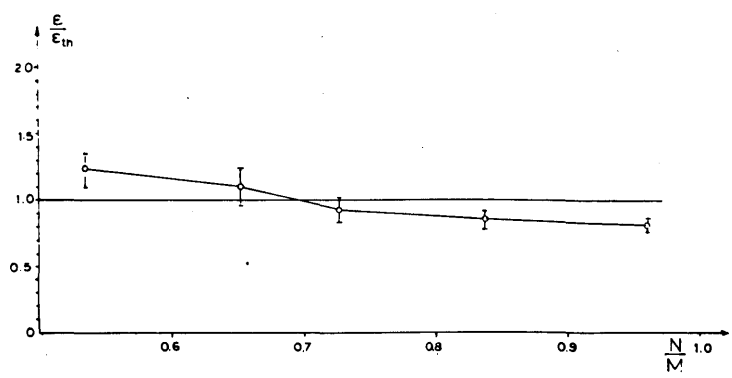

Fig. 7
Verification of formula (45) by laboratory experiments (after HORST 1969); N/M in the figure means ν/μ in the text.

Bild 7
Nachprüfung der Formel (45) durch Laboratoriumsexperimente (nach HORST 1969); N/M in der Figur bedeutet ν/μ im Text.

One should remember, that besides some other assumptions for the formula (45) orthogonality of the two vortex systems has been assumed; in the experiments the angle between the axes of the two vortex systems has not been measured, it is estimated to be about 60°–70°; this may be a reason for the systematic deviation. Also one should keep in mind that the assumption (23a) of an axi-symmetric basic current is inadequate for HORSTs experiments where the basic current has a radial component depending on height and therefore is similar to an EKMAN boundary layer flow.

VII. The orientation of cloud streets and seif-dunes

There is no doubt that the cloud streets are formed by more or less longitudinal vortex rolls due to instability of the EKMAN layer; for the destabilisation the Coriolis forces may be responsible as well as buoyancy forces may do when convection occurs. If both vortex systems are perceptible and the two wavenumbers are evaluable (as for instance from figure 5) the direction of the geostrophic flow can be determined; this would differ only very little from the direction of the mean wind at the cloud base.

Cloud streets will be reorientated immediately when the mean wind changes its direction.

A completely different situation exists with respect to the seif-dunes. These are probably formed also by the helical motion in vortex rolls due to Ekman layer instability. But the formation of seif-dunes takes a very long time in which climatic changes are possible including changes of the direction of the prevailing wind. Therefore the orientation of seif-dunes should give with about 14° to the right the direction of the wind averaged over the whole time of the formation of these dunes except those periods in which the boundary layer has not been unstable. Comparison of this direction with the wind direction given by climatological data of our time should allow conclusions on long term climatic changes.

Since the interior part of the seif-dunes is firm (only the sand of the outer part can be moved by wind) these dunes are fixed. When EKMAN layer instability occurs, the formation of vortex rolls does not take place over a plane earth surface as assumed in the theory of instability but over a waved topography prescribing already the angle ϵ and the wavenumber μ in the lateral direction, for which the amplitude of velocity perturbations will amplify. This means only the wavenumber ν in the more longitudinal direction is not prescribed directly by the topographic features but, of course, is determined by ϵ and μ according to (45). It should be

$$\nu = \mu \frac{\exp\{2\pi \operatorname{tg} \epsilon\}}{2\pi}, \quad \epsilon > 0 \tag{46}$$

Some values of the wavenumber ratio are given in the following table

ϵ	$\frac{\nu}{\mu}$	ϵ	$\frac{\nu}{\mu}$
10°	0.485	30°	5.31
15°	0.850	35°	13.0
20°	1.57	40°	31.9
25°	3.39	45°	86.6

To give an example: If $\epsilon = 40°$ and the wavelength in the transversal direction $L_\eta = 3.5$ km, a wavelength in the direction along the dunes $L_\sigma = 110$ m should occur. In figure 8, after CLOS-ARCEDUC (1968), one notices long chains of dunes showing a structure along these chains, which already have been cut to pieces. It seems possible to explain such a structure as the effect of the superimposed second vortex system having a rather high wavenumber because of a large value of ϵ. This would mean that the prevailing winds which had originally an almost east-west direction (from 85°, whereas the chains of dunes run 72° to 252°) would have turned to get a southerly component, say from 110° to 290° (i.e.: $\epsilon = 38°$) and remained in that direction. The effect of the superimposed second vortex system now is supported by the basic current clearly shown by the sand blown to the right of the chain. It has been formed a "lefthand side type" of an Elb (after CLOS-ARCEDUC 1968).

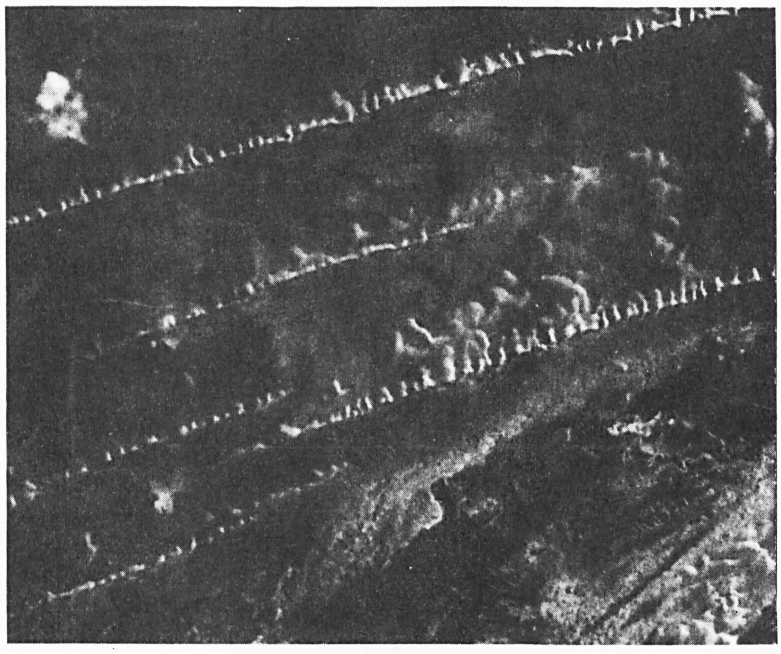

Fig. 8 "Left-hand side" type of seifdunes (after CLOS-ARCEDUC 1968).

Bild 8 „Linksseitiger" Typ ovn Seifdünen (nach CLOS-ARCEDUC 1968).

The use of the logarithmic spirals for the coordinate system in the foregoing derivation excludes cases with $\epsilon < 0$; however the reasoning is also possible for $\epsilon < 0$ and allows also an explanation of the so-called "righthand side type" of an Elb.

If the prevailing wind would change for more than 45° from the original direction the vortices with their axis in the lateral direction and the vortices perpendicular to them would have to change their rôles. In this case ϵ and ν would be prescribed by the existing seif-dunes where μ would be determined by (45).

It is felt that the gross-features of seif-dunes can be explained by the two vortex systems due to an instability of the EKMAN boundary layer.

VIII. Acknowledgment

The author wishes to thank Dr. H. FRANZ for his helpful assistance on the transformation of the equations into the (σ, η, z)-coordinate system.

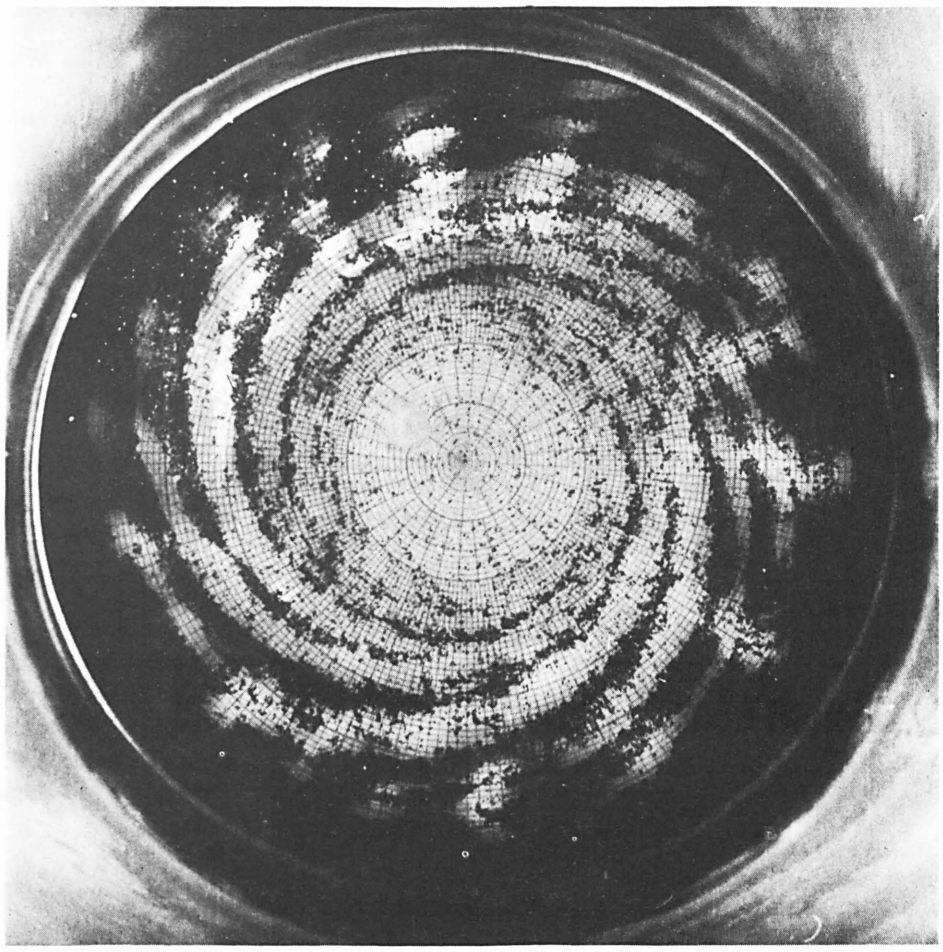

Fig. 9. The double vortex system due to boundary layer instability as produced in laboratory experiments by HORST (1969).

Bild 9. Zweifaches Wirbelsystem infolge Grenzschichtinstabilität erzeugt in Laborexperimenten von HORST (1969)

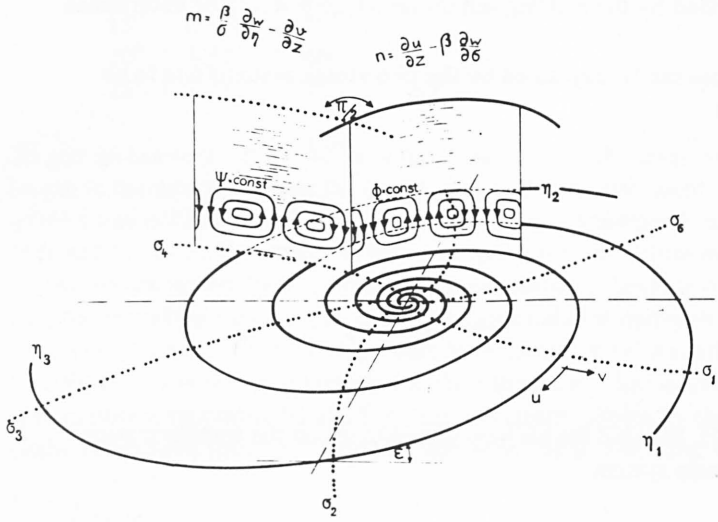

Fig. 10
Schematic representation of the (σ, η, z)-coordinate system.

Bild 10
Schematische Darstellung des (σ, η, z)-Koordinatensystems

IX. References

ANGELL, J. K., PACK, D. H. and DICKSON, C. R., 1968, A Langrangian Study of Helical Circulations in the Planetary Boundary Layer. J. Atm. Sc. **25**, 707–717.

AVSEC, D., 1939, Tourbillons thermoconvectifs dans l'air, application à la météorologie. L'Académie de Paris, Thèse Dr. Sc. Serie A 1910, No. d'ordre 2777.

BAGNOLD, R. A., 1945, The Physics of Blown Sand and Desert Dunes. London, Methuen and Co. pp. 265.

BARCILON, V., 1965, Stability of a Non-divergent Ekman Layer. Tellus **17**, 53–68.

CLOS-ARCEDUC, A., 1968, Emploi des couvertures photographiques aériennes pour la vérification des théories relatives à la formation des dunes allongées dans une direction voisine de celle du vent. XI^{e}Congrès International de Photogrammetrie Lausanne 8–20 Juillet 1968, pp. 8.

FALLER, A. J., 1963, An Experimental Study of the Instability of the Laminar Ekman Boundary Layer. J. Fluid Mech. **15**, 560–575.

FALLER, A. J. and KAYLOR, R. E., 1965, A Numerical Study of the Laminar Ekman Boundary Layer. Techn. Note BN 410, July 1965, 26 pp. Inst. Fluid Dyn., Univ. of Maryland.

FALLER, A. J. and KAYLOR, R. E., 1966, Investigations of Stability and Transition in Rotating Boundary Layers. in: Dynamics of Fluids and Plasmas edited by S. Pai a. o., 309–329, Academic Press New York.

GÖRTLER, H., 1940, Über eine dreidimensionale Instabilität laminarer Grenzschichten an konkaven Wänden. Nachr. Ges. Wiss. Göttingen, Nachr. aus der Mathmatik **2**, 1, 26 pp.

GÖRTLER, H., 1959, Über eine Analogie zwischen den Instabilitäten laminarer Grenzschichtströmungen an konkaven Wänden und an erwärmten Wänden. Ing. Archiv **28**, 71–78.

GREGORY, N., STUART, J. T. and WALKER, W. S., 1955, On the Stability of Threedimensional Boundary Layers with Application to the Flow Due to a Rotating Disk. Phil. Trans. Roy. Soc., London, A **248**, 155–199.

HORST, W., 1969, Experimentelle Untersuchungen der Wirbelstruktur in einer instabilen Ekman-Grenzschicht. Ph. Thesis, Inst. f. Meteorologie, Techn. Hochschule Darmstadt, Germ.

KUO, H. L., 1963, Perturbations of Plane Couette Flow in Stratified Fluid and Origin of Cloud Streets. Phys. of Fluids, **6**, 195–211.

LILLY, D. K., 1966, On the Instability of Ekman Boundary Layer. J. Atm. Sc. **23**, 481–494.

MALKUS, J. S. and RONNE, C., 1960, Cloud distributions over the Tropical Oceans in Relation to Large Scale Flow Patterns. Geophys. Monogr., Am. Geophys. Union Nr. 5, 45–56.

PLANCK, V. G., 1966, Wind Conditions in Situations of Patternform and Non-pattern-form Cumulus Convection. Tellus **18**, 1–12.

STERN, M. S., 1960, Instability of Ekman Flow at Large Taylor Numbers. Tellus **12**, 399–417.

WOODCOCK, A. H., 1940, Convection and Soaring over the Open Ocean. J. Mar. Res. **3**, 248–253.

Beiträge zur Physik der Atmosphäre, 44. Band, 1971, S. 168–186

Einfluß der thermischen Schichtung auf die Stabilität einer Ekman'schen Grenzschichtströmung

The Stability of an Ekman Boundary Layer Flow as Influenced by the Thermal Stratification

D. Etling

Technische Hochschule Darmstadt Institut für Meteorologie

Eingegangen am 7. April 1971

Zusammenfassung: Die dynamische Instabilität einer Ekman'schen Grenzschichtströmung in Form von horizontalen Wirbelrollen wird mit Hilfe einer Störungsanalyse untersucht. Zwei Faktoren bestimmen die Bildung solcher Wirbel in der Grenzschicht. Bei labiler Schichtung macht sich der Einfluß der thermischen Konvektion mit einer kritischen Wellenzahl von etwa $\alpha = 0.5$ bemerkbar, während bei stabiler Schichtung ein reiner Scherungseinfluß mit einer kritischen Wellenzahl von $\alpha = 0.2$ überwiegt.

Es wird gezeigt, daß die kritische Reynoldszahl beträchtlich mit der statischen Stabilität variiert. Bei labiler Schichtung setzt die dynamische Instabilität schon bei kleinen Reynoldszahlen ein, bei stabiler Schichtung erst bei sehr großen.

Außerdem kann gezeigt werden, daß die kritische Reynoldszahl noch von der Orientierung des Grundstroms zur Ost-West Richtung abhängt, was auf den Einfluß der oft vernachlässigten Vertikalkomponente der Coriolis-Kraft zurückzuführen ist.

Summary: The dynamical instability of an Ekman boundary layer appearing as vortex rolls is investigated by a perturbation analysis. The formation of such vortex rolls is caused by two effects. With unstable stratification the influence of thermal convection is observed with a critical wave number of about $\alpha = 0.5$, with stable stratification shearing instability dominates according to a critical wave number of $\alpha = 0.2$.

It is shown that the critical Reynolds number varies considerable with the thermal stratification. With unstable stratification the dynamical instability appears even at low Reynolds numbers, with stable stratification high Reynolds numbers are needed.

Besides it is shown that the critical Reynolds number is a function of the orientation of the mean flow to the east-west direction, due to the vertical component of the Coriolis force, which is often neglected.

Résumé: A l'aide de la théorie des perturbations, l'auteur étudie l'instabilité dynamique qui apparaît dans un courant de la couche limite d'Ekman sous la forme d'une suite de tourbillons à axes horizontaux parallèles (rouleaux). Deux facteurs déterminent la formation de tels tourbillons dans la couche limite. Pour une stratification instable, l'influence de la convection thermique se marque lorsque le nombre d'ondes critique est d'environ $\alpha = 0.5$. Par contre, pour une stratification stable, une nette influence de l'instabilité du vent n'est prépondérante que pour un nombre d'ondes critique de $\alpha = 0.2$.

L'auteur démontre que le nombre critique de Reynolds varie considérablement avec la stabilité statique. Dans le cas d'une stratification instable, l'instabilité dynamique apparaît à partir de petits nombres de Reynolds, dans une stratification stable, que pour les grands nombres de Reynolds.

En outre, l'auteur démontre également que le nombre critique de Reynolds peut dépendre de l'orientation du courant de base par rapport à la direction $W \rightarrow E$, ce qui résulte de la composante verticale de la force de Coriolis, laquelle est souvent négligée.

Symbolverzeichnis

Stehen 2 Symbole nebeneinander, so bedeutet der kleine Buchstabe eine dimensionsbehaftete, der große eine dimensionslose Größe.

$c, C = \frac{c}{\lvert \mathbf{v}_g \rvert}$	Phasengeschwindigkeit, C_i = Imaginärteil, C_r = Realteil
$D = \sqrt{\frac{2k_m}{f}}$	charakteristische Länge
$f = 2\omega \sin\varphi,\ F = \frac{fD}{\lvert \mathbf{v}_g \rvert}$	Coriolisparameter
$f^* = 2\omega \cos\varphi,\ F^* = \frac{f^*D}{\lvert \mathbf{v}_g \rvert}$	
g	Erdbeschleunigung
H	charakteristische Höhe
k_h	turbulenter Diffusionskoeffizient für Wärme
k_m	turbulenter Diffusionskoeffizient für Impuls
$l, L = \frac{l}{D}$	Wellenlänge
N	Intervallzahl
$p, = \frac{p}{\rho v_g^2}$	Druck
Pr_t	turbulente Prandtlzahl
S	Maß für die statische Stabilität, s. Gl. (9c)
$t, T = \frac{t \lvert \mathbf{v}_g \rvert}{D}$	Zeit
u, U	Geschwindigkeitskomponente in x- oder X-Richtung
v, V	Geschwindigkeitskomponente in y- oder Y-Richtung
$\mathbf{v}, \mathbf{V}$	Geschwindigkeit
$\mathbf{v}_g$	geostrophischer Wind
w, W	Geschwindigkeitskomponente in z- oder Z-Richtung
α	dimensionslose Wellenzahl
∂	Operator
Δ	Intervalldistanz
ϵ	Ablenkungswinkel
λ	Orientierungswinkel des Koordinatensystems
μ	komplexe Amplitude im Wellenansatz für U'
φ	1. komplexe Amplitude im Wellenansatz für die Stromfunktion ψ'
ψ	dimensionslose Stromfunktion
ρ	Dichte
σ	komplexe Amplitude im Wellenansatz für Θ'
$\vartheta, \Theta = \frac{\vartheta}{\frac{\partial \bar{\vartheta}}{\partial z} H}$	potentielle Temperatur
$\xi = (\nabla \times \mathbf{V})_x$	dimensionslose Vorticity
ω	Winkelgeschwindigkeit der Erdrotation

1. Einleitung

Als Wolkenstraßen bezeichnet man die Erscheinung bänderförmig angeordneter Cumulusbewölkung, die sich bis über 100 km Länge erstreckt. Untersuchungen von PLANK (1966) und KUETTNER (1967) haben gezeigt, daß der Abstand der Wolkenbänder 2–5 km beträgt und diese einen Winkel $\epsilon = 13°–16°$ mit der Richtung des geostrophischen Windes bilden. An der Erdoberfläche findet man ähnlich angeordnete Dünenketten, sogenannte Seifdünen, die in Arbeiten von HANNA (1969) und WIPPERMANN (1969) näher beschrieben sind.

Beide Phänomene sind möglicherweise durch das Auftreten von Wirbeln mit horizontaler Achse in der atmosphärischen Grenzschicht zu erklären. Die Bildung solcher Wirbelrollen kann durch Scherungsinstabilitäten der Ekmanschen Grenzschichtströmung oder durch thermische Konvektion ausgelöst werden. Einen direkten Nachweis dieser Zirkulationen in der Atmosphäre erbrachten ANGELL, PACK und DICKSON (1968) durch Bahnvermessungen von Tetroons.

Eingehender konnte die Wirbelbildung in der Ekman-Schicht in Laborexperimenten untersucht werden. FALLER (1963), FALLER und KAYLOR (1966) machten die Wirbelrollen in einem rotierenden Wassertank durch Farbstoff sichtbar, HORST (1970) wies diese durch Anhäufung von Sand nach. TATRO und MOLLO-CHRISTENSEN (1967), CALDWELL und v.ATTA (1970) untersuchten rotierende Luftströmungen mit Hitzdrahtanemometern. Von allen Autoren übereinstimmend wurden 2 Arten von Wirbelsystemen gefunden.

Mit Typ I werden allgemein fast stationäre Wirbel bezeichnet, deren Achse gegen die geostrophische Strömung um $\epsilon = 14°$ nach links gedreht ist. Die mit der Ekman-Länge D normierte Wellenlänge beträgt $L = 12$, die kritische Reynoldszahl $Re_{krit} = 125$. Wirbel mit großer Phasengeschwindigkeit und Wellenlängen von $L = 22–33$ treten bei $Re_{krit} = 65$ auf. Diese mit Typ II bezeichneten Wirbel bilden einen Winkel zwischen $0°$ und $-20°$ mit der Richtung der geostrophischen Strömung.

Diese Ergebnisse werden durch theoretische Arbeiten von FALLER und KAYLOR (1966), LILLY (1966) und BROWN (1970) im wesentlichen bestätigt.

Wirbel mit horizontaler Achse, die rein thermischer Natur sind, wurden für den Fall einer einfachen Scherströmung und ohne Berücksichtigung der Coriolis-Kräfte in Laborexperimenten von AVSEC (1939) und auf theoretischem Wege von OGURA (1969) untersucht. Es treten hier vorwiegend Wirbel mit der Wellenzahl $\alpha = 0.5$ auf ($\alpha = \frac{2\pi}{L}$), wobei die Wirbelachse parallel zur Strömungsrichtung ist.

Es ist bisher weitgehend ungeklärt, ob die in der Atmosphäre auftretenden Wirbel mit horizontaler Achse hauptsächlich auf Konvektion zurückzuführen sind, oder ob es sich meist um Scherungsinstabilitäten der Ekman-Schicht handelt.

In der folgenden Arbeit soll daher untersucht werden, wie sich eine Ekmansche Grenzschichtströmung unter dem zusätzlichen Einfluß der thermischen Konvektion verhält.

Aus einer Störungsanalyse der thermohydrodynamischen Grundgleichungen erhält man als Ergebnis Wachstumsraten αC_i der Störungen in Abhängigkeit von der Reynoldszahl Re, der Wellenzahl α, dem Orientierungswinkel ϵ und der thermischen Schichtung.

2. Formulierung des Problems

Das x, y, z Koordinatensystem ist so orientiert, daß die Wirbelachse mit der x-Achse, die mit der Ostrichtung und Winkel λ bildet, zusammenfällt. Ein weiteres Koordinatensystem $x°, y°, z$ ist im Uhrzeigersinn um den Winkel ϵ um die z-Achse gedreht, so daß die $x°$-Achse die Richtung des geostrophischen Windes hat.

Für Feldgrößen, die durch eine übergreifende Mittelbildung geglättet sind, lauten im x, y, z-System die Bewegungsgleichungen, die Kontinuitätsgleichung, sowie die Adiabatengleichung für eine inkompressible Strömung entsprechend den Gleichungen (1a)–(1e); dabei wurde die molekulare Reibung gegenüber der turbulenten Reibung vernachlässigt.

$$\frac{\partial u}{\partial t} + (\mathbf{v} \cdot \nabla) u - fv + f^* w \cos\lambda + \frac{1}{\rho}\frac{\partial P}{\partial x} - k_m \nabla^2 u = 0 \tag{1a}$$

$$\frac{\partial v}{\partial t} + (\mathbf{v} \cdot \nabla) v + fu - f^* w \sin\lambda + \frac{1}{\rho}\frac{\partial P}{\partial y} - k_m \nabla^2 v = 0 \tag{1b}$$

$$\frac{\partial w}{\partial t} + (\mathbf{v} \cdot \nabla) w + f^* v \sin\lambda - f^* u \cos\lambda + \frac{1}{\rho}\frac{\partial P}{\partial z} - k_m \nabla^2 w + g = 0 \tag{1c}$$

$$\nabla \cdot \mathbf{v} = 0 \tag{1d}$$

$$\frac{\partial \vartheta}{\partial t} + (\mathbf{v} \cdot \nabla) \vartheta - k_h \nabla^2 \vartheta = 0 \tag{1e}$$

Es sind $f = 2\omega \sin\varphi$ und $f^* = 2\omega \cos\varphi$ die Coriolis-Parameter, worin ω die Winkelgeschwindigkeit der Erdrotation und φ die geographische Breite ist. k_m und k_h sind die als konstant angenommenen turbulenten Diffusionskoeffizienten für Impuls und Wärme. ϑ ist die potentielle Temperatur. Die übrigen Bezeichnungen haben die übliche Bedeutung.

Für die potentielle Temperatur wird vorausgesetzt, daß sich ihr (horizontales) Flächenmittel nur linear mit der Höhe ändert.

$$\vartheta = \bar{\vartheta}_0 + \frac{\partial\bar{\vartheta}}{\partial z} z + \vartheta' \tag{2}$$

$\bar{\vartheta}_0$ ist der Wert für $z = 0$, $\frac{\partial\bar{\vartheta}}{\partial z}$ der als konstant angenommene Gradient der mittleren potentiellen Temperatur und ϑ' die Abweichung vom Mittelwert.

Die Variablen in (1a)–(1e) werden dimensionslos gemacht, wobei die einzelnen Symbole durch ihre Großbuchstaben ersetzt werden. Benutzt man $|\mathbb{v}_g|$, den Betrag des geostrophischen Windes, als Normierungsgeschwindigkeit, und bezeichnet man mit D eine charakteristische Länge sowie mit H eine charakteristische Höhe, so sind die dimensionslosen Größen gegeben durch:

$$X = \frac{x}{D}, \qquad Y = \frac{y}{D}, \qquad Z = \frac{z}{D}, \tag{3a}$$

$$U = \frac{u}{|\mathbb{V}_g|}, \qquad V = \frac{v}{|\mathbb{V}_g|}, \qquad W = \frac{w}{|\mathbb{V}_g|} \tag{3b}$$

$$T = \frac{|\mathbb{v}_g|}{D} t, \qquad \mathbb{V} = \frac{\mathbb{v}}{|\mathbb{V}_g|}, \qquad \Pi = \frac{1}{\mathbb{V}_g^2} \frac{P}{\rho} \tag{3c}$$

$$F = \frac{D}{|\mathbb{V}_g|} f, \qquad F^* = \frac{D}{|\mathbb{V}_g|} f^*, \qquad \Theta = \frac{\vartheta}{-\frac{\partial\bar{\vartheta}}{\partial z} H} \tag{3d}$$

Alle folgenden Betrachtungen gelten für eine barotrope Grenzschicht $\left(\frac{\partial \mathbb{v}_g}{\partial z} = 0\right)$, so daß $|\mathbb{v}_g|$ als Normierungsgröße verwendet werden kann. D ist die sogenannte Ekman Länge.

$$D = \sqrt{\frac{2k_m}{f}} \tag{4}$$

Mit den Gleichungen (1a)–(1e) wird für die dimensionslos gemachten Größen eine Störungsrechnung durchgeführt; es sei:

$$\mathbb{V} = \bar{\mathbb{V}} + \mathbb{V}', \quad \Theta = \bar{\Theta} + \Theta', \quad \Pi = \bar{\Pi} + \Pi' \tag{5}$$

Außerdem wird in (1c) von der Boussinesq-Approximation

$$\frac{\rho'}{\bar{\rho}} = -\frac{\vartheta'}{\bar{\vartheta}} \tag{6}$$

Gebrauch gemacht.

Unter den Voraussetzungen eines stationären Grundzustandes

$$\frac{\partial\bar{\Theta}}{\partial T}=\frac{\partial\bar{V}}{\partial T}=0 \tag{7a}$$

eines horizontalen und horizontal homogenen Grundstromes

$$\bar{W}=0 \tag{7b}$$

$$\frac{\partial\bar{U}}{\partial X}=\frac{\partial\bar{U}}{\partial Y}=\frac{\partial\bar{V}}{\partial X}=\frac{\partial\bar{V}}{\partial Y}=0 \tag{7c}$$

sowie der Barotropiebedingung

$$\frac{\partial\bar{\Theta}}{\partial X}=\frac{\partial\bar{\Theta}}{\partial Y}=0 \tag{7d}$$

und einer Bedingung für die Unveränderlichkeit von Störgrößen entlang der in der X-Richtung liegenden Wirbelachse

$$\frac{\partial}{\partial X}(\ldots)'=0 \tag{7e}$$

lauten die vollständigen Störungsgleichungen:

$$Re\left[\frac{\partial U'}{\partial T}+\bar{V}\frac{\partial U'}{\partial Y}-FV'+F^*W'\cos\lambda+W'\frac{\partial\bar{U}}{\partial Z}\right]-\frac{\partial^2U'}{\partial Y^2}-\frac{\partial^2U'}{\partial Z^2}=0 \tag{8a}$$

$$Re\left[\frac{\partial V'}{\partial T}+\bar{V}\frac{\partial V'}{\partial Y}+FU'-F^*W'\sin\lambda+W'\frac{\partial\bar{V}}{\partial Z^2}+\frac{\partial\Pi'}{\partial Y}\right]-\frac{\partial^2V'}{\partial Y^2}-\frac{\partial^2V'}{\partial Z^2}=0 \tag{8b}$$

$$Re\left[\frac{\partial W'}{\partial T}+\bar{V}\frac{\partial W'}{\partial Y}+F^*V'\sin\lambda-F^*U'\cos\lambda+\frac{\partial\Pi'}{\partial Z}\right]-\frac{\partial^2W'}{\partial Y^2}-\frac{\partial^2W'}{\partial Z^2}-\frac{S}{Pr_t\,Re}\Theta'=0 \tag{8c}$$

$$\frac{\partial V'}{\partial Y}+\frac{\partial W'}{\partial Z}=0 \tag{8d}$$

$$Re\,Pr_t\left[\frac{\partial\Theta'}{\partial T}+\bar{V}\frac{\partial\Theta'}{\partial Y}+W'\frac{\partial\bar{\Theta}}{\partial Z}\right]-\frac{\partial^2\Theta'}{\partial Y^2}-\frac{\partial^2\Theta'}{\partial Z^2}=0 \tag{8e}$$

Als dimensionslose Parameter wurden hier verwendet:

$$Re=\frac{|\mathbb{V}_g|D}{k_m} \quad \text{Reynoldszahl} \tag{9a}$$

$$Pr_t=\frac{k_m}{k_h} \quad \text{turbulente Prendtlzahl} \tag{9b}$$

$$S=-\frac{g\frac{\partial\bar{\vartheta}}{\partial z}HD^3}{\bar{\vartheta}k_m k_h} \quad \text{Maßzahl für die thermische Schichtung} \tag{9c}$$

Übrigens hängt S mit der häufig benutzten Rayleighzahl Ra wie folgt zusammen

$$S=Ra\frac{D^3}{H^3}, \quad Ra=-\frac{\partial\bar{\vartheta}}{\partial z}\frac{gH^4}{\bar{\vartheta}k_m k_h} \tag{9d}$$

Die Randbedingungen für die Gleichungen (8a)–(8e) lauten

$$Z = 0 : U' = V' = W' = \Theta' = 0 \tag{10a}$$

$$Z \to \infty : \frac{\partial U'}{\partial Z} = \frac{\partial V'}{\partial Z} = W' = \frac{\partial \Theta'}{\partial Z} = 0 \tag{10b}$$

Wegen (8d) kann eine dimensionslose Stromfunktion ψ' eingeführt werden, wobei für die Störungen V' und W' gilt

$$V' = -\frac{\partial \psi'}{\partial Z}, \qquad W' = \frac{\partial \psi'}{\partial Y} \tag{11}$$

Differenziert man (8b) nach Z und (8c) nach Y, so läßt sich durch Subtraktion der Gleichungen der Druck Π' eliminieren. Nach Einführung der dimensionslosen Vorticity ξ'

$$\xi' = \frac{\partial W'}{\partial Y} - \frac{\partial V'}{\partial Z} = \nabla^2 \psi' \tag{12}$$

erhält man das Gleichungssystem

$$\mathrm{Re}\left[\frac{\partial}{\partial T}(\nabla^2 \psi') + \overline{V}\frac{\partial}{\partial Y}(\nabla^2 \psi') - \frac{\partial^2 \overline{V}}{\partial Z^2}\frac{\partial \psi'}{\partial Y} - F\frac{\partial U'}{\partial Z}\right.$$
$$\left. - F^*\frac{\partial U'}{\partial Y}\cos\lambda\right] - \frac{\partial^2}{\partial Y^2}(\nabla^2 \psi') - \frac{\partial^2}{\partial Z^2}(\nabla^2 \psi') - \frac{S}{\mathrm{Pr_t\,Re}}\frac{\partial \Theta'}{\partial Y} = 0 \tag{13a}$$

$$\mathrm{Re}\left[\frac{\partial U'}{\partial T} + \overline{V}\frac{\partial U'}{\partial Y} + \frac{\partial \overline{U}}{\partial Z}\frac{\partial \psi'}{\partial Y} + F\frac{\partial \psi'}{\partial Z} + F^*\frac{\partial \psi'}{\partial Y}\cos\lambda\right] - \frac{\partial^2 U'}{\partial Y^2} - \frac{\partial^2 U'}{\partial Z^2} = 0 \tag{13b}$$

$$\mathrm{Re\,Pr_t}\left[\frac{\partial \Theta'}{\partial T} + \overline{V}\frac{\partial \Theta'}{\partial Y} + \frac{\partial \overline{\Theta}}{\partial Z}\frac{\partial \psi'}{\partial Y}\right] - \frac{\partial^2 \Theta'}{\partial Y^2} - \frac{\partial^2 \Theta'}{\partial Z^2} = 0 \tag{13c}$$

Die Störungen ψ', U', Θ' sollen durch Wellen mit der Wellenlänge l und der Phasengeschwindigkeit c dargestellt werden. Die Wellenansätze lauten mit den komplexen Amplituden φ, μ, σ, der komplexen Phasengeschwindigkeit C und der Wellenzahl α in dimensionslosen Größen:

$$\psi'(Y, Z, T) = \varphi(Z)\exp[i\alpha(Y - CT)] \tag{14a}$$
$$U'(Y, Z, T) = \mu(Z)\exp[i\alpha(Y - CT)] \tag{14b}$$
$$\Theta'(Y, Z, T) = \sigma(Z)\exp[i\alpha(Y - CT)] \tag{14c}$$

mit

$$\alpha = \frac{2\pi}{l}D = \frac{2\pi}{L}, \quad C = \frac{c}{|v_g|} \tag{15}$$

Setzt man (14a)–(14c) in (13a)–(13c) ein und bezeichnet die Vertikalableitung durch einen Punkt, so erhält man die folgenden Stabilitäts- oder Frequenzgleichungen:

$$\ddddot{\varphi} - 2\alpha^2\ddot{\varphi} + \alpha^4\varphi - i\alpha\,\mathrm{Re}\,[(\overline{V} - C)(\ddot{\varphi} - \alpha^2\varphi) - \ddot{\overline{V}}\varphi - \mu F^*\cos\lambda] + \mathrm{Re}\,F\dot{\mu} + i\alpha\frac{S}{\mathrm{Pr_t Re}}\sigma = 0 \tag{16a}$$

$$\ddot{\mu} - \alpha^2\mu - i\alpha\,\mathrm{Re}\,[(\overline{V} - C)\mu + \dot{\overline{U}}\varphi + \varphi F^*\cos\lambda] - \mathrm{Re}\,F\dot{\varphi} = 0 \tag{16b}$$

$$\ddot{\sigma} - \alpha^2\sigma - i\alpha\,\mathrm{Pr_t}\,\mathrm{Re}\,[(\overline{V} - C)\sigma + \dot{\overline{\Theta}}\varphi] = 0 \tag{16c}$$

Die zugehörigen Randbedingungen (10a), (10b) lauten:

$$Z = 0 : \mu = \varphi = \dot{\varphi} = \sigma = 0 \tag{17a}$$

$$Z \to \infty : \dot{\mu} = \varphi = \ddot{\varphi} = \dot{\sigma} = 0 \tag{17b}$$

Für die Amplituden φ, μ, und σ der Störgrößen ψ', U', Θ' erhält man mithin ein System von 3 gekoppelten gewöhnlichen Differentialgleichungen, von denen die erste (16a) vierter Ordnung, die beiden anderen (16b), (16c) zweiter Ordnung sind. Für $F = F^* = 0$, also eine nichtrotierende Erde, entfällt die Kopplung zwischen Gleichung (16a) und (16b), für $S = 0$, d.h. adiabatische Schichtung, entfällt die Kopplung zwischen Gleichung (16a) und (16c). Wenn beide Fälle gleichzeitig erfüllt sind ($F = F^* = S = 0$) reduziert sich Gleichung (16a) auf die ORR-SOMMERFELD-Gleichung und behandelt reine Scherungsinstabilität in der (dann zweidimensionalen) Grenzschicht.

Zur Lösung der Gleichungen (16a)–(16c) benötigt man noch die Grundstromkomponenten $\overline{U}$ und $\overline{V}$. Im x^0, y^0, z-System lauten die Gleichungen (1a), (1b) für die gemittelten horizontalen Geschwindigkeitskomponenten unter den Voraussetzungen (7a)–(7d) in dimensionslosen Größen:

$$\mathrm{Re}\left[-F\overline{V}^0 + \frac{\partial \overline{\Pi}}{\partial X^0}\right] - \frac{\partial^2 \overline{U}^0}{\partial Z^2} = 0 \tag{18a}$$

$$\mathrm{Re}\left[F\overline{U}^0 + \frac{\partial \overline{\Pi}}{\partial Y^0}\right] - \frac{\partial^2 \overline{V}^0}{\partial Z^2} = 0 \tag{18b}$$

Voraussetzungsgemäß ist die X^0-Richtung senkrecht zum Druckgradienten orientiert.

$$\frac{\partial \overline{\Pi}}{\partial X^0} = 0 \tag{19a}$$

Die (dimensionslose) Beziehung für die geostrophische Windgeschwindigkeit in der X^0-Richtung lautet:

$$\frac{1}{F}\frac{\partial \overline{\Pi}}{\partial Y^0} = -1 \tag{19b}$$

Weiterhin ist gemäß (3d), (4) und (9a):

$$\mathrm{Re}\, F = 2 \tag{19c}$$

Es ergibt sich als Lösung von (18a), (18b) die bekannte Ekman-Spirale

$$\overline{U}^0(Z) = 1 - \exp(-Z)\cos(Z) \tag{20a}$$

$$\overline{V}^0(Z) = \exp(-Z)\sin(Z) \tag{20b}$$

oder im X, Y, Z Koordinatensystem

$$\overline{U}(Z) = \cos(\epsilon) - \exp(-Z)\cos(Z + \epsilon) \tag{21a}$$

$$\overline{V}(Z) = -\sin(\epsilon) + \exp(-Z)\sin(Z + \epsilon) \tag{21b}$$

Die Untersuchung des Stabilitätsproblems besteht nun in der Lösung der Stabilitätsgleichungen (16a)–(16c) für verschiedene Wertekombinationen von Re, ϵ, α, C und S unter Verwendung der in den Gleichungen (21a), (21b) angegebenen Vertikalprofile für die beiden Grundstromkomponenten $\overline{U}(Z)$ und $\overline{V}(Z)$.

3. Das Lösungsverfahren

Die Stabilitätsgleichungen (16a)–(16c) mit den Randbedingungen (17a), (17b) und den Grundstromkomponenten (21a), (21b) stellen ein Eigenwertproblem dar. Bei vorgegebenen Parametern Re, α, ϵ, S werden die zu den Eigenwerten $C = C_r + i\,C_i$ gehörenden Eigenvektoren φ, μ, σ bestimmt. Es werden Eigenwerte mit $C_i > 0$ gesucht und die Wachstumsrate αC_i als Funktion von Re, α, ϵ, S dargestellt. Das System (16a)–(16c) reduziert sich bei neutraler Schichtung (S = 0) auf (16a), (16b). Bis auf die Terme $F^* \cos\lambda\varphi$ und $F^* \cos\lambda\mu$ ist dies das von LILLY (1966) gelöste Gleichungssystem.
Wie schon gesagt erhält man für $F = F^* = S = 0$ als Stabilitätsgleichung für eine zweidimensionale Grenzschicht die bekannte ORR-SOMMERFELD-Gleichung

$$\ddddot{\varphi} - 2\alpha^2\ddot{\varphi} + \alpha^4\varphi - i\alpha\,\mathrm{Re}\,[(\overline{V} - C)(\ddot{\varphi} - \alpha^2\varphi) - \ddot{\overline{V}}\varphi] = 0$$

die von zahlreichen Autoren behandelt wurde. BETCHOV und CRIMINALE (1967) geben einen Überblick über Lösungen dieser Gleichung. Zur Lösung des vollständigen Gleichungssystems (16a)–(16c) werden die Differentialgleichungen durch Differenzengleichungen ersetzt. Dabei wird die Grenzschicht, wie in Bild 1 dargestellt, in N-Intervalle der Länge Δ aufgeteilt, so daß sich die untere Grenze bei Z = 0 und die obere bei $Z = N\Delta$ befindet. Bei der Diskretisierung werden die Funktionen μ, σ nur an den Stellen $Z = (n - \frac{1}{2})\Delta$ und φ bei $Z = n\Delta$ für n = 1,2, . . . , N definiert.

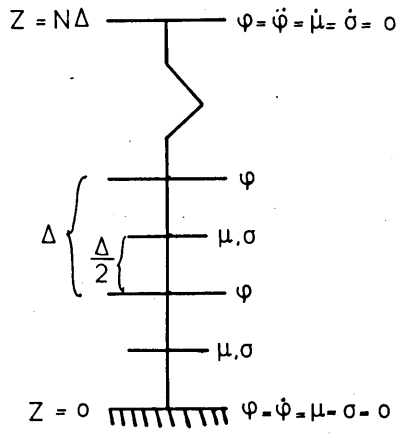

Bild 1
Aufteilung der Z-Koordinate in diskrete Intervalle.

Fig. 1
Division of the Z-coordinate in discrete intervals.

Nach dem Ersetzen der Differentiale durch zentrierte Differenzen erhält man ein lineares Gleichungssystem mit 3N-1 Gleichungen für die Unbekannten $\mu(\frac{\Delta}{2}, \frac{3}{2}\Delta, \ldots)$, $\sigma(\frac{\Delta}{2}, \frac{3}{2}\Delta, \ldots)$, $\varphi(\Delta, 2\Delta, \ldots)$.
In Matrixschreibweise lautet es:

$$(A - B\lambda_n)\,X_n = 0 \tag{22}$$

wobei A und B komplexe Matrizen, λ_n der n-te Eigenwert und X_n der n-te Eigenvektor sind.
Das System (22) ist lösbar, wenn

$$|B^{-1}A - \lambda_n E| = 0 \tag{23}$$

E = Einheitsmatrix
(23) ist das Matrixeigenwertproblem, wobei λ_n die Eigenwerte der Produktmatrix $B^{-1}A$ sind. Die Eigenwerte wurden mit dem L-R Algorithmus für komplexe Matrizen berechnet, wie er von WILKINSON und MARTIN (1968) entwickelt wurde.

Bei 20 Intervallen Δ erhält man eine 59 x 59 Matrix, so daß sich 59 Eigenwerte $C = C_r + iC_i$ ergeben. Es wurde der Wert verwendet, bei dem $C_i > 0$ war. Für die Rechnungen mit $S = 0$ und $S < 0$ ergab sich jeweils nur 1 Wert mit $C_i > 0$, während bei $S > 0$ mehre positive C_i auftreten konnten.

Die Rechnungen wurden für mehrere hundert Kombinationen der Parameter Re, α, ϵ, S durchgeführt. Die Lösungsmethode wird ausführlicher im Anhang beschrieben.

4. Ergebnisse der Stabilitätsuntersuchungen

Bei der Lösung der Stabilitätsgleichung wurden folgende Vereinfachungen vorgenommen:

$Pr_t = 1$ (24a)

$\lambda = 0°$ X-Achse in Ostrichtung (24b)

$\varphi = 45° \rightarrow F = F^* \rightarrow ReF^* = 2$ (24c)

Sodann wurden Fälle unterschieden mit (A) statisch indifferenter Schichtung ($S = 0$), statisch stabiler Schichtung ($S < 0$) und schließlich (C) statisch instabiler Schichtung ($S > 0$). Im Falle der statisch indifferenten Schichtung wurde auch noch die Voraussetzung (24b) fallen gelassen und untersucht, wie sich das Stabilitätsverhalten mit einer Umorientierung des Koordinatensystems ändert.

A. Statisch indifferente Schichtung (S = 0)

Es wird $\epsilon = 14°$ gesetzt und $C = C_r + iC_i$ in Abhängigkeit von Re und α berechnet. Das Ergebnis sind Linien gleichen Amplitudenwachstums αC_i = konst., wie in Bild 2 dargestellt. Innerhalb der Kurve $\alpha C_i = 0$ ist die Grenzschichtströmung instabil, die gestrichelte Linie zeigt $C_r = 0$ an.

Als Resultat läßt sich aus Bild 2 entnehmen:

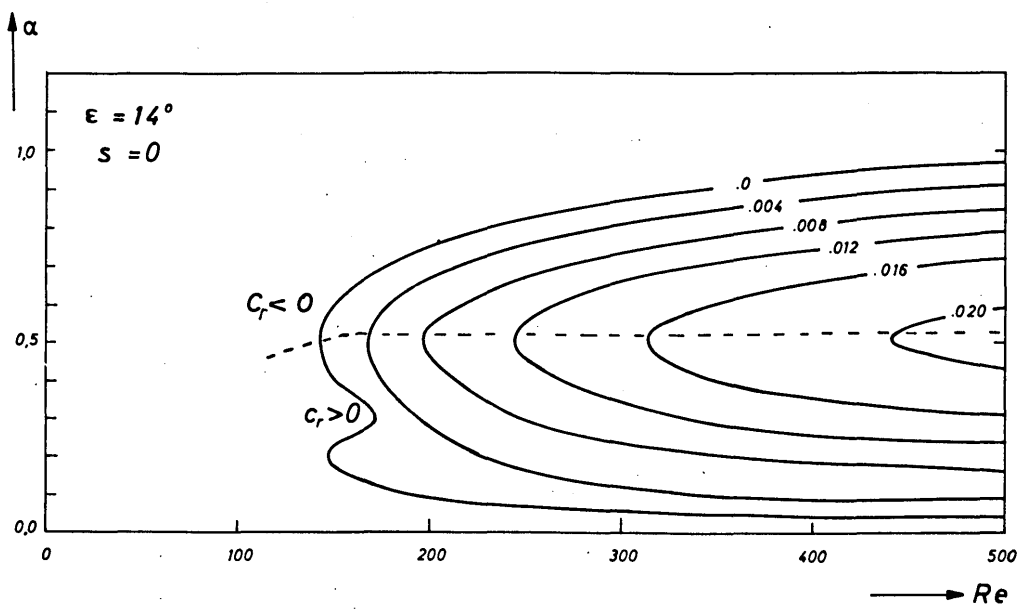

Bild 2. Wachstumsrate αC_i (ausgezogene Linien) als Funktion der Wellenzahl α und der Reynoldszahl Re für den Ablenkungswinkel $\epsilon = 14°$ und den Schichtungsparameter $S = 0$. Gestrichelte Linie: Phasengeschwindigkeit $C_r = 0$.

Fig. 2. Growth rates αC_i (solid) as a function of wave number α and Reynolds number Re for orientation angle $\epsilon = 14°$ and stability number $S = 0$. Dashed line: phase velocity $C_r = 0$.

Für alle berücksichtigten Reynoldszahlen liegt das jeweilige Maximum von αC_i bei etwa $\alpha = 0.5$, stationäre Wirbel ($C_r = 0$) treten bei $\alpha = 0.53$ auf. Auffällig sind 2 Maxima in der Kurve $\alpha C_i = 0$, die 2 kritische Reynoldszahlen zur Folge haben.

$$Re_{krit,1} = 143 \text{ bei } \alpha = 0.5$$
$$Re_{krit,2} = 145 \text{ bei } \alpha = 0.2$$

Wie LILLY zeigen konnte, ist $Re_{krit,2}$ auf den Unterschied zwischen der ORR-SOMMERFELD-Gleichung und dem System (16a), (16b) zurückzuführen, in dem bei LILLY allerdings auch noch $F^* = 0$ ist. Er stellte fest, daß $Re_{krit,2}$ bei einem Winkel $\epsilon = -20°$ und $Re_{krit,1}$ bei $\epsilon = 8°$ auftraten, während bei der Lösung der ORR-SOMMERFELD-Gleichung (allerdings mit dem Ekmanschen Grundstrom) sich eine kritische Reynoldszahl in der Nähe von $Re_{krit,1}$ ergab.

Ein Vergleich von Bild 2 mit den Ergebnissen von LILLY für $\epsilon = 15°$ zeigt, daß für eine gegebene Reynoldszahl ($Re > Re_{krit}$) die von LILLY berechneten zugehörigen Werte von αC_i größer sind. Es wird vermutet, daß dieser Unterschied auf die Berücksichtigung des bei LILLY fehlenden Termes $F^* \cos\lambda$ in den Stabilitätsgleichungen zurückzuführen ist. Für $\lambda = 90°$ wäre das hier verwendete Gleichungssystem mit dem von LILLY identisch. Dabei wurden auch die αC_i für $\alpha = 0.5$ und verschiedene Reynoldszahlen berechnet. Die Ergebnisse stimmen mit denen von LILLY gut überein. Zusätzlich wurde eine Rechnung mit $\lambda = 180°$ durchgeführt. Das Ergebnis ist in Bild 3 dargestellt. Für eine gegebene Reynoldszahl haben Längswirbel in einem Grundstrom, der nahezu nach Osten gerichtet ist, den kleinsten, in einem solchen, der nahezu nach Westen orientiert ist, den größten Wert von αC_i. Für die kritischen Reynoldszahlen ergibt sich:

λ	Re_{krit}
0°	143
90°	110
180°	70

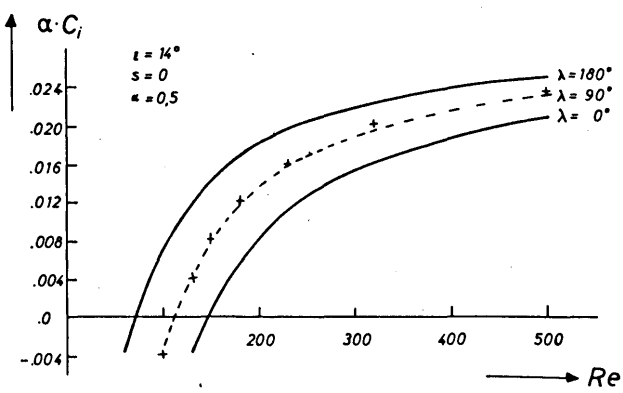

Bild 3
Wachstumsrate αC_i als Funktion der Reynoldszahl Re für $\alpha = 0.5$, $\epsilon = 14°$, $S = 0$ und verschiedene Werte des Orientierungswinkels λ.
++ = Ergebnisse von LILLY (1966) für $\epsilon = 14°$ und $\lambda = 90°$.

Fig. 3
Growth rate αC_i as a function of Reynolds number Re for $\alpha = 0.5$, $\epsilon = 14°$, $S = 0$ and different values of the deviation angle λ.
++ = results by LILLY (1966) for $\epsilon = 14°$ and $\lambda = 90°$.

Eine Ekman'sche Grenzschichtströmung wird am frühesten instabil, wenn die Achse der Längewirbel zonale Richtung hat und der Grundstrom nach Westen gerichtet ist. An diesem Verhalten macht sich der Einfluß der Vertikalkomponente der Coriolis-Kraft bemerkbar, der bei anderen dynamischen Problemen oft vernachlässigt wird.

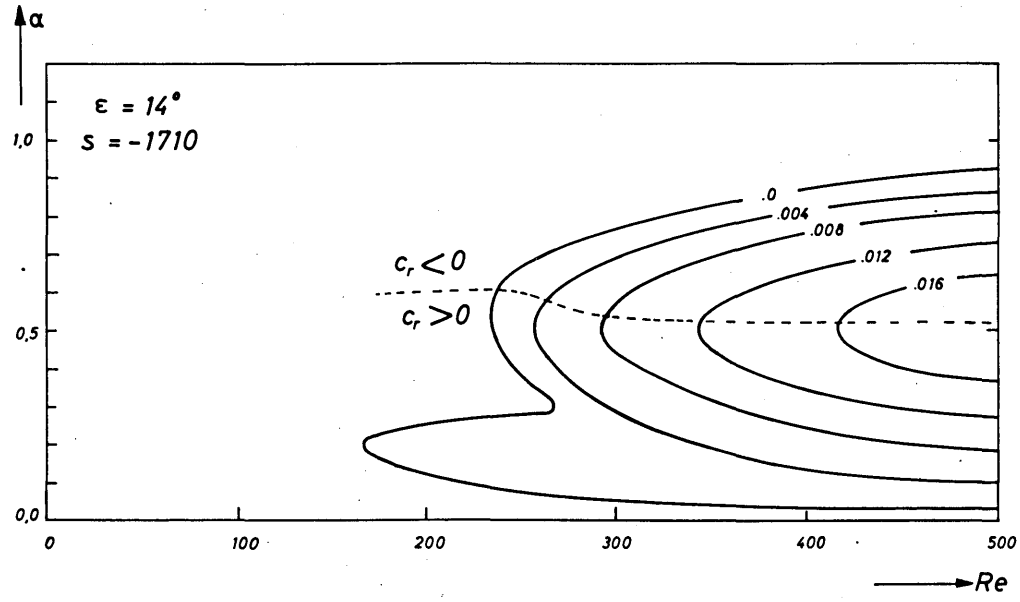

Bild 4. Wie Bild 2, jedoch für S = - 1710 (stabile Schichtung).

Fig. 4. Same as Fig. 2 except S = - 1710 (stable stratification).

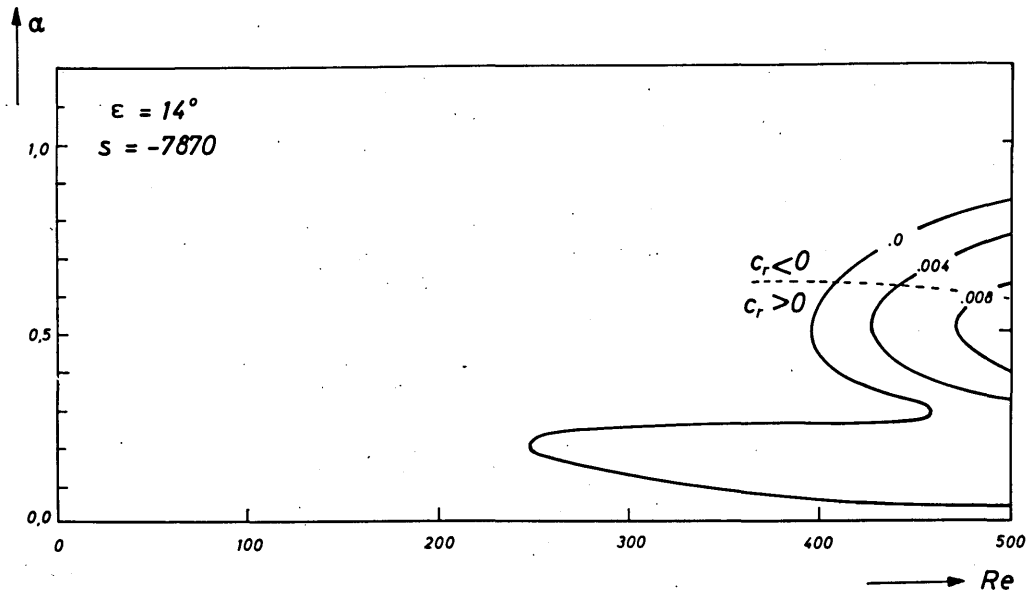

Bild 5. Wie Bild 2, jedoch für S = - 7870 (stabile Schichtung).

Fig. 5. Same as Fig. 2 except S = - 7870 (stable stratification).

B. Statisch stabile Schichtung (S < 0)

Für die aus Zweckmäßigkeitsgründen gewählten beiden negativen Werte S = – 1710 und S S = – 7870 wurde das vollständige Gleichungssystem (16a)–(16c) ebenfalls gelöst. Die Ergebnisse in Bild 4 und Bild 5 sind wie in Bild 2 dargestellt. Übereinstimmend mit dem neutralen Fall liegt (αC_i)max bei $\alpha = 0.5$. Die Kurven $C_r = 0$ sind zu größeren Werten von α verschoben, d.h., mit zunehmendem S werden die Phasengeschwindigkeiten der Wirbel mit maximalem Amplitudenwachstum größer. Für die kritischen Reynoldszahlen ergibt sich nachstehende Tabelle.

S	$Re_{krit,1}$	$Re_{krit,2}$	$Re_{krit,1} - Re_{krit,2}$
-1710	235	167	68
-7870	395	250	145

Während sich die kritische Reynoldszahlen mit zunehmender Stabilität der Schichtung zu höheren Werten verschieben, vergrößert sich dabei die Differenz $Re_{krit,1} - Re_{krit,2}$.

Die Ekman'sche Grenzschicht kann also auch im statisch stabilen Fall (dynamisch) instabil werden, die Anfangsstörungen haben aber bevorzugt größere Wellenlängen.

Die Vermutung liegt nahe, daß das 2. Maximum bei $\alpha = 0.2$ wie im indifferenten Fall mit negativen Werten von ϵ gekoppelt ist. Für den Fall S = – 1710 wurden deshalb für die feste Reynoldszahl Re = 275 Werte von αC_i in der α, ϵ-Ebene berechnet und in Bild 6 dargestellt.

Der maximale Wert von αC_i liegt bei $\epsilon = 20°$ und bei $\alpha = 0.5$. Störungen mit $\alpha = 0.1$–0.3 und großen Phasengeschwindigkeiten liegen bevorzugt zwischen $\epsilon = 0°$ und $\epsilon = -50°$.

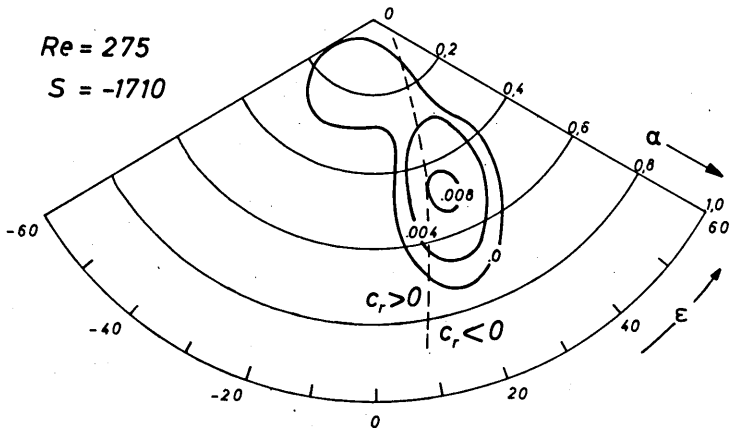

Bild 6
Wachstumsrate αC_i (ausgezogene Linen) als Funktion der Wellenzahl α und des Ablenkungswinkels ϵ für Re = 275 und S = - 1710. Gestrichelte Linie: Phasengeschwindigkeit $C_r = 0$.

Fig. 6
Growth rates αC_i (solid) as a function of wave number α and orientation angle ϵ for Re = 275 and S = - 1710. Dashed line: physe velocity $C_r = 0$.

C. Statisch labile Schichtung (S > 0)

Bei ausreichender Erwärmung der Erdoberfläche tritt in der Grenzschicht kleinräumige thermische Konvektion auf, die sich in einer Erhöhung von k_m äußert; sie führt zu einer statisch instabilen Schichtung. Auch in einer solchen Grenzschicht können Längswirbel entstehen, natürlich modifiziert durch die wirksam werdenden Auftriebskräfte. Physikalisch handelt es sich um das gleiche Phänomen wie die erstmals von GÖRTLER (1959) untersuchten Längswirbel an erwärmten Wänden.

Für 2 verschiedene thermische Schichtungen, charakterisiert durch S = 170 und S = 460 wurden die Wachstumsraten der Störungen berechnet und in Bild 7 und Bild 8 dargestellt.

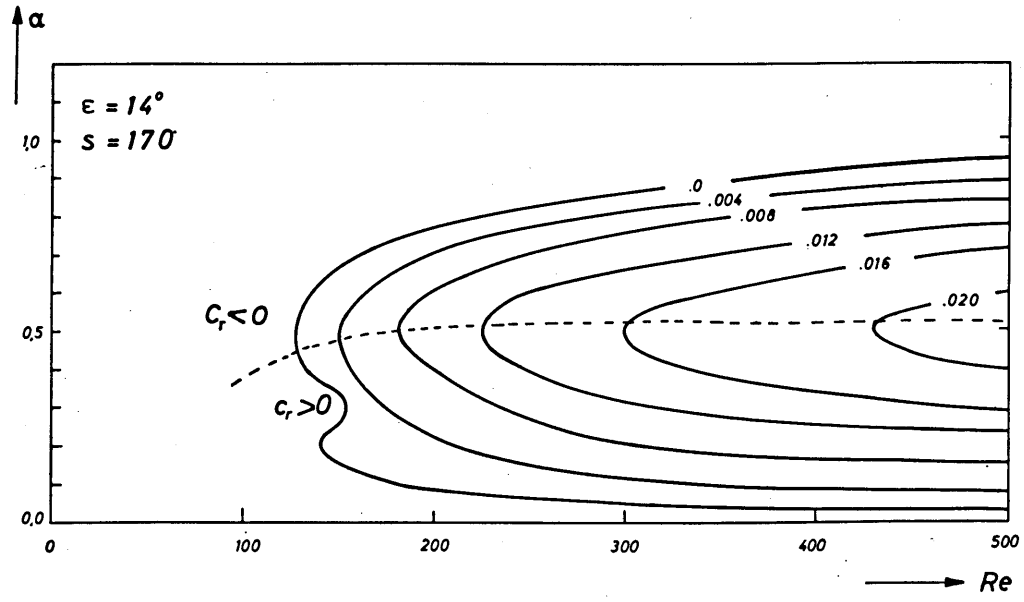

Bild 7. Wie Bild 2, jedoch für S = 170. (Labile Schichtung.)

Fig. 7. Same as Fig. 2 except S = 170 (unstable stratification).

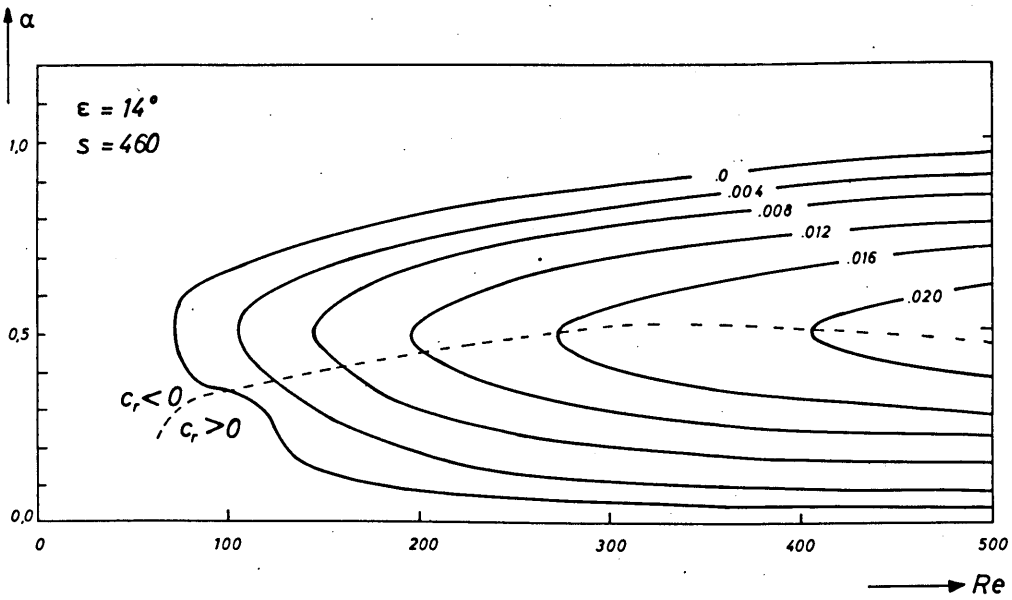

Bild 8. Wie Bild 2, jedoch für S = 460 (labile Schichtung).

Fig. 8. Same as Fig. 2 except S = 460 (unstable stratification).

Im Vergleich zur indifferenten Schichtung sind die Kurven αC_i = konst. zu kleineren Reynoldszahlen verschoben. Die Extremwerte findet man wie im neutralen und stabilen Fall bei etwa $\alpha = 0.5$. Die Linie $C_r = 0$ ist zu kleineren Werten von α verschoben, d.h., die Störungen mit maximalen αC_i haben negative Phasengeschwindigkeiten, bewegen sich also gegen den Grundstrom. Das im neutralen Fall noch ausgeprägte 2. Maximum bei $\alpha = 0.2$ verschwindet mit zunehmender Labilität der Schichtung, was besonders deutlich bei S = 460 zu erkennen ist.

Für die kritischen Reynoldszahlen ergibt sich:

S	$Re_{krit,1}$	$Re_{krit,2}$	$Re_{krit,1} - Re_{krit,2}$
170	128	140	-12
460	75	–	–

5. Diskussion der Ergebnisse

Die Lösungen der Frequenzgleichungen haben gezeigt, für welche Werte α und C einer Anfangsstörung eine Ekman'sche Grenzschichtströmung, charakterisiert durch Re und ϵ, instabil wird.

Der Einfluß der thermischen Schichtung auf das Stabilitätsverhalten wird beim Vergleich der Indifferenzkurven $\alpha C_i = 0$ deutlich. Bild 9 zeigt, daß bei statisch stabiler Schichtung die kritischen Reynoldszahlen zu größeren Werten, bei statisch labiler Schichtung zu kleineren Werten von Re verschoben sind.

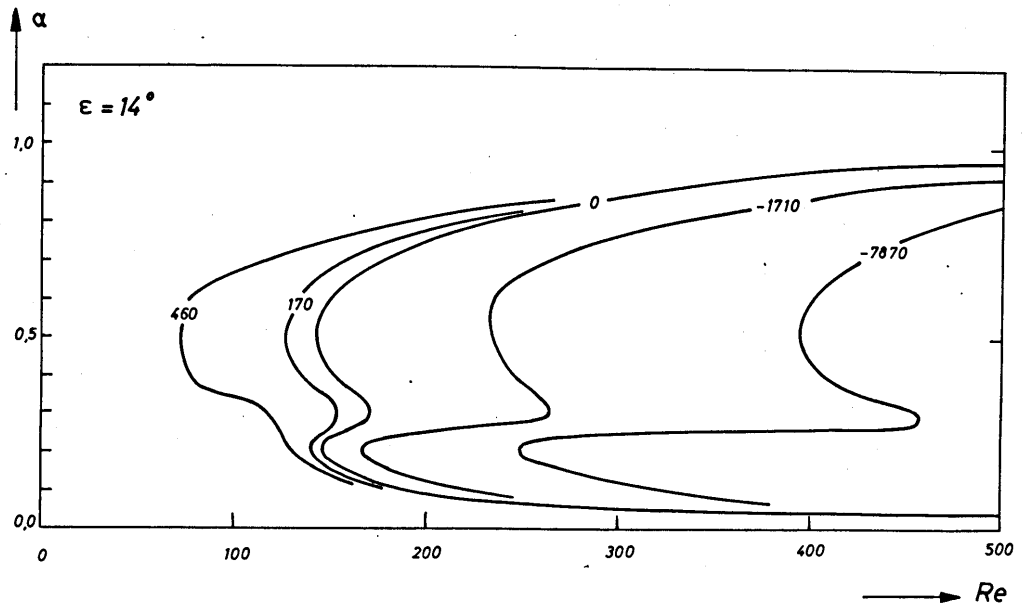

Bild 9. Indifferenzkurven $\alpha C_i = 0$ für verschiedene Werte des Schichtungsparameters S. (S > 0 instabile, S = 0 neutrale und S < 0 stabile Schichtung.)

Fig. 9. Neutral curves $\alpha C_i = 0$ for different values of stratification number S. (S > 0 unstable, S = 0 neutral and S < 0 stable stratification.)

Während das Maximum bei $\alpha = 0.2$ für eine statisch stabile Schichtung sehr stark ausgeprägt ist, verschwindet es unter dem Einfluß der thermischen Konvektion.

Anfangsstörungen haben im neutralen und labilen Fall bevorzugt Wellenlängen von L = 12, entsprechend einem $\alpha = 0.5$, im stabilen Fall L = 31, entsprechend $\alpha = 0.2$.

Für die Phasengeschwindigkeiten der Störungen bei den kritischen Reynoldszahlen ergibt sich folgendes Bild:

S	-7870	-1710	0	170	460
C_r ($\alpha = 0.5$)	0.020	0.016	0.0004	-0.0047	-0.040
C_r ($\alpha = 0.2$)	0.297	0.230	0.136	0.122	–

Störungen mit großen Wellenlängen haben eine weit größere Phasengeschwindigkeit als solche mit dem maximalen αC_i-Wert. Allgemein nimmt C_r ($\alpha = 0.2$) mit wachsender Stabilität der Schichtung zu. Störungen mit $\alpha = 0.5$ haben im neutralen Fall die geringste Phasengeschwindigkeit, sie können hier als fast stationär bezeichnet werden. Bei stabiler Schichtung nimmt C_r ($\alpha = 0.5$) zu positiven Werten, bei labiler Schichtung zu negativen Werten zu.

Negative Phasengeschwindigkeit bedeutet, daß die Störungen entgegen der V-Komponente des Grundstroms wandern.

Speziell läßt sich zu den einzelnen Ergebnissen sagen:

A. Statisch stabile Schichtung ($S < 0$)

Mit wachsendem S wird das 2. Maximum bei $\alpha = 0.2$ stärker ausgeprägt, d.h., bei der kritischen Reynoldszahl können nur Störungen mit großen Wellenlängen auftreten. Die Tendenz der Rechnungen für $S = -1710$ und $S = -7870$ läßt vermuten, daß für ein weiteres Wachsen von S das sekundäre Maximum bei $\alpha = 0.5$ gänzlich verschwindet. Wie aus der Rechnung für variables ϵ zu sehen ist, treten Wirbel mit großen Wellenlängen, bzw. kleinen Wellenzahlen, bevorzugt bei negativen Werten von ϵ auf.

Dieses Ergebnis stimmt mit den Untersuchungen von FALLER und KAYLOR (1967) überein. Sie erhalten für Re = 600, $\alpha = 0.25$ und $Ra = -2.4 \cdot 10^7$ ein primäres Maximum von αC_i bei $\epsilon = +20°$ und ein sekundäres Maximum bei $\epsilon = -20°$.

Die mit dem sekundären Maximum verbundene Phasengeschwindigkeit der Störungen liegt dabei im Bereich der Phasengeschwindigkeiten für interne Schwerewellen. Die Autoren vermuten, daß das bevorzugte Auftreten von Typ II Wirbeln bei statisch stabiler Schichtung möglicherweise auf Resonanzerscheinungen mit internen Schwerewellen zurückzuführen ist.

Die hier durchgeführten Untersuchungen geben über diese Vermutung keinen Aufschluß, jedoch können in den Lösungen der Frequenzgleichungen bei stabiler Schichtung interne Schwerewellen enthalten sein. Es ist nicht auszuschließen, daß Schwerewellen bei dem Entstehungsmechanismus von Störungen mit großer Wellenlänge und großer Phasengeschwindigkeit, die bevorzugt bei stabilen Verhältnissen auftreten, beteiligt sind.

B. Statisch labile Schichtung ($S > 0$)

Während beim stabilen Fall zusätzlich interne Schwerewellen auftreten können, ist im labilen Fall eine Kopplung von Konvektionswirbeln mit den Wirbeln, die auf Grund von Schwerungsinstabilität entstehen, möglich. Der Einfluß der thermischen Schichtung bedingt, daß die kritischen Reynoldszahlen kleiner werden, d.h., die Grenzschichtströmung früher instabil wird als im neutralen Fall.

Die Kurven αC_i = konst. verschieben sich mit wachsendem S zu kleineren Reynoldszahlen, wobei dieser Effekt bei kleinen αC_i-Werten stärker ist als bei großen. Quantitativ läßt sich der unterschiedliche Einfluß von thermischer Konvektion einerseits und reiner Scherung andererseits auf das Instabilwerden der Grenzschicht am besten zeigen, indem man $\alpha C_i(th) = \alpha C_i(S > 0) - \alpha C_i(S = 0)$ bildet. Für die maximale Wachstumsrate bei $\alpha = 0.5$ und für S = 170 und S = 460 wurde $\alpha C_i(th)$ als Funktion von Re in nachfolgender Tabelle dargestellt.

	$\alpha C_i(th)$	
Re	S = 170	S = 460
150	0.0026	0.0061
175	0.0019	0.0050
200	0.0014	0.0038
250	0.0009	0.0024
300	0.0006	0.0018
400	0.0003	0.0009
500	0.0002	0.0006

In Übereinstimmung mit Ergebnissen von FALLER und KAYLOR wird die durch die thermische Schichtung bedingt Wachstumsrate $\alpha C_i(th)$ mit wachsendem S größer und nimmt dabei mit steigender Reynoldszahl stark ab.

Die Stabilität der Grenzschichtströmung wird durch thermische Effekte am stärksten bei kleinen und damit kritischen Reynoldszahlen beeinflußt, während bei großen Reynoldszahlen Scherungsinstabilität wie im neutralen Fall vorherrscht.

Aus den Rechnungen kann allerdings nicht geschlossen werden, ob dieses Verhalten der thermischen Konvektion direkt zuzuschreiben ist, oder ob das durch sie bedingte Vorhandensein einer labilen Temperaturschichtung die Grenzschichtströmung früher instabil werden läßt.

Obwohl die Rechnungen nur für 2 Werte von S durchgeführt wurden, kann man annehmen, daß bei S = 460 thermische Konvektion auftritt. Hier verschwindet nämlich das 2. Maximum bei $\alpha = 0.2$, so daß nur noch eine kritische Wellenzahl $\alpha = 0.5$ auftritt. Dieser Wert von α stimmt mit der in den Arbeiten von AVSEC (1939) und OGURA (1969) erhaltenen Wellenzahl für rein thermische Wirbel überein.

Wegen der Störungsrechnung geben die vorstehenden Stabilitätsuntersuchungen zwar Aufschluß über das anfängliche Amplitudenwachstum, sowie Wellenlängen und Phasengeschwindigkeiten beim ersten Auftreten der Störungen, sie können aber nicht den zeitlichen Ablauf der Wirbelbildung wiedergeben. Mit diesem Problem haben sich FALLER und KAYLOR näher befaßt.

Die Autoren untersuchen die zeitliche Entwicklung von Störungen der Ekman'schen Grenzschichtströmung. Als Resultat erhalten sie Stromfunktionen der Störungen in der Y, Z-Ebene für verschiedene Zeitintervalle. Im Fall einer labilen Temperaturschichtung mit Re = 300, Ra = 10^5 und $\epsilon = 14°$ bilden sich als Endzustand der Entwicklung Wirbel mit einer Wellenlänge von L = 12, entsprechend $\alpha = 0.5$, und negativer Phasengeschwindigkeit.

Diese, mit einer völlig anderen Untersuchungsmethode gewonnenen Ergebnisse, stimmen mit den Resultaten der Stabilitätsrechnungen für $S > 0$ überein.

Man kann deshalb vermuten, daß die in der Grenzschicht entstehenden Wirbel schließlich die Abmessungen derjenigen Störungen annehmen, die bei Erreichen der kritischen Reynoldszahl als erste auftreten, zumal diese Wirbel auch noch die maximale Wachstumsrate besitzen.

Schlußbemerkung

Um den Rechenaufwand in Grenzen zu halten, wurden in dieser Arbeit keine ausführlichen Untersuchungen für variables ϵ durchgeführt, so daß nur ein kleiner Teil der möglichen Wirbelbildungen erfaßt wurde. Die hier durchgeführten Rechnungen und die Ergebnisse anderer Autoren zeigen aber, daß zumindest im neutralen und labilen Fall, Störungen mit $\alpha = 0.5$ und $\epsilon = 10°–20°$ die maximalen Wachstumsraten besitzen, also für Wirbelbildung hauptsächlich verantwortlich sind. Durch die Festlegung auf $\epsilon = 14°$ wurden vor allem Wirbel des Typ I erfaßt. Dieser Wirbeltyp scheint die in der Atmosphäre auftretenden Phänomene am besten zu erklären. BROWN findet für die atmosphärische Grenzschicht D-Werte von 200–400 m, was mit $\alpha = 0.5$ eine Wellenlänge von 2,4–4,8 km für Längswirbel ergibt. Dieser Wert stimmt mit den gemessenen Abständen der Wolkenstraßen gut überein.

Bei stabiler Schichtung scheinen Wirbel des Typ II für vertikale Transporte hauptsächlich in Frage zu kommen. Für eine genauere Klärung dieser Frage sind noch weitere Untersuchungen für verschiedene Wertekombinationen von S und ϵ erforderlich.

6. Literaturverzeichnis

ANGELL, J. K., PACK, D. H., DICKSON, C. R., 1968: A Langrangian study of helical circulations in the planetary boudary layer. J. Atm. Sc. **25**, 707–717.

AVSEC, D., 1939: Tourbillons thermoconvectifs dans l'air, application à la météorologie. L'Academie de Paris, Thèse Dr. Sc. Serie A 1910, No. d'ordre 2777.

BETCHOV, R., CRIMINALE, W. O., 1967: Stability of parallel flows. Applied Mathematics and Mechanics, Vol. **10**, Academic Press.

BROWN, R. A., 1970: A secondary flow model for the planetary boundary layer, J. Atm. Sc. **27**, 742–757.

CALDWELL, D. R., VAN ATTA, C. W., 1970: Characteristics of Ekman boundary layer instabilities. J. Fluid Mech. **44**, 79–95.

FALLER, A. J., 1963: An experimental study of the instability of the Laminar Ekman boundary layer. J. Fluid Mech. **15**, 560–575.

FALLER, A. J., KAYLOR, R. E., 1966: A numerical study of the instability of the laminar Ekman boundary layer. J. Atm. Sc. **23**, 466–480.

FALLER, A. J., KAYLOR, R. E., 1966: Investigation of stability and transition in rotating boundary layers. In Dynamics of fluids and plasmas, edited by S. Pai, 309–329, Academic Press New York.

FALLER, A. J., KAYLOR, R. E., 1967: Instability of the Ekman spiral with applications to the planetary boundary layers. Phys. of Fluids, **10**, 212–219.

GÖRTLER, H., 1959: Über eine Analogie zwischen den Instabilitäten laminarer Grenzschichtströmungen an konkaven Wänden und an erwärmten Wänden. Ing. Archiv, **28**, 71–78.

HANNA, S., 1969: The formation of longitudinal sand dunes by large helical eddies in the atmosphere. J. Appl. Meteor. **8**, 874–883.

HORST, W., 1970: Experimentelle Untersuchungen der Wirbelstruktur in einer instabilen Ekman-Grenzschicht. Beitr. Phys. Atmos. **43**, 1–34.

KUETTNER, J., 1967: Cloudstreets, theory and observations. Aero Revue, **42**, 52–56, 109–112.

LILLY, D. K. 1966: On the stability of Ekman boundary layer. J. Atm. Sc. **23**, 481–494.

MARTIN, R. S., WILKINSON, J. H., 1968: The modified LR algorithm for complex Hessenberg matrices. Numer. Math. 12, 349–368, 369–376.

OGURA, Y., YAGIHASCHI, A., 1969: A numerical study of convection rolls in a flow between horizontal parallel plates. J. meteor. Soc. Japan, 47, 205–217.

PLANK, V. G., 1966: Wind conditions in situations of patternform and non-pattern-form cumulus convection. Tellus 18, 1–12.

TATRO, P. R., MOLLO-CHRISTENSEN, E. L., 1967: Experiments on Ekman layer instabilities. J. Fluid Mech. 28, 531–544.

WIPPERMANN, R., 1969: The orientation of vortices due to instability of the Ekman boundary layer. Beitr. Phys. Atmos. 42, 225–244.

7. Anhang

Numerische Lösung der Stabilitätsgleichungen

Die Z-Koordinate wird, wie in Kapitel 3 dargestellt, in diskrete Intervalle der Länge Δ unterteilt. An Stelle der Differentiale werden zentrierte Differenzen eingeführt. Die Umwandlung erfolgt durch folgende Beziehungen, wobei die Vertikalableitungen wieder durch einen Punkt bezeichnet werden.

$$\dot{\varphi} = \delta_1 \varphi, \quad \ddot{\varphi} = \delta_2 \varphi, \quad \dddot{\varphi} = \delta_4 \varphi \tag{A1}$$

Dabei bedeutet:

$$\delta_1 \varphi = \frac{1}{\Delta}\left[-\varphi\left(Z - \frac{\Delta}{2}\right) + \varphi\left(Z + \frac{\Delta}{2}\right)\right] \tag{A2a}$$

$$\delta_2 \varphi = \frac{1}{\Delta^2}\left[\varphi(Z - \Delta) - 2\varphi(Z) + \varphi(Z + \Delta)\right] \tag{A2b}$$

$$\delta_4 \varphi = \frac{1}{\Delta^4}\left[\varphi(Z - 2\Delta) - 4\varphi(Z - \Delta) + 6\varphi(Z) - 4\varphi(Z + \Delta) + \varphi(Z + 2\Delta)\right] \tag{A2c}$$

An den Stellen $Z = (n - \frac{1}{2})\Delta$ für $n = 1, 2, \ldots N$, an denen φ nicht definiert ist, wird ein Mittelwert φ_m verwendet.

$$\varphi_m = \frac{1}{2}\left[\varphi\left(Z - \frac{\Delta}{2}\right) + \varphi\left(Z + \frac{\Delta}{2}\right)\right] \tag{A3}$$

In den mit dem relativ großen Parameter α Re multiplizierten Termen der Stabilitätsgleichungen werden für die Differenzenbildung Mehrstellenformeln verwendet. Diese erhöhen die Ordnung des Gleichungssystems nicht, reduzieren aber beträchtlich anfallende Rundungsfehler. Sie lauten für die 2. Ableitung

$$\ddot{\varphi} = \left(\delta_2 - \frac{\Delta^2}{12}\delta_4\right)\varphi \tag{A4a}$$

und für die Mittelbildung

$$\varphi_m = \left(\frac{1}{2} - \frac{\Delta^2}{16}\delta_2\right)\left[\varphi\left(Z - \frac{\Delta}{2}\right) + \varphi\left(Z + \frac{\Delta}{2}\right)\right] \tag{A4b}$$

Analog werden Differenzenformeln für μ und σ gebildet. Setzt man die so erhaltenen Beziehungen zwischen Differentialen und Differenzen in die Stabilitätsgleichungen (16a)–(16c) ein, so erhält man das folgende System von Differenzengleichungen:

$$(\delta_4 - 2\alpha^2\delta_2 + \alpha^4)\,\varphi - i\alpha\,\mathrm{Re}\left[(\bar{V} - C)\left(\delta_2 - \frac{\Delta^2}{12} - \alpha^2\right)\varphi - \ddot{\bar{V}}\varphi\right]$$

$$+ i\alpha\, 2\mu_m + 2\delta_1\,\mu + i\alpha\frac{S}{\mathrm{Re}}\left(\sigma_m - \frac{\Delta^2}{8}\delta_2\,\sigma_m\right) = 0 \qquad \text{(A5a)}$$

$$(\delta_2 - \alpha^2)\,\mu - i\alpha\,\mathrm{Re}\left[(\bar{V} - C)\,\mu + \dot{\bar{U}}\left(\varphi_m - \frac{\Delta^2}{8}\delta_2\,\varphi_m\right)\right] - i\alpha\, 2\varphi_m - 2\delta_1\varphi = 0 \qquad \text{(A5b)}$$

$$(\delta_2 - \alpha^2)\,\sigma - i\alpha\,\mathrm{Re}\left[(\bar{V} - C)\,\sigma + \dot{\bar{\Theta}}\left(\varphi_m - \frac{\Delta^2}{8}\delta_2\,\varphi_m\right)\right] = 0 \qquad \text{(A5c)}$$

Die Randbedingungen lauten in Differenzenschreibweise:

$$Z = 0 \quad : \varphi = \delta_1\varphi_m = \mu_m = \sigma_m = 0 \qquad \text{(A6a)}$$

$$Z = N\Delta \; : \varphi = \delta_2\varphi = \delta_1\mu = \delta_1\sigma = 0 \qquad \text{(A6b)}$$

Die Umwandlung des Differentialgleichungssystems in ein System gekoppelter linearer Gleichungen führt, wie in Kapitel 3 beschrieben, auf ein Matrixeigenwertproblem, das nach einem Verfahren von MARTIN und WILKINSON (1968) gelöst wurde.

Die Genauigkeit der gefundenen Eigenwerte hängt im wesentlichen von der Intervalldistanz Δ und von der Grenzschichthöhe $N\Delta$ ab. Bei konstantem N und Δ wäre bei kleinen Wellenlängen der Störungen die Maschenweite zu groß, während bei großen Wellenlängen die Höhe $N\Delta$ zu gering wäre.

Es wurde daher bei festem N = 20 ein variables Δ gewählt, für das LILLY (1966) eine empirische Formel angibt.

$$\Delta = \frac{1}{\sqrt{N\alpha}} \qquad \text{(A7)}$$

Die Formel bewirkt, daß bei wachsender Wellenlänge Δ und damit $N\Delta$ größer wird.

Obwohl die wegen der Speicherkapazität der Rechenanlage begrenzte Anzahl der Intervalle von 20 gering erscheint, ist die Übereinstimmung mit den Werten von LILLY, der 35 Intervalle verwendete, recht gut. Eine Vergrößerung der Intervallzahl wird sicher eine Verbesserung der einzelnen αC_i Werte bringen, die allgemeine Tendenz der Ergebnisse wird aber erhalten bleiben.

CHAPTER 7

The Dispersion of Windborne Material in the Planetary Boundary Layer

In recent years the efforts at environmental protection have pushed forward the investigations of the turbulent diffusion in the atmospheric boundary layer; the turbulent diffusion from an isolated continuous point source as well as that from multiple sources (urban pollution) is studied. A great many papers appeared on this topic and their number is still increasing every year.

In this chapter, however, the reproduced papers are restricted to special aspects of the turbulent diffusion. As mentioned in the foreword, this chapter is concerned with such problems of the dispersion of material, in which parameters of the planetary boundary layer are involved.

In almost all diffusion formulae the assumption has been made that the mean wind does not vary with height and that the turbulent diffusion coefficients $k_{s,y}$ and $k_{s,z}$ (or in the statistical theory expressed by σ_y and σ_z) are independent on z . Very few attempts only have been made to take into account a vertical wind profile and a vertical profile of the diffusion coefficient. Such theories are restricted to the surface layer; they may be sufficient, if the source is located at the ground or has a low elevation only. For very elevated sources (e.g. tall stacks with a large over-rise of the plume) the turning of the mean wind with height and the vertical profile of the diffusion coef-

ficient (with a maximum) should be taken into consideration.

For this purpose it may be advantageous to make use of some results of the theory of the PBL: if correctly nondimensionalized, the vertical profiles of the eddy diffusion coefficient k_m and of the velocity defect are universal. These profiles should be applied in the diffusion theory.

The first of the reproduced papers attempts such an application. Unfortunately, the resulting field of the mean concentration S of the dispersed material is not universal, although it is non-dimensionalized correctly. This is due to the fact that the mean velocity $\mathbb{V}$ has not a universal profile but only the shear $d\mathbb{V}/dZ$ or the defect $\mathbb{V}-\mathbb{V}_g$. Therefore the non-dimensional concentration field remains depending on external parameters, expressed by the nondimensional roughness-length Z_o. This, of course, enables to take into account the surface roughness of the area over which the diffusion takes place.
The second paper studies the difference in the maximum concentration $\hat{s}_{max}$ at the ground when either a PBL-model is applied or a time-dependent boundary layer model. For this in both cases are formed vertical averages of the mean wind velocity and of the turbulent diffusion coefficients; these averages are inserted in the common diffusion formula.
In the third paper, finally, should those meteorological parameters be found, which are relevant in a statistical analysis of air quality data. Here again use is made of the Rossby-number similarity in the PBL.

It is believed that there are many points beside these three examples where the results of the PBL-theory can be applied to problems of the turbulent diffusion and that improvement can be achieved by that.

Atmospheric Environment Pergamon Press 1972. Vol. 6, pp. 877–888. Printed in Great Britain.

A PERSPECTIVE FOR A ROUTINE PREDICTION OF CONCENTRATION PATTERNS

F. WIPPERMANN and D. YORDANOV*

Department of Meteorology, Technical University Darmstadt, Germany

(*First received* 27 *January* 1972 *and in final form* 10 *May* 1972)

Abstract—A method by which it should be possible to predict the steady-state concentration pattern in the lee of one (or more) point sources is suggested. The height and strength of the sources, together with some characteristic parameters for the area over which the diffusion takes place (e.g. the roughness–length and the Coriolis parameter) must be given. If in addition some parameters which are important for the planetary boundary layer (PBL) can be predicted by the methods of numerical weather forecast, corresponding internal parameters for the PBL can be computed. Provided that the actual atmospheric boundary layer can be considered as a PBL (e.g. horizontal homogeneity and a steady state exists), these internal parameters determine completely the turbulent state in the PBL and therefore the turbulent diffusion in the PBL; that means the predicted concentration pattern depends on these (predicted) internal PBL parameters only. To each set of (predicted) internal PBL parameters belongs one and only one (predicted) concentration field. In order to get the latter a relationship between both has still to be established, either by measurements or by a numerical solution of the three-dimensional diffusion equation. Both aspects are discussed. In the final section those parameters are discussed which should be used as independent variables in evaluating long term measurements of concentrations at a fixed point.

Zusammenfassung—Es wird ein Verfahren beschrieben, welches es gestattet, die stationäre Konzentrationsverteilung im Lee einer (oder mehrerer) Punktquellen vorherzusagen, für welche die jeweilige Höhe und die Quellstärke gegeben sind. Weiterhin müssen einige für das Ausbreitungsgelände charakteristische Parameter gegeben sein wie z.B. die Rauhigkeitslänge und der Coriolisparameter. Wenn zusätzlich noch einige für die planetarische Grenzschicht (PBL) wichtige Parameter mit den Methoden der numerischen Wettervorhersage vorausberechnet werden, lassen sich (vorhergesagte) sogenannte innere Parameter für die PBL berechnen. Wenn man für die aktuelle atmosphärische Grenzschicht die Voraussetzungen der PBL (Stationarität und horizontale Homogenität) gelten läßbt, dann bestimmen diese inneren Parameter eindeutig den Turbulenzzustand der Grenzschicht und damit auch die turbulente Diffusion in ihr; d.h. die vorhergesagte Konzentrationsverteilung hängt nur von diesen (vorhergesagten) inneren Parametern der PBL ab. Zu jeder Kombination von vorhergesagten inneren Parametern der PBL gehört eine und nur eine (vorhergesagte) Konzentrationsverteilung. Um letztere zu erhalten, muß allerdings noch eine Beziehung zwischen beiden hergestellt werden; dies kann entweder durch Messungen oder durch eine numerische Lösung der dreidimensionalen Diffusionsgleichung erreicht werden. Beide Möglichkeiten werden erörtert. In einem letzten Abschnitt werden diejenigen Parameter erörtert, welche als unabhängige Variable benutzt werden sollten, wenn man über längere Zeit reichende Messungen der Konzentration an einer festen Station auswerten will.

NOMENCLATURE

a_{h0}	$(k_h/k_m)_0$
b	strength of the source [$g\ s^{-1}$]
C_g	$u_*/(\lvert \hat{\mathbf{v}}_g \rvert)_0$ Geostrophic drag coefficient
C_{th}	$\vartheta_*/\{\hat{\vartheta}(z_1) - \hat{\vartheta}(z_0)\}$ Thermal drag coefficient
f	$2\,\Omega \sin \phi$ Coriolis parameter
g	acceleration of gravity
H	$\kappa u_*/f$ Internal scale height of the PBL
$\mathbf{k}$	unit vector in the vertical direction (z-coordinate)

* On leave from the Bulgarean Academy of Science, Department of Geophysics, Sofia, on a fellowship by the A. von Humboldt-Foundation.

k_m	eddy viscosity
k_h	turbulent diffusion coefficient for heat
K_m	$k_m/(\kappa^2 u_*^2/f)$ nondimensional eddy viscosity
K_x, K_y, K_z	nondimensional diffusion coefficients
L_*	$-c_p \bar{\rho}\tilde{\vartheta} u_*^3/(\kappa g q_0)$ Monin–Obukhov stability length
$M_m(\mu, \lambda_x, \lambda_y)$	Universal function in the resistance law
$M_h(\mu, \lambda_x, \lambda_y)$	Universal function in the resistance law
$N(\mu, \lambda_x, \lambda_y)$	Universal function in the resistance law
PBL	Planetary Boundary Layer
P	$\kappa(\hat{u} - u_g)/u_*$ nondimensional velocity defect in the x-direction
Q	$\kappa(\hat{v} - v_g)/u_*$ nondimensional velocity defect in the y-direction
Ro_0	$\lvert \hat{\mathbf{v}}_g \rvert_0/(f z_0)$ surface Rossby number
$\hat{s}$	mean concentration $[g\ \mathrm{cm}^{-3}]$
S	$\hat{s}\, g^3/(b f^5)$ nondimensional mean concentration
$\hat{u}$	mean wind velocity in the x-direction
u_g	geostrophic wind in the x-direction
u_*	friction velocity
$\hat{v}$	mean wind velocity in the y-direction
$\hat{v}_g$	geostrophic wind in the y-direction
$\hat{\mathbf{v}}_g$	vector of the geostrophic wind velocity
$\mathbf{x}^\circ$	unit vector in the direction of the surface stress
$X = x/H$. $Y = y/H$	nondimensional horizontal coordinates
z	vertical coordinate
z_0	roughness-length
z_1	approximative height of the PBL
Z	z/H nondimensional vertical coordinate
Z_b	z_b/H nondimensional height of the point source
Z_0	z_0/H nondimensional roughness-length
α_0	cross-isobar angle (between $\hat{\mathbf{v}}_{g0}$ and the surface stress)
η_{x*}	$\kappa^2/f\, d\hat{\mathbf{v}}_g/dz \cdot (\hat{\mathbf{v}}_{g0})^\circ$ } external parameters for the
η_{y*}	$\kappa^2/f\, d\hat{\mathbf{v}}_g/dz \cdot [\mathbf{k} \times (\hat{\mathbf{v}}_{g0})^\circ]$ } baroclinicity (x^* has the direction of $\hat{\mathbf{v}}_{g0}$)
$\hat{\vartheta}$	time averaged potential temperature
$\tilde{\vartheta}$	reference value of the potential temperature (average over the whole PBL)
ϑ_*	$-q_0/(\kappa c_p \bar{\rho} u_*)$ characteristic potential temperature
κ	0·4 von Karmans constant
λ_x	$\kappa^2/f\, d\hat{u}_g/dz$ } internal parameters for the
λ_y	$\kappa^2/f\, d\hat{v}_g/dz$ } baroclinicity
μ	H/L_* internal parameter for the thermal stratification
σ	$\kappa^2 g\{\hat{\vartheta}(z_1) - \hat{\vartheta}(z_0)\}/(\tilde{\vartheta} f \lvert \hat{\mathbf{v}}_{g0} \rvert)$ external parameter for thermal stratification

1. INTRODUCTION

THE PLANETARY boundary layer (PBL) is defined as a steady state and horizontally homogeneous boundary layer of the atmosphere. In recent years our knowledge of the PBL has grown considerably and the authors believe that one is now able to predict the vertical profiles of the wind and of the eddy viscosity in the whole PBL, if the values of some external PBL-parameters can be predicted. These external parameters may now be calculated by the methods of numerical weather prediction (NWP) on a routine basis.

The vertical profiles of wind and of the diffusion coefficients appear in the diffusion equation as variable coefficients, they determine the concentration pattern in the lee of a continuous point source, if stationarity can be assumed. Therefore the concentration patterns can be predicted by solving this equation, in which the predicted profiles of wind and of the eddy viscosity (for the coefficient of turbulent diffusion of matter) have been used. It will be demonstrated, that the concentration pattern depends on five parameters only, namely on the height of the point source, on the roughness-length, on an (internal) parameter for the thermal stratification and on two (internal)

parameters for the baroclinicity. For each possible set of these five parameters the diffusion equation has to be solved (only) once in order to be able to apply the method proposed here.

By a simple superposition one is also able to compute the concentration pattern caused by multiple sources.

Any prediction of the concentration patterns will apply to that time for which the external parameters have been determined by NWP. At that time, of course, stationarity has to be assumed; any variation with time, for instance the daily variation, has to be understood as a sequence of different steady states.

The procedure described in the following sections remains in part empirical; nevertheless the authors believe that it will be superior to the present procedures, which apply classifications of dispersion types and make a much larger use of empiricism.

2. THE PROPOSED METHOD

The method of calculation follows the flow-diagram shown in FIG. 1. It gives the sequence of steps (solid lines with arrows), which have to be followed in order to obtain the concentration pattern $S(X, Y, Z)$.

In this section a description of each step is given.

The parameters which have to be given are listed on the left-hand side of the diagram. There are three kinds of parameters, namely the local ones, the technical ones and the flow parameters predicted by NWP. The first category include the acceleration of gravity g, the Coriolis parameter $f = 2\Omega \sin(\varphi)$ ($\Omega = 7{\cdot}29\ 10^{-5}\ s^{-1}$

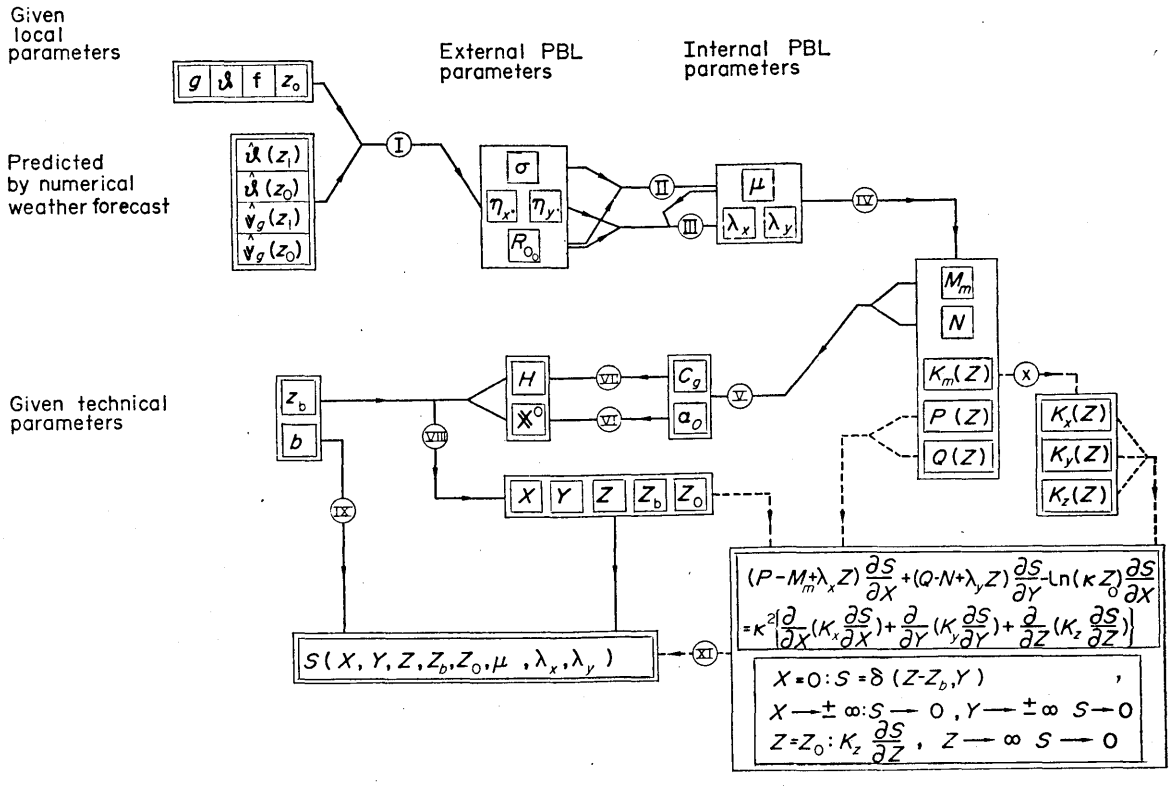

FIG. 1. A flow-diagram showing a sequence of steps to be done in order to predict concentration patterns by the proposed method. (The steps are described in section 2).

speed of rotation of the earth, φ the geographical latitude), a reference potential temperature $\tilde{\vartheta}$ (for example the potential temperature averaged over the whole PBL) and the roughness-length. z_0. This length must be determined once for each site by conventional methods (e.g. measurements of the wind profile in the surface layer for neutral stratification); if z_0 varies with the wind direction it has to be determined for different sectors, if it varies with the cycle of vegetation it has to be determined for different seasons too.

The technical parameters are the height z_b of the point source and the strength b $[g\ s^{-1}]$ of this continuous source. In the case of a source of hot gases the height z_b must be replaced by the effective height $z_{b,\mathrm{eff}}$ which consists of z_b and the rise Δz_b of the plume. Δz_b can be computed by one of the numerous formulae, in which of course the quantities have to be made nondimensional in the same way as described later.

The third category of input parameters contains the predicted flow parameters; they can be obtained by NWP. These comprise the geostrophic wind and the potential temperature on the lower and on the upper border of the PBL. In most cases the upper border z_1 will not coincide with that level next to the ground (z_0), for which the NWP-model predicts the flow parameters. The difference in height between this level and the upper border z_1 of the PBL depends on the surface Rossby number $Ro_0 = |\hat{\mathbf{v}}_{g0}|/(f z_0)$, which is available.* In the case of no coincidence the values at z_1 have to be inter- or extrapolated from the values at the lowest levels of the NWP-model. The potential temperatures $\hat{\vartheta}(z_1)$ and $\hat{\vartheta}(z_0)$ as well as the geostrophic winds $\hat{\mathbf{v}}_g(z_1)$ and $\hat{\mathbf{v}}_g(z_0)$ are representative of an area of about 300×300 km^2, since the usual grid size in the present NWP-models is about 300 km. Of course, meteorologists are developing so-called nesting-models, which allow reduction of the grid size to about 50 km over a restricted area. Applying such a NWP-model the predicted flow parameters would be representative of an area of about 50×50 km.^{2} This is almost the scale needed for diffusion processes. It should be mentioned, that the roughness-length z_0 should not be representative of the area of about 50×50 km^2, but rather for the site where the concentration patterns are to be determined.

Step I. From the given parameters mentioned before one has to form the surface Rossby number

$$Ro_0 = |\hat{\mathbf{v}}_{g0}|/(f z_0), \tag{1}$$

the external parameter for the thermal stratification

$$\sigma = \kappa^2 g\{\hat{\vartheta}(z_1) - \hat{\vartheta}(z_0)\}/(f\tilde{\vartheta}\,|\hat{\mathbf{v}}_{g0}|) \tag{2}$$

and two external parameters for the baroclinicity

$$\eta_{x*} = \kappa^2/f\, d\hat{\mathbf{v}}_g/\mathrm{d}z.(\hat{\mathbf{v}}_{g0})^0 \tag{3a}$$

$$\eta_{y*} = \kappa^2/f\, d\hat{\mathbf{v}}_g/\mathrm{d}z.[\mathbf{k} \times (\hat{\mathbf{v}}_{g0})^0] \tag{3b}$$

where the vertical shear of the geostrophic wind is approximated by

$$\mathrm{d}\,\hat{\mathbf{v}}_g/\mathrm{d}z \approx \{\hat{\mathbf{v}}_g(z_1) - \hat{\mathbf{v}}_g(z_0)\}/z_1 \tag{4}$$

* Actually the difference between z_1 and the lowest level in the NWP-model depends also on an internal parameter for the thermal stratification and on two internal parameters for the baroclinicity. However this dependence can be obtained iteratively only, since these parameters are not known in advance. For the purpose of an application of the method to be described it may be sufficient to consider the dependence on Ro_0 only.

κ is the Karman constant. Now these external parameters (2, 3a and 3b) have to be converted into the corresponding internal parameters, namely into an internal parameter μ for the thermal stratification

$$\mu = H/L_* \quad \text{or} \quad \mu = \kappa^3 g \vartheta_*/(f \tilde{\vartheta} u_*) \tag{5}$$

and into two internal parameters for the baroclinicity

$$\lambda_x = \kappa^2/f \, d\, \hat{\mathbf{v}}_g/\mathrm{d}z . \mathbf{x}^0 \tag{6a}$$

$$\lambda_y = \kappa^2/f \, \mathrm{d}\, \hat{\mathbf{v}}_g/\mathrm{d}z . [\mathbf{k} \times \mathbf{x}^0] \tag{6b}$$

where

$$H = \kappa u_*/f \tag{7}$$

is the internal scale height of the PBL, u_* the friction velocity and

$$L_* = - c_p \bar{\rho} \tilde{\vartheta} u_*^3/(\kappa g q_0) \tag{8}$$

the Monin–Obukhov stability-length.

$$\vartheta_* = - q_0/(\kappa c_p \bar{\rho} u_*) \tag{9}$$

is a characteristic potential temperature describing the turbulent heat flux q_0 at the ground. $\mathbf{x}^0$ is the unit vector in the direction of the surface stress. The angle between this direction and the direction of the geostrophic wind at the ground is the so-called cross-isobar angle α_0.

The next two steps provide the conversion from the external into the internal parameters.

Steps II *and* III. The relation between the external parameter σ for the thermal stratification and the internal parameter μ for it can be written

$$\mu/\sigma = \kappa C_{th}/C_g \tag{10}$$

where

$$C_g = u_*/ \mid \hat{\mathbf{v}}_{g0} \mid \tag{11}$$

is the geostrophic drag coefficient and

$$C_{th} = \vartheta_*/\{\hat{\vartheta}(z_1) - \hat{\vartheta}(z_0)\} \tag{12}$$

is the thermal drag coefficient. Unfortunately C_g and C_{th} are not yet known but they can be obtained from the (predicted) inputparameters by applying the resistance laws for a PBL (see YORDANOV and WIPPERMANN, 1972):

$$\kappa/C_g \sin(\mid \alpha_0 \mid) = N(\mu, \lambda_x, \lambda_y) \tag{13a}$$

$$\ln(Ro_0 C_g) - \kappa/C_g \cos(\alpha_0) = M_m(\mu, \lambda_x, \lambda_y) \tag{13b}$$

$$\ln(Ro_0 C_g) - a_{h0}/C_{th} = M_h(\mu, \lambda_x, \lambda_y). \tag{13c}$$

These resistance laws permit computation of C_g, C_{th} and α_0 for a given Ro_0. Of course, the functions $N(\mu, \lambda_x, \lambda_y)$, $M_m(\mu, \lambda_x, \lambda_y)$ and $M_h(\mu, \lambda_x, \lambda_y)$ have to be known, they can be determined only by measurements or for special models of the PBL. Evaluations of measurements in order to obtain N, M_m and M_h have been reported by MONIN

and ZILITINKEVICH (1967) and by CLARKE (1970, a); unfortunately the baroclinicity has been disregarded in these evaluations. ZILITINKEVICH (1970), FIEDLER (1972) and WIPPERMANN (1972) have computed N and M_m by using models of the PBL; almost all of these computations are restricted to barotropic conditions. Nevertheless further research work on the PBL will provide us in the future with a satisfying knowledge of the functions N, M_m and M_h, so that an application of the resistance laws will be possible in order to obtain C_g, C_{th} and α_0 also in baroclinic conditions.

However, the resistance laws can be applied only if the internal parameters μ, λ_x and λ_y are already known. In steps II and III the laws are applied in order to obtain C_g, C_{th} and α_0 and to use these in equation (10) for obtaining μ, which itself is needed for an application of the resistance laws. That means the procedure of conversion of σ into μ has to be applied iteratively. ZILITINKEVICH (1970) gives a preliminary diagram for this conversion, the construction of the diagram is based on the O'Neill data. In order to obtain a more correct conversion diagram, which takes into account the baroclinicities too, much more precise measurements are needed. Nevertheless correct conversion diagrams should be available in a not too far future.

The iterative procedure of the construction of a conversion diagram has also to include the parameters of baroclinicity, for which the same difficulties arise. For the conversion of the (predicted) external parameters η_{x*} and η_{y*} into the needed internal parameters and λ_x and λ_y of the baroclinicity the following formulae should be applied

$$\lambda_x = \eta_{x*} \cos(\alpha_0) - \eta_{y*} \sin(\,|\,\alpha_0\,|\,) \tag{15a}$$

$$\lambda_y = \eta_{x*} \sin(\,|\,\alpha_0\,|\,) + \eta_{y*} \cos(\alpha_0). \tag{15b}$$

That means that the cross-isobar angle α_0 has to be already known; but it is obtained by an application of the resistance law (13a, 13b) for which λ_x and λ_y itself already have to be known. Again the determination has to be done iteratively. At the present time a diagram for the conversion of external into internal parameters of baroclinicity is not yet available, but certainly it will be available in the future.

It should be noticed that the construction of such conversion diagrams or conversion tables has to be done only once; they will be used then in the procedure to predict the concentration patterns in steps II and III.

Step IV. When the internal parameters μ, λ_x and λ_y are obtained one has to find the values of N and M_m belonging to these parameters. For this purpose the evaluations of datas or the results of numerical computations with PBL-models will be used which have been mentioned in the steps II and III; of course, these sets of measurements as well as the mentioned BPL-models have to be improved considerably.

Step V. With the value of Ro_0 obtained by step I and with the values of N and M_m obtained by step IV the geostrophic drag coefficient C_g and the cross-isobar angle α_0 will be computed by using the resistance law (13a, 13b).

Step VI *and* VII. With the cross-isobar angle α_0 obtained by step V and with $\hat{\mathbf{v}}_{g0}$ as predicted by NWP the x-direction of the coordinate system (= direction of the surface stress) can be fixed. The unit vector in this direction is $\mathbf{x}^0$. Furthermore, with the geostrophic drag coefficient C_g also obtained by step V and with $\hat{\mathbf{v}}_{g0}$ the friction velocity u_* can be obtained. With this friction velocity and with the Coriolis parameter f the internal scale height H of the PBL can be formed according to equation (3).

Step VIII. The internal scale height H of the PBL as obtained by step VII is used

in order to non-dimensionalize the three coordinates as well as the height of the point source and the roughness-length:

$$X = x/H \qquad Y = y/H \tag{16a}$$

$$Z = z/H \qquad Z_b = z_b/H \qquad Z_0 = z_0/H. \tag{16b}$$

Step IX. The mean concentration $\hat{s}$ [$g\ \mathrm{cm}^{-3}$] is made dimensionless by using the strength b [$g\ \mathrm{s}^{-1}$] of the source

$$S = \hat{s}\, g^3/(b f^5). \tag{17}$$

3. THE CONCENTRATION PATTERNS

In the assumed conditions (steady state and horizontally homogeneous) for one set of the four parameters Z_0, μ, λ_x, λ_y there is one and only one set of the statistical characteristics of the turbulence in the PBL. That means that for one set of these four parameters the turbulent state of the PBL is completely determined and therefore also the turbulent diffusion in the PBL is completely determined. It follows that also the field of the nondimensional concentration S in the lee of one (or more) point source(s) must be determined completely (in the nondimensional coordinates X, Y and Z) if an additional fifth, sixth or more parameter(s) is (are) given, namely the nondimensional height(s) of the point source(s) Z_b.

Actually the problem would be solved, if for each possible set of these five parameters the concentration field $S(X, Y, Z)$ were measured in diffusion experiments; in this way $S(X, Y, Z, Z_b, Z_0, \mu, \lambda_x, \lambda_y)$ would be obtained, which is the final box in the flow diagram FIG. 1.

However, it is quite unrealistic to expect the problem to be solved in this way. Although for each set of these five parameters only one diffusion experiment with measurements has to be made there are too many possible sets of these parameters and also too many difficulties since the actual boundary layer during a diffusion experiment does not satisfy the conditions of a PBL (stationary and horizontal homogeneity). Even if one assumes that for a practical application measurements in only one level z_M close to the ground may be satisfying, there are still too many measurements required. Therefore some other way must be chosen to obtain $S(X, Y, Z, Z_b, Z_0, \mu, \lambda_x, \lambda_y)$. A possible way seems to be a numerical solution of the steady state three-dimensional diffusion equation, in which the velocities and the diffusion coefficients are consistent with the conditions in the PBL. Such an approach is represented in the flow diagram FIG. 1 by those boxes, which are connected by broken lines with arrows; it will be discussed in the section V.

Diffusion experiments cannot be carried out for each possible set of the five parameters $Z_b, Z_0, \mu, \lambda_x, \lambda_y$ but only for very few of the possible combinations of these parameters; such measurements can be used to verify the $S(X, Y, Z, Z_b, Z_0, \mu, \lambda_x, \lambda_y)$ obtained in other ways. If diffusion experiments are carried out for this purpose they have to include, of course, measurements which allow to determine z_0 of the site as well as the meteorological parameters μ, λ_x, λ_y and H; the latter will be used to nondimensionalize the x, y, z, z_b and z_0.

The five parameters Z_b, Z_0, μ, λ_x, λ_y are a minimum of the parameters to be considered, except one assumes barotropy ($\lambda_x = \lambda_y = 0$). In more realistic conditions

other parameters have to be added, for instance for the absorption of diffusing gases at the ground or for a loss of diffusing gases by chemical reactions.

It should be noted that diagrams are available (ZILITINKEVICH, 1970; CLARKE, 1970b), which allow (at least in the barotropic case) to obtain C_g and α_0 for given σ and Ro_0. Although these diagrams combine the steps II, III, IV and V to one step they cannot be applied in the proposed procedure, since finally also μ, λ_x, λ_y are needed and therefore the steps II and III cannot be done together with steps IV and V.

4. THE USE OF THE DIFFUSION EQUATION

As mentioned before a possible way to obtain $S(X,Y,Z,Z_b,Z_0,\mu,\lambda_x,\lambda_y)$ is a numerical solution of the three-dimensional diffusion equation.

$$\hat{u}\frac{\partial \hat{s}}{\partial x} + \hat{v}\frac{\partial \hat{s}}{\partial y} = \frac{\partial}{\partial x}\left\{k_x \frac{\partial \hat{s}}{\partial x}\right\} + \frac{\partial}{\partial y}\left\{k_y \frac{\partial \hat{s}}{\partial y}\right\} + \frac{\partial}{\partial z}\left\{k_z \frac{\partial \hat{s}}{\partial z}\right\} \tag{18a}$$

which is in non-dimensional notation

$$\begin{aligned}(P - M_m + \lambda_x Z)\frac{\partial S}{\partial X} + (Q - N + \lambda_y Z)\frac{\partial S}{\partial Y} - ln\,(\kappa Z_0)\frac{\partial S}{\partial X} = \\ = \kappa^2\left[\frac{\partial}{\partial X}\left\{K_x \frac{\partial S}{\partial X}\right\} + \frac{\partial}{\partial Y}\left\{K_y \frac{\partial S}{\partial Y}\right\} + \frac{\partial}{\partial Z}\left\{K_z \frac{\partial S}{\partial Z}\right\}\right].\end{aligned} \tag{18b}$$

In this notation are

$$P = \kappa\,(\hat{u} - \hat{u}_g)/u_* \qquad Q = \kappa(\hat{v} - \hat{v}_g)/u_* \tag{19a, b}$$

the non-dimensional velocity defects and

$$K_x = k_x/(\kappa^2 u_*^2/f) \qquad K_y = k_y/(\kappa^2 u_*^2/f) \qquad K_z = k_z/(\kappa^2 u_*^2/f) \tag{20a, b}$$

the non-dimensional coefficients of turbulent diffusion. In the PBL exists for $Z \gg Z_0$ Rossby number similarity (see WIPPERMANN and YORDANOV, 1972a), which means that P, Q, M_m and N as well as the turbulent diffusion coefficients K_x, K_y, K_z (if they are proportional to the eddy viscosity K_m) are universal functions of μ, λ_x, λ_y and (for the vertical profiles) of Z only.

In FIGS. 2 and 3 such universal profiles are shown of the eddy viscosity K_m and of the velocity defects P and Q. In FIG. 2 datas (dots) are given from the Leipzig wind profile, which probably resembles a barotropic and near-adiabatic case; in FIG. 3 the data from the profile Helgoland II are plotted valid for an unstable stratification and a moderate baroclinicity (cold air advection). In both figures the observations are compared with the universal profiles (solid lines) computed with the aid of a model for the PBL (see WIPPERMANN, 1972). In this model the parameter for the thermal stratification is L_∞, the non-dimensional asymptotic mixing-length; an empirical relationship between L_∞ and μ has been found.

Incidentally, it may be mentioned, that the vertical profiles of the turbulent diffusion coefficient K_m can be modified considerably by baroclinic effects. FIG. 3 gives an example showing a reduction of the diffusion coefficients to $\frac{1}{4}$, the minimum occurs at $Z = 0{\cdot}35$ which corresponds to $z = 325$ m in this case. A more detailed description of such minima in the vertical profiles of the turbulent diffusion coefficients are

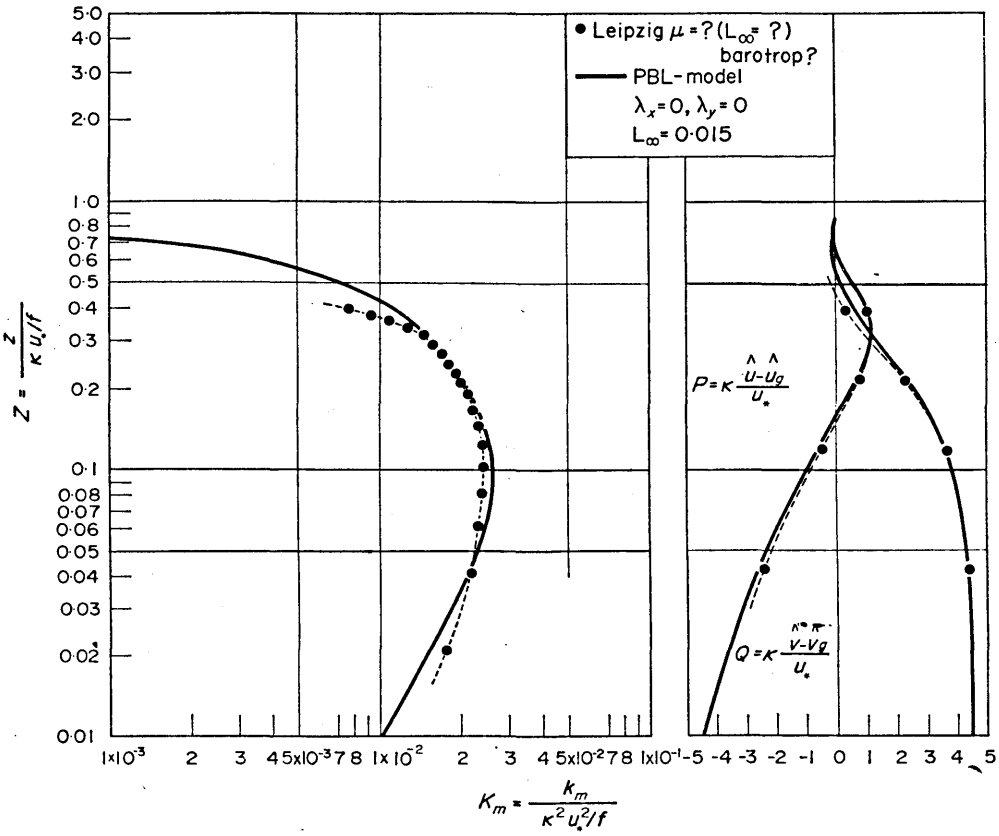

FIG. 2. Universal vertical profiles of the eddy viscosity K_m and the velocity defects P and Q for a probably barotropic and near-neutral case.

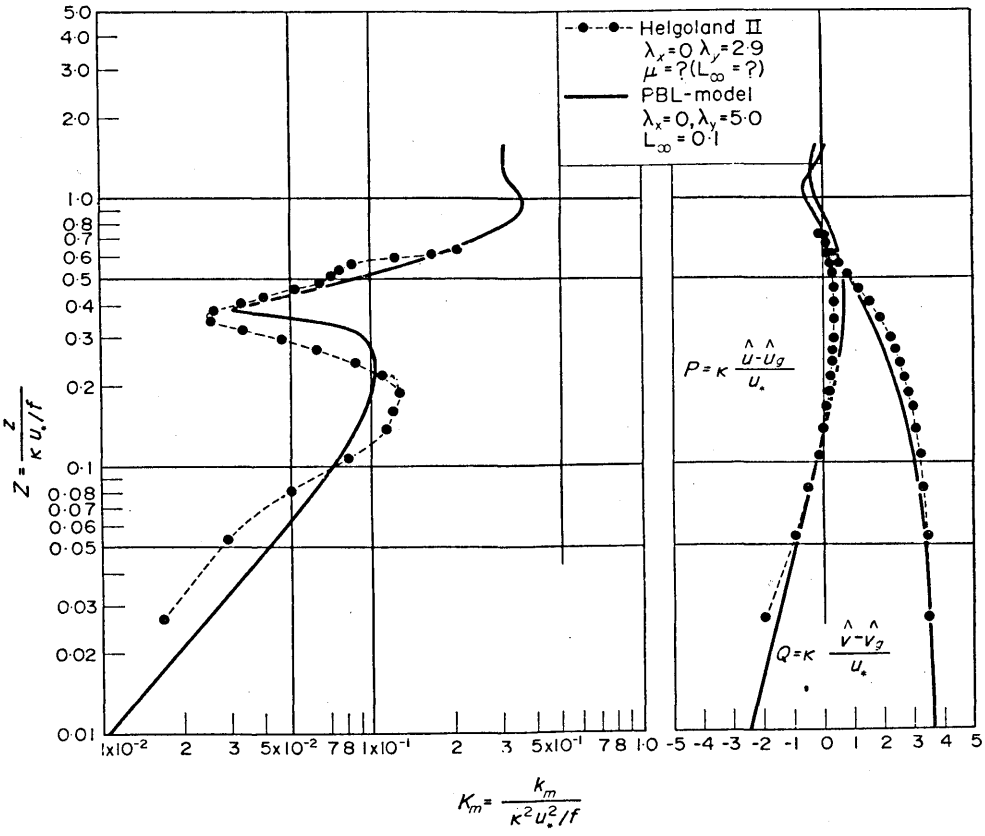

FIG. 3. Universal vertical profiles of the eddy viscosity K_m and the velocity defects P and Q for a baroclinic (cold air advection) and unstable case. In the profile $K_m(Z)$ appears a minimum caused by the baroclinicity.

discussed in another paper, WIPPERMANN and YORDANOV (1972b); this paper also contains citations of the sources of data. Such layers with a reduced diffusion coefficient may be important for the diffusion of noxious gases emitted from tall stacks.

The last term on the left-hand side of equation (18b) contains the non-dimensional roughness-length Z_0, which is by definition, see (16b),

$$Z_0 = (\kappa\, C_g\, Ro_0)^{-1}. \tag{21}$$

It is the only term which depends on the surface Rossby number. With regard to this term the resulting concentration patterns will also depend on the surface Rossby number and therefore not obey Rossby number similarity.

The following steps have to be done in order to obtain $S(X, Y, Z, Z_b, Z_0, \mu, \lambda_x, \lambda_y)$ as a solution of the diffusion equation (18b) with the boundary conditions given in the flow diagram FIG. 1.

Step IV. To each set of the three internal parameters μ, λ_x and λ_y belong not only the values of the two functions M_m and N but also the three universal profiles $K_m(Z)$, $P(Z)$ and $Q(Z)$, for which examples are given in FIGS. 2 and 3. These universal profiles can be obtained only by measurements or in an approximative form by models of the PBL. At the present time the measurements of the structure of the PBL are still too rare and too deficient to obtain these profiles in a satisfying form. Therefore such profiles must be used, which are obtained by numerical integrations of the equations of a PBL-model. Such integrations are described by WIPPERMANN (1972).

Step X. The turbulent diffusion coefficients K_x, K_y, K_z in equation (18b) are those for matter, they are not identical with the turbulent diffusion coefficient for momentum K_m, i.e. with the eddy viscosity. Since profiles $K_x(Z)$, $K_y(Z)$ and $K_z(Z)$ are not known it seems reasonable to use $K_m(Z)$ instead of these. This may be justified most easily for the coefficient $K_z(Z)$. For the two others it is proposed to put $K_x(Z) = K_y(Z) = c\, K_z(Z)$, where the factor of proportionality c must be determined empirically.

At some time or other in the future vertical profiles $K_h(Z)$ will be available, where K_h is the turbulent diffusion coefficient for heat. At that time, $K_z(Z)$ should be put equal to $K_h(Z)$ instead to $K_m(Z)$.

A disadvantage of the proposed use of the diffusion equation would be that the increase of the turbulent diffusion coefficients with travel time would not be considered. To overcome this disadvantage the turbulent diffusion coefficients should depend also on a nondimensional travel time $[(X^2 + Y^2)/\{(P - M_m + \lambda_x Z - ln(\kappa Z_0))^2 + (Q - N + \lambda_y Z)^2\}]^{1/2}$ until they reach their asymptotic value. Of course, this dependence, which is different for K_z and K_y (or K_x), is determined by the parameters Z_0, μ, λ_x and λ_y, it varies with Z. Since one is not able at the present time to get this dependence by theoretical reasoning one should attempt to obtain it empirically.

Step XI. Several difficulties will arise in attempting to solve the diffusion equation (18b) numerically, some of them should be listed here:

(a) A numerical solution could be easier obtained when the equation would be parabolic. In order to have a parabolic type of equation the turbulent diffusion in the direction of the mean wind has to be neglected (compared with the turbulent advection in this direction) as it is done usually. But by using the universal profiles for the wind velocity (with vanishing $\hat{v}$ at $Z = Z_0$) such an assumption is no longer justified in the lowest part of the PBL.

(b) The boundary conditions for $X \to \pm\infty$, $Y \to \pm\infty$, $Z \to +\infty$ cannot be

applied in a numerical solving procedure, since only a finite volume can be considered in which the diffusion takes place. That means that at the border of this finite volume new artificial boundary conditions have to be defined.

(c) The δ-function in the boundary condition at $X = 0$ cannot be handled in a numerical scheme; the point source at $X = 0$ has to be replaced by an equivalent area-source in the (Y,Z)-plane at $X = \alpha\, \Delta X$.

(d) Since after discretization $Z_0 \ll \Delta Z$ (with ΔZ the grid size in the vertical direction) it is probably necessary to use a logarithmic vertical coordinate in the lowest part of the PBL and a linear one in the upper part.

If one overcomes these difficulties equation (18b) can be solved by applying an appropriate numerical solving procedure, the solution $S(X, Y, Z, Z_b, Z_0, \mu, \lambda_x, \lambda_y)$ will be obtained.

For a routine prediction of concentration patterns this solution must be available for each possible set of the five parameters Z_b, Z_0, μ, λ_x, λ_y. That means many integrations have to be carried out; nevertheless, it is believed that in this way the problem can be solved easier than by a very large number of diffusion experiments as described in the preceding section.

If an approximative solution is satisfactory the diffusion equation (18b) may be simplified by additional assumptions, for instance by the restriction to barotropic cases (justified for sources at the ground or with small z_b) or by the use of Gaussean distributions in the lateral direction.

5. STATISTICAL EVALUATION OF CONCENTRATION MEASUREMENTS

Today many measurements of concentration are carried out at many places in the industrial countries. The evaluations of these measurements are as different as the places are, mostly the concentrations are considered as depending on the surface wind (speed and direction) and on the surface temperature. These three parameters are not able to describe completely the turbulent state of the PBL and therefore the diffusion conditions in the PBL. One has a similar situation with the so-called diffusion categories as introduced by PASQUILL (1961).

For continuous recording of the concentration of a specific gas at a fixed point the sources causing this concentration are not known. If one assumes that the positions and the strengths of the sources are constant with time, the concentration at the point under consideration must depend only on the external parameters as given in the flow-diagram of TABLE 1. These parameters determine the turbulent state of the PBL completely and therefore also the turbulent diffusion in the PBL. That means it is recommended to evaluate such measurements as

$$\hat{s}/\hat{s}_m \text{ depending on } Ro_0,\ (\hat{\mathbf{v}}_{g0})^0,\ \sigma,\ \eta_{x*},\ \eta_{y*}.$$

The non-dimensional concentration $\hat{s}/\hat{s}_m$ should not be mixed up with the non-dimensional concentration $S = \hat{s}/(b\, f^5/g^3)$; the former one is non-dimensionalized by a mean concentration $\hat{s}_m$ measured at the point. $(\hat{\mathbf{v}}_{g0})^0$ is the unit vector of the geostrophic wind at the ground. The external parameters are defined in the equations (1, 2, 3a and 3b), they can be obtained from the parameters g, $\tilde{\vartheta}$, f, z_0 given for the fixed point and from the parameters $\hat{\mathbf{v}}_g(z_1)$, $\hat{\mathbf{v}}_g(z_0)$, $\hat{\vartheta}(z_1)$ and $\hat{\vartheta}(z_0)$ computed by a NWP-model for the time of the concentration measurement.

If one neglects the baroclinicity η_{x*}, η_{y*} as a first approximation there are only three parameters left, on which $\hat{s}/\hat{s}_m$ will depend:

$$\hat{s}/\hat{s}_m = f(Ro_0, (\hat{\mathbf{v}}_{g0})^0, \sigma). \tag{22}$$

This is the same number of parameters for which evaluations of concentration measurements are made usually, namely for the speed and the direction of the surface wind and for the surface temperature. These latter parameters are chosen arbitrarily or conditioned by the possibilities of measurements; they do not describe the turbulent state of the PBL completely and therefore also not the turbulent diffusion. For that reason it seems to be more logical to evaluate measurements of concentrations at a fixed point as depending on the three external parameters given in (22).

REFERENCES

CLARKE R. H. (1970a) Observational studies in the atmospheric boundary layer. *Q. J. R. met. Soc.* **96**, 91–114.

CLARKE R. H. (1970b) Recommended methods for the treatment of the boundary layer in numerical methods. *Austral. Meteor. Mag.* **18**(2), 51–73.

FIEDLER F. (1972) The effects of the baroclinicity on the resistance law in a diabatic Ekman layer. Paper presented at the Meeting Germ. Meteor. Soc., Essen 26 Sept.–2 Oct. 1971. (To be published).

MONIN A. S. and ZILITINKEVICH S. S. (1967) Planetary boundary layer and large scale atmospheric dynamics. Report GARP Study Conf. Stockholm. Append. V, pp. 37.

PASQUILL F. (1961) The estimation of dispersion of wind-borne material. *Meteor. Mag.* **90**, 33.

WIPPERMANN F. (1972) Universal profiles in the barotropic planetary boundary layer. *Beitr. Phys. Atm.* **45**(2), 148–163.

WIPPERMANN F. and YORDANOV D. (1972a) A note on the Rossby similarity for flows of barotropic planetary boundary layers. *Beitr. Phys. Atm.* **45**(1), 66–71.

WIPPERMANN F. and YORDANOV D. (1972b) Layers with a reduced eddy viscosity caused by baroclinicity. *Beitr. Phys. Atm.* **45**(3), 148–163.

YORDANOV D. and WIPPERMANN F. (1972) The parameterization of the turbulent fluxes of momentum heat and moisture at the ground in a baroclinic planetary boundary layer. *Beitr. Phys. Atm.* **45**(1), 58–65.

ZILITINKEVICH S. S. (1970) *The Dynamics of the Atmospheric Boundary Layer* (in Russian) p. 290. Gidrometeoizdat, Lenningrad.

Atmospheric Environment Pergamon Press 1973. Vol. 7, pp. 671–672. Printed in Great Britain.

ERRATA

F. WIPPERMAN and D. YORDANOV; A perspective for a routine prediction of concentration patterns. *Atmospheric Environment* **6,** 877–888.

IN this paper the concentration $\hat{s}$ [g cm^{-3}] has been non-dimensionalized arbitrarily, see equation (17) by

$$S = \hat{s}g^3/(bf^5)$$

where g is the acceleration of gravity, f the Coriolis parameter and b the strength [g sec^{-1}] of the source. However, the equation of continuity in the stationary case

$$\int\int \hat{u}\,\hat{s}\,\mathrm{d}y\,\mathrm{d}z = b$$

tells, how the concentration has to be non-dimensionalized, namely

$$S = \hat{s}\,\kappa\,u_*^3/(bf^2)$$

with κ the Karman constant and u_* the friction velocity. This should be used instead in equation (17); results and conclusions remain unaffected by this change.

Meteorol. Rdsch. 26, 11–18 (1973)
©by Springer-Verlag 1973

Ein Vergleich zeitlich veränderlicher Konzentrationen von Luftbeimengungen mit denjenigen der entsprechenden stationären Fälle

F. Wippermann
Technische Hochschule Darmstadt

Zusammenfassung. In den derzeitigen Modellen zur quantitativen Erfassung der Ausbreitung luftfremder Stoffe werden die Ausbreitungsbedingungen nach Klassen (im wesentlichen der thermischen Schichtung entsprechend) eingeordnet; zu jeder Klasse kennt man empirisch gewonnene Diffusionsparameter. Für jede Klasse muß man den Ausbreitungsvorgang als einen stationären Vorgang ansehen, es wird nicht unterschieden, ob und in welchem zeitlichen Abstand der betrachteten Ausbreitungsklasse eine solche mit stabilerer oder mit weniger stabiler Schichtung vorangegangen ist. In Wirklichkeit hängen die zu einer Ausbreitungsklasse gehörenden Diffusionsparameter nämlich sehr merklich von der „Vorgeschichte" ab; es wird gezeigt, daß an einem normalen Strahlungstag der turbulente Diffusionskoeffizient sich für eine Ausbreitungsklasse maximal um den Faktor 2 unterscheiden kann, je nachdem ob die zeitlich vorangehende Klasse eine stabilere oder weniger stabile Schichtung aufwies. Der tägliche Gang der relevanten meteorologischen Parameter wird durch die numerische Integration eines zeitabhängigen Grenzschichtmodelles erhalten, für welches als Input der Tagesgang der thermischen Schichtung vorgegeben wird. Die Ergebnisse werden nach einer vertikalen Mittelbildung auf die Maximalkonzentration (am Boden) eines sich von einer kontinuierlichen Punktquelle ausbreitenden luftfremden Stoffes und auf die Quellentfernung dieser Maximalkonzentration angewandt.

Summary. In the present models for the turbulent diffusion of polluting material "dispersion categories" are used which vary mainly with the thermal stratification. For each of these categories diffusion parameters are known which have been obtained empirically. For each category the process of dispersion has to be considered as a stationary one; neither the influence of the category preceding in time is considered nor the time, in which the change from one category to another takes place. In reality the diffusion parameters of any of these categories depend on the "history" of the considered category, namely if the preceding category had a less stable or a more stable stratification. It will be shown that on a day with normal conditions of radiation the coefficient of turbulent diffusion for a certain category can differ by a factor of 2 depending on the category preceding in time. The diurnal variation of the relevant meteorological parameters has been obtained by a numerical integration of a time-dependent boundary layer model; the input for this model was the diurnal variation of the thermal stratification. The results (averaged in the vertical) are applied to the formulas for the maximum concentration at the ground of a material dispersing from a continuous point source and for the distance of this maximum.

I. Einleitung

Ausnahmslos ist allen Modellen zur quantitativen Erfassung der Ausbreitung luftfremder Stoffe die Voraussetzung zu eigen, daß es sich um einen stationären Ausbreitungsvorgang handelt, d.h. daß die meteorologischen Parameter (Diffusionskoeffizienten und Horizontalwind) wie auch die Quellstärke des oder der Emittenten zeitlich konstant bleiben. Einer zeitlichen Veränderung, etwa dem Tagesgang der meteorologischen Parameter, pflegt man dadurch Rechnung zu tragen, daß man diese als eine Folge von stationären Zuständen auffaßt; dabei ist natürlich der stationäre Zustand zur Zeit t völlig unabhängig von dem zur Zeit $t-\Delta t$ betrachteten. Dies wird einigermaßen zutreffen, wenn einmal die beiden Zustände nicht sehr verschieden voneinander sind, und wenn die Zeitpunkte, an denen sie gelten, beträchtlich auseinander liegen. Im Allgemeinen sind aber die zeitlichen Veränderungen (z.B. durch den normalen Tagesgang) so stark, daß der Zustand zum Zeitpunkt t merklich beeinflußt ist von dem vorangehenden Zustand, also von demjenigen zur Zeit $t-\Delta t$.

Bei den meisten Modellen der Ausbreitungsrechnung bedient man sich einer Einordnung der zu behandelnden Fälle in sogenannte Ausbreitungsklassen, z.B. solche nach Pasquill (1961), für welche dann die Diffusionsparameter, in diesem Falle σ_y und σ_z gegeben sind. Die Ausbreitungsklasse charakterisiert die thermische Schichtung der Grenzschicht, in welcher die Ausbreitung erfolgt; die zu einer thermischen Schichtung (zu dieser Ausbreitungsklasse) gehörenden Diffusionsparameter sind aus Messungen bei Diffusionsexperimenten gewonnen worden und müssen wohl als zum jeweiligen stationären Zustand gehörig angesehen werden. Betrachtet man z.B. die Ausbreitungsklasse für neutrale Schichtung, so wird diese an einem Tage mit überdurchschnittlicher Einstrahlung sowohl am Vormittage auftreten, wenn die stabile Schichtung der Nacht und des frühen Morgens abgebaut ist, als auch am späten Nachmittage, wenn der überadiabatische Temperaturgradient verschwunden ist, der um die Mittagszeit und am frühen Nachmittage herrschte. In beiden Fällen hätte man in den derzeitigen Modellen der Ausbreitungsrechnung die gleiche Ausbreitungsklasse und damit die gleichen Diffusionsparameter zu berücksichtigen. Ganz sicher sind aber die Diffusionsparameter verschieden, je nachdem ob man sich dem (hier betrachteten) neutralen Fall von der Seite der stabilen Schichtung oder derjenigen der labilen Schichtung genähert

hat; im ersten Fall werden die Diffusionsparameter kleiner, im zweiten Fall jedoch größer sein als im stationären Fall mit neutraler Schichtung. Ähnliches gilt für alle andern Schichtungen natürlich auch.

In dieser Arbeit werden die Ergebnisse einer Untersuchung vorgelegt, in welcher die Differenzen zwischen den Diffusionskoeffizienten im instationären Fall (bei Vorgabe eines normalen Tagesganges) einerseits und im entsprechenden stationären Fall andererseits ermittelt worden sind; die gleichen Differenzen sind auch für die horizontale Windgeschwindigkeit ermittelt worden. Mit diesen Differenzen in den meteorologischen Parametern lassen sich dann die entsprechenden Differenzen für die Maximalkonzentration am Boden im Lee einer hochgelegenen kontinuierlichen Punktquelle (z. B. Schornsteinmündung) und für die Quellentfernung dieses Konzentrationsmaximums berechnen.

II. Ein Beispiel für den Tagesgang der relevanten meteorologischen Parameter

Im Zusammenhang mit Untersuchungen des Effektes der Instationarität auf die planetarische Grenzschicht (d.h. auf eine als stationär und horizontal homogen definierte Grenzschicht) wurden für einen vorgegebenen Tagesgang der thermischen Schichtung der zugehörige Tagesgang gewisser meteorologischer Parameter mit einem numerischen Modell ermittelt. Einzelheiten über dieses Modell, nämlich über die Schließung des Gleichungssystems und über das numerische Lösungsverfahren, findet man bei Wippermann, Etling und Leykauf (1973); hier soll sich auf die Wiedergabe einiger in diesem Zusammenhang wichtiger Ergebnisse beschränkt werden.

Vorgegeben wird in diesem Modell der Tagesgang der thermischen Schichtung, welche durch den internen Schichtungsparameter μ repräsentiert wird

$$\mu = H \,/\, L_{M0} \tag{1}$$

μ ist das Verhältnis der internen charakteristischen Grenzschichthöhe H (internal scale height)

$$H = \varkappa\, u_* \,/\, f \tag{2}$$

zur Monin-Obukhov'schen Stabilitätslänge

$$L_{M0} = -\, c_p\, \bar{\varrho}\, u_*^3 \,/\, (\varkappa\, \beta\, q_0) \tag{3}$$

Es ist die übliche Bezeichnungsweise gewählt worden, nämlich $u_* = \sqrt{|\tau_0| / \bar{\varrho}}$ für die Schubspannungsgeschwindigkeit, f für den Coriolisparameter und $\varkappa$ für die von Karman'sche Konstante; es ist c_p die spezifische Wärme, ϱ die Dichte, $q_0 = c_p\, \overline{\varrho\, w''\, \vartheta''}$ der turbulente Wärmestrom am Boden und schließlich ist $\beta = g/\vartheta$ mit g der Schwerebeschleunigung und ϑ einer (potentiellen) Referenztemperatur.

Die μ-Werte werden für jede halbe Stunde vorgegeben, in Tabelle 1 sind aus dieser Vorgabe die Werte zu jeder vollen Stunde zusammengestellt.

Man erkennt in dieser Tabelle, daß der Parameter für die thermische Schichtung symmetrisch zu 12 Uhr mittags vorgegeben ist; zu diesem Zeitpunkt soll die stärkste Instabilität der Schichtung herrschen. Um 06 Uhr morgens und um 18 Uhr abends ist nach der Vorgabe die Schichtung neutral, die ganze Nacht über herrscht eine stabile Schichtung, die von 21 Uhr bis 03 Uhr konstant bleibt. Diese Stabilität während der Nacht ist betragsmäßig gering verglichen mit der Instabilität am Tage.

Wie vom Verfasser früher dargelegt (Wippermann 1972) existiert in der planetarischen Grenzschicht eine obere Grenze für den abwärts gerichteten turbulenten Wärmestrom am Boden und damit für positive Werte des Schichtungsparameters μ; dieser Grenzwert ist von der Boden-Rossby-Zahl $Ro_0 = |\mathbf{V}_{g0}| \,/\, (z_0 f)$ abhängig, für kleine Boden-Rossby-Zahlen ist es etwa der für die Nacht vorgegebene Wert. (Es bedeuten $|\mathbf{V}_{g0}|$ den Betrag der geostrophischen Windgeschwindigkeit am Boden und z_0 die Rauhigkeitslänge).

Inwieweit diese Vorgabe realistisch ist, läßt sich am besten durch einen Vergleich mit Messungen beurteilen. Zu diesem Zweck wird der zu jedem Schichtungsparameter μ gehörende turbulente Wärmestrom am Boden q_0 betrachtet; es besteht folgender Zusammenhang

$$\mu = -\, q_0 \,/\, (b\, C_g) \tag{4}$$

wobei $C_g = u_* \,/\, |\mathbf{V}_{g0}|$ der geostrophische Widerstandskoeffizient (drag coefficient) ist und b eine Abkürzung für

$$b = c_p\, \bar{\varrho}\, f\, |\mathbf{V}_{g0}|^2 \,/\, (\varkappa^2\, \beta) \tag{5}$$

Mit $c_p = 0.24$ cal g^{-1} grad^{-1}, $\beta = 3.5$ cm sec^{-2} grad^{-1}, $\varkappa = 0.4$, $\bar{\varrho} = 1.2\ 10^{-3}$ g cm^{-3}, $f = 1.1\ 10^{-4}$ sec^{-1}, $|\mathbf{V}_{g0}| = 1 \cdot 10^3$ cm sec^{-1} hat b den Wert $b = 56.6$ mcal cm^{-2} sec^{-1}. Die Werte für C_g können im stationären Fall für eine gegebene Boden-Rossby-Zahl Ro_0 aus dem sogenannten Widerstandsgesetz für die planetarische Grenzschicht erhalten werden. Der sich damit ergebende Wärmestrom q_0 ist wiederum zu 12 Uhr symmetrisch, er ist als kräftig ausgezogene Kurve in der Abb. 1 eingetragen. Die übrigen Kurven sollen den Vergleich mit Messungen von q_0 ermöglichen; es sind die Meßergebnisse dargestellt worden, die Berz (1969) bei Messungen in der Nähe von München erhielt. Man erkennt, daß ein durchaus vernünftiger Tagesgang vorgegeben wurde. Die kräftige, gestrichelte Linie in Abb. 1 erhält man, wenn in Gl. (4) diejenigen Widerstandswerte C_g benutzt werden, die sich im instationären Fall ergeben und mit denjenigen des stationären Falles nicht mehr übereinstimmen; insbesondere zeigt sich, daß mit diesen Werten der Tagesgang schon nicht mehr zu 12 Uhr symmetrisch ist.

Die vorgegebenen μ-Werte reichen aus, um in einer horizontal homogenen Grenzschicht den Tagesgang

Tabelle 1

Tages-zeit	00	01 23	02 22	03 21	04 20	05 19	06 18	07 17	08 16	09 15	10 14	11 13	12
μ	13.4	13.4	13.4	13.4	12.4	9.0	0	−11.0	−20.6	−29.1	−34.7	−37.7	−39.1

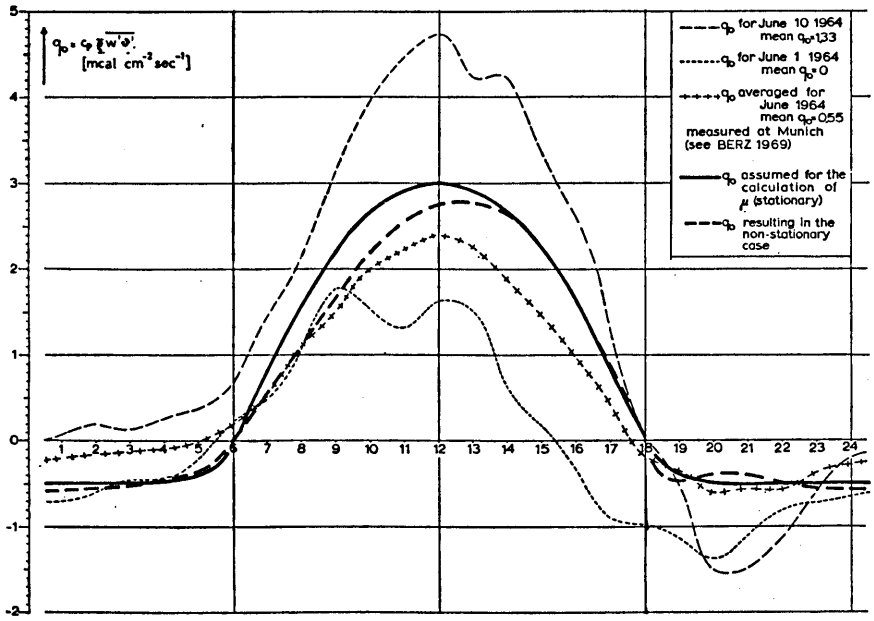

Abb. 1. Der vorgegebene Tagesgang des turbulenten Wärmestromes am Boden, verglichen mit Meßergebnissen

einer Reihe anderer meteorologischer Parameter zu berechnen, man erhält diese in Abhängigkeit von der Höhe z und der Zeit t. Dabei wird mit einer dimensionslosen Zeit $F = tf$ und einer dimensionslosen Vertikalkoordinate $Z_* = z/H_*$ operiert. Die charakteristische Grenzschichthöhe H gem. (2) ist ja zu jeder Zeit eine andere, da die Schubspannungsgeschwindigkeit u_* natürlich auch einen Tagesgang hat. Wenn also die Vertikalkoordinate z mit H dimensionslos gemacht würde, hätte man zu jeder Zeit eine andere Normierung. Um aber alle Werte miteinander vergleichbar zu machen, wurde diejenige charakteristische Höhe $H_* = \varkappa\, u_{**}/f$ verwendet, die sich im stationären Fall bei neutraler Schichtung ergibt. Der zugehörige Widerstandskoeffizient ist $C_{g*} = 0.0324$ für das verwendete $Ro_0 = 1\ 10^7$, d.h. $u_{**} = 32.4$ cm sec^{-1} für ein angenommenes $|\mathbf{V}_{g0}| = 1 \cdot 10^3$ cm sec^{-1} und $H_* = 1180$ m, wenn weiterhin angenommen wird, daß $f = 1.1\ 10^{-4}$ sec^{-1}.

Die berechneten meteorologischen Parameter sind einmal die von der Zeit F abhängigen Größen

$$C_g(F) = u_*(F) / |\mathbf{V}_{g0}| \quad \text{und} \quad \alpha_0(F) \tag{6}$$

und zum andern diejenigen, die sowohl von der Höhe Z_* als auch von der Zeit F abhängen

$$L_*(Z_*, F) = l/H_* \tag{7a}$$
$$K_{m*}(Z_*, F) = k_m/(H_*^2 f) \tag{7b}$$
$$X_*(Z_*, F) = \tau_x/(\bar{\varrho}\, u_{**}^2) \tag{7c}$$
$$Y_*(Z_*, F) = \tau_y/(\bar{\varrho}\, u_{**}^2) \tag{7d}$$
$$P_*(Z_*, F) = \varkappa(\hat{u} - \hat{u}_g)/u_{**} \tag{7e}$$
$$Q_*(Z_*, F) = \varkappa(v - v_g)/u_{**} \tag{7f}$$
$$\Theta_*(Z_*, F) = \hat{\vartheta}\, q_0/q_{0*} \tag{7g}$$
$$K_{h*}(Z_*, F) = k_h/(H_*^2 f) \tag{7h}$$

Es ist α_0 der sogenannte Ablenkungswinkel, der von der Bodenschubspannung τ_0 und dem geostrophischen Wind am Boden $\mathbf{V}_{g0}$ eingeschlossen wird. Weiterhin sind L_* der dimensionslose Mischungsweg, K_{m*} der dimensionslose turbulente Diffusionskoeffizient für Impuls, X_* und Y_* die dimensionslosen Komponenten der Reynolds'schen Schubspannung, P_* und Q_* die dimensionslosen Komponenten des Geschwindigkeitsdefektes, Θ_* die dimensionslose potentielle Temperatur und K_{h*} der dimensionslose turbulente Diffusionskoeffizient für Wärme. Es ist noch anzumerken, daß das Koordinatensystem mit der x-Achse in die Richtung der Bodenschubspannung τ_0 orientiert sein muß.

Im Zusammenhang mit den Luftbeimengungskonzentrationen interessieren vor allem die Größen K_{m*} gem. (7b), welche anstelle des benötigten turbulenten Diffusionskoeffizienten k_z verwendet werden soll, und die horizontale Windgeschwindigkeit, welche aus den Defekten (7e) und (7f) bestimmt werden kann:

$$|\mathbf{V}| / |\mathbf{V}_{g0}|(Z_*, F) = C_g(F) \cdot \{ [P(Z_*, F) - P(Z_{0*}, F)]^2 + [Q(Z_*, F) - Q(Z_{0*}, F)]^2 \}^{1/2} / \varkappa \tag{8}$$

Gl. (8) gilt nur für eine barotrope Grenzschicht, die bei den Rechnungen immer vorausgesetzt wurde. Es sind

$$P(Z_{0*}, F) = -\varkappa \cos\{\alpha_0(F)\} / C_g(F) \tag{9a}$$
$$Q(Z_{0*}, F) = \varkappa \sin\{|\alpha_0(F)|\} / C_g(F) \tag{9b}$$

Die Gln. (9a) und (9b) sind nichts anderes als die untere Randbedingung für die Geschwindigkeiten, wonach diese bei $z = z_0$ verschwinden.

Sowohl für $K_{m*}(Z_*, F)$ als auch für $|\mathbf{V}| / |\mathbf{V}_{g0}|(Z_*, F)$ sind in der bereits zitierten Arbeit (Wippermann u.a. (1973) Isoplethendarstellungen gegeben, aus welchen der Tagesgang der beiden Größen in jeder Höhe entnommen werden kann. In der Abbildung 2 sind die

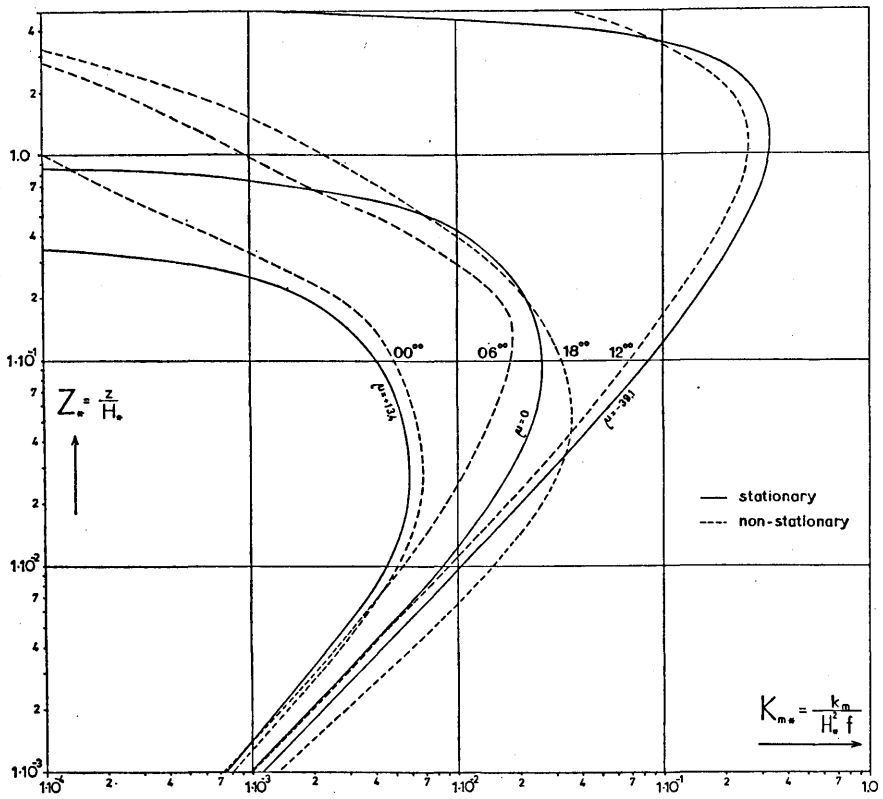

Abb. 2. Errechnete Vertikalprofile des turbulenten Diffusionskoeffizienten K_{m*} für die Tageszeiten 00, 06, 12 und 18 Uhr jeweils verglichen mit den K_{m*}-Profilen des entsprechenden stationären Falles

resultierenden Profile $K_{m*}(Z_*)$ für 00, 06, 12 und 18 Uhr als gestrichelte Linien dargestellt und verglichen mit denjenigen Profilen, die man in den entsprechenden stationären Fällen (ausgezogene Kurven) erhält. Man sieht, daß mittags K_{m*} kleiner ist als im entsprechenden stationären Fall, um Mitternacht hingegen größer. Um 06 Uhr und um 18 Uhr herrscht die gleiche thermische Schichtung (entsprechend der Vorgabe Tabelle 1 nämlich neutrale), die K_{m*}-Profile sind jedoch sehr verschieden. Wie man sieht, hängt es davon ab, ob der Zustand neutraler Schichtung von der stabilen Seite aus (morgens) oder von der instabilen Seite aus (abends) erreicht worden ist. Zu den bemerkenswerten Unterschieden gehört auch die Lage des Maximums: es findet sich um 06 Uhr bei $Z_* = 0.14$ (d.h. $z = 119$ m für $H = 1180$ m, siehe oben) um 18 Uhr bei $Z_* = 0.05$ (d.h. $z = 42$ m), während es im stationären Fall bei neutraler Schichtung bei $Z_* = 0.09$ (d.h. $z = 76$ m) festzustellen ist.

Eine ähnliche Abbildung ist für $|\mathbb{V}| / |\mathbb{V}_{g0}|$ in der bereits zitierten Arbeit (Wippermann u.a. 1973) als Figur 12 gegeben; sie zeigt, daß um Mitternacht der Horizontalwind stärker ist als im entsprechenden stationären Fall, mittags jedoch schwächer. Freilich ist der Unterschied zur Mittagszeit beträchtlich geringer als in der Nacht, wofür zur Erklärung wohl die zu den beiden Terminen unterschiedliche thermische Schichtung herangezogen werden muß.

In allen derzeitigen Diffusionsmodellen benutzt man einen höhenkonstanten Horizontalwind und höhenkonstante turbulente Diffusionskoeffizienten k_y und k_z (oder entsprechende mittlere Verschiebungsquadrate σ_y^2 und σ_z^2 der Partikel). Eine Anwendung der zuvor genannten Ergebnisse auf die Diffusionsmodelle nötigt also zu einer vertikalen Mittelbildung von K_{m*} einerseits und $|\mathbb{V}| / |\mathbb{V}_{g0}|$ andererseits; derartige Mittelwerte können dann als höhenkonstante Werte benutzt werden. Solche vertikalen Mittelbildungen sind durchgeführt worden für den Höhenbereich zwischen dem Boden und $Z_* = 0.15$ (d.h. $z = 170$ m für $H_* = 1180$ m). Die erhaltenen Mittelwerte sind in Tabelle 2 zusammengestellt. Aus der Tabelle 3 sind die Verhältnisse von jeweils zwei turbulenten Diffusionskoeffizienten K_{m*} oder von zwei Horizontalgeschwindigkeiten $|\mathbb{V}|$, die bei gleicher thermischer Schichtung auftreten, ersichtlich. Es zeigt sich, daß Diffusionskoeffizienten, die zur gleichen thermischen Schichtung, also zur gleichen „Ausbreitungsklasse" gehören, um den Faktor 2 verschieden sein können, nur aufgrund der Instationarität. Durch die zeitliche Veränderlichkeit, also durch die Kopplung mit dem vorangegangenen Zustand, hinkt die wirkliche Entwicklung immer etwas hinter derjenigen hinterher, welche durch den stationären Zustand bei dieser thermischen Schichtung gegeben ist. Wenn in zwei zu vergleichenden Fällen der zeitliche Ablauf so ist, daß der betrachtete Zustand (also die betrachtete thermische Schichtung) von den beiden unterschiedlichen Seiten her, also einmal von der mehr stabilen Schichtung und zum andern von der mehr labilen erreicht worden ist, wird ein besonders großer Unterschied zwischen den dann auftretenden K_{m*}-Werten bemerkbar.

Tabelle 2. *Vertikale Mittelwerte (zwischen Boden und etwa 170 m) für den turbulenten Diffusionskoeffizienten K_{m*} und die horizontale Windgeschwindigkeit $|\mathbf{V}|/|\mathbf{V}_{g0}|$. Außerdem ist das Verhältnis dieser Größen im instationären Fall zu denjenigen im entsprechenden stationären Fall angegeben. Daß sich für $|\mathbf{V}|/|\mathbf{V}_{g0}|$ ein Maximum während der Nacht, also bei verminderter vertikaler Durchmischung, ergibt und nicht wie erwartet am Tage, muß mit dem starken Überschießen des geostrophischen Windes während der Nacht (z.B. 20% in etwa 200 m Höhe) erklärt werden*

Tageszeit	$K_{m*,\,\mathrm{inst}}$	$K_{m*,\,\mathrm{stat}}$	$\frac{K_{m*,\,\mathrm{inst}}}{K_{m*,\,\mathrm{stat}}}$	$\frac{\lvert\mathbf{V}\rvert}{\lvert\mathbf{V}_{g0}\rvert}$ instat.	$\frac{\lvert\mathbf{V}\rvert}{\lvert\mathbf{V}_{g0}\rvert}$ stat.	$\frac{\lvert\mathbf{V}\rvert_{\mathrm{inst}}}{\lvert\mathbf{V}\rvert_{\mathrm{stat}}}$
00	0.0047	0.0039	1.22	0.97	0.90	1.08
01	0.0047	0.0039	1.22	0.96	0.90	1.07
02	0.0045	0.0039	1.16	0.95	0.90	1.06
03	0.0042	0.0039	1.10	0.94	0.90	1.05
04	0.0046	0.0045	1.02	0.92	0.89	1.03
05	0.0064	0.0070	0.93	0.89	0.87	1.02
06	0.0153	0.0217	0.71	0.84	0.82	1.02
07	0.0314	0.0519	0.61	0.81	0.82	0.99
08	0.0460	0.0713	0.65	0.79	0.82	0.97
09	0.0537	0.0780	0.69	0.80	0.82	0.97
10	0.0588	0.0802	0.73	0.81	0.82	0.98
11	0.0637	0.0807	0.79	0.82	0.82	1.00
12	0.0687	0.0813	0.84	0.82	0.82	1.00
13	0.0737	0.0807	0.91	0.83	0.82	1.01
14	0.0782	0.0802	0.97	0.83	0.82	1.01
15	0.0816	0.0780	1.05	0.82	0.82	1.00
16	0.0817	0.0713	1.14	0.82	0.82	1.00
17	0.0693	0.0519	1.34	0.80	0.82	0.97
18	0.0276	0.0217	1.27	0.74	0.82	0.90
19	0.0074	0.0070	1.07	0.74	0.87	0.84
20	0.0034	0.0045	0.75	0.78	0.89	0.88
21	0.0031	0.0039	0.80	0.86	0.90	0.96
22	0.0038	0.0039	0.97	0.92	0.90	1.02
23	0.0044	0.0039	1.13	0.95	0.90	1.06
24	0.0047	0.0039	1.22	0.97	0.90	1.08

Tabelle 3. *Das Verhältnis der turbulenten Diffusionskoeffizienten K_{m*} zu denjenigen, die bei gleicher thermischer Schichtung auftreten; das gleiche für die horizontale Windgeschwindigkeit $|\mathbf{V}|$ (Vertikale Mittelwerte zwischen Boden und etwa 170 m). Die Klammer- von 21 Uhr bis 03 Uhr soll andeuten, daß in dieser Zeit ständig die gleiche thermische Schichtung herrscht und daher das Verhältnis auch zwischen andern Stunden als den zu 12 Uhr symmetrisch liegenden gebildet werden könnte*

Tageszeit (I)	Tageszeit (II)	$\frac{K_{m*,(\mathrm{I})}}{K_{m*,(\mathrm{II})}}$	$\frac{\lvert\mathbf{V}\rvert_{(\mathrm{I})}}{\lvert\mathbf{V}\rvert_{(\mathrm{II})}}$
00		—	—
01	23	1.07	1.01
02	22	1.18	1.03
03	21	1.39	1.09
04	20	1.35	1.18
05	19	0.87	1.20
06	18	0.55	1,13
07	17	0.45	1.01
08	16	0.56	0.96
09	15	0.66	0.98
10	14	0.75	0.98
11	13	0.86	0.99
12		—	—

In der Abb. 3 sind die zur jeweils gleichen thermischen Schichtung gehörenden Werte des turbulenten Diffusionskoeffizienten (vertikal gemittelt) bezogen auf denjenigen des jeweils entsprechenden stationären Falles dargestellt. Beim Ordinatenwert 1.0 ist gerade derjenige K_m-Wert erreicht, der im entsprechenden stationären Fall auftritt; dies ist morgens kurz nach 04 Uhr und am Nachmittage zwischen 14 und 15 Uhr der Fall. Die vielen unterschiedlichen K_{m*}-Werte bei gleicher thermischer Schichtung während der Nacht sind dadurch bedingt, daß bei der Vorgabe von μ dieses zwischen 21 und 03 Uhr konstant gehalten wurde.

Die verglichenen Werte sind natürlich auch etwas davon abhängig, bis zu welcher Höhe die vertikale Mittelbildung vorgenommen wurde. An einem kleinen Beispiel läßt sich der Unterschied demonstrieren: bei einer Mittelbildung zwischen Boden und 170 m ist das Verhältnis $K_{m*(06)} / K_{m*(18)} = 0.55$, bei einer Mittelbildung zwischen Boden und 85 m erhält man für dieses Verhältnis den Wert 0.46. Für das Verhältnis der Werte um 07 Uhr und 17 Uhr (beide male $\mu = -11.0$) erhält man für die beiden entsprechenden Zahlen 0.45 bzw. 0.42.

An dieser Stelle sei dem Verfasser noch eine Anmerkung erlaubt, die zwar nur mittelbar im Zusammenhang mit dem Übrigen steht, die aber nichts desto weniger sehr wichtig ist. Nach seiner Meinung ist die in Gl. (1) definierte Größe μ derjenige meteorologische Parameter, der anstelle der bislang verwendeten empirischen Ausbreitungsklassen zu benutzen wäre. Dieser Parameter μ würde eine korrekte Quantifizierung der Ausbreitungsverhältnisse erlauben. Einer Verwendung von μ steht nicht so sehr die Schwierigkeit gegenüber, aus den gemessenen externen Parametern zu dem benötigten internen Parameter μ zu gelangen (für diese Konvertierung hat z.B. Zilitinkevich 1970 bereits Diagramme angegeben) als vielmehr die Schwierigkeit, für eine durch Messungen gegebene Situation die einer planetarischen Grenzschicht (stationär und horizontal homogen) äquivalente zu finden. Die planetarische Grenzschicht ist ja eine fiktive Grenzschicht, die — solange die Divergenzen von Strahlungsflüssen nicht berücksichtigt werden, wie das z.Z. noch der Fall ist — nur monoton mit der Höhe sich ändernde Temperaturen, aber beispielsweise keine Inversionen kennt. Für eine irgendwie gegebene Grenzschicht müßte also die zugehörige fiktive planetarische Grenzschicht gefunden werden, um an dieser den zugehörigen μ-Wert abzulesen. Diese Schwierigkeiten werden in absehbarer Zukunft sicher wesentlich geringer,

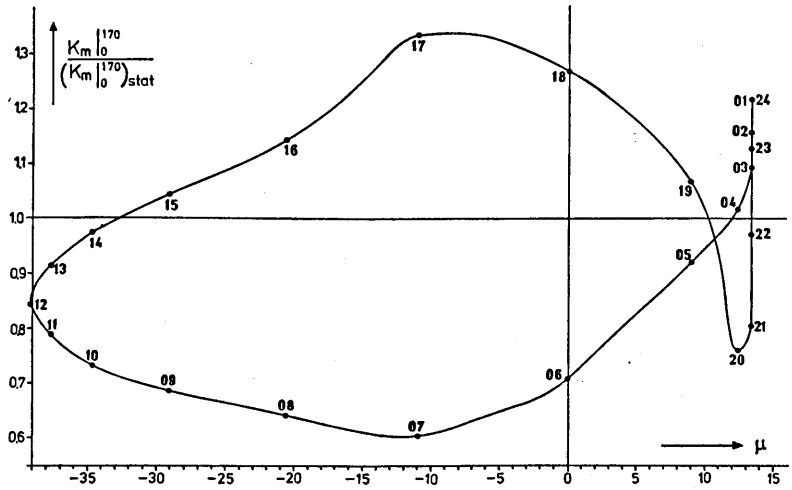

Abb. 3. Das Verhältnis des turbulenten Diffusionskoeffizienten K_{m*} im instationären Fall zu demjenigen im entsprechenden stationären Fall. Die Zahlen geben die Tageszeit an

wenn es durch weitere Forschungen auf dem Gebiet der Grenzschicht gelingt, in diese quantitativ die Divergenzen der Strahlungsströme aufzunehmen; damit ließe sich die fiktive planetarische Grenzschicht der wirklichen bedeutend ähnlicher machen.

III. Eine Abschätzung des Effektes der Instationarität auf die Ergebnisse der Ausbreitungsrechnung

Fast ausnahmslos wird in den heute benutzten Formeln für die Ausbreitung luftfremder Stoffe eine zweidimensionale Gauß'sche Verteilung in der Ebene senkrecht zur mittleren Rauchfahnenachse angenommen:

$$\bar{s}(x,y,z) = \frac{Q}{4\pi (k_y k_z)^{1/2} x} \exp\left(-\frac{\bar{u} y^2}{4 k_y x}\right) \cdot \left\{ \cdot \left\{ \exp\left(-\frac{\bar{u}(z-h)^2}{4 k_z x}\right) + \exp\left(-\frac{\bar{u}(z+h)^2}{4 k_z x}\right) \right\} \right. \tag{10}$$

Dabei ist s die Konzentration des sich ausbreitenden luftfremden Stoffes, x ist die Entfernung von der Quelle in Richtung des mittleren Windes $\bar{u}$, d.h. in Richtung der Rauchfahnenachse, y ist die horizontale Koordinate senkrecht zu x, und z ist die Vertikalkoordinate. h ist die Höhe der Quelle und Q die Quellstärke. k_y und k_z sind die beiden Diffusionskoeffizienten in den Richtungen senkrecht zur Rauchfahnenachse. Die obige Formel (10), übrigens die Lösung der Fick'schen Diffusionsgleichung für das Konzentrationsfeld im Lee einer kontinuierlichen Punktquelle, benutzt räumlich konstante Diffusionskoeffizienten, obwohl man weiß, daß diese von der Reisezeit der emittierten luftfremden Stoffe und damit von der Quelldistanz x abhängen. Wie schon zuvor erwähnt wird daher in den meisten Formeln für die Ausbreitung luftfremder Stoffe

$$k_y x = \frac{\bar{u}}{2} \sigma_y^2(x) \tag{11a}$$

$$k_z x = \frac{\bar{u}}{2} \sigma_z^2(x) \tag{11b}$$

gesetzt, wobei für die $\sigma_y(x)$ und $\sigma_z(x)$ empirische Werte benutzt werden, welche zu der jeweils angewandten Ausbreitungsklasse gehören.

Für das, was hier betrachtet werden soll, ist es jedoch völlig unerheblich, ob mit den konstanten Diffusionskoeffizienten k_y und k_z operiert wird oder mit den sich ändernden $\sigma_y(x)$ und $\sigma_z(x)$; wir betrachten daher die Konzentration auf der Projektionslinie der Rauchfahnenachse auf den Boden ($y=0$, $z=0$) in der Form mit k_y und k_z

$$\bar{s}(x,0,0) = \frac{Q}{2\pi (k_y k_z)^{1/2} x} \exp\left(-\frac{\bar{u} h^2}{4 k_z x}\right) \tag{12}$$

Gl. (12) gestattet mit der Bedingung

$$d\bar{s}/dx = 0 \tag{13}$$

eine Festlegung der Entfernung x_{max}, in welcher das Maximum der Konzentration $\bar{s}_{max}$ am Boden auftritt,

$$x_{max} = \bar{u} h^2 / (4 k_z) \tag{14}$$

und des maximalen Konzentrationswertes $\bar{s}_{max}$ selbst

$$\bar{s}_{max} = \frac{2Q}{e\pi h^2 \bar{u}} \left[\frac{k_z}{k_y}\right]^{1/2} \tag{15}$$

Um die im Tagesgang erhaltenen meteorologischen Parameter in den Formeln (14) und (15) anwenden zu können, soll der turbulente Diffusionskoeffizient k_z für luftfremde Stoffe gleichgesetzt werden dem turbulenten Diffusionskoeffizienten k_m für Impuls. Der dabei entstehende Fehler ist sicher sehr klein in dem Höhenbereich, in dem die Ausbreitungsvorgänge im Allgemeinen betrachtet werden; dieser Fehler braucht um so weniger berücksichtigt zu werden, als im folgenden nur noch Verhältnisse der Art $k_{m(1)} / k_{m(2)}$ betrachtet werden. Es wird also k_z durch den vertikalen Mittelwert (Boden bis 170 m) von k_m ersetzt, $\bar{u}$ wird durch den vertikalen Mittelwert von $|\mathbb{V}|$ ersetzt. k_y betrachten wir

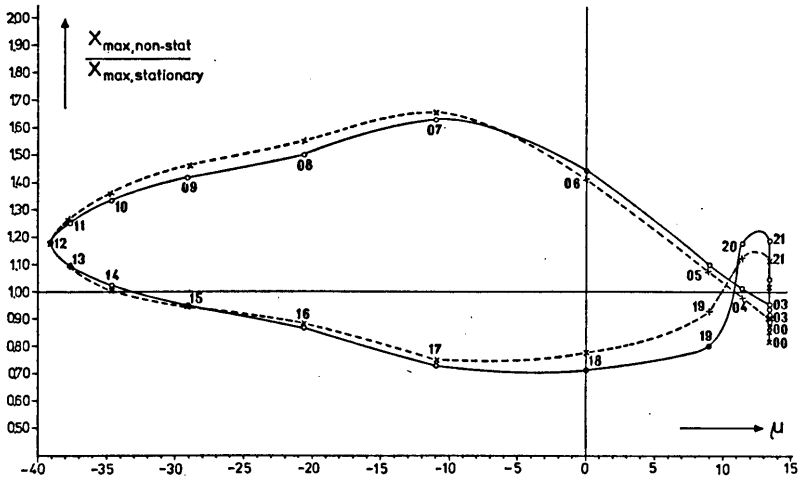

Abb. 4. Das Verhältnis der Entfernungen x_{max} im instationären Fall zu denjenigen im entsprechenden stationären Fall. Die Zahlen geben die Tageszeit an. Die ausgezogene Kurve gilt für das Verhältnis im Falle (a), die gestrichelte im Falle (b) entsprechend den Gln. (16) bzw. (18)

als zeitlich unverändert, da Angaben hierüber aus dem Grenzschichtmodell nicht zu erhalten sind; wenn jedoch eine zeitliche Veränderung auch von k_y berücksichtigt würde, könnte diese in Formel (15) den Effekt der zeitlichen Änderung von k_z zum Teil auskompensieren (bei gleichgerichteter zeitlicher Änderung, vermutlich bei instabiler Schichtung) oder aber noch verstärken (bei entgegengesetzter zeitlicher Änderung von k_y und k_z, vermutlich bei stabiler Schichtung).

Es müssen jetzt zwei Fälle unterschieden werden, nämlich

(a) sowohl k_z als auch $\bar{u}$ werden der entsprechenden Ausbreitungsklasse (für den stationären Fall) entnommen

(b) nur k_z wird der Ausbreitungsklasse für den stationären Fall entnommen, für $\bar{u}$ wird ein beobachteter Wert eingesetzt.

Dann ergeben sich für den Fall (a):

$$\frac{x_{max,instat}}{x_{max,stat}} = \frac{|V|_{instat}}{|V|_{stat}} \frac{K_{m^*,stat}}{K_{m^*,instat}} \tag{16}$$

$$\frac{\bar{s}_{max,instat}}{\bar{s}_{max,stat}} = \frac{|V|_{stat}}{|V|_{instat}} \left[\frac{K_{m^*,instat}}{K_{m^*,stat}}\right]^{1/2} \tag{17}$$

und für den Fall (b)

$$\frac{x_{max,instat}}{x_{max,stat}} = \frac{K_{m^*,stat}}{K_{m^*,instat}} \tag{18}$$

$$\frac{\bar{s}_{max,instat}}{\bar{s}_{max,stat}} = \left[\frac{K_{m^*,instat}}{K_{m^*,stat}}\right]^{1/2} \tag{19}$$

In der Abb. 4 ist das Verhältnis der Entfernungen der Maximalkonzentration im instationären Fall zu demjenigen im stationären Fall sowohl für den Fall (a) — ausgezogene Kurve — als auch für den Fall (b) — gestrichelte Kurve — im Tagesablauf dargestellt. Da die Abszisse entsprechend dem Parameter μ für die thermische Schichtung geteilt ist, kann man sofort erkennen, welche Tageszeiten die gleiche Schichtung aufweisen; diese müßten auch den gleichen Wert für x_{max} haben, wenn der Effekt der Instationarität nicht spürbar wäre. Die Abbildung 5 enthält die gleiche Darstellung für die Maximalkonzentration $\bar{s}_{max}$.

Zu den Tageszeiten mit der gleichen thermischen Schichtung lassen sich die in Tabelle 4 mitgeteilten Verhältnisse der Maximalkonzentrationen bzw. der Entfernungen x_{max} berechnen.

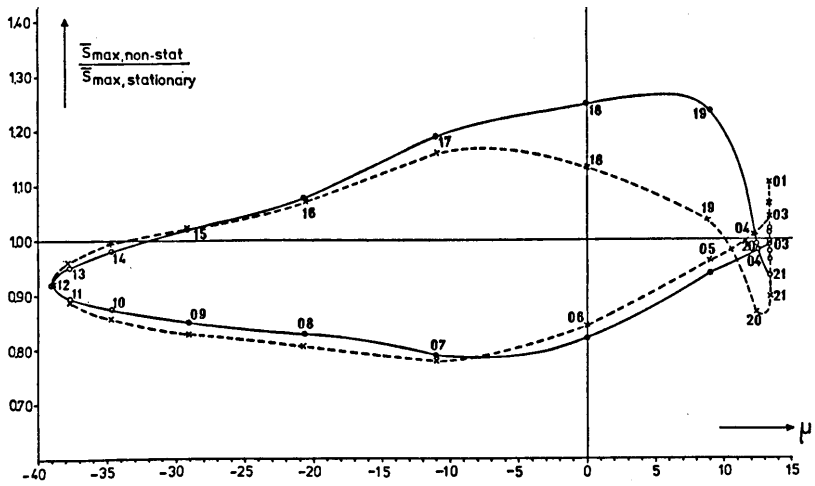

Abb. 5. Das Verhältnis der Maximalkonzentrationen $\bar{s}_{max}$ im instationären Fall zu denjenigen im entsprechenden stationären Fall. Die Zahlen geben die Tageszeit an. Die ausgezogene Kurve gilt für das Verhältnis im Falle (a), die gestrichelte im Falle (b) entsprechend den Gln. (17) bzw. (19)

Tabelle 4. *Das Verhältnis der Maximumsentfernungen x_{max} zu Zeiten mit der gleichen thermischen Schichtung; ebenso das Verhältnis der Maximalkonzentrationen selbst. Die Unterscheidung in die Fälle (a) und (b) gilt entsprechend den Gln. (16), (17) bzw. (18), (19). Wegen der Klammer von 21 Uhr bis 03 Uhr siehe die Unterschrift der Tabelle 3*

Tageszeit (I)	Tageszeit (II)	$x_{max,(I)}$ / $x_{max,(II)}$ (a)	$x_{max,(I)}$ / $x_{max,(II)}$ (b)	$\bar{s}_{max,(I)}$ / $\bar{s}_{max,(II)}$ (a)	$\bar{s}_{max,(I)}$ / $\bar{s}_{max,(II)}$ (b)
00		—	—	—	—
01	23	0.97	0.93	0.99	1.04
02	22	0.87	0.84	1.05	1.09
03	21	0.80	0.73	1.07	1.16
04	20	0.86	0.73	1.00	1.16
05	19	1.38	1.16	0.76	0.93
06	18	2.04	1.80	0.63	0.75
07	17	2.24	2.20	0.66	0.67
08	16	1.73	1.77	0.75	0.75
09	15	1.49	1.53	0.83	0.81
10	14	1.30	1.34	0.89	0.87
11	13	1.14	1.16	0.94	0.93
12		—	—	—	—

Um einen extremen Fall herauszugreifen: man sieht, daß $\bar{s}_{max,(a)}$ um 18 Uhr um mehr als die Hälfte größer ist als diejenige Maximalkonzentration, die (bei gleichen Schichtungsverhältnissen) um 06 Uhr auftritt. Da dies nur für einen normalen Strahlungstag gilt (vgl. den dem μ-Wert äquivalenten turbulenten Wärmestrom in Abb. 1) muß an Tagen mit einer noch größeren Amplitude von μ mit auch noch größeren Unterschieden der Maximalkonzentrationen bei gleicher thermischer Schichtung gerechnet werden. Für das Verhältnis der Maximumsentfernungen wird bereits bei dem hier behandelten Tagesgang der Faktor 2 überschritten.

IV. Schlußfolgerungen

Für einen (hier behandelten) „normalen Strahlungstag" ergeben sich Maximalkonzentrationen $\bar{s}_{max}$ und Quellentfernungen x_{max} dieser Maxima zu den einzelnen Tageszeiten, die z. T. sehr verschieden sind von denjenigen Werten, welche zu diesen Tageszeiten im stationären Zustand gelten würden und welche mit den derzeitigen Diffusionsmodellen bestimmt werden. Wie die Abbildungen 4 und 5 zeigen, kann die Maximalkonzentration $\bar{s}_{max}$ zwischen dem 1.25fachen (18 Uhr) und dem 0.79fachen (07 Uhr) derjenigen im entsprechenden stationären Zustand schwanken; für die Maximumsentfernung x_{max} tritt eine Schwankung zwischen dem 1.63-fachen (07 Uhr) und dem 0.71fachen (18 Uhr) auf. An Tagen mit einem noch ausgeprägteren Tagesgang, d. h. an „reinen Strahlungstagen", werden diese Abweichungen noch größer sein.

Es sind hier — wohl erstmals — quantitative Angaben über diejenigen Fehler gemacht worden, die man mit den derzeitigen Diffusionsmodellen dadurch begeht, daß man nur stationäre Verhältnisse betrachtet. Gleichzeitig scheint die vorgelegte Untersuchung auch eine Möglichkeit aufzuzeigen, wie diese Fehler künftig gemindert werden könnten: aufgrund einer größeren Anzahl von Modellrechnungen mit verschiedenen Tagesgängen müßte sich eine empirische Beziehung für einen Korrekturfaktor (abhängend von der Art des Tagesganges) für $\bar{s}_{max}$ und für x_{max} ermitteln lassen.

Literatur

1. Berz, G.: Untersuchungen zum Wärmehaushalt der Erdoberfläche und zum bodennahen Transport Wiss. Mitt. **16**, Meteor. Inst. Univ. München (1969). — 2. Pasquill, F.: The estimation of the dispersion of windborn material. Meteor. Magaz. **90**, 33 (1961). — 3. Wippermann, F.: Empirical formulae for the universal functions $M_m(\mu)$ and $N(\mu)$ in the resistance law for a barotropic and diabatic planetary boundary layer. Beitr. Phys. Atm. **45**, (1972). — 4. Wippermann, F., Etling, D., Leykauf, H.: The effects of non-stationarity on the planetary boundary layer. Beitr. Phys. Atm. **46**, (1973). — 5. Zilitinkevich, S. S.: Die Dynamik der atmosphärischen Grenzschicht (in russ.), Leningrad Gidrometeoriz. 290 S. (1970).

Meteorological Parameters Relevant in a Statistical Analysis of Air Quality Data*)

A b s t r a c t : Applying the arguments of Rossby-number similarity to a planetary boundary layer (steady state and horizontally homogeneous) it can be concluded, that the concentration of a polluting material is determined uniquely by two parameters: the internal parameter μ (i.e. the ratio of the internal scale height of the PBL to the Monin-Obukhov stability length) for the thermal stratification and the surface Rossby-number. Two additional parameters have to be considered in the case of a baroclinic PBL, however for much elevated sources only.
The considerations are made for the concentration (a) of a horizontal area source, (b) of a continuous point source and (c) of multiple sources.

Introduction

Today many measurements (continuous or at discrete times) of the air quality are carried out at many places in the industrial countries. The statistical evaluations of these measurements are as different (and therefore incomparable) as the places are. Mostly the concentration of a gaseous component or of particulate matter are considered as depending on the surface wind (speed and direction), on the surface temperature and sometimes on the humidity. However these three or four parameters are not able to describe completely the turbulent state in the atmospheric boundary layer and therefore not the diffusion conditions in it.

This paper intends to show which meteorological parameters can be considered as relevant in a statistical analysis

---

*) Paper presented at the Symposium "Statistical Analysis of Air Quality Data" Nov. 9-10 1972 Chapel Hill, N.C., USA sponsored by the Triange Universities Consortium on Air Pollution (TUCAP)

of air quality data. However, the drawn conclusions are valid only if the atmospheric boundary layer satisfies the conditions of a planetary boundary layer (PBL), i.e. stationarity and horizontal homogeneity. In general the actual boundary layer differs from the PBL, the conclusions are therefore only approximatively correct.
The basic concept has been developed together with D. YORDANOV (Sofia, Bulgaria) and is subject of a recent joint paper (WIPPERMANN and YORDANOV 1972).

The planetary boundary layer (PBL) and Rossby-number similarity

The PBL is defined as a stationary and horizontally homogeneous boundary layer. In a PBL exists for $z >> z_o$ (z_o = roughness-length) the so-called Rossby-number similarity, which means that the vertical profiles of certain variables (non-dimensionalized correctly by internal parameters) are independent of the given external parameters; they depend only on an internal parameter μ for the thermal stratification and on two internal parameters λ_x and λ_y for the baroclinicity in the PBL. Of course, also the height above the ground as the independent variable has to be made non-dimensional by a scale height H of the PBL

$$Z = z/H \qquad H = \varkappa u_*/f \qquad \text{(1a),(1b)}$$

where $\varkappa$ is the von Karman constant, $u_* = \sqrt{\tau_o/\bar{\varrho}}$ the friction velocity, τ the Reynolds stress, ϱ the density and f the Coriolis parameter. Variables for which the Rossby-number similarity is valid are for instance

$$P = \varkappa(\hat{u}-\hat{u}_g)/u_* \qquad Q = \varkappa(\hat{v}-\hat{v}_g)/u_*$$

$$T = \tau/(\bar{\varrho}\, u_*^2) \qquad \mathcal{E} = \varkappa^2\varepsilon/(f\, u_*^2)$$

$$K_m = k_m/(H^2 f) \qquad E_x = \overline{\varrho(u'')^2}/(\bar{\varrho}\, u_*^2)$$

$$E_y = \overline{\varrho(v'')^2}/(\bar{\varrho}\, u_*^2) \qquad E_z = \overline{\varrho(w'')^2}/(\bar{\varrho}\, u_*^2)$$

$$E_x \varphi_x(n) \qquad E_y \varphi_y(n) \qquad E_z \varphi_z(n) \tag{2}$$

$$\delta\Theta = (\hat{\vartheta}_T - \hat{\vartheta})/\vartheta_* \qquad \delta S = (\hat{s}_T - \hat{s})/s_*$$

P and Q are the non-dimensional velocity defects, $\hat{u}$ and $\hat{v}$ are the velocity components in a coordinate system, the x-axis of which coincides with the direction of the surface stress τ_o (an internal parameter); ε is the rate of the dissipation of turbulent kinetic energy. u" , v" and w" are the velocity fluctuations, E_x , E_y and E_z are the three parts of the turbulent kinetic energy. φ_x , φ_y and φ_z are the spectral density functions with the frequency n . $\delta\Theta$ is the non-dimensional difference of the potential temperatures at the top ($_T$) and the bottom ($_o$) of the PBL. δS is the analogous difference for the water vapor content. $\vartheta_* = - q_o/ /(\varkappa\, \bar{\varrho}\, c_p\, u_*)$ is a characteristic temperature fluctuation with c_p the specific heat and q_o the turbulent heat flux at the ground. $s_* = - j_o/(\varkappa\, \bar{\varrho}\, u_*)$ is a characteristic moisture fluctuation with j_o the turbulent moisture flux at the ground, i.e. the rate of evaporation.

All these variables listed in (2) have universal vertical profiles, depending only on the three internal parameters μ , λ_x , λ_y , for instance

$$T = T(Z, \mu, \lambda_x, \lambda_y) \qquad \text{for} \quad Z >> Z_o \tag{3}$$

where

$$\mu = H / L_* \tag{4}$$

is the internal parameter for the thermal stratification with $L_* = - c_p\, \bar{\varrho}\, u_*^3/(\varkappa\, \beta\, q_o)$ the Monin-Obukhov stability-length; $\beta = g/\tilde{\vartheta}$ with $\tilde{\vartheta}$ a reference temperature.

$$\lambda_x = \varkappa^2/f\; d\hat{u}_g/dz \qquad \lambda_y = \varkappa^2/f\; d\hat{v}_g/dz \tag{5a),(5b}$$

are the two internal parameters of the baroclinicity of the PBL; they are internal ones because they have components of $d\hat{v}_g/dz$ in a coordinate system orientated with the x-axis in the direction of the internal parameter τ_o.

For all the variables listed in (2) the same as in (3) is valid; that means the vertical profiles depend only on μ, λ_x; λ_y. That means furthermore that the state of turbulence in the PBL and therefore also the turbulent diffusion is completely determined by these three parameters.

The vertical profile of concentration caused by a horizontal surface source

The condition of horizontal homogeneity of the PBL is satisfied as long as the source of a gas or of particulate matter is a horizontal and infinite surface source. That means, that the concentration $\hat{r}_s$ $[g\ cm^{-3}]$, made dimensionless by the characteristic fluctuation of the concentration $r_* = i_o/(\varkappa\ \bar{\varrho}\ u_*)$, with i_o $[g\ cm^{-2}\ sec^{-1}]$ the source strength, must have a universal vertical profile

$$R_s = \frac{\hat{r}_s}{r_*}(Z, \mu, \lambda_x, \lambda_y) \quad \text{for} \quad Z >> Z_o \qquad (6)$$

Actually the Rossby-number similarity is valid for the non-dimensional difference $(R_s)_T - R_s$ only; here $(R_s)_T$, the concentration at the top of the PBL, is put zero (vanishing background concentration).

Examples for natural sources of that kind are an evaporating sea surface or a very large sand desert with sustained strong winds. Water vapor, respectively sand, is added to the air; the vertical profile of the concentration of these admixtures depends only on the three parameters μ, λ_x and λ_y.

The concentration in the case of a continuous point source

If one considers a continuous point source the condition of horizontal homogeneity is violated, Rossby-number similarity can not longer be used in order to conclude on which meteorological parameters the concentration pattern depends. (In the case of an instantaneous point source also the condition of stationarity is violated).

One can attempt to make a statement concerning the relevant meteorological parameters by assuming that the diffusion process is described by the steady state Fickian diffusion equation

$$\hat{u}\frac{\partial}{\partial x}\hat{r}_p + \hat{v}\frac{\partial}{\partial y}\hat{r}_p = \frac{\partial}{\partial x}\left\{k_x\frac{\partial}{\partial x}\hat{r}_p\right\} + \frac{\partial}{\partial y}\left\{k_y\frac{\partial}{\partial y}\hat{r}_p\right\} + \frac{\partial}{\partial z}\left\{k_z\frac{\partial}{\partial z}\hat{r}_p\right\} \tag{7}$$

and by replacing the velocities $\hat{u}$ and $\hat{v}$ and the turbulent diffusion coefficients k_x, k_y, k_z by variables, for which universal vertical profiles exist. The horizontal coordinates should be non-dimensionalized by the internal scale height H given in (1b), $X = x/H$ and $Y = y/H$ and the diffusion coefficients by $H^2 f$.

Since

$$\hat{u}_g(z) = \hat{u}_{go} + \left[d\hat{u}_g/dz\right]_c z = \hat{u}_{go} + u_*/\varkappa\ \lambda_x Z$$

$$\hat{v}_g(z) = \hat{v}_{go} + \left[d\hat{v}_g/dz\right]_c z = \hat{v}_{go} + u_*/\varkappa\ \lambda_y Z$$

and

$$\hat{u}_{go} = |\hat{w}_{go}|\ \cos(\alpha_o)$$

$$-\hat{v}_{go} = |\hat{w}_{go}|\ \sin(|\alpha_o|)$$

it results

$$\hat{u}/(Hf) = \{ P + \varkappa \cos(\alpha_o)/C_g \} / \varkappa^2 \tag{8a}$$

$$\hat{v}/(Hf) = \{ Q - \varkappa \sin(|\alpha_o|)/C_g \} / \varkappa^2 \tag{8b}$$

α_o is the cross-isobar angle and $C_g = u_*/|\hat{v}_{go}|$ the geostrophic drag coefficient. Both, α_o and C_g, can be eliminated in (8) by making use of the resistance law for the PBL.

$$\varkappa \cos(\alpha_o)/C_g = - M_m(\mu, \lambda_x, \lambda_y) + \ln(RO_o\, C_g) \tag{9a}$$

$$\varkappa \sin(\alpha_o)/C_g = N(\mu, \lambda_x, \lambda_y) \tag{9b}$$

Herein $RO_o = |\hat{v}_{go}|/(f\, z_o)$ is the surface Rossby-number, a non-dimensional combination of the given external parameters. The functions N and M_m appearing in this law are universal functions, i.e. they are independent of the external parameters and depend only on μ, λ_x and λ_y. The resistance law was first derived by KAZANSKII and MONIN in 1961 for the barotropic and neutral case, it was extended to the diabatic case by BLACKADAR (1967) and by MONIN and ZILITINKEVICH (1967); recently it was extended to baroclinic cases by YORDANOV and WIPPERMANN (1972). By using the resistance law (9a), (9b) and the definition

$$Z_o = (\varkappa\, RO_o\, C_g)^{-1} \tag{10}$$

one obtains for the diffusion equation (7) the following non-dimensional form

$$\begin{aligned}(P - M_m + \lambda_x Z)\frac{\partial}{\partial X}R_p + (Q - N + \lambda_y Z)\frac{\partial}{\partial Y}R_p - \\ - \ln(\varkappa Z_o)\frac{\partial}{\partial X}R_p = \\ = \varkappa^2\left[\frac{\partial}{\partial X}\left\{K_x\frac{\partial}{\partial X}R_p\right\} + \frac{\partial}{\partial Y}\left\{K_y\frac{\partial}{\partial Y}R_p\right\} + \frac{\partial}{\partial Z}\left\{K_z\frac{\partial}{\partial Z}R_p\right\}\right]\end{aligned} \tag{11}$$

The boundary conditions are

$$\left.\begin{array}{l} X \longrightarrow +\infty \\ Y \longrightarrow \pm\infty \\ Z \longrightarrow +\infty \end{array}\right\} \quad : \quad R_p = 0 \qquad (12a)$$

$$X = 0 \;,\; Y = 0 \;,\; Z = Z_b \quad : \quad R_p = 1 \qquad (12b)2$$

$$Z = Z_o \quad : \quad \partial R_p/\partial Z = 0 \qquad (12c)$$

It is $R_p = \hat{r}_p/(b\, f^5\, g^{-3})$ the non-dimensional concentration caused by a continuous point source $(_p)$, b $[g\ sec^{-1}]$ is the strength of the source, $Z_b = z_b/H$ is the non-dimensional effective height of the source.

If one assumes that the vertical profiles of the nondimensional diffusion coefficients for matter K_x, K_y and K_z are universal ones like the vertical profile of the diffusion coefficient K_m for momentum, all coefficients in the eq. (11) - except Z_o - depend only on μ, λ_x and λ_y and, of course, some of them on the independent variable Z. They all are universal functions. However the non-dimensional roughness-length Z_o depends on RO_o and C_g as seen in eq.(10), C_g itself depends on RO_o, μ, λ_x, λ_y as seen in the resistance law (9a), (9b). Since therefore Z_o depends on RO_o, μ, λ_x, λ_y the non-dimensional concentration R_p must depend on RO_o also:

$$R_p = R_p(X, Y, Z, Z_b, RO_o, \mu, \lambda_x, \lambda_y) \qquad (13)$$

The universality is now lost; the dependence from RO_o (i.e. from external parameters) enters because of the violation of the condition of horizontal homogeneity by having a continuous point source. A comparison of R_p in (13) with R_s in (6) shows the difference.

The concentration at a fixed point caused by multiple sources

A statement can be made only if one assumes that all the sources do not change their coordinates and their strengths

during the period of measurement. Furthermore one has to assume that this period of measurement is long enough to cover all possible cases (wind direction, Rossby-number, thermal stratification and possibly the baroclinicity) to almost equal parts. This later assumption has to be made in almost all statistical analyses of measured concentrations; however the first assumption will be satisfied only incompletely and causes therefore errors.

For each direction $(_d)$ (of the geostrophic surface wind) the mean concentration $\bar{r}_d$ at the point under consideration should be evaluated and a non-dimensional concentration

$$R_d = \hat{r} / \bar{r}_d \tag{14}$$

should be formed herewith. Fluctuations of R_d should be independent of the source positions $(x_b)_i$, $(y_b)_i$, $(z_b)_i$ and of the source strengths b_i , they should depend only on the parameters remaining in (13)

$$\boxed{R_d = R_d(RO_o , \mu , \lambda_x , \lambda_y)} \tag{15}$$

The surface Rossby-number RO_o can be determined directly from the given geostrophic surface wind, when z_o in the denominator is known; that can be obtained by the conventional measurements of the wind profile near the ground, but it should be representative for the whole area in which diffusion takes place. It may vary with the wind direction (and is therefore a "meteorological" parameter) and possibly with the vegetation period.
The internal parameter μ for the thermal stratification has to be found by converting the external parameter σ for the thermal stratification

$$\sigma = D / \Lambda \tag{16}$$

into the internal one. D is the external scale height of the

PBL and Λ is the external stability length of the PBL

$$D = \kappa^5 \left|\hat{v}_{go}\right| / f \tag{17a}$$

$$\Lambda = \kappa^3 \left|\hat{v}_{go}\right|^2 / (\beta \delta\hat{\vartheta}) \tag{17b}$$

with $\delta\hat{\vartheta} = \hat{\vartheta}_T - \hat{\vartheta}_o$. When the (potential) temperature difference $\delta\hat{\vartheta}$ from top to bottom and $\hat{v}_{go}$ the geostrophic wind at the ground are given, the parameter σ then can be formed; this must be converted into the parameter μ. ZILITINKEVICH (1970) for instance gives diagrams for the conversion of the given external parameter σ into the wanted internal parameter μ ; for this conversion again RO_o is needed.

Of course, difficulties will arise in forming the external parameter σ from the given parameters $\hat{\vartheta}_T$, $\hat{\vartheta}_o$, $\hat{v}_{go}$ because the first two are difficult to find. A PBL can only have a monotonically decreasing or increasing temperature profile $\hat{\vartheta}(z)$, it does not know temperature inversions or layers with unstable stratification or similar things frequently observed in the real atmospheric boundary layer. Therefore an observed temperature profile has to be smoothed in order to obtain the corresponding profile belonging to the PBL. From such a profile the difference $\hat{\vartheta}_T - \hat{\vartheta}_o$ should be taken.

The baroclinicity seems to be less important, it has to be considered only for much elevated sources, for instance for very tall stacks. An example has been given by WIPPERMANN and YORDANOV (1972) showing a cse with a pronounced minimum of the eddy diffusivity k_m in 320 m caused by the baroclinicity. When the baroclinicity must be considered one has to form first the two external parameters (in a coordinate system x^*, y^* orientated with the x-axis in the direction of the geostrophic wind at the ground)

$$\eta_{x^*} = \frac{\varkappa^2}{f\, z_T} \left\{ (\hat{\mathbb{v}}_{go})^{o} \cdot \hat{\mathbb{v}}_{gT} - \hat{\mathbb{v}}_{go} \right\} \tag{18a}$$

$$\eta_{y^*} = \frac{\varkappa^2}{f\, z_T} \; \mathbb{k} \cdot \left[(\hat{\mathbb{v}}_{go})^{o} \times \hat{\mathbb{v}}_{gT} \right] \tag{18b}$$

where z_T is the height of the top of the PBL. For a conversion into the internal parameters λ_x , λ_y of the baroclinicity the cross-isobar angle α_o is needed:

$$\lambda_x = \eta_{x^*} \cos(\alpha_o) + \eta_{y^*} \sin(|\alpha_o|) \tag{19a}$$

$$\lambda_y = - \eta_{x^*} \sin(|\alpha_o|) + \eta_{y^*} \cos(\alpha_o) \tag{19b}$$

The cross-isobar angle α_o can be obtained from the resistance law (9a),(9b). (For this purpose, however, λ_x and λ_y have to be known already; again an iterative procedure is necessary).

Concluding remarks

The baroclinicity of the boundary layer has an effect on the concentration pattern only when this is caused by much elevated sources; the effect can be neglected in most cases. The remaining meteorological parameters are the internal parameter μ for the thermal stratification of the boundary layer and the surface Rossby-number RO_o. Both these parameters determine the concentration uniquely (as long as the assumptions of a PBL are satisfied).

It seems that the parameter μ is just that one which is searched as a measure for the diffusion characteristics depending mainly on the thermal stratification; the empirical "dispersion categories" can be replaced possibly by this parameter, if one succeeds to determine that PBL, which is equivalent to the measured actual boundary layer.

References

BLACKADAR, A.K. 1967 External Parameters of the Wind Flow in the Barotropic Boundary Layer
GARP Study Conf. Stockholm, Rep. Append. IV, 11 pp

KAZANSKII, A.B.
MONIN, A.S. 1961 On the Dynamic Interaction between the Atmosphere and the Earth Surface
Bull. (Izv.) Acad. Sci. USSR, Geophys. Ser. Nr. 5, 786-788, engl. transl. 514-515

MONIN, A.S.
ZILITINKEVICH, S.S. 1967 Planetary Boundary Layer and Large Scale Atmospheric Dynamics
GARP Study Conf. Stockholm, Rep. Append. V, 37 pp

WIPPERMANN, F.
YORDANOV, D. 1972 A Perspective of a Routine Prediction of Concentration Patterns
J. Atm. Environm. 6, 877-888

YORDANOV, D.
WIPPERMANN, F. 1972 The Parameterization of the Turbulent Fluxes of Momentum, Heat and Moisture at the Ground in a Baroclinic Planetary Boundary Layer
Beitr. Phys. Atm. 45,58-65

ZILITINKEVICH, S.S. 1970 The Dynamics of the Atmospheric Boundary Layer (in Russ.)
Hydrometeorological Press, Leningrad, pp 291

Note added in reproduction

The non-dimensionalization of r_p following eq. (12c) on page 328 is not correct; a correction can be found on the page 313.

List of Symbols

The symbols used in chapter 6 have not been entered in this list, since they are somewhat different from those used in the chapters 1 - 5 and 7. Of course, they are explained in the papers reproduced in this chapter.

A_1, A_2, A_3, A_4 = abbreviations (pages 51-52)

A^* = $2.389\ 10^{-8}$ cal g^{-1} cm^{-2} sec^2, mechanical equivalent of heat

a = 0.4343

a = abbreviation in eq. (6b) on page 181, = b on page 234 and 315

a_h = k_h/k_m

a_s = k_s/k_m

B^2 = b^2/u_*^2, nondimensional turbulent kinetic energy, (pages 46 - 57, 106)

B_x = $1/f\ d\hat{v}_g/dz$ = $\lambda_y/\varkappa^2$ } Internal parameters for

B_y = $-1/f\ d\hat{u}_g/dz$ = $-\lambda_x/\kappa^2$ } the baroclinicity

b = abbreviation in eq. (40) on page 234 and eq.(5) on page 315, = a on page 181

b = $\overline{\varrho(\mathbb{v}'')^2}/(2\bar{\varrho})$, turbulent kinetic energy per mass unit [cm^2 sec^{-2}]

b = $\overline{(\mathbb{v}'')^2}$, twice the turbulent kinetic energy per mass unit [cm^2 sec^{-2}], pages 66-75

b^2 = $\overline{(\mathbb{v}'')^2}/2$, turbulent kientic energy per mass unit, used on pages 46 - 57 and 106

b_m = $\bar{\varrho}\,\hat{\mathbb{v}}^2/2$, kinetic energy (of the mean flow) per unit volume, pages 111 - 119

b_t = $\overline{\varrho(v'')^2}/2$, turbulent kinetic energy per unit volume, pages 111 - 119

C_g = $u_*/|\hat{\mathbb{v}}_{go}|$, geostrophic drag coefficient

C_{g*} = 0.0324, i.e.: C_g for $\mu = 0$, $\lambda_x = 0$, $\lambda_y = 0$ and for stationary condition

C_d = C_g, used on pages 46-57, 66-75, 89-94, 167-176, 184-191

C_h, C_{th} = $\vartheta_*/\delta\hat{\vartheta}$, "thermal drag coefficient", Stanton number

C_s = $s_*/\delta\hat{s}$, "drag coefficient for moisture"

$C\langle E_1,E_2\rangle$ = rate of the conversion of energy E_1 into energy E_2

c_p = specific heat at constant pressure [cal g^{-1} $grad^{-1}$]

c_v = specific heat at constant volume [cal g^{-1} $grad^{-1}$]

D = $\varkappa^5|\hat{\mathbb{v}}_{go}|/f$, external scale height of the PBL

D = $|\hat{\mathbb{v}}_{go}|/f$, external scale height of the PBL, used on pages 46-57, see also Λ

D_{xz}, D_{yz} = abbreviations for terms containing the molecular friction, see page 32

d = zero plane displacement

$\mathbb{E}$ = $\mathbb{i}\,\mathbb{i} + \mathbb{j}\,\mathbb{j} + \mathbb{k}\,\mathbb{k}$, unit tensor

E_x = $\overline{\varrho(u'')^2}/(\bar{\varrho}u_*^2)$

E_y = $\overline{\varrho(v'')^2}/(\bar{\varrho}u_*^2)$ nondimensional parts of the turbulent kinetic energy, page 324

E_z = $\overline{\varrho(w'')^2}/(\bar{\varrho}u_*^2)$

F = $f\,t$, nondimensional time, independent variable

$\mathbb{F}$ = tensor of molecular friction, see eq. (1) on page 8

$F_u, F_v, F_\vartheta, F_s$ = nondimensional functions in eq. (7), page 186

f = $2\Omega\sin(\varphi)$, Coriolis parameter

f^* = $2\Omega\cos(\varphi)$, second Coriolis parameter

$G_u, G_v, G_\vartheta, G_s$ = nondimensional functions in eq. (9) on page 187

g = gravitational acceleration, 981 cm sec^{-2}

H = $\varkappa u_*/f$, internal scale height of the PBL

H' = scale height in Lettau's mixing-length hypothesis page 48

h = height of the Prandtl-layer, defined by $\tau(h) = 0.9\tau_0$, pages 66-75

h = z_T , height of the PBL (pages 184-191)

h = z_b , height of the point source (page 319)

I = $\bar{\varrho}\{c_v\hat{T}+\Phi\}$, averaged internal and potential energy

I_x, I_y = Integrals in eqs.(35a),(35b) on page 203

i_o = strength of a surface source [g cm^{-2} sec^{-1}]

$\mathbb{i}$ = unit vector in the x-direction

$j = \overline{\varrho w''s''}$, turbulent vertical flux of water vapor [g cm^{-2} sec^{-1}]

$\mathbf{j}$ = unit vector in the y-direction

$K_h = k_h/(H^2 f)$, nondimensional turbulent diffusion coefficient for heat

$K_m = k_m/(H^2 f)$, eddy viscosity nondimensionalized by internal parameters

$K_{mn} = k_m/(D^2 f)$, eddy viscosity nondimensionalized by external parameters

$K_s = k_s/(H^2 f)$, nondimensional turbulent diffusion coefficient for moisture

$K_x, K_y, K_z = k_i/(H^2 f)$ $i = x,y,z$, nondimensional turbulent diffusion coefficient for matter

$k = (c_p - c_v)/c_p = 0.285$

k = integer for the vertical steps in the iterative procedure on pages 227-230

$\mathbf{k}$ = unit vector in the vertical (z-) direction

k_m = eddy viscosity, turbulent diffusion coefficient for momentum [cm^2 sec^{-1}]

k_h = turbulent diffusion coefficient for heat [cm^2 sec^{-1}]

k_s = turbulent diffusion coefficient for the water vapor [cm^2 sec^{-1}]

k_b = turbulent diffusion coefficient for the turbulent kinetic energy [cm^2 sec^{-1}]

k_x, k_y, k_z = turbulent diffusion coefficients for matter (for the diffusion in the directions x, y and z) [cm^2 sec^{-1}]

$L = 1/H$, nondimensional mixing-length

$L_n = 1/D$, mixing-length nondimensionalized by external parameters

$L_* = -c_p \bar{\varrho} u_*^3/(\varkappa \beta q_o)$, Monin-Obukhov stability length

$L_* = -c_p \bar{\varrho} u_*^3/\{\varkappa \beta (q_o + q_{so})\}$, Monin-Obukhov stability length including the latent heat flux (used on pages 184-191)

$L_{MO} = L_*$, Monin-Obukhov stability-length, used on page 315

L^* = condensation heat per unit mass [cal g^{-1}]

l = mixing-length

l_∞ = asymptotic mixing-length for $z \longrightarrow \infty$

M, M_m = universal function in the resistance law (for momentum)

δM_m = $M_m(\mu, \lambda_x, \lambda_y) - M_m(\mu, 0, 0)$, see page 191

M_h = universal function in the resistance law (for heat)

M_s = universal function in the resistance law (for water vapor)

m = coefficient in the Ekman solution, page 45-50 or eq. (23) page 70; see also n

N = universal function in the resistance law (for momentum)

δN = $N(\mu, \lambda_x, \lambda_y) - N(\mu, 0, 0)$, see page 191

n = power in the stress profile (24), page 71

n = $(f/2k_{mE})^{1/2}$, coefficient in the Ekman solution eq. (15) page 195, see also m

n = frequency , page 324

P = $\varkappa(\hat{u}-\hat{u}_g)/u_*$, nondimensional velocity defect, x-component

PBL = Planetary Boundary Layer

p = pressure

p = power in the vertical profile of k_m

p = power in the mixing-length hypothesis by Wippermann, page 45, = q on page 90

p_N = p/τ_0 , nondimensional pressure

Q = $\varkappa(\hat{v}-\hat{v}_g)/u_*$, nondimensional velocity defect, y-component

Q = source strength [g sec^{-1}] of a point source, in diffusion formula on page 319

δQ^* = diabatic heating per unit mass per unit time [cal g^{-1} sec^{-1}]

q = power in the vertical profile of k_m , page 39

q = abbreviation for a power in eq. (26) on page 51

q = power in the mixing-length hypothesis by Wippermann eq. (5) on page 90, = p on page 45

q = integer in the iterative procedure, pages 59-62

q = $c_p \overline{\rho w'' \vartheta''}$, turbulent vertical flux of sensible heat [cal cm^{-2} sec^{-1}]

R = gas constant, 2.868 10^6 cm^2 sec^{-2} $grad^{-1}$ for dry air

IR = radiative flux [cal cm^{-2} sec^{-1}]

Ri_f = Richardson flux number, page 118

RO_o, Ro_o = $|\hat{v}_{go}|/(f\, z_o)$ surface Rossby number

R_d = $r/\bar{r}_d$, nondimensional concentration from multiple sources for the direction d of the surface geostrophic wind

R_p = $\hat{r}_p\ g^3/(b\ f^5)$ = S , nondimensional concentration of dispersed matter from a continuous point source, see note on page 313

R_s = $\hat{r}_s/r_*$ nondimensional concentration of dispersed matter from a surface source

r = abbreviation (35) on page 72

r = abbreviation in eq. (27) on page 52

r = integer in the iterative procedure, pages 59-62

r = integer for the time steps in the iterative procedure pages 227-230

$\hat{r}$ = concentration of dispersed matter [g cm^{-3}]

r_d = mean concentration of dispersed matter for a fixed direction of the surface geostrophic wind

$\hat{r}_p$ = concentration of dispersed matter from a continuous point source

$\hat{r}_s$ = concentration of dispersed matter from a surface source

r_* = $i_o/(\varkappa\bar{\varrho}\ u_*)$, characteristic fluctuation of the concentration

S = $\hat{s}/s_*$, nondimensional content of water vapor

S = $\beta\ \delta\hat{\vartheta}/(f\ |\hat{v}_{go}|)$, external parameter for the thermal stratification, see eq. (10c) on page 187

S = stability parameter in the hypothesis for $k_m(z)$ by Kovetz et al., page 38

S = $\hat{s}\ g^3/(b\ f^5)$ = R_p , nondimensional concentration of dispersed matter, see the note on page 313

s = abbreviation in eq. (29) on page 52

s = integer in the iterative procedure (pages 227-230)

s = moisture (specific humidity or mixing-ratio)

s = concentration of dispersed matter [g cm^{-3}]

s_* = $-\ j_o/(\varkappa\bar{\varrho}\ u_*)$, characteristic fluctuation of the moisture

$\delta\hat{s}$ = $\hat{s}_T - \hat{s}_o$, used in the resistance laws

$\delta\hat{s}$ = amount of water vapor condensated ($\delta s < 0$) or evaporated ($\delta s > 0$); used in the energy equations

T = temperature [grad K]

$\mathbb{T}$ = τ / τ_o nondimensional Reynolds stress

t = time (independent variable)

U = $\varkappa \hat{u}/u_*$, nondimensional velocity component in the direction of the surface stress

U_n = $\hat{u}_n / |\hat{\mathbb{v}}_{go}|$, nondimensional velocity component in the direction of the surface geostrophic wind

$\hat{u}$ = velocity component in the x-direction

$\hat{u}_g$ = component of the geostrophic wind in the x-direction

u_* = $(\tau_o / \bar{\varrho})^{1/2}$, friction velocity

V = $\varkappa \hat{v}/u_*$, nondimensional velocity component in the direction perpendicular to the surface stress

V_n = $\hat{v}_n / |\hat{\mathbb{v}}_{go}|$, nondimensional velocity component in the direction perpendicular to the surface geostrophic wind

$\mathbb{V}$ = $\varkappa \hat{\mathbb{v}}/u_*$, vector of the nondimensional wind velocity

$\hat{v}$ = velocity component in the y-direction

$\hat{v}_g$ = component of the geostrophic wind in the y-direction

$\hat{\mathbb{v}}$ = vector of the wind velocity

$\hat{\mathbb{v}}_g$ = vector of the geostrophic wind

$\hat{\mathbb{v}}_h$ = vector of the horizontal wind

W = $\varkappa w/u_*$, nondimensional vertical component of the velocity

w = vertical component of the velocity

X = x/H , nondimensional horizontal coordinate, used in chapter 7 only

X = $\tau_x / (\bar{\varrho}\, u_*^2)$ nondimensional stress-component in the direction of the surface stress

X_n = $\tau_x / (\bar{\varrho}\, \varkappa^8 |\hat{\mathbb{v}}_{go}|^2)$ nondimensional stress-component in the direction of the surface geostrophic wind

x = horizontal coordinate in the direction of the surface stress

x^* = horizontal coordinate in the direction of the surface geostrophic wind

x = horizontal coordinate in the direction of the mean wind (used in chapter 7 only)

x_{max} = distance of the maximum ground concentration from the source, used in chapter 7 only

Y = y/H , nondimensional horizontal coordinate, used in chapter 7 only

Y = $\tau_y/(\bar{\varrho}\, u_*^2)$ nondimensional stress component in the direction perpendicular to the surface stress

Y_n = $\tau_{y*}/(\bar{\varrho}\, \varkappa^8 |\hat{\mathbb{v}}_{go}|^2)$ nondimensional stress-component in the direction perpendicular to the surface geostrophic wind

y = horizontal coordinate perpendicular to the surface stress

y^* = horizontal coordinate in the direction perpendicular to the surface geostrophic wind

y = horizontal coordinate in the direction perpendicular to the mean wind (used in chapter 7 only)

Z = z/H vertical coordinate nondimensionalized by internal parameters

Z_n = z/D vertical coordinate nondimensionalized by external parameters

Z_o = $(\varkappa\, C_g\, RO_o)^{-1}$, nondimensional roughness-length

z = vertical coordinate

z_b = height of a point source

z_g = height where the wind $\hat{\mathbb{v}}_h$ for the first time has the direction of the geostrophic wind (for barotropic cases only)

z_o = roughness-length

z_R = height above which Rossby-number similarity exists

z_* = upper boundary for the $k_m(z)$-hypothesis by Rossby, see pages 35-36

α = angle between $\hat{\mathbb{v}}_g$ and τ

α_o = cross-isobar angle (between $\hat{\mathbb{v}}_{go}$ and τ_o)

β = angle between $\hat{\mathbb{v}} - \hat{\mathbb{v}}_{go}$ and $\hat{\mathbb{v}}_{go}$

β = $g/\tilde{\vartheta}$

β = undetermined constant, pages 175-176

Γ = abbreviation in eq. (9c), page 60

Γ = abbreviation according to eq. (33c), page 228

γ = factor in the (log + linear) profile, page 212

γ = factor in the linear dependence of Φ_m on the stratification, page 102

γ = angle between $\hat{\mathbb{v}}_{go}$ and $\nabla_h \hat{\vartheta}$

δ^* = displacement thickness of the boundary layer

δ_1, δ_2 = exponents in expressions for l_∞ , eq.(8), p. 182

$\mathcal{E}$ = $\varepsilon \varkappa^2/(f\, u_*^2)$ the rate of kinetic energy dissipated per unit volume per unit time, nondimensionalized by internal parameters

ε = rate of kinetic energy dissipated per unit volume per unit time, [$cm^2\ sec^{-3}$]
index m for the kinetic energy of the mean motion,
index t for the turbulent kinetic energy

ε_N = $u_*^2 f/\varkappa^2$ dissipation rate for nondimensionalization [$cm^2\ sec^{-3}$]

ζ = z/z_o nondimensional vertical coordinate

η = angle between τ and τ_o (pages 66-75)

η = $(Z - Z_o)/K_{mo}$, abbreviation on pages 129-135

η_{x*} = $\varkappa^2/f\ d\hat{v}_g/dz \cdot (\hat{v}_{go})^o$ External parameters for the baroclinicity

η_{y*} = $\varkappa^2/f\ |k \cdot [(\hat{v}_{go})^o \times d\hat{v}_g/dz]$

Θ = $\hat{\vartheta}/\vartheta_*$ nondimensional potential temperature

ϑ = $T\,(p_o/p)^k$, potential temperature

$\tilde{\vartheta}$ = a (potential) reference temperature

ϑ_* = $-\,q_o/(\varkappa\, c_p\, \bar{\varrho}\, u_*)$, characteristic fluctuation of the temperature

ϑ_* = $-\,(q_o + q_{so})/(\varkappa\, c_p\, \bar{\varrho}\, u_*)$, here the turbulent flux of latent heat is included, pages 184-191

$\varkappa$ = 0.4 , von Karman's constant

Λ = $|\hat{v}_{go}|/f$, external scale height of the PBL, pages 184-191, see also D

Λ = $\varkappa^3 |\hat{v}_{go}|^2/(\beta\, \delta\hat{\vartheta})$ external stability length, see eq. (17b) on page 330

λ = factor in the stress-profile (26a) on page 71

λ_x = $\varkappa^2/f\ d\hat{v}_g/dz \cdot (\tau_o)^o$ Internal parameters for the baroclinicity

λ_y = $\varkappa^2/f\ |k \cdot [(\tau_o)^o \times d\hat{v}_g/dz]$

μ = viscosity, 1.81 10^{-4} $g\ cm^{-1}\ sec^{-1}$ for air at 20°C

μ = factor in the stress-profile (25a) on page 71

μ = H/L_* , internal parameter for the thermal stratification

μ_* = $\mu\,(q_{o,min})$, see pages 181-182

ν = $\mu/\bar{\varrho}$, kinematic viscosity, 0.15 $cm^2\ sec^{-1}$ for air at 20°C

ν = power in the stress-profile (25a) on page 71

ν_h = coefficient of molecular heat transfer $[cm^2\ sec^{-1}]$

ν_s = molecular diffusion coefficient for water vapor $[cm^2\ sec^{-1}]$

ξ = $\log_{10}(Z)$, on pages 59-62, 227-230

ϱ = density

Φ_h = $z/\vartheta_*\ d\hat{\vartheta}/dz$ = $Z\ d\Theta/dZ$, nondimensional function for the temperature profile in the surface layer

Φ_m = $\kappa\ z/u_*\ d\hat{u}/dz$ = $Z\ dU/dZ$ nondimensional function for the wind shear in the surface layer

Φ = geopotential $[cm^2\ sec^{-2}]$

Φ = abbreviation in eq. (48) on page 75

φ = geographical latitude

$\varphi_u, \varphi_v, \varphi_\vartheta, \varphi_s$ = universal functions in eqs. (15a)-(15d) page 189

$\varphi_x(n), \varphi_y(n), \varphi_z(n)$ = spectral density functions (n = frequency), page 324

ψ = ε_t/k_m used in the mixing-length hypothesis page 44

ψ = angle between $-(\hat{\mathbf{v}}-\hat{\mathbf{v}}_g)$ and τ , pages 66-75

$\psi_u, \psi_v, \psi_\vartheta, \psi_s$ = universal functions in the eqs. (14a) - (14d), page 188

σ = $\beta\ \delta\hat{\vartheta}/(|\hat{\mathbf{v}}_{go}|\ f)$ external parameter for the thermal stratification, see also S

σ_x, σ_y = mean square deviations of particles, diffusion parameter, see page 319

τ = $-\overline{\varrho w''\ \mathbf{v}''}$, Reynolds stress

Ω = vector of the angular velocity of the earth

Ω = $|\Omega|$ = $7.29\ 10^{-5}\ sec^{-1}$

Indices

ad = adiabatic

BL = by BLACKADAR

b = for turbulent kinetic energy

E = for Ekman's spiral

F = by an empirical formula, pages 105-106

g = geostrophic; Z_g means the height where the wind $\hat{w}_h$ for the first time has the direction of the geostrophic wind

H , h , th = for heat ; H is used on pages 184-191 only, th is used as index to C only

h = horizontal

L = for the logarithmic profile (pages 100-102)

m = for momentum

m = for the kinetic energy of the mean motion

s = for water vapor

s = at the sea surface

T = taken at Z_T , i.e. at the top of the PBL

x = the x-component

y = the y-component

z = the z-component

o = taken at z_o , i.e. at the lower boundary

10 = taken at 10 m above the sea surface

∞ = as index to l means the asymptotic mixing-length

$(..)'$ = $d(..)/dz$, pages 66-75, 129-135

$(..)^*$ = $d(..)/dZ$; pages 66-75

$(..)^*$ = final iteration in the iterative procedure on the pages 227-230

$(..)^{(n)}$ = $d^n(..)/dZ^n$, used on the pages 129-135

$(..)_*$ = normalized by C_{g*}/C_g , see pages 145-150, 234-243

The integers in the several iterative procedures are not listed in this table.

Author Index

Akerblom F.A. 34
Angell J.K. 259 263 281
Antonia R.A. 252 253
Appleby J.F. 43 47 49 50 58 60 90 102 143 170 172
Arago L.R. 246
Armendariz M. 137 138 139
Atwell N.P. 249
Avsec D. 266 282 295

Bagnold R.A. 262
Barcilon V. 266
Berliand M.E. 37
Bernhardt K. 114
Berz G. 182 233 234 315 316
Betchov R. 287
Bhumralkar Ch.H. 60 250 252
Blackadar A.K. 38 42 43 48 50 58 60 89 90 96 102 122 123 137 138 140 157 160 168 172 177 181 189 193 204 249 327
Blinova E.N. 36 172
Blom J. 250
Bobileva I.M. 44 49 50 96 107 172
Boldizeva N.A. 43 49
Bonner W. 137 138 140 141 147
Bradley E.F. 30 134 225 247 249
Bradshaw P. 250
Boogard J.F. 249
Brocks K. 209
Brooks F.A. 246
Brown R.A. 259 282 296
Businger J.A. 30 134 225

Caldwell D.R. 282
Chalikov V. 217
Charnock H. 124 156 209 216
Ching J.K. 43
Clarke R.M. 54 108 109 156 170 178 190 201 217 218 306 308
Clos-Arceduc A. 264 276 277
Coté O.R. 32 112
Counihan J. 252
Crawford T.V. 248
Criminale W.O. 287
Csanady C.T. 157 164 168 170 172 177 189 193

Daberdt W.F. 74
Deardorff J.W. 174
Dickson C.R. 281
Dmitrev A.A. 245
Donev E. 221 251 252
Druce A.J. 246
Dyer A.J. 247 248

Echols W.T. 252 253
Ekman V.W. 34
Elliott W.P. 246
Ellison T.H. 37 172
Estoque M.A. 60 246 250 252
Etling D. 4 142 148 222-244 257 280-298 315

Faller A.J. 256 257 258 263 275 282 294 295
Farquharson S.J. 138
Ferris D.H. 249
Fiedler F. 45 108 109 178 179 200 206 306
Findlater J. 138
Francis J.R.D. 124
Frost R. 37

Gandin L.S. 245
Gill A.E. 89 100 157 168 171 177 189 193
Glaser A.H. 246
Glass P.E. 249
Godev H. 39 221 252
Görtler H. 264 266 291
Gordon A.L. 259
Goualt J. 138
Gregory N. 263
Gutman L.N. 57

Hanna S.R. 73 168 250 259 281
Hasse L. 212 213
Haugen D.A. 2
Hidy G.M. 249
Hill G.E. 259
Hoeber H. 112 124 170
Hoecker W.H. 259
Horst W. 263 275 278 282

Izumi Y. 30 112 134 225

Jacobs W. 245
James J.R. 212 213
Johnson P.W. 212 213
Jones J.B. 247

Kaylor R. 256 257 258 263 275 282 294 295
Kazanskii A.B. 67 89 92 157 168 172 177 189 193 327
Khajeh-Nouri B. 32
Kibel I.A. 36 172
Klyuchnikova L.A. 39
Köhler H. 36
Kolmogorov A.N. 71
Kovetz A. 38
Kraus H. 112 114
Krishna K. 141
Kruegermeyer L. 209
Kuettner J. 281
Kung E.C. 48 52 176
Kung R. 252
Kuo H.L. 263
Kurosaki A. 44 50 238
Kutzbach J. 246

Laikhtman D.L. 1 39 44 49 50 96 107 171 172 173 252
Lettau H.H. 42 48 50 60 74 87 90 96 99 102 104 105 112 124 138 170 172 180 247 250

Leykauf H. 4 142 148 222-244 315
Lilly D.K. 263 267 282 289 298
Logan E. 247
Lumley J.L. 2 32
Luxton R.E. 252 253
Lykosov V.N. 57 237 238

Mahrt L.J. 138
Malkus J.S. 256 264
Martin R.S. 287 298
Merbt H. 245
Mildner P. 124
Miyake M. 246 248
Möller F. 35 172
Mollo-Christensen E.L. 282
Monin A.S. 1 41 54 55 67 71 87 89 92 108 109 153 157 162 168 171 172 176 177 178 189 193 217 218 248 305 327
Montgomery R.B. 36 94 96 172
Moroz W.J. 249

Nadejdina E.D. 248 251
Neumann J. 38
Neumann G. 212 213
Nickerson E.C. 250
Novikova E.D. 251

Obukhov A.M. 71 87 92
Ogura Y. 282 295
Ohmstede W.D. 43 47 49 50 58 60 90 102 143 170 172
Onishi G. 250
Orlenko L.R. 38 172

Pack D.H. 281
Panchev S. 221 252
Panofsky H.A. 2 178 179 247 249
Pasquill F. 311 314
Petersen E.L. 254
Peterson E.W. 251 253
Philip J.R. 247
Pierson W.J. 212 213
Planck V.G. 263 281
Plate E.J. 2 221 249
Prandtl L. 35 71 94
Priestley C.H.B. 2

Radikevich V.M. 253
Rao K.S. 32
Rider L.J. 137 138 139
Rider N.E. 247
Ronne C. 256 264
Rooke F.N. 138
Rossby C.G. 35 36 94 96 192
Roux L. 245
Ruszin M.I. 42 43 49

Sabeleva T.A. 43 49
Sakakibara S. 35
Schwerdtfeger W. 138
Sheppard P.A. 124 170
Shimanuki A. 44 104 172
Shir C.C. 253
Smith F.B. 44 50 249
Sokolova I.N. 245

Stearns C.R. 247 248

Stern M.S. 263

Stuart J.T. 263

Suzi R. 38

Svetz M.E. 36 37 96

Takaya S. 35

Tani I. 250

Tatro P.R. 282

Taylor G.I. 34 172

Taylor R.J. 102 155 175 176 247

Taylor P.A. 249 251 252 253 254

Tennekes H. 89 157 168 177 189 193

Tkachenko A.V. 248

Tollmien W. 35 94

Townsend A.A. 247 248

Tseitin G.Kh. 38 39 172

Tsverava V.G. 138

Van Atta C.W. 282

Wagner E.K. 253

Wagner N.K. 249

Wagner V. 212 213

Walker W.S. 263

Warenta L. 250

Wilkinson J.H. 287 298

Woodcock A.H. 262

Wyngaard J.C. 30 32 112 134 225

Yagihashi A. 282 295

Yamamoto G. 44 104 172

Yasuda N. 44 104 172

Yordanov D. 4 39 51 56 85 89-94 95 99 120-128 131 157 162 177 184-191 202 301-313 323 327 330

Yudin M.I. 36 96

Zabransky J. 250

Zaitsev A.S. 247

Zilitinkevich S.S. 1 44 49 50 54 55 89 96 107 108 109 156 157 162 171 172 173 177 178 181 190 193 209 217 218 242 243 306 308 318 327 330

The authors of the papers listed in the bibliography on the low-level jet (pages 151-153) have not been entered in the author index.